Cooperative Air Traffic Optimisation for Minimum Overall Fuel Usage

A thesis submitted in fulfilment of the requirements for the degree of Doctor of Philosophy

Paul N. Simon

B.Eng B.Bus.

School of Aerospace, Mechanical and Manufacturing Engineering.
College of Science, Engineering and Health
RMIT University

March 2013

DECLARATION

I certify that except where due acknowledgement has been made, the work is that of the author alone; the work has not been submitted previously, in whole or in part, to qualify for any other academic award; the content of the thesis is the result of work which has been carried out since the official commencement date of the approved research program; any editorial work, paid or unpaid, carried out by a third part is acknowledge; and, ethics procedures and guidelines have been followed.

Paul N Simon
Date: 06/02/14

ACKNOWLEDGEMENTS

I would like to express my gratitude to all those who enabled this thesis to come about. Foremost of these is my family for their support and understanding. Next, my supervisor A/Prof Cees Bil is due considerable thanks for his expertise and patience throughout this thesis and the research shown in it. Lastly, my fellow pursuers of ATM advancement, Greg Macdonald and Jesper Bronsvoort of Air Services Australia, are deeply appreciated for their insight and guidance in all things ATC.

TABLES & LISTS

Table of Contents

Table of Tables

Table of Figures

List of Abbreviations

AC #	Aircraft Number #
ANSP	Air Navigation Service Provider
ATC	Air Traffic Control
ATD	Along Track Distance
ATFM	Air Traffic Flow Management
ATFU	Air Traffic Fuel Usage
ATM	Air Traffic Management
ATS	Air Traffic System
BFF	BADA Fuel Function
BFO	BADA assisted PCO
BSO	BFO using a ‘schedule’ optimizer instead of a fuel optimizer.
CAS	Calibrated Airspeed
CTD	Cross Track Distance
CDR	Conflict Detection and Resolution
DAM	Discrete Area Method
DSM	Discrete route Segment Method
DTM	Discrete Time Method
FIR	Flight Information Region
OFF	Original Fuel Function used with PCO.
nmi	Nautical Mile
PCO	Prototype Core Optimizer
PDO	PCO or BFO based Dynamic Optimizer
Q#	Research Question # (refer to 2.4.2)

TAS	True Airspeed
TEM	BADA Total Energy Model
UPT	User Preferred Trajectories

List of Symbols

A	Set of NMD Areas or Nodes	-
A_{NN}	Set of potentially conflicting aircraft pairs for each and all A	-
Alt	Optimizer Variable - Altitude	ft
Alt_{MAX}	Optimizer Variable - Maximum Altitude	ft
AR	Aspect Ratio	-
ATD_i	ATD Baseline for Fuel/Performance Calculation.	nmi
ATD_A	ATD Baseline for NMD Data Transfer	nmi
ATD_n , ATD_{nN}	ATD Baseline for Individual Aircraft Control Nodes.	nmi
ATD_N	ATD Baseline for All Aircraft Control Nodes.	nmi
ATD_{NN}	Set of ATD_{nN} - ATD_{nN} pairs representing each element of A_{NN}	nmi
ATD_{R1}	ATD_N with no nodes representing the linear portion of cruise	nmi
ATD_{R2}	ATD_{R1} with a constant altitude cruise.	nmi
ATD_{R3}	ATD_{R2} but with all *TAS* reintroduced.	nmi
a_l	Longitudinal Acceleration	$m.s^{-2}$
a_n	Normal Acceleration	$m.s^{-2}$
C_D	Drag Coefficient	-
C_{D_i}	Drag Coefficient at Trajectory Calculation Node *i*	-
C_{D0}	Profile Drag Coefficient	-
C_{f1}	1st Thrust Specific Fuel Consumption Coefficient	$kg.(min.kN)^{-1}$
C_{f2}	2nd Thrust Specific Fuel Consumption Coefficient	kt
C_{fcr}	Cruise Fuel Flow Correction Coefficient	-
C_L	Lift Coefficient	-
C_{Li}	Lift Coefficient at Trajectory Calculation Node *i*	-
C_{Lmax}	Maximum Lift Coefficient	-
C_{Lmin}	Minimum Lift Coefficient	-
C_{T1}	1st Thrust Coefficient	N
C_{T2}	2nd Thrust Coefficient	ft
$C_{tc,4}$	1st Thrust Temperature Coefficient	$° C$
C_{Vmin}	BADA Defined Minimum Speed Coefficient	-
D	Aerodynamic Drag	N
e	Oswald's Wing Efficiency	-
FC_T	Total Fuel Capacity Weight	N
F_i	Initial on board fuel volume as a proportion of total fuel capacity	-
G_T	Temperature Gradient for Maximum Altitude	$ft/° C$
G_W	Weight Gradient for Maximum Altitude	ft/kg
g	Acceleration on Earth Surface due to Gravity (constant)	$m.s^{-2}$
H_{MAX}	BADA Defined Maximum Altitude	ft
H_{MO}	BADA Defined Maximum Operating Altitude	ft
h	Altitude	ft

h_i	Altitude at Trajectory Calculation Node *i*	ft
h_{MAX}	Maximum Altitude Optimizer Bounds	ft
h_{MIN}	Minimum Altitude Optimizer Bounds	ft
i	Fuel/Performance Calculation Interval Index for an Aircraft.	-
i_{max}	Total Number of *i* values for an aircraft.	-
k	Isentropic expansion coefficient	-
M_{MO}	Maximum Operating Mach Number	-
$MTOW$	Maximum Take Off Weight	N
m	Mass	kg
m_{act}	Actual Aircraft Mass	t
m_{max}	Maximum Aircraft Mass	t
N	Individual Aircraft Index	-
N_{MAX}	Total Number of Aircraft to be Optimized	-
n	Individual Aircraft Control Node Index	-
n_{max}	Total Number of Control Nodes for an Individual Aircraft	-
R	Universal Gas Constant	$m^2.K^{-1}.s^{-2}$
S	Aircraft Wing Area	m^2
S_y	Cross Track Distance (CTD)	nmi
S_{FLIGHT}	Total Route Distance Covered by a Trajectory	nmi
TAS	Optimizer Variable - True Air Speed	$nmi.min^{-1}$
TAS_{MAX}	Optimizer Variable - Maximum True Air Speed	$nmi.min^{-1}$
T	Thrust	N
T_{local}	Local Temperature	$^\circ C$
T_{req}	Required Thrust	N
$T_{req\ MAX}$	Maximum Required Thrust	N
$T_{req\ MIN}$	Minimum Required Thrust	N
t	time	sec
V_{MO}	Maximum Operating Calibrated Air Speed (knots)	kt
V_{TAS}	True Air Speed	$m.s^{-1}$
W	Aircraft Weight	N
W_1	Initial Aircraft Weight	N
W_i	Aircraft Weight at Trajectory Calculation Node *i*	N
X	Optimizer Variable Matrix	10^{-5}ft, 10^{-1} $nmi.min^{-1}$
X_{MIN}	Minimum Limits or Bounds on X	10^{-5}ft, 10^{-1} $nmi.min^{-1}$
X_{MAX}	Maximum Limits or Bounds on X	10^{-5}ft, 10^{-1} $nmi.min^{-1}$
ΔATD_i	Spacing between ATD_i elements.	nmi
$\Delta ATD_{i\ IDEAL}$	User Preferred Spacing between ATD_i elements.	nmi
ΔATD_N	Spacing between ATD_N elements.	nmi
$\Delta ATD_{N\ IDEAL}$	User Preferred Spacing between ATD_N elements.	nmi
Δh	Altitude Separation	ft
Δh_{min}	Minimum Altitude Separation	ft

$\Delta h_{A,\,N1,\,N2}$	Altitude Separation between AC N_1 and N_2 at A	ft
ΔT_{ISA}	Local Sea Level and ISA Temperature Difference	$^{\circ}K$
ΔS_y	CTD Separation	nmi
$\Delta S_{y\,min}$	Minimum CTD Separation	nmi
$\Delta S_{y,\,A,\,N1,\,N2}$	CTD Separation between AC N_1 and N_2 at A	nmi
Δt	Longitudinal Time Separation	min
Δt_{min}	Minimum Longitudinal Time Separation	min
$\Delta t_{A,N1,N2}$	Longitudinal Time Separation between AC N_1 and N_2 at A	min
γ	Aircraft Climb Angle	rad
γ_i	Aircraft Climb Angle at Trajectory Calculation Node i	rad
μ	Specific Fuel Consumption	$kg.(N.s)^{-1}$
ρ	Ambient Density	$kg.m^{-3}$
ρ_i	Ambient Density at Trajectory Calculation Node i	$kg.m^{-3}$

ABSTRACT

The objective of this research was to demonstrate that a continental-scale air traffic model, featuring cooperative user preferred trajectories (UPT), can be optimized to minimize total fuel usage. The model was based on the premise that the flight plans, i.e. routes with departure and arrival times, for all aircraft within a continental-scale region were known and their altitude and speed profiles were determined for minimum overall fuel burn, subject to conflict resolution; the resulting set of trajectories would require actions for all involved aircraft and thus be cooperative in nature. The model was also based on the premise that these flight plans would also contain information on the aircraft's, and its corresponding airline's, trajectory preferences in the form of UPT; preferences that did not prevent minimization of total fuel usage, or cooperative action towards it, were incorporated into the model. To facilitate this demonstration, three phases were followed:

1. Selection of optimisation methodology and aircraft performance models.
2. Development of an efficient model for air traffic prediction.
3. Testing, evaluation, and improvement.

The first phase reviewed pertinent literature for optimization methodologies and aircraft performance models that were, or could be, used for the purpose of minimizing air traffic fuel usage. In the review, the tacit limitations and advantages of different optimization processes, suitable for air traffic optimisation, were analysed and discussed.

The second phase saw the integration of optimization methodologies and aircraft performance models and the resulting optimisation methodology was developed around an Interior Point Optimisation technique. Each aircraft's speed and altitude along the aircraft's route, was treated as a free variable within aircraft performance limits; the optimisation methodology determined the speed and altitude schedule for each aircraft to ensure total fuel usage was minimum. Constraints on minimum separation, aircraft performance limits and arrival time, were also included; unexpected heading changes and deviation due to adverse weather conditions were included in the optimisation. Further, the integration utilized a means of data transfer which was also found to efficiently define separation required by air traffic; this led to the development of a more efficient form of air traffic optimization. In order to take advantage of this new form, several novel concepts were tested and used, such as fuel usage optimization via Interior Point based algorithms, hyper ellipse based definitions of air traffic separation, and flexible trajectory control node distribution to suit different purposes.

The third phase developed the model further and developed three additional functionalities that improved its utility as an ATC tool. The three functionalities consisted of, the use of the Base of Aircraft Data (BADA) for aircraft performance modelling, the Dynamic re-optimization of air traffic flow to account for aircraft going off-track or changes in flight plan e.g. diversion due to bad weather or unintended pilot actions, and the intentional restrictions on trajectory profile to cater for likely user preferences, e.g. to create trajectories with descents and climbs that are less frequent or more attuned to passenger comfort.

The final result of this research was an air traffic optimizer with several notable attributes. First is that it optimizes individual aircraft trajectories to minimize fuel usage; no fuel usage inefficiencies due to aircraft clustering. Second is that it optimizes air traffic covering a continental sized area in a time frame that makes it

feasible for actual use. Lastly is that it facilitates incorporation of all forms of Air Navigation Service Provider (ANSP), Airline, and Aircraft information into the optimization process; i.e. the process is holistic and accommodate a variety of air traffic stakeholder interests. ANSP data is incorporated as a model of ground and airspace specific properties and restrictions, airline and aircrew data are incorporated as properties of customizable UPT, and individual aircraft information are incorporated as the mechanics and constraints of air traffic and its fuel usage.

1. INTRODUCTION

The main task of Air Traffic Control (ATC), Air Traffic Management (ATM) and, Air Navigation Service Providers (ANSP) is to ensure the safety of air traffic, and a large part of this is to ensure aircraft stay sufficiently separated. Over time, these organizations incorporated various technologies, such as radar and radio communications to better perform the task. As these technologies changed and improved, concern began to grow on how they could be integrated efficiently and effectively. The US based Radio Technical Commission for Aeronautics (RTCA) suggested improving Air Traffic System (ATS) efficiency by decentralizing ATC via the use of computer and aircraft based separation technologies [1]. Almost a decade later the Advisory Council for Aeronautics Research in Europe (ACARE), suggested that significant reduction in fuel usage could be achieved by ATS improvements [2]. Subsequent to these reports the USA and Europe embarked on the development of a new ATM system, Next Generation Air Transportation System (NextGen) [3], and the Europe based Single European Sky ATM Research (SESAR) [4].

A common requirement in both systems was the aim to offer greater flexibility to airspace users. For example, aircraft are no longer required to follow pre-determined airways, but can choose their own User Preferred Trajectories (UPT). However, the current implementation of UPT is simplified and, achieves only a limited mix of user preferences and ATC requirements. This research includes the provision of UPT by developing a methodology where an ideal mix of user preferences and ATC requirements can be fully realized.

1.1 Conceptual Approach

From a user perspective the UPT defined by NextGen [3] and SESAR [4] are quite similar; a flight plan proposed by a flight crew is submitted to ATC that modifies it for safety, and then sends it back for re-modification. These steps are repeated until the proposal is accepted or cancelled, and given that the flight crew has incomplete ATS knowledge, this negotiation does take considerable time. Consider a situation where both aircrew and ATC had sufficiently complete knowledge so as to remove the time spent negotiating during flight. In this situation both aircrew and ATC would require the following abilities; being able to track all aircraft, knowing the performance limits and preferences of each aircraft and their associated airlines, and most importantly having negotiated all potential cooperative actions prior to flight so that all aircraft would know what to do under both normal and unpredicted situations to satisfy ATS requirements. The RTCA, believing that these requirements were possible, proposed a decentralized control in an ATS based on technologies that supported ATC via aircraft to aircraft communications [1]. These technologies gave aircraft improved situational awareness, as well as a sufficiently complete list of self-separation rules that defined a singular action to be taken in almost all situations, meaning that users had ‘sufficiently complete knowledge’ to obviate the need for trajectory negotiation during flight. However, even without testing, the apparent issue was that the ‘sufficiently complete knowledge’ was not sufficiently representative of all user preferences and ATC requirements; the generic nature of the list of self-separation rules meant they could not recognize aircraft specific limits and preferences, and the purely localized situational awareness granted to aircraft could not prevent them from moving into unsafe situations that are outside that situational awareness e.g. a time delay in the current sector leading to a sector capacity breach two sectors away. These highlighted a need for any future attempts at removing real time negotiated trajectory changes to be considerably more holistic in terms of both individual

aircraft specific requirements and of ATC requirements over the entirety of the trajectory rather than just in the visible near term.

The inclusion of sufficiently holistic knowledge does complicate the removal of trajectory negotiation; both the means of determining the best way of adhering to a UPT given ATC requirements, and the means of comparing such for multiple aircraft to allow their simultaneous resolution, would have to be sufficiently comprehensive so as to allow appropriate understanding and handling of the holistic knowledge. Assuming the determination of an ideal UPT requires simultaneous resolution of the desired UPT of all aircraft, then this complication boils down to the appropriate selection of a baseline for comparison that is sufficiently pervasive as to notice changes in all parameters of the ATS. Currently, the only known baseline that can do this is monetary cost; the ability to model variation in everything as variation in expense, marking it as the only baseline with sufficient pervasiveness. Unfortunately the use of monetary cost as a baseline for variation in ATS can be difficult due to differences between the comparative worth of a single aspect of the ATS to the fiscal policies of multiple, and potentially competing, stakeholders. Fortunately, there is a baseline that is more readily acceptable as a means of comparison to most stakeholders and has a sufficient level of pervasiveness to allow appropriate testing of the removal of trajectory negotiation; this baseline is the fuel consumed by all aircraft comprising air traffic of concern, or more aptly, Air Traffic Fuel Usage (ATFU). AFTU is more readily acceptable because, firstly, aircraft fuel is a recognized commodity that has a specific and easily understood worth, and secondly, the consensus driven ATM reports and programmes have marked its reduction as a universal desirable for both environmental and economic reasons [1], [2], [3], [4]. ATFU is sufficiently pervasive because, while it cannot be used to compare the maintenance, labour, and management, costs of a particular flight, it does allow comparisons of the trajectory shapes that do cause those, and other non-fuel related parameters, to vary. Lastly, because of its recognition as a commodity, its correlation to monetary cost is clear, thus variation in ATFU can be directly convertible to variation in monetary cost; this in combination with its sufficient level of pervasiveness allows it to be an appropriate test bed for future means of avoiding trajectory negotiation and therefore the provision of more beneficial UPT.

1.2 Issues and Challenges

Even with a known baseline and a means of application, there are a considerable number of issues that could prevent this form of improved UPT from being feasible. While section 2 and 3 will go over these issues in greater detail, the ACARE report's perspective on the means of reducing ATFU do give an appropriate overview of the major issues that could cause such infeasibility. Another ACARE report [5] indicates that a reduction of 10~15% in ATFU is possible through preparing for six particular concepts; Efficient Route Network, Free Routes, Flexible Use of Airspace, Optimised Routes, Reduced Holding, and Reduced Taxiing. ATFU, itself, can be modelled as a function of several parameters; flight planned trajectories, aircraft performance data, separation requirements, and weather. As a consequence of using ATFU as a Figure of Merit, each of these concepts and parameters had to be correlated with each other in a correct and synergistic manner. In addition to complicating the variation in ATFU significantly, failure to perform the correlation correctly would have resulted in either incorrect or untimely output which would render the method infeasible. The two issues that consistently appeared, when correlating the concepts, was the possibility of improper Air Traffic Modelling and inaccurate Selection of Ideal Air Traffic; these are discussed in the next two subsections.

1.2.1 Air Traffic Modelling

Efficient Route Network determines the trajectory based on the placement of land marks and other ground based navigation aids, or Nav Aids, which may differ from the UPT [5]. In Free Routes, flight routes are planned irrespective of ground based Nav Aids, and other non-ground based Nav Aids are used in their place [5]. The technological solution, as earmarked by SESAR, is to use an aircraft based situational awareness system, referred to as Automatic Dependant Surveillance - Broadcast (ADS-B), that is backed up by a Global Positioning System (GPS) and a network of ground-based stations with sufficient area density that an aircraft is always within reach. Australia is the first to effectively apply such a system over a continental land mass [6]. For aircraft that are equipped and certified to use ADS-B or some other technological equivalent, the use of ground based Nav Aids was no longer necessary. However this created a problem for ATM, as the Nav Aids were also used to simplify ATM representations of air traffic [1]; because aircraft were required to fly past Nav Aids, aircraft routes were defined as connections between airports and these Nav Aids. Even without radar, an aircraft's progress could be accurately determined by when they passed these Nav Aids. Aircraft conflict resolution was also similarly simplified to scheduling sufficient times or altitude differences between aircraft as they passed the same Nav Aid. If these Nav Aids are no longer followed, the ATM system for modelling air traffic falls apart; these Nav Aids still exist today [3] and still restrict air traffic. To fully utilize ADS-B technology and allow aircraft to fly a straight line between airports rather than past a list of waypoints, a new way of modelling air traffic and airspace must be developed. Flexible Use of Airspace refers to the ability to grant civilian air traffic partial usage of airspace normally dedicated to military or non-civilian activities [5]. While handling of this seems fairly trivial, the details required of it do mean that various grades and shapes of airspace, each with different ATC requirements [7], can be made available for civilian usage. As a consequence, Flexible Use of Airspace can significantly reduce flight distances at the cost of stricter ATC requirements. As [5] indicated, air traffic is directed through pre-established routes and deviation away can either be allowed or disallowed based on the state of the airspace and how long air traffic would be in that area. While useful in current ATM, it can be non ideal where straight aircraft trajectories are allowed, e.g. an aircraft flying a straight route between airports may find a portion of their trajectory along the edge of an Airspace of Flexible Use; with the current model of air traffic and airspace, the aircraft would have to fly around the airspace, or through its pre-established set of routes. Either option incurs additional fuel usage and is reason to develop a new model of air traffic and airspace; however this situation also poses a question for this new model in terms of how it would deal with Flexible use of Airspace. Consequently any new model for air traffic and airspace must also find a way to incorporate the various shapes of these airspaces with the broad variety of straight paths that could exist between airports.

1.2.2 Determination of Fuel Optimized Air Traffic

Optimized Routes, Reduced Holding, and Reduced Taxiing, refer respectively to the alteration of the route, profile, or ground, aspect of air traffic trajectories so as to reduce the impact such would have on either the environment or air traffic itself. While ACARE raised concerns on the impact of aircraft contrails on atmospheric chemistry, the closer concern was the safe control of trajectories so as to reduce ATFU and therefore CO_2 generation. For the purposes of improved UPT, while these do touch on the air traffic modelling issues mentioned above, the key issue these highlight is that industry recognized that methods that could support selection of an ideal form of various aspects of air traffic needed to be defined. This is true for the research here as well; even if the issues mentioned above were solved and the sufficiently pervasive baseline could be

holistically represented as a function of fully modelled air traffic, there would still be the issue of how to select that ideal set of air traffic from that modelling.

The problem is complex and simple methods of finding an ideal set of air traffic cannot be used. A comparison or ranking of all alternative sets of air traffic is not possible because a great many of the variables inside the problem are not discrete in nature, and even if they were made to be so, would involve checking of an incomprehensibly large number of alternatives. The use of analytical solutions is problematic as well, as various components of the air traffic model are highly non-linear, with solutions being highly dependent on how these components are correlated. The only other field of assessment available to the problem is the use of numerical optimization methods. Numerical optimization methods try to determine a point at which a function is either a maximum or minimum; given the aim of reducing ATFU as much as possible the methods used in this research focus on the application of optimization methods to reduce ATFU.

The issue with numerical optimization methods is the selection of an optimizer that best suits the problem at hand; as discussed in section 2.3, several optimization methods exist each with specific capabilities. However these methods may also have downsides, e.g. lack of repeatability due to necessary randomness, or lack of timeliness due to slow computation. Thus on top of handling the issues mentioned above and developing a comprehensive model of air traffic, the research must also consider the negative impact the optimizer could have on the problem and therefore seek ways to either mitigate or rationalize such an impact.

1.3 Thesis Outline

Given the issues mentioned in sections 1.1 and 1.2, this research is structured in three phases:

- Perform a comprehensive review of pertinent literature to understand the current state-of-the-art
- Develop a methodology for modelling air traffic so as to show correct variation in ATFU.
- Integrate the air traffic model with an optimisation technique, and apply the resulting methodology to realistic air traffic scenarios to evaluate its effectiveness.

The chapters in this thesis follow these steps, and show how they result in a methodology capable of avoiding real time trajectory negotiation.

2. LITERATURE REVIEW

The intent of this literature review is to define the state of the art regarding the optimization of ATFU. Section 1.2 defines the key issues as surrounding either the modelling or optimization of air traffic. The issues in air traffic modelling are concerned with the variable representation of certain aspects of air traffic, particular where such have been known to require intensive calculations, or be unsuitable for particular types of optimization, or were insufficiently accurate. The issues in air traffic optimization are concerned with how air traffic could be optimized in terms of the optimization methods used, the suitability of various methods to aspects of the ATS, and the resultant accuracy of these methods if applied. In both cases the state of the art is largely defined by previous attempts to optimize air traffic, irrespective of the baseline of optimization; while optimization of ATFU has been attempted, very few methods exist and research into the broader context of air traffic was necessary. Thus, to focus review of air traffic modelling, the objectives and their requisite parameters were collected from those previous attempts and categorized for usefulness. Similarly, to focus review of air traffic optimization, the optimization methods used in those previous attempts were also collected and ranked for desirability.

While the nomenclature used by these two fields are different they can overlap; to avoid confusion a subsection on conventions used to define aspects of these fields is provided in the next section, with the review of literature shown afterwards. Further, to avoid confusion regarding the relevance of ATC technology to the optimization of ATFU, only necessarily important aspects of ATC technology are mentioned in the main body of this thesis; for more information Appendix A contains a full overview of the technology and policies used by ATC, ATM, and ANSP. Further to avoid confusion with the large amount of ATM research concepts that do exist in the literature, only the concepts that were used to develop and guide the research are shown in the main body of the thesis; a bibliography of sources that gave insight into the field but were not directly used can be found in Appendix M.

2.1 Standard Conventions used in Defining Air Traffic Optimization

The optimization of fuel consumption can be broken down into three topics; first is the history of ATM and its impact on fuel usage optimization, second is the control of individual trajectories, and third is the application of optimization methods to ensure minimum fuel is consumed. Each of these topics have specific conventions, terminologies, and tacit assumptions that they use to discuss their concepts. The following subsections go over these and discuss their relevance to the research in the thesis.

2.1.1 Conventions for Air Traffic Management (ATM)

The field of ATM covers all the management practices used to govern the interaction of aircraft while they exist in a system of airspaces and airports; consequently, it has a broad variety of academic and research disciplines to support it. The engineering and natural sciences are obviously required given the field's focus on aircraft control, however social sciences are also necessary given the impact of aircrew and controllers on ATM [8]. Each time a new approach for ATM was announced, research on the corresponding human factors was put forward; externally in [9] for [1], but as a result of community derived consensus in [4]. Consequently, it should not be surprising that the field of ATM has developed a set of terms and definitions that is specific to them. This section will thus define and discuss the subset of these that have relevance to the research in this thesis.

The first set of definitions regard parameters of an aircraft's flight. The terms 'trajectory', 'route', 'profile', and 'flight plan', are used frequently and have specific meanings [4] which are also used in this thesis. Firstly, the term 'trajectory' refers to a list of four dimensional (altitude, time, latitude and longitude) points that define the path taken by an aircraft flying to its destination. Next, the term 'route' refers only to the latitude and longitude dimensions of any potential trajectory, and is set with the altitudes and times associated with those points as being unknown or variable. The term 'profile' refers to the altitude and speed values that correlate to an aircraft's state at points in that aircraft's trajectory or route. Lastly, the term 'flight plan', in its most basic form refers to a list of airports and waypoints that an aircraft plans to fly past during its trajectory; more sophisticated forms do exist and varies around the world as they include more information depending on what data airlines wish to convey, and what data ANSP can process.

The next set of definitions regard the type of ATM that can be applied to an airspace. In all of these regimes a common feature is that ANSP have further divided their ACAO allocated Flight Information Regions (FIR) into sectors and aerodromes based on the demands of the location. It should be noted that NextGen [3] and SESAR [4] are not types of ATM, but rather ATM improvement programmes; it is their aim to introduce the ability to apply the best ATM types, or combinations thereof. The ATM types discussed here include classic ATM, free flight, and Air Traffic Flow Management (ATFM). The first type is the classic, stereotypical, ATM [7] in which air traffic through sectors and aerodromes are controlled strictly by individuals trained for that type of airspace; en-route controllers guide aircraft as they fly between sectors aerodromes, while aerodrome controllers guide aircraft descending to, and climbing away from aerodromes. Due to minimal aircraft surveillance information, high air traffic demand, or a combination of both, en-route or cruise flight is limited to constant altitudes and headings with changes to these always requiring ATC approval.

The next type of ATM, categorised as “Free Flight” was the regime put forward by the RTCA in [1]. While never applied as directed in that document, it was nevertheless the conceptual beginning of advanced ATM. The Free Flight ATM in [1] was fairly similar to classic ATM, however it had several notable differences. The most important of these was that aircrews could facilitate separation and conflict avoidance by themselves; this was allowed by the introduction of improved on-board aircraft surveillance hardware that gave aircrew situational awareness whilst in air traffic. In this regime, aircraft would still fly with constant altitudes, however, by broadcasting their intent to change direction or altitude, aircraft could better follow its most fuel efficient trajectory. However it was shown in [10] that pilots, when in such a scenario, have a tendency to fly relatively dangerous trajectories to ensure they reach conflict points before others; in free flight, aircraft that reached a point of conflict after others effectively “gave way” to preceding aircraft, and lost flight efficiency as a result. This lack of co-operation also occurred in other aspects of the regime and consequently free flight was never applied. Later research efforts [11] learnt from this and aimed research at defining ways of facilitating co-operative aircraft actions; they had recognized that the lack of co-operation stemmed from both aircrew and ATC being unable to negotiate a fair compromise in trajectories in the time between recognizing a conflict and it actually occuring. It was consequently a major facet of the research in this thesis, that this concept of “co-operative trajectories” be somehow facilitated when optimizing air traffic.

The next type of ATM is, in terms of scale, the closest to the aims of the research in this thesis; Air Traffic Flow Management (ATFM) and its methods is the only type currently capable of managing aircraft on a continental scale. ATFM does this by defining air traffic as a fluid flowing through routes already present in the FIR [12]; airspace would define the fluid volume, and airports would define the source and drain of the fluid. The resulting model of air traffic is sufficiently simple in complexity that Linear programming methods can be used to control allowed speeds and altitudes in routes to ensure separation and sector capacity limits. However as a consequence of its air traffic simplication, it has difficulty in handling individual trajectories [12]; firstly because results have to be discretised back into individual aircraft and incurs de-optimizations in the process, and secondly because ATFM assumes that sufficient separation occurs when sector capacity limits are not broken. For these reasons, as well as other reasons mentioned and fully discussed in section 2.2, the research discussed in this thesis could only rarely apply the concepts developed in ATFM and hence is not mentioned significantly in this thesis.

The next set of definitions cover a means of categorizing various ATC functions. The definition of the terms "Strategic" and "Tactical" with the most consensus currently is the one put forward by SESAR [4]:

"Tactical relates to means employed to help achieve a certain goal (while strategic relates to the preparation of a plan, which may involve complex patterns of individual tactics)."

At the time of research completion, NextGen had yet to commit to a particular definition, however from the perspective of the research, no significant differences from the SESAR definition have been seen in NextGen’s usage of the two terms. Regardless, these terms are important as they define where specific ATC functions occur with respect to real time usage. For example classic ATM, as defined above, is almost entirely made of tactical functions as controllers choose and directly apply appropriate separation; the definition of routes, waypoints and separation and sector limits can be considered as the only strategic element of the ATM type. In constrast, ATFM is entirely strategic, it creates speeds and altitudes allowances for entire routes; it relies on controllers to apply tactical functions akin to classic ATM in order to be a complete ATM type. The research in this thesis can

be considered similarly; the optimization of air traffic performed here is entirely strategic and also relies on the tactical functions of classic ATM in order to be a complete ATM type. Consequently there is no discussion in this thesis on changing the tactical methods already present in ATC. The last thing to note regarding these terms is the existence of the term “Pre-Tactical” which also occurs in [4] however is less clearly defined; from its usage, its assumed to refer to functions that occur just prior to tactical implementation and have the benefit of having more uptodate situational awareness. While it would be ideal for the functions defined in this thesis to be categorized as such, the categorization itself is irrelevant, and the research will use tests of performance computational performance to indicate if a function can be used in a Pre-tactical manner.

The last term to be defined and discussed is User Preferred Trajectory or UPT. The US uses [13] the term to refer to aircraft trajectories that were designed by the aircraft’s user, i.e. the aircraft’s airline and aircrew, to contain user preferred properties not normally facilitated by ANSP. SESAR has a similar term, i.e. “Business Trajectories” [14], which is functionally the same, however as Australia uses UPT [15] in its equivalent of NextGen and SESAR, this thesis will do the same. The term is important as fuel usage is not the only cost that airlines need to minimize; in this thesis there is an aim to facilitate the minimization of these non-fuel related parameters via the provision of UPT. More information on how this can be performed starts in section 2.2.3. However, it should be mentioned here that the concepts of Cooperative and User Prefferred Trajectories do not align well; the purpose of a cooperative trajectory is to perform a trajectory in coordination with other trajectories for the simultaneous benefit of all, e.g. lower ATFU, whereas the purpose of a UPT is to introduce trajectory properties to a single trajectory to make it more economically feasible, e.g. faster flight speeds to reduce flight time. As commercial aircraft all prefer to make their trajectories more economically feasible, and because aircraft can have similar properties (e.g. cargo mass, aircraft model, and destination airport), the UPT of different aircraft can conflict. However this is no different from how the fuel-efficient trajectories of multiple aircraft can also conflict; the key is to find a baseline for cooperation. The baseline for cooperation in this thesis is the minimization of ATFU; therefore the provision of UPT in this thesis can be translated into the investigation of UPT parameters that do not prevent the minimization of ATFU. Again, more information on how this can be performed starts in section 2.2.3.

2.1.2 Conventions for Trajectory Control

The process of trajectory control involves changing the elements of a trajectory’s route or profile so as to achieve a desired property of that trajectory; this can be, for example, creating sufficient space between it and another aircraft, or, exiting a heavily congested sector early to decrease controller workload. While there are many means of controlling trajectories, the research covered by this thesis could be alternatively perceived as finding a method of Conflict Detection and Resolution (CDR) that supports fuel usage optimization; definitions pertinent to CDR would therefore be useful for discussion of issues that may arise. A comprehensive study [12] carried out in 1999 showed that a variety of viable CDR methods exist that could carry out the role of autonomous CDR in support or replacement of ATC. As substantial time has passed since then, other CDR methods have been created and the current state of CDR methods with respect to each other is not exactly known. However the categories and definitions it set forward for defining CDR methods are still applicable and are used here for clarity and as an introduction to air traffic optimization. These categories also shaped the review of air traffic optimization in the literature as it effectively defined what kind of methods could and could not achieve the research’s goals.

According to [12] CDR methods could be categorized according to their properties in terms of modelling method, dimension, detection, resolution, manoeuvres, and conflict multiplicity. Modelling Method referred to how the state propagation in a trajectory is modelled; under nominal state propagation only the intended trajectory is prepared for, under worst case propagation all possible trajectories are prepared for equally, and under probabilistic state propagation pre-defined portions of all possible trajectories are prepared for in a pre-rationalized manner. Dimension referred to how CDR methods could use either, or both, the horizontal (route) or vertical (profile) planes to determine CDR. Detection referred

to whether or not conflict detection was explicitly carried out. Resolution referred to how proscribed, optimized, force field, and manual, methods could be used to define the manoeuvres used to resolve conflict. Manoeuvres referred to the changes in heading, altitude, speed, or a combination of any, that could be used to resolve conflict. Conflict multiplicity referred to the number of aircraft controlled in conflict resolution; so either global i.e. between all manoeuvrable aircraft, or pair wise i.e. between successive pairs of aircraft considered according to a specific ranking or order.

Further, [12] also mentioned certain implicit issues that needed to be addressed to ensure the feasibility of a particular CDR method. These included, but are not limited to, issues regarding operational robustness, pilot and controller coordination requirements, computational requirements, implementation issues, source data integration, and stakeholder acceptance. Any and all of the categories and implicit issues can be used to define a particular CDR method. Note that while this research could be defined as optimized resolution, lessons obtained from resolution methods that were not optimized still held pertinence during development. Similarly, consideration of all categories and implicit issues were required for decisions carried out later during the development of a fuel usage based air traffic optimizer.

2.1.3 Conventions for Optimization

Optimization can occur via a variety of ways, however at the core it is a mathematical process of finding an optimal value for an objective function and its constraints, in terms of variables which correlate the three. A simple example is the shortest path between two points given the avoidance of obstacles in between; the optimal value is the shortest distance of the path, the objective function is the calculation of that distance, the constraints are the increases to distance caused by avoiding the obstacles, and the variables could be the sequence of waypoints which define the path. However the problem itself can get more complicated and different optimization methods can be more suited to particular problems. To aid appropriate application of optimization methods, classifications were developed in the field of optimization in order to better define the problems they could or should face.

According to [17], an optimization problem's objectives and constraints can be characterized in terms of their number, function form, landscape, variables, and determinacy.

- The number of objectives is either singular or multiple; while singular objectives would define singular optimums, multiple objectives can give a range of optimum from which a user can choose from. For constraints, if none exist the problem is unconstrained; otherwise existing constraints are further segregated to equality and inequality constraints.

- The function form of the objectives and constraints are defined via their linearity or non-linearity; different methods are usually required to handle different combinations of objective and constraint function forms. Constraints are also allowed to be constant, and these are known as bounds.

- The landscape as experienced by the objective can be defined as unimodal or multimodal; the former describes a landscape that slopes towards a minimum or maximum from all points, whereas the latter can have multiple minimums or maximums in the landscape, thereby creating what are known as local minima or maxima. It is possible for constraints to cause a unimodal landscape to resemble a multimodal one.

- The variables that are optimized can be continuous, discrete, or a mix of both; continuous variables are any number in the real domain and as such are prepared for generally, whereas discrete or integer based variables are those that can only be particular numbers or integers in the real domain and would require some variant of integer programming or combinatorial optimization to aid optimization with or without the presence of other continuous variables.

- Determinacy refers to the problem being exact or containing an element of randomness or noise; the former defines the problem to be deterministic and generally prepared for, the latter is defined as a stochastic approach and may require the use of statistical parameters to aid in optimization.

After a problem is defined, and an optimization process is applied, there are several implicit issues that need consideration for actual usage; these are tied to the computational requirements of the process itself. While there are intellectual property issues to be handled whenever applying a particular optimization method in practice, the only computational issues discussed in this paper regard the usage of computational resources; the most pertinent of these being central processing unit (CPU) speed and random access memory (RAM) size. As a consequence three key concepts need to be made aware of; computation time, parallelization, and scalability.

Computation time is the time required to perform the optimization process and is proportional to the size of the process against the number and speed of available CPU; parallelization and scalability determine how proportional it is. Parallelization refers to the division of the process into small parts that can be processed on separate CPU in parallel with each other so as to reduce overall computation time. However Amdahl's argument [18] states that the decrease in computation time due to the presence of multiple available CPU is limited by the portion of necessarily sequential, i.e. not parallelizable, operations in the process; thus, when defining the parallelizability of a process, focus is placed on the sequential operations within the process so as to define the maximum gain from increasing the number of available CPU. Scalability can be defined in various ways [19] but in general it refers to how computation time changes as problem size increases; here it specifically refers to the applicability of the process in light of larger problem sizes. In other words a process can be deemed scalable if increases in computation time, due to increases in problem size, can be rationalized as applicable within a reasonable time frame. While this concept has many similarities with the concept of parallelization it focuses more on the impact due to variation in the problem, rather than in variation in how the problem is solved.

Much like the characteristics of trajectory control, any and all of the classifications and implicit issues mentioned previously can be used to define any optimization problem and method. Further, the previously mentioned classifications and implicit issues are encountered in a number of ways and combinations in this research and consequently do have specific ramifications on particular parts of it; further details on these ramifications are

mentioned in the sections that are affected by them so as to aid understanding of how they occurred and correspondingly mitigated.

2.2 Optimization Objectives

With conventions for trajectory control and optimization established, it is now possible to discuss the topic of optimization for the purpose of reducing ATFU. A notable parameter of cooperative trajectories is that they require simultaneous optimization to be ideal, i.e. they must all be optimized with respect to each other and at the same time; allowing an aircraft to be optimized later prevents earlier aircraft from cooperating with later aircraft. This concept of simultaneous handling of aircraft is also known as global conflict multiplicity, which was defined in 2.1.2. Consequently when reviewing literature for useful optimization objectives, it is important to ensure they have this parameter. A literature review of air traffic optimizations methods that prepare for global conflict multiplicity [12] showed that it is not necessary to reduce fuel usage directly; reduction in ATFU can occur via optimization of other aircraft and air traffic parameters that do not require fuel usage to be known; e.g. minimized difference from an initial flight plan, minimized deviation required to avoid conflict. While these methods cannot be individually used to optimize ATFU, they give insight to how to approach optimization of ATFU and thus their details and merits are discussed in section 2.2.1. After considerations of non ATFU based objectives, summaries of previously attempted ATFU based objectives are provided in section 2.2.2 with their usefulness in providing sufficiently complete knowledge in modelling air traffic.

2.2.1 Trajectory, Conflict, and Traffic Flow based Objectives

The standard equations for defining fuel consumption, as mentioned both in [20] and [21] do allow an individual aircraft to determine the specific values for altitudes and speeds along its intended route that would reduce the fuel usage for that trajectory. However during a flight, unforeseen weather, arrival time restrictions, and interaction with other aircraft, do prevent this fuel efficient trajectory from being performed, and the expected fuel reduction is not fully achieved. However as the aircraft would be experiencing near optimal speed and altitude combinations for uninterrupted portions of its flight, some of the intended fuel reductions would still be gained. This is the basis of objectives in the literature that focus on optimizing trajectory parameters; they focus on the restrictions that would prevent their previously established fuel efficient trajectories from being performed, as opposed to changing the trajectory parameters directly to try and find a more fuel efficient alternative. For instance [22] defined a method of defining optimal combinations of speed and heading changes that would, in the presence of separation requirements, minimize the aggregate delay experienced by all aircraft being optimized; by minimizing the delay, the difference in flight time frame is reduced and the difference in trajectory becomes marginal. The method defined in [23] was similar but more direct in that it had the objective of minimizing the difference between the speed required to satisfy separation requirements, and the speed required by a pre-defined, supposedly optimal, trajectory. The theme of reducing restriction goes even further in [24] which had the objective of minimizing a metric quantifying the restriction, or nearness to undesirable flight modes, experienced by all aircraft, again while avoiding unsafe separation states.

This trend of reducing restrictions is also seen in methods optimizing aircraft conflict. In these methods it is the interrelationships between aircraft that are focused upon because of their greater impact among causes for trajectory deviation. Trajectory deviations due to weather can affect large regions but can be predicted, and catered for, in advance. Trajectory deviations due to aircraft conflict can be considerably less predictable as cooperation is required between a set of mutually conflicted aircraft that may or may not be able to follow ATC

guidance exactly; as an inability to follow ATC guidance occurs randomly, the resulting air traffic structure after conflict resolution tends to be unplanned for. Trajectory deviations due to aircraft are not small either as the separation requirements mentioned in [25] suggest that even in well surveyed regions that conflict resolution between a single pair of aircraft can span a distance of 80nm or a timeframe of 15minutes; in less surveyed areas these numbers can grow larger. Among methods that optimize conflict between pairs of aircraft, two types of methods should be mentioned. The first type focuses on direct control of aircraft experiencing conflict. The method defined in [26] optimizes against conflict as well as the efficacy of the resolution that occurs afterwards; the ability to search and optimize of the efficacy of the resolution being an indicator that optimization could better enhance air traffic if more direct application of control were allowed. The method in [27] while performed in a very different way has a very similar goal. The second type focuses on the shape, existence, or placement of the conflict itself, i.e. without much consideration on the resulting trajectory of aircraft inside the conflict. The method in [28] epitomizes this distinctly by removed itself away from control optimization and optimized towards a holistically acceptable list of predefined aircraft relationships; the assumption being that the problem of defining aircraft trajectories becomes deterministic once a relationship is held, and that it is only these relationships that need, or can afford, optimization in the first place. This particular method was later improved on in [29] via the introduction in various levels of autonomy.

Optimization methods applied to ATFM are different to those previously mentioned due to the different way they handle conflict. At the ATFM level, conflict is defined in terms of capacity and throughput limits; this assumes that trajectories are largely static and that minor perturbations can be handled, to the satisfaction of separation requirements as per [25] and with comparatively insignificant cost, at the controller level provided capacity limits are obeyed. Considering the tendency of airports to be bottlenecks in ATFM, these optimization efforts tend to be centred on them. For instance, [30] attempts to maximize the arrival rate for a particular airport while recognising a minimum time limit between arrivals. The method defined by [12] expands upon this concept greatly by defining ATFM in terms of an Eulerian network density problem constrained by density limits on flyable route segments; it therefore is capable of maximizing throughput, i.e. arrivals and departures combined, for a particular airport. Again however, concern was raised regarding the additional responsibility such efforts would have on aircrew hence some mixing of trajectory parameter and ATFM based objectives; a method shown in [31] defines a network of traffic flows between airports but, instead of maximizing throughput for a sector or airport, minimizes the aggregate delay experienced by aircraft instead.

The issue with all the methods mentioned above is that they minimize fuel usage indirectly. And since none of the objectives' variable parameters correlate exactly with variation in fuel usage, there is the distinct possibility that following any of them may lead to increases in fuel usage. However, the fact they all control air traffic somehow makes them invaluable sources for inspiration on developing a means of fuel usage optimization.

2.2.2 Fuel Usage based Objectives

The review indicated that there are few CDR methods that directly consider fuel usage, and fewer still do it at a level that correctly follows standard equation, i.e. as in [20] and [21], for aircraft fuel consumption. So in terms of the CDR dimensions mentioned in 2.1.2, the dimension of importance here is the modelling method used to determine or predict aircraft performance as this determines the applicability of the optimized result. In terms of prior literature, two methods were found to contain fuel based objectives that do follow standard equations for

fuel consumption and are discussed here in terms of their benefits and issues. The first is discussed in 2.2.2.1 and defines an idealistic analytical method that encapsulates the problem well, but has certain issues to it. The second is discussed in 2.2.2.2 and is more current and does cover some of the issues of the first, but also create issues that prevent it from being directly applied. Besides these methods, two more were found that contained useful characteristics that while not directly beneficial to the optimization of ATFU, could aid in supporting it. The first of these is discussed in 2.2.2.3 developed a means of discretising airspace so as to appropriately define previously ill-defined aspects of the ATS and thus improve the accuracy of any calculation of ATFU. The second is discussed in 2.2.2.4 and developed a means of modelling air traffic that enabled it to use a particular form of optimization that gives insight as to how the problem could be efficiently performed.

2.2.2.1 A Reference Method for the Optimization of Fuel Consumption

The method presented in [32] is the earliest comprehensive attempt at fuel usage minimization. In terms of the CDR classifications mentioned in 2.1.2 it provided 3D trajectory manoeuvres, global conflict multiplicity, and optimized ATFU under both aircraft performance limits and ATC separation requirements.. However it had three issues which made it difficult to use in modern ATC; it used basic flight mechanics to calculate fuel consumption, it favoured changing headings over changing speed or altitude, and it could not facilitate time based separation requirements. Without these issues, this method could have been directly used to explore the characteristics of fuel optimized collaborative trajectories. The details of these issues are discussed below.

The classical, i.e. as derived from basic flight mechanics, equations for fuel consumption have been utilized for a considerable time as they do accurately define fuel usage for trajectories where all flight performance parameters, and pilot actions, are known. However, this information includes data that is commercially sensitive; how an airline's pilots fly their aircraft, and what assumptions an aircraft manufacturer has used to optimize their aircraft, is information that is not publicly released. Consequently newer methods, such as in [33], were designed to work backwards; i.e. they took trajectory and fuel usage information from previous flights, and combined it with public knowledge of aircraft, to create representative models that can be used to predict the aircraft's fuel usage. As these models use only publicly available information to define the flight mechanics of an aircraft, they do not require knowledge of all flight performance parameters, and pilot actions, of a trajectory to calculate that trajectory's fuel usage. However, as these models were based on data from trajectories flown for commercial activities, their resulting calculation of fuel usage would be more accurate than what [32] had chosen to do; i.e. calculating classical fuel consumption without knowing all flight performance parameters. Consequently, if cooperative fuel usage minimization is to be fully explored accurate for actual usage, it will require either a) the full disclosure of flight performance parameters, and schedules of pilot action, from the manufacturers and airliners involved, or b) the use of methods similar to [33]. As b) can be provided for a large number of aircrafts [33], and a) has yet to occur in the public domain, these newer updated methods are needed to properly define fuel optimization in a collaborated context.

The methods detailed in [32] were developed during a period in time when [1] was still being considered for use in ATM; consequently [32] mirrors the rules defined in [1] that allow heading changes to resolve conflict. However this was never formally allowed in ATM, and the newer programmes, i.e. [3] and [4], show no indication of facilitating it; consequently [32] could never be applied in ATM. Further, as [32] allowed heading changes to resolve conflict, such conflict resolutions were tested and found to be the dominant choice for conflict

resolution in their results; no trends could be discerned from [32] regarding fuel usage optimization where heading changes are disallowed.

Regarding the lack of a minimum time separation between aircraft passing the same point, at the time of [32], the set of separation constraints it utilized was heavily influenced by regulatory properties set out in [1]. This caused conflict to be completely spatial in nature, i.e. it was the distance measured between aircraft that determined if conflict was to occur or not. Time separation did exist in [32], but only as something to be minimized in tandem with minimized fuel consumption; i.e. solutions that had the simultaneous objective of minimal fuel and airspace usage. However in later papers, some of the authors of [32] adopted methods that could prepare for time separation, i.e. akin to that in [30] and [12], via defining traffic as Eulerian networks [34] or similar; this suggested heavily that time separation as a constraint was desirable and would need to be added to [32] in order for it to be made current. It should be noted that the later works of the authors of [32] did not consider fuel usage optimization again; reasons for such are unknown, however experiences found in the course of this research did provide answers to this.

2.2.2.2 A Method for Improved Accuracy in Estimating Fuel Consumption

The method shown in [35] did improve upon on all the issues previously associated with the method in [32]; it did utilize more accurate information to optimize towards minimum fuel usage, it did restrict aircraft trajectories to a particular route, and because of the pre-arranged nature of the routes being used, it did also apply an arguably acceptable time separation between aircraft. The ability of [35] to calculate fuel usage was granted via the use of the Base of Aircraft Database, or BADA [33]. This database, and the methods that supported it, were intended to provide accurate ways of determining both the fuel usage and performance required of a particular aircraft flying a known trajectory; thus it would be ideal if it were used directly as an optimizer for trajectories instead of the classical method used in [32]. The method described in [35] did do this, but was focused on the resolution of conflict in a single sector and in the near future, so it did not grant any further insight as to what ATFU optimization in a continental setting may entail. Further, it resorted to a couple of questionable assumptions that disallowed it from being directly applied in this research.

The first of these assumptions regards the acceptability of integers as variables of the problem, i.e. that aircraft relationships can be defined in binary terms along pre-specified dimensions, and that applicable altitudes can be defined from a set of predefined flight levels. The issue is that this does significantly suggest that no direct benefit to the objective could be obtained from allowing non-integer based answers. In the case of set altitudes this would be erroneous since an aircraft's optimal trajectory does not have a constant altitude in it; forcing a set altitude would therefore automatically de-optimize fuel usage. The case of binary aircraft relationships is not so clear since the required separation in only one dimension out of a pair of almost completely orthogonal separation dimensions i.e. time and altitude, implies that it's binary modelling should be acceptable. However if the same relationship could be described using a smooth function akin to the spheroids used in [32], one would have to wonder if the binary modelling is necessary given the additional work required to optimize integers; more discussion on the issues associated with this are found in 2.3.

The second of the questionable assumptions refers to accepted accuracy of the linearized components of the problem; i.e. in fuel usage optimization, as well as separation and performance constraints. The linearized representation of fuel consumption should be correct when calculating fuel consumption, however given the non-

linearity of the actual function one has to wonder if the linearized representation would give accurate predictions for feasible variables for fuel consumption. The issue regarding the accuracy of the separation and performance constraints is that they may not be complete. In general, checking separation at common waypoints, or points of conflict, should be sufficient; however in cases with trailing or close to trailing traffic, there is a distinct possibility of separation being breached between waypoints. Without changing the separation constraint, more waypoints would be needed to appropriately define separation. The issue with the performance constraints was that, despite their availability and clear definition by BADA in [38], such were not incorporated into the method. This is likely due to the non-linear nature of the constraints; these performance constraints are of particular importance as they define what forms of trajectory can actually be performed.

2.2.2.3 A Method for Improved Ground Data Correlation

The methods outlined in [36] are for the purpose of simulating air traffic so as to assess the impact and efficiency of recently developed ATC rules. However, in supporting such, it covered two of the issues associated with [32]; it had facilitated the methods defined in [33] to accurately define fuel usage, and had developed methods that correlated trajectories to limitations associated to regions or fixed locations; e.g. weather or restricted airspace . The latter method was of particular interest as it discretised airspace into static rectangular prisms that would allow association of ground based limits to trajectory segments where they are applicable; while [36] only used these prisms for the purposes of heading change and weather avoidance, it was theoretically possible to use them for other data. However the methods used by [36] did not include fuel usage optimization and thus did not give any insight on how the prisms could be adapted to such. The team behind its development did reach a state where fuel usage optimization was incorporated in [40] however this did not use the prism method shown in [36]. Without this link between the calculation of fuel consumption and an air traffic model that can handle both separation and other location based constraints, the research in this thesis had no choice but to develop its own.

2.2.2.4 A Method for Defining ATFU Optimization Subproblems

While the method mentioned in [37] does optimize BADA defined ATFU, it does so in combination with a variety of other objectives that can prevent optimization of fuel usage. Its aim was to optimize cooperative conflict avoidance, so its distinct correlation with current ATM priorities was intended. Consequently it does mean that it cannot be directly applied for the purposes of this research. However in performing its optimization it used what is known as “dynamic programming”; this involves the division of an overarching optimization problem into overlapping subproblems which are individually optimized to find an optimum for the overarching problem. Thus [37] divided its optimization of ATFU into multiple subproblems that could be optimized separately. Considering this was done in a forward stepping manner, the problem was likely to have been divided into optimizations that assessed optimum aircraft positions at discrete points in time. Thus again, this could not initially be directly used in this research; however the fact that it could do this suggested that it might be a viable approach for defining subproblems of optimizing ATFU that could be isolated and performed elsewhere.

2.2.3 Important Non-Fuel Usage based Objectives

As mentioned in section 2.1.1, the provision of the UPT in this thesis occurs by investigating the parameters of airline and aircrew preferences that do not prevent fuel usage minimization. A useful starting place to understand the expenditures that an airline might incur, and correspondingly the preferrences they may request, can be seen

in the Airline Cost Index published by the American Transport Association of America (ATA); an example of this can be seen in Table 1 which shows the average distribution of costs incurred by an American airline in the first quarter of 2004 [39]. However, it should be noted that the information in Table 1 is only a snapshot of costs at that time, and percentages, and their associated impact, will change over time.. Looking at the list of cost items and removing the ones that have little to no relationship with an aircraft trajectory, four cost items become significant; Labor, Fuel, Aircraft Ownership, and Profressional services. The ATA uses the following definitions [39] for these terms:

- *Labor: Wages, employee benefits (e.g., annuity payments, educational, medical, recreational and retirement programs) and payroll taxes (e.g., FICA, state and federal unemployment insurance). General management, flight personnel, maintenance labor, and aircraft and traffic handling personnel are all included in the calculation of labor costs.*

- *Fuel: Cost of aviation fuel used in flight operations, excluding taxes, transportation, storage and into-plane expenses.*

- *Aircraft Ownership: The cost of aircraft rentals, depreciation and amortization of flight equipment, including airframes and parts, aircraft engine and parts, capital leases and other flight equipment.*

- *Professional Services: The cost of legal fees and expenses (e.g., attorney fees, retainer fees, witness expenses, legal forms, litigation costs), professional and technical fees and expenses (e.g., engineering and appraisal fees, consultants, market and traffic surveys, laboratory costs), as well as general services purchased outside (e.g., aircraft and general interchange service charges).*

With these terms defined, discussion should be made on how these can affect an aircraft's trajectory, and consequently how the optimizer can incorporate them as part of a UPT. However before that, the matter of including fuel preferences into a UPT must be discussed. While it is possible to include fuel preferences into a fuel optimization, e.g. minimum onboard fuel limits to ensure sufficient fuel required for safe landing [38], care must be taken to ensure they do not allow the prevention of cooperation. An example of this would be of a user artificially raising the aforementioned amount of fuel required by their aircraft for safe landing. If this amount is misrepresented by an aircraft participating in ATFU minimization, and this misrepresentation prevents the aircraft from performing a trajectory that would have reduced ATFU further, then this misrepresentation has allowed the aircraft to save fuel at the expense of other air traffic. In essence, this aircraft did not cooperate with air traffic undergoing ATFU minimization because it was allowed to misrepresent the amount of onboard fuel it could use during flight. This can occur with any fuel based preference and is thus why this thesis did not include fuel based preferences as part of UPT.

Table 1 – ATA Airline Cost Index, 1st Quarter 2004.

Cost Item	% of Operating Expense	Cost Item (cont)	% of Operating Expense
Labor	32.4	Aircraft Insurance	0.2
Fuel	15.0	Non-Aircraft Insurance	0.8
Aircraft ownership	9.5	Passenger Commissions	1.6

Non-aircraft ownership	4.6	Communication	1.1
Professional services	8.3	Advertising & Promotion	0.8
Food & Beverage	1.9	Utilities & Office Supplies	0.8
Landing fees	2.3	Other Op.	19.2
Maintenance Material	1.6		0.2

With the fuel category of cost items removed from consideration, focus needs to be placed on the other three categories. Each of these categories contain items that are affected by parameters of an aircraft trajectory. Further, the trajectory can affect these items differently. The discussion below covers three different methods by which a trajectory can affect cost. Due to the complexity of airline economics, the discussion is not exhaustive and is only meant for illustrative purposes.

The first method of impact refers to items whose cost is determined on a per flight basis, i.e. their cost is proportional to the number of airport-airport transfers undertaken by the aircraft; the majority of the examples listed under Professional Services and some listed under Labor, particularly the wages of flight and maintenance crew, fall into this category. These items generally would not be affected by aircraft trajectory, except where the aircraft fails to makes it destination; in which case, the cost of these items are effectively doubled as the aircraft must make another flight if it wishes to reach its destination. There are numerous causes for failing to reach a destination, however two such causes are directly affected by an aircraft trajectory; a) using too much fuel and not reaching the destination, and b) arriving outside runway operation hours. While the main objective of the optimizer should help in preventing a), it is possible for an optimizer to prevent b); section 3.4 discusses the impact of including on-time arrivals as part of the UPT. This inclusion assists in ensuring aircraft do reach their destination on-time and within runway operating hours.

The second method of impact refers to items whose cost is determined by the length in time of the flight trip; the majority of the examples listed under Labor, as well as some of the examples listed under Aircraft Ownership, fall into this category. As flight time is directly affected by having a scheduled arrival time, the inclusion of on-time arrivals as part of the UPT also assists in reducing the cost of items affected by this method of impact. Again, section 3.4 will discuss how on-time arrivals affect ATFU optimization as part of the UPT.

The last method of impact refers to items who are affected by the flight performance of the aircraft during a trajectory; the majority of the examples listed under Aircraft Ownership, and some of the items under Labor and Professional Services, fall under these categories. For these items, it's the time spent at increased levels of aircraft performance that may increase the cost of a flight; increased aircraft structural damage occurs as a function of increased loading and frequency [20]. This causes aircraft to devalue faster and requires more maintenance. Consequently a facet of UPT must include a means of proactively limiting performance, especially where that performance would prove costly. Chapter 6 will be used to discussthe inclusion of constant altitudes, speeds, and climb angles for user specified portions of the UPT; while these inclusions were meant for other reasons, the chapter does shows how these reduce the impact of aircraft performance limits in resulting cooperative trajectories. Chapter 6 also shows why these inclusions come at the cost of increased fuel usage; this gives credence towards their fairness as an aspect of UPT undergoing ATFU minimization. .

2.3 Optimization Methods

In order to support the list of objectives mentioned previously, a similarly varied list of optimization methods were used. These methods are the mathematical and numerical processes used to define the optimum for the desired objective. Ideally, the optimization objective would suit the optimization method, and vice versa, with no concessions made by either to facilitate the other; however this is an ideal, with either or both the objective and optimization method normally making concessions to accuracy, or applicability, in order to prepare for the other. In some cases, the objective and the problem it defined were sufficiently simple that optimums could be reached via non-recursive methods, i.e. solving a single analytical expression [12], or a single comparison of already ranked alternatives [27]; while it is distinctly possible for these methods to be sufficiently accurate for the problem they faced, given the experiences of [32], and [36], it is likely that the methods would be unable to handle the complexities of optimizing fuel usage and thus not discussed here. The remaining optimization methods all find an optimum by recursively adjusting variables to reach better optimums and are therefore more capable of handling such complexities. Further, these can be categorized according to one, or a combination, of four effective categories for which the experienced concession is similar; random search and evolution based algorithms, integer programming and combinatorial optimization algorithms, linear programming algorithms, or non-linear programming algorithms.

Random searches and evolutionary or genetic optimization algorithms all have the common component that they randomly adjust variables in order to search for better optimums; this is advantageous when the correlation between variation in variables and optimal value is deemed counter-indicative, as in [26], or not easily observable as in [28] and [29]. This ability to not consider such correlations allows these methods, as optimization algorithms, to be more efficient in finding optimums [41] and also be more widely applicable since such correlations do not have to be known for the method to be applied. Further, in terms of computation they benefit from and support parallelization; all other algorithms are sequential in nature and suffer significant diminishing returns when parallelization is applied. However there is a theoretical loss in accuracy when using it; the randomness of the algorithms ensures that the final result may not be an optimum, whereas others would find a local optimum at the least if it exists. In terms of its use with fuel usage optimization, the concern is that [32], in using a nonlinear program algorithm, did show that correlation exists between an optimal fuel usage value, and cooperatively de-conflicted aircraft trajectories. Such correlation could be used to either hasten optimization, or create control laws outside of an optimization process; thus utilizing methods from this optimization category without fully exploring methods that could use such correlation seems unwise. However if it is shown that the correlation between variation in variables and optimal value is counter-indicative or not easily observable, random searches and evolutionary or genetic algorithms would be reconsidered.

The commonality held by integer programming [42] and combinatorial optimizations [43] is that the methods focus on variables that can only be integers. This makes such algorithms highly applicable for optimizing fuel usage due to the ease with which the trajectory and traffic parameters can be represented as integers; as in [31] with singular selection of pre-set route structures or as in [35] with flight levels and separation modes, all are easily considered if indexed as integers. Further, even smooth phenomena, such as weather and other earth surface correlated data, are often necessarily discretised and indexed as integers. However, again as in the discussion of the objective in [35], this also presents an issue in the correctness of the representation of the

problem if it becomes integer based; optimum modes, e.g. slight deviations from route structures, cruising between levels, or variations in separation modes over time, could all be avoided because they are not integers. There are further issues when these methods are considered as algorithms; considerable computation time in these algorithms is devoted to defining optimum integers [43], i.e. a premium is paid for calculating them. If the problem did not have to rely on integers, optimization computation time decreases and, simultaneously, the correctness of the result improves and the chance of improved understanding of the problem is gained. The counterpoint to this line of thought is that the use of integers as optimized variables is unavoidable in the control of air traffic; while that could be true, attempts must be made to fully explore options in situations where integers appear to be necessary and only when none are found should these methods be used.

Linear Programming algorithms are very specific in that they only handle problems with objectives and constraints that are entirely linear [44]. Given the non-linearity of fuel consumption, and other aspects of trajectory optimization, linear programming would be inappropriate as an optimizer by itself, however as seen in [35], it can be used in conjunction with the two previously mentioned categories to handle aspects that can be defined in a linear manner. Further, again as per [35], under certain conditions, particularly where optimization occurs over a very small time frame, normally non-linear aspects of trajectory optimization can be treated as linear with a decent level of accuracy. In effect, when combined with an algorithm from either of the two previous categories, linear programming reduces the broad applicability of the other algorithm in return for increased accuracy where ever it's applied. It should be noted however that the same trade off does not occur in combination with Non Linear Programming due to the ease of treating linear problems as non-linear problems. Thus, Linear Programming would only ever be considered for use if integer or random search based algorithms are considered for use as the primary optimizer.

Non Linear Programming is a general term that includes all optimization algorithms that can handle non linear problems. Consequently the random, evolutionary, integer and combinatorial algorithms mentioned previously, can all be considered a form of Non Linear Programming. However, there is a subset of Non Linear Programming algorithms that do not have their own classification and these are the algorithms that only handle problems with objectives and constraints that are mostly smooth and non-linear [45]; for the purposes of this research, Non Linear Programming refers to these methods. These methods are clearly restricted to problems where every aspect has to be defined in smooth terms, i.e. no singular aspect inside the problem is allowed to be random, unpredictable or undefinable. It is possible to combine nonlinear programming algorithms with integer and random based algorithms [46], but usually only in capacity akin to linear programming in doing the same, i.e. the issues associated with nonlinear programming in such a combination become secondary to the issues experienced by whatever it was combined with. Excluding this possibility, the use of only a nonlinear programming algorithm equates to having really low applicability due to the difficulty of framing problems as a group of smooth functions, but with high accuracy due to the ability to use information embedded in that 'smoothness' to aid optimization. If it is possible to create smooth functions for all aspects to the problem, then a nonlinear programming algorithm should be used; even if the resulting optimization process is slow, lessons gathered from understanding the process can be extracted and used in quicker optimization methods, or directly applied in control laws outside of an optimization process.

Within Non Linear Programming, two particular algorithms of note should be mentioned due to their applicability as optimization methods for problems encountered during the research; sequential quadratic

programming algorithms and interior point based algorithms. Sequential quadratic programming, or SQP, optimization involves the improvement of a set of variables that define an objective function, by representing the objective function and the constraints surrounding those variables with a quadratic model from which a more optimum point can be calculated from; the process is repeated till an optimum is found [47]. Interior point methods find new optimums by taking the gradient of the current set of variables and combining that with a logarithmic barrier function representation of the constraints; as the representation is lessened an optimum is reached [45]. Detailed testing and discussion between SQP and Interior Point methods can be found in section 3.3.1, however a couple of statements can be made here. Firstly, SQP was found to be incompatible with the combination of ATFU minimization objective and separation constraints; resulting trajectory shapes were clearly non-ideal and manual creation of trajectories could yield lower ATFU. Conversely, Interior Point methods were found to function acceptably in this thesis; resulting trajectory shapes showed properties of optimized trajectories, i.e. smooth climbs and transitions to cruise, as well as quick linear descents, which molded closely around points of conflict. Fuel consumption with altitude and distance separation constraints was shown to be optimizable via SQP in [32] thus the inclusion of time based separation constraints must have been the cause of SQP incompatibility; the exact mechanics are not known however it was clearly responsible. Again, more information can be found in 3.3.1.

2.4 Research Objectives

With all pertinent issues having been discussed in the review of the literature, this section summarizes the challenges to the optimization of continental ATFU.

2.4.1 Summary of Issues

To perform ATFU minimization, an algorithm that models cooperative air traffic over a continental region and supports minimum total fuel usage, must first be developed. While the methods presented in [32] and [35] are suitable, both have shortcomings. Firstly, both methods do not take aircraft performance limits into account; therefore the optimized trajectory may not take full considerations of those limits. Secondly, both methods do not accurately calculate fuel consumption; one algorithm required integration with more accurate calculations, while the other assumed constant speeds and altitudes to simplify the calculation and its consequent optimization. The solutions to these shortcomings is to introduce an accurate aircraft performance model and ensure all elements of the model are correctly integrated with an optimization method. Finding an optimization method that can cater for the accuracy of the performance model may be difficult, but the broad variety of optimization methods available does ensure an effective method would be found. However in planning these solutions a deeper issue was noticed and the two previously mentioned shortcomings were recognized as being symptomatic of the same issue; i.e. that the dimensions in which trajectories are defined can place limitations on how trajectories can be controlled. To enable understanding of this issue, two of the previous optimization methods capable of ATFU minimization provide apt analogies for the cause of it.

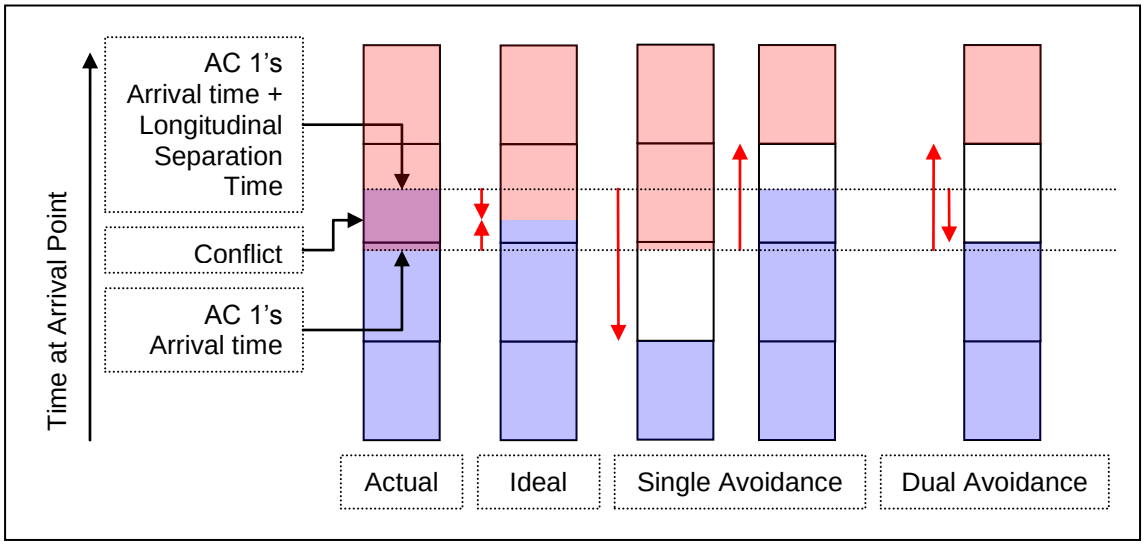

Figure 1 - Graphical Example of Time Deviations due to assigning Arrival Times to Discrete Times.

The method defined in [32] used a time discretised assessment of air traffic to check constraints and perform optimized resolutions of conflict. While the equations that supported this were appropriate, it did mean difficulty in incorporating other data, e.g. region and time separation based requirements. The correlation of region based data can be performed via the 4D positional data inherently required by fuel calculations but can be computationally inefficient; the number of aircraft-aircraft comparisons are large due to their non-fixed nature, and their resultant optimization would be significantly non-linear. However the accuracy and freedom of

movement required to satisfy time based separation requirements would be restricted by the discretised time steps that are used, i.e. conflicts that are resolved via time separation could incur additional unnecessary time separation due to time separation being only checked at a time step as opposed to during it. The same applies to trying to prepare for a variable landing or airspace exit time; unless aircraft are allowed to land or exit at a non-discrete time step, landing and exit times will be fixed upon the nearest discrete time step. Figure 1 characterizes the presence of multiple aircraft arriving at the same point; the preceding aircraft is in pink, and the following aircraft in blue.Due to time separation requirements [25], an aircraft's presence at a point begins when it gets there and ends after the time separation limit has passed and the aircraft is consequently far enough away from the point that another aircraft can travel through it. However Figure 1 shows examples of time losses in conflict resolutions where one or both of these aircraft must resolve conflict or arrival time using a discrete time system. An easy solution to these would be to use sufficiently small time steps; however this has a multiplicative effect on the number of conflict checks required and can, for other additional reasons, slow down optimization significantly.

In contrast, the method defined in [35], due to its CDR representation from an ATFM perspective, uses a distance discretised assessment of air traffic; time and distance separation were checked and resolved at pre-defined waypoints and intersections. Accordingly, this does not have any difficulties with trajectory correlation to ground based data, or the adherence to time based air traffic relationships. It does however have other issues in terms of an inability to handle route changes and inaccuracy in conflict resolution. The issues with route changes in a predefined list of intersection points is that the intersection points must change to suit; however where a single route has multiple aircraft where some need to change route and some do not, the number of necessary intersection points also increases. This has a multiplicative effect similar to the one experienced by [32]. The inaccuracy of conflict resolution stems from conflict only being checked at waypoints and intersection points; this was acceptable in [35] because it used only level flight altitude assignments, so conflict between waypoints and intersection points would always be detected and resolved. However since optimal fuel consumption inherently requires non-constant flight level assignments, doing the same allows possible undetected conflicts to occur between intersections and waypoints. Resolving this can be problematic as it requires additional waypoints to be used to cover gaps; the appropriate distribution and number of these would need to be researched and developed especially in light of desirable route changes. Further, it would experience a multiplicative effect greater than that required of [32], but, as a positive, would prepare for smooth variation in time separation based conflicts.

Given a desire for cooperative aircraft behaviour and the sensitivity of fuel consumption calculation to the speeds and altitudes experienced during flight, enforcing a static waypoint time that does not correlate directly to another aircraft, should be avoided. However without an apparent means of introducing waypoints that simultaneously covers undetected conflicts while handling significant route variation, an optimization process built upon [32] was almost a necessary choice. The algorithm shown in [36] provides sufficient inspiration to create an alternative. In order to perform ground data correlation, [36] had a means of dividing airspace to correlate wind as well as to provide necessary heading changes; i.e. using this discretised airspace it was possible for discrete airspace locations to store data and perform checks that are specific to it. This led to the possibility of treating discrete airspace locations, initially defined irrespective of trajectories that could fly through or pass it, as checkpoints; using data stored by these locations, aircraft and ground location specific checks could be carried out with ease. This did imply significant computational resources, but the more accurate fuel optimization in an

easily expandable means of defining air traffic, and all the benefits such implies, did warrant a fuel consumption optimization process to be developed along those lines.

2.4.2 Research Questions

Since the apparent solution to the last obstacle was the use of an alternate means of defining air traffic, and since this can effectively alter how other obstacles mentioned before it are handled, it's application and development became the core of the research. This also meant that a considerable number of already existing functions had to be redeveloped to check and ensure fitness for purpose. Consequently, collating these issues with the intended goals of the research would therefore create the research questions below to be answered. These research questions are reassesed in each chapter of this thesis to chart progress in answering them, as well as to give rationale for key decisions made during research and defined later in the thesis.The conclusion will give a final summary of the progress in answering each question.

Q1: Can a co-operative and sufficiently informed air traffic optimisation methodology achieve a reduction in total fuel usage compared to current ATM?

While the ability to model and control traffic via a discretised airspace approach is apparent, its process must be shown in formal terms and in consideration of a wide range of issues. This is important as UPT requirements do shape the optimizer's method of controlling air traffic. Similarly, as co-operative actions require simultaneous optimization of all aircraft trajectories, optimization results must clearly show, and rationalize, the reasonable involvement of all air traffic; up to and including air traffic created by current ATM.

Q2: What information is required to achieve such an optimisation methodology and how sensitive are the results to the accuracy of the input information?

The purpose of this optimization methodology was to be utilized in the minimization of ATFU to control and optimize air traffic; consequently information regarding fuel consumption, flight mechanics, and trajectory control, are required to facilitate it. The key focus then is to assess potential sources of this information in terms of its applicability in minimizing ATFU. Airspace [7] and trajectory [25] control methods do have regulations that can and should be followed, however a variety of fuel consumption and flight mechanic information sources exist and should be compared. Once the optimization methodology, and its requisite sources of information, are fully integrated, it can be comprehensively tested against a set of simple, extreme and critical conflict scenarios; these scenarios would utilize a range of data, in the form of multiple aircraft models, from those data sources to see if ATFU can still be minimized with them.

Q3: How can constraints such as aircraft performance limitations, minimum separation and on-time arrival be incorporated into an optimizable UPT, and how do these affect total fuel usage?

Once there is sufficient confidence in the optimization process, development will then aim for improving any already existing constraints on the process as well as including more constraints so as to more realistically describe an ATS. Aircraft performance limitations were to be improved via the integration of an updated and more comprehensive means of calculating fuel consumption. Minimum separation constraints were to be improved via the addition of functions that better enable it, inside the optimization process, to lead to ideal

ATFU. On-time arrival, and other user preferences were to be included via the transformation of the trajectory optimizer variable to a UPT optimizer variable. At each stage, their impact on fuel usage will be tested and discussed.

Q4: How can a dynamic environment, such as deviation from or in-flight changes to the flight plan, airspace closure, and emergency diversion, be accommodated in an optimisation methodology?

Is the performance of the optimisation methodology acceptable for real-time use and, if not, what improvements can be made to make it more suitable for use in an ATC environment? Given the results in the previous research steps, trends and benefits and issues associated with the optimization process can be gathered and summarized to define its impact in actual application, and to see if it can accomodate in-flight changes to the flight plan, airspace closures and emergency diversions.

3. MODELLING AND OPTIMIZATION OF AIR TRAFFIC FUEL CONSUMPTION

In order to develop a system that could optimize air traffic to minimize total fuel usage, two tasks had to be performed. The first is the characterization of the ATS so as to allow modelling of the behaviour of its elements. The second is the fitting of the resulting model into a set of functions that can reflect the modelling, whilst being able to optimize it towards minimum fuel usage; this group of functions is considered as the resulting "optimizer" of this research and should not be confused with the "optimisation method" which is the mathematical optimisation technique discussed in sections 2.3 and 3.3.1. The discussion of these two tasks are summarized via five sections and presented in this chapter.

In characterizing the ATS, two models of air traffic are required for its control. Section 3.1 develops a model that defines the separation held between every potential pair of aircraft being controlled; i.e. how the state of separation between a pair of aircraft changes as the trajectories of the pair are controlled. Section 3.2 develops a model that defines the actual trajectories of the individual aircraft that make up the traffic; i.e. how the aircrafts' heading, altitudes, and speeds, vary as they travel across their intended paths. The models defined in these sections are similar in that they are affected by external requirements, and that within the same control mechanism, can have the same baseline, or index, from which they are defined. These two sections will look at the external requirements in terms of their impact with each of the modellings, however for ease of explanation this will be done in comparison with the modellings used in [32] since such is shared with almost all non-ATFM based representations of the CDR problem. This comparison is allowed due to the modellings of [32] having a purely discrete time index and therefore being representative of almost all Discrete Time based Methods (DTM). In contrast, the new modelling of air traffic developed here was based on ATFM developed Discrete route Segment based Methods (or DSM) via the inclusion of a dimension lateral to the route segment; the new method can therefore be described as having a discrete area index that allow Discrete Area based Methods (DAM). With these baselines in mind the differences between DTM and DAM, in terms of their means of correlating between, and within, their modellings of air traffic, should become readily apparent and give reason for the use of DAM.

With the first two sections having defined a holistic ATS model, it was possible to develop a means of optimizing ATFU. However since the modellings of air traffic are new, there was little indication of where problems could come from; therefore it seemed prudent to first try optimizing a simplified means of calculating fuel consumption. The general trends in such are well known and easily seen; checking to see if the optimizer was working properly would be the task of finding such trends in the results. To distinguish the efforts here from those later on, the optimizer developed in the latter sections of this chapter was defined as a Prototype Core Optimizer, or PCO; so named because of it being an initial attempt at NMD based fuel optimization, and because it only contained the components that were necessary for future ATFU optimizers with placeholder functions for components that were not. The discussion of it and its results are covered in the last three sections of this chapter. Section 3.3 contains discourse on each of the requisite components of the PCO and the experiences each had during development. Section 3.4 shows three case studies that were considered representative of all the scenarios that were trialled under the last version of the PCO; discussing and rationalizing all the trends found in

such results. Lastly, section 3.5 concludes this chapter by summarizing the achievements, lessons and recommendations caused by the work herein.

3.1 Modelling Air Traffic Separation

The reason a traffic separation model and a trajectory control model should have the same baseline within the same algorithm or program is due to the need of the separation model to understand and use information from the trajectory model. If the index for both is different, the process for data transfer becomes more convoluted with increased chance of being inaccurate or incorrect. However if the index is the same, data is merely transferred and not transformed to fit. In DTM, for instance, separation as experienced by air traffic is checked via an assessment of their relative position at discrete points in time, then for ease of correlation, variations to altitude, speed and heading would only occur with reference to some or all of those points in time; or vice versa depending on which model needed to provide information. If however, the DSM in [35] was used to define trajectory, transferring data to a discrete time index would first require the variation in trajectory parameters to be defined in terms of time, then because of the likely differences in time step size, would then require extrapolation or interpolation methods, and all the inaccuracies such may imply, to transfer the necessary data.

The development of DAM was necessary to grant DSM a means to control air traffic to the same extent that DTM could, i.e. to not be reliant on a static list of waypoints to define conflict, whilst maintaining the ease of correlating location based data, such as sector capacity limits, that DSM have. With DSM the point of correlation is either the start or end of a route segment; these would be defined by intersection points and the expected need for variation in trajectory. Essentially this means that if the point of conflict is allowed to vary, the model of separation is lost since conflict is no longer aligned to the start and end points where conflict was checked. To maintain conflict assessment, it needs to be performed from a perspective that does not change, yet can prepare for changes in trajectory should such occur. A useful reference point is the original point of conflict; provided aircraft fly sufficiently close to the original point so as to be considered as having passed it, then the times and altitudes it experienced when doing so can be used to determine conflict with other aircraft doing the same. The issue with this is that aircraft trajectories can be sufficiently deviated that they no longer fly close enough to the original conflict point; trying to calculate time separation using the same method would create an inaccurate result. The solution is to have a pre-existing set of reference points cover the entirety of the map; points that have multiple aircraft fly sufficiently close to them can then compare those aircraft against each other to see if they flew close enough to each other in terms of time or altitude so as to be in conflict. This can be difficult to imagine so the rest of this section will go into detail as to how this occurs.

As mentioned previously, external requirements affect air traffic modelling; in the case of separation, the pertinent requirements stem from the ANSP associated regulations or policies that define such. The common DTM of using radial distance and altitude between separate pairs of aircraft to assess separation came from the aircraft based situational awareness policies defined in [1], though [32] did show that an elliptical separation could be used in place of a simple circle to better represent longitudinal limits. In contrast DAM based separation was developed to accurately reflect currently accepted ATC defined separation; i.e. Δt, Δh, and ΔS_y, correlate directly and respectively to the standard definitions of longitudinal time [25], altitude [25], and cross track distance [48], between separate pairs of aircraft. Consequently, the minimum allowed values for those separation modes can also be transferred directly from those sources and are defined here respectively as Δt_{min}, Δh_{min}, and $\Delta S_{y\,min}$. This also allows, using the terminology defined in section 2.1.2, a nominal state propagation to define intended trajectories; as emergency scenarios are defined using ATC definitions for separation, probabilistic or

worst case propagation, and the calculation methods they use, are not required to handle them. Figure 2 compares DAM and DTM visually and in terms of the separation requirements involved.

	DTM, or *t* based, Separation	DAM, or *A* based, Separation
Separation per discrete dimension	*At discrete time step, t:* 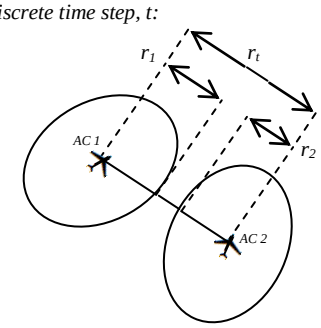	*At discrete area, A:* 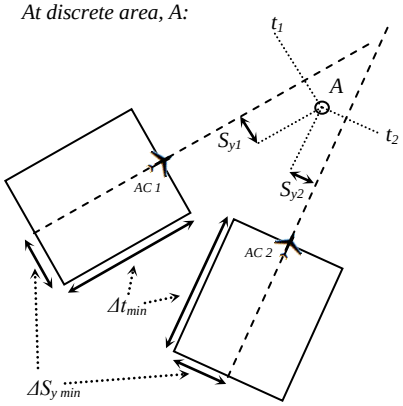
Minimum Longitudinal Dist. Separation, $\Delta S_{x\,min}$	Covered via: $r_1 + r_2 < r_t$	Covered via Δt_{min}
Minimum Longitudinal Time Separation, Δt_{min}		$\Delta t_{A,1,2} = \lvert t_1 - t_2 \rvert_A$ $\Delta t_{A,N1,N2} > \Delta t_{min}$
Minimum Cross Track Separation, $\Delta S_{y\,min}$		$\Delta S_{y,A,1,2} = \lvert S_{y1} - S_{y2} \rvert_A$ $\Delta S_{y,A,1,2} > \Delta S_{y\,min}$
Minimum Altitudinal Separation, Δh_{min}	$\Delta h_{t,1,2} = \lvert h_1 - h_2 \rvert_t$ $\Delta h_{t,1,2} > \Delta h_{min}$	$\Delta h_{A,1,2} = \lvert h_1 - h_2 \rvert_A$ $\Delta h_{A,1,2} > \Delta h_{min}$

Figure 2 - Comparison of Separation Constraints per discrete dimension

The details in Figure 2 are for a single discrete baseline interval and do need to be replicated for all other intervals for each base line; how this is done in the case of DAM separation has considerable ramifications throughout the entirety of the research and is mentioned in the next section. However, one discrete interval from the two baselines is sufficient to see significant differences already. The foremost of these is in the holistic state of DTM separation and the separated state of the DAM separation. The DTM separation limits are coupled such that individual separation limits cannot be easily isolated from each other; optimization processes have no choice but to handle all such limits at the same time due to the performance of the aircraft affecting them all in an unpredictable manner. In contrast DAM separation isolates Δt_{min}, Δh_{min}, and $\Delta S_{y\,min}$ from each other; this is useful as, under particular conditions, these separation modes can become constant and therefore reduce the complexity and computation time of the optimization process.

One last thing to note from Figure 2 is the distribution of discrete areas that DAM would require. For DTM, the equivalent issue is the size or frequency of time steps; there must only be enough to cover any inaccuracies in the problem, anymore would cause unnecessary computer workload. Due to the two dimensional nature of discrete areas, the issue of their size and frequency has two elements. The first element is the maximum distance between the centre points of discrete areas; since ΔS_y is referenced from the centre points of those areas, the space between them would thus impact on the accuracy of ΔS_y checks. Given that for en route air traffic [48] defines $\Delta S_{y\,min}$ as 5 nautical miles, and [25] defines Δh_{min} as 2000ft and Δt_{min} as 5 minutes, a maximum distance between centre points of 1 nautical mile was deemed sufficient enough to model differences between various modes of conflict at the en route level. The second element was the earth surface distribution of these areas; trying to maintain areas with the same consistent area would have required convoluted and cumbersome techniques in order to manage them. For simplicity and because other earth surface discretised data did similar, the maximum distance between nodes was redefined to be one nautical minute in either longitude or latitude; this allowed definition of discrete areas to be in terms of a matrix correlating discrete nautical minutes of longitude with discrete nautical minutes of latitude. Figure 3 shows a comparison of two baselines using multiple separation checks.

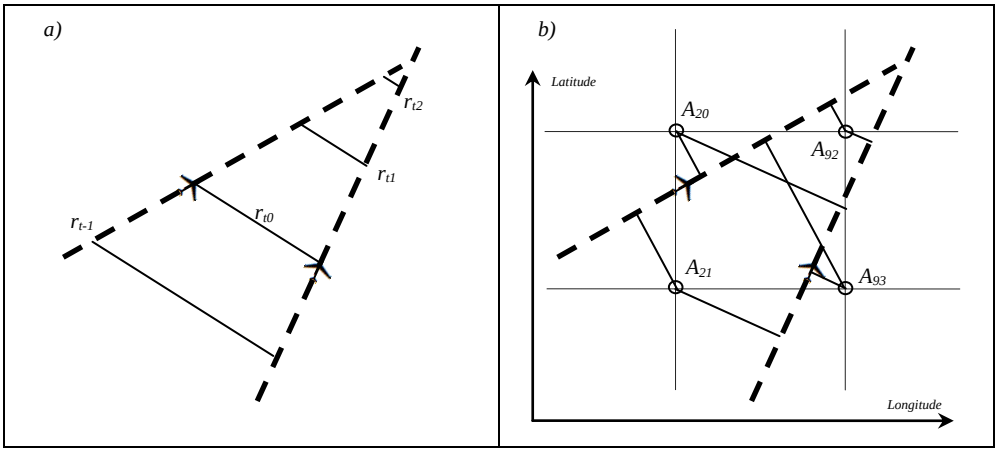

Figure 3 - Characteristic Separation for multiple a) time steps and b) discrete areas

A nautical minute is 1/60th of a degree of either longitude or latitude, and is equivalent to a nautical mile when measured along any great circle of earth. The lines of longitude are always great circles and thus a nautical minute is always a nautical mile when measured in the latitudinal direction, but the lines of latitude, with the exception of the equator, are small circles so a nautical minute in the longitudinal direction reduces from one nautical mile at the equator, to zero at the poles. Regions with higher magnitude of latitudes may need to increase the step size of their discrete areas along the longitude dimension to offset the reduction in distance per nautical minute that is experienced there and ensure more uniformly sized discrete areas. As the majority of research here has occurred irrespective of location, the one nautical minute discrete step size has been maintained throughout with all mechanisms using such being described as having Nautical Minute Discretisation, or NMD. Figure 4 shows how NMD interacts with allowable cross track deviations to describe time separation in NMD terms.

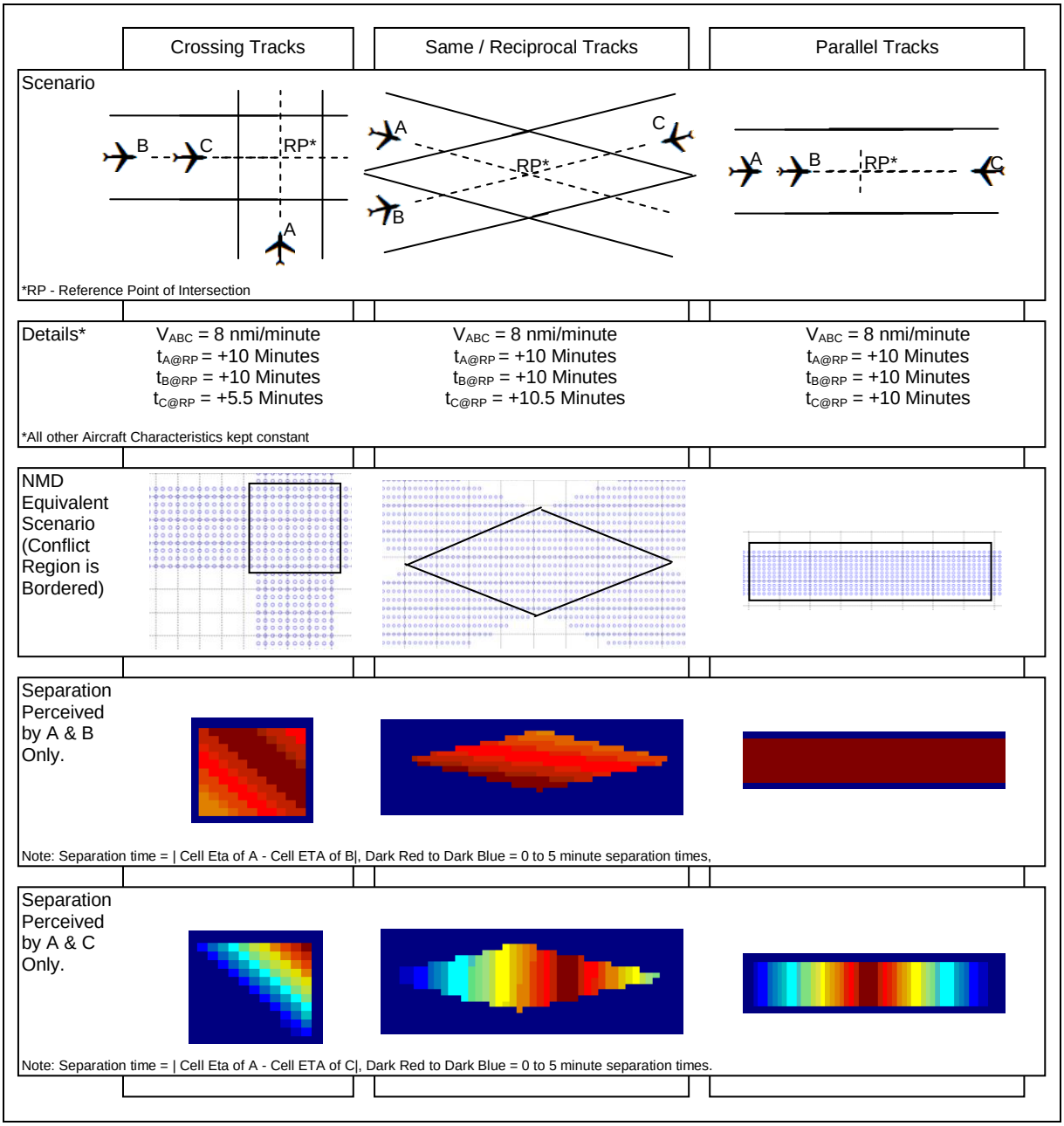

Figure 4 - Modelling of Separation Times via NMD

3.2 Modelling Trajectory Control

There are two elements to the trajectory model; actual and potential. Actual merely refers to an aircraft's actual or intended trajectory; given its simplicity, discussions on it mostly go over how its information is transferred to other components that need it. Potential modelling is considerably more complex as it defines a trajectory in terms of what it could be, given known limits; this is of significant importance as its definition both allows and limits the ability of anything to control the trajectory.

3.2.1 Actual Trajectory Modelling

As mentioned in 3.1, minimizing unnecessary data transfer requires that Trajectory and Separation models have the same index. While NMD based separation does appear to be modelled by the minutes of longitude and latitude, from the perspective of aircraft they are also modelled by the along track distance, or ATD, required to travel pass them. It is also possible to use ATD as the baseline for variation in aircraft altitude and speed, thus its use as a common baseline here makes sense. Figure 5 shows how the ATD for particular areas are gathered to form a list of discrete ATD distances from which a trajectory can be defined.

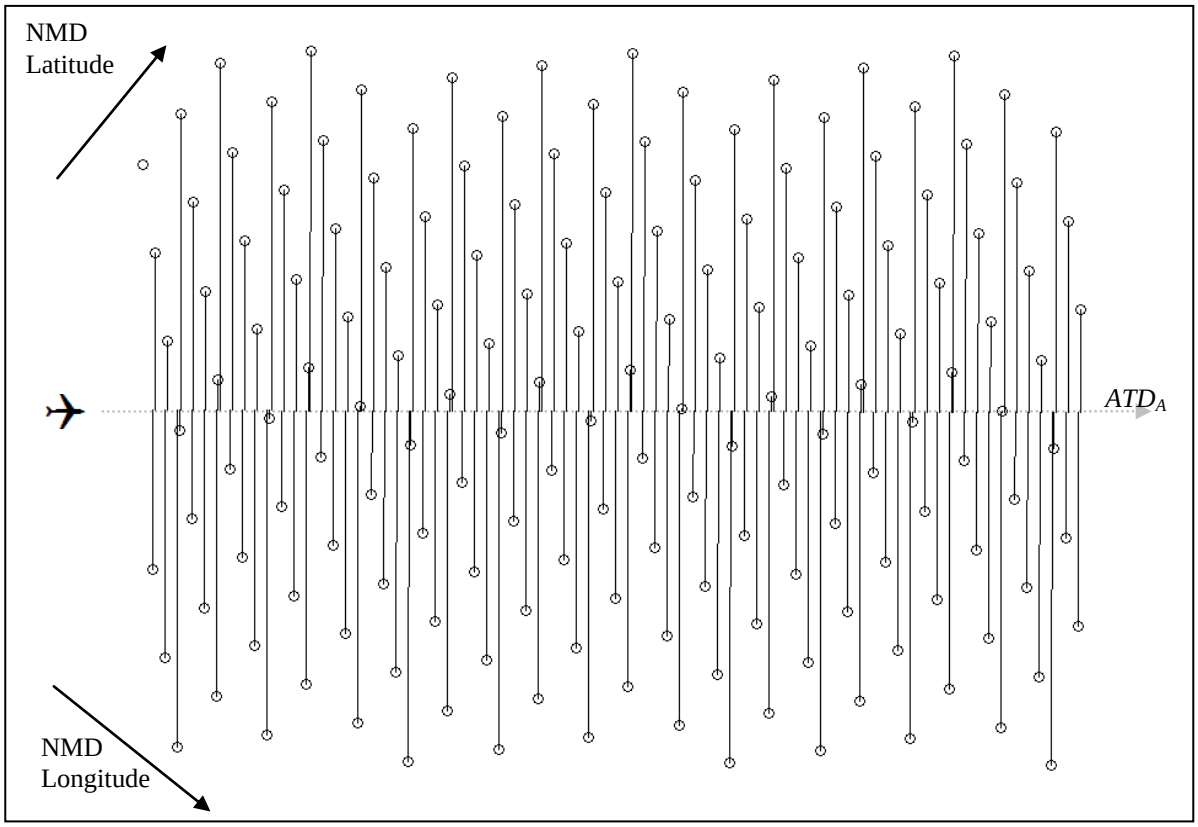

Figure 5 - ATD_A from NMD describing an aircraft heading N53E

However there are several issues that prevent this list of discrete area ATD, or ATD_A, an example of which is shown in Figure 5, from being directly used to calculate aircraft performance over them. The first and foremost issue is that ATD_A is prohibitively non-uniform over its range; even ignoring variation due to earth curvature, the two dimensional nature of their modelling implies that elements of ATD_A can have equal or near equal ATD values, particularly where a route travels along a meridian or temporarily along a circle of latitude. This is

problematic since route segments with zero distance are nonsensical, and route segments with near zero distance can experience extreme rounding off errors. The other issue is that the sheer number of ATD_A elements is significantly greater than that required to accurately perform trajectory prediction; particularly since the research here uses a 5 nautical mile cross track deviation on an NMD field, it is possible to have ten or more ATD_A elements occur within a nautical mile.

While not introduced to deal with these issues, two further ATD based dimensions were created that did prepare for inability of ATD_A to appropriately index trajectory prediction. The most pertinent one is ATD_i which uses an ATD step size of roughly four nautical miles which creates just enough ATD steps to accurately predict trajectory. The other is ATD_N which uses the significantly larger step size of roughly 20 nautical miles for the purposes of control, as it would be inappropriate to expect pilots to cause trajectory changes every 4 nautical miles. While they do have different step sizes, they were still made to align with ATD that exist in ATD_A hence the 'rough' step sizes. This ensures that separation checks can be performed with minimal interpolation or unnecessary data alteration. With the persistent use of ATD as a baseline for trajectory modelling, the times, altitudes, cross track distances, and speeds experienced at specific ATD within ATD_A, ATD_i, and ATD_N, can easily be determined and transferred.

3.2.2 Potential Trajectory Modelling

The main aim of modelling potential trajectories is in determining which of, and how, its parameters are allowed to be variable for the purpose of optimization via trajectory control. The reason for the discussion of this stems from two things. The first is the desire to reduce the significant number of separation checks that NMD separation in optimization intuitively suggests. The second is NMD separation's ability to define and check separation in uncoupled dimensions. Possibilities provided by the second allowed partial satisfaction of the first. Accordingly the parameters discussed here are only of the trajectory limits definable in terms of airspace dimensions. However external regulations and policies, as well as aircraft performance limits, do come into consideration and have significant ramifications. The apparent parameters given an ATD baseline are the altitudes, h, times, t, and cross track distances, S_y, of aircraft with respect to their existing ATD_A indices. The values for h and t set by an aircraft as it passed various ATD_A were, due to their impact on fuel calculation, allowed and intended to be completely variable; however certain performance related limits do exist for both that reduce the number of separation checks. The reduction of separation checks stemmed largely from the variability of an aircraft's S_y; certain ranges of S_y allow a large number of separation checks to be completely avoided.

3.2.2.1 Limits of Variable Cross Track Distance (S_Y)

As the core issue, the initial discussion needs to be of the limits of S_Y as a variable. If A is the set of discrete areas that define a region of air traffic, then it is possible to define, for any pair of non-equal N, a subset of A over which both N fly; collecting this subset for all non-equal pairs of N yields A_{NN} which lists in total all discrete area and aircraft pair combinations for which separation must be checked. Given that S_y defines the region over which an aircraft can fly, it has a direct correlation to the size of A_{NN}. To aid understanding of the issue, several two aircraft scenarios of differing S_Y variability and their resultant A_{NN} are shown in Figure 6. Figure 6a) shows how DTM modelling of separation requires one separation check for each pair of aircraft for each discrete time step. Figure 6b) shows air traffic with unlimited S_Y variability causes A_{NN} to be the same size as A. Figure 6c) shows

how air traffic with limited S_Y, e.g. via a known maximum aircraft range, restricts A_{NN} to the overlap of their potential routes. Figure 6d) shows air traffic with no S_Y variation would cause A_{NN} to be restricted to a region that is also known as the 'area of conflict' [25] defined by lateral or cross track separation requirements. Figure 6e) shows how, if S_Y variation were allowed in places that did not create overlapping areas of conflict, then only the A_{NN} shown in Figure 6d) would be required.

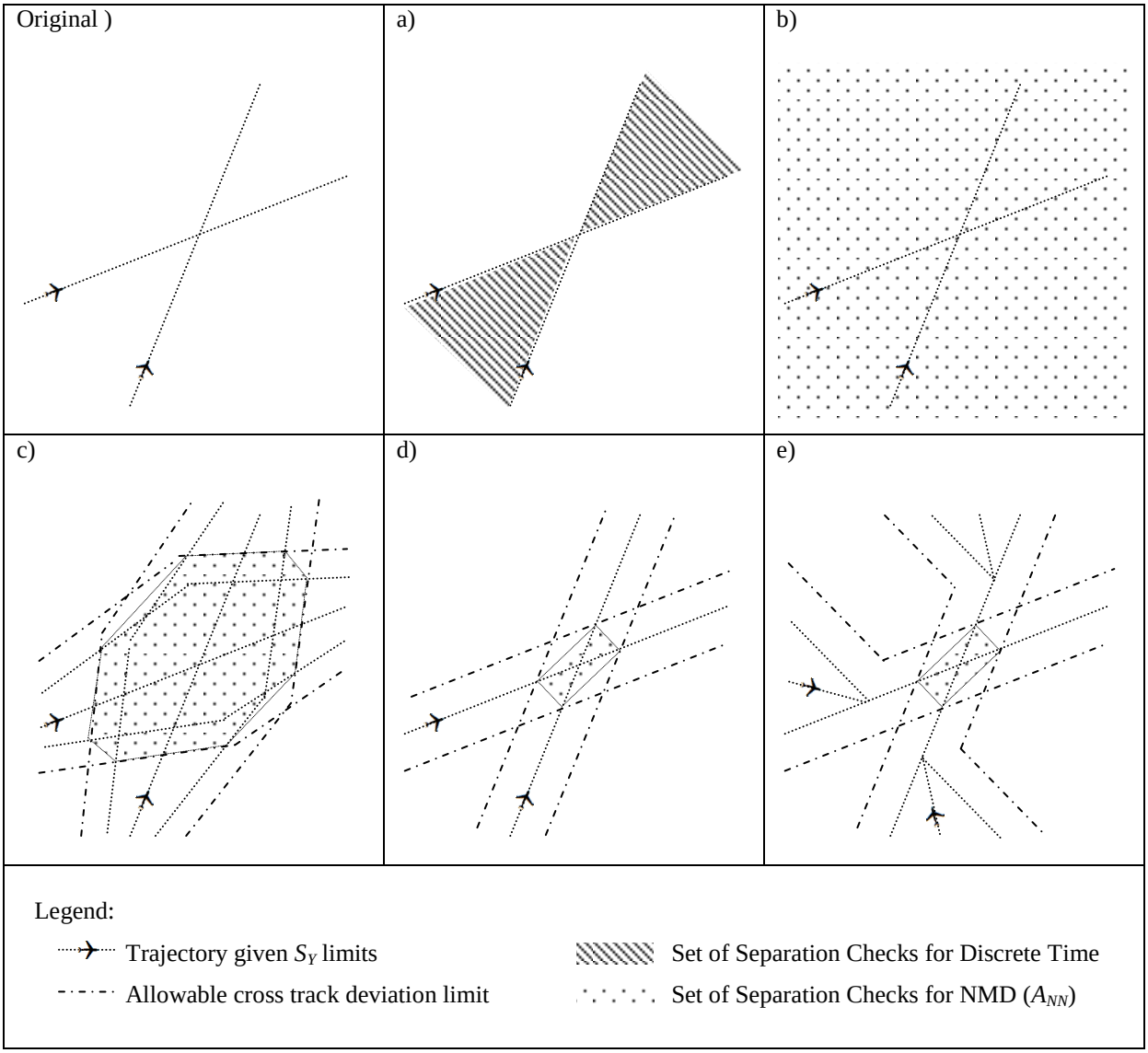

Figure 6 - Visual Representation of Requisite Separation Checks for discrete time (a) and NMD (b ~ e) assuming different levels of S_Y variability.

The issue then is to determine to what level of S_Y variation should be allowed as part of the optimization process. Clearly the A_{NN} in Figure 6b) is undesirable; a choice therefore had to be made between allowing a degree of S_Y variation as in Figure 6c) or making S_Y variation a matter external to fuel optimization and only allow the altitude and time of an aircraft to be variable thereby resulting in intersections as in Figure 6d). While the inclusion of S_Y variation was warranted, several issues kept it from being so.

The first and foremost was a concern for computational requirements. Prior to developing the methods in Appendix B, using NMD was equivalent to carrying out the separation checks for Figure 6b); a continental region can be thousands of nautical minutes wide along both longitude and latitude dimensions, which implied millions of checks would be necessary just for a single pair of aircraft. However given the work in Appendix B,

methods were developed that efficiently and accurately picked up the NMD nodes that would model conflict between a pair of aircraft experiencing Figure 6d); this drastically dropped the number of separation checks to be, in the case of cross tracks, proportional to the square of the number of nodes across a trajectory, and in the case of reciprocal or same tracks, proportional to the number of nodes along their trajectories where they were on reciprocal or same tracks that overlapped. In contrast, trying to do the same for Figure 6c) proved doable, but troublesome as it required defining S_Y variation given an aircraft range limit; even assuming public knowledge on range limits were accurate for all conditions, such still created potential flight regions that covered a large fraction of continental airspace thus still leading to undesirable numbers of separation checks.

The second issue was the randomness that allowing S_Y variation could create. The methods defined in [26] and [28] decided to use random search and genetic algorithm based optimization methods because some conflict modes had multiple resolutions that were equally, or near equally, as cost efficient as each other. This is particularly true in the case of S_Y variation, where performing a roundabout in either clockwise or counter clockwise directions usually required the same amount of additional fuel. From the perspective of a non-linear optimizer this is equivalent to starting at a point with zero gradient with the apparent option of travelling along increasing gradients in two opposing directions; assuming the initial point is invalid due to separation, an optimizer would have to choose between the two with the choice being defined by either irrelevant rounding error or the order in which the directions are presented [17]; this is highly undesirable since two equivalent scenarios with slightly different orientations can experience different results.

The defining point that settled the matter came from investigatory research that doubled as trials for the method in Appendix B. The research in Appendix C looked at projected air traffic density for the United States as defined in NMD terms for a variety route structures. The structures that were used included those that prepared for direct unaltered flights, flights that were locally dispersed to avoid air traffic, and flights that wanted to use routes that guaranteed an optimal or near optimal flight level but over a considerably longer distance. The research showed, using very rough methods, that given increasing air traffic, the perceived amount of fuel lost to handling air traffic would cause pilots and airlines to use the third route structure since its ‘highway’ like properties would help to ensure near optimal operating conditions. The research indicated that even though locally dispersed routes could achieve the same, the increasing traffic would eventually cause dispersions of traffic to reach each other and thereby nullify and benefit the dispersion had. Even though Appendix C was rough in methodology, the mere possibility that heavily structured routes could be more efficient than anything done on local scale suggested that S_Y variation, or any other form of route control, should be handled external to the fuel optimization process.

The above issues did mean that S_Y variation was excluded from the optimization in this research. However it should be noted that the issues mentioned above do not define the inclusion of S_Y variation with DAM as impossible or infeasible; only that it is computationally expensive, likely to be irrespective of fuel optimization, and possibly inappropriate in the future. That it can handle S_Y variation, and is one of only a few DSM that could do so, is true; as is the significant ease of re-introducing it in the future should the need arise. Also just for clarity, S_Y variation is still possible outside of optimization; several scenarios used later for trailing various optimizers do contain flights that change heading. For the purposes of the research, only assessing scenarios that disallowed S_Y variation did grant several benefits. First is that it becomes more readily suitable for the purpose of aiding ATC directly; route control only requires the prediction of the intersection of linear routes. In contrast,

altitude and time controls require understanding and experience of the aircraft's performance limits; considering the difficulty of calculating such with accuracy, the provision of an optimizer that can handle such should be more useful to ATC than one that optimizes via route control. The second is that it provides a clear, non-stochastic, path to testing fuel optimization; primarily because components capable of random output have been removed, but also because it allows focus on altitude and time controls which do have a significant impact on fuel usage.

3.2.2.2 Limits of Variable Altitude and Time

With the DAM in this research now confined to zero S_Y variation in optimization, it would be prudent to consider any means of reducing separation checks that the other intentionally variable dimensions could confer. In the case of DTM, due to aircraft position at a time step being coupled to its performance, the only consistently reliable way to further reduce the number of requisite separation checks inside optimization was to only consider the separation checks for time steps where both aircraft were part of air traffic to be optimized. In contrast DAM has two further apparent means of reducing separation checks; each of the two is based on the limitations that can be experienced by an aircraft in the *t* and *h* domain. In the case of *h*, aircraft or airline preferences on maximum climb and descent angles create regions in airspace where an aircraft cannot be; e.g. the altitudes above an aircraft as it tries to reach maximum altitude or descend to land or exit optimized airspace. Considering that these regions are generally associated to entries and exits, they are as useful as the DTM separation check reduction just mentioned. The *t* domain in DAM, on the other hand, has considerable ability to reduce numbers of separation checks.

Aircraft have a maximum and minimum achievable ground speed; the maximum is defined by the thrust and drag aspects of its performance, whereas the minimum is defined by the aircraft's stall speed. When combined with the aircraft's entry time to optimized airspace, they create a region, as shown in Figure 7, of *t* in which the aircraft could have passed a particular ATD; the size of the region increases as further ATD locations determine the earliest (blue line) and latest (green line) *t* that the aircraft could pass them, including where necessary the Δt_{min} (light blue line) and assuming the aircraft's optimal ATD pass times (red line). These earliest and latest times can then be defined for each A_{NN} to check to see if their point of conflict could ever actually occur assuming aircraft cannot breach maximum or minimum ground speeds. This reduction works well if the difference between minimum and maximum speeds is small, such as in the case of an aircraft with a really high stall speed; the resulting feasible region becomes smaller thereby reducing the region of overlap in which potential conflict could occur. Further reductions are feasible by combining maximum and minimum ground speeds with a predefined landing or exit time; the feasible region then reduces in such a way, as shown in Figure 8, as to ensure that the exit time can always be met. It should be noted that the narrowest feasible time region can only be obtained with trajectories that have to maintain a maximum speed in order to make their exit time; delaying the exit time results in increasing feasible time regions. However having a fixed entry and exit time can cause significant reductions in feasible time regions, which results in smaller overlap between aircraft, and consequently a smaller number of requisite separation checks.

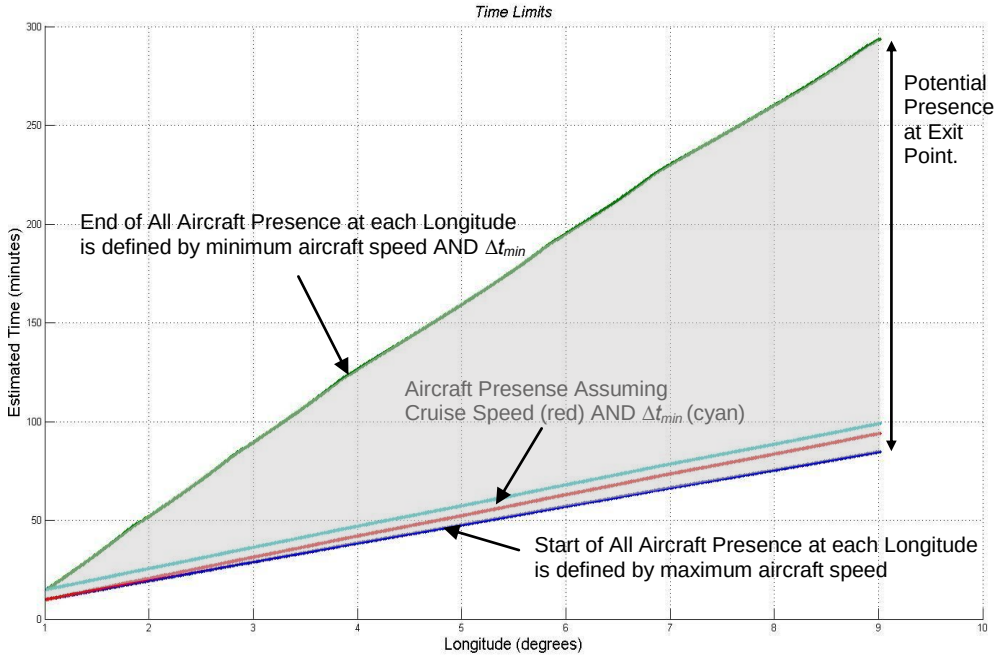

Figure 7 - Feasible Time Regions (shaded area) for an aircraft travelling from (1, 1) to (9, 9) with an unspecified arrival time.

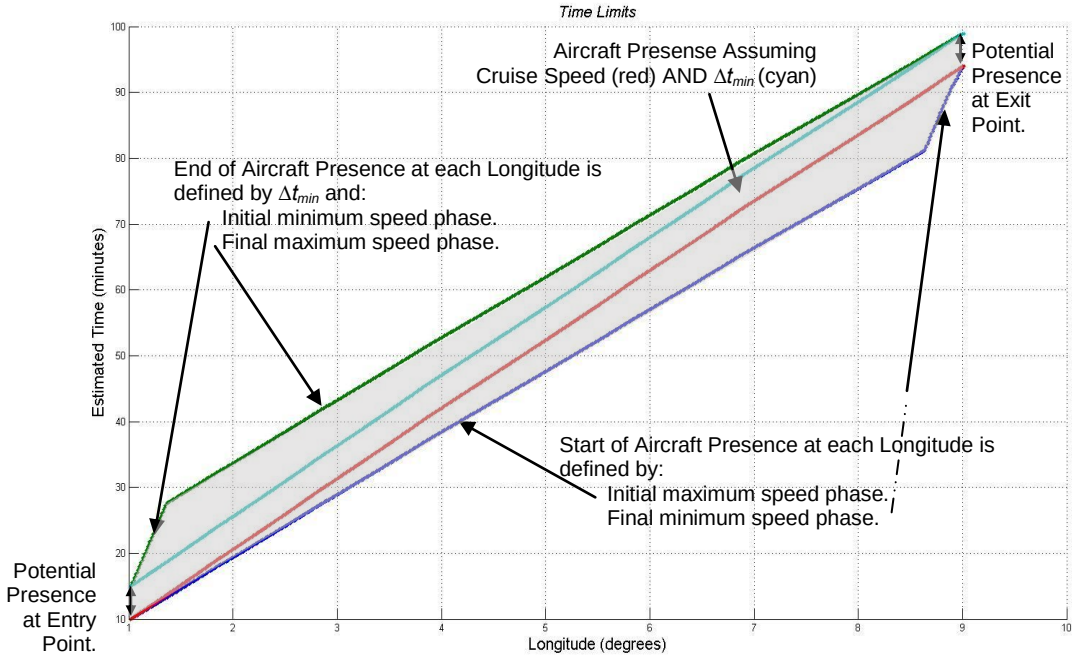

Figure 8 - Feasible Time Regions (shaded area) of Figure 7 but with specified arrival time.

3.3 Prototype Core Optimizer (PCO) Components

As mentioned previously, this version of the optimizer only contains the basic components required for optimization of an area based model of air traffic; i.e. a set of initial air traffic trajectories, a means of ATFU calculation, aircraft performance limits, air traffic separation limits, and a framework for optimizing ATFU assuming those limits. In order to create these components, a staggered approach was taken; each stage development would focus on the aspects of these components that would be needed in the next stage of development. For example, the means of ATFU calculation and aircraft performance limits had to mirror research done in [32] to enable comparison of their results in section 3.4; this provided an objective method with known results that could be used to ensure the effectiveness of the PCO as defined in Chapter 3. This was needed as the objective function is further improved in Chapter 4 using the method in [38] the optimization of which has no comparable results in the literature; removing as much unexpected variation from the PCO as possible was thus important for Chapter 4.Similarly, the PCO was developed without a means to handle subsequent changes to an air traffic scenario; i.e unpredicted and de-optimizing events that occur after trajectories were optimized, but before aircraft had exited optimized airspace. In theory, the optimizer would only need to re-optimize the scenario to re-introduce optimality, however this requires data transfer between re-optimizations. During PCO development, the amount and type of data to be transferred was not known and it was only through testing of the PCO that a complete list of such data was created. Chapter 5 discusses development of functions that solve subsequent scenario changes.

For the purposes of development, the PCO is the interface between the airspace model and navigation data, i.e. NMD, and an optimisation function that gives it decision making capability to minimize ATFU. Given the range of applicable optimization methods that could facilitate PCO, the MatLab® computing environment, and in particular it's Optimization Toolbox which contained most of the applicable optimizers, was used for development. Further, previously attempted optimizations mentioned in 2.2 did not have NMD's cohesive and comprehensive data structure, as mentioned in 3.1, nor the aircraft representation that NMD supports, as mentioned in 3.2. This meant that various functions of the optimizer were unique and had to be specifically developed to suit the components they serve. However, because DTM, DSM and DAM all have commonalities with each other and DTM and DSM were used in previously attempted optimizations, concepts outlined in 2.2 were used as some of the optimizer's components, and were useful in defining any previously non-existant function. The discussions below focus on the six major components of PCO and in each discusses their 1) issues in initial development, 2) discussion of alternatives, 3) issues in optimizer integration, and 4) current form in terms of equations, settings and functional flow; discussions will focus heavily on any novel or unique functions that occur in that component. One final section will bring all equations together and show the optimizer as a whole mathematical function.

It should be noted that potential optimizer components had to be repetitively trialled as a whole, with representative functions and placeholders for more complex fuel optimization issues, to make sure they worked together. Ineffective combinations of components were altered or replaced per trial, till an effective set of components was reached. The process is not optimal, and more effective or efficient combinations of components do exist; some have already been found via the development here and in the literature, and were or were not used for reasons outlined in the following sections. Nonetheless, the holistic development of the

optimizer allowed the current form of PCO, to be the core prototype of NMD based fuel optimization; further development was merely extensions or optimizations of capabilities already present in PCO.

3.3.1 Optimisation Method

Section 2.3 concluded that the process for negotiating conflict separation should be an optimization algorithm, as opposed to a manual, proscribed, or any other means of resolving conflict. This implied a computational solution which would need to be assessed at multiple stages of development to define its fitness for purpose. During initial development, the key issue was in how much of the algorithm could be developed from existing software and in choosing a software package that would be the best environment for the optimizer's development. This would consequently determine the range of readily available optimization methods, and the next key issue would be to determine the optimizer method to be used from the alternatives in this range. Once all of these have been decided, the limits of the method itself would have to be recognized in order to ensure smooth integration with the other components of the optimizer's design.

3.3.1.1 Issues in Initial Development

A prior issue to the selection of an optimizer method was whether or not to rely on methods developed previously or to develop one from scratch. Previously developed optimizers were, thanks to the MatLab®; readily available, had consistent input methods, and comprehensive documentation. However, there was also the possibility that the optimizers would be insufficiently specialized to handle the problem, or were noticeably inefficient in operation. Ultimately, developing a specialized optimizer from scratch would have ignored the already present literature surrounding DTM and DSM and could have extended development times significantly. It is assumed that effort can be put into optimizing the optimization process once the processes of the optimizer have been tested thoroughly.

3.3.1.2 Discussion of Alternative Optimisation Methods

The discussion on an ideal optimization method from four major categories of optimization can be found in section 2.3; it indicated that non linear programming methods were preferred over linear methods, which were preferred over random and integer based methods. Further, as is discussed later in section 3.3.3 and chapter 4, both the separation and objective functions were planned to be non linear, which meant non-linear programming methods had to be comprehensively investigated lest the research resort to random or integer based methods. Two non-linear methods, i.e. SQP and Interior Point, were available in MatLab® and it was its 'Interior Point Algorithm' that became the preferred optimizer method in this research. This was primarily because the quadratic model used by the 'Active-Set Algorithm', which was the MatLab® implementation of SQP, was not as effective or as efficient as the interior point barrier function at guiding optimisation for the PCO. This was shown at three separate points during development of the optimizer and similar occurrences were partially documented in literature [49]. The first realisation of this issue was when the 'Active-Set Algorithm' had difficulty in dealing with the initial value for this problem. The initial value, as defined in section 3.3.2, consists of a set of optimal trajectories that are infeasible due to unapplied separation modes; however 'Active-Set' requires a feasible initial value and so had to rely on other functions to perform the initial optimization to a feasible value. The next occurrence was in handling scenarios fairly simple scenarios; while the separation functions are smooth and simple enough to be modelled using a quadratic model, their number and distribution

as constraints to the objective function made determination of new optimum using the model, irrational. The last occurrence, while not directly related to the quadratic model, did show how similar calculations could not be used efficiently for determining new optimums. During the process of improving the results of the 'Interior Point Algorithm', an option for the algorithm was tested for its effect on the optimisation; the option defined whether or not a new optimum was calculated using a direct Newtonian step. By default, a conjugate gradient would be used, but in some stages, a direct step was definable and was applied instead. The conjugate gradient includes the barrier terms, while the direct Newtonian step is a simpler form of the quadratic model. It was found that forcing Newtonian steps to be never used led to improved computation times and smoother results. There are other possible reasons for this occurrence; however it does suggest that the usage of the barrier terms in new optimum calculation leads to better results.

3.3.1.3 Issues in Optimizer Integration

Given the utility of the MatLab® optimization toolbox, no changes were necessary of its internal calculation methods. Thus any issues with the integration of the other components stem from the component needing to fit the optimization toolbox's simple input and output requirements; hence those issues are found in their respective component discussions. For ease of understanding section 3.3.1.4 defines how various components give data as inputs to the optimizer method in Figure 9, it also shows what settings are used in the current form of the optimizer in Table 2. Given that the PCO is developed during this stage, the 'MaxFunEvals' and 'MaxIter' values, which respectively describe the maximum number of times the objective function could be evaluated as well as the maximum number of optimization steps the optimizer method could use during optimization, were set high so as to allow assessment of the optimizer in situations that had the potential to not be solvable. Due to an inability to estimate these values, purely nominal values were used and set only to be maginudes greater than the preset defaults. It should be noted that the optimizer method does not perform this number of evaluations or iterations unless the program has failed to find an optimum and therefore would only be an indicator of performance if the system was allowed to fail in actual use; however later testing indicated that successful optimizations were likely and thus more holistic assessments of the performance and computational costs of the optimizer can be found for simple scenarios in section 4.3.2, and for high capacity scenarios in section 6.3. The optimizer inputs shown in Figure 9 were consistent among the optimizers available within MatLab®, so testing against various optimizer methods, as was performed in 3.3.1.2, only involved changing the defined method and its settings whilst keeping the size, shape, and data of all inputs the same. For clarity, the constraints shown in Figure 9 all had formats to ensure only constraints of that type could be used in its place.

3.3.1.4 Current Form

Table 2 - Non-Default Optimizer Settings

Option Name	Input Value	Explanation
'Algorithm'	'interior-point'	See section 3.3.1.2.
'MaxFunEvals'	30000000	Maximum Function Evaluations and Iterations. Nominal numbers were used.
'MaxIter'	300000	
'TypicalX'	Speed Variables = 10 nmi/min Altitude Variables = .5 (10000's)ft	Indication of magnitude of expected values. Used to scale gradients.
'Subproblem	'cg'	'cg' requests that only Conjugate Gradients are used

Algorithm'		in optimization. Please refer to section 3.3.1.2.

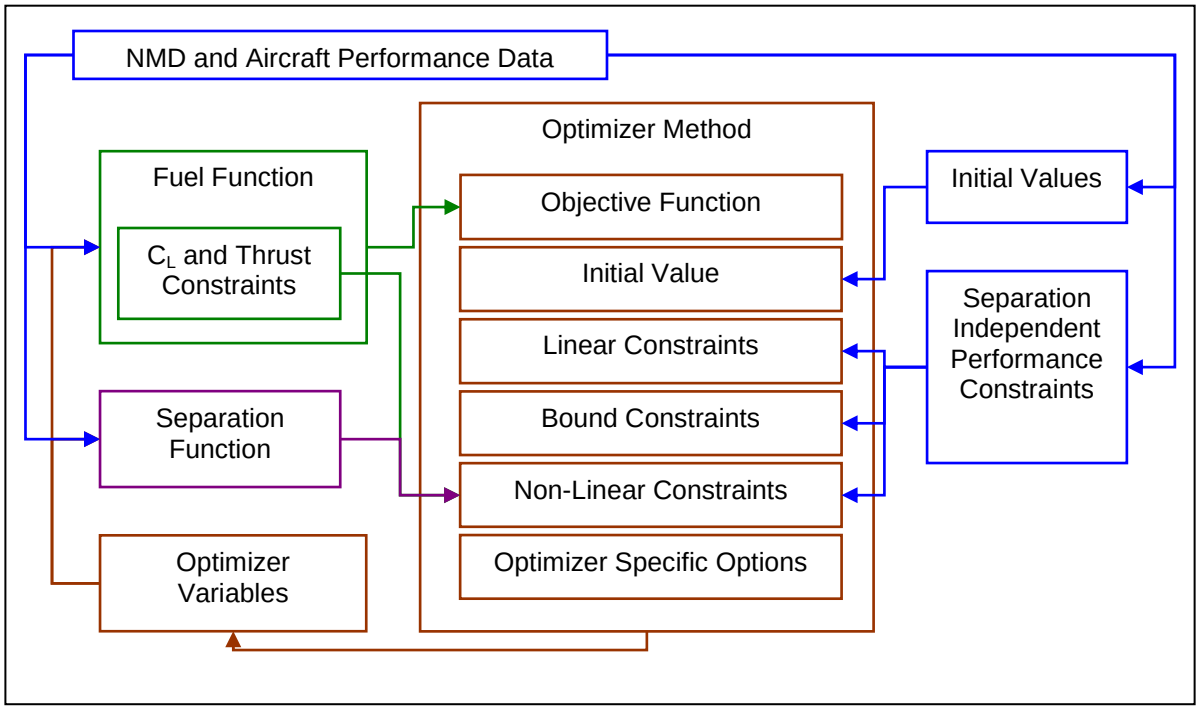

Figure 9 - Functional Data Flow between Optimizer Method and Optimizer Components

3.3.2 Optimizer Variables

The optimizer variables are the free variables that the optimiser can vary within certain limits. They are passed on to the air traffic simulation to calculate total fuel usage and to determine if any aircraft performance or separation constraints have been violated. The issue with choosing optimizer variables is that the optimizer has almost complete freedom in varying the variables to generate an optimal result. As the following sub sections show, granting complete freedom in certain dimensions may not be conducive to reaching an optimal set of trajectories.

3.3.2.1 Issues in Initial Development

The issue encountered during initial development, prior to the rationalizations in sections 3.1 and 3.2, was in deciding what parameters describing a set of air traffic should be controlled to minimize fuel usage. While the control of trajectory parameters was the logical choice, previous optimization attempts mentioned in section 2.2 did indicate that the control of aircraft interaction modes, i.e. modes of cooperative behaviour between two potentially conflicting aircraft, could also be used to minimize fuel usage. However the use of aircraft interaction modes as an optimizer variable was not pursued as it required an assumed trajectory between points of potential conflict; this was considered undesirable as there was potential for irregular trajectory shapes between points of conflict to cater for more fuel efficient conflict avoidance. As the direct control of trajectory parameters was the only means of allowing these irregular trajectory shapes to form, it was chosen as the outline for optimizer variable development. Further, as per section 3.2.2.1, even though heading change via CTD variation was

feasible and could be performed using the model developed for this optimizer, it was not due to concerns of available computing power for testing purposes.

3.3.2.2 Discussion of Alternative Optimizer Variables

Optimizer variables have three aspects that can impact the efficacy of any optimization process; its dimensions with respect to the optimization problem, its feasible regions in those dimensions, and its initial value in those dimensions. As the second and third are subset to the first, the alternatives to the optimizer variable's dimensions are discussed first. As aircraft performance properties and limits are often defined by the trajectory parameters of altitude and true air speed, or TAS, it was logical for aircrew and aircraft engineers to have the optimizer variable be in terms of the speeds and altitudes experienced by the aircraft over route segments, and this was adhered to throughout thesis. However from an ATS perspective, conflict avoidance and separation assurance is defined by the altitudes and times that aircraft experience as they pass a potential conflict point and this consequently posed an alternative that had to be investigated; i.e. altitudes and times of aircraft as they pass all potential conflict locations. As the difference between altitude and TAS, and altitude and time, as optimizer variables is minor, it was in the frequency of either that made the biggest difference. As mentioned in section 3.2.1 use of altitude and time as variables was abandoned due to the large number of variables it required; a large number of conflict locations could occur in a single nautical mile, and it was deemed grossly inefficient to have a pair of optimizer variables, i.e. altitude and time, along the straight route to represent each of these. Consequently speeds and altitudes over a series of reasonably and equally sized route segments, the discussions of which is in section 3.3.2.3, were selected as the optimizer variable.

With the dimensions of the optimizer variable defined, the bounds and initial values of the optimizer variable can now be discussed. The main purpose of the optimizer variable bounds was to put a hard limit on where, in the optimizer variable dimensions, the optimizer could search for an optimum. While the limit to each of the optimizer variable's dimensions do seem obvious, each did have an alternative and the initial selection of bounds was determined by their availability of information rather than any merit of fitness. In the case of the speed dimensions, the limits were determined by their associated aircraft's minimum and maximum capable TAS. However because it was recognized that the maximum and minimum could change throughout a flight due to aircraft mechanics as well as airline and pilot preferences, a unique pair of speed bounds was made for every speed variable. Further however, because exact information on the variation of the maximum and minimum speeds is limited, each of these unique pairs is still only set to the aircraft's minimum and maximum capable TAS. In the case of the altitude dimensions, limits were defined by the aircraft's predefined minimum and maximum cruising altitudes; thought was given to including altitudes outside of this range that the aircraft could fly at, if only temporarily, but the flight mechanics in such situations were deemed to be too different to cruise flight for them to be realistically incorporated in the optimization process. As with the speed dimensions, it was recognized that the minimum and maximum cruising altitude could also change throughout a flight, these being due to regional weather variation and region specific airspace regulations. Similarly, a unique pair of altitude bounds is made for every altitude variable, and again due to a lack of information, almost all of these were all made to equal the aircraft's predefined minimum and maximum cruising altitudes; the only time a different altitude limit was used was at points where the aircraft was known to leave or enter cruise, i.e. just after takeoff or just before landing, in which case an equivalency constraint (i.e. where the minimum and maximum bound are the same) was used to ensure the aircraft entered or left optimized airspace at the minimum cruising altitude for

the sake of realism. One last point to make about these bounds is that they are all specific to a particular situation and will change if the aircraft and airspace involved, or the information regarding them, are changed for any reason.

The initial optimizer variable values, i.e. the first set of optimizer variables to undergo optimization, required certain properties to make them sufficiently realistic; since the optimizer was intended to optimize an actual scenario, it was important that the initial optimizable value be representative of a pre-existing trajectory so as to understand the optimizer's ability to handle such. There was also a desire to minimize optimization times and since it was recognized that trajectories were often optimized for the trip, if not the exact traffic involved, it was assumed that pre-planned trajectories would require less optimization to reach the most fuel efficient set of air traffic. However as such well-defined flight plans are not readily available, a composite flight plan had to be made from publicly available information; given that this consisted of only singular values for aircraft preferred cruising altitudes and speeds, the majority of the initial optimizer variable's altitude and expected speed pairs had been set to match and were thus largely uniform for the trajectory. The only time where this was not the case was wherever an equivalency constraint was expected on an altitude value, in which case a mild climb or descent angle of 3° was used to bridge the preferred altitude to the or from the equivalency. As the 3° was well within reasonable climb and descent values, it was expected that the optimizer would have no difficulty in altering the climb's, or descent's, associated altitude values to reach a more optimum climb or descent rate.

3.3.2.3 Issues in Optimizer Integration

There are two notable issues that were specifically due to the optimizer variable and its definition. One refers to the fact that the use of a series of reasonably and equally sized route segments, here defined as ATD_N, with a conflict check system that is based on a closely space and randomly sized list of route points, i.e. ATD_A, requires a data transfer mechanism to be developed between the two. Due to the separation associated issues involved, this is discussed and developed in 3.3.3.3. The other notable issue is in the size of the segments defined in ATD_N, or more accurately, the distance between elements of ATD_N. This is of particular importance as this value is tied the aircrew or airline's preferences. Smaller values would enable more optimal solutions, but may require the aircraft to fly frequent trajectory changes. Conversely, larger values would decrease the frequency of trajectory changes, but may require less optimal trajectories. Consequently this value must be treated as an input variable, and consideration given to how its potential range could affect anything else. The issue found stems from the need to have the trajectory solely defined in the pre-defined airspace. If a trajectory is divided into route segments with length exactly equal to its preference, then one of two situations occur. The first has segments where all segments, bar one, are equally sized, with the exception carrying the remainder; this causes an undesirable and uneven weighting on route segments which increases as the preferred step size increases. The second has all segments equally sized, but with a segment having a portion outside of pre-defined airspace; inferences that require environmental data would be incomplete, and any trajectory changes made assuming so would therefore be dangerous or non-optimal.

To deal with this issue, the trajectory has to be divided into segments sizes that are all equally sized but still close to the trajectory's preferred value. To do this the total number of control nodes used in a trajectory, n_{max}, is defined using the total route distance, S_{FLIGHT}, and the user preferred step size, $\Delta ATD_{N\ IDEAL}$, as:

$$n_{\max} = ceil\left(\frac{S_{FLIGHT}}{\Delta ATD_{N\ IDEAL}}\right) \quad \textbf{(1)}$$

This is then used in equation (3) to generate an ATD_N composed of steps that have a size, ΔATD_N , that is constant yet close to the users preferred segment size, i.e.:

$$\Delta ATD_N = \frac{S_{FLIGHT}}{n_{\max}} \quad \textbf{(2)}$$

3.3.2.4 Initial Formulation

In its last form, the PCO optimizer variable was based on an individual trajectory being defined via *n* number of control nodes, with their total defined by n_{max} and the ATD spacing between them set to ΔATD_N. These nodes were equally spaced out, but for efficient retrieval of environmental data, they were made to align with elements in the ATD_A for that trajectory, as per Figure 5. This was done by comparing the nodes of ATD_N with the elements of ATD_A, and altering the nodes of ATD_N to match the position of their nearest element in ATD_A. While this may appear to be against the desire for equally spaced route segments mentioned in 3.3.2.3, the variation brought by aligning to ATD_A is sufficiently small as to be negligible. The ATD_N for an individual aircraft trajectory, ATD_n, can therefore be described as:

$$ATD_n \approx \begin{bmatrix} 0 \\ \vdots \\ n \\ \vdots \\ n_{\max} \end{bmatrix} \times \frac{Total\ \ Flight\ \ Dist}{n_{\max}} \quad \textbf{(3)}$$

Assuming each individual aircraft can be defined as an element of *N*, with N_{max} representing the total number of aircraft to be controlled, the collective list of ATD control nodes can be defined, given MatLab© input requirements, as the vertical concatenation of the ATD_n of all aircraft:

$$ATD_N = \begin{bmatrix} ATD_{n1} \\ \vdots \\ ATD_{nN} \\ \vdots \\ ATD_{nN\max} \end{bmatrix} \quad \textbf{(4)}$$

Given that both *Alt* and *TAS* has to be optimized for each ATD_N, the optimizer variable, X, must therefore contain both. Due to MatLab© input requirements, X is the vertical concatenation of these two:

$$X = \begin{bmatrix} Alt(ATD_N)\ \ ft/100000 \\ TAS(ATD_N)\ \ nmi.\min^{-1}/10 \end{bmatrix} \quad \textbf{(5)}$$

Note the existence of the scaling factors for the two sets of variables. These were introduced to 'centre and scale' the optimization problem; this assists in ensuring that variation in the variables is comparable. Without it, there is sufficient difference in the magnitude of the two sets of values that determination of new optimums can become

inappropriate. Consequently, and given the discussion in 3.3.2, the resulting constraints have the same shape as the optimizer variable and are:

$$X_{MAX} = \begin{bmatrix} Alt_{MAX}(ATD_N) & ft/100000 \\ TAS_{MAX}(ATD_N) & nmi.\min^{-1}/10 \end{bmatrix} \quad \textbf{(6)}$$

And:

$$X_{MIN} = \begin{bmatrix} Alt_{MIN}(ATD_N) & ft/100000 \\ TAS_{MIN}(ATD_N) & nmi.\min^{-1}/10 \end{bmatrix} \quad \textbf{(7)}$$

For ease of understanding, a representation of the process as outlined in 3.3.2 is presented in Figure 10.

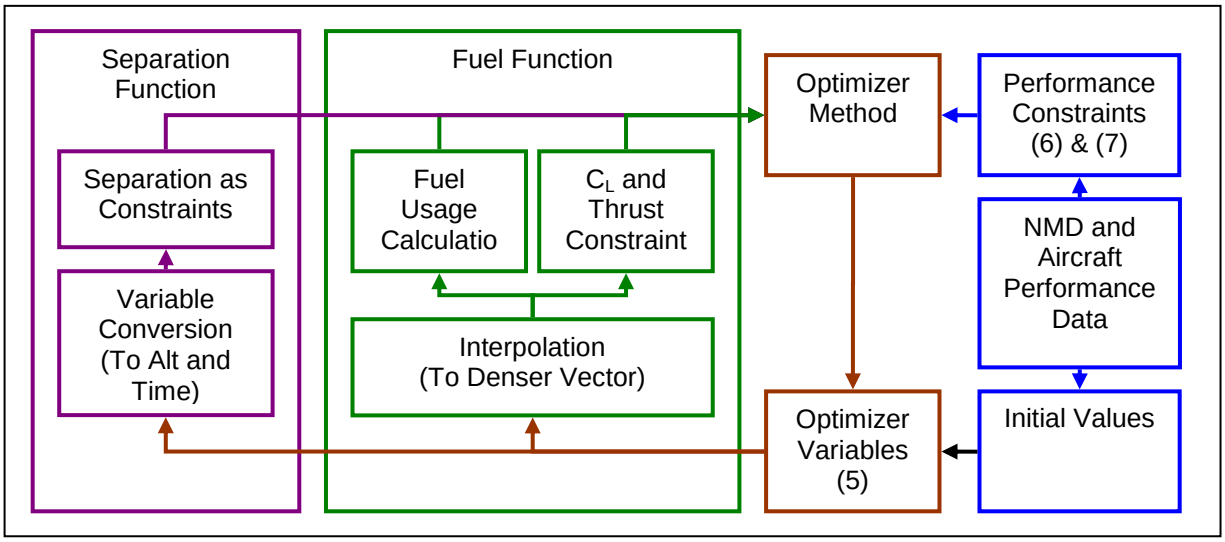

Figure 10 - Functional Data Flow for Optimizer Variables

3.3.3 Separation Function

Requisite separation between aircraft is the raison d'être for ATC; a sufficient representative of it must be present in the PCO. Given statements in section 2.2.1, this representative must be a constraint and not an objective; the policies in [25] only define minimum separation requirements with no further benefit gained from improving on such separation. Further, the conceptual DAM separation using NMD mentioned in 3.1 was sufficiently developed so as to only worry about fitting issues with the optimizer method; all minimum separation values mentioned in 3.1 were used consistently throughout all optimizer development efforts. However, by far the biggest issue to using these separation modes, which were incorporated into NMD separation, was their conversion into mathematic functions that could be used by the optimizer as constraints.

3.3.3.1 Issues in Initial Development

The primary issue in using a state based form of separation, as allowed by DTM, DSM, and now DAM is that it is possible for separation to be insufficiently defined between states; i.e. between discrete time steps in DTM, between route segment start points in DSM, and between discrete NMD locations in DAM. There are two ways of handling this; the use of successive points to define separation between states, or the use of buffers and limiters to prevent separation violations from occurring in between states.

The former was of particular interest as it would allow consideration of an array of correlated separation points rather than just each individual point by itself. The baseline for the array was created by defining the ATD region for both aircraft in which conflict could occur; these would be the diagonals of the 'area of conflict' shown in Figure 6e). The aircrafts' variation in altitude and time with respect to ATD in this region would then be normalized against the ATD travelled in the region, then combined together to allow definition of overlapping dimensions, i.e. conflict. This is combination is possible since the NMD information does distinctly tell where and when conflict starts and ends. However results from trials using this method showed that combining data this way hid pertinent information from the optimizer; a singular value representing the group of separations had to primarily define the separation mode closest to being breached, which meant that changes elsewhere in the ATD like dimension could not be seen by the optimizer.

The separation function had to use state based methods in combination with limitations on trajectories between NMD locations to prevent separation violation there. As S_Y variation was excluded from consideration, variation across ATD is constant in the S_Y dimension and separation violation could only vary across ATD; thus only linear constraints between successive ATD were required to prevent separation violation. That said, as minimum altitudinal separation when compared to the allowable range of altitudes, is significantly smaller than the minimum longitudinal time separation when compared to the allowable range of intersection arrival times given aircraft speeds, the actual constraints can be treated differently between dimensions. Figure 11 shows a graphic analogy of how variations in the optimizer variables could cause violations between determinations of separation at each of the NMD locations. Figure 11a) shows how the greater freedoms of the Altitude variable can lead to unknown separation violation, while Figure 11b) shows how the lesser freedoms of the Time variable (which is constrained through and as TAS) almost ensure all violations in that dimension are picked up.

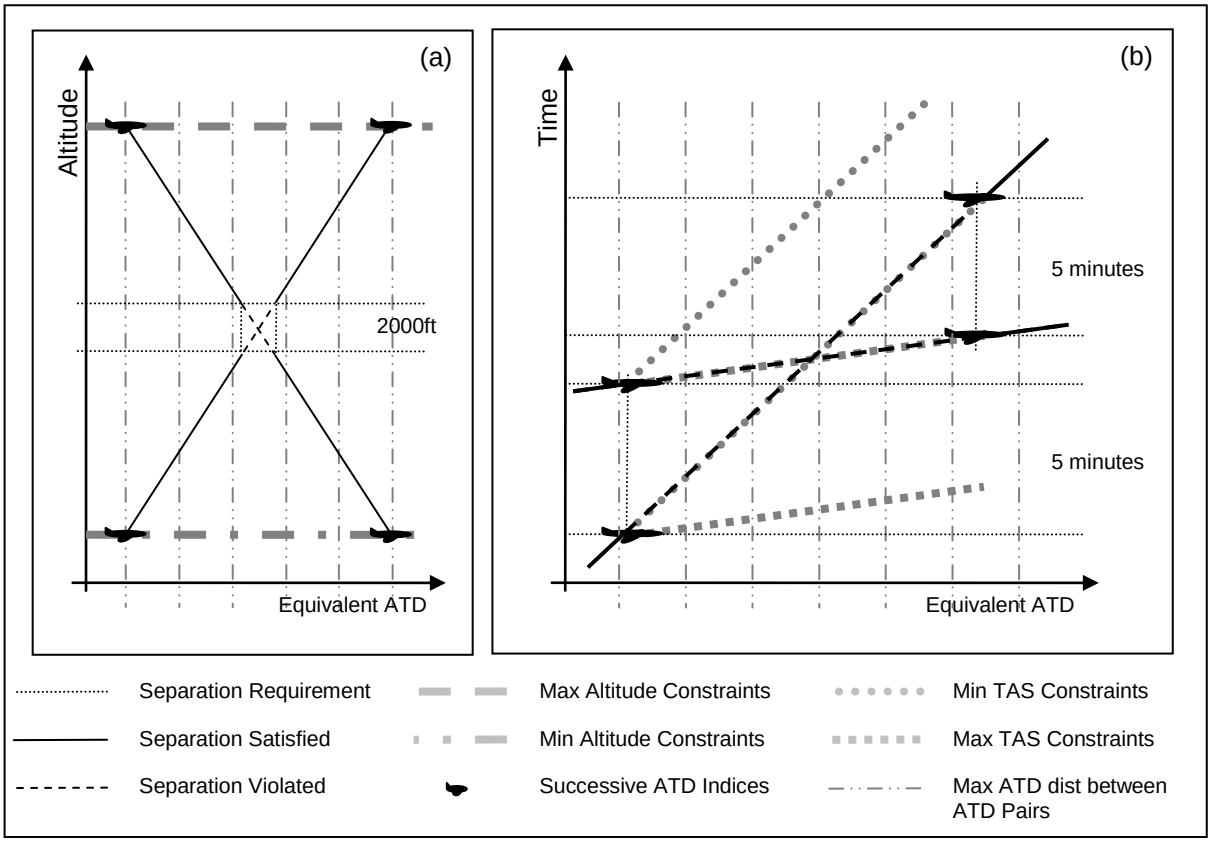

Figure 11 - Examples of Separation Mode Violation in terms of a) Altitude and b) Time assuming State Based Separation

For these reasons a blanket linear climb angle constraint of ±18.2°, or a maximum variation of 2000ft, i.e. Δh_{min} as required by [25], per nautical mile, was applied to ensure that aircraft could not violate Δh_{min} between conflict checks. A similar blanket constraint for Time or TAS was developed but after determining how Figure 11b) was constantly true for the constraints and dimensions given, there was no apparent need for it and it was consequently removed. It should be noted that the decision to not apply a similar blanket constraint on TAS is only to ease computational issues; should the dimensions of the area discretization change, its application would have to be reassessed. It should be mentioned that an alternative to these linear constraints is the use of smaller discrete areas; this was avoided as NMD presented a sufficiently decent definition of separations already.

3.3.3.2 Discussion of Alternative Separation Functions

The section covers the mathematical algorithms that were considered for the purpose of modelling separation. The core issue here came from the multi-dimensional nature of satisfying separation. For a collision to occur the separation minima, Δt_{min}, Δh_{min}, and $\Delta S_{y\,min}$, must be simultaneously breached for at least one element of A_{NN}. An example of the concurrent breach of the separation minima can be seen in Figure 12; as 3.2.2.1 caused A_{NN} to currently only contain elements where $\Delta S_{y\,min}$ is already breached, collision only requires that Δt_{min} and Δh_{min} be breached in the h - t domain of any of the known A_{NN}, which is shown in Figure 12. However, referring to the same figure, if AC 2 had flown 1kft higher, then while Δt_{min} would still be breached, AC 1 and AC 2 would not be in conflict. Thus, even though Δt_{min}, Δh_{min}, and $\Delta S_{y\,min}$ are linear constraints and could be used as such directly, the appropriate satisfaction of separation requires that they be combined in a nonlinear manner to allow acceptable breach of the separation minima, i.e. when one is already satisfied.

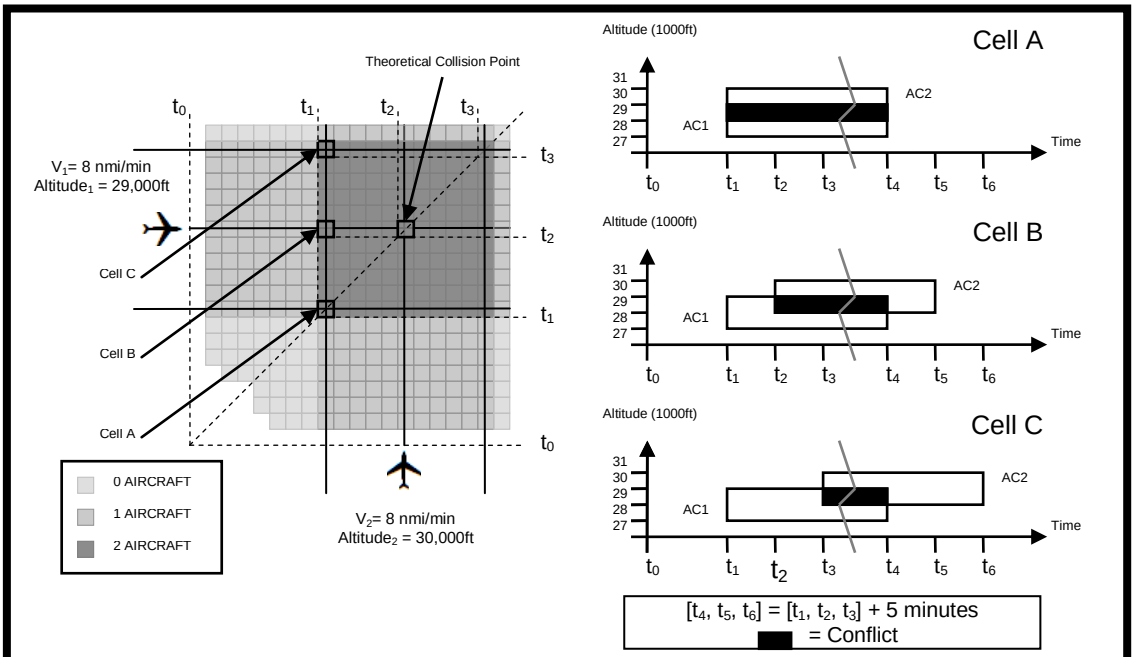

Figure 12 - Conflict Modelling and Detection at NMD locations (Simplified S_Y Requirement of Presence instead of Distance).

Four variants were developed; three of which were considered prior to PCO inclusion, and one that was developed afterwards. This later one is discussed in 3.3.3.3 as its creation was a direct result of integration issues rather than just the PCO concept. The three developed concurrently consisted of a binary linear variant, a four integer separation variant, and a four linear plane separation variant. As these were developed during a period

when optimizer method had yet to be set, each provided a different output that correlates to a particular type of optimizer method. While the methods are different, each is dedicated to modelling aircraft separation as per 3.1.

The binary linear variant required the two dimensional discretisation of the *h* - *t* graphs shown in Figure 12 ; the discrete points on the graph could then define if two aircraft were simultaneously present at a discrete altitude and time, thereby giving a value of one for such points and zero for anything else. Consequently this becomes a binary constraint and can only be performed using an integer or combinatorial optimization method. The primary reason for not using this variant is that it necessitates discretisation of the *h* - *t* domain; the positions of aircraft within would align themselves with the discrete times and altitudes of *h* - *t* domain. This could be acceptable if the step sizes were small enough, however the fact a discretised domain would have to be created for each NMD Aircraft ATD pair gives concern for how an optimizer would attempt aligning aircraft positions with different steps in different fields. If the fields were sufficiently harmonized in such a way as to ensure a patterned alignment between aircraft for each field then perhaps the method could work; however such a method is not known so the optimizer can encounter objective and constraint combinations that infinitely repeat trials that try to align with different steps in different fields. For that reason this variant was not used.

The four integer separation variant was inspired by Vela et al. [35] and developed with the understanding that Δt_{min} and Δh_{min} could be re-interpreted as four alternate separation modes, again with only one mode needing to be satisfied for all A_{NN}. This re-interpretation saw that a pair of aircraft only had to be separated by having one aircraft be earlier than, later than, above, or below, the other. These would be ordered according to appropriate transitions between them; if zero represents above, then, one represents earlier than, two represents below, and three represents later than. Variation between these modes would thus represent aircraft considering placement via 'circling' another aircraft in the *h* - *t* domain for each A_{NN}. However, because only one of the integers had to be true and that values between integers did not distinctly mean a combination of them, it meant that the variant also required an integer or combinatorial optimization method. Further, it would have to be complemented with another constraint that ensures that the aircraft are sufficiently separated in the relative position that was chosen for them at that point. Despite all this, the method is feasible, and if an integer or combinatorial optimization method were used a variant of this method would have been used with it. The concept of aircraft 'circling' each other was valid and if it could be developed in such a way as not to require integers that it would be useful in non-linear programming.

The four linear plane separation variant was developed to combine the four integer separation variant with the linear and smooth aspects required by non-linear programming; i.e. so that 'circling' provides non-integer results. Consider that the checks for Δt_{min} and Δh_{min}, as listed in Figure 2, share the same form:

$$\left| [t,h]_1 - [t,h]_2 \right|_{A_{NN}} \geq \Delta[t,h]_{\min} \qquad \textbf{(8)}$$

If applied individually for the four previously mentioned separation modes, each would remain linear provided the other three are not considered. In the Constraint-Altitude-Time domain, an example of which can be found in Figure 13, the left hand side of equation (8) would be a slanted plane; decreasing linearly in either *t* or *h* as separation between the two aircraft decreases in that dimension. As the separation minima on the right hand side are constant, it would be a flat plane represented by a constant constraint value throughout the Constraint-Altitude-Time domain. It becomes possible to combine the four planes if their version of equation (8) scaled in

such a way that indication of sufficient separation is consistent and that their simultaneous intersection defines only a single location. The constraint input for the optimization method requires that constraints give a scalar value which would indicate the constraint is satisfied if the returned value is less than or equal to zero; which makes an acceptable consistent separation value. As per the 'centre and scale' issue, their combined intersection is set to be equal to one at origin. Adhering to these changes turns (8) to:

$$1 - \frac{\left| [t,h]_1 - [t,h]_2 \right|_{A_{NN}}}{\Delta[t,h]_{\min}} \leq 0 \qquad \textbf{(9)}$$

This is merely a scaled and inverted version of (8); to combine them the four were calculated and the minimum value between the four was found and returned as a result. As a separation function it defined the separation modes exactly and did so in a quasi linear manner. However it did have certain failings that lead to its eventual removal and creation of the fourth variant.

3.3.3.3 Issues in Optimizer Integration

The issues with the four linear plane separation variant were fully understood during trials and development of the Fuel Function as in 3.3.4. Given a scenario of two aircraft crossing each other at the same altitude with one slightly faster than the other, the separation function was expected to ensure that one or both of the aircraft would change altitude; the necessary change in speed to ensure separation in time costing more fuel in comparison. Instead the optimizer proceeded with a speed change and incurred the extra fuel. The reason for this was that optimizer modelling of the four linear plane separation function only gave indication of the plane that the current values of the optimizer variable where on. This meant projections for new optimum values only followed the incline of the plane that was being used to define the constraint. To fix this the four planes that made the third variant had to include a slight difference in indicative gradient that would suggest that other regions for sufficient separation existed. To define how this could be done, the common DTM separation was considered; i.e. heading change was controlled via avoidance of a separation region defined by a cylinder of constant radius and predefined height. This cylinder allowed understanding of alternative routes because gradients on each point on the surface of the circular side of the cylinder suggested that the surface curved in other dimensions and that those alternative points did exist. Unfortunately, the DAM separation modes form a rectangular region and a normal circular or elliptical form could not be directly applied; however a super ellipse could work. A super ellipse is an ellipse, for which the dimensions are raised to powers not equal to two; the more they are raised above two, the more the edges of the super ellipse become closer to defining a rectangle defined by the major and minor axes of the ellipse. Converting equation (8) to fit a super ellipse creates equation (10):

$$\left(\left(\frac{t_1 - t_2}{\Delta t_{\min}} \right)^{10} + \left(\frac{h_1 - h_2}{\Delta h_{\min}} \right)^{10} \right)_{A_{NN}} \geq 1 \qquad \textbf{(10)}$$

Altering (10) in the same way (9) was created gives equation (11) and a comparison of output for the two given variation in difference in altitude and time is given in

Figure **13**. There is a circular area in the corners of the super ellipse which can be minimized by raising the powers even more; however this has to be balanced against the ability of the super ellipse to give information regarding alternative separation modes.

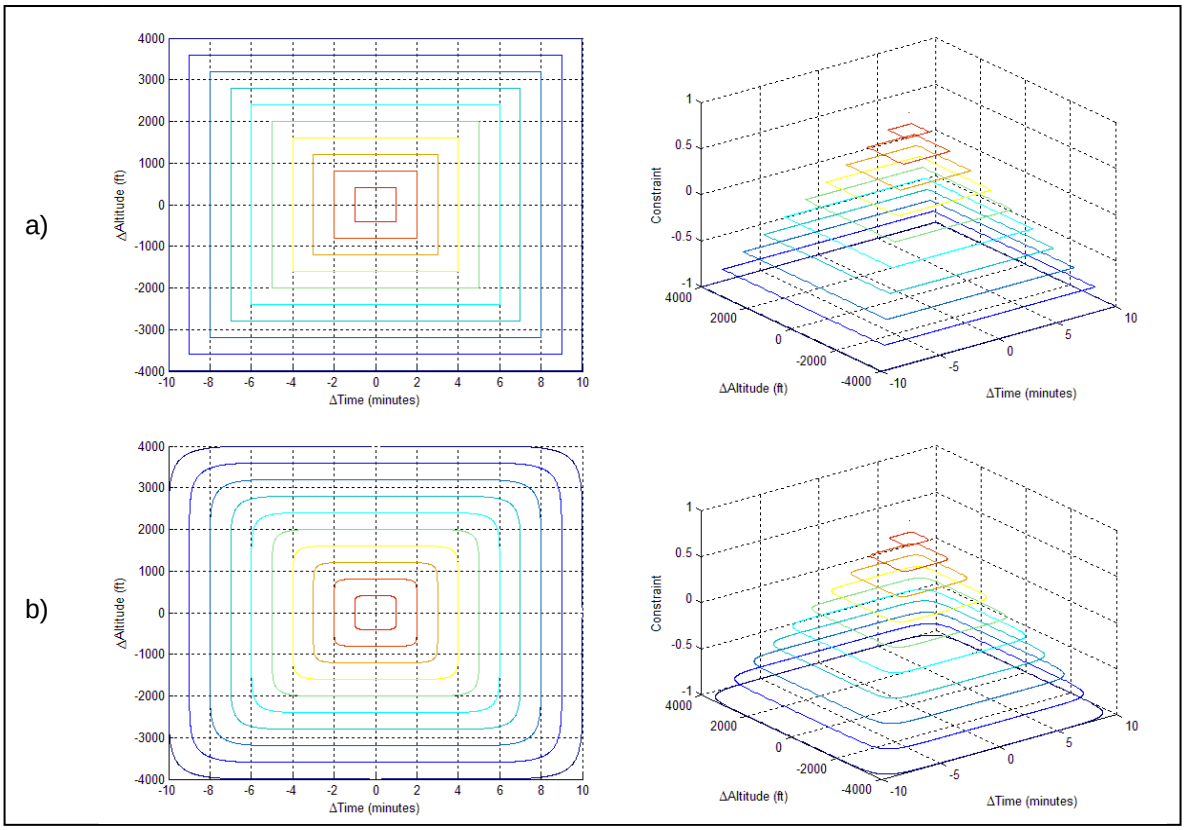

Figure 13 - Contour Plots of the output of a) the Four Linear Planes Separation Function and b) the Super Ellipse based Separation Function, as constraints. Separation is satisfied when constraint <= 0, or outside the olive green contour.

One last thing to mention is the impact of issues discussed in 3.2.1 for the development of ATD_A, and in 3.3.2.3 for the development of X. In these, a discrepancy was created in how data was transferred from X to the separation checks required for A_{NN}. X had initially been developed to suit separation checks and was in terms of h and t, and used ATD_A as a baseline. X now was in terms of h and TAS, and used ATD_N as a baseline, which meant transforms on X were required to perform separation checks accurately. However because variation in h and TAS along ATD_N was linear, the transform to h and t along ATD_A was reduced to a sampling problem with little to no additional computational effort required. Further, because separation only required checking on A_{NN} which is based on a small subset of A, the transform to ATD_A was skipped and instead transformed into ATD_{NN}, which is the respective ATD position of only the indices defined by A_{NN}. The transform to ATD_i is exactly the same, though the rationale behind the difference between it and ATD_N is mentioned in 3.3.5.

3.3.3.4 Initial Formulation

The super ellipse formulae in equation (11) rewritten as a constraint gives:

$$1-\left(\left(\frac{t_1-t_2}{\Delta t_{\min}}\right)^{10}+\left(\frac{h_1-h_2}{\Delta h_{\min}}\right)^{10}\right)^{\frac{1}{10}}_{A_{NN}} \leq 0 \qquad \textbf{(11)}$$

Which is calculated for each A_{NN}. Note that the 1/10 power was used to 'centre and scale' output.

For ease of understanding, a representation of the process as outlined in 3.3.3 above is present in Figure 14.

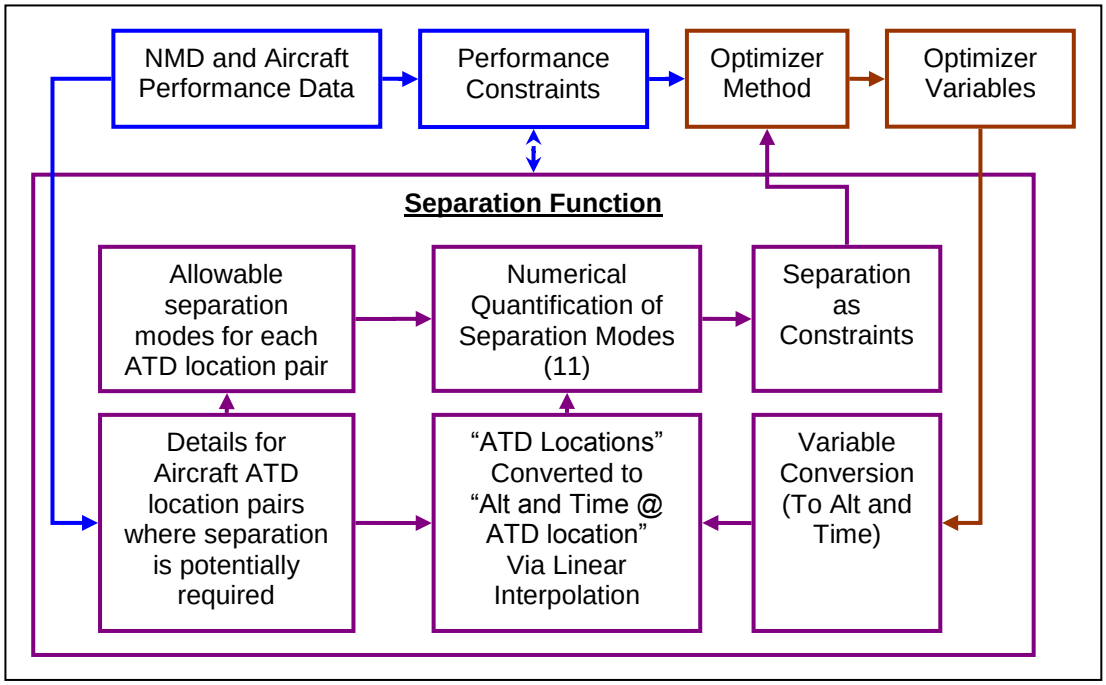

Figure 14 - Functional Data Flow between Separation Function and Optimizer Components

3.3.4 Fuel Function, as an Objective Function

The fuel function serves two purposes; the first is as an objective function that defines the common and comparable measure of fuel consumption among optimizable air traffic, and the second is as a constraint function that defines nonlinear aircraft performance limits. The reason for this dual purpose is because the process of calculating fuel usage and of calculating the state of aircraft performance limits are based on the same data and use the same equations, the initial formulation of which can be seen in section 3.3.4.4. Thus, for the sake of simplicity and to ensure the two are correctly synchronized during development, a singular function is used to perform both. However for the purposes of discussion of the optimization process, the fuel function as an objective function is discussed here, with the fuel function as a constraint function discussed in section 3.3.5.

3.3.4.1 Issues in Initial Development

Total fuel usage was selected as the objective function to minimize total fuel cost and emissions, as discussed in section 1.1. Other factors could be included in the objective function, provided they can be translated into a cost factor. For example, significant cost is incurred if an aircraft is delayed causing major disruptions and inconvenience to passengers. In this study, on-time arrival was incorporated by treating it as a constraint.

However, it should typically be included in the objective function as a cost item allowing the optimizer to make the trade-off between the cost of flying at high speed and delayed arrival. Other cost factors are crew cost, navigation costs and other direct operating costs that can be included in the objective function.

3.3.4.2 Discussion of Alternatives Objective Fuel Functions

Given the variety of acceptable assumptions on fuel usage, a sample of which is seen in section 2.2.2, it is likely that many different methods for calculating fuel consumption exist, with most not being in the public domain and available for research and development. The foremost of methods that are in the public domain and available for research and development is BADA [33] which was used in [35], however close examination of its methods [38], reveal that it is similar to the standard flight mechanics used for fuel usage calculation in [20] and [21]. Further, the research in [32] also uses equations directly derived from these standard flight mechanics. Thus in order to gain sufficient understanding of the optimization problem without venturing into the complexities that make BADA more accurate, the standard method of fuel usage calculation shown in [20] and [21] was used at this stage of the optimizer's development. The actual equations used to define fuel usage are defined in 3.3.4.4 for clarity.

3.3.4.3 Issues in Optimizer Integration

As an objective function, the fuel function is linked to the optimizer via the optimizer variable; i.e. the optimizer creates or updates the optimizer variable, sends it to the objective function to be evaluated, which in turn sends its result to the optimizer so that the optimizer can determine the values of the next iteration of the optimizer variable. As passing a result to the optimizer only requires transferring a singular data value, the source of any integration issues stems from the fuel function receiving and interpreting the optimizer variable. As the optimizer variable already consists of altitude and speed values, the fuel function only requires that standard unit conversions be applied to the optimizer variable so that it can evaluate ATFU. However due to issues experienced with the fuel function as a constraint function, as described and discussed in section 3.3.5, a different ATD index had to be used to calculate ATFU, hence the intervening interpolation shown in Figure 15 between the optimizer variables and the other components of the fuel function.

3.3.4.4 Initial Formulation

Figure 15 is a flow chart of data going between the Fuel Function, its own functions and the optimizer method.

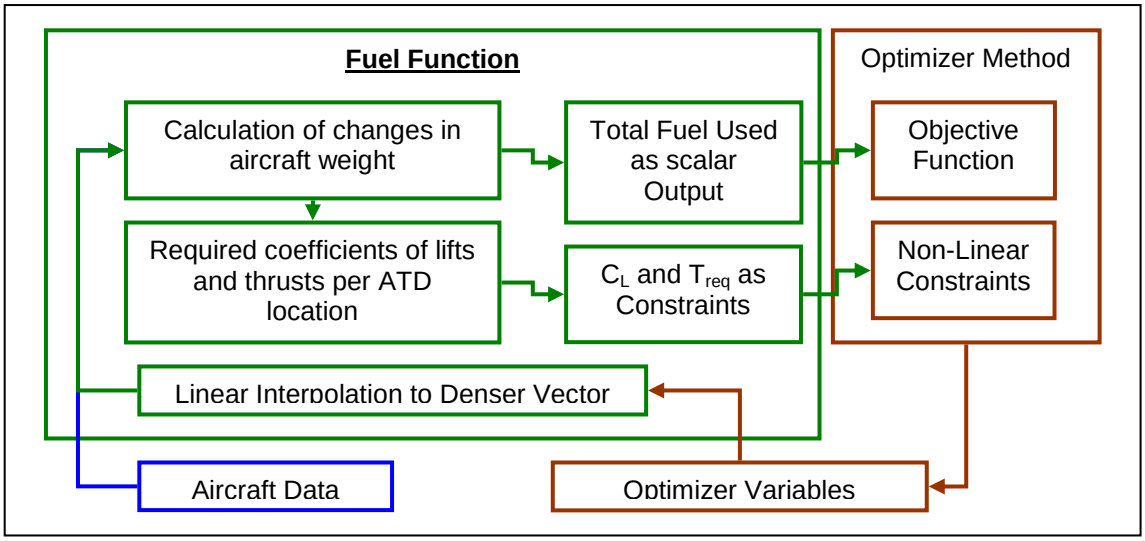

Figure 15 - Functional Data Flow between Fuel Function and Optimizer Components

The equations for fuel usage calculation are defined below in equations (12) to (17). Those equations can generate the necessary terms to define fuel usage if given a table of data containing: the combined ATD index of all aircraft, the Optimizer Variable in terms of the same index, and the conversion methods to turn TAS into time and altitude into density. It should be noted that the environmental data necessary to perform the conversions were present in the NMD data store and linearly interpolated if the location did not exist as an NMD index.

Assuming an ATD baseline, ATD_i, that is similar to ATD_N but with increment $i \in Z\{1,\ldots,i_{max}\}$ that is denser due to model accuracy issues, trajectory based values of Altitude (h_i), TAS (V_{TASi}), time (t_i), and density (ρ_i), can be combined with the aircraft based constants of initial aircraft weight (W_1, derived from an initial percentage fuel capacity, $\%FC_1$, Maximum Take Off Weight, $MTOW$, and Total Fuel Capacity, FC_T), fuel consumption rate (μ), skin drag (C_{D0}), aircraft wing area (S), aspect ratio (AR), and wing lift efficiency (e), to calculate aircraft performance properties of Climb Angle(γ_i), Coefficient of lift (C_{Li}), Coefficient of drag (C_{D_i}), Thrust required ($T_{req\,i}$), and Weight (W_i). For simplicity a constant C_{D0} was assumed even though it does become variable at high Mach numbers. A free body diagram of aerodynamic forces as applied between successive ATD_i is shown in Figure 16. The values used for aircraft based constants in PCO testing, as gathered and appropriately converted from [50], [51], [52], and [53], are shown in Table 3 and the equations used to calculate the resulting performance properties are shown in equations (12) through (17).

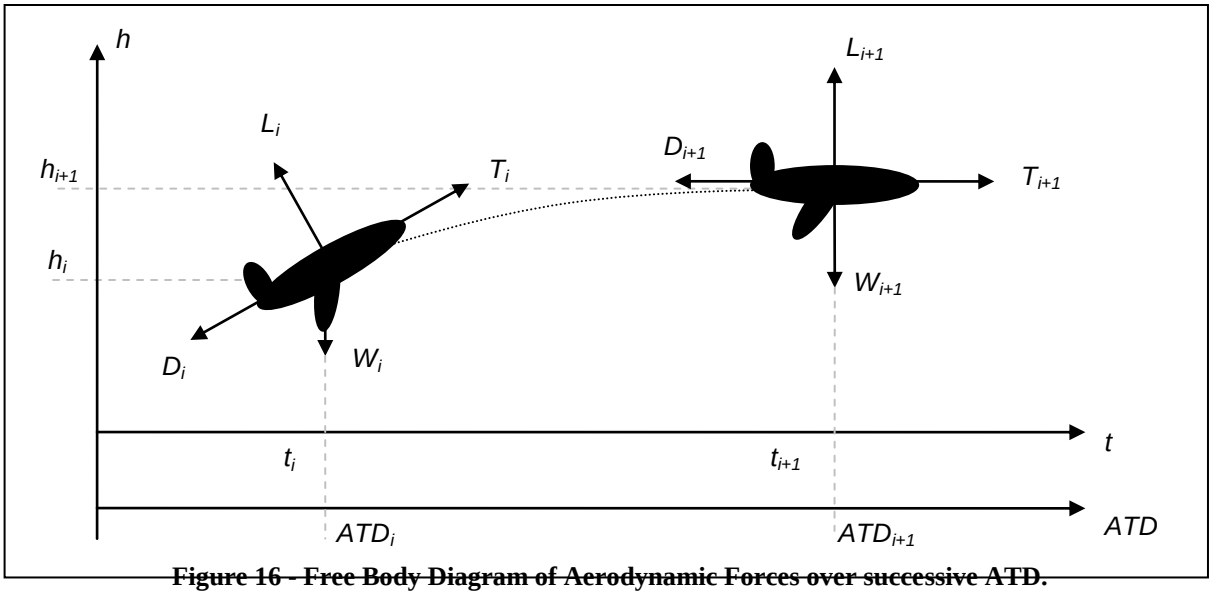

Figure 16 - Free Body Diagram of Aerodynamic Forces over successive ATD.

Table 3 - Aircraft Simulation Constants for a Boeing 747-300 [50], [51], [52], and [53]

Symbol	Units	Value
W_1	N	*Weight of Aircraft when entering optimized airspace (externally defined)*
μ	kg.(N.s)$^{-1}$	*1.71 e-5* kg.(N.s)$^{-1}$
C_{D0}	-	*0.031*
S	m^2	*511* m^2
AR	-	*6.9*
e	-	*0.9*

$$\gamma_i = \tan^{-1}\left(\frac{(h_{i+1} - h_i)nmi}{ATD_{i+1} - ATD_i}\right) \quad \textbf{(12)}$$

$$C_{L\,i+1} = \frac{W_i.\cos(\gamma_{i+1})}{1/2.\rho.V_{TAS\,i+1}^{\;2}.S} \quad \textbf{(13)}$$

$$C_{D\,-i} = C_{do} + \frac{C_{Li}^2}{\pi.AR.e} \quad \textbf{(14)}$$

$$T_{req_{i+1}} = C_{D\_i+1}.\frac{1}{2}.\rho.V_{TAS\,i+1}^{\;2}.S + W_i\sin(\gamma_{i+1}) \quad \textbf{(15)}$$

$$W_{i+1} = W_i - \mu.T_{req_{i+1}}.(t_{i+1} - t_i).g \quad \textbf{(16)}$$

Fuel usage for a flight, F_N, is then:

$$F_N = W_{i\max} - W_1 \quad \textbf{(17)}$$

With ATFU being the sum total of fuel usage among all air traffic being optimized.

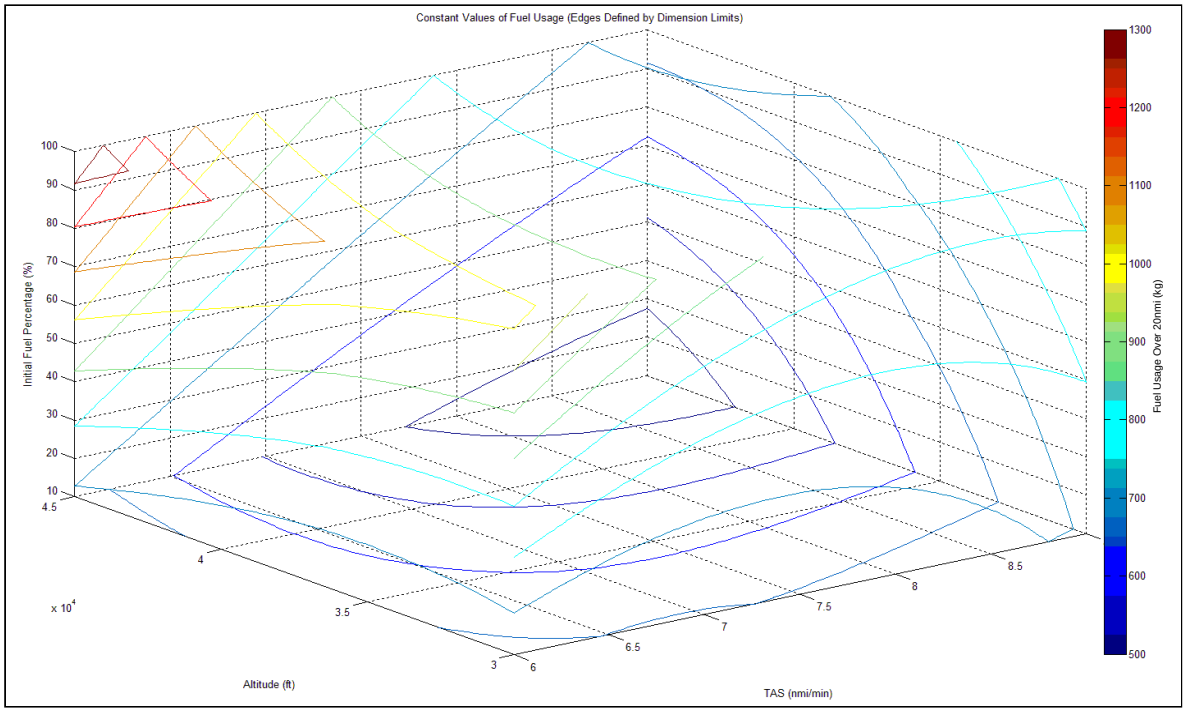

Figure 17 - Fuel Usage for a hypothetical B747-300 over 20nmi.

To enable understanding of how the optimizer perceives ATFU minimization, the data shown in Figure 17 was gathered. Figure 17 shows the fuel usage of a Boeing 747-300 defined in Table 3 covering a 20nm flight with full payload, at various combinations of valid $\%FC_1$, h_i and TAS_i. Both h_i and TAS_i were kept constant over the 20nm, and the fuel percentage at the beginning of the 20nm was set to $\%FC_1$. Figure 17 indicates that ATFU minimization for a lone Boeing 747-300 with this fixed flight profile would seek lower speeds at higher altitudes, i.e. the dark blue region. Actual optimization will be different as it will have to deal with performance constraints and the impact of other aircraft.

3.3.5 Fuel Function, as a Constraint Function

As mentioned in section 3.3.4, the fuel function also acts as a constraint function; Figure 15 showed how the C_L and T_{req} constraints were transferred as constraints, and equations (13) and (15) showed how C_L and T_{req} were calculated. As the fuel calculation method is a first order model, and has limits on where it is accurate [21], these constraints ensure that those limits are not breached and the accuracy of the calculation remains acceptable. During fuel function optimization trials that occurred during development, it was clear these limits needed to be actively enforced. Without C_L constraints, impossible C_L values gave aircraft the ability to fly higher than what their weight allowed them to. Without T_{req} constraints, T_{req} values above the maximum engine thrust allowed aircraft to climb much faster than in reality, while T_{req} values below zero allowed aircraft to slow down significantly and still maintain steady flight. Further, in those same trials, it was shown that the constraints

themselves were insufficient to prevent unrealistic phenomena and measures, in the form of a different ATD index, had to be introduced to ensure realistic results.

3.3.5.1 Issues in Initial Development

The initial application of the T_{req} constraints had encountered no prohibitive issues during its implementation as the information for maximum thrust of particular aircraft was publicly available. However, while information on C_L constraints was publicly available, the issue was in which C_L constraint to apply. Maximum C_L values existed for multiple modes of operation, from low speed, low altitude flight, through to high altitude, high speed cruise. Given that the highest of these values were from flight modes that were not technically cruise, and since the maximum values for cruise flight were not publicly known, the only solution was to use the maximum of the C_L values that were indicated as being necessary for cruise flight, e.g. as in [53].

3.3.5.2 Discussion of Alternative Aircraft Performance Constraints

As equations (12) to (17) are directly taken from the standard method of fuel usage calculation shown in [20] and [21], the C_L and T_{req} constraints represent the entirety of aircraft performance based constraints that can be assessed without improving the aircraft model defined by equations (12) to (17). The equations behind BADA [38] do show that a broader variety of limits do exist, but simultaneously show that to support them requires a more sophisticated or complete aircraft performance model. Consequently the only aircraft performance based constraints used in PCO development were those implemented via the optimizer variable, as in section 3.3.2.2, or via the fuel function, which is discussed here.

3.3.5.3 Issues in Optimizer Integration

The pertinent handling issue regards a known occurrence when using these constraints, particularly when an upper bound is restricting increases in altitude as well as C_L, is the formation of height oscillated cruise sections, i.e. successive ATD_N oscillating between high and low altitude values and causing route segments to experience repeatedly steep climbs and descents. It was highly suspected that the formation of these height oscillated cruise sections was due to the direct control of the flight nodes by the optimizer, as well as a minor but noticeable influence of climb angle in the C_L constraint calculation; i.e. if an aircraft's current max altitude due to C_L was sufficiently close to the upper altitude bound set for the optimizer (i.e. representing an aircraft's maximum operating altitude), the optimizer would allow a climb to and descent from the max altitude bound, rather than allow a shallower cruise climb at the max altitude due to the C_L limit. The optimizer's action is not infeasible; it resembles an aircraft climbing at its C_L limit, stalling, and then diving down to pick up speed and maintain C_L and consequently lift. The action is not practical due to the aircraft and its occupants experiencing intolerable stresses due to acceleration; variables not limited in the optimization. Examples can be found in Appendix F.

To check that this was the case, a version of the optimizer variable was made using a much smaller distance step, and was used as the interface between the optimizer variable and the fuel function. It was hoped that this conversion would impose a flight segment at the peaks of height oscillated cruise which are at a smaller climb angle than what was required to reach the peak of the height oscillation. During this period, the C_L constraints could be violated and the optimizer is forced to reduce the oscillation in height till it becomes a cruise climb. This was the reason why the Fuel Function used an ATD index based on i and i_{max}, rather than the n and n_{max}

used by the optimizer variable. The optimizer variable in terms of ATD_N, would be linearly interpolated to become a denser optimizer variable in terms of ATD_i, using a function similar to that discussed in 3.3.3.3; the denser optimizer variable would then be used to calculate fuel usage and related constraints. The implementation was shown to be successful provided that the periods of smaller climb angle were properly created at the control nodes; i.e. that none of ATD_i were sufficiently close to any of ATD_N to allow the optimizer to exploit any ATD_i. To ensure this and maintain the equally sized route segments defined in 3.3.2.3, ATD_i spacing, ΔATD_i, is defined from an ideal ATD_i spacing, $\Delta ATD_{i\,IDEAL}$ and the ΔATD_N for that trajectory:

$$\Delta ATD_i = \frac{\Delta ATD_N}{ceil\left(\frac{\Delta ATD_N}{\Delta ATD_{i\,IDEAL}}\right)} \quad \textbf{(18)}$$

This ensures an equal number of fuel calculation segments for each optimizer control segment. To ensure distance between elements of ATD_i and ATD_N, an offset equal to half of ΔATD_i is added to all ATD_i elements. It should be noted that the $\Delta ATD_{i\,IDEAL}$ is, like $\Delta ATD_{N\,IDEAL}$, a stakeholder preference as well, as increasing its size allows faster computation time in return for less fuel calculation accuracy, and vice versa.

The reason this separation of ATD_i and ATD_N is so important is not only did it result in appropriate handling of fuel function discontinuities; it also caused a necessary split between the optimizer variable and the fuel function as ATD_N was originally used instead of ATD_i. Previously, issues that affected the fuel function inherently caused issues in setting up the optimizer variable, and vice versa. With this split, changes can occur in either with relative ease; simultaneous combinations of increasing the size of ATD_i for improved Fuel Function accuracy, and decreasing the size of ATD_N to minimize the number of variables and cause faster optimizations, were distinctly possible. A notable possibility was that the combination of a user preferred number of trajectory changes, as set by a predefined ATD_N size, and the optimized variation in ATD values via their inclusion in the optimizer variable, could lead to the fuel optimized placement of trajectory changes given separation and performance constraints; it also inherently allowed user preferred limits and constraints to be specified for each ATD_N step, where previously such would have to be defined in terms of an invariable location. The possibilities granted by this particular combination could quite drastically improve the ability of pilots and airlines to adhere to an optimizer set trajectory, and therefore also the appeal of using the optimizer itself.

3.3.5.4 Current Form

The data flow diagram for these components in their current configuration has been given in Figure 15. Given equations (13) and (15), a maximum for C_L and the minimum and maximum values for T_{req}, the equations for constraints, given the format required by MatLab® and as applied in equations (9) and (11), are:

$$\frac{C_{Li} - C_{L\max}}{C_{L\max}} \leq 0 \quad \textbf{(19)}$$

And

$$\frac{T_{req_i} - T_{req_{\max}}}{T_{req_{\max}}} \leq 0 \quad \textbf{(20)}$$

$$\frac{T_{req_{\min}} - T_{req_i}}{T_{req_{\max}}} \leq 0 \qquad \textbf{(21)}$$

These are applied for each element of ATD_i. Note the use of scaling factors for the purposes of the optimizer method; particularly in equation (20) where the possibility of $T_{req\ min}$ being equal to or very close to zero requires its scaling factor be $T_{req\ max}$. For subsequent testing, the values shown in Table 4, as gathered and appropriately converted from [54] and [55], were used.

Table 4 - C_L and T_{req} Constraints for a Boeing 747-300

Constraint	Units	Value
C_{Limax}	-	0.50
$T_{req\ min}$	N	0 N
$T_{req\ max}$	N	936315 N

3.3.6 PCO as a Mathematical Function

For the sake of clarity, the mathematical definition of the PCO's main algorithm, when utilizing all the functions defined in this subsection creates:

minimize $\underset{X \in R}{\sum_N F_N(X)}$ … as per section 3.3.4

Subject to: $X_{MIN} \le X \le X_{MAX}$ … as per section 3.3.2

and: $1 - \left(\left(\frac{t_1 - t_2}{\Delta t_{\min}} \right)^{10} + \left(\frac{h_1 - h_2}{\Delta h_{\min}} \right)^{10} \right)_{A_{NN}}^{\frac{1}{10}} \le 0$ for all A_{NN} … as per section 3.3.3

and:

$$\frac{C_{Li} - C_{L\max}}{C_{L\max}} \le 0,$$

$$\frac{T_{req_i} - T_{req_{\max}}}{T_{req_{\max}}} \le 0, \text{ and}$$

$$\frac{T_{req_{\min}} - T_{req_i}}{T_{req_{\max}}} \le 0 \text{ for all } i$$

… as per section 3.3.5

3.4 Prototype Core Optimizer Results

The majority of optimizer component specific issues have been addressed previously in 3.3; however section 3.4 will focus on trends as found in results obtained with the PCO when applied to a number of case studies. Three cases are presented; first is a four aircraft case for discussion of basic issues and to guide interpretation of graphical results, then two sets of ten aircraft in different situations to highlight complex issues and the potential strengths and weaknesses of the optimizer. These cases were selected from a group of eleven hypothetical and extreme scenarios which were all purposely used to test the optimizer's performance. The rationale, explanations and descriptions of all of these scenarios are presented in Appendix E, with results for all eleven scenarios, as obtained for this section, found in Appendix G. All situations trailed using the PCO used a $\Delta ATD_{N\ IDEAL}$, of 20nmi, $\Delta ATD_{i\ IDEAL}$ of 5nmi and a test field between 0 to 10° latitude and longitude. The 20nmi for $\Delta ATD_{N\ IDEAL}$ was a simple number that offered sufficient trajectory fidelity even with short flights, with a comfortable frequency of trajectory changes that amounted to one change every two minutes even at high speeds. The 5nmi for $\Delta ATD_{i\ IDEAL}$ ensured at least four fuel calculation nodes for each route segment. The test field location ensured that the distances between NMD were at their longest to increase possibility of separation violation, and its size, which roughly equated to a square region 600 nmi on a side, was sufficiently large enough to handle the entire trajectories of short ranged commercial flights without requiring the conflict check pre-processing of a continental region. All aircraft are models of the Boeing 747-300 defined in Figure 17, with the arbitrarily defined optimizer variable bounds defined in Table 5. While most of these values were made to encompass the maximum values associated to a Boeing 747-300, the h_{min} had further importance as aircraft were also constrained to enter and exit optimized airspace at this value. This was done to ensure aircraft did not suddenly and unintentionally appear at higher levels of optimized airspace.

Table 5 - Optimizer Variable Bounds for a Boeing 747-300

Altitude Constraints	
h_{min}	30000 ft
h_{max}	50000 ft

Velocity Constraints	
V_{min}	360 kts
V_{max}	600 kts

Also, while the introduction of ATD_i in 3.3.5.3 did prevent frequent altitude variation from forming, the optimizer's tendency to pursue high magnitude climb angles was still present, particularly when changing between portions of the trajectory that did or did not require separation assessment. This consequently meant aircraft pursuing climb angles equal to the blanket climb angle constraint required to ensure vertical separation, as per 3.3.3.1. While this was physically feasible, it is possible for such results to be against user preferences; allowing aircraft to climb at the maximum allowed climb angle at any point in the trajectory may result in a more fuel efficient trajectory overall, but it would also prevent aircrew and passenger actions, such as food distribution or access to ablutions, whenever such climb angles are used. To cater for the possibility that a lower climb angle may be user desired, the blanket climb angle constraint was further reduced to a nominal 1.5°, i.e. half the standard angle of decent for final approach, and therefore midway between the lack of discomfort incurred when completely level, and the discomfort experienced during landing.

To further support inquiry into the impact of user preferences on fuel usage optimization, departure and arrival time constraints were considered for application for this stage of testing. The departure time constraint, i.e. a

constraint on what time aircraft needed to enter optimized airspace, was completely rejected as it would have required knowledge of the aircraft trajectory, and of aircraft performance, prior to cruise. While possible, this requires aircraft performance models more sophisticated than that defined in section 3.3.4 and was therefore avoided at this stage of development; consequently the optimized airspace entry time for aircraft became a necessary scenario based input that could not be varied. The arrival time constraint, i.e. a constraint on what time aircraft needed to leave optimize airspace, was given more consideration as it is common practice for ANSP and airlines to schedule aircraft to arrive at a destination at certain times, and further, because the application of an arrival time constraint did not need any other performance based information. Counter to the application of the constraint was the knowledge that the optimizer could generate better fuel usage optimums if arrival time is not constrained; aircraft with a planned arrival time must cater for any time lost or gained in ensuring separation with other aircraft, aircraft without a planned arrival time do not. The most realistic solution would be to have a combination of both, i.e. instead of a set arrival time, an arrival time window made of a maximum and minimum arrival time; this would allow aircraft to not always have to make up for time lost or gained from ensuring separation, and would ensure aircraft can adhere to their destination's schedule for arriving aircraft. The issue with this is the window planned by ANSP and airlines for scheduled arrival time is not fixed nor determined by any standard or publicly availably list of preferences, yet aircraft adhere to them as much as they adhere to avoiding other aircraft; optimization results would thus vary dramatically between having an infinitely sized arrival time window, i.e. no arrival time constraint, and a small arrival time window, i.e. a specific arrival time constraint, with the trends for any optimization result in between being difficult to establish. As the optimizer is still being developed and this level of trend analysis is not yet necessary, it is sufficient to trial scenarios only with and without a constraint which would cause aircraft to exit airspace at a specific time; this would allow results to be generated for either arrival window size extreme and allow prediction of results of scenarios where arrival windows have a pre-defined value. For the purposes of the scenarios discussed in this section, exit times constraints were applied to all aircraft in a time constrained situation and were predefined as an aircraft's start time plus the time required flying its route at a TAS of 8 $nmi.min^{-1}$; this value being a generic rule of thumb representing average flying speeds for Boeing 747's in commercial traffic.

3.4.1 Scenario '4acCO': A Four Aircraft Cross Over

Figure 18 and all figures like it in the thesis, shows the air traffic situations in terms of the routes taken by individual aircraft inside the situation, and is accompanied with data table that indicates how corresponding trajectories were modelled. The 'Start Time' column specifies when that aircraft entered the airspace test field; given that separation is also time based, the start time of aircraft in some test scenarios was altered to simulate critical forms of separation. The 'Distance Covered' column gives the trip length and due to the relationship of S_{FLIGHT} , $\Delta ATD_{N\ IDEAL}$, and $\Delta ATD_{i\ IDEAL}$, to ATD_N and ATD_i, also gives indication of the number of nodes per aircraft used for optimizer control (e.g. AC1 had a trip length of 480 MM, AC 1 would therefore have 480/20 = 24 ATD_N elements) and fuel calculation (e.g. AC 1 would have 480/5 = 96 ATD_i elements). The 'Initial Weight' column indicates the weight of the aircraft when they entered airspace. Referring back to the scenario under discussion, Figure 18 specifically shows a 4 aircraft intersection at (5, 5).

Figure 19, and all figures like it, presents three perspectives of the optimizer variable defined by the optimizer to be the optimum for that scenario. The first perspective is a combined plot of the initial value, and the optimizer variable as returned by the optimizer, against the ATD_N used as their base; it is therefore a horizontal

representation of equation (5) with the gridlines therein representing the concatenation in equation (4), and from left to right, the trajectory of the aircraft as it flies its route. The second and third perspectives are the optimizer variable transposed to an NMD field to allow three dimensional assessment of separation in terms of time and altitude respectively; for each location on the field, separation in terms of a constant value, must be maintained in at least one of the two. Figure 19, specifically, shows a typical optimizer result; aircraft reach maximum sustainable altitude quickly, carry out a prolonged cruise climb, then descend rapidly. The noticeable preference for altitude separation, as defined by the larger variation in altitude data as compared to variation in TAS data, is often due to the comparative fuel cost of speed changes required for time separation, as previously indicated in Figure 17. Necessary altitude change is further reduced due to already present separation caused by carrying different amounts of fuel. Another typical optimizer characteristic is the sharp changes in TAS and altitude due to the large step size; intersection areas can be small enough that ATD steps cannot mould around it, and suffer a sharp transition as a result, as AC 4 did in Figure 19. However, if separation requirements are present above and below, as was for AC 2 and 3, trajectories during intersection can be flattened to allow aircraft below them to reach higher altitudes.

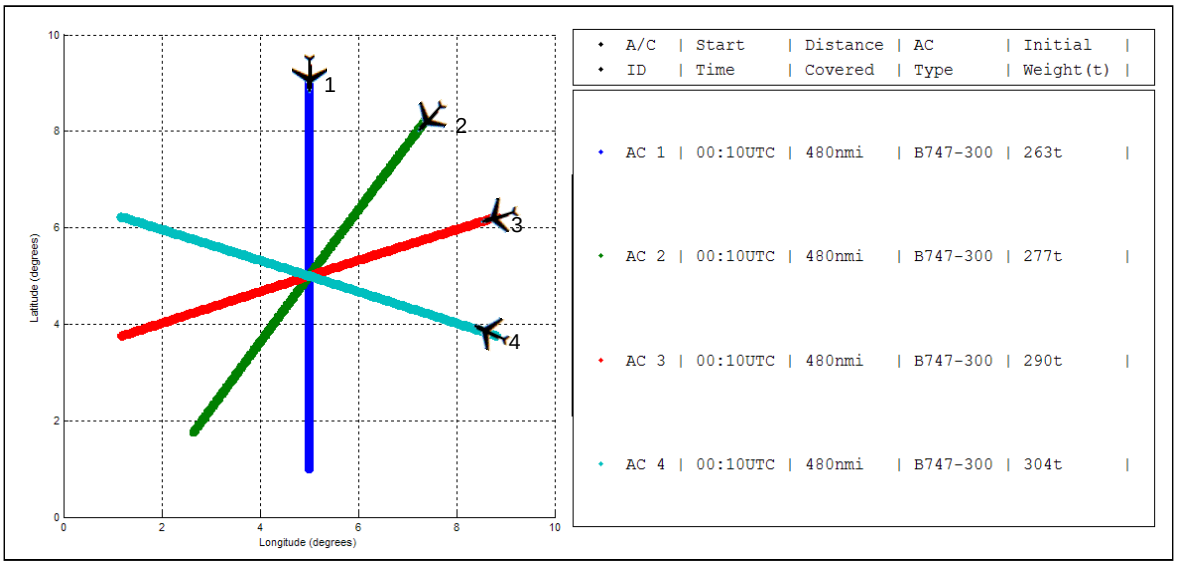

A/C ID	Start Time	Distance Covered	AC Type	Initial Weight(t)
AC 1	00:10UTC	480nmi	B747-300	263t
AC 2	00:10UTC	480nmi	B747-300	277t
AC 3	00:10UTC	480nmi	B747-300	290t
AC 4	00:10UTC	480nmi	B747-300	304t

Figure 18 - Situational Details for a Four Aircraft Crossover

Figure 20 shows a typical time constrained result; aircraft still reach a maximum altitude, but one that is lower due to lowered TAS required to exit on time. Preferences for altitude changes are still present, and largely enhanced by the increase in already present altitude separation due to the lower TAS. Another notable difference caused by the time requirement is the continuousness of the result; the resulting optimizer variable in both altitude and velocity was continuous, whereas the unconstrained arrival time result was discontinuous at the intersection. This would be indicative of the optimizer's attempt to distribute the difference in exit time across the entire trajectory. Figure 21 and all figures like it, show comparative information between the two optimizer results as well as an optimization result where separation had not been taken into consideration, i.e. if it did not have to avoid other aircraft. Its main purpose is to show the impact on fuel usage and flight time that separation, even when optimized, would cause. Figure 21, specifically, is a typical comparison; as the time constraint requires aircraft to fly a less optimal profile its fuel usage increases significantly and their flight time becomes uniform, in contrast, without a time constraint the influence of interactions are minimal and this usually causes only slight increases in flight time and fuel usage.

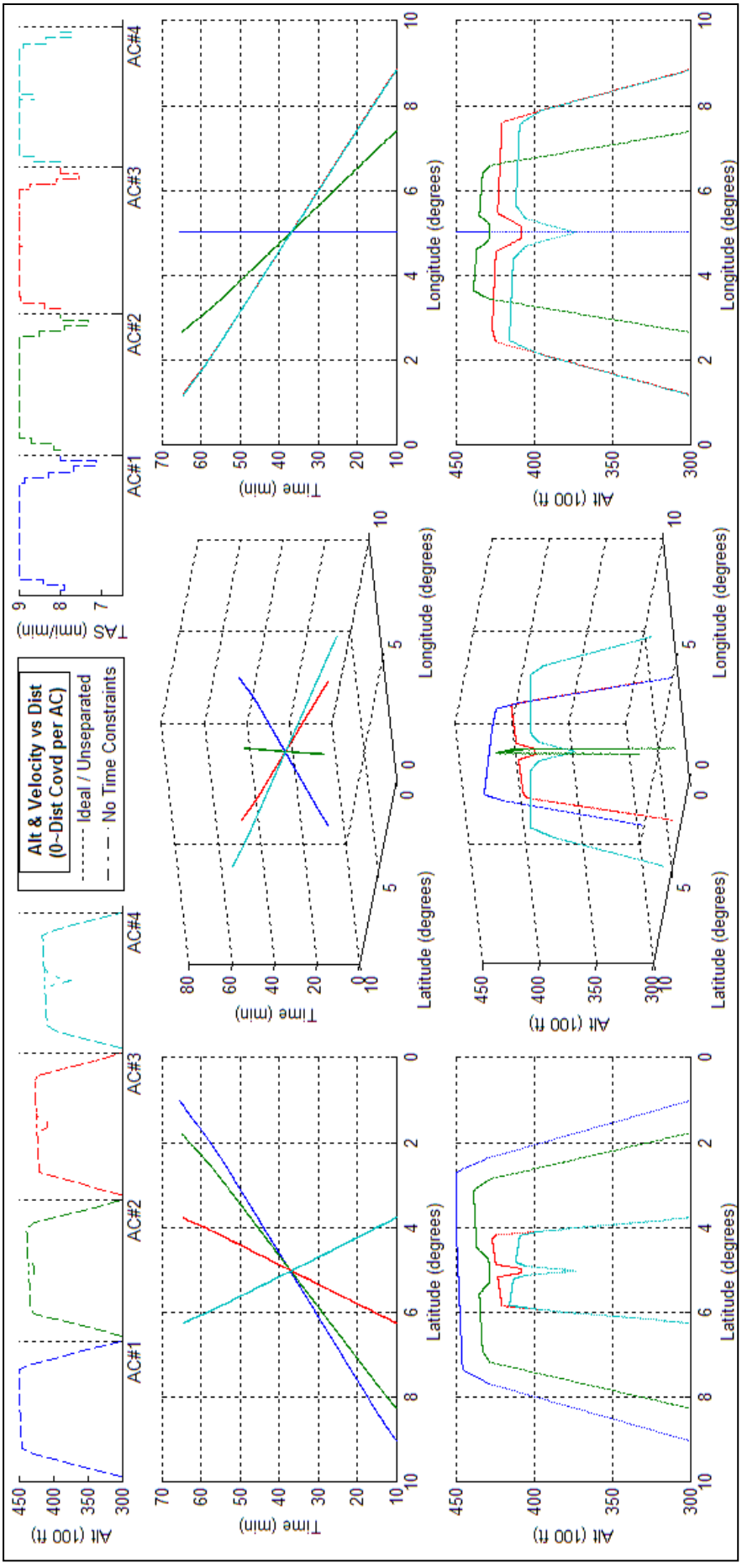

Figure 19 - Optimized Four Aircraft Crossover.

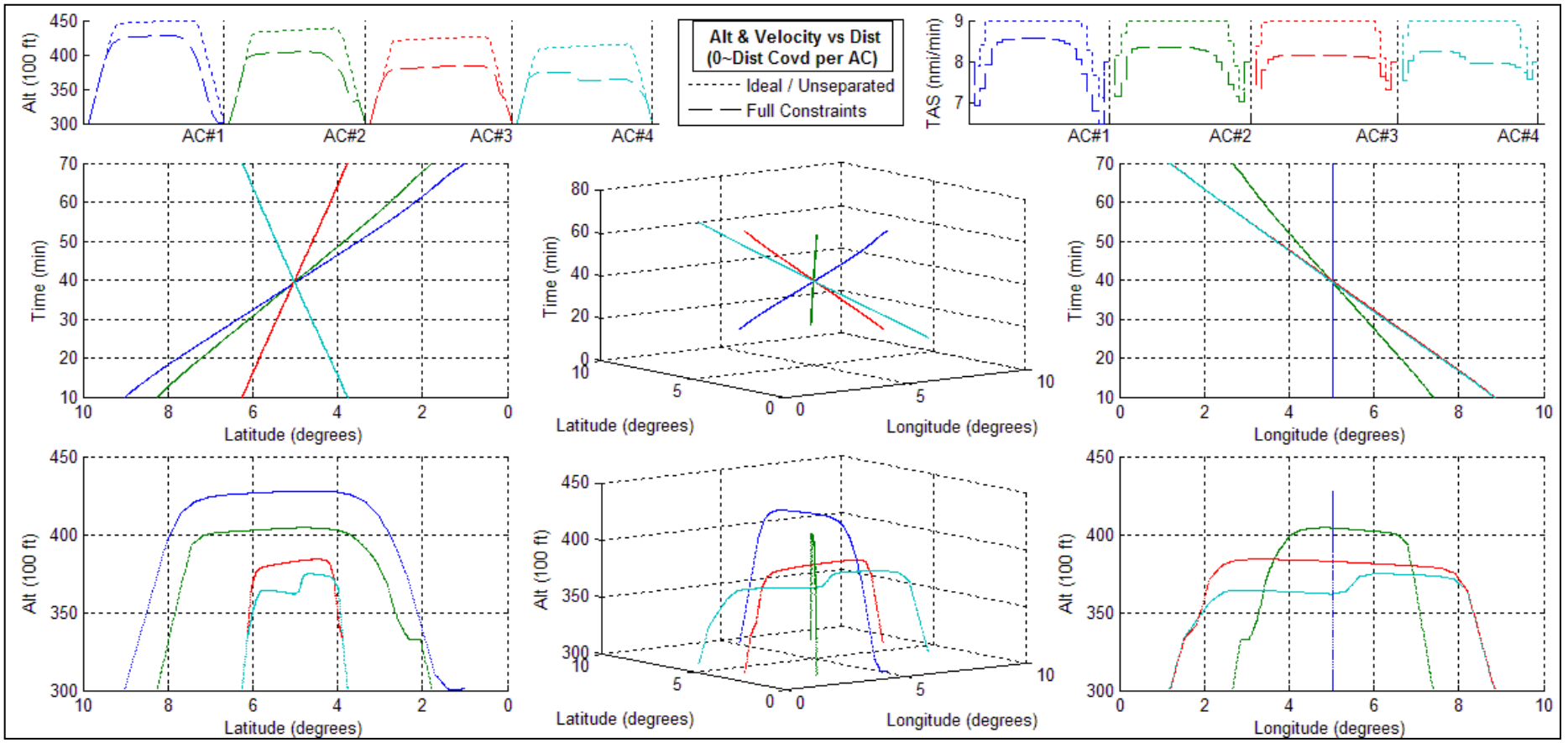

Figure 20 - Optimized Four Aircraft Crossover assuming an exit time constraint.

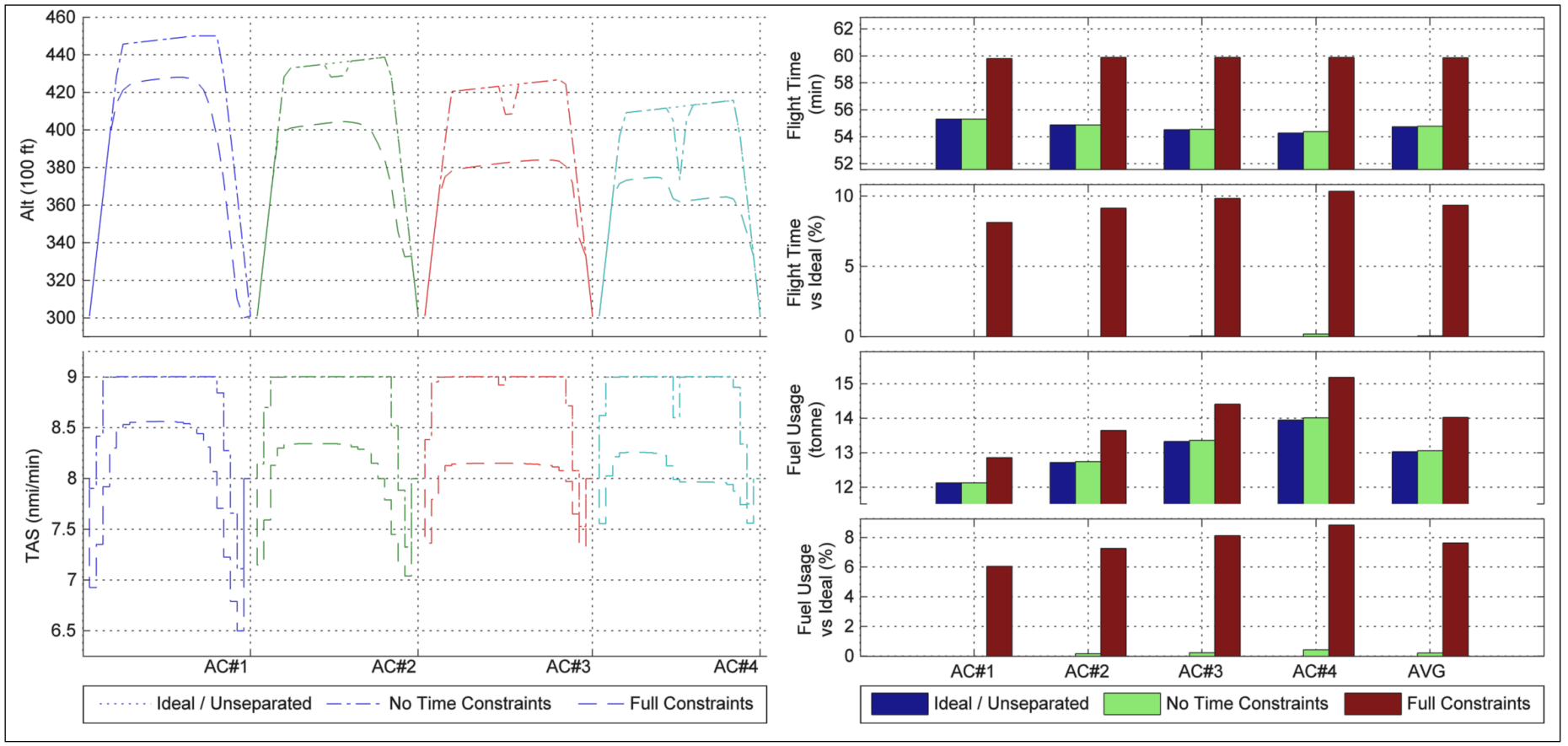

Figure 21 - Comparisons of Optimizer Variable (left) and Flight Data (right) between various optimizations of the Four Aircraft Crossover.

3.4.2 Scenario '10acCO': A Ten Aircraft Cross Over

Figure 22 describes an exaggerated situation; while possible, the use of route structures and sector aircraft limits prevent this kind of occurrence. However on the premise that optimizations like PCO can provide additional air traffic controller capability, scenarios that could occur without those limits have to be considered. This particular scenario is even more pertinent as one of the two PCO optimizations conducted on it failed to find an optimum.

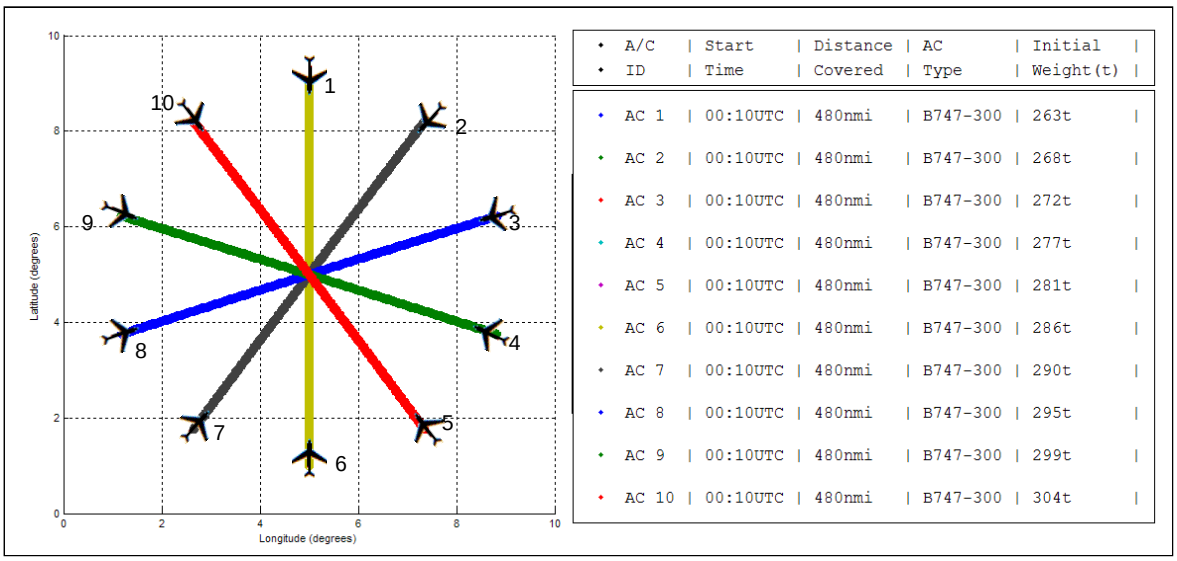

A/C ID	Start Time	Distance Covered	AC Type	Initial Weight(t)
AC 1	00:10UTC	480nmi	B747-300	263t
AC 2	00:10UTC	480nmi	B747-300	268t
AC 3	00:10UTC	480nmi	B747-300	272t
AC 4	00:10UTC	480nmi	B747-300	277t
AC 5	00:10UTC	480nmi	B747-300	281t
AC 6	00:10UTC	480nmi	B747-300	286t
AC 7	00:10UTC	480nmi	B747-300	290t
AC 8	00:10UTC	480nmi	B747-300	295t
AC 9	00:10UTC	480nmi	B747-300	299t
AC 10	00:10UTC	480nmi	B747-300	304t

Figure 22 - Situational Details for a Ten Aircraft Cross Over

The failure was in an optimization of 3.4.2 that did not constrain arrival time. Figure 24 shows the last iteration that the optimizer method took before it determined that it could not find an optimum; it shows a couple of incongruities that are not expected in a successful result and that could also give indication of why the optimizer could not find an optimum. The first incongruity is the presence of optimizer variable altitudes higher than the initial value; while not impossible it does require a significant expenditure of fuel prior to higher altitudes to prepare for the lesser aircraft weight required. The optimizer variable shows no initial trajectory which could cause excessive fuel usage so it must be a remnant of the optimizer's methods; this makes sense as these higher altitude values decrease fuel usage and therefore aid in the optimization. Being infeasible, the higher altitude values were pushed down by the barrier functions to ensure C_L and T_{req} constraints are met; that it has not occurred suggests it may have caused the failure. However this is unlikely as nothing is stopping it from being applied; the regions of higher altitudes do not have separation constraints holding them in place.

The other incongruity here is a separation violation; the time data in Figure 24 shows that the aircraft arrived at the same point at the same time thus altitude separation was required for all, which is impossible as nine separation distances of 2000ft would have to fit in the 15000ft of available altitude (minimum global altitude was 30000ft, maximum global altitude was 45000ft; both set purely to constrain the scenario). Thus the optimizer needed to shift at least two of the aircraft in time via speed changes to satisfy separation, but did not. Other scenarios showed that the optimizer could do that, but something in this scenario prevented it. It is possible that the separation function may not have sufficiently indicated a new optimum; if so, performing the optimization with the powers in equation (10) being gradually decreased from 10, would find a new optimum. However, a more likely reason is that the optimizer trapped itself; as separation in terms of altitude was gradually applied,

the resulting altitude changes prior to and after an intersection could not perform simultaneous TAS changes because such would clash the separations above and below it during the intersection and thus be considered as increases in infeasibility by the optimizer. The only way to get out of this is to perform a TAS change with the only aircraft without an altitude change, i.e. the aircraft at the top, and give it separation in terms of time rather than altitude; however this too is rendered infeasible because at high altitudes the C_L and T_{req} constraints are easily breached. The solution to this would be to remove the global minimum altitude initially, then replace it after optimization; the resulting freedom would allow complete vertical separation which would then lead to changes in time as smaller fuel usage costs are recognized at different speeds at higher altitudes. While the solutions are obvious, the seldom occurrence of situations that warrant them suggests their further research before a specific solution is made integral to PCO.

Contrary to Figure 24, Figure 25 shows how this scenario is optimized. The indicators of a time constrained result are present; the only peculiarity is the significant variation in TAS and altitude throughout each flight's trajectory. This is easily explained via the combined effects of the exit time and separation constraints; due to their definition in terms of time, separation constraints can partially act as time constraints causing distortions, similar to those in Figure 20, in ATD before and after the region where the constraint is applied. These distortions are further enhanced by the separation's impact on altitude which, due to its change and the optimum variation seen in Figure 17, requires alternate simultaneous speeds to be considered. Figure 23 confirms that without time constraints, a feasible optimum was not found; the lesser fuel usage amounts being impossible in this form of optimization. What was surprising, and still needs to be checked, is the lower than expected increase in fuel usage in the time constrained result; in 3.4.2, comparative fuel usage varied between +6~9% and averaged at +7.5%, while here, fuel usage varied between +6~12% and averaged at +9%. This increase in fuel usage, due to having more aircraft in the air in a more complex scenario, as compared to the time constrained 3.4.2, is smaller than the percentage increase in fuel that the time constraint had caused in 3.4.2 over its non-constrained counterpart. This heavily suggests that imposing less optimal arrival times has a greater effect on fuel usage than the impact that the traffic itself could impart once optimized.

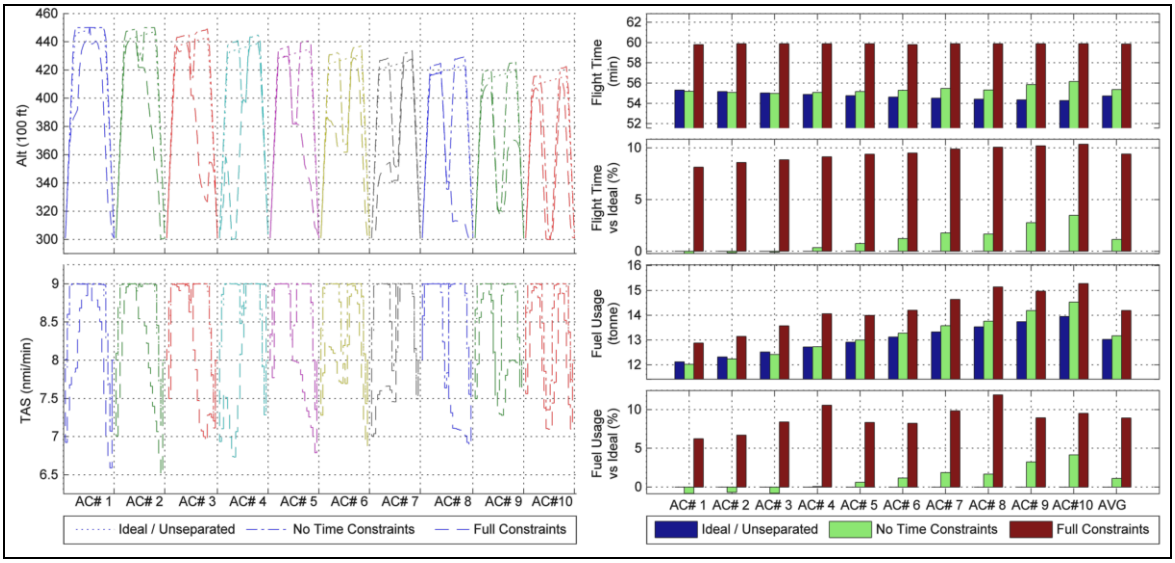

Figure 23 - Comparisons of Optimizer Variable (left) and Flight Data (right) between various optimizations of the Ten Aircraft Cross Over.

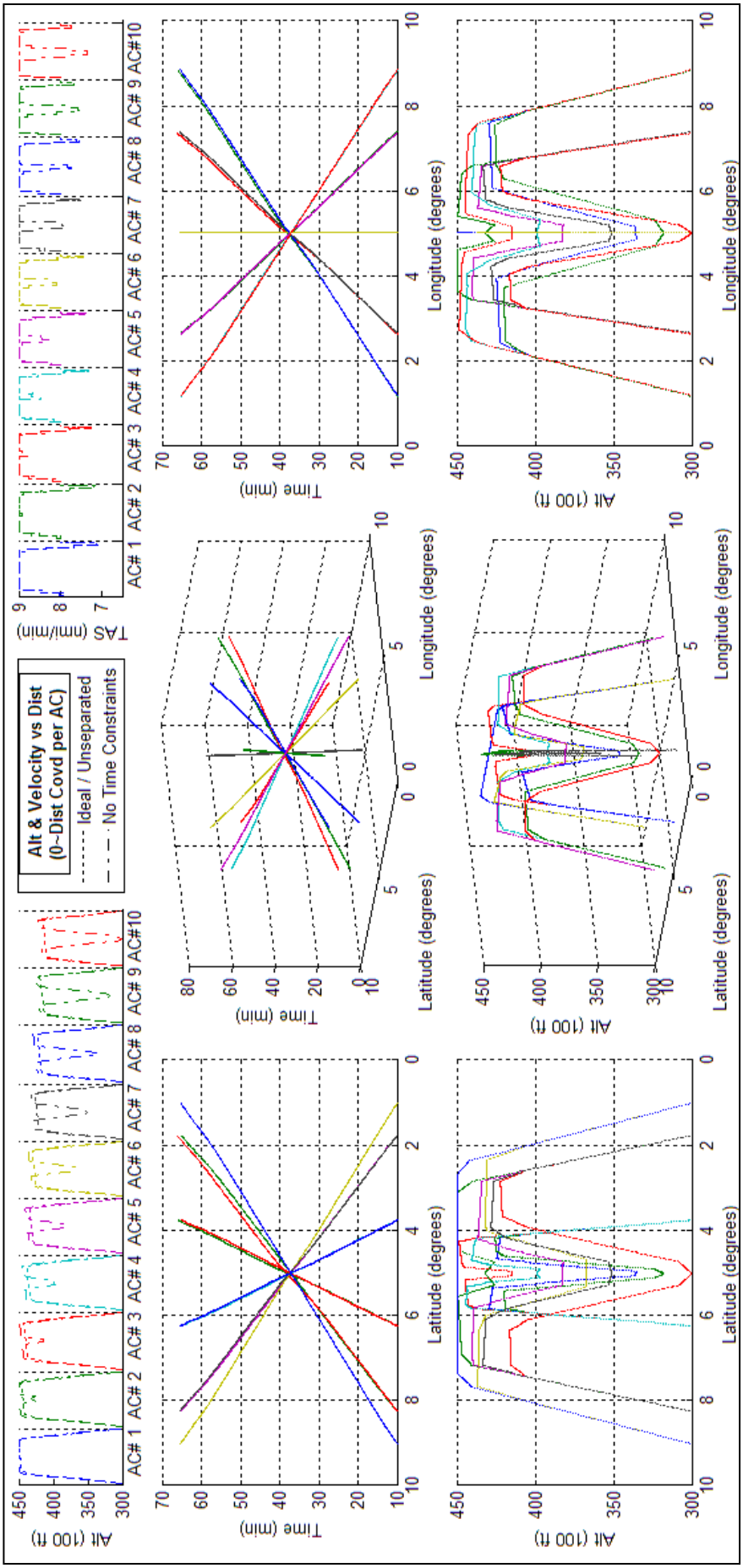

Figure 24 - Optimized Ten Aircraft Cross Over.

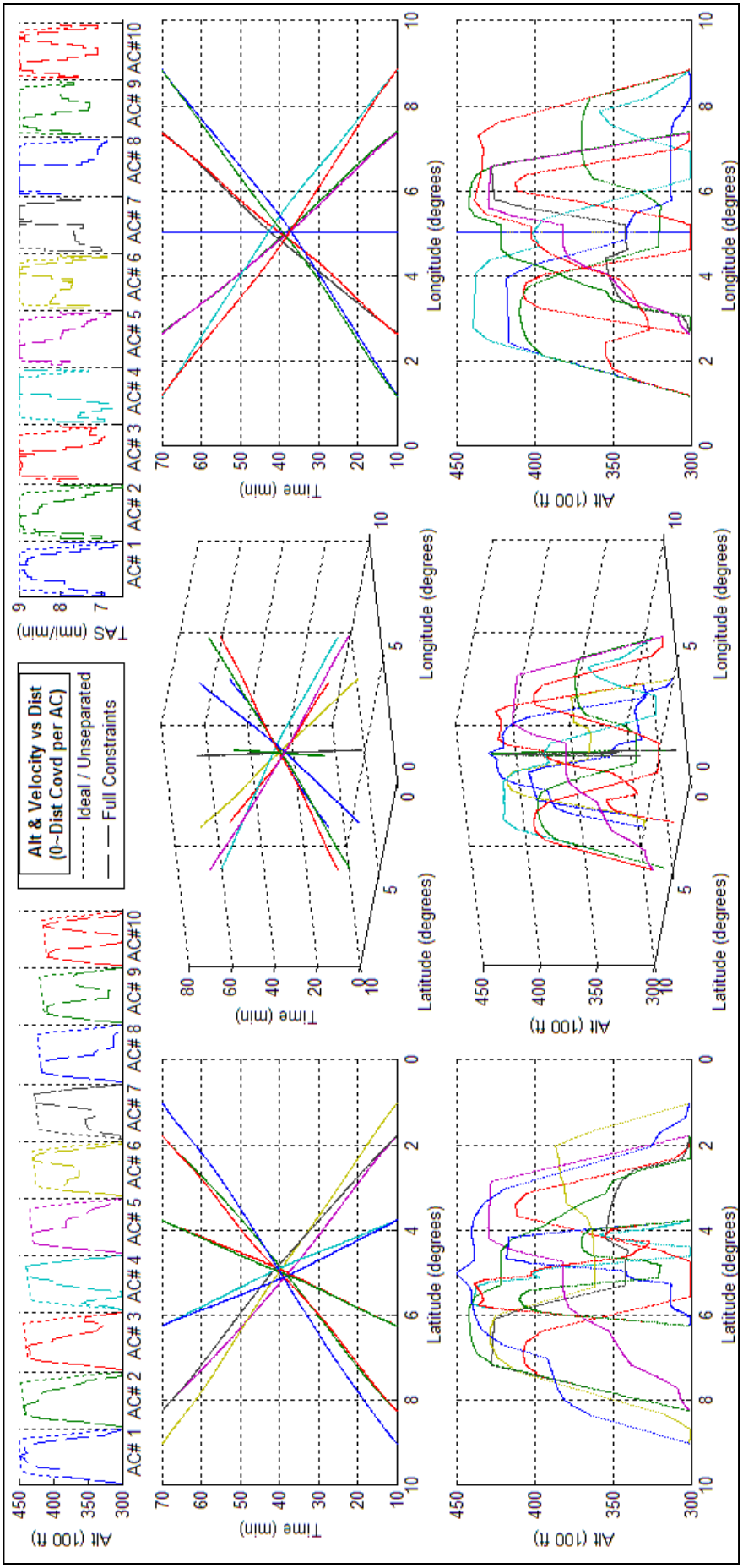

Figure 25 - Optimized Ten Aircraft Cross Over assuming an exit time constraint.

3.4.3 Scenario '10acPH2H': Five Pairs of Parallel Head-Head Crossover

Before discussing the results of this scenario, the impact of reciprocal and parallel routes needs to be discussed. As Figure 4 showed, as intersection trajectories become increasingly parallel, the number of NMD locations where collision could occur increases and becomes proportional to the ATD the two aircraft existed in. As the potential region of conflict is significantly large, initiation of separation does not have to occur outside the potential region of conflict. Thus for the optimizer the use of parallel routes supports knowledge gain in two areas; the first is the trends of the optimizer's results given the greater number of constraints these routes use, the second are the deviations that the optimizer can apply when it can freely control the relative placement of the initial points of separation. The scenario shown in Figure 26 was developed to assess optimization of air traffic interaction along parallel routes; it consisted of five pairs of aircraft, with each pair in a head to head collision.

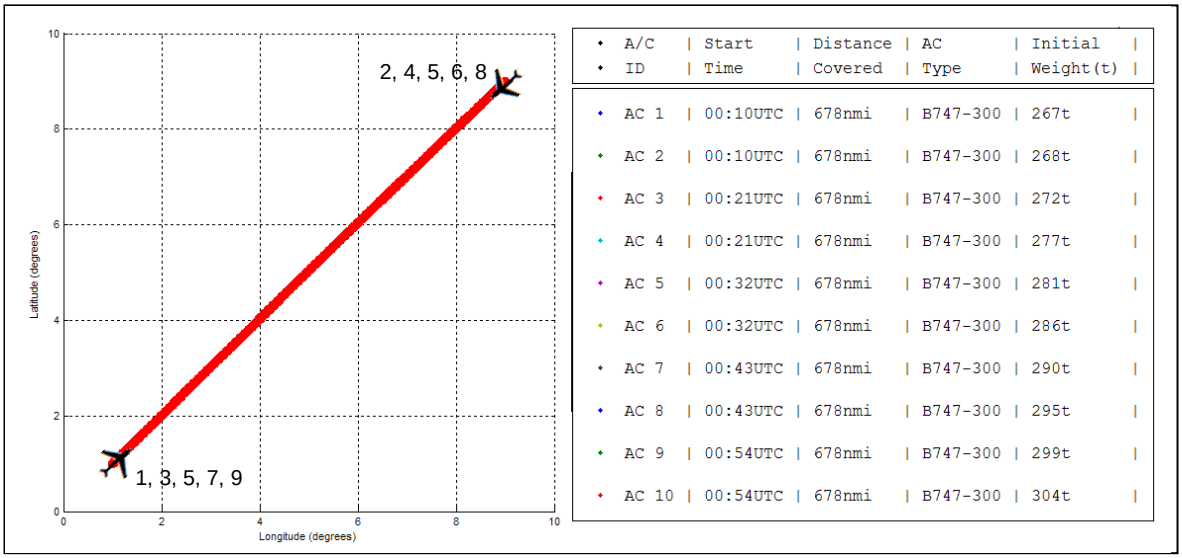

A/C ID	Start Time	Distance Covered	AC Type	Initial Weight(t)
AC 1	00:10UTC	678nmi	B747-300	267t
AC 2	00:10UTC	678nmi	B747-300	268t
AC 3	00:21UTC	678nmi	B747-300	272t
AC 4	00:21UTC	678nmi	B747-300	277t
AC 5	00:32UTC	678nmi	B747-300	281t
AC 6	00:32UTC	678nmi	B747-300	286t
AC 7	00:43UTC	678nmi	B747-300	290t
AC 8	00:43UTC	678nmi	B747-300	295t
AC 9	00:54UTC	678nmi	B747-300	299t
AC 10	00:54UTC	678nmi	B747-300	304t

Figure 26 - Situational Details for Five Pairs of Parallel Head-Head Crossover

To simulate a critical form of parallel route interaction, an eleven minute gap was placed between successive pairs of aircraft to allow a third aircraft to be in the middle. This ensures that aircraft can exit and enter at the same 3 dimensional location despite the entry point for trajectories being unalterable once optimization begins. It also has an effect on separation; if the gap was greater than 15 minutes then aircraft would have sufficient time to fly around oncoming aircraft such that their deviation only impacts one other aircraft and results in trajectories similar to those in Figure 19, if the gap were less than ten minutes aircraft with the same heading in Figure 26 would adhere to the same flight level for the duration of the flight resulting in a similarly simple trajectory. The results in Figure 27 show why the eleven minutes are special; between the two time values is a transition from small intersection deviations to massive intersection deviations, in other words the initiation of a cascade effect. That the optimizer results show this is a good indication that it can show other similarly critical points as well.

Figure 28 mirrors the ability to show the cascade effect as well, however with the time constraint present the effect extends to the time dimension as well, and the initial desire to 'shift away' from the rest is apparent in that. Further with the demands on time being so excessive the lower altitude limit also forms a barrier to the ability to reach a slower speed as such requires lower altitudes to satisfy C_L constraints.

The information in Figure 29is similar to that in Figure 23. The only notable difference is the presence of reduced flight times for some of the aircraft. As indicated by Figure 17 fuel usage optimums suggested by the fuel function are generally at maximum altitudes and TAS; however as aircraft enter and exit upper level airspace at a lower altitude, achieving higher TAS does not lessen fuel usage during those segments and a lower TAS is used instead. Due to variation in position of separation, these aircraft were forced to reach higher altitudes faster in order to minimize cascade effect. This is a fairly expensive operation so even though their trajectory is only slightly controlled in comparison to the rest, their additional fuel usage is comparable to those who experienced even greater deviation.

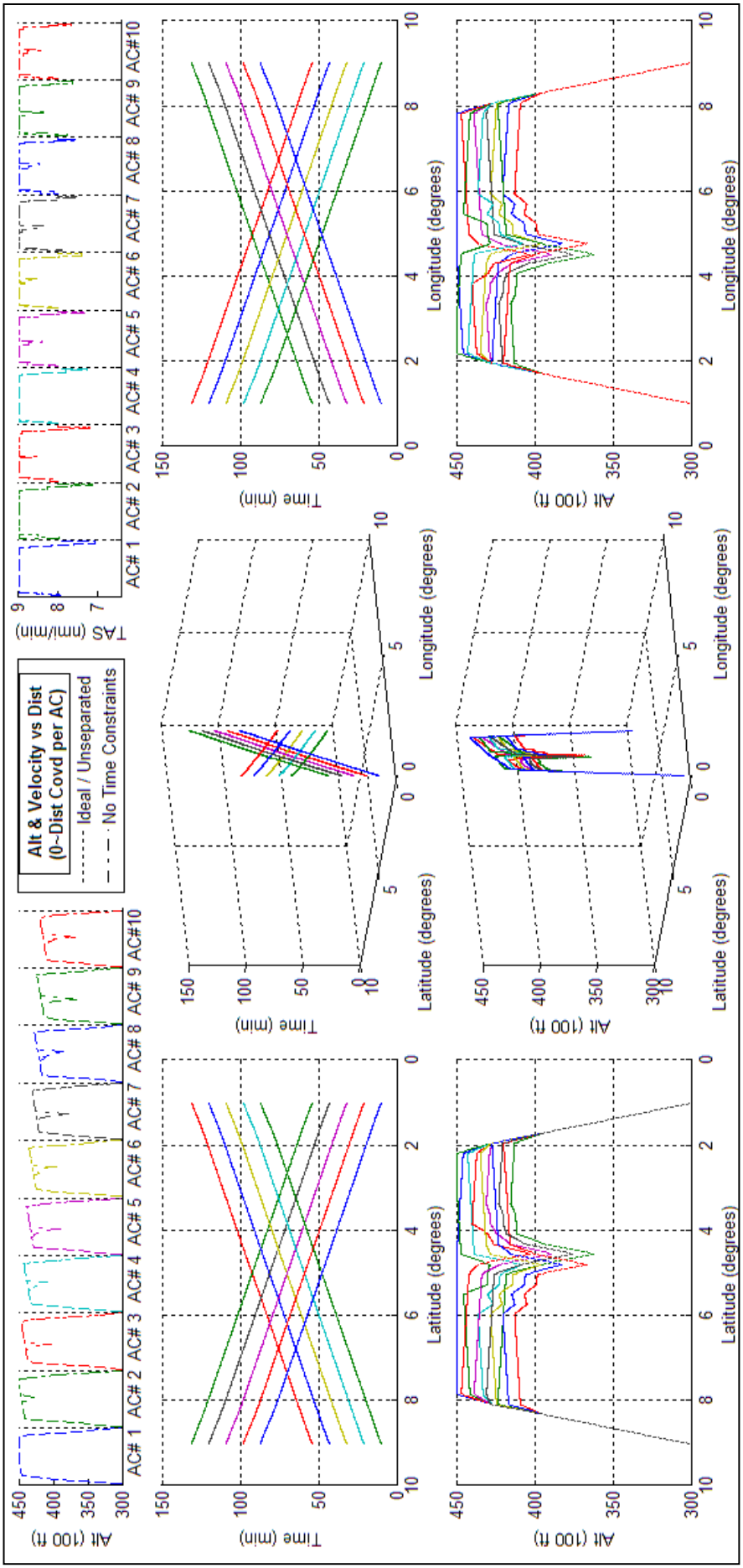

Figure 27 - Optimized Five Pairs of Parallel Head-Head Crossover.

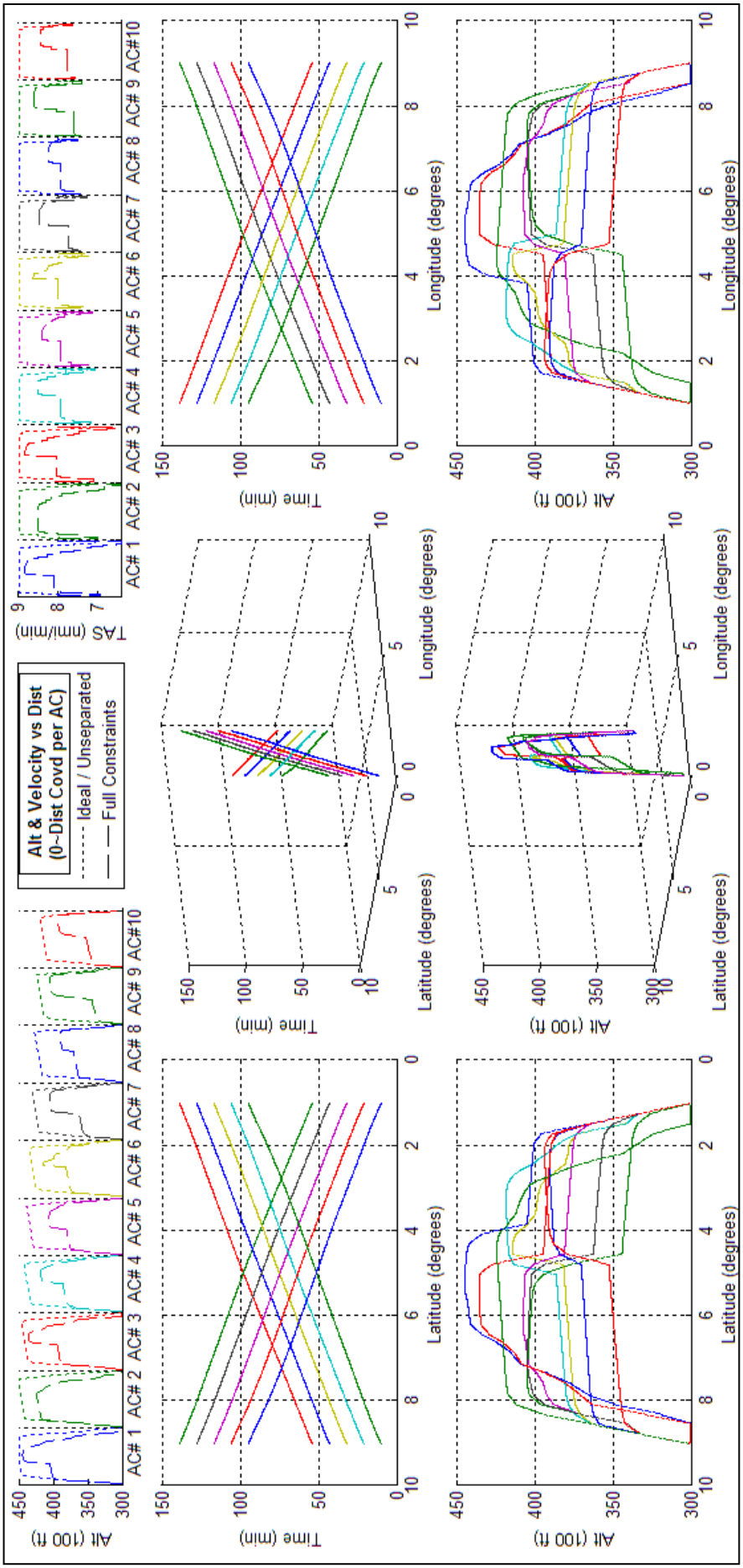

Figure 28 - Optimized Five Pairs of Parallel Head-Head Crossover assuming an exit time constraint.

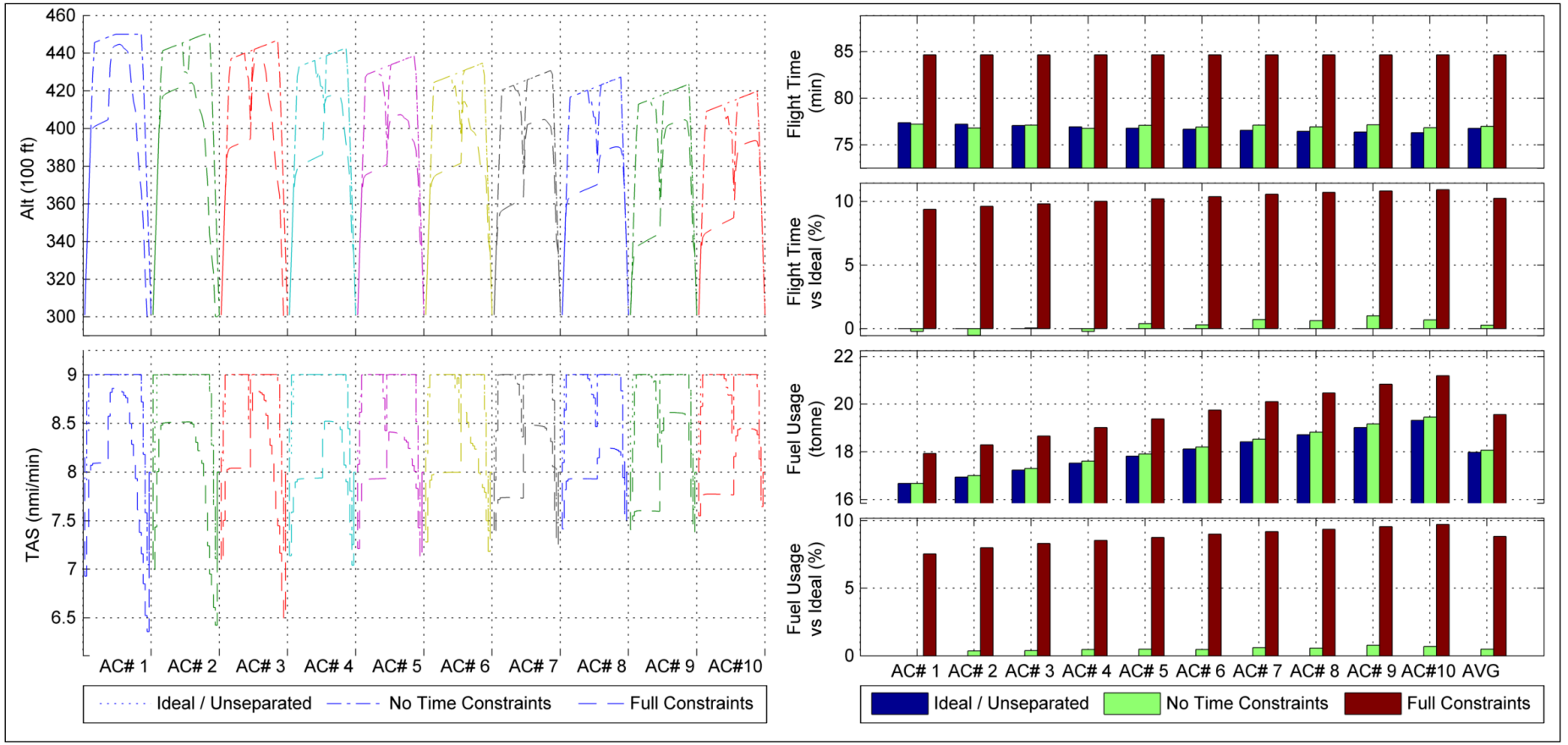

Figure 29 - Comparisons of Optimizer Variable (left) and Flight Data (right) between various optimizations of Five Pairs of Parallel Head-Head Crossover.

3.5 Conclusions

The purpose of this section is twofold. The first purpose is to give a summary of the research contributions performed in this chapter and this is performed in section 3.5.1. The second purpose is to highlight the impact the work had on the Research Questions mentioned in section 2.4.2 and this is discussed for each research question in section 3.5.2.

3.5.1 Chapter Summary of Research Contributions

Given airspace containing aircraft that could benefit from optimization of their fuel consumption, a means of modelling their trajectories and their conflict with each other was developed and presented in the first two sections of this chapter. The methodology was developed as an extension of DSM so as to combine in one package the desirable traits of DTM and DSM. The result was a DAM that used locations, which were separated according to the minutes of longitude and latitude, to accurately assess conflict that occurred near them. The modelling of separation was akin to knowing the intersection point of a pair of aircraft, then using checks in altitude and time at the point of intersection to determine if conflict occurred; this being the norm in ATC application of separation. The only difference is the inclusion of a lateral deviation check to see if conflict could occur at that point or not. The DAM modelling of actual trajectory, due to its root s in DSM and the ability for NMD to be described in ATD, meant that the baseline for DAM modellings was ATD. However the variation in step size between successive elements of the directly gathered ATD_A meant that it could not easily be used as a baseline and additional layers of ATD_i and ATD_N, developed for other reasons, had to be used instead. In order to avoid significant computational expenses, randomness in fuel optimization, and future inapplicability, the modelling of potential trajectories for the purpose of researching fuel optimization disallowed any S_Y variation. Further, in a continued desire to reduce computational effort, and due to the uncoupled nature of DAM separation, means of reducing separation checks in the time and altitude dimensions were developed and implemented. Unfortunately, due to the importance and difficulty of the optimization of fuel consumption, a considerable portion of NMD capability that was developed had to be ignored. However in consideration of the possibility that such capability could be used in future research in fuel optimized air traffic, or in any other area of air traffic control, a summary is included in Appendix D.

In the last three sections of this chapter, a PCO was developed that combined all key components and data transfer mechanisms required for a complete tool that can carry out cooperative optimization of the fuel consumption of air traffic over a continental region. The optimizer method, optimizer variables, separation function, and fuel function were all tested as a united algorithm, with placeholder functions present for future components. All components were found to have flaws that required improvements in their form and integration with each other. All flaws were sufficiently improved upon so as to allow modelling of air traffic that had been optimized using simplified fuel calculation equations. The general trends found in scenarios with an unrestricted airspace exit time did show the expected properties that the Breguet range and endurance usually cause, and did show sharp trajectory changes that modelled the results of [32]; the combination of these do suggest that future versions that incorporate the PCO would yield useful and accurate results. Additionally, scenarios with restricted airspace exit times showed how the interior point algorithm will try to distribute time losses due to the required

exit time over the entirety trajectory so as to maintain a close to optimum trajectory; this is an unintended result that positively indicates that the optimization of fuel consumption is being modelled appropriately.

3.5.2 Current State of Research

3.5.2.1 Q1: Can a co-operative and sufficiently informed air traffic optimisation methodology achieve a reduction in total fuel usage compared to current ATM?

In this chapter, an optimization methodology was setup to optimize the fuel usage of air traffic via the control of their trajectories and under the assumption that aircraft could cooperate with each other in accordance with the optimized trajectories to safely reduce fuel usage. The results of trials of this optimization methodology did show that a reduction in total fuel usage was possible, in fair utilization of all aircraft involved, and as compared to current ATM scheduling methods (i.e. the PSO). Further, this was despite the different ATS model and the additional information it contained that had hitherto been unincorporated in air traffic optimization. The key issue therefore revolves around whether or not the optimization methodology was "sufficiently informed"; i.e. did it have a sufficient understanding of the actual ATS such that its results could be directly used to optimize air traffic?

The answer is that the optimizer's understanding of the actual ATS could be sufficient for actual application of the optimizer result. However this is only true if, and only if, airlines and aircrew were willing to accept equations (12) to (17) and (19) to (21) as representative of the functional capability of their aircraft, and as such, always fly their aircraft as the equations predicted. As it is possible for the representation to be sufficiently true in reality, Q1 therefore also becomes possible in reality. However the representations are not always true thus Q1 is only partially answered. It will require, as anticipated in Q4, at least the development of an ATS model that incorporates a dynamic environment and a robust optimizer methodology that can handle such.

3.5.2.2 Q2: What information is required to achieve such an optimisation methodology and how sensitive are the results to the accuracy of the input information.

It was expected that the ATS model information listed and discussed in sections 3.1, 3.2, and 3.3, as well as the requisite information anticipated for Q4 would be the entirety of the information required to achieve the optimization methodology desired in Q1. Thus Q2 is also only partially answered at this stage. However the research in sections 3.1, 3.2, and 3.3, did highlight several pieces of previously unconsidered ATS information that, when included, were capable of causing significant variation in the optimization results in terms of either the values of the result, or in the time required to compute them.

The key information incorporated in section 3.1 was airspace region based data; i.e. weather and airspace regulation information that can vary unpredictably across a trajectory. This information became important to the accuracy of the results as it led to aircraft conflict being defined the same way, i.e. as airspace region based data. While variation in weather and airspace regulation information had not been tested for, it was clear from the results seen in section 3.4 that optimized trajectories would conform tightly to the avoidance of aircraft conflict so as to minimize as much as possible their impact on the trajectory. Thus if aircraft conflict had been defined using airspace regions with a larger area, in lieu of the square nautical minute currently being used, then it would have a corresponding increase in aircraft conflict size and in aircraft trajectory distance spent avoiding conflict.

However it would also have a corresponding decrease in requisite computation time, so direct theoretical trade-offs between accuracy and optimization calculation time could also be made if so desired.

The key information incorporated in section 3.2 was potential trajectory data; i.e. the individual definition of the domains of each and every optimized parameter of a given trajectory. As section 3.2 discussed, these limits on the optimizer variable were originally intended to minimize the size of the optimization problem and to prevent unrealistic results, however when combined with the airspace region definition of aircraft conflict developed in section 3.1, the size of the optimization problem was further reduced by being able to recognize, before the optimization process began, which aircraft conflicts could and could not happen. Due to the spherical nature of the earth surface, all trajectories have the ability to intersect any other trajectory, thus determination of potential conflicts would require comparative checks for each aircraft against all other aircraft. However as the optimizer variable limits are known in terms of time and altitude for every individual airspace region, conflict can be recognized as only occurring when an individual airspace region contains within it multiple aircraft with overlapping optimizer variable limits. This thus causes optimizer computation times to be more affected by the peak four dimensional densities of air traffic within the region, rather than the total number of aircraft within the same.

The key information incorporated in section 3.3 was the superelliptical separation model and the correlation methods between aircraft performance and optimizer control of air traffic trajectories. As section 3.3.3 showed, the superelliptical separation model was introduced because nonlinear optimization methods were not sensitive to the existence of alternate separation modes in any particular conflict. Introducing superelliptical separation provided the optimizer with additional gradient information that indicated the existence of those alternate separation modes, thereby allowing the optimizer to appropriately switch between those modes. This also prevented the requisite use of a combinatorial or random type of optimizer which, as discussed in section 2.3, can cause further accuracy issues yet were the dominant method of automatically handling separation. The impacts on optimizer sensitivity due to the optimizer's correlation methods are twofold and simultaneously due to the disassociation of the ATD index for calculating aircraft performance from the ATD index for the optimizer's control of air traffic trajectories, which was discussed in section 3.3.5. The first impact stemmed from allowing user defined values for the ATD interval between trajectory changes in climb angle and speed; lower ATD intervals would require more computation time but result in reduced impact of conflict avoidance by allowing trajectories that mould closer to conflict, while higher ATD intervals would increase the impact of conflict avoidance but would require less computation time and could facilitate improved aircrew and cabin conditions as well. The second impact stemmed from the disassociation of ATD indices allowing significantly smaller ATD intervals for performance calculation; while the expected improvement in performance accuracy was not measured, section 3.3.5 did show how proper synchronization of the two ATC indices did limit the unrealistic exploitation of discontinuities (i.e. where pilots are expected to change climb angle and speed to follow an optimized trajectory) to reach lesser ATFU values.

3.5.2.3 Q3: How can constraints such as aircraft performance limitations, minimum separation and on-time arrival be incorporated into an optimizable UPT, and how do these affect total fuel usage?

While Q3 was intended for research on improvements on the optimizer that are not discussed in this chapter, the results of this chapter do highlight how these constraints can be incorporated and what kind of affect they would

have on optimized fuel usage. As shown in section 3.3, most of these constraints are applied as non-linear constraints; they could not be simplified enough so as to approximate a linear relationship with the optimizer variables. Even the linear constraints and bounds that are currently used can be argued as being rough approximations of nonlinear interpretations of the physical limiting phenomena they represent, e.g. the optimizer speed and altitude bounds that are independent of aircraft state. Consequently the following chapters will show that as the definition of constraints become necessarily more non-linear, the impact on optimization results due to linear and bound constraints decreases, while the impact due to the interaction between non-linear constraints increases. It should be noted that this trend towards non-linearity is preferable, as it allows the non-linear optimizer to more correctly interpret the interaction between constraints, which is necessary for accurate optimizations of ATFU.

Each of these limitations, in their current formulation, always caused ATFU to increase; as Figure 17 showed, the most optimum aircraft fuel usage was always beyond the extremes of the optimizer variable, and therefore always on the infeasible side of a constraint. However as they constrain different aspects of a trajectory, their associated ATFU increases are carried out in different ways, each of which is shown in the results in section 3.4. The most significant of the constraints is minimum separation as it forces aircraft to avoid each other; assuming the flight plan prior to conflict avoidance had optimal fuel efficiency, carrying out the conflict avoidance will create a sub-optimal trajectory. The optimizer will mitigate the loss in fuel efficacy by optimizing the flight prior to and after the conflict, however the cause for efficiency loss is the conflict and cannot be entirely removed without also removing the conflict. The aircraft performance limitations, in terms of T_{req} and C_{lmax}, restrict variation in trajectory profile by limiting climb angles and speeds; this increases the loss of fuel efficiency due to conflict as a lesser ability to vary trajectory profile means more flight time and distance spent away from an optimum trajectory. The on-time arrival constraint is similar in that it causes portions of a trajectory to be less fuel efficient in order to facilitate the time difference required to arrive at a destination at a particular time. The arrival time constraint is different in that the impact of aircraft performance constraints on trajectory is proximate to the points of conflict during the trajectory due to the need to mitigate undesirable fuel usage caused by avoiding conflict; however as time difference can be acquired from any part of the trajectory, the necessary change to the trajectory is distributed over the entirety of the trajectory as minute speed changes that cause the necessary time difference to appear at the end of the trajectory.

3.5.2.4 Q4: How can a dynamic environment, such as deviation from or in-flight changes to the flight plan, airspace closure, and emergency diversion, be accommodated in an optimisation methodology?

Like Q3, Q4 was not intended to be answered at this stage of the research; however, unlike Q3, none of the necessary research to facilitate it had been attempted before this stage of the research and consequently goes unanswered at this point.

4. BADA AIRCRAFT PERFORMANCE MODEL

In PCO, the fuel function was based on standard flight mechanic equations for fuel usage and assumed a constant specific fuel consumption to allow more advanced methods for calculating fuel consumption to be superimposed on it. BADA, given its depth in modelling a comprehensive range of aircraft performance phenomena for a broad variety of aircraft, was an ideal representation of such advanced methods and was thus a logical choice for improving the accuracy of the optimizer further. It was also the only database, at the time of research, which publicly disclosed its fuel usage calculation methodology [38], which effectively excluded other databases, including Flight Simulator X, for consideration in this research as the validity of their methods could not be confirmed. Consequently this chapter describes how the Original Fuel Function, OFF, and a BADA Fuel Function, BFF, have noticeable differences in calculation despite performing the same function, How these differences are overcome, and the pertinent lessons learned, are described in the first two parts of this section. In the last part a functional assessment will show the capability of the resulting BFF based PCO, or BFO, via mapping its results over the entirety of the optimizer variable domains, and through reruns of optimizations used to test the original optimizer. Throughout testing and development the raw data file [56] shown in Figure 30 was used to define the B747-300, which in turn is used in this chapter to explain the mechanics and expectations of the improvements brought about in using BADA. Other aircraft were used for testing and validation and are defined in detail in section 0 where their results are discussed.

```
CCCCCCCCCCCCCCCCCCCCCCCCCCCCCCCCCCCCCCC B743__.OPF CCCCCCCCCCCCCC/
CC                                                                /
CC                AIRCRAFT PERFORMANCE OPERATIONAL FILE           /
CC                                                                /
...
CD                                                                /
CC====== Actype ================================================/
CD   B743__          4 engines    Jet                      H     /
CC           B747-306                                    wake    /
CC                 (source = KLM OPS manual & BOEING data)       /
CC====== Mass (t) ==============================================/
CC    reference      minimum      maximum     max payload  mass grad  /
CD     .31000E+03   .17400E+03   .37780E+03   .69100E+02   .71400E-01 /
CC====== Flight envelope =======================================/
CC     VMO(KCAS)        MMO        Max.Alt       Hmax       temp grad  /
CD     .36000E+03   .90000E+00   .45000E+05   .32200E+05  -.28300E+03 /
CC====== Aerodynamics ==========================================/
CC Wing Area and Buffet coefficients (SIM)                        /
CCndrst Surf(m2)     Clbo(M=0)       k          CM16              /
CD 5   .51123E+03   .10700E+01   .39000E+00   .00000E+00           /
CC   Configuration characteristics                                /
CC n Phase  Name    Vstall(KCAS)    CD0          CD2        unused    /
CD 1 CR   Clean     .19300E+03   .20000E-01   .50000E-01   .00000E+00 /
CD 2 IC   Flap05    .14900E+03   .00000E+00   .00000E+00   .00000E+00 /
CD 3 TO   Flap20    .13700E+03   .00000E+00   .00000E+00   .00000E+00 /
CD 4 AP   Flap20    .13700E+03   .00000E+00   .00000E+00   .00000E+00 /
CD 5 LD   Flap30    .12200E+03   .00000E+00   .00000E+00   .00000E+00 /
...
CC====== Engine Thrust =========================================/
CC         Max climb thrust coefficients (SIM)                    /
CD     .57342E+06   .58255E+05   .99400E-12   .96566E+01   .68000E-02 /
CC      Desc(low)    Desc(high)   Desc level   Desc(app)    Desc(ld)  /
CD     .52000E-01   .26900E-01   .15000E+05   .00000E+00   .00000E+00 /
CC      Desc CAS     Desc Mach    unused       unused       unused    /
CD     .30000E+03   .85000E+00   .00000E+00   .00000E+00   .00000E+00 /
CC====== Fuel Consumption ======================================/
CC   Thrust Specific Fuel Consumption Coefficients                /
CD     .95260E+00   .10000E+15                                    /
CC   Descent Fuel Flow Coefficients                               /
CD     .38197E+02   .53810E+05                                    /
CC   Cruise Corr.    unused       unused       unused       unused    /
CD     .99560E+00   .00000E+00   .00000E+00   .00000E+00   .00000E+00 /
...
CC=================================================================/
FI                                                                /
```

Figure 30 - Extract from the BADA Aircraft Performance File of the B747-300 [56].

4.1 Differences for the purposes of calculating fuel usage

BADA, particularly version 3.6 which is used here, derives its ability to define fuel usage through curve fitting accumulated performance data of particular aircraft makes and models, to a Total Energy Model, or TEM, with coefficients therein being varied to match the data [38]. The TEM, as shown in equation (22), is an assessment of the known forces acting upon an aircraft, but modified for the perspective of energy use; as such, the methods of calculating fuel consumption in a BFF would be similar to the classical methods previously used in the OFF. Assuming T as thrust, D as aerodynamic drag, m as aircraft mass, h as altitude, g as gravitational acceleration, V_{TAS} as true airspeed, and d/dt as the time derivative, the TEM equation as used by BADA is:

$$(T - D).V_{TAS} = m.g.\frac{dh}{dt} + m.V_{TAS}.\frac{dV_{TAS}}{dt} \quad \textbf{(22)}$$

BADA also incorporated engine specific data into determining fuel consumption, which is a notable difference between it and the OFF. The fuel consumption formula for jets is shown in equation (23), with the moulded coefficients therein representing a particular aircraft's performance; different formula and coefficients are used for aircrafts with turboprops and piston engines, with a full listing of all such shown in Appendix H. Combining V_{TAS} with the thrust specific fuel coefficients, C_{f1} and C_{f2}, a cruise fuel flow cruise correction coefficient, C_{fcr}, and appropriate dimensional converters, yielded the BADA formula for μ:

$$\mu = \frac{C_{f1}}{60 \times 1000} \times \left(1 + \frac{V_{TAS_i} \times 1.9438}{C_{f2}}\right) \times C_{fcr} \quad \textbf{(23)}$$

Other than incorporating more accurate engine specific data, the original and BADA method of calculating fuel consumption were had no other pertinent differences. The TEM, rearranged for required thrust at a particular ATD_i and assuming that $D = C_D.\rho.V_{TAS}^2.S / 2$, $W = m.g$, $dV_{TAS}/dt = a$, and $dh/dt = V_{TAS}.\sin\gamma$, yields:

$$T_{req_i} = C_{D\_i}.\frac{1}{2}.\rho.V_{TAS\,i}^{\,2}.S + W_{i-1}.\sin\gamma_i + m.a_i \quad \textbf{(24)}$$

Which, assuming acceleration of zero is functionally no different from equation (15) and the thrust calculations currently in the OFF. Thus, with only the modified fuel consumption rate and a swap of all aircraft specific data, as shown in Table 3, with their corresponding BADA equivalents, as shown in Figure 30, it is possible to initially modify the OFF to use BADA information of a Boeing 747-300 and thereby ensure that the resultant fuel usage amounts were in the same order as the OFF. The visual results of the comparison are shown in Figure 31 and Figure 32 and assume the aircraft took off with *MTOW*. The magnitudes of the two Fuel Functions indicate that the initial interpretation of the BADA methods and the OFF are roughly similar, thus suggesting that the BADA information and coefficients were correctly used. Further, the BFF generally calculated slightly lower fuel usage estimates than the OFF; these were more in line with publicly known Boeing 747-300 fuel usage rates and so caused greater confidence in the correctness of the BFF.

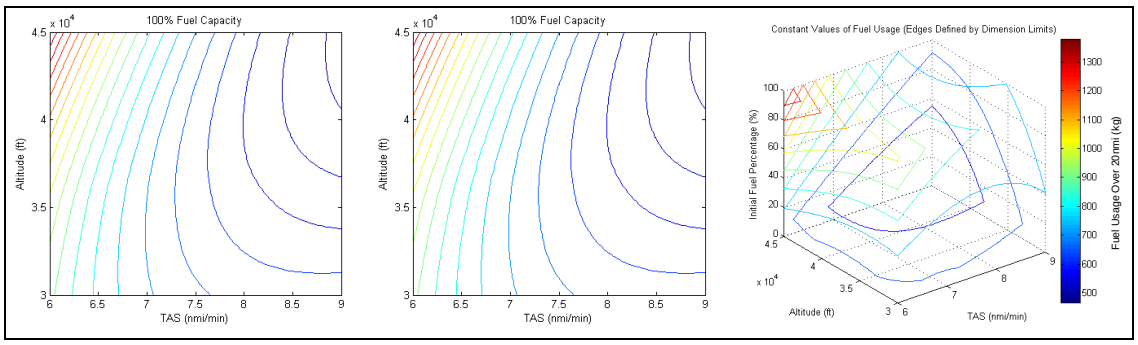

Figure 31 - OFF or Original Fuel Usage Contours over 20nmi assuming 100%, 40%, and variable Initial Fuel Capacities.

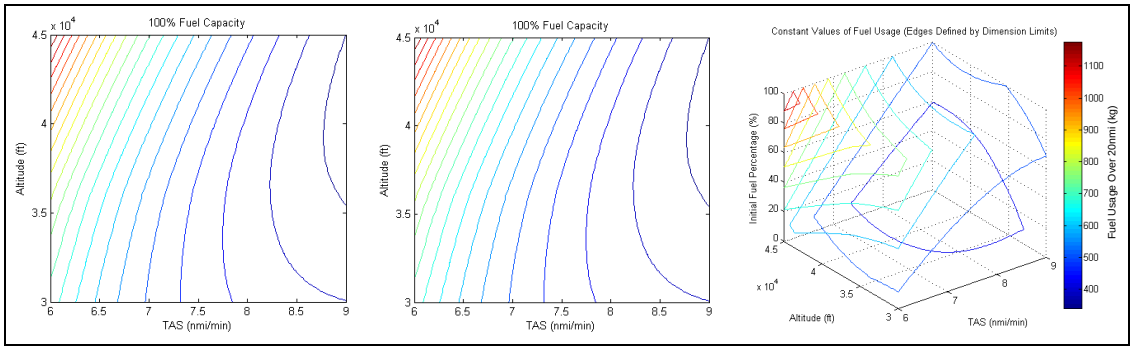

Figure 32 - BFF or BADA Fuel Usage Contours over 20nmi assuming 100%, 40%, and variable Initial Fuel Capacities.

4.2 Differences for the purposes of optimizing fuel usage

With the BFF providing results with improved accuracy, a few components in the optimizer had to be checked, and altered if necessary, to ensure the capabilities of the optimizer. These checks were required due to differences in the way BADA handled data as compared to PCO. The components that required checking included the optimizer variable and its limits, the variable converters present in the fuel and separation functions, the constraints present in the fuel function, and the requisite optimizer tolerances for them; all other components were not altered in any way.

4.2.1 Optimizer Variable and its Limits

While developing the original, the optimizer variable was a concatenation of the altitudes (in 10k ft) and velocities (True Airspeed, TAS, in nmi/min) that an aircraft would adhere to whilst flying a predefined route; the velocity and altitude pairs are defined using an ATD control node index, or ATD_N, which sets the pairs at roughly 20 nmi intervals. Constant bounds were placed on altitudes in the form of a 30kft lower limit and a maximum altitude defined by the maximum known operating limit for a Boeing 747-300. Constant bounds were placed on velocities in the form of the known stall and maximum TAS speeds for a Boeing 747-300. No linear limits were applied to TAS variables; however a maximum climb or descent angle of 1.5 degrees was used to prevent passenger and crew discomfort due to frequent variations in altitude. For the BFO, all of these were checked for necessary changes. The use of altitudes and TAS for the optimizer variable was kept the same however there was significant reason to do otherwise; keeping altitude as part of the optimizer variable was required to ensure that the bounds and linear limits placed on it were maintained, however the BADA limits that existed on aircraft speed were defined by Mach number and Calibrated Airspeed (CAS) limits and not TAS.

A minor but notable question that was researched at this stage was the validity of using CAS as a replacement for TAS in the optimizer variable; the rationale being that CAS was related directly to more of the BADA defined performance constraints than TAS was and could thus lead to optimums that were either faster to compute or were more fuel efficient. Trials were thus performed with TAS and its limits replaced by CAS and its limits, alongside the necessary converters to allow TAS based calculations to work. However the resulting optimizations showed a lack of robustness that the PCO optimizer had; a large number of optimizations failed to converge or to satisfy all constraints. It was suspected that because resultant TAS was defined by an aircraft's current CAS as well as altitude, using CAS as an optimizer variable placed a greater number of restricting constraints on varying altitude thereby preventing optimizations to reach previously achieved optimums; given this, the optimizer was changed again to use TAS, and the potential use of CAS in the optimizer was abandoned.

The bounds that were previously used on CAS, when it was trialled as an optimizer variable, were thus transferred to the Fuel Function as a performance constraint alongside the Mach limits that were also introduced for CAS. The only changes that were effectively required were in the bounds and limits of the optimizer variable. The maximum altitudes were altered to reference BADA data on the maximum operating altitude for the aircraft concerned. Minimum altitudes had to be dropped to allow interaction between jet, turboprop and piston aircraft (i.e. the engine types defined by BADA), yet still be above the maximum known transition level so as to allow focus on cruise and minor variations in altitude (i.e. the maximum 1.5 degree climb/descent angle

that was kept) rather than fast climbs and descents. The transition level is the lowest flight level that occurs after an aircraft reaches an altitude where it switches between defining altitude as a distance above sea level to altitude as a distance defined by variation in pressure i.e. flight level; as a consequence it is a common point in a trajectory where an aircraft switches from post take off climb to steady state cruise. The highest known transition altitude is observed in North America at 18kft, thus with a buffer defined by Δh_{min}, the minimum altitude set for the research from this chapter onwards is 20kft. As velocity bounds were now performance based and sitting in the Fuel Function, the range of allowable TAS was widened to prepare for the variation allowed by the program, the maximum and minimum TAS are, respectively and nominally, 2 and 20 nmi/min; no scenarios where either of these constraints have been actively used has been encountered.

4.2.2 Variable Conversion

Perhaps the biggest change from the PCO was the inclusion of acceleration. The TEM does take into consideration the impact of acceleration on fuel usage, whereas the OFF and optimizer variable converters relied on velocity being constant; this assumption allowed the use of fuel calculation methods reliant on near zero acceleration to also be used. It is possible, given the range of forces acting on the aircraft, for the acceleration it experiences to be significantly non-linear; if so, it would require the use of computationally expensive solvers or interpolators to handle accurate extraction of time and acceleration data from the optimizer variable. However even with the additional computational expense, the accuracy of the solvers or interpolators would be unknown, and the usefulness of having that accuracy becomes debatable. As a temporary compromise, constant acceleration during an ATD step is assumed; this allows extraction of time and acceleration data to become linear and avoids the use of expensive solvers or interpolators. Only trials with real data can determine if this sufficiently accurate or not.

4.2.3 Aircraft Performance Constraints

While the method of fuel calculation between the original and BFF are similar, the way BADA created its data causes it to have different performance based constraints. The OFF had constraints on minimum and maximum thrust as well as on maximum coefficient of lift. The BFF had nonlinear constraints on maximum altitude, Mach number and longitudinal and normal acceleration, as well as minimum and maximum velocity and thrust; it did not have a direct constraint on coefficient of lift but this was satisfied via a combination of the other constraints. The subsections below show how the original BADA aircraft performance limits, i.e. equations (25), (28), (30), (32), (34), (37), and (38), were recreated as constraints, i.e. equations (26), (27), (29), (31), (33), (35), (36), (39), and (40), in the BFF, whilst discussing their physical correctness and potential improvement. Each constraint would be calculated for each element in ATD_i.

4.2.3.1 Maximum Altitude

The BADA maximum altitude constraint is based on the minimum between two values; a static maximum operating altitude, H_{MO}, or a formula representing a possibly lower maximum altitude defined by the aircraft's current state and environment. The latter is defined by an aircraft's maximum altitude at maximum take-off weight, H_{max}, the difference between local sea level and ISA temperature, ΔT_{ISA}, a thrust temperature coefficient,

$C_{tc,4}$, the maximum and actual aircraft masses, m_{max} and m_{act}, and the corresponding temperature and mass gradients, G_t and G_w, to turn them into a maximum altitude. The full combined constraint on altitude, h, is:

$$h \le MIN\left[H_{MO}, H_{\max} + G_t \times \left(\Delta T_{ISA} - C_{tc4}\right) + G_w \times \left(m_{\max} - m_{act}\right)\right] \quad \textbf{(25)}$$

The BADA manual did indicate that G_t and G_w were derived from historical data of the aircraft model regarding the maximum altitudes achieved at various temperatures and aircraft weight; this limit is therefore a combined representation of the performance limits of the aircraft engine and aerodynamics under those conditions, and thus at least partially covers the PCO thrust and coefficient of lift constraints. However given that it does not require data of the aircraft's current velocity it can be considered as only a domain limit on the altitudes of the optimizer variable and does not affect how the optimizer satisfies thrust and coefficient of lift constraints within that domain.

While MatLab optimizers have some capability of handling combined constraints like above, given previous experience in 3.3.3.1, it was deemed better to separate constraints that would, when combined, create discontinuities that could hamper optimization. Further, the components of the maximum altitude constraint create an upper bound and a non-linear constraint, which are different optimizer inputs and thus had to be separated anyway. The combined minimum of the two is inherently satisfied by the fact that both must be true after optimization. The bound and non-linear constraints, reconfigured for optimizer use, are respectively:

$$h \le H_{MO} \quad \textbf{(26)}$$

$$\frac{h}{H_{\max} + G_t \times \left(\Delta T_{ISA} - C_{tc4}\right) + G_w \times \left(m_{\max} - m_{act}\right)} - 1 \le 0 \quad \textbf{(27)}$$

4.2.3.2 Mach Number Limit

The BADA maximum Mach number is defined by a maximum operational Mach number, M_{MO}, which is taken from the aircraft manufacturer's intended Mach limit for that aircraft model. As a constraint, it only requires that any experienced Mach number be less than M_{MO}. Given that the Mach number is defined by V_{TAS}, the universal gas constant, R, the isentropic expansion coefficient for air, k, and the altitude dependant local temperature, T_{local}, this combined constraint is defined as:

$$V_{TAS} \times \left(k \times R \times T_{local}\right)^{-0.5} \le M_{MO} \quad \textbf{(28)}$$

As an optimizer constraint, despite T_{local} being discontinuous at a point in allowable altitude (temperature is constant above tropopause and linear below it), no undesirable optimizer results have yet been seen that were linked to this issue and the constraint has been left as:

$$\frac{V_{TAS} \times \left(k \times R \times T_{local}\right)^{-0.5}}{M_{MO}} - 1 \le 0 \quad \textbf{(29)}$$

4.2.3.3 Acceleration Limits

BADA has a limit, $a_{lmax(civ)}$, on longitudinal accelerations for civil flights that is defined for a time interval, Δt, via change in V_{TAS} during that interval, ΔV_{TAS}. It and its corresponding global constraint equivalent are:

$$\left|\Delta V_{TAS}\right| \le a_{l\max(civ)} \times \Delta t \quad \textbf{(30)}$$

$$\frac{\left|\Delta V_{TAS}\right|}{a_{l\max(civ)} \times \Delta t} - 1 \le 0 \quad \textbf{(31)}$$

The BADA limit on normal acceleration, $a_{nmax(civ)}$, is similar to longitudinal acceleration but based on change in γ, $\Delta\gamma$, as well. It and its corresponding global constraint equivalent are:

$$\left|\Delta\gamma\right| \le \frac{a_{n\max(civ)} \times \Delta t}{V_{TAS}} \quad \textbf{(32)}$$

$$\frac{V_{TAS} \times \left|\Delta\gamma\right|}{a_{n\max(civ)} \times \Delta t} - 1 \le 0 \quad \textbf{(33)}$$

It should be noted that these are BADA defined limits and, while derived from known safe human limits, have no correlation with the acceleration limits that crew and airlines may wish to use during flight. As for their correctness as acceleration limits, their weak point of using average acceleration to question the limit is offset by the optimizer's assumption of constant acceleration; if the optimized had assumed nonlinear, or even linear, acceleration modes between ATD_i, then these equations would have had to change.

4.2.3.4 Thrust Limits

The required thrust, T_{req}, for a given ATD_i was found by calculating equation (24) for that interval, after fuel usage calculations had been performed so as to give a more accurate figure. Maximum thrust, T_{MAX}, like equation (23), is based on the aircraft engine type, as well as the current flight phase. For a jet in cruise:

$$T_{req} \le T_{MAX} \Rightarrow T_{req} \le C_{Tcr} \times C_{Tc1} \times \left(1 - \frac{h}{C_{Tc2}} + C_{Tc3} \times h^2\right) \quad \textbf{(34)}$$

Where C_{Tcr} was the aircraft's cruise thrust coefficient, and C_{Tc1}, C_{Tc2}, C_{Tc3}, were the first through third climb thrust coefficients; all such coefficients being BADA defined and constant for an aircraft. This, like the Maximum Altitude limits in section 4.2.3.1, is also derived by BADA from the collective trajectory histories of the aircraft model in terms of what thrusts were sustained at which altitudes. It should be noted that the Turboprop version of this equation does contain a velocity parameter so the lack of one in this equation for Jets implies that it was considered as unnecessary. This is particularly important as coefficient of lift is constrained, through T_{req}, in this equation, and therefore concern is made on its correctness as a coefficient of lift constraint. However, this issue remains unsolved as, from one perspective coefficient of lift is treated as a setting for various modes of flight and thus has discontinuities in the way it changes, while from another other perspective coefficient of lift always has a technological limit which should be observed. Out of respect for its non-appearance in BADA a direct limiter on coefficient of lift is not applied at this stage, however if one should ever be considered, its interaction with equation (34) would have to be assessed for phenomena that could cause the optimizer to not find an optimum.

Regardless of its issues with coefficient of lift, equation (34) was needed, and the corresponding optimizer constraint was initially similar in form to other constraints, i.e. T_{req} over T_{MAX} minus one. However it was found that this form was too highly non-linear for the optimizer; as h increases T_{MAX} can approach zero and T_{req} can increase via increase in climb angle, thereby giving divisions drastically greater than one. This caused the constraint to be highly sensitive to variations in X and restricted any optimization that significantly affected thrust. To prevent this, the actual and maximum were separated and had appropriate normalizing coefficients applied before being combined linearly to represent the constraint; this reduced the likelihood of an unexplained breached constraint by minimizing the impact of vastly different actual and maximum thrusts being combined. The final constraint is shown below with all other similarly derived thrust constraints shown in Appendix H:

$$\frac{T_{req}}{C_{Tcr} \times C_{Tc1}} - \left(1 - \frac{h}{C_{Tc2}} + C_{Tc3} \times h^2\right) \leq 0 \quad \textbf{(35)}$$

While BADA did not specify a minimum thrust for the aircraft, one was necessary due to the ability of the optimizer to create situations where T_{req} was calculated to be negative. Thus on the assumption that all aircraft would not cause negative thrust during cruise, i.e. via control surfaces that increase drag, a constraint requiring T_{req} to be above zero was needed:

$$-\frac{T_{req}}{C_{Tcr} \times C_{Tc1}} \leq 0 \quad \textbf{(36)}$$

4.2.3.5 CAS Limits

As mentioned previously in 4.2.1, an attempt had been made to switch the TAS in the optimizer variable to CAS; the process would have used the following BADA equation and its inverse:

$$V_{CAS} = \left[\frac{2.(P_0)_{ISA}}{\mu.(\rho_0)_{ISA}}\left\{\left(1 + \frac{P}{(P_0)_{ISA}}\left[\left(1 + \frac{\mu.\rho}{2.P}V_{TAS}^2\right)^{1/\mu} - 1\right]\right)^{\mu} - 1\right\}\right]^{1/2} \quad \textbf{(37)}$$

Where P is local pressure, ρ is local density, μ is $(k-1)/k$, and $(*_0)_{ISA}$ are the ISA sea level equivalents. P and ρ are similar to T_{local}, and therefore are discontinuous at tropopause and linear or non-linear elsewhere. While CAS is not used for the purposes of trajectory and fuel usage prediction, BADA limits on velocity are CAS based, and so used there. Further, these limits are taken from the manufacturer limits of the aircraft so goes unquestioned in terms of physical correctness. The BADA defined minimum and maximum velocity are respectively; the stall speed, V_{stall}, at cruise for aircraft modified with a global minimum speed coefficient, C_{Vmin}, and the maximum operating speed, V_{MO}, both in CAS. I.e.:

$$\left(C_{V\min} \times V_{stall}\right) \leq V_{CAS} \leq V_{MO} \quad \textbf{(38)}$$

The constraints are nonlinear due to equation (37) and respectively are:

$$1 - \frac{V_{CAS}}{\left(C_{V\min} \times V_{stall}\right)} \leq 0 \quad \textbf{(39)}$$

$$\frac{V_{CAS}}{V_{MO}} - 1 \leq 0 \quad \textbf{(40)}$$

4.2.4 Optimizer Settings

Using the previously list of alterations with the BFO without any further alterations was possible, and decent results were the norm. However, in some cases, particularly where points in the optimizer variable were pushing against multiple constraints, it was possible for the point to remain fixed at a clearly non-optimum position. After consideration of the accuracy of the BADA model, it was shown that the default settings in the BFO were expecting BADA to be overly accurate; the default setting was 1e-6, the minimum number of significant figures in BADA, i.e. 2, suggested that a tolerance of somewhere between 1e-1 and 1e-2 would be appropriate for constraints that are critical between ±1, with 1e-1 supposedly granting more flexibility with constraints, while 1e-2 would grant greater accuracy. After trials using 1e-1 were performed, it was found that a high percentage of scenarios still maintained an accuracy of greater than 1e-2. Thus as a compromise between flexibility and accuracy, the BFO was setup to perform one or two optimizations. The first optimization was set to 1e-1 constraint tolerance; if it was successfully optimized and adhered to 1e-2 constraint tolerance, then no further optimization would run. If the first failed to optimize or adhere to the lower constraint tolerance, then the optimizer would be run again using the previous optimizer result as an initial point and with the constraint tolerance set to 1e-2. If the optimization fails again, then it would be considered a thoroughly infeasible scenario.

4.2.5 Diagrammatic Representation of the BFO

Combining Figure 9, Figure 10, Figure 14, and Figure 15 into a functional flow diagram for PCO yields Figure 33, unaltered components of the PCO have been greyed out to show modifications.

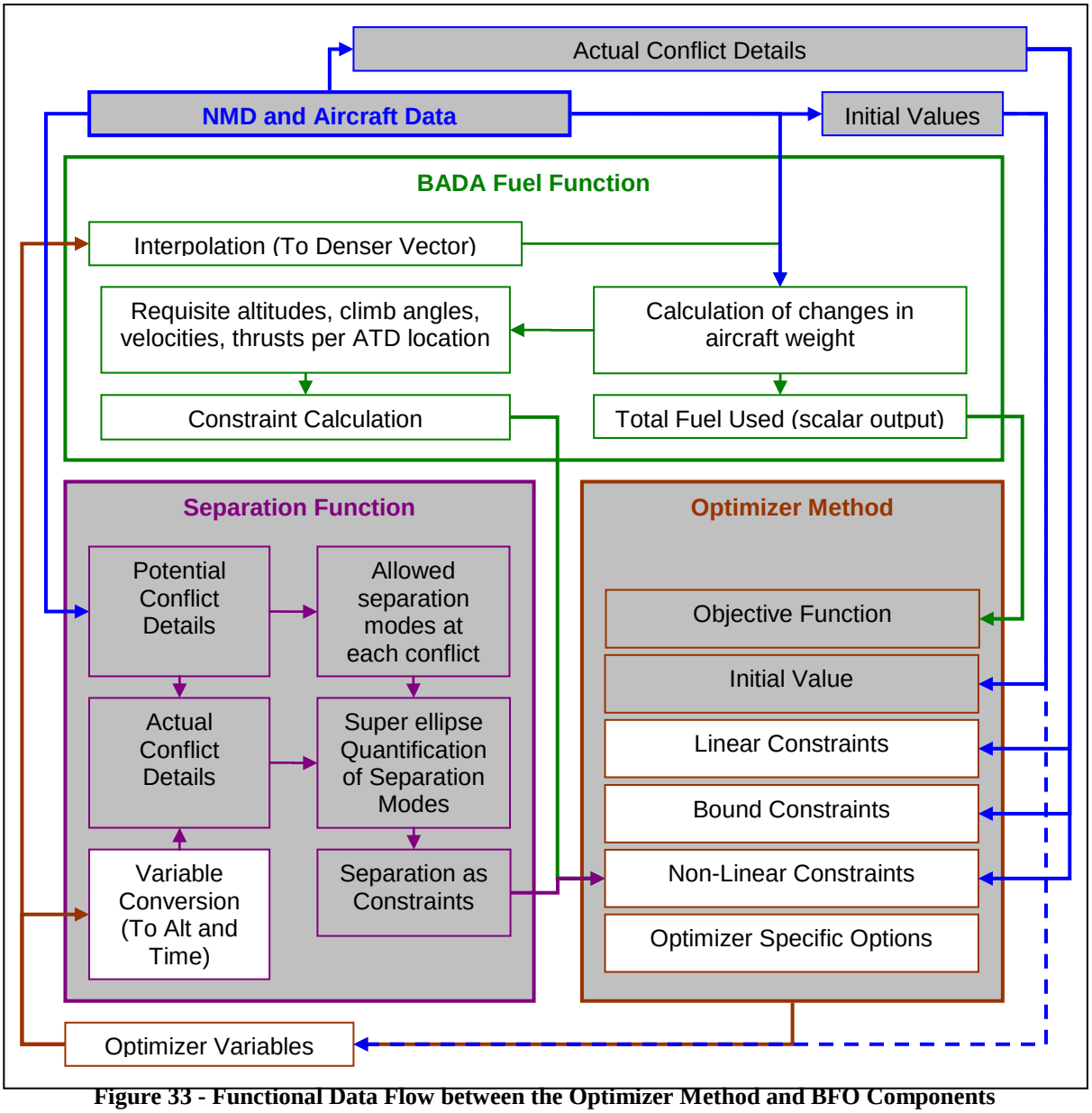

Figure 33 - Functional Data Flow between the Optimizer Method and BFO Components

4.3 Functional Assessment

To ensure correct BFO implementation four assessments were performed; the first was a simple feasibility study of the flight envelope using the BFF to determine fuel usage and performance constraints, the second was a study of the BFO sensitivity to varying numbers of control nodes, and the third and fourth were scenario trials of the BFO when using BADA data. The first assessment involved simultaneously determining the fuel usage and feasibility of various initial weights, velocities and altitudes, on scenarios of varying climb angles and accelerations. This assessment would act as validation for the accurate optimization of the BFF, as well as give indications of the kind of actions that the BFO would take to reduce ATFU. The second checks to see if the 20nmi step length hitherto used is the most effective in terms of optimizing fuel usage; it does by optimizing trajectories of the same route and aircraft properties but with different numbers of control nodes and consequently differently sized step lengths. The third and forth assessments are merely reruns of the same tests performed on the PCO prior to BFO; the third leaves the tests unchanged and focuses on ensuring that the same functionality is retained, while the forth trials the tests with alternative aircraft models that are available within BADA.

4.3.1 Validation of BADA based Fuel Usage Calculations

Given that the optimizer currently uses a non-linear optimization methodology, a key concern surrounds the sensitivity of BFF results due to variation in the optimizer variable; i.e. is it possible for variation in the optimizer variable to cause BFF results to become sufficiently discontinuous so as to prevent a true optimum from being reached? As an issue, this was ignored during OFF implementation for three reasons: first is because the literature, including [32], tacitly indicated that it would not be a problem; second is because the assessment in Figure 17 showed OFF variation to be continuous and well scaled over the entirety of the optimizer variable domain; and third was because the T_{req} and C_{lmax} limits were the only two active nonlinear constraints and both of these, even together, are not known for creating discontinuous flight envelopes. However for BFF development this could not be ignored for two reasons. The first is because there is no literature on non-linearly optimizing the BADA equations for minimum fuel usage and in consideration of BADA constraints; the closest alternative to the optimizer developed here, i.e. the method in [35], did use a linear optimization methodology however this was in combination with a Mixed Integer method that can handle discontinues, which, as mentioned in section 2.3, was already established in this research as being undesirable. Consequently, even though the OFF and BFF are similar, there is a need to ensure that the BFF, as an optimization problem, is as continuous as the OFF. The second reason is that it is not known if the combination of all BADA constraints on aircraft performance would cause discontinuities in the feasible region of the optimizer variable domain; i.e. regions in the optimizer variable domain where an optimum that satisfies all constraints could be found become separated by regions wherein all constraints cannot be satisfied. Were this to occur it would slow down optimization as the interior point methodology would also focus on the satisfaction of the unsatisfied constraint, rather than just the BFF result with respect to the constraints, to determine better optimums. Failure of the optimization process could also occur when the unsatisfied constraint gives no indication of the existence of feasible regions elsewhere; thus preventing the assessment of potentially better optimums.

As only the BFF model is being tested, there is no need to test entire trajectories or the interaction between them; the entirety of the BFF's output, given its current formulation, can be defined by simulating an aircraft's trajectory over a single ATD_n interval and using discrete combinations of initial and final speed, initial and final altitude, and initial fuel capacity, to define its performance over that interval in terms of its fuel usage and satisfaction of constraints. The initial and final speeds and altitudes are taken from the optimizer variable, and it is through these that the optimizer can control any individual trajectory segment. The initial fuel capacity, or the amount of fuel the aircraft has at the beginning of an interval, is the only property that the BFF carries between segments and thus by varying this property, a single ATD_n interval can become representative of any ATD_n segment in a complete trajectory. By design, and as mentioned in section 4.2.3, all other aircraft properties, e.g. thrust and Mach settings, are defined as that required to achieving the final speed and altitude set by the optimizer for that ATD_n interval assuming constant acceleration and are thus entirely dependent on these five variables. Therefore, by assessing various combinations of these five variables it becomes possible to assess how the BFF will react to being controlled by the optimizer variable. For the sake of simplicity these variables are reformulated in terms of initial fuel weight, average speed, average altitude, acceleration, and climb angle; this allows variation in BFF fuel usage and feasibility to be described in terms of varying initial fuel weight, average speed, and average altitude, while keeping acceleration and climb angle constant. The impact of various accelerations and climb angles can then be studied by doing the same for different yet still constant values of acceleration and climb angle. This reformulation is preferable as it is comparable to Figure 17, Figure 31, and Figure 32, which themselves are assessments of the OFF and BFF in the optimizer variable domain, and it gives insight into the impact of climb, descent, acceleration and deceleration, on a segment's fuel usage and feasibility.

To graph variation in BFF fuel usage and feasibility, the domain for initial fuel capacity (10%~100%) was divided into 15% increments and the domains for average speed (2nmi/min ~ 10nmi/min) and average altitude (20kft ~50kft) were divided into 100 increments each; the initial fuel capacity domain limits were defined by physical limitations and the average speed and altitude limits were taken from section 4.2.1. With a specific acceleration and climb angle set, the BFF was applied for each three value combination of initial fuel capacity, average speed, and average altitude, over a single ATD_n segment; as per previous testing, the ATD_n segment was set to 20nmi. To improve graphical resolution, the process was repeated three times, but each time reducing the domain limits to a domain increment just outside the feasible region for that domain; while this does improve graphical resolution it also means that regions in the optimizer variable domain are removed from the graph by virtue of no feasible BFF results being found in that part of the domain. Figure 34 describes the results of this process in specific detail for the same aircraft in Figure 32, i.e. a Boeing 747-300, while assuming zero acceleration and climb angle. Figure 35 through Figure 38 do the same but with non-zero accelerations and climb angles.

Figure 34 is a dual view of the flight envelope of a B743 as defined by its feasible fuel usage, i.e. that satisfies all constraints, over 20nmi with no acceleration or climb angle, at various altitudes, h, velocities, V_{TAS}, and initial on-board fuel volume as a proportion of total fuel capacity, F_i. It shows the expected and usually continuous tendency of the aircraft to reach lower fuel usages at faster speeds and higher altitudes. For this particular feasibility assessment five of eight constraints were present in the optimizer variable domain, but with only four forming the envelope. M_{MO} was responsible for the upper V_{TAS} limit above 280FL; the intersection between the varying and constant V_{TAS} limits occurring at tropopause. In contrast V_{MO} was responsible for the upper V_{TAS} limit below 280FL; the variation due to the effect of ρ on V_{CAS}. The upper h limit is formed by h_{MAX}; the effect of

reducing F_i on h_{MAX} visible in the rising upper h limit that is constant for a particular F_i. Lastly, V_{stall} was responsible for all lower V_{TAS} limits with its intersection with h_{MAX} defining feasible high altitude low speed trajectories; note that where h_{MAX} is greater than tropopause, its effect can be seen in the variation of V_{stall}. Further, it should be noted that the V_{stall} and V_{MO} induced limits are similar due to their similar method of calculation. The fifth constraint present but not visible was that of T_{MAX}.

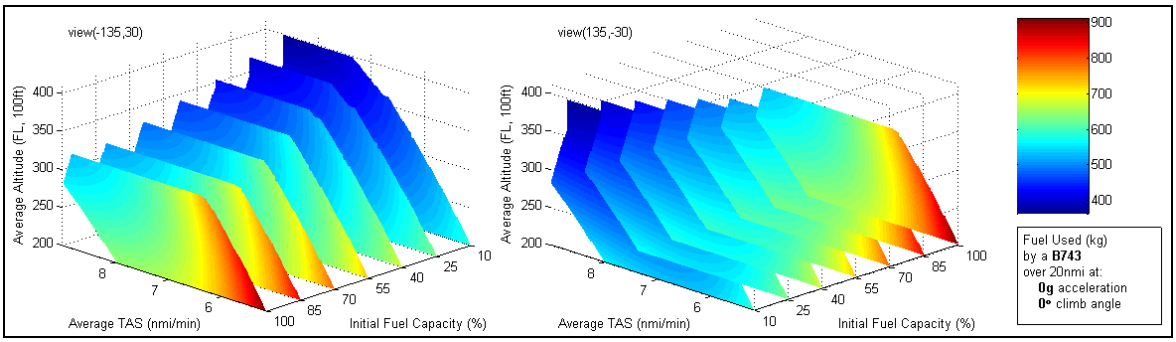

Figure 34 - Feasible Fuel Usage over 20nmi with no acceleration or climb angle.

Figure 35 and Figure 36 are similar to Figure 34 in that they all have five constraints active within the feasible optimizer variable domain, but with only four or less actually forming the envelope; however the two assessments describe an optimizer variable domain under positive acceleration and the slight differences can be taken as being indicative of that. In Figure 35 the typical impact of V_{MO} and V_{stall} can be seen respectively on the upper and lower V_{TAS} limits. The overarching constraint however comes from T_{MAX}; the positive acceleration and climb angle causing the T_{MAX} limit to only allow faster V_{TAS} at fairly low flight levels. While the M_{MO} and h_{MAX} limits are present, the T_{MAX} limit overshadows both. Figure 36 shows the impact a climb angle of any sort has on effective V_{TAS}; the severe V_{MO} and V_{stall} limits significantly reducing the feasible region between the upper and lower V_{TAS} limits, and V_{stall} limits completely overshadowing T_{MAX} limits. The other primary envelope edge is determined by the constant h_{MAX} limits, with M_{MO} limits affecting lower Fuel Capacities where the h_{MAX} limit is higher.

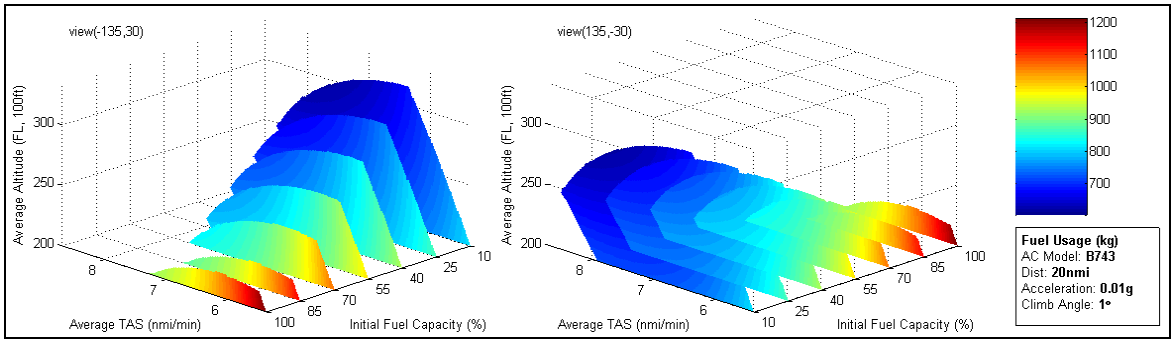

Figure 35 - Feasible Fuel Usage at a_l = 0.01g and γ = 1°

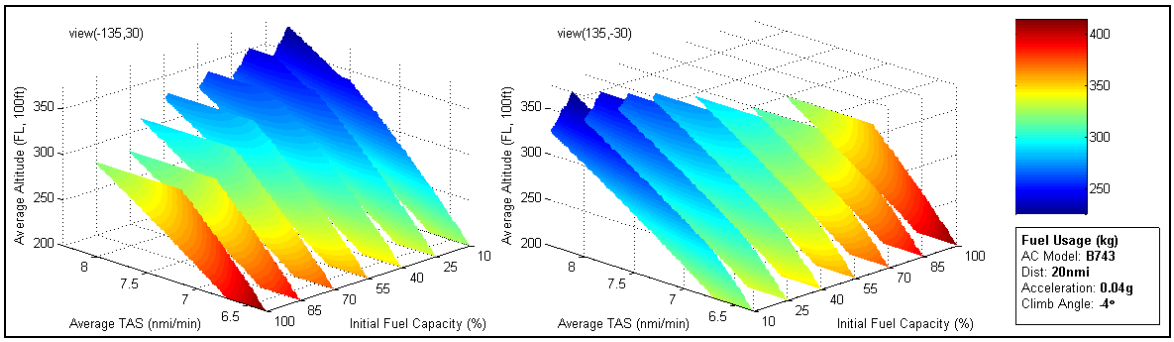

Figure 36 - Feasible Fuel Usage at a_l = 0.04g and γ = 4°

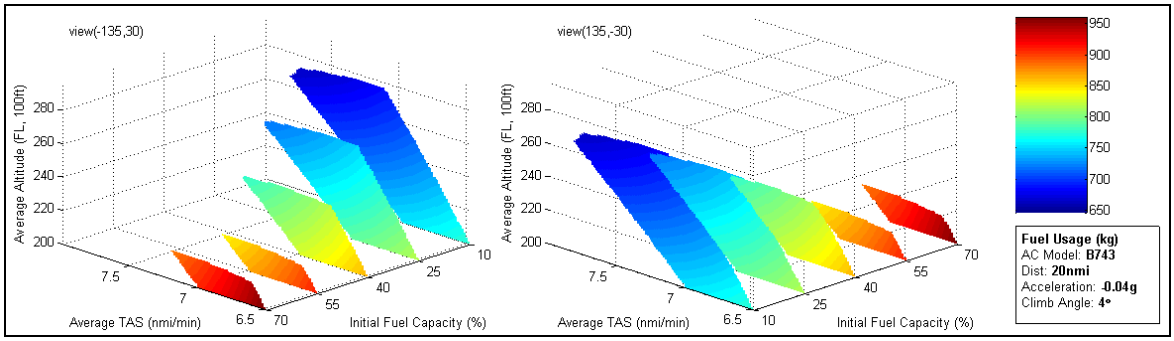

Figure 37 - Feasible Fuel Usage at a_l = -0.04g and γ = 4°

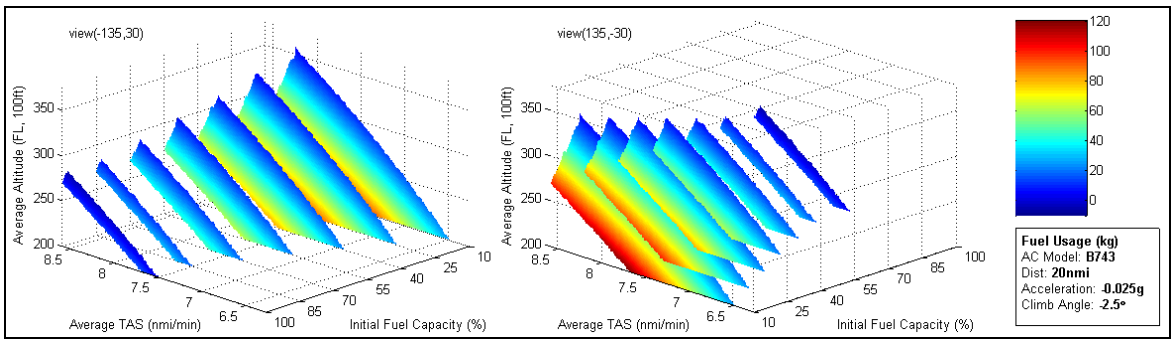

Figure 38 - Feasible Fuel Usage at a_l = -0.025g and γ = -2.5°

Figure 37 and Figure 38 are unique assessments that only have negative acceleration in common. Figure 37 only had three active constraints within feasible phase space with each forming an edge on the envelope. The V_{MO} and V_{stall} limits and their impact on the upper and lower V_{TAS} limits are similar to that in Figure 36 though deceleration is causing V_{MO} breaches to occur at higher average V_{TAS}, and V_{stall} breaches to occur at lower average V_{TAS}. The h limit between the two velocity limits possesses the similarly curved nature of the T_{MAX} limit shown in Figure 35 and is caused by the same, though significantly enhanced by the steep positive climb. Figure 38 describes a phase space that is similar to a pre-descent situation where the aircraft has built up speed that it no longer needs and is effectively gliding to the bottom of cruise airspace before it exits; the envelope edges are therefore formed with the V_{MO} and M_{MO} limits forming the upper V_{TAS} limit, and the lower V_{TAS} limit caused by T_{MIN} limits. The T_{MIN} limits are significantly enhanced due to the negative acceleration and climb angle to the point where they overshadow the h_{MAX} and V_{stall} limits that are also active within the same phase space.

The four examples above give perspective on the six aircraft specific performance constraints and how they vary according to requisite accelerations and climb angles. It should be noted however that the process is not exhaustive and, under extreme points in the altitude-speed-weight domain, can encounter non-realistic fuel usages and constraint regions; however that is a matter regarding the accuracy of the model and not discussed

here. It is sufficient for the purposes of the optimizer that the above five show results that, firstly, are continuous enough to be counted as continuous output, and secondly, have interactions between constraints that are not chaotic or are capable of creating separate feasible regions. Appendix I provide more detailed versions of these assessments for the B743. It should be known that this process was carried out for all aircraft from BADA 3.6 and did show that the trajectories of all sufficiently defined aircraft in BADA 3.6 could be optimized using the BFO. Consequently actual optimizations based on any of the models that Appendix I defines as acceptable, can be run with confidence in accurate results.

4.3.1 Second Assessment: BADA Fuel Optimization Sensitivity Analysis.

The main purpose of this assessment is to determine an effective step length for the purposes of fuel usage optimization. Before now, as mentioned in section 3.3.2, a step length of 20nmi was used as a rule of thumb for defining the number of control nodes in a trajectory. However with a different means of calculating fuel, the effectiveness of that distance may have changed; consequently there is a need to reassess the optimization of other step lengths to see if their differing number of control nodes can can generate similar or better fuel optimizations; the smaller the number of control nodes, the smaller the number of iterations the optimizer has to perform.

To perform this assessment of step length a BADA defined B747-300, with enough fuel to fill 25% of its total fuel capacity, is flown over the 678nmi route shown in section 3.4.3, and its trajectory is fuel optimized using the BFO. Step length variation occurred by varying the number of control nodes in the ATD_N; these control nodes were evenly distributed along the total flight distance and resulted in the step length between each ATD_N node decreasing as the number of nodes increased; e.g. at six control nodes there were five discrete trajectory 136.9nmi long steps, and, at 64 control nodes there were 63 discrete trajectory 10.86nmi long steps. Note that the PCO, and consequently the BFO, used two baselines for discretising a trajectory and that can be varied independently as a user input; these are ATD_N, which is the optimizer variable defined in section 3.3.2, and ATD_i, which is the index for fuel usage calculation defined in section 3.3.5. As the purpose of the second assessment was to test the sensitivity of the optimizer due to differing step lengths, there was a need to limit the impact of varying ATD_N against varying ATD_i, i.e. the trajectory optimization issues experienced and discussed in section 3.3.5 that allowed the optimizer to exploit inconsistencies at control nodes if fuel calculation nodes were placed in the same spot. Thus, this test maintained a four to one ratio between the number of nodes in ATD_N and ATD_i; i.e. four fuel calculation nodes in each step length, with one quarter of a step length between each subsequent fuel calculation node, and one eighth (i.e. one half of a quarter) of a step length between each control node and its neighboring fuel calculation nodes. The BFO results of increasing the number of control nodes from six to 64 for a 678nmi route is shown in Figure 39.

The expectation in increasing the number of control nodes, and consequently in decreasing the step length, was to further improve the optimization result by providing more points in the trajectory at which the optimizer can determine fuel efficient speed and altitude properties. However it is also expected that the improvement in optimizer result due to the addition of a control node will decrease as more control nodes are added; there will eventually be a point where the addition of a control node will have negligible improvement to the optimization result. Both of these expectations are shown in Figure 39. As the number of trajectory steps increased from five to ten, the amount of fuel used over the 678nmi fell by about 0.4% of the B747-300's total fuel capacity. As the

number of trajectory steps further increased from ten to 34, the amount of fuel used over the 678nmi only fell by another 0.05%. As the number of trajectory steps increased above 34, the amount of fuel used began to oscilliate and generated fuel usage values both higher and lower than when there were only 34 trajectory steps.

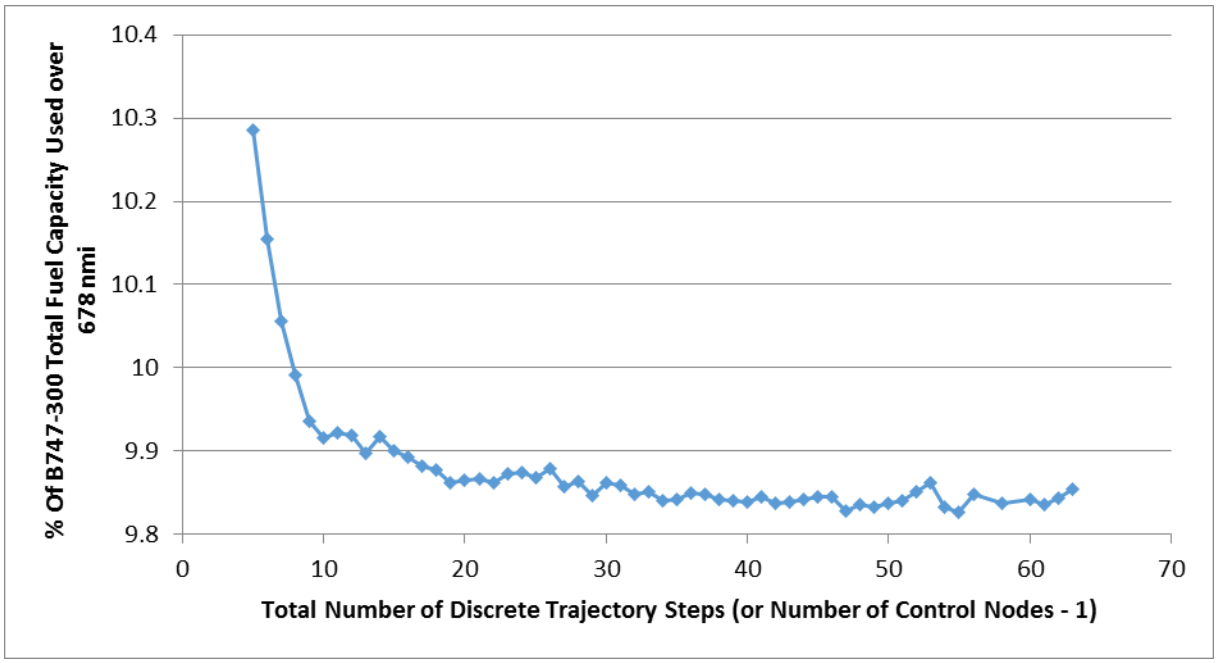

Figure 39 - The Impact of Step Length and Control Node Customization on Fuel Usage Minimization

Consequently, the step length created from having 34 trajectory steps over 678nmi is the optimal step length. At 34 trajectory steps, the step length was 20.13nmi, which only differs from the rule of thumb by 0.13nmi. With these results, it can be concluded that BFO optimizations of air traffic scenarios featuring the B747-300 can be effectively optimized by using control node step lengths of 20nmi. Remember however that this current system requires a trajectory's entire route to be divided into steps of equal length; unless the route length is an exact multiple of 20nmi, the step length actually used will differ slightly. Thus this 20nmi distance can only be used as a guide in determining the ideal number of control nodes for any trajectory; the methods shown in 3.3.2 for determining actual step length from ideal step length would still need to be applied to determine ATD_N.

4.3.2 Third Assessment: BFO interpretations of previous PCO trials.

The main purpose of this assessment is to ensure that the BFO can successfully perform the same scenarios that were trailed on the PCO. To do that, those same scenarios were rerun using the BFO. For these trials, many of the global constraints and settings used for the PCO remained the same. The BFO still used a $\Delta ATD_{N\ IDEAL}$, of 20nmi, $\Delta ATD_{i\ IDEAL}$ of 5nmi and a test field between 0 to 10° latitude and longitude. The blanket climb angle constraint of 1.5° was kept, but it was never noticed in any of the results as an active constraint during optimization and so was not considered relevant in the following discussions. The 8nmi/min speed used to schedule constrained arrival times was also kept and the results of using such are shown here alongside optimizations without a constrained arrival time. However because the aircraft model was different there were differences in what data was used for fuel and performance calculation as well as in the global constraints used on them; all of which was mentioned and discussed in sections 4.1 and 4.2. For clarity, the specifics of these

changes are detailed below with Table 6 showing the BADA data for a Boeing 747-300, i.e. Figure 30, in terms of the variables used in sections 4.1 and 4.2, and Table 7 showing the global constraints that were altered due to previous PCO results as well as the incorporation of BADA.

Table 6 - BADA Performance and Constraint Data for a Boeing 747-300 [56]

Thrust and Fuel Usage Calculation		**Height Constraint Calculation**	
Engine Type	Jet	h_{MO}	45000 ft
C_{f1}	0.953 kg.min^{-1}.kN^{-1}	H_{max}	32200 ft
C_{f2}	1e14 kt	G_t	-283 ft.C^{-1}
C_{fcr}	0.996	C_{tc4}	9.66 deg.C
C_{D0}	0.02	G_w	0.0714 ft.kg^{-1}
$1/(\pi.AR.e)$	0.05	M_{max}	378 t
S	511 m^2	**Thrust Constraint Calculation**	
Speed Constraint Calculation		C_{Tcr}	0.95
M_{MO}	0.9	C_{Tc1}	573000 N
V_{stall}	193 KCAS	C_{Tc2}	58300 ft
V_{MO}	360 KCAS	C_{Tc3}	9.94e-13 ft^{-2}

The constraints shown in Table 7 were discussed in section 4.2.1. To cater for BADA capabilities, h_{min} was reduced to allow greater variation in cruise altitude, while the range between V_{min} and V_{max} bounds were drastically increased as they were no longer the primary means of constraining speed. Further, BADA itself had constraints that were applied irrespective to aircraft type; these are important as BADA results become inaccurate outside of them.

Table 7 - Global Constraint Data for the BFO and BSO

Due to BADA Integration		**As required by BADA Methods**	
h_{min}	20000 ft	$a_{lmax(civ)}$	2 ft.s^{-2}
h_{max}	50000 ft	$a_{nmax(civ)}$	5 ft.s^{-2}
V_{min}	120 kts	C_{Vmin}	1.2
V_{max}	1200 kts		

Summarized information on the PCO test scenarios, in terms of their intended relative 4 dimensional positioning and in terms of the number of trajectory variables that had to be optimized to find minimum fuel usage, can be found in Table 8. For simplicity of discussion each of these scenarios have been designated with an abbreviation formed from the number of aircraft in the scenario (i.e. 2ac, 4ac, 10ac, respectively refer to 2, 4 or 10 aircraft) and a simple description of the situation itself (i.e. PSd for parallel and same direction scenarios, CO for cross over scenarios, CH for cross hatch scenarios, and PH2H for parallel and head to head scenarios). Further information on the scenarios in terms of their specific intended purposes can be found in Appendix F and in this and later chapters where specific scenarios are discussed; their general purpose however is to define scenarios that use as much of the test field as possible to setup comparable trajectories in conflict scenarios that test the optimizer's capabilities.

Table 8 - Summarized Details of Optimizer Test Scenarios trialled using the PCO

Scenario	Scenario Details
'2acPSd'	Two aircraft covering 678 nmi on the same route with departure time difference of 6 minutes. 136 trajectory variables to be optimized.
'4acPSd'	Two consecutive instances of 2acPSd occurring 5 minutes from each other. 272 trajectory variables to be optimized.
'10acPSd'	Five consecutive instances of 2acPSd occurring every 5 minutes. 660 trajectory variables to be optimized.
'2acCO'	Two aircraft covering 678 nmi and the same departure time, intersecting at ≈90°. 136 trajectory variables to be optimized.
'4acCO'	Four aircraft covering 480 nmi and the same departure time, conflicting with each other at the same surface point 240 nmi from their starting position. The bearing difference between each successive aircraft at the point of conflict is ≈36°. 192 trajectory variables to be optimized.
'10acCO'	4acCO with six more aircraft. Each aircraft is on a head on collision with another aircraft. 480 trajectory variables to be optimized.
'4acCH'	Four aircraft covering ≈ 340 nmi and the same departure time; four two aircraft ≈90° intersections. 128 trajectory variables to be optimized.
'10acCH'	10 aircraft covering ≈ 480 nmi and the same departure time, setup in a cross hatch fashion. Aircraft head either south or east, and aircraft with the same heading have a minimum cross track separation of ≈ 90 nmi. 476 trajectory variables to be optimized.
'2acPH2H'	Two aircraft covering 678 nmi and the same departure time, conflicting head on. 136 trajectory variables to be optimized.
'4acPH2H'	Two consecutive instances of 2acPH2H occurring 11 minutes from each other. 272 trajectory variables to be optimized.
'10acPH2H'	Five consecutive instances of 2acPH2H occurring every 11 minutes. 660 trajectory variables to be optimized.

For the purpose of this third assessment, the scenarios in Table 8 were optimized again, with and without an arrival time constraint, and pertinent details of their optimization are found in Table 9. The table shows the key points of each scenario; its total fuel usage once optimized, if a minimum was found, if all constraints were satisfied, and the effective number of requisite reruns (as defined in 4.2.4). Further visual information on these results can be found in Appendix J. It should be noted that Table 9 only contains results created by the BFO; while comparisons were run between these and the results created by the PCO, no meaningful conclusions were made given the difference in fuel calculation between the two, and thus those comparisons were not displayed here. However, there were notable differences in the trajectory shape between BFO and PCO results and these are discussed later in this section. As an aid to understanding Table 9, an objective function that minimizes disruption from an ideal trajectory was applied to the same scenarios and its results were also shown for comparison. Similarly, more visual detail on these results are presented in Appendix J. This disruption is calculated as the difference between the ideal and current position of the aircraft in terms of time and altitude, t_{i_ATDi}, h_{i_ATDi}, t_{c_ATDi}, and h_{c_ATDi}, then normalized against the minimum separation requirement in the relevant dimension, t_{minsep} and h_{minsep}, then squared and summed for all fuel calculation points, ATD_i. As a minimized objective function it equates to:

$$\min_{V_{TAS\_ATDn},h_{ATDn}} \sum_{ATDi}\left(\left(\frac{t_{c\_ATDi}-t_{i\_ATDi}}{t_{\min sep}}\right)^2+\left(\frac{h_{c\_ATDi}-h_{i\_ATDi}}{h_{\min sep}}\right)^2\right) \quad \textbf{(41)}$$

V_{TAS_ATDn} and h_{ATDn} being the respective velocity and altitude values in the optimizer variable that control variables defined in ATD_i. As this objective method tries to improve adherence to the original trajectories' schedule, it's nominally defined as a 'BADA Schedule Optimizer' or BSO, and is intended to mimic the ability of ATC to facilitate an aircraft's desired trajectory as much as possible given aircraft limits.

That Table 9 shows an almost complete list of scenarios that were successfully optimized is not surprising; the original optimizer was almost as successful, and the integration work defined in 4.2 was aimed to support this level of functionality. The sole failure in the list is reasonable because the 4acCH scenario has the shortest route distances with points of potential conflict intentionally placed where descents and climbs are usually desired; time deviations to avoid conflict are consequently larger, and the shorter route distances would not be able provide or absorb the time deviations required to ensure the scheduled arrival time is still met. In all other arrival time constrained scenarios, successful optimization was achieved using the same distribution of time deviations that was seen in the PCO trials for the same. Unfortunately given the smoothness of the BFO results and the closeness of the 8nmi/min average speed used for scheduling arrival times to the actual average speed of the BADA defined 747-300, there is very little difference between the arrival time constrained and unconstrained results, which makes for poor comparison between the two. Fortunately for the purposes of comparison, the BSO results were shown to use up more fuel than their BFO equivalents; this is also expected as maintaining the most fuel efficient trajectory, at the cost of drastic manoeuvres at conflict points, should use more fuel than following a less efficient trajectory that does not use significantly disruptive manoeuvres. The result of fuel inefficient portions of trajectories being dispersed along the entire trajectory was present in PCO but not easily seen; with the BSO the effect becomes visible and can be confirmed to exist in the BFO. To display this effect and other changes caused by using BADA data, Figure 40, Figure 41, andFigure 42, show results for the arrival time unconstrained scenario presented in Figure 22, i.e. '10acCO' in Table 8, to highlight the effectively similar

capabilities of PCO and BFO, as well as the differences that the BSO would or would not cause in the same situation. Further discussion on the implications of the BSO as compared to BFO is given later in section 5.3.

Table 9 - Details and Results of Optimizer Test Scenarios using BADA based Fuel Function

Scenario	Schedule Optimized (BSO)			Fuel Optimized (BFO)			Fuel Optimized (w/ ETA)		
	Fuel Used (tonnes)	Convergence?	#Runs	Fuel Used (Δ% v.BSO)	Convergence?	#Runs	Fuel Used (Δ% v.BSO)	Convergence?	#Runs
'2acPSd'	28.14	Yes	1	-2.88%	Yes	1	-3.01%	Yes	0
'4acPSd'	56.20	Yes	1	-3.13%	Yes	1	-2.90%	Yes	0
'10acPSd'	140.30	Yes	0	-2.42%	Yes	1	-2.78%	Yes	0
'2acCO'	28.05	Yes	1	-2.70%	Yes	1	-2.73%	Yes	0
'4acCO'	40.44	Yes	1	-3.20%	Yes	1	-3.23%	Yes	1
'10acCO'	109.13	Yes	1	-7.57%	Yes	1	-8.21%	Yes	1
'4acCH'	28.60	Yes	1	-0.83%	Yes	2	-3.96%	No	2
'10acCH'	99.62	Yes	1	-2.11%	Yes	1	-1.26%	Yes	1
'2acPH2H'	28.05	Yes	1	-2.69%	Yes	1	-2.73%	Yes	0
'4acPH2H'	56.85	Yes	1	-3.85%	Yes	1	-3.79%	Yes	1
'10acPH2H'	153.58	Yes	1	-10.20%	Yes	1	-8.71%	Yes	1

The first notable difference between Figure 40 and the PCO result of '10acCO' shown in Figure 24 is in the way altitude climb is treated. In PCO, provided maximum lift coefficient and thrust was not violated, any climb angle could be used; this resulted in harsh climb angle changes that stem from the need to maintain maximum altitude for as long as possible, it also required the use of a climb angle limit to prevent chaotic climb angle combinations. In contrast, the BFO has to cover a greater number of constraints to create a feasible climb; thus only climb angle changes prior to descent are equally as harsh and the climb portion is persistently gradual even upon returning from a lower altitude required to avoid conflict. Further, trajectories above this calm climb are clearly possible but given their rarity suggest significantly increased fuel usage. One other difference between Figure 40 and Figure 24 is in the variation in velocity for one aircraft. The original optimizer had acceleration equal to zero during segments; this allowed fuel efficiencies to accumulate or disperse for greater periods of time, thus causing great velocity changes over a small number of key points. In both Figure 40 and Figure 41, possibly due to the acceleration being allowed or the improved accuracy BADA infers, velocity variation occurs more frequently but with smaller variations; it suggests that more chaotic manoeuvres could be attempted for conflict avoidance or fuel minimization using the BFF. In all other aspects, PCO and BFO are the same; the same ability to control velocity when a particular altitude is required due to conflict, as well as the stagger on effect where altitudes and velocities just prior and after conflict prefer other values for themselves which leads to the same preference to control portions of the trajectory much larger than what conflict would originally require.

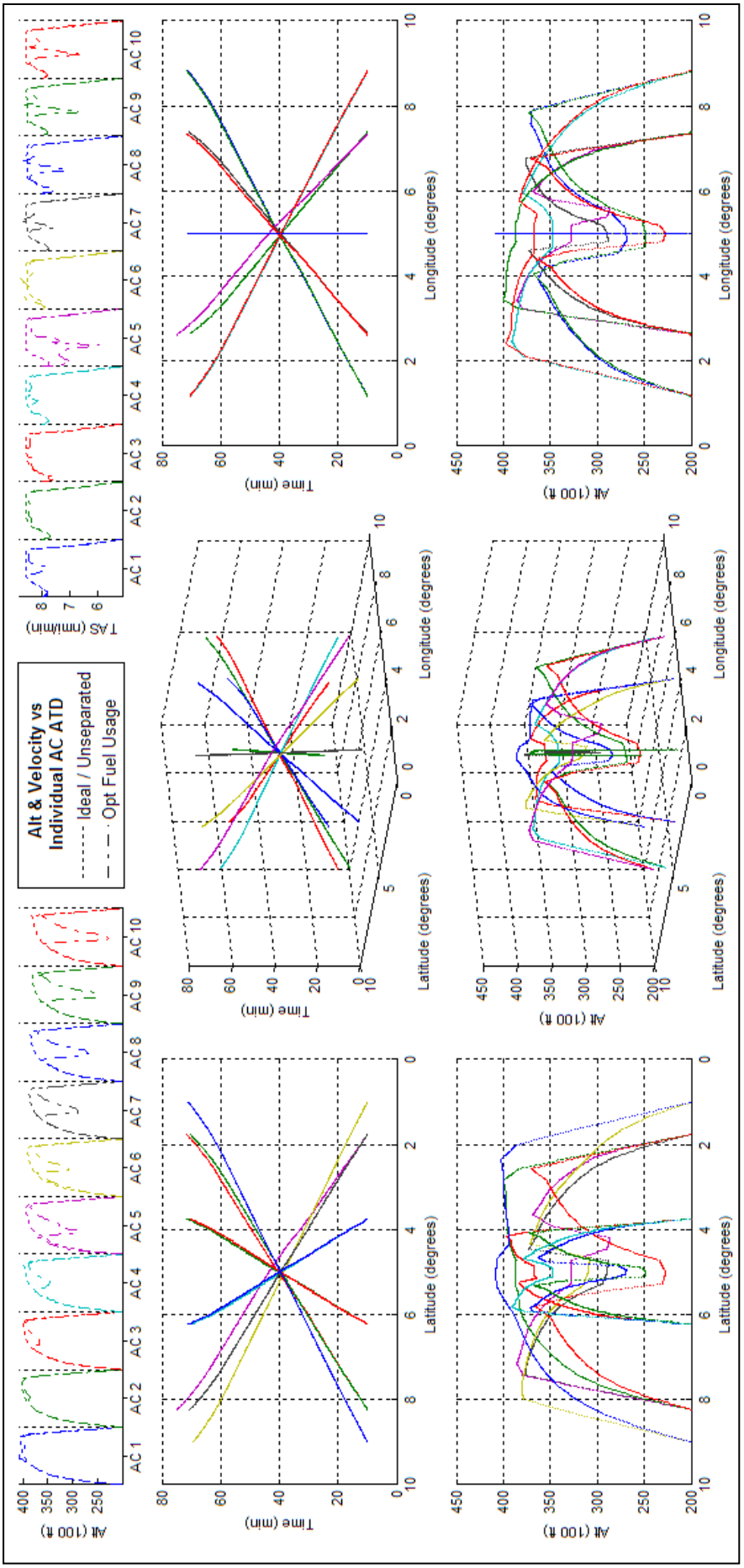

Figure 40 - BADA based Fuel Optimizer result for 10acCO.

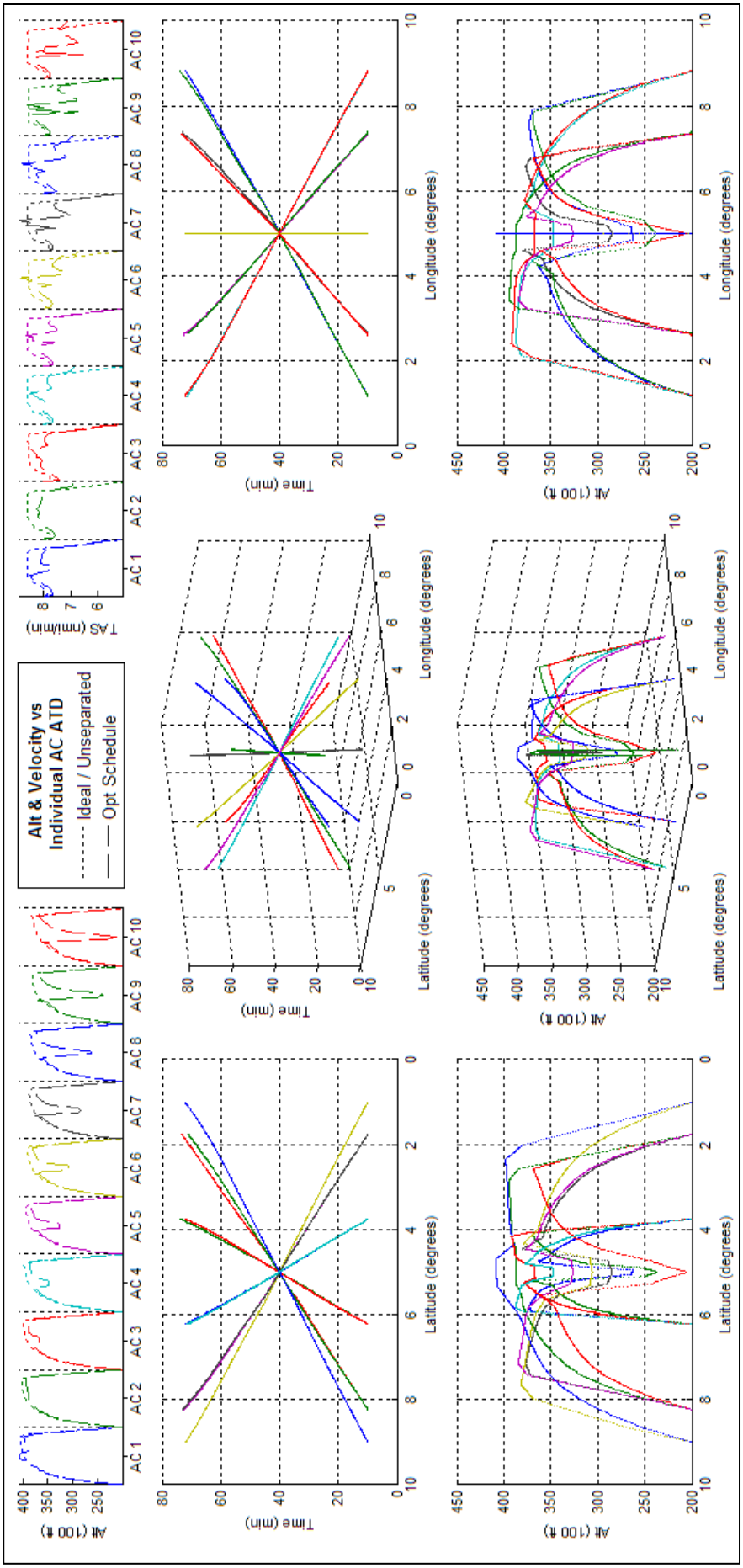

Figure 41 - BADA based Schedule Optimizer result for 10acCO.

The differences between BFO and BSO, as represented by Figure 40 and Figure 41, are less noticeable; they adhere to the same performance constraints so they should look considerably similar in terms of trajectory so Figure 42is needed to show differences. The biggest and most indicative difference between the two is the willingness of BFO to increase the fuel usage of one aircraft if it would decrease the fuel usage of all aircraft in the scenario; in this scenario, the BFO result has Aircraft 5 flying lower cruising altitudes and flight speeds despite it making and using the same separation slot its BSO counterpart flew. This is most likely due to Aircraft 5 being the most capable of inducing significant fuel usage reduction; by slowing it down its impact on the aircraft just below and above it after the main intersection, is minimized, allowing them to take on trajectories that are beneficial to ones further away. On the other hand the BSO result was consistent; the same patterns in both altitude and TAS being repeated for each aircraft, with the amplitude and relative position of each being suited to the weight, and resultant h_{MAX}, of their specific aircraft. In terms of flight time and fuel usage there is a clear zigzagging pattern that suggests that aircraft were alternately slowed down or hastened to allow aircraft to be, on average, closer to their original schedules while preparing for separation. It can be debated which of the two optimums would be preferred in use; however for the purposes of the research here, it is sufficient that both are possible and, due to the confirmed functionality presented in this section, available in the optimizer as different optimization methods.

The last comment to be made of the BFO in comparison to the PCO regards its computation time and scalability; consequently the data in Table 10 was collected. This table shows the computation times of BFO optimizing the scenarios mentioned in Table 8 whilst using one core of an AMD Quad Core Opteron™ 2.3ghz processor with each core having 4GB of RAM and 160GB of scratch space. The cores communicated via Infiniband Interconnect on a CentOS 5 Linux based network. As this data was expected to be used to determine if the process could be scaled to higher numbers of aircraft in situations comprising multiple scenarios, the times were sorted against scenario type and number of aircraft involved.

Table 10 – Comparison of Scenario Computation Time (hrs) versus Number of Aircraft Involved

Scenario / #AC	PSd	CO	CH	PH2H
2ac	0.13	0.04	0.04	0.14
4ac	1.23	0.08	0.31	1.09
10ac	21.82	2.41	1.33	68.26

The key trend taken from Table 10 is that computation time drastically increases as the number of aircraft increases, as well as between scenario types, thereby disallowing any significant correlation to be made. However, if the same data is defined using a logarithmic scale, as in Figure 43, several trends can be defined. Firstly, given the linearity of results in this scale, computation time is clearly exponential based on the number of aircraft. Further, given that an order of magnitude separates the CO and CH scenario types from the PSd and PH2H scenario types, the number of aircraft is likely to not be the sole parameter.

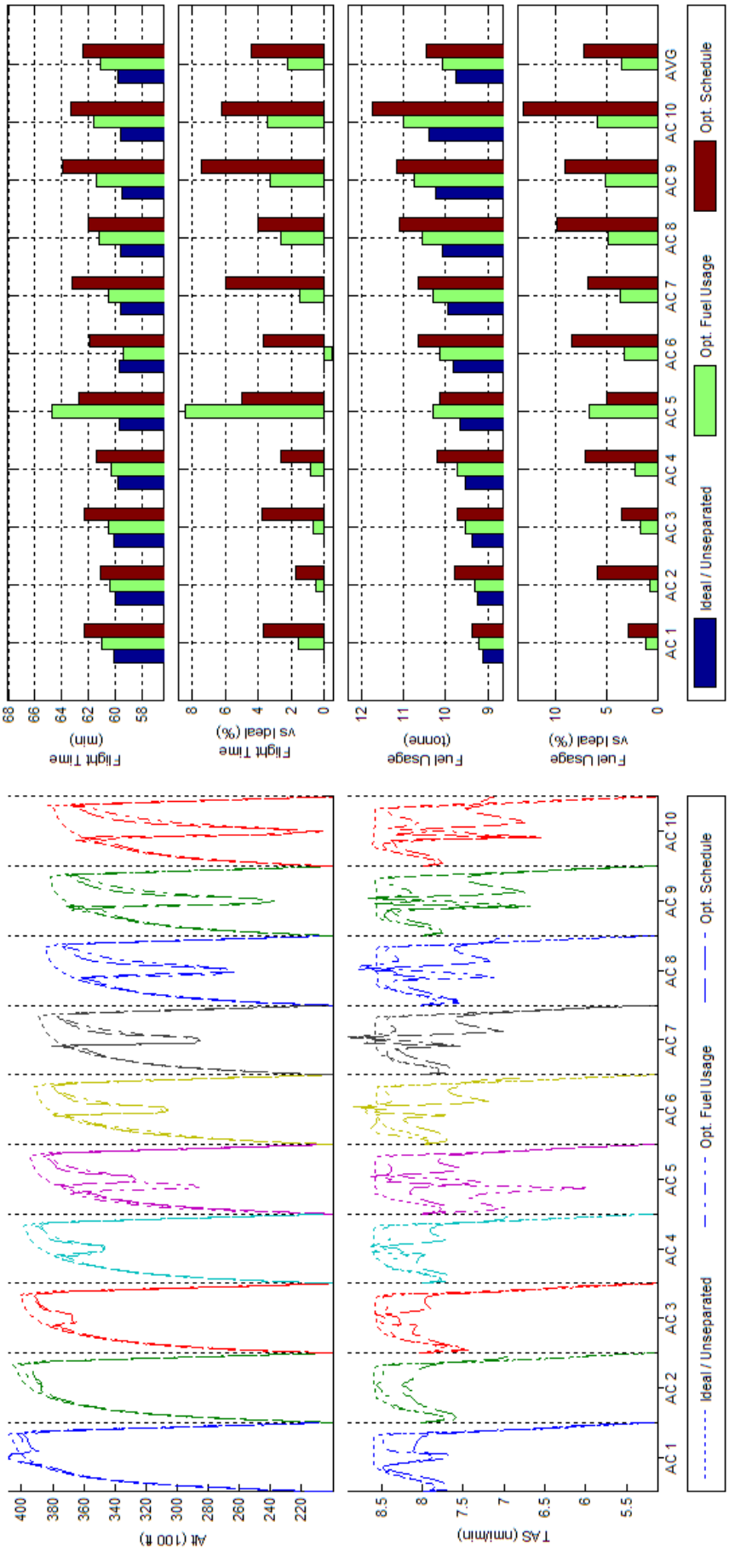

Figure 42 - Comparisons of Optimizer Variable (left) and Flight Data (right) between Fuel and Schedule Optimizations of 10acCO.

Given the optimizer's focus on the discretization of airspace in which conflict occurs, the more relevant scaling parameter should be the sum of the active nodes required to ensure that each individual conflict's appropriate separation occurs. For example, Figure 6 indicated how the area of conflict varies with the conflict type; i.e. how perpendicular aircraft intersections would have the smallest area, while parallel intersections would have the largest area due to the amount of space spent in proximity to each other. The trends in Figure 43 align with this theory and show that the PSd and PH2H scenario types do take an order of magnitude longer than the CO and CH scenario types to optimize. The theory also correlates with the exponential increase in computation time with aircraft numbers, as each additional aircraft in conflict must check its separation with all other aircraft already being considered inside the optimization. This thus indicates that the exponential increase in computation time is primarily due to the problem itself, and not necessarily the way it is optimized.

This exponential increase in computation time caused by the linear increase in the number of aircraft presents a difficult obstacle to the scalability of this optimizer. An exponential increase would suggest that if a 10 aircraft scenario takes a day to solve, a 100 aircraft scenario would take a month or longer to solve; this is heavily undesirable, as the latter scenario occurs on a daily, if not hourly, basis around the world. However, a partial solution presents itself in the fact that the CO and CH scenarios took less time to optimize; i.e. that reductions in the amount of conflict airspace can yield time savings an order of magnitude in size. It was not clear how this might be utilized at this stage of the research, however later in section 5.2.2, it was used to enable the optimizer at higher aircraft numbers.

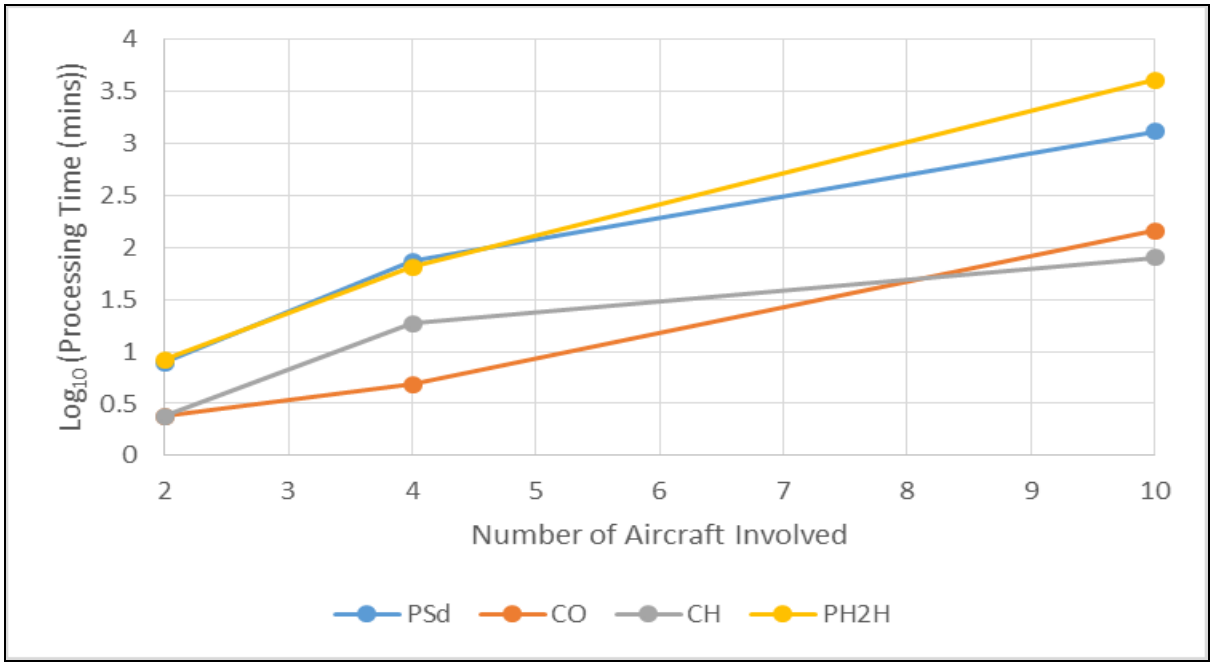

Figure 43 – Variation in Scenario Computation Time using a Logarithmic Scale

4.3.3 Fourth Assessment: Aircraft Model Variation Trials.

The trials shown here were intended to be exactly the same as the trials in 4.3.2, just with different aircraft. The aim being to show that the optimizer could utilize all BADA data and not just that for a 747. Consequently the global constraints, scenarios, and environmental data are all the same as that in 4.3.2, however instead of a 747, the trials used an Airbus A320, a Boeing 737, or a mix of the two. The necessary BADA data of the two aircraft are shown respectively in Table 11 and Table 12. While it was originally intended to run the trials with both constrained and unconstrained arrival times, the results for the optimizations with unconstrained arrival times indicated that the scenarios were heavily constrained already and that attempts to add further constraints would likely result in failed optimizations across the 11 scenarios and thereby provide poor comparative data. As a consequence all scenarios within this assessment have no constraints on arrival times.

Table 11 - BADA Performance and Constraint Data for an Airbus A320

Thrust and Fuel Usage Calculation		**Height Constraint Calculation**	
Engine Type	Jet	h_{MO}	39000 ft
C_{f1}	0.94 kg.min^{-1}.kN^{-1}	H_{max}	34354 ft
C_{f2}	100000 kt	G_t	-130 ft.C^{-1}
C_{fcr}	1.06	C_{tc4}	10.29 deg.C
C_{D0}	0.024	G_w	0.28 ft.kg^{-1}
$1/(\pi.AR.e)$	0.0375	M_{max}	77 t
S	122.6 m^2	**Thrust Constraint Calculation**	
Speed Constraint Calculation		C_{Tcr}	0.95
M_{MO}	0.82	C_{Tc1}	136050 N
V_{stall}	145 KCAS	C_{Tc2}	52238 ft
V_{MO}	350 KCAS	C_{Tc3}	2.66e-11 ft^{-2}

Table 12 - BADA Performance and Constraint Data for a Boeing 737

Thrust and Fuel Usage Calculation		**Height Constraint Calculation**	
Engine Type	Jet	h_{MO}	41000 ft
C_{f1}	0.9468 kg.min^{-1}.kN^{-1}	H_{max}	37700 ft
C_{f2}	1E+14 kt	G_t	-131 ft.C^{-1}
C_{fcr}	0.9737	C_{tc4}	10.7 deg.C
C_{D0}	0.0235	G_w	0.3138 ft.kg^{-1}
$1/(\pi.AR.e)$	0.0445	M_{max}	70.8 t
S	124.65 m^2	**Thrust Constraint Calculation**	
Speed Constraint Calculation		C_{Tcr}	0.95
M_{MO}	0.82	C_{Tc1}	145730 N
V_{stall}	143 KCAS	C_{Tc2}	55638 ft
V_{MO}	340 KCAS	C_{Tc3}	1.42E-11 ft^{-2}

Due to BADA Conditions of Use it is not possible to publicly compare fuel usage data between two different aircraft models. However it is possible to compare the computational resources used in performing those optimizations, as shown in Table 13, as well as their resulting trajectories post optimization, as shown in Figure 44, Figure 45, and Figure 46. Table 13 is similar to Table 9 but compares Processing Time instead of Fuel Usage. Figure 44, Figure 45, and Figure 46, use the 10acCO scenario which was discussed in 4.3.2.

Table 13 - Computational Details of Optimizer Test Scenarios using Multiple BADA Aircraft Models

Scenario	Airbus A320			Boeing 737			A320 & 737 Mix		
	Processing Time (Δ% v. mix)	Converged?	#Runs	Processing Time (Δ% v. mix)	Converged?	#Runs	Processing Time (hours)	Converged?	#Runs
'2acPSd'	-19%	Yes	0	-4%	Yes	0	0.61	Yes	0
'4acPSd'	-99%	Yes	0	-99%	Yes	0	118.37	No	2
'2acCO'	-46%	Yes	0	-33%	Yes	0	0.92	No	2
'4acCO'	-16%	Yes	1	-73%	Yes	1	0.41	Yes	1
'10acCO'	-3%	Yes	1	100%	Yes	1	46.39	Yes	1
'4acCH'	5%	Yes	1	41%	Yes	2	0.08	Yes	1
'10acCH'	54%	Yes	1	309%	Yes	1	0.69	Yes	1
'2acPH2H'	-59%	Yes	0	-49%	Yes	0	1.21	No	2
'4acPH2H'	121%	No	2	22%	No	2	24.68	No	2

While the trials for the alternate aircraft models lacks the overall convergence rate experienced in section 4.3.2, this is largely explained by the fact all 11 scenarios set the fuel initially available to all aircraft in the scenario to linearly vary between 15~45% of their total fuel capacity. For a 747 this is significantly above that needed to travel across the test field, however for a 737 or A320, this is only just above the amount needed. When combined with comparatively fuel expensive trajectory deviations, it increases the likelihood of optimizations failing due to a lack of available fuel. Consequently this was what was seen as the primary cause of the failed results as all such results indicated that the ‘must have fuel’ constraint as being consistently unsatisfied. It also explains why the ‘10acPSd’ and ‘10acPH2H’ scenarios, the results of which are not shown in Table 13, experienced unexpectedly high computation times per optimizer iteration that prevented their completion; the combination of a severely constrained scenario with severely constrained fuel usage would vastly increase computation times. However overall, the large number of convergences and explainable failures shown in Table 13 do indicate that the usage of alternative aircraft model data within BADA as being possible and this is further supported by the trajectory shapes shown in Figure 44, Figure 45, and Figure 46, having properties akin to, and not significantly different, than that seen in Figure 40 and Figure 41.

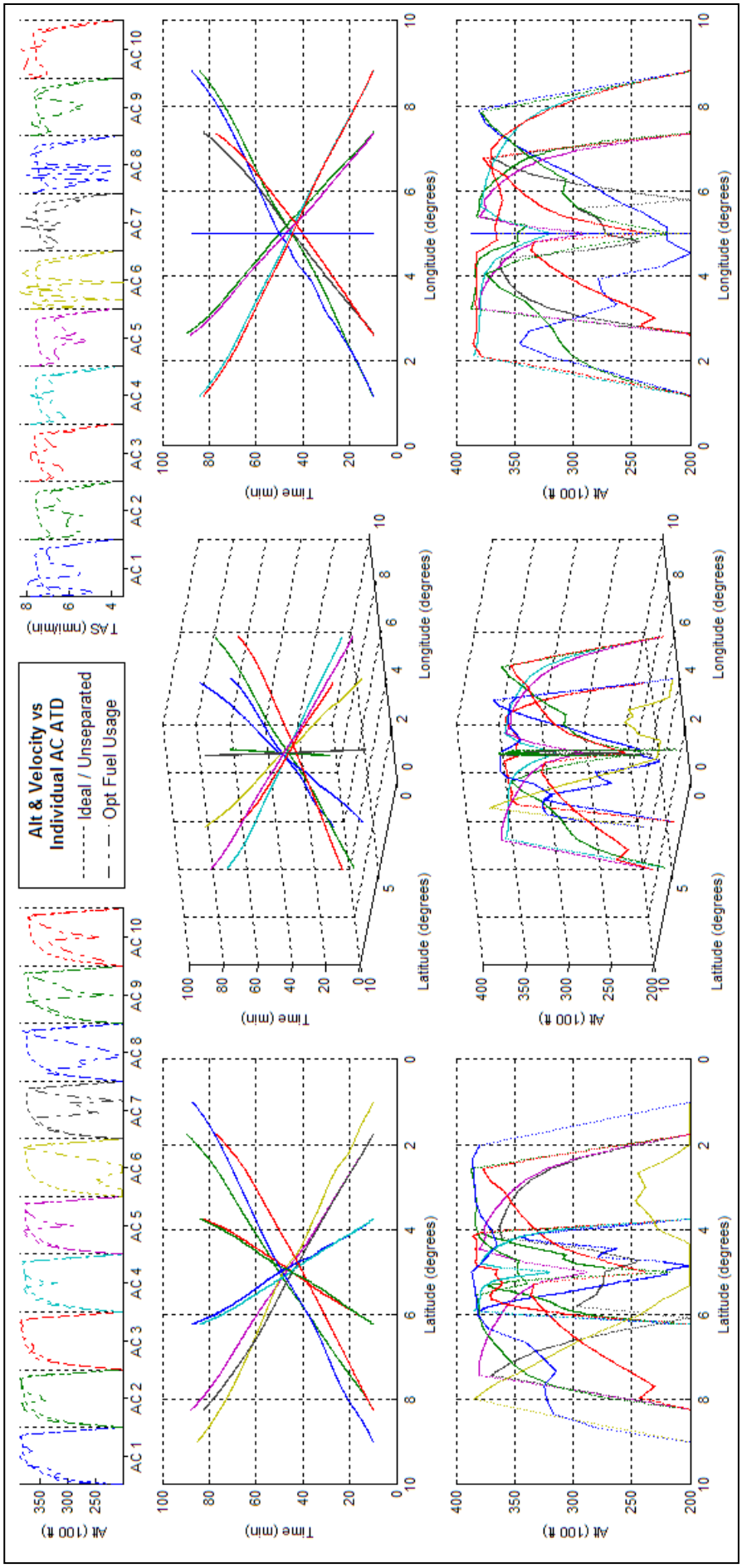

Figure 44 - BADA based Fuel Optimizer result for 10acCO using only A320s.

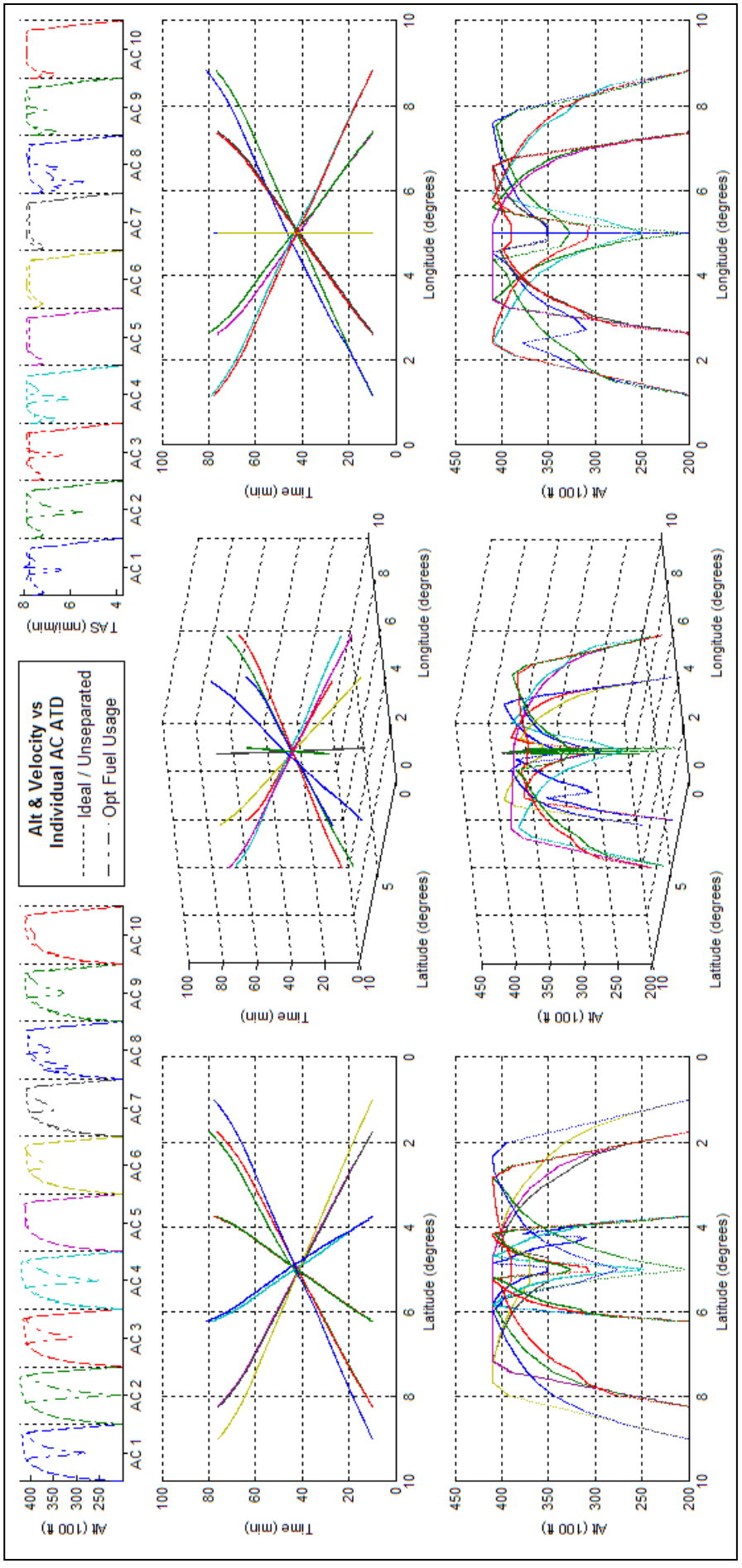

Figure 45 - BADA based Schedule Optimizer result for 10acCO using only 737s.

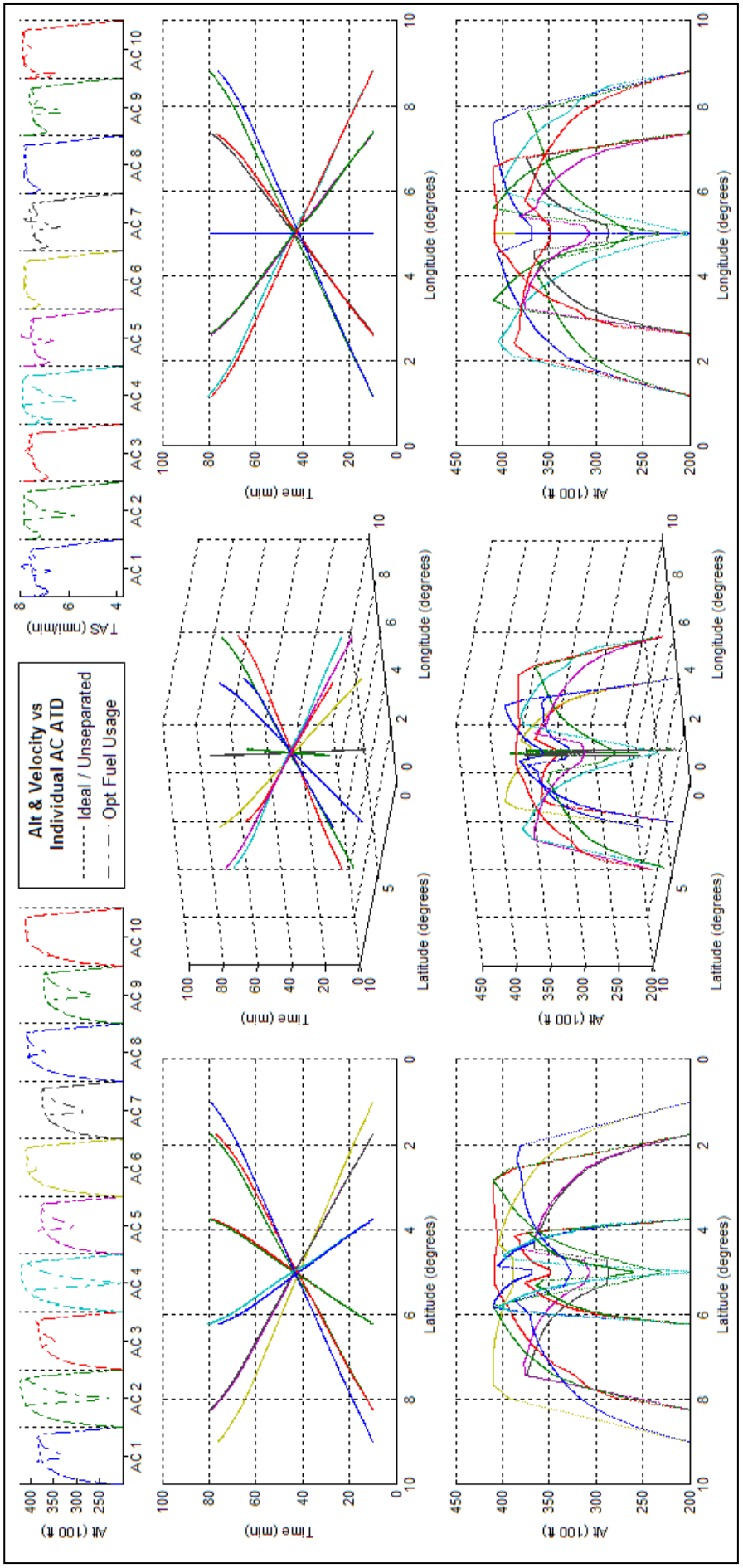

Figure 46 - BADA based Schedule Optimizer result for 10acCO using a mix of A320s and 737s.

4.4 Conclusions

The purpose of this section is twofold. The first purpose is to give a summary of the research contributions performed in this chapter and this is performed in section 4.4.1. The second purpose is to highlight the impact the work had on the Research Questions mentioned in section 2.4.2 and this is discussed for each research question in section 4.4.2.

4.4.1 Chapter Summary of Research Contributions

In this chapter BADA methods of trajectory and fuel prediction were taken and incorporated into the PCO, as a test of the optimizer's ability to handle more accurate and more complex forms of aircraft performance and fuel usage modelling. To do this, the BADA REM and its associated performance limits were first reformulated into the BFF defined in section 4.1 and the series of optimizer constraints defined in section 4.2. Simultaneously, due to concerns regarding the optimizability of the BFF given its interaction with its potentially highly nonlinear constraints, a method of mapping feasible BFF results, i.e. Fuel Usage values that satisfy all constraints, was developed and used to study variation of BFF results specific to a Boeing 747-300 as allowed by the domains of the optimizer variable. The results of the mapping indicated that feasible BFF results, particular to the Boeing 747-300, are largely concave and continuous; this therefore significantly reduced concerns regarding selection of incorrect fuel usage minimums for specific aircraft and thus allowed focus on the results of doing the same in a coordinated traffic scenario. A side consequence of being able to map BFF results was that it also allowed quick assessment of the feasibility of optimizing other specific aircraft models that are present in BADA without requiring their optimization; thus the same reduction in optimizer concerns were made of all sufficiently complete BADA models and this allowed optimization tests involving aircraft other than the Boeing 747-300.

To finalize BADA incorporation into the PCO, the resulting BFO underwent the same trials that the PCO had experienced in Chapter 3, i.e. fuel usage minimization of multiple B747-300 in construed air traffic and conflict scenarios, with and without arrival time constraints. The optimization results showed that the BFO generated simular concerted conflict avoidance solutions as the PCO with most differences being associated to the more accurately defined cruise climb profiles that the BFF would have indicated as being optimum. To support understanding of optimized concerted separation, an alternate schedule based objective function was also developed to compare fuel usage minimization with minimizing deviation from a previously fuel optimized flight plan; the BFO Boeing 747-300 trials showed that minimizing disruption or enforcing a schedule, as opposed to a defined concerted ATFU optimum, can cause increased fuel usage. For completeness the same trials were performed with two other aircraft that are similar to each other and commonly seen in air traffic; the Airbus A320 and Boeing 737. The purpose of the trials was to ensure the BFO could work with other aircraft, and to see what happens when you simultaneously optimize different aircraft models in the same conflict scenario. While the scenarios were shown to be severely constrained due to a lack of fuel initially available to each aircraft, it did indicate that the BFO could optimize different aircraft combinations.

4.4.2 Current State of Research

4.4.2.1 Q1: Can a co-operative and sufficiently informed air traffic optimisation methodology achieve a reduction in total fuel usage compared to current ATM?

In chapter 3 Q1 was partially answered by showing that the PCO could minimize ATFU. However, the PCO was based on flight mechanic derivations of fuel consumption and could not be compared to current ATMHowever, this chapter incorporated BADA, which is used worldwide for the purposes of optimally planning the fuel usage of current commercial air traffic. Further, this chapter also created the BSO which simulated the optimal impact of current ATC scheduling on ATFU. The comparison of results between the BFO and BSO showed that the BFO achieved ATFU values lower than those achieved by the BSO. In essence the cooperative air traffic optimization methodology developed in this thesis can achieve a reduction in ATFU compared to current ATM.

However this is all based on the premise that the optimized set of cooperative trajectories can be, and is, followed accurately by the air traffic involved; i.e. that the trajectory variation allowed of aircraft is not restricted by non-aircraft performance related parameters, e.g. crew and passenger requirements, and that the optimized scenario does not experience future events which would invalidate the optimized result, e.g. unanticipated weather or other aircraft. Assuming that BADA aircraft performance modelling is as accurate as it will ever get, which is untrue as improvements are still being researched by Eurocontrol, the research here will still have to deal with the possibility of crew and passenger requirements on trajectories, as well as unanticipated weather and aircraft, before answering Q1 fully.

4.4.2.2 Q2: What information is required to achieve such an optimisation methodology and how sensitive are the results to the accuracy of the input information.

Section 3.5.2.2 showed the information associated with the PCO that is required to achieve ATFU optimization, as well as how sensitive its results are respect to that information, in terms of correlatable relationships and impact on computation time. As these aspects do not change in the BFO, there is no need to go over the same information and their sensitivity again. The question that needs to be answered here is how sensitive are the results to variation in the BADA data. The variation shown in this chapter occurs in two ways; within the aircraft performance model itself, i.e. as caused by the optimizer variable, and between different aircraft performance models, i.e. as caused by optimizing different aircraft types.

Regarding the former variation, due to the similarity of the BFF with the standard fuel equations shown in Chapter 3, the BFO can reach simular fuel savings and computation times as the PCO. However this is only true if the BADA constraints are not active during optimization; the increased number of constraints, when active as a barrier during optimization, will cause slower computation times but does ensure that the result accurately reflects the impact of the constraint. Regarding the latter variation, given that the performance equations are the largely the same between aircraft, computation times are more determined by the severity of the scenario on the aircraft rather than the aircraft itself, and this was shown in section 4.3.3. However it is clear from the same section that results do change based on what aircraft is being flown in the scenario.

4.4.2.3 Q3: How can constraints such as aircraft performance limitations, minimum separation and on-time arrival be incorporated into an optimizable UPT, and how do these affect total fuel usage?

The means of incorporating aircraft performance limitations, minimum separation and on-time arrival, are exactly the same as mentioned in 3.5.2.3; consequently this section focuses on how their impact on ATFU differs due to the incorporation of BADA methods. The aircraft performance limitations are the most noticeable with height, thrust and velocity requirements limiting potential conflict avoidance solutions that could have allowed more fuel efficient results. The characteristic impact of minimum separation remains unchanged but is heavily affected by aircraft performance limitation. The characteristic impact of on-time arrival constraints is also unchanged; however it is less noticeable now given the existence of similarly encompassing aircraft performance constraints which require trajectory wide changes to satisfy e.g. the more pronounced height limitations on cruise climb.

4.4.2.4 Q4: How can a dynamic environment, such as deviation from or in-flight changes to the flight plan, airspace closure, and emergency diversion, be accommodated in an optimisation methodology?

Chapter 4 does not answer this question however, as 4.4.2.1 mentioned, this is the stage in the research where Q4 starts to become a concern. With a static optimization like BFO being as good as it can get given the state of aircraft performance modelling in air traffic, research focus needed to shift to issues like Q4.

5. DYNAMIC ASSESSMENT AND OPTIMIZATION

The optimization efforts thus far shown have all been based on the assumption that the scenario would not change; i.e. that ATS is fully defined and that the aircraft involved would fully and consistently follow the resulting optimized trajectories. That aircraft always follow a planned trajectory is an unrealistic assumption, so effort was placed into preparing for variation in scenario over time. The method mentioned in 2.2.2.4 provided guidance in this endeavour as it prepared for such via defining subproblems as resolution of states at discrete points in time. While the holistic trajectory coverage of the PCO would prevent it from doing the same, what can be isolated into subproblems is the scenario as seen during particular intervals of time throughout the scenario. The optimization process could then be rerun for these sub-scenarios, and provided that these are also run in an earliest sub-scenario manner with results being passed on to subsequent sub-scenarios, a semblance of overall optimization that could handle variation in scenario, could be gained. Further, this division may have further benefits. The holistic perspective used when optimizing air traffic over the entire scenario, including even those not yet in the air, would be the most computationally intensive due to the amount of traffic to be considered, and the most computationally wasteful as not all scheduled flights fly at their intended times. In contrast, the minimalist perspective of the sub-scenarios only controls aircraft that are currently flying, or about to enter optimized airspace, during that sub-scenario; this would have computational intensity that is reduced, and computational efficiency that is increased as only truly necessary optimizations would occur. However the inability to consider scheduled flights does suggest a price in terms of an inability to reach viable optimums.

Given that the holistic perspective is already possible via PCO or BFO, a minimalist perspective was chosen for emphasis during the development of a PCO based Dynamic Optimizer or PDO; the ability to compare against an already well developed holistic perspective would, as the level of dynamic variation increases, give information on fuel efficiency losses and their corresponding reductions in computation time if any. This also allows the simulation of changing or dynamic scenarios to be simple; where an optimizer with a holistic perspective requires knowledge of all future flight changes, an optimizer with a minimalist perspective need only have a list of deviations between what it had optimized, and what had actually happened. Consequently, in terms of functional programming, the dynamic scenario is represented as an initial scenario, i.e. one of the eleven scenarios mentioned in Table 8, combined with a list of "trigger" events that occur at prespecified times. At these events, the optimizer modifies the scenario at that time by forcing trajectory re-optimization. The optimization and re-implementation of trajectories by later event triggers facilitates dynamic optimization.

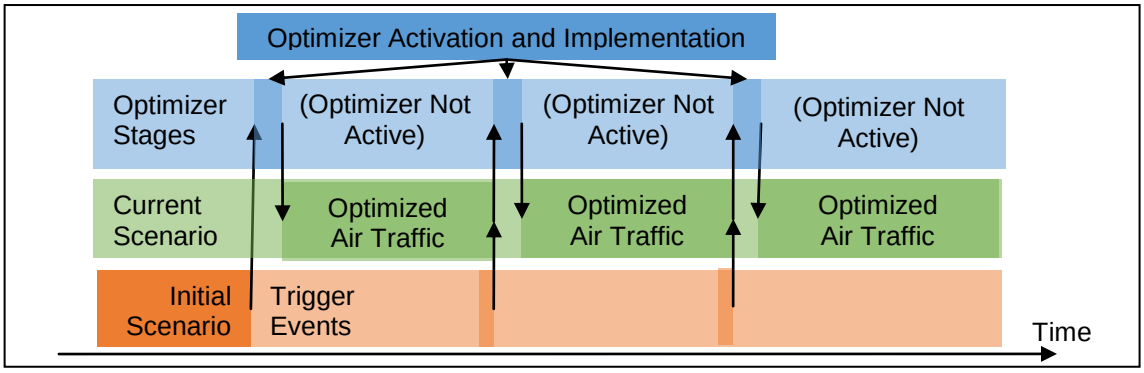

Figure 47 – Functional Representation of Dynamic Environment (Arrows indicate Data Flow)

5.1 Requirements and Additional Functionality for a Dynamic Optimizer

The conceptual process of letting PCO or BFO assess and optimize dynamic scenarios is conceptually simple and consists of only two stages. The first requires the current scenario to be defined from a minimalistic perspective and transferred to the optimizer to be assessed and optimized; the trajectories therein only being optimized for times well after the optimizer is finished. The second requires that the optimizer's results be applied, adhered to, and monitored, till another event requires the first stage to be reiterated. Only the first stage is defined here; while considerable inference was made on second stage elements that could affect the first stage, it would be unwise to develop processes for the second stage till the first is well understood. To that end, the six steps that were developed to support PDO implementation of the first stage are discussed below.

5.1.1 Define Trajectories of Currently Flying Aircraft

The first step of a reiterated optimization is to update PDO understanding of the scenario; the first part of that is to retrieve data previously created or used that is still in effect. Thus all environmental data and the potential and actual presence of the aircraft as defined by NMD data are all considered for inclusion as currently useful data. As mentioned previously a minimalist perspective is being emphasized, so certain parts of this data will be left behind; essentially, the potential and actual presence of the aircraft are compared to the intended time of application of the PDO results and all presence data that occurs prior to that time, less any necessary to ensure time separation, are excluded. This creates two sources for reduced computation time for the optimization process. The first is that the portion of the trajectory being optimized for each currently flying aircraft is reduced; this leads to reduction in the number of variables being optimized and thus a reduction in overall optimization time. The second source is that the region of potential presence is also reduced; the reduction in optimization time comes from the reduced number of separation checks stemming from the removal of already resolved and actioned collision avoidance.

5.1.2 Define New Entrants and Alterations to Currently Flying Aircraft

The disallowance of route changes in optimization is dependent on allowing route changes outside of optimization. Thus it was important to develop basic capability to support this in the PDO; the second part of updating PDO understanding of the scenario is therefore to define new additions or alterations to the current understanding of the scenario. These can be either environmental or aircraft related alterations. If the only alterations are changes in the environmental data, then this step and the one after it are skipped because all aircraft in need of re-optimization are already in the potential and actual presence format, and the optimization process occurs directly from that state. Usually, the trajectories of new entrants to the optimized airspace, as well as modifications to the routes of those currently flying there, will be in terms of a flight plan based on a sequence of surface coordinates; these have to be reconstituted into the necessary potential and actual presence format and such takes place in the next step. For currently flying aircraft, their potential and actual presence data has to be altered to correctly define the situation at the point of reoptimization; all presence data, except for actual presence data in effect at the point of optimization, is archived to allow creation of presence data based on a trajectory that uses the aircrafts' position at the point of optimization as a new start point.

There are two important things to note about this capability. The first is that the changes occur at the flight plan level, i.e. changes are defined as alterations to the list of coordinate waypoints; this allows interoperability between trajectory change methods that are based on such. The second is that this could have been performed at the NMD store level, the data therein representing the situation as best understood at any moment in time; that it was not allowed here was due to preference of interoperability over untested capability. That said if methods for direct usage of NMD data were sufficiently developed, their use in the optimizer would be ideal.

5.1.3 Define Unseparated Fuel Optimized Parameters for New or Altered Trajectories

The rationale for this step is spread over three different sources; the original, conceptual, and practical need of it. The original need for it was due to the tendency of gradient based optimizers, the interior point algorithm used here being one, to find local as opposed to global optimums. This is particularly noticeable in optimizations of the spatial relationship between three or more entities; the possibility of a 'locked' spatial relationship being carried throughout the optimization becomes higher. For the variables of an individual aircraft, this 'locked' state can be created, but not as readily so; thus aircraft variables are optimized individually first, then collectively combined to create a global optimum that satisfies all constraints except for separation. The de-optimisation required to reach the true global optimum should therefore be minimal, and the gradient information at the initial point accurate enough to get the correct local optimum. Conceptually speaking however, even before the original need was realized, this process was meant to act as a simulacrum of airline and pilot preferences input prior to ATC interference; to show how such could be used or treated in the cooperative fuel optimization effort. That the original need showed a requirement for the same means of determining aircraft fuel usage and performance between airline, pilot and ANSP, was a very important conclusion in the development of PCO. That the same step be well defined and developed in the PDO therefore goes without saying.

From a practical perspective, the same process does provide information that is necessary for testing the PDO, but that cannot be readily obtained elsewhere. While a flight plan can be stitched together using publicly available data on preferred cruising levels, speeds, climb and descent rates, there would be no confirmation such would ever be planned, and it is possible that the preferences used maybe incorrect for that flight, or the traffic expected during it. Thus being able to determine 'an' optimum trajectory that satisfied known performance constraints was inherently useful. The same was true for the amount of fuel an aircraft should carry for a particular trip; no readily available data existed on it, and at the least, a means including it as an airline preference was needed. Thus an initial fuel capacity variable was added to the individual aircraft optimizations with constraints on how much should be left to prepare for ATC interference and other traffic requirements; this allowed in one simple step the calculation of an aircraft's preferred trajectory and the amount of fuel it had to carry, and caused no latent issues elsewhere.

5.1.4 Perform Initial Separation Assessment.

After each individual optimization has been completed, they are linearly interpolated (through constant acceleration and constant climb angle) as NMD data so that their potential and actual presence can be defined. When this has been completed for all new and altered trajectories, these presences are combined with those from the remaining currently flying aircraft and a scenario wide separation assessment occurs. There are three stages

to this process; a potential presence conflict assessment, an actual presence conflict assessment, and a conflict grouping assessment. The first two determine and define the need for optimized separation at all, while the last, if activated and where possible, reduces the size of the optimization problem; all stages can provide reductions in optimization time.

Potential presence defines, via the trajectory dimension limitations mentioned in 3.2.2.2, the complete phase space of an aircraft's trajectory assuming minimum and maximum speeds and altitudes and adjusted for the requisite separation limits such would require; thus if the potential presence of two aircraft overlap each other, then there is the 'potential' for conflict between the two aircraft. If no potential for conflict exists, separation optimization is completely bypassed; if potential conflict exists; the check for conflict among actual presences occurs. The actual presence of an aircraft is merely the aircraft's 'actual' trajectory extended via requisite separation limits to define a 4d presence in optimized airspace. Clearly if these overlap there is an actual conflict and the separation optimizer must run, otherwise the separation optimization is completely bypassed again.

Defining potential presence and conflict does seem redundant; however the information defined there is then used in two other areas that help reduce optimization time. The most important usage is in the separation optimization process itself; as potential presence is a complete representation of an aircraft's phase space, conflict interaction between two aircraft can only occur in their overlap, thus the state based separation nodes that define separation constraints only exist in the longitudinal and latitudinal region of that overlap. Consequently, reduction of optimization time comes from the critical number of separation constraints; any less and the assumptions that underpin the state based separation fall apart, while the inclusion of any more would provide useless data.

The second usage of the potential presence data, and the last stage of the scenario wide separation assessment, stems from an assessment of the first usage of the potential presence data. There, a critical number of nodes are created for the assessment of separation constraint; if none are needed, none are created. Thus, it is possible for individual, or groups of, trajectories to not have any connected separation constraint with other aircraft. In the case of individual trajectories with no separation constraint, the separation optimization for that aircraft could be bypassed as the aircraft would usually already be on a trajectory that fully satisfies all other constraints. In the case of isolated groups, separation optimization of the isolated group could be performed away from all other aircraft: firstly, it would allow parallel computation of multiple sub scenarios which could reduce computation in actual time, and secondly, as computation time for this optimization process is likely to be polynomial based on the number of variables, even sequential optimization of multiple sub scenarios could be faster than simultaneous optimization of all variables in the same scenario. The assessment of conflict groups therefore defines isolated groups and individual trajectories so as to further reduce computation time in those ways.

5.1.5 Perform Global Concerted Optimization, if required.

The global concerted optimization performed here can either be the PCO or the BFO developed in section 4; whatever the choice, it is reiterated separately for each isolated group found. It only runs if the previous step indicated an actual conflict, or if a previously conflicted aircraft has had its trajectory altered. The rationale behind the former is obvious, however further explanation is needed in the case of the latter: an aircraft that had its trajectory altered via a flight plan change would necessarily go through the individual optimization step in

5.1.3, however no such optimization would occur for the aircraft it conflicted with previously. It was possible to use previous conflict assessment data to also tag those it was in conflict with to also go through individual optimization; however it was simpler to tag them for separation optimization instead. Separation optimization in this situation is preferred as individual optimization would have reset and lost the separation that was achieved in previous separation optimizations, therefore requiring more computation time to reacquire those separation modes. The removal of one trajectory from a conflict group has not lead to a grossly erroneous separation optimization result yet, however in the event it does, enforcing individual optimization for an entire conflict group, even if only one trajectory from the group was altered, may be reconsidered.

5.1.6 Apply new trajectories, and wait for next event.

Once the optimization in the previous step has been completed, the resultant trajectories are then converted to their potential and actual presence formats and stored. This data is then used to allow comparison between actual and intended arrival times at particular NMD nodes. Further, the data is sufficiently dense that accurate assessment of how ahead or behind time the aircraft is should be available at any point during the trip; it should therefore be possible to setup an automatic execution of a re-optimize event if an aircraft becomes too far ahead or behind its schedule. That said, as the optimizer handles the 4D control of all trajectories in optimized airspace, re-optimization events do not have to occur at the time they are needed; there is sufficient data management capability currently within the optimizer to support prediction of a future re-optimization event and the scheduling of the necessary re-optimization to occur at a set time before it. This would prevent frequent unnecessary re-optimizations, and would allow various updates and alterations to accrue before re-optimization; therefore taking advantage of the optimizer's ability to assess multiple new and altered trajectories in one optimization process.

5.1.7 Resultant PCO Based Dynamic Optimizer Architecture

Applying all the steps mentioned above into a working architecture creates yields the diagram below.

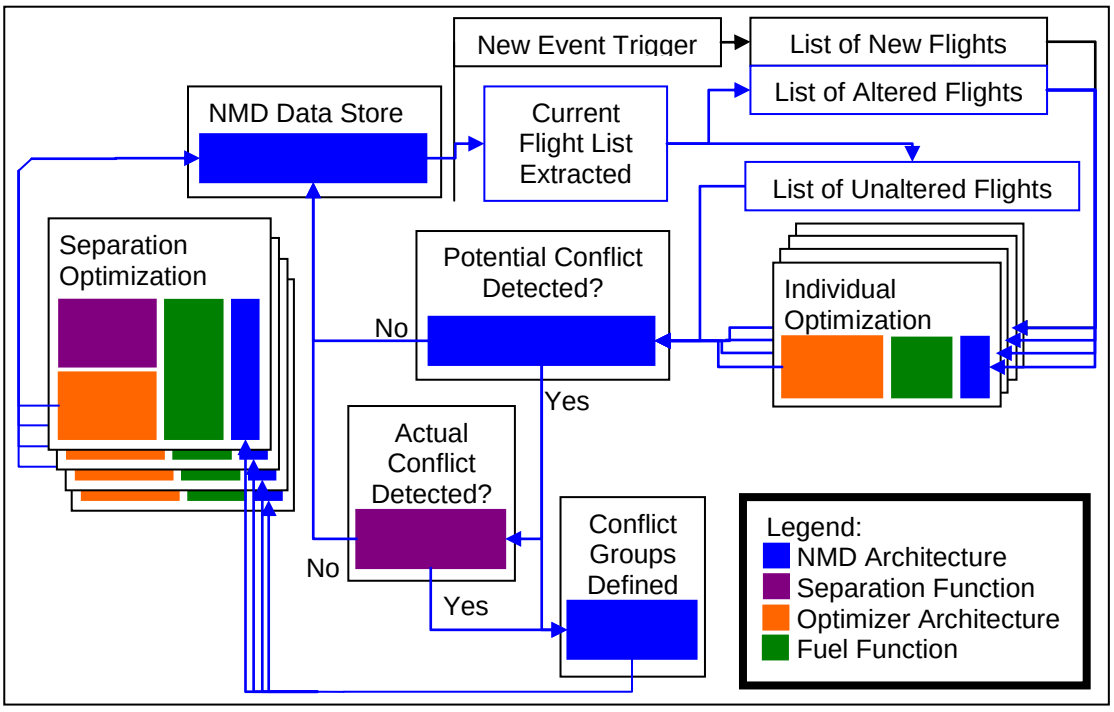

Figure 48 - Functional Data Flow and Architecture during a first stage implementation of PDO

5.2 Dynamic Optimizer Case Study Assessment

For this section there are two forms of assessments to be made. The first uses scenarios to showcase the additional functionality that the dynamic optimizer gives; the ability to perform and optimize changes in trajectories, and the ability to assess and isolate mutually exclusive scenarios. The second uses another scenario to show efficiency differences between a static and dynamic optimization.

5.2.1 Handling Route Changes

For this assessment '10acPSd', as shown in Figure 49, was taken and altered to allow PDO specific operation; i.e. each of the 10 aircraft therein were placed into separate trigger events denoted by their start time, which is defined as when that aircraft entered airspace. Assuming no unpredicted scenario changes, the results in Figure 51 occur. '10acPSd' was intended to be representative of a common scenario; however when it first ran it showed how aircraft travelling on the same route, even with sufficient initial separation between aircraft, could still affect each other en route. Minor speed adjustments were necessary to slow aircraft down when those ahead of them were slowing down to enable an efficient glide to descent. The PDO version of Figure 51 is similar in nature. However, the PDO version of 10acPSd was then run again, but with another trigger event occurring at the 80th minute; the destination for all aircraft at (9, 9) was closed down for some reason and all aircraft heading there had to be diverted to another destination at (1, 9). The results of this optimization are shown in Figure 52.

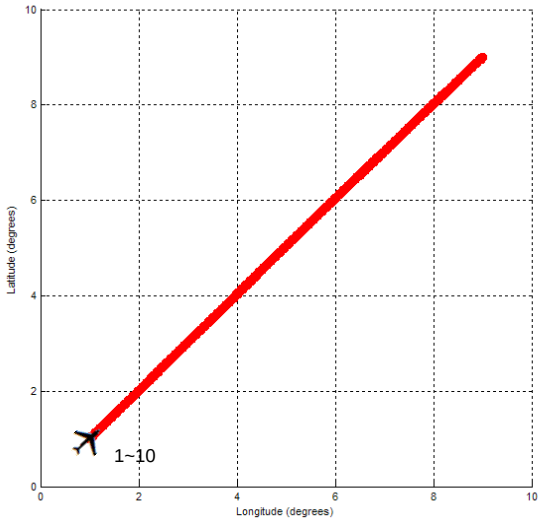

A/C ID	Start Time	Distance Covered	AC Type	Initial Weight(t)
AC 1	00:10UTC	678nmi	B747-300	267t
AC 2	00:10UTC	678nmi	B747-300	268t
AC 3	00:21UTC	678nmi	B747-300	272t
AC 4	00:21UTC	678nmi	B747-300	277t
AC 5	00:32UTC	678nmi	B747-300	281t
AC 6	00:32UTC	678nmi	B747-300	286t
AC 7	00:43UTC	678nmi	B747-300	290t
AC 8	00:43UTC	678nmi	B747-300	295t
AC 9	00:54UTC	678nmi	B747-300	299t
AC 10	00:54UTC	678nmi	B747-300	304t

Figure 49 - Situational Details for '10acPSd' unchanged

Where the situation in Figure 51 allowed trajectories quite close to their optimums, Figure 52 did not; an orderly stream of aircraft was suddenly forced to reach the same destination at the same time, causing a disruptive choke point to occur. Figure 52 shows how the BFO had to resort to high and frequent climb angle changes to slow aircraft and gain sufficient time separation between successive aircraft when exiting airspace; high-lift devices could provide more appropriate alternatives, but insufficient information on their application prevented their use in the aircraft performance model. However the optimization was successful and is indicative of the handling capability of the PDO even in harsh dynamic scenarios. It should be noted that the harshness of the result was due to the intentionally challenging destination change; changes that are backed up with pre-set emergency

handling methods or route structures are not as likely to lead to similarly harsh results. That said if no externally created route change is supplied, and trajectory control is left to the optimizer which successfully performs it, then even though the trajectory may look severe and chaotic, it should still be performable by the aircraft.

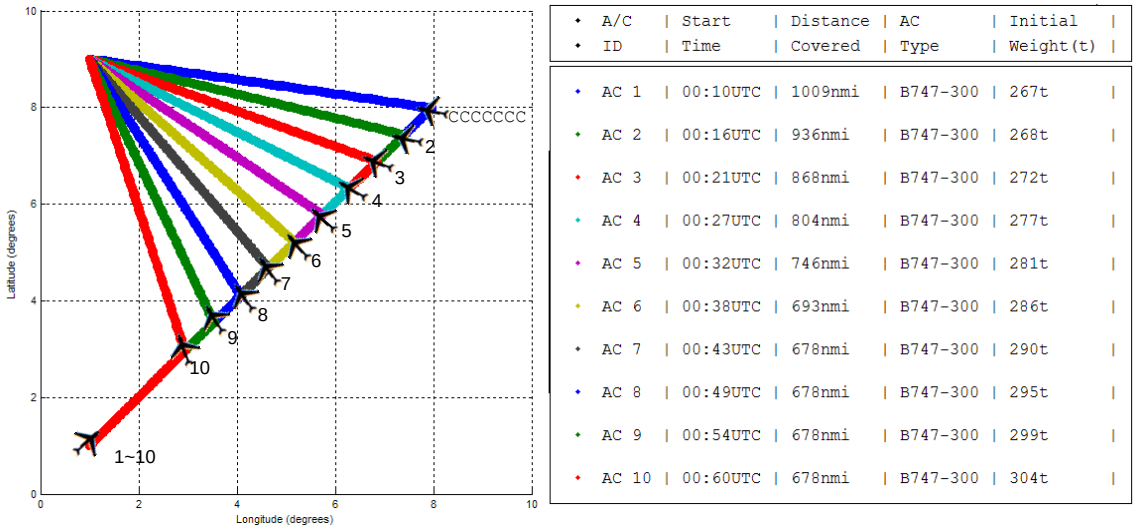

A/C ID	Start Time	Distance Covered	AC Type	Initial Weight(t)
AC 1	00:10UTC	1009nmi	B747-300	267t
AC 2	00:16UTC	936nmi	B747-300	268t
AC 3	00:21UTC	868nmi	B747-300	272t
AC 4	00:27UTC	804nmi	B747-300	277t
AC 5	00:32UTC	746nmi	B747-300	281t
AC 6	00:38UTC	693nmi	B747-300	286t
AC 7	00:43UTC	678nmi	B747-300	290t
AC 8	00:49UTC	678nmi	B747-300	295t
AC 9	00:54UTC	678nmi	B747-300	299t
AC 10	00:60UTC	678nmi	B747-300	304t

Figure 50 - Situational Details for '10acPSd' redirected to (1, 9) at t = 80

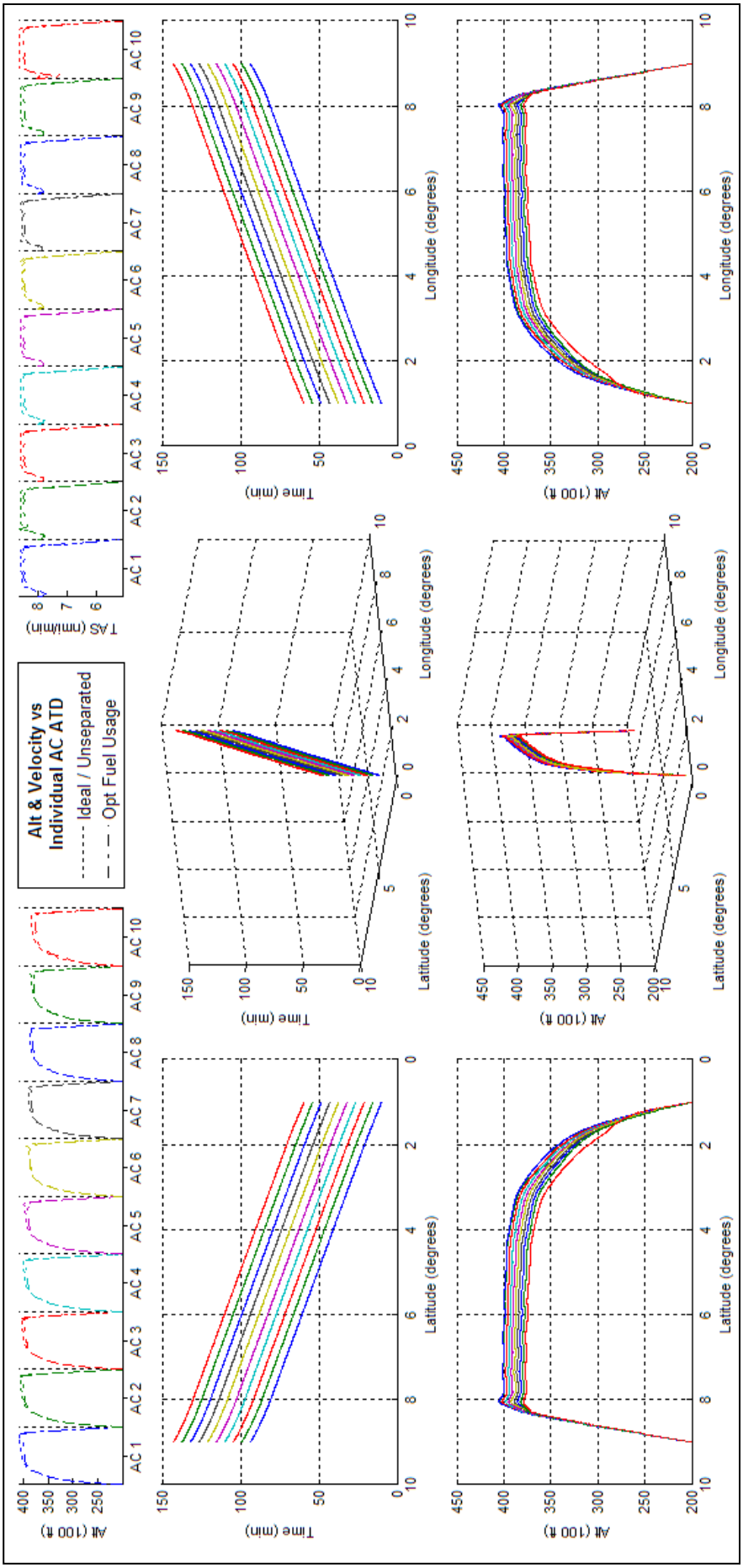

Figure 51 - BFO Result of '10acPSd' unchanged.

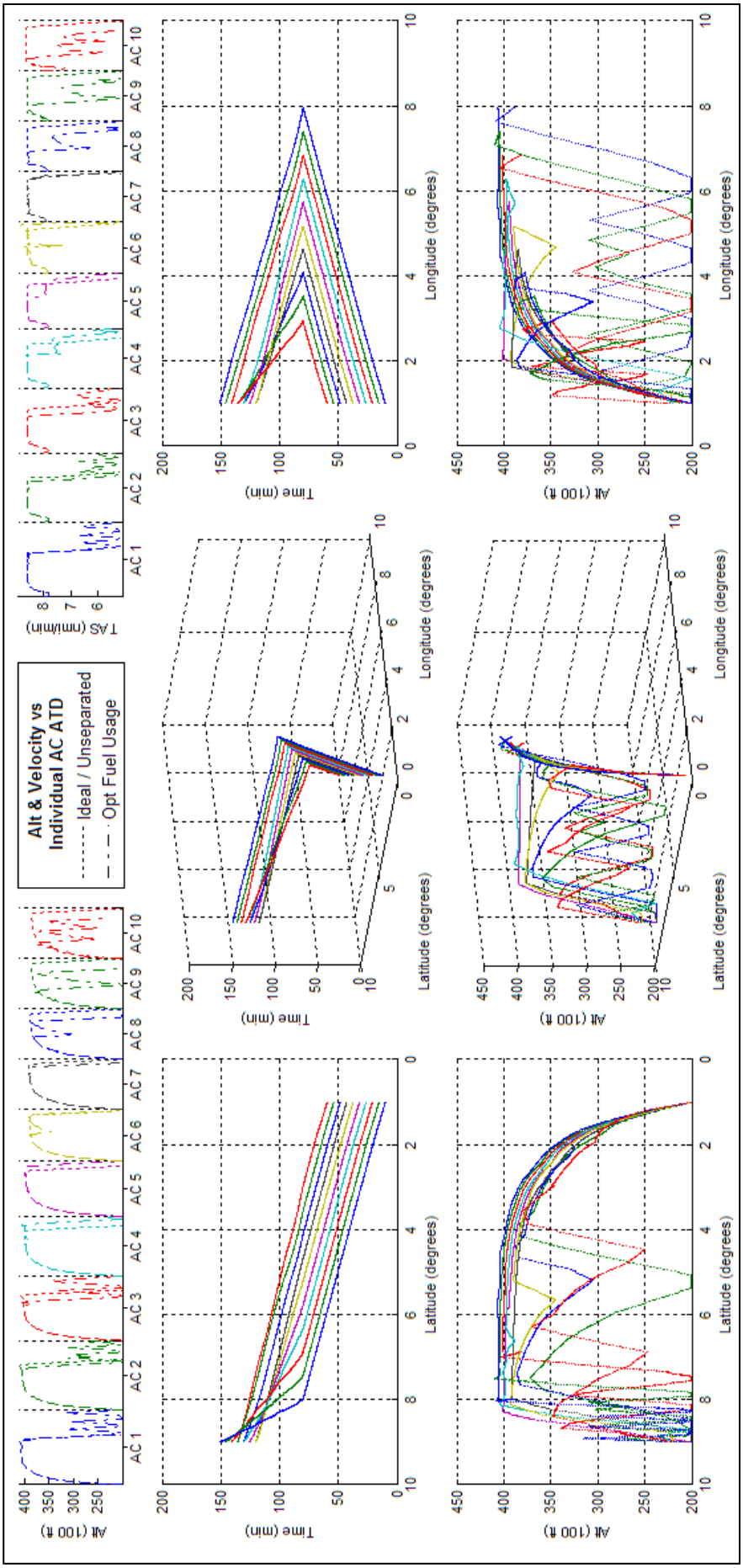

Figure 52 - BFO Result for '10acPSd' redirected to (1, 9) at t = 80

These diversions do not always create severe and chaotic trajectories; a simpler scenario was created and trialled to show how. The simpler scenario had six aircraft travelling the same route, but with three aircraft east bound and staying 30nm north of the route, and three aircraft west bound and staying 30nm south of the route. Before the 17th minute, the three aircraft in each group maintained 5 minutes of longitudinal time separation from each other aircraft in the group. At the 17th minute, unflyable weather was recognized in the region between 3° and 7° longitude, and above 4.25° latitude; this therefore required an externally applied route change to force all east bound traffic to converge on the west bound route temporarily until they could travel direct to their exit point. As a result however, their route change caused significant potential conflict with aircraft on that route. This scenario has a couple of distinct differences from the scenario in Figure 52. The first is the lesser number of aircraft; the impact of any unpredicted scenario grows significantly as more aircraft are involved due to an inability to respond exactly to it, thus lesser impacts would occur with lesser numbers of aircraft. The second difference is that the conflict occurs at a distance away from the entry and exit points; this provides additional freedom to resolve conflict as travel through entry and exit points are constrained in altitude to the minimum of the airspace. As can be seen in the optimization of this scenario in Figure 54, even though there is still some height oscillation being experienced, the majority of the trajectories are smooth and only distorted where required to ensure separation.

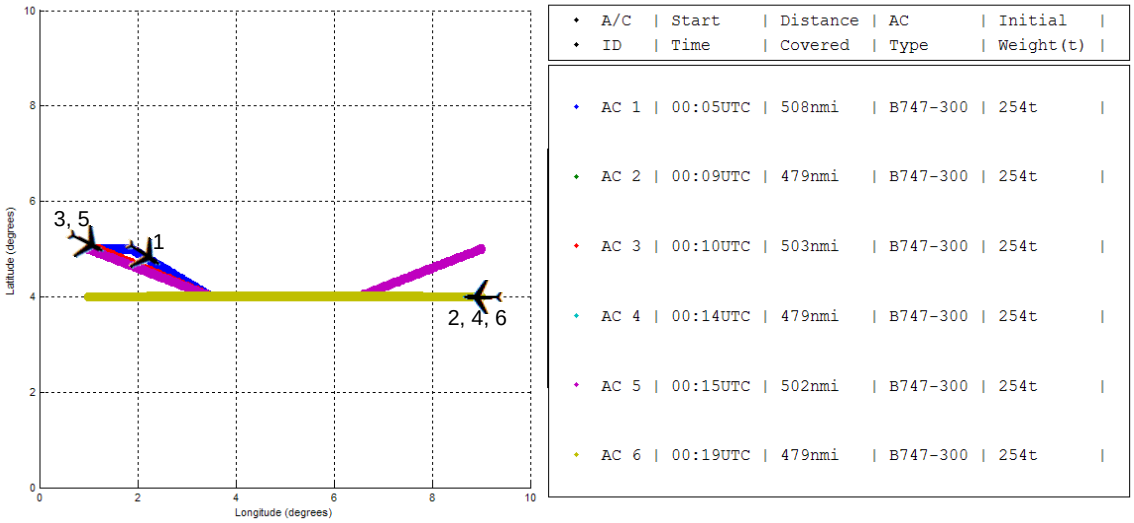

A/C ID	Start Time	Distance Covered	AC Type	Initial Weight(t)
AC 1	00:05UTC	508nmi	B747-300	254t
AC 2	00:09UTC	479nmi	B747-300	254t
AC 3	00:10UTC	503nmi	B747-300	254t
AC 4	00:14UTC	479nmi	B747-300	254t
AC 5	00:15UTC	502nmi	B747-300	254t
AC 6	00:19UTC	479nmi	B747-300	254t

Figure 53 - Situational Details for a Weather Diversion (at t = 17) causing two opposite heading groups of three trailing aircraft to travel on the same route.

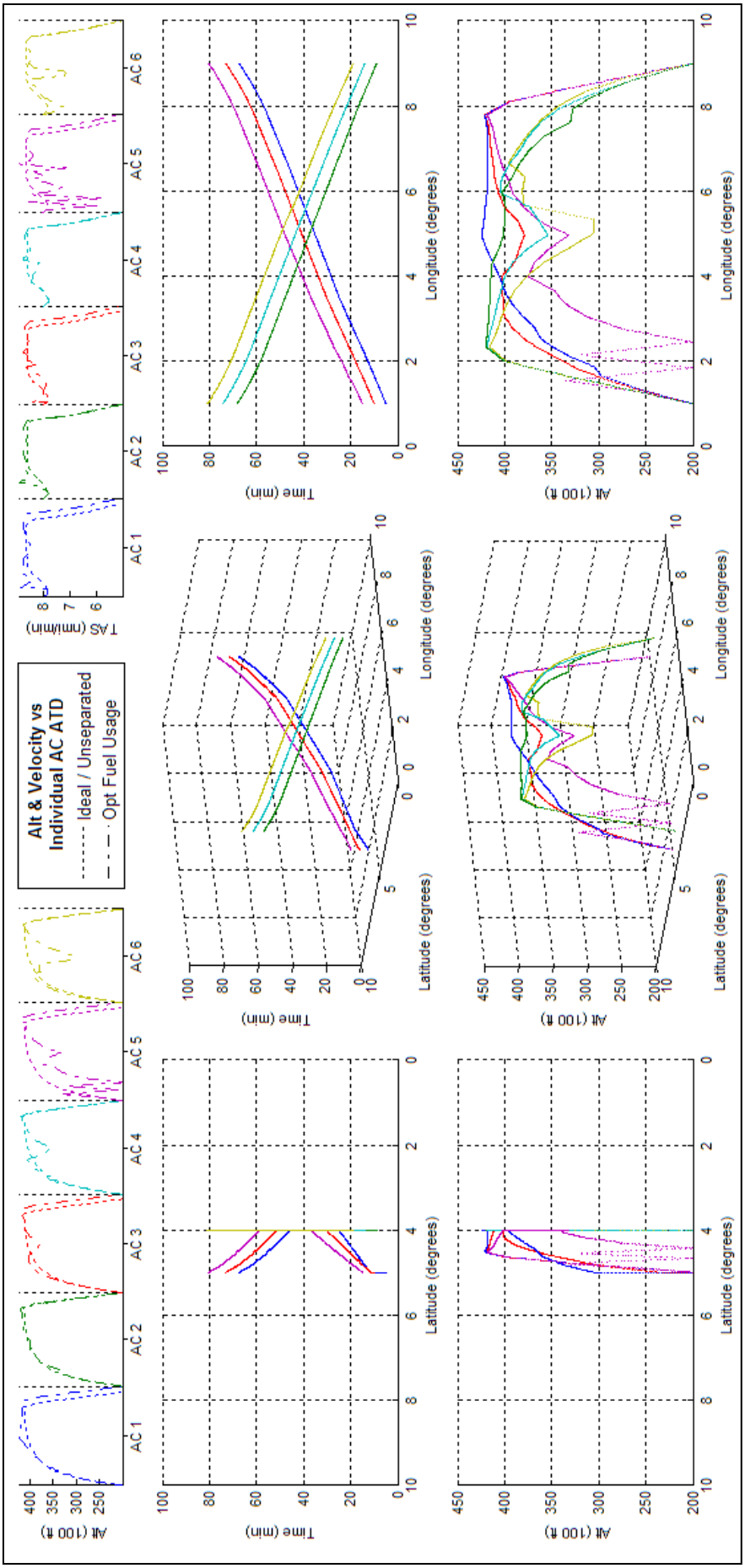

Figure 54 - PDO Result for a Weather Diversion (at t = 17) causing two opposite heading groups of three trailing aircraft to travel on the same route

5.2.2 Isolation of Mutually Exclusive Scenarios

Performing a conflict group assessment on any of the scenarios listed in Table 8 is redundant as they are all intentionally within the same conflict group; to show how it works a larger scenario featuring many more aircraft over a larger area has to be assessed. To this end, 2007 domestic flight statistics [57] were used to simulate an average day's worth of air traffic for Australia; the number of trips between destinations were averaged on a day then evenly distributed over 24 hours. As per the optimizer's current requirement of only optimizing cruise phases, these trips were modified to begin and end at 20,000ft, 30 nautical miles out from their departure point and destination. Rather than the usual practice of setting cruise flight levels depending on east or west heading, aircraft were set on trajectories that maintain a greater than 7 nautical mile cross deviation from (i.e. 7 nmi left of) their departure aerodrome centre to destination aerodrome centre great circle path. An initial check was run to ensure that separation constraint between the entry points of all aircraft was satisfied; the optimizer cannot control when and where an aircraft enters optimized airspace, thus any of its optimizations will fail if entering aircraft are not sufficiently separated from other nearby entering aircraft. The same would be true for exit points if a constraint on exit time was required. The check found four aircraft with conflicting entry points and these were removed for future optimization efforts; if a larger percentage was found to have such a conflict, the most likely solution would have been to use alternating entry points that are all within 30nm of the departure airport and parallel to either the original or connecting trajectory. On the assumption all aircraft within were Boeing 747-300s, the results of the potential conflict assessment of the entire scenario and the definition of mutually exclusive scenarios such would create, are shown below in Figure 55 and Figure 56.

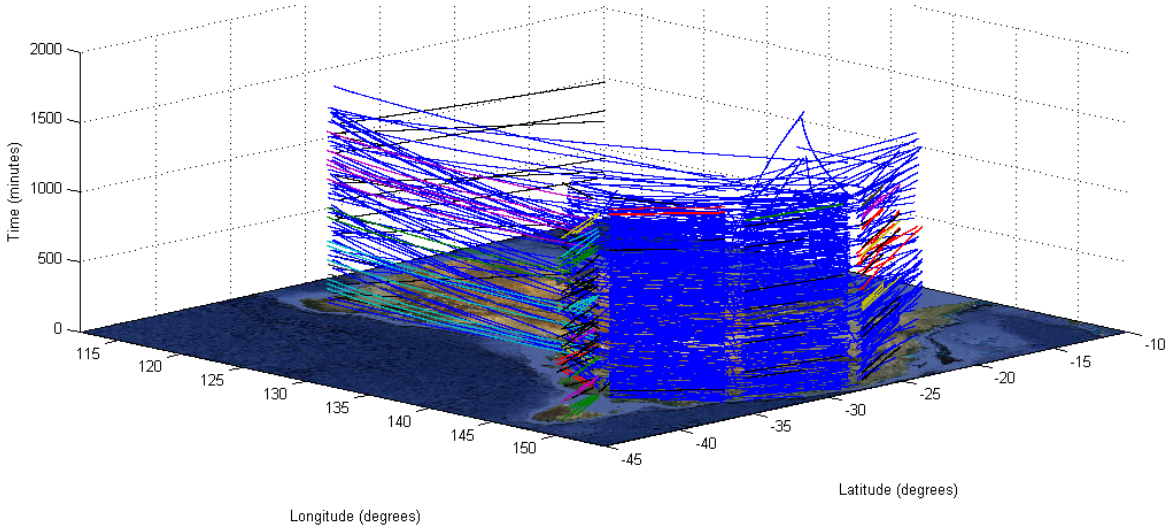

Figure 55 - Average Day of Australian Domestic Air Traffic against Time; colours indicate conflict groups.

The time dimension in Figure 55 refers to the concurrent time everywhere on the map; thus an individual trajectory would appear to be increasing in time as it travels along its ATD, the gradient of the increase indicating the TAS of the aircraft at that time. The colours shown do indicate separate conflict groups, however the colour black is special in that it shows trajectories that are completely separated from all other trajectories;

these do not share potential conflict with any other aircraft and would therefore be exempt from separation optimization. Finally, any curvature perpendicular to the time dimension is due to earth curvature and nothing else. There are several observations to be made of Figure 55. The first is that the majority of the trajectories therein exist in the same potential conflict group; i.e. the blue mass of lines. The dense air traffic on the south eastern side effectively act as hubs for most domestic traffic thereby requiring entry and exit points to have barely enough time separation between them; it would be expected that these, and all aircraft that cross them, would therefore become part of the same group. What was not expected was the proliferation of the same blue group; while maintaining a slightly 'left-sided' trajectory and the exclusion of the aerodromes directly over airports are warranted for real reasons, they also do act as barriers to aircraft interaction. That the blue group has incorporated so many aircraft indicates how far in time a single group can extend; the causative relationships both forward and backward in time, as well as through non-hub junctions, can force even previously separated groups to be considered at the same time. Figure 56, which shows the corresponding numbers of aircraft for each of the colours shown in Figure 55, also confirms the majority share that the blue group consists of.

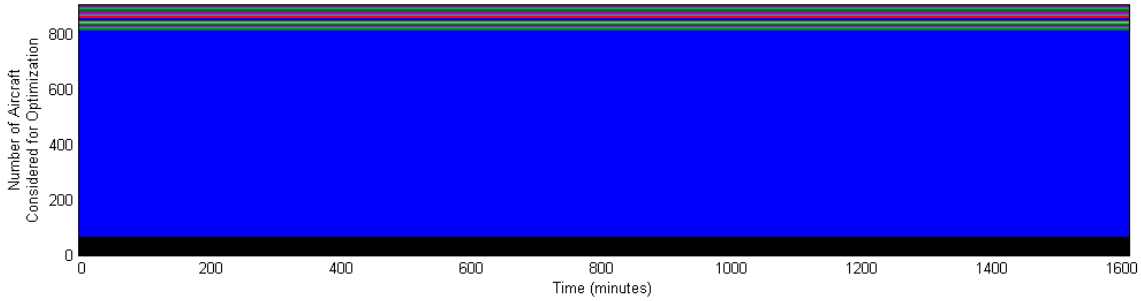

Figure 56 - Overall Conflict Group Distribution for an average day of Australian Domestic Air Traffic

It is important to note that Figure 55 is resultant of the conflict group assessment of the entire day's worth of traffic considered in one go, as confirmed by the static nature of Figure 56. This can mean different results for the PDO in actual usage for two reasons. The first reason is due to the likelihood of unexpected occurrences; previously unknown flight plan alterations either intentional or not can cause groups to join or break depending on the action. Aircrafts in unplanned holding patterns increase the 4D volume of their potential presence so will combine groups together; whereas aircraft that forego a busy airport for any reason increase the likelihood of the conflict group at the airport being broken up. Thus even if a conflict group assessment was carried out for a day, it is unlikely to remain the same for the duration; this inherently implies that a conflict group assessment could only realistically occur in a PDO type setup, hence its inclusion at this stage rather than any earlier. The second reason for difference of the PDO in actual usage is that when using the PDO in its current minimalist perspective the entire day would not be considered at the same time, only aircraft that are in, or about to enter, optimized airspace would be included; potential presence overlap between existing and non-existing aircraft, as well as between existing and previously existing presences, i.e. presences that have been past, will not occur. This can fragment the conflict group assessment even further causing even greater number of mutually exclusive groups, and even smaller numbers per group, than those shown in Figure 56. To show such fragmentation the same traffic assessed above was altered to be seen through a minimalist perspective. The traffic scenario was divided and sorted according to their upper level airspace entry times and an update interval every five minutes; the PDO would then treat each interval with new entrants as a new event that would trigger re-optimization. The equivalents of Figure 55 and Figure 56 in this perspective are respectively Figure 57 and Figure 58.

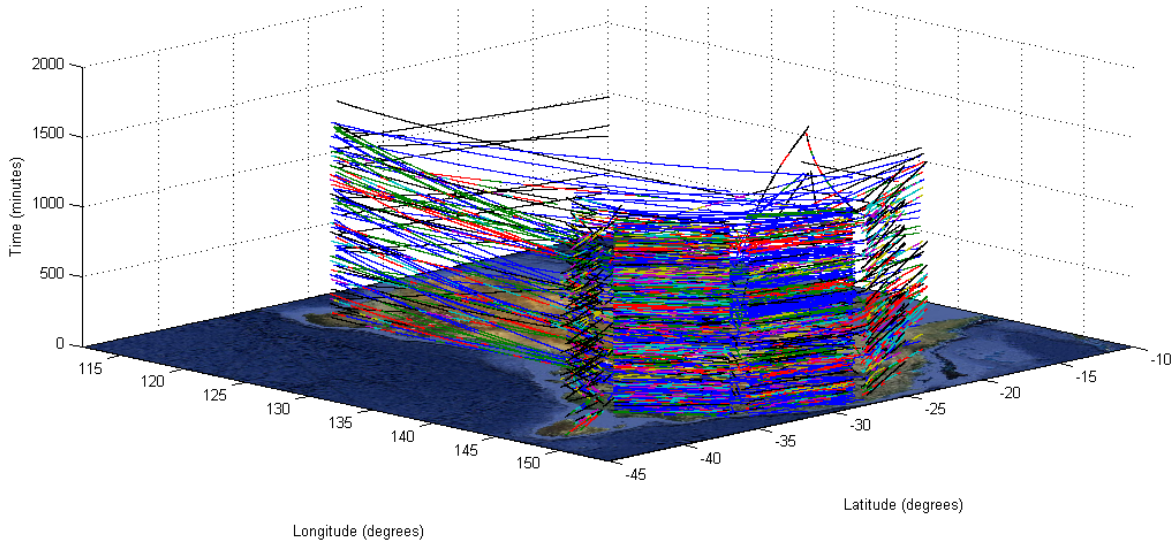

Figure 57 - Average day of Australian Domestic Air Traffic against Time; colours indicate Dynamic Conflict Groups.

Many notable differences exist between Figure 55 and Figure 57 however it should be remembered that a dynamic scenario requires multiple re-optimizations; the apparently greater number of conflict groups is caused by the unique potential conflict group assessment that is performed by each re-optimization. The number of overall conflict groups does not actually change, merely that the minimalist perspective that causes the need for the re-optimizations limits their ability to become whole groups. That Figure 57 contains individual trajectories with multiple group colourings is further indication that the variation in conflict groups is time based; it is also indicative of the ability of the optimizer to exclude aircraft that were optimized previously from future optimizations, as shown by trajectories with partially black colouring.

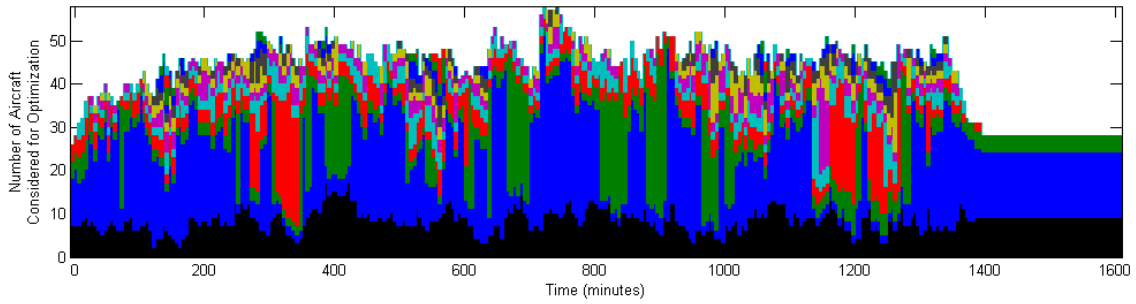

Figure 58 - Dynamic Conflict Group Distribution for an average day of Australian Domestic Air Traffic

Figure 58 confirms all of the statements regarding Figure 57 as it shows the distribution of conflict groups and how they change in size over time; despite the continued reassessment, the blue group still has a large share of the number of aircraft undergoing separation optimization. However Figure 58 does also show the key differences between the holistic and minimalist perspectives in PDO optimization; where Figure 56 is constant and comprised of large numbers of large groups, Figure 58 is chaotic and comprised of small numbers of small groups but reiterated a large number of times. This last point emphasizes the usefulness of the minimalist perspective in the PDO in terms of handling computational requirements; the optimization of small numbers of small groups likely to require less computation time and resources.

Another point to mention is that Figure 57 and Figure 58 assume that an aircraft is removed from potential conflict, i.e. becomes ‘black’, either when it is no longer in potential conflict, or it reaches its destination and no

longer has any trajectory left to be optimized. In the latter, it is still possible for the aircraft to cause potential conflict because the time aspect of its presence is still required to ensure time separation between it and aircraft close behind it. As the trajectory has been completed, its presence becomes immutable; i.e. its actual presence cannot be changed, and any separation requirements would be ensured purely by the movement of other aircraft. This also means that it cannot facilitate interaction between aircraft that are separated by it; its presence becomes much like the barriers to interaction mentioned previously. The point of discussion here is where and when can an aircraft be effectively assumed to be at its destination and therefore be defined as immutable and become a barrier to aircraft interaction; in terms of logical rationale and coding this point would be when the aircraft has passed all NMD points in the aircraft's presence that are not at the destination, however from an ATC and pilot perspective trajectory may well be considered immutable at a noticeable time before, or distance ahead, of the destination. In recognition of this, as well as to avoid optimizing extremely small trajectories, the PDO was coded to set any trajectory with a remaining ATD less than 2.5nmi to be immutable; where 2.5nmi represents half the desired fuel calculation interval and a reasonable distance at which no more variation would realistically occur. Under this setting, the equivalent of Figure 57 looks largely the same; however the equivalent of Figure 58, as seen in Figure 59, does display some useful data.

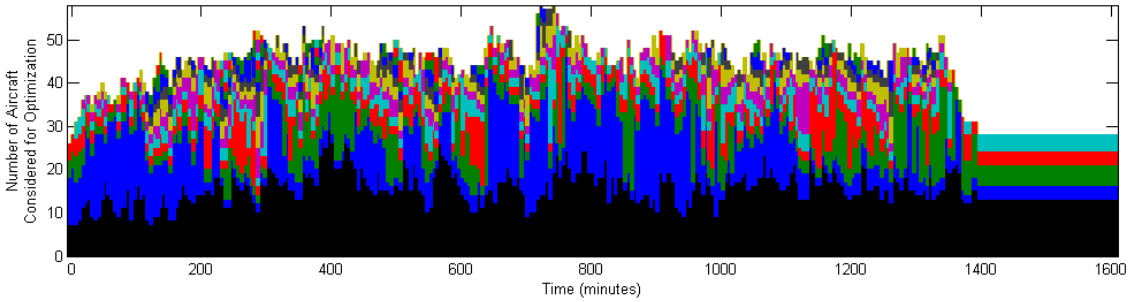

Figure 59 - Figure 58 assuming trajectories become immutable 2.5nm before exiting optimized airspace

As expected, the amount of aircraft classified as being non-optimized has increased, but it has done so far more than expected; in some events doubling and tripling its value compared to that in Figure 58. Further, the numbers of the blue conflict group are significantly diminished, with the other groups slightly increasing in number and size to pick up the slack. It can therefore be inferred that the 2.5nmi region prior to exiting airspace is a common means of allowing interaction between aircraft and of connecting conflict groups. From a computational view point it is very tempting to further increase the distance of immutability so as to fragment conflict groups further to gain additional decreases in requisite computation times.

5.2.3 Efficiency Differences

In theory, the inability to consider future scenarios, i.e. due to the minimalist perspective of the PDO, should cause fuel losses; e.g. if aircraft A had to maintain a lower cruise altitude for longer because a previously unseen aircraft B had to take aircraft A's intended position should mean that aircraft A had to use more fuel than intended. The situation discussed here however shows how the near opposite occurred in the PDO test trial; a result that used less fuel than its holistic counterpart. To be fair the difference is sufficiently small enough to be within the allowable error of the BFO, however the fact that it can occur requires discussion on what can cause it, and what such would mean for future optimizations. This occurred in '10acPH2H', which has been shown previously in Figure 26; its BFO result can be seen in Figure 61.

The critical scenario defined in Figure 26 was designed to show how an optimizer would deal with two chains of five aircraft heading along the same track in a head on manner; the time separation between aircraft in a chain was set to be slightly greater than two times the minimum separation requirement to see how the optimizer would utilize that region of empty space. Of the scenarios in Table 8, only those that had aircraft entering optimized airspace at different times could be reinterpreted using a minimalist perspective; if all aircraft are present, there remains no ability to create a hither to unexpected intersection. Further to ensure sufficient displacement is created to allow visual observation of PDO method influences, only those with complex intersections could be used. In other words '10acPH2H' was the only applicable scenario to initially test the PDO; other scenarios could be developed, but there was insufficient knowledge on the subject to suggest how scenario parameters should be changed to properly test the PDO.

The BFO result in Figure 61 is typical for scenarios with head on trajectories between aircraft with different weights; these led to differing ideal altitudes and the eventual usage of the empty space between chained aircraft to allow ‘sequencing’ of aircraft in the time dimension. To prepare for the sequencing aircraft had to expand the time separation they had, via the noticeable pattern of frequent climb angle changes, as well as diverting to an alternate altitude to avoid collision; further, due to the differing ideal altitudes, the effect was propagated downwards and lower level aircraft had to experience greater altitudinal diversions to compensate. If this scenario was re-interpreted using a minimalist perspective a new event would be triggered each time an aircraft pair departed, i.e. every 11 minutes, as each pair was set to depart at the same time. The PDO result for this interpretation can be seen in Figure 62.

The PDO result in Figure 62 tells a very similar story to that in Figure 61; timed sequencing of aircraft and the propagation of altitude changes increasing downwards. The difference was the smaller overall altitudinal deviation. At first glance there could be a number of optimizer acceptable reasons for this; altered TAS to increase time separation and allow expedited returns to ideal altitude, being the most likely. However if such were the case, then a comparison of fuel usages should indicate that the PDO result incurred additional fuel costs to support those mechanisms. Figure 60 suggests otherwise.

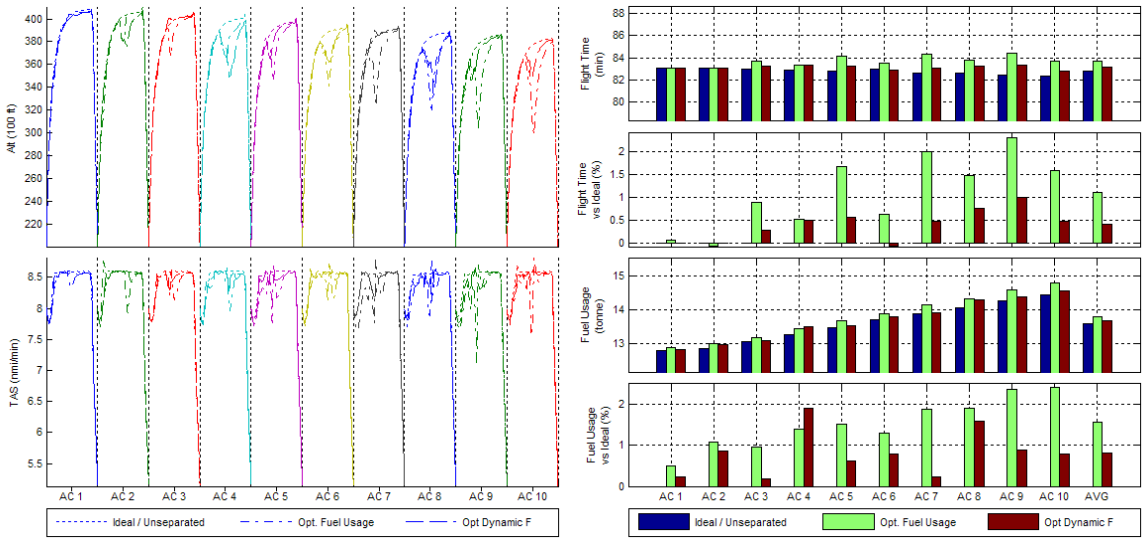

Figure 60 - Comparisons of Optimizer Variable (left) and Flight Data (right) between BFO, or ‘Opt Fuel Usage’, and PDO, or ‘Opt Dynamic F’, Optimizations of ‘10acPH2H’.

The comparison of result data in Figure 60 allows several conclusions to be made. The most apparent is that the PDO ATFU was less than in its BFO counterpart, and even more startling, it was less for each aircraft except aircraft four. The difference in average fuel percentage was less than 1% which is the equivalent of the error allowed for the BFF; however the distribution in fuel usage does indicate that the PDO did find a way to 'sacrifice' aircraft four fuel to allow lower fuel usages for all other aircraft as well as overall. This is backed up by the altitude variable data which shows the PDO resorting to lesser altitude deviations except in the case of aircraft four. While chaotic, the variation in the TAS variable can be considered minimal due to the relatively small deviations in flight time compared to the ideal; however the flight time data does show that the PDO did resort to lesser TAS deviations as well. That there are no increases in fuel usage automatically forces the question: how did the PDO get a result that is more optimal than its BFO counterpart in effectively the same situation? Given the lack of any randomness in the PDO methods, the answer must have something to do with the fact the PDO re-assesses each new event. Due to the NMD architecture, trajectory data fields stay the same unless a significant route change has occurred; hence any variation must occur with how the optimizer uses the data. As the portion of a trajectory that can be optimized reduces as the aircraft travels along it, so too must the control and fuel calculation node indices, ATD_i and $ATD_{N,}$ change to suit; thus the most likely cause of the difference lies with those two indices.

In previous testing with the PCO it was shown that having a vastly varying ATD interval could cause highly erroneous results for ATD intervals that are significantly smaller than the rest; the calculated fuel usage in such small segments being so low as to return inaccurate or nonsensical results, or be invisible to the optimizer. Having a pre-specified constant ATD interval for all intervals meant that one interval would have to represent a remainder that could become significantly smaller as the total remaining ATD reduced. Thus to avoid issues caused by having significantly smaller ATD intervals, the ATD was split so as to have the same number of equivalently sized intervals; these would be slightly smaller than the pre-specified constant ATD interval and would suffer variation as remaining ATD reduced, but would not carry any of the issues associated with intervals that are too small. This does mean that periods of constant climb and acceleration would differ for each new event, and that the resulting initial trajectory could be noticeably different than what was stored; further, the difference in ATD positions meant it would be impossible to return to exactly the same trajectory via optimization, making it certainly possible to get a different optimum.

Due to the accuracy of the BFF, provided no separation optimization is required, re-optimization to prepare for the new ATD_i and ATD_N should bring it back to within 1% of the fuel usage of the original trajectory. However, the possible side effects of using it with separation optimization are disconcerting; aircraft keep minimal separation to achieve optimum fuel usage, however the placement of the ATD_N has a direct effect on how an aircraft deals with an intersection. If a node from ATD_N is in the very middle of an intersection and the intersection does not expand to its connective nodes, then high climb angle changes usually result; separation is satisfied at the beginning and end of the intersection and the control node in the middle excessively satisfies the separation constraint so as to allow trajectory portions outside of the intersection to become significantly more fuel efficient. In contrast, if two nodes bound an intersection so as to produce a snug fit, the interval in between remains flush against the separation constraint it experiences since doing so would lead to the least fuel usage. In other words, if the PDO changes the ATD_N over time, the separation optimization result may also change over time.

While this does mean increased computational time, one has to wonder if this functionality is truly undesirable. In terms of positives, it should first be noted that such variation in separation optimization result has very little bearing on the actual flight other than the selection of an optimum trajectory; aircraft can only fly the flight plan that is set for them, which here is the result of the last separation optimization that was run. Thus it is unlikely for aircraft, under average conditions, to experience a chaotic trajectory; chaotic variation of optimized separation modes is not transferred to reality unless the scenario demands it (i.e. as in 5.2.1). Also, in optimization theory terms, the use of a varying ATD_N is slightly akin to using alternate initial values; the chances of finding a global minima is greater when using multiple initial values instead of just one, even if they occur sequentially in time. That it does this in its current form may provide an alternate means of reaching a global optimum for separation optimization; if it's too computationally difficult to reach it as soon as possible using multiple different initial ATD_N, allowing several iterations to change ATD_N and close in on it over time might be more feasible.

As a minor recheck to see if this occurrence was truly created by the use of new events, the re-interpreted scenario was further adjusted to have four more pseudo new events; new events placed halfway in time between each successive pair of previously used new events. These pseudo new events do not introduce any new aircraft entrants and serve only to mark where and when untriggered re-optimizations are required. With these in place, the interval between re-optimizations was reduced to a constant 5.5 minutes. The PDO result for this interpretation can be seen in Figure 63.

Comparing Figure 62 and Figure 63 the only significant difference was in the distribution of altitudes between aircraft eight, nine, and ten, which comprise three of the four aircraft in the last group to leave, and, due to linear distribution of initial fuel weights, are also the heaviest of the group, and thus perform the three lowest altitudes during their cruise. Reviewing the Figure 63 equivalent of Figure 60 found that aircraft eight bore the grunt of the fuel loss as it did in Figure 62; however this time, aircraft nine and ten adopted slightly less fuel efficient trajectories that resulted in aircraft eight flying a more efficient trajectory. This difference resulted in 56kg of fuel being saved as compared to the previous interpretation. It also gives more credence to the possibility that the variation in ATD_N and ATD_i does introduce a mild global optimization effect over time, as again, it was only possible due to the new ATD granted by the extra re-optimizations. To appropriately test this possibility however, further scenarios with comparable levels of conflict complexity and dynamic variation would have to be created; as the list of test scenarios currently stands, only '10acPH2H' had sufficient complexity to test such out, and further scenarios are required to gain confidence in the possibility as well as to compare against a non-varying ATD to see if the fuel savings justify the additional computational effort.

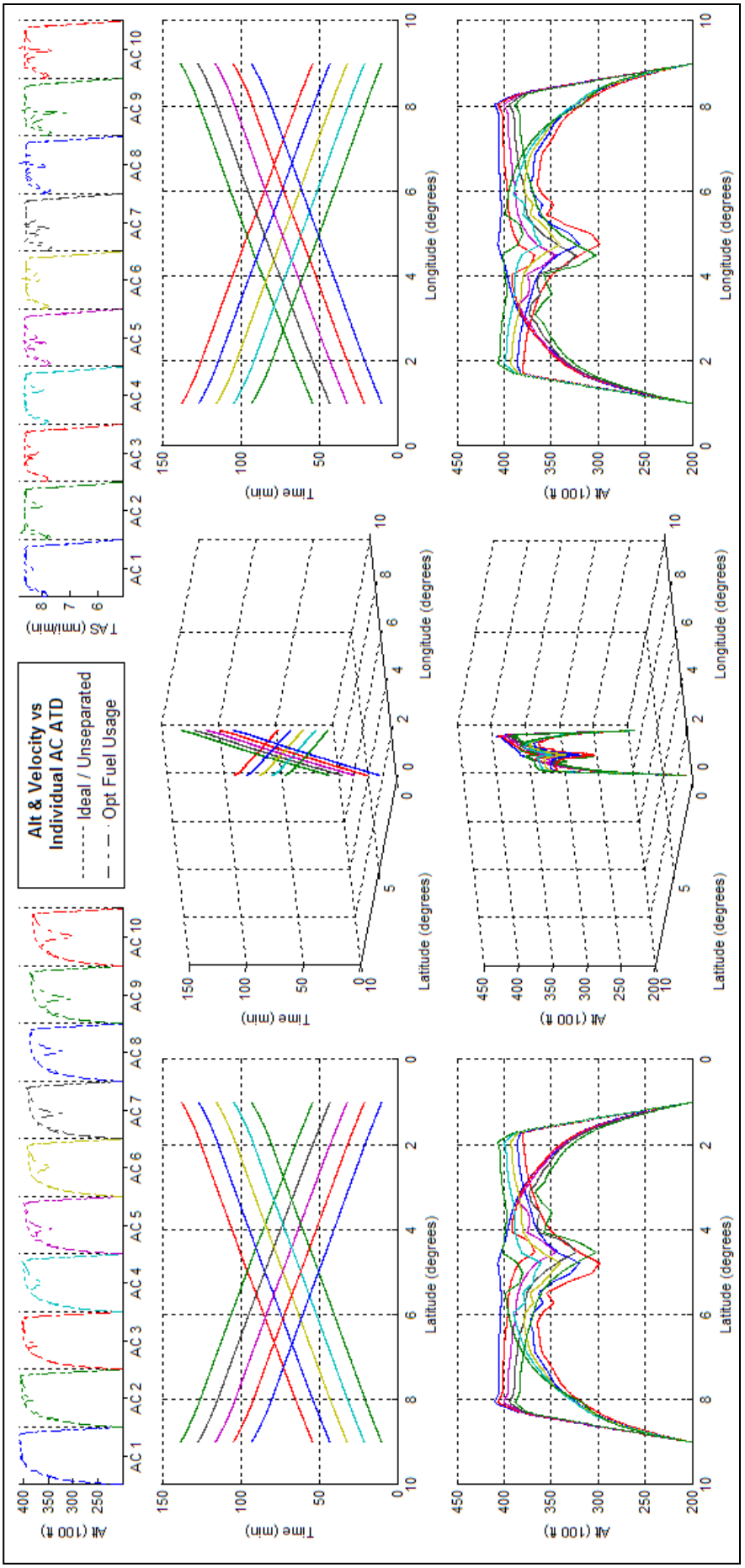

Figure 61 - BFO result for '10acPH2H': situational details (top), optimized results as a variable (middle), conversion of results into time and altitude in terms of longitude and latitude (bottom).

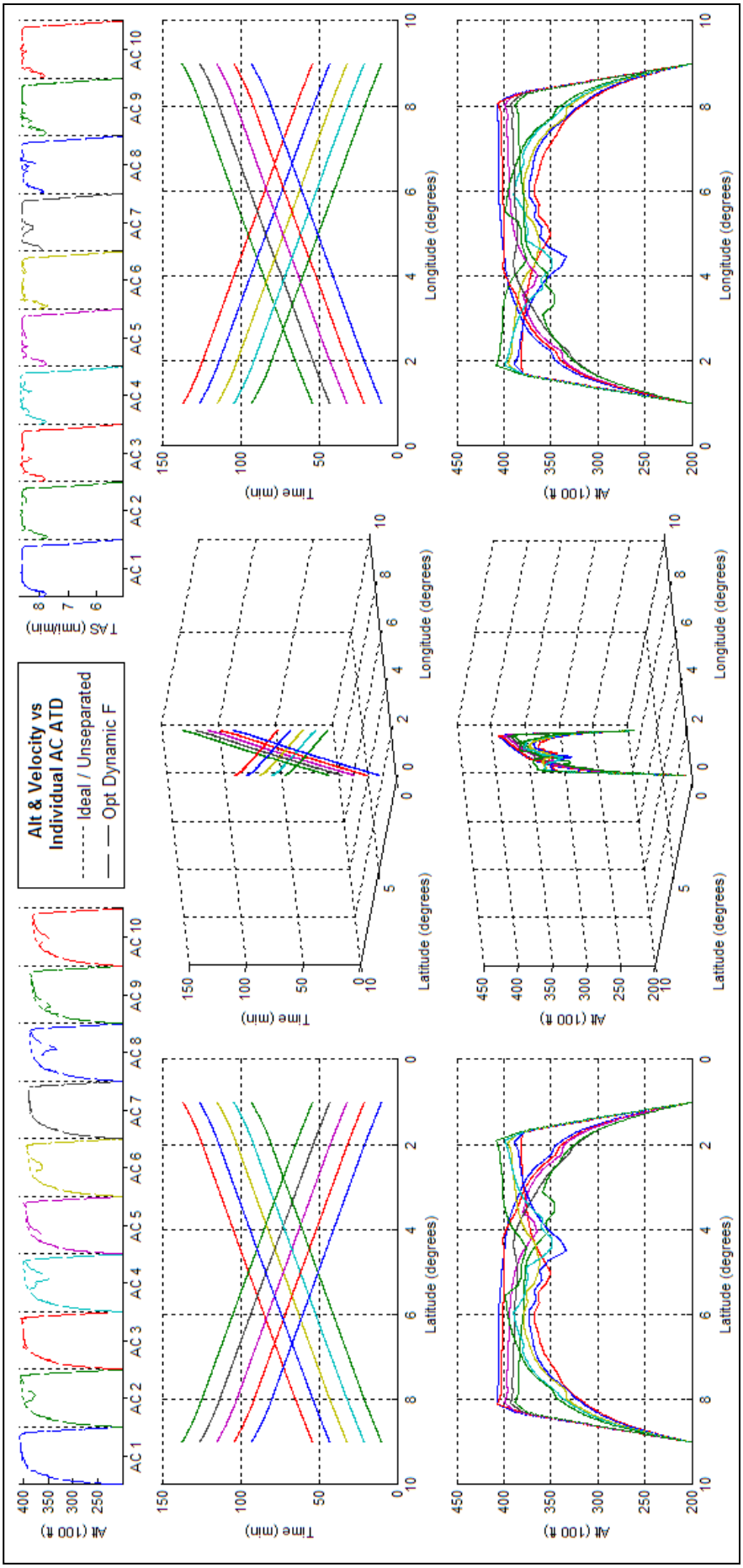

Figure 62 - PDO result for '10acPH2H' with event interval synchronized to aircraft entry.

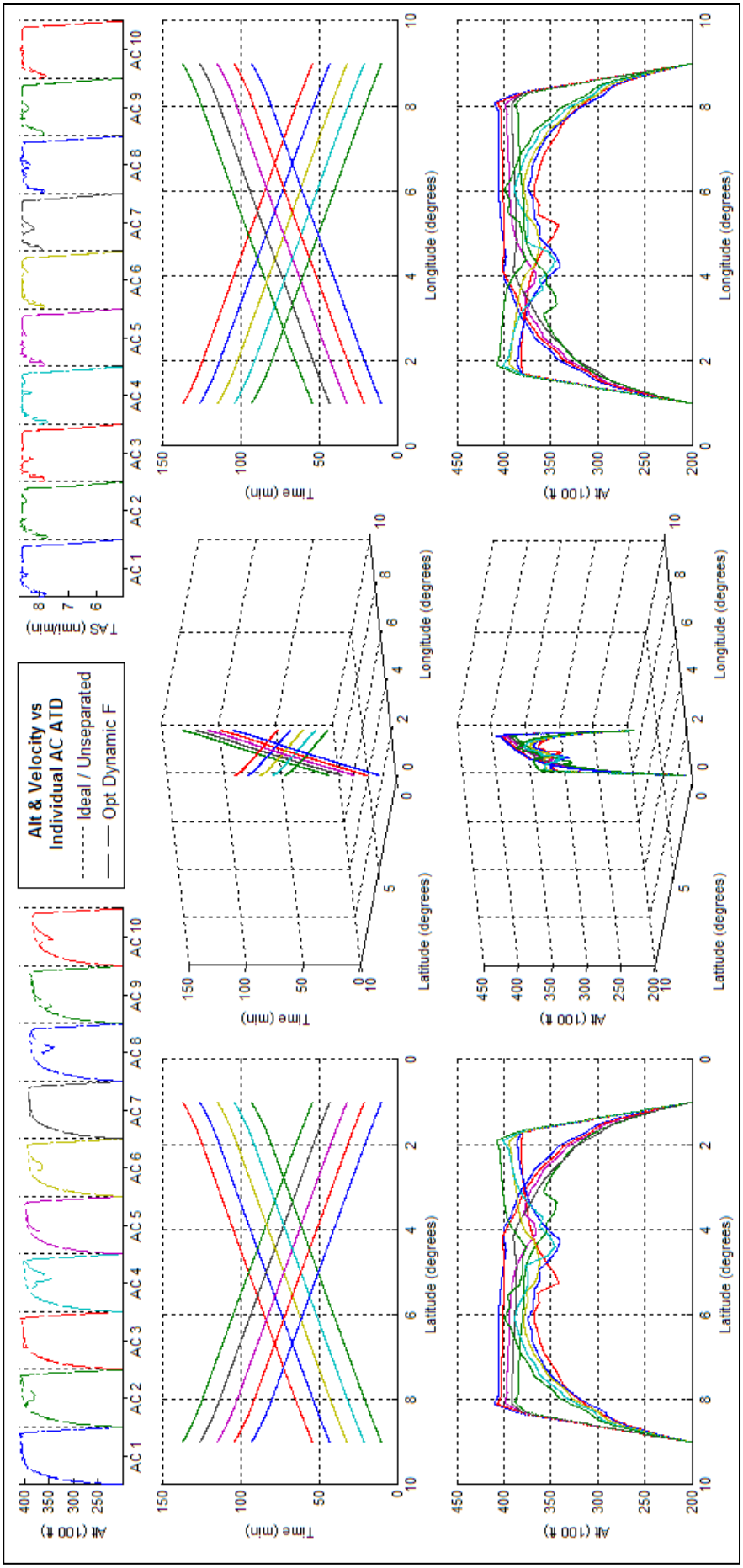

Figure 63 - PDO result for '10acPH2H' with event interval of 5.5 minutes.

5.3 Conclusions

The purpose of this section is twofold. The first purpose is to give a summary of the research contributions performed in this chapter and this is performed in section 5.3.1. The second purpose is to highlight the impact the work had on the Research Questions mentioned in section 2.4.2 and this is discussed for each research question in section 5.3.2.

5.3.1 Chapter Summary of Research Contributions

In this chapter, in consideration of the weaknesses of using a primarily static optimization, attempts at handling dynamic situations were carried out. As a result the PDO was created; this structure allowed the PCO to be applied in a time sequential manner and in consideration of only aircraft that were in, or just about to enter, optimizable airspace. Further, several new additional functionalities were introduced that could significantly reduce computation time for any scenario, including those that were primarily static. One new function of note was the use of potential conflict assessments to fragment the situation in mutually exclusive scenarios that could be optimized separately to reduce computational requirements. Unfortunately because of the minimalist perspective chosen for defining the optimizer realm of consideration, the resulting ATFU could be greater than if a static optimization had been taken; however the reduction of ATFU was also found to be possible, the variation in control node intervals creating a partial global optimization effect that finds optimums previously unreachable due to previous control node limitations.

5.3.2 Current State of Research

5.3.2.1 Q1: Can a co-operative and sufficiently informed air traffic optimisation methodology achieve a reduction in total fuel usage compared to current ATM?

In chapter 3 Q1 was partially answered by showing that the PCO could minimize ATFU. However, the PCO was based on flight mechanic derivations of fuel consumption and could not be compared to current ATM. In chapter 4, the BFO had improved upon the representation of the air traffic model by using more accurate data, i.e. BADA, to define optimum trajectories, and also included the creation of the BSO which simulated current ATM methods for scheduling aircraft. These two inclusions allowed the BFO to be more realistic and to allow comparison with current ATM; the consequence was that chapter 4 did show that it was possible for a cooperative air traffic optimization methodology to reduce ATFU. Chapter 5 improves the answer to this question by building upon the "sufficiently informed" aspect of the optimization; i.e. it tries to improve upon the air traffic model by enabling the model to change in a dynamic manner and thereby be representative of unforeseen changes to air traffic. Thus the question to be asked at this stage is whether or not the air traffic optimization methodology is now "sufficiently informed" compared to current ATM The answer is that it can be considered as being as sufficiently informed as current ATM; as it can now also be updated with unexpected changes to the ATS and perform the necessary re-optimizations to re-introduce optimality.

However, whether or not the PDO can generate more of a reduction in ATFU than current ATM, depends on whether it can be applied in real time. If so, the fact that BFO results achieved better ATFU than the BSO suggests that real time usage of the PDO would be more fuel efficient than current ATM. If not, then it is

possible that the optimization process will suffer further de-optimizations due to it lagging behind. The research here will have to find ways that allow the PDO to be applied in real time; if these are found then Q1 is possible, if they are not, then Q1 will remain impossible. .

5.3.2.2 Q2: What information is required to achieve such an optimisation methodology and how sensitive are the results to the accuracy of the input information.

The capability developed in this chapter was the ability to optimize new unforeseen events, thus the new input information required to enable dynamic optimization is merely knowledge of when, where, and which, new events occur in the future. In summary, the PDO optimizes an initial scenario and uses the result to control air traffic till an unforeseen event occurs, whereupon it will update the scenario and its data on the current states of all optimized air traffic and optimize again; this process of reoptimization reoccurring whenever an unforeseen event occurs. Given its ability to find an ATFU optimum, the PDO is sensitive to the series of unforeseen events that occur and can cause subsequent reoptimizations to reassess the situation in its entirety. In order to make this re-optimization computationally more efficient and less sensitive to new events, the method of isolating mutually exclusive air traffic was introduced which allowed the same numerical sensitivity to a new event, without having to re-optimize uninterrupted air traffic and thereby reduced the computational workload of subsequent re-optimizations.

5.3.2.3 Q3: How can constraints such as aircraft performance limitations, minimum separation and on-time arrival be incorporated into an optimizable UPT, and how do these affect total fuel usage?

The means of incorporating aircraft performance limitations, minimum separation and on-time arrival, are exactly the same as mentioned in 3.5.2.3; consequently this section focuses on how their impact on ATFU differs due to PDO reiterations caused by new events. However it is because of how well the optimizer achieves minimal ATFU with these constraints already incorporated, i.e. as developed in chapters 3 and 4, which can allow the PDO to be oversensitive. As the optimization ability of each PDO reiteration remains the same as applying a BFO to a new scenario, achieving the optimum for each scenario does come at the cost of completely changing all air traffic trajectories involved, which can therefore cause apparently illogical variation in air traffic trajectories where aircraft follow an optimum result that becomes non-applicable in the next reiteration.

5.3.2.4 Q4: How can a dynamic environment, such as deviation from or in-flight changes to the flight plan, airspace closure, and emergency diversion, be accommodated in an optimisation methodology?

The research in chapter 5 was specifically performed to investigate how to answer Q4. The core issue that this research has tried to deal with, and the common facet of the events mentioned in Q4, is that they can be unforeseen; hence the development of a dynamic optimizer in the form of the PDO and consequently chapter 5 does show, in detail, how these events are accommodated for. However while the PDO effectively succeeds in handling new events, it is apparent from the optimization trials in section 5.2 that the optimization can be a bit oversensitive by requiring trajectory changes directly after a new event has been recognized, which can be ideal but only if no other unexpected events occur afterwards. This suggests that the PDO could become more robust, and be more computationally efficient, by somehow decreasing the optimizer's ability to react quickly to new events.

6. CONTROL NODE CUSTOMIZATION

In the previous section, effort was placed on hastening the optimization process via either the division of the scenario into mutually exclusive parallel optimizations, or the removal of scenario components that do not require optimization. A possible avenue for improvement would be the fine tuning of trajectory step length and other optimizer parameters to generate faster results. However within the PDO, the value of the fidelity provided by having equidistant variable altitudes and velocities in the optimizer variable for the duration of all flights, is unknown; particularly as such are re-calculated by the PDO when it creates a new ATD_N be optimized for each new event. From another perspective, a key criticism of the optimized flights, even in a purely static optimization, is their complexity in terms of altitude variation can make them unsafe; in previous chapters, resultant trajectories avoid conflict with only the bare minimum separation, requiring constant attention and concentration from both an ATC and aircrew perspective to be safe. Given the stress these types of trajectories place on ATC, aircraft and aircrew, users may desire periods of constant altitude and speed to alleviate pilot or controller workload via reduced air traffic complexity. These issues with the optimizer variable suggest a need to develop a computationally efficient way in which trajectories can be optimized whilst respecting ATC required or aircrew/airline preferred flight modes.

The solution was to have a user customizable optimizer variable; i.e. a flight plan in which aircrew and ATC pre-specify trajectory step lengths in which the climb angle, altitude, speed, acceleration, or a combination of these, is constant. The actual values of these parameters would still be calculated by the optimizer, however the optimizer would save computational effort as regions of constant altitude or speed are likely to cover entire sectors rather than the nominal 20nmi used as a basic step length during optimization. This level of customizability would normally add prohibitive amounts of complexity to the optimizer, however it is possible here due to the division between correlative indices, ATD_i and ATD_N, that occurred in section 3.3.5.3; ATD_N no longer needed equidistant step lengths for the purpose of accurate aircraft performance modelling since ATD_i was created to serve that role to an extent that ATD_N could not. Consequently the step lengths defined by ATD_N could be altered individually to define constant parameter trajectory lengths that correlate with ATC and airline/aircrew preferences. The optimizer variable, X, which has variable h and TAS after each step length in ATD_N, would then be optimized directly, with additional constraints indicating which trajectory length is experiencing which constant parameter.

As the introduction of these customizations increases the complexity of any performance improvements that could have been made on the optimizer variable, section 6.1 thus discusses the impact of various implementations of this customisation when used by the BFO and PDO. The scenarios used in section 4.3.2 are used again and the customizations' collective impact on fuel usage optimization and computational performance are compared. In section 6.2, a unique functionalityoccured between the customizations and the PDO; this functionality allowed ATFU minimizations of customized UPT, to have similar trajectory properties of ATFU minimizations of ATD_N. This functionality was investigated further, and assessed as a replacement for dynamic ATFU minimizations of ATD_N. In section 6.3, the entire optimizer, as developed in this thesis, is tested in a high capacity air traffic scenario resembling current domestic air traffic in Australia.

6.1 Customised Control Node Lists for Static Scenarios

Another way to describe the rationale for customized control nodes is to provide stakeholders with the ability to define where and when *h-TAS* variation can occur. By forcing constant altitudes and minimal longitudinal accelerations in ATD_A with high through traffic, ATC assurance of separation is reduced to watching for any deviations in *h* and *TAS* as such would indicate significant problems for ATC. Conversely, the portions of trajectory that require non-constant altitudes and significant accelerations, can be relegated to ATD_A with low through traffic; the absence of other traffic giving stakeholders more freedom to perform trajectory variation safely. Thus ideally, a customized control node list would be derived from known ATC and airline preferences i.e.; under what traffic densities and numbers would ATC demand constant altitude flight, and under what frequency and duration of segments with *h-TAS* variation can airlines and aircrew handle. These could then be checked against each other, and ATD_A defined traffic data, to create altitude and velocity constraints on route segments that require them, as well as to remove ATD_N based variables that are no longer necessary due to those constraints. Unfortunately, such data was not available, and an alternative had to be made. Given that ATD_N defined complete *h-TAS* variability, and a customized control node list removes a portion of this variability, an acceptable alternative could be defined from an ATD_N that defined minimum *h-TAS* variability; by using a list of the most constrained yet feasible control nodes, the effects of control node redistribution can be maximised and assessed for usefulness. Thus, three customizations of ATD_N with their corresponding constraints were created and tested; a visual comparison of them can be seen in Figure 64.

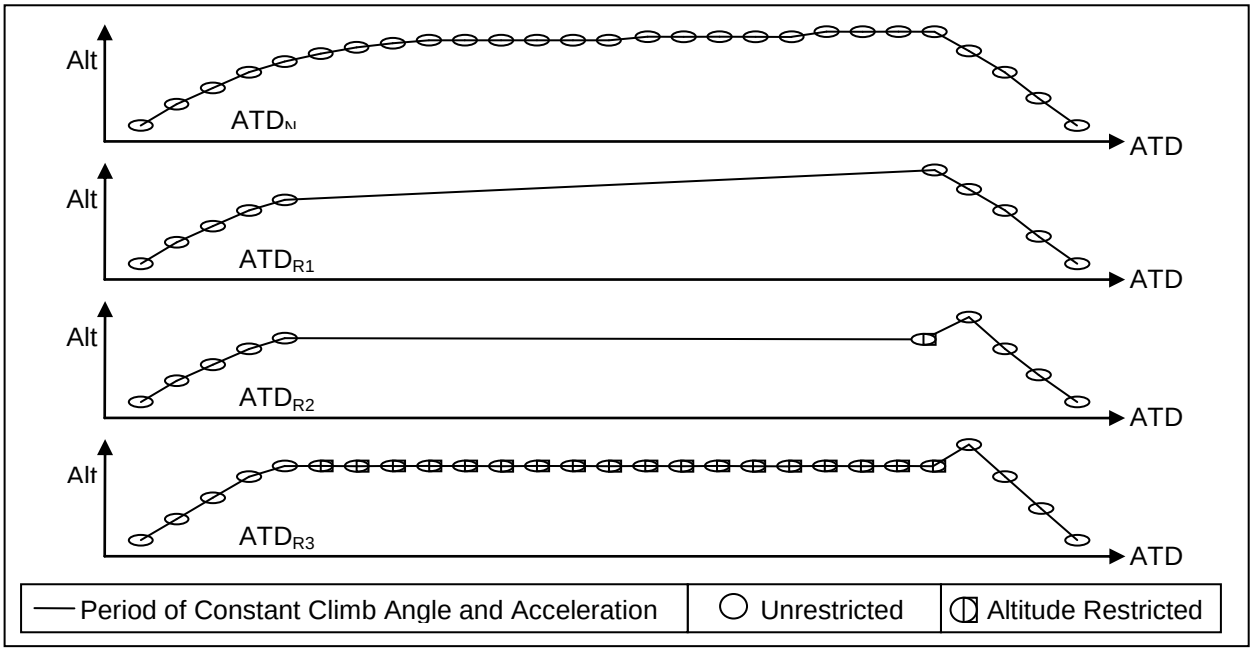

Figure 64 - Typical results for control node, ATD_N, and the three customized control node lists, ATD_{R1}, ATD_{R2}, & ATD_{R3}.

All three customized control node lists were based on the premise that portions of the trajectory after the initial climb and before the descent to exit optimized airspace were largely level and suffered little deviation from being linearly represented; thus suggesting their possible removal as variables. Thus each of the three control node lists retain altitude and velocity variability for the first and last five control nodes (roughly speaking, the first and last 80nmi of the trajectory), but lose to some extent the variability in the middle remaining portion. The

first control node list, ATD_{R1}, completely removes any variables other than the first and last five control nodes, assuming a constant climb angle and acceleration for the periods between nodes. The second list, ATD_{R2}, does the same but enforces equality between the altitudes of the middle nodes, thereby causing the middle portion to be level for its duration. The third list, ATD_{R3}, does the same as the second, but allows velocity to be variable during the middle portion. Example results when using the three on the same scenario as in Figure 22 leads to the results in Figure 65, Figure 66, and Figure 67. Appendix L shows the same for all eleven test scenarios.

ATD_{R1} was a by-product of tests on ATD_{R2} that intended to see what happens when the trajectory of an aircraft is forced to have a constant climb angle and acceleration during the middle portion of its trip. The result was the allowance of a partial cruise climb; without the altitude restrictions in ATD_{R2}, the optimizer would seek to raise the altitude of the node representing the end of the middle portion, as exemplified by every aircraft in Figure 65, resulting in reduced fuel usage therein. As a consequence of the usually positive climb angle, acceleration had to also be positive to prepare for the higher speeds necessary at higher altitudes. A possibility not shown in Figure 65 is that of constant climb angles that cause descents; such are possible but usually only occur where significant conflict is being avoided in the last 80nmi of the flight. One last thing to mention is that the altitude spikes, that occur frequently in Figure 65 during the initial and final part of the aircrafts' trajectories, are merely the optimizer's desire to minimize ATFU; while the trajectories' middle portion would need lowered altitudes to satisfy separation requirements, the first and last portions would not, and the optimizer would further minimize fuel usage by increasing the altitude of the first and last portions of the trip.

Enforcing a level altitude during potential conflict was the main reason for developing ATD_{R2} and is seen clearly in all of its results; a level altitude would give ATC and airlines an easily monitored trajectory. The optimized ideal for each aircraft would have the aircraft reach the highest altitude it could in the first 80 nmi, then maintain that altitude for the middle portion till the beginning of the final 80 nmi where it will take advantage of allowed altitude change to reach its maximum altitude and descend to the exit from there. Resultant accelerations tend to be positive; the effect of reducing weight on maximum thrust allowing higher velocities, and overall lower flight times and fuel usages, to be reached. It should be noted that the result in Figure 66, while indicative of ATD_{R2} results, was also one that failed to optimize; the reason was lack of separation space. Travelling at a constant altitude causes separation to be in terms of altitude whenever purely time separation is impossible, as intended in Figure 66; however as altitudes are level, the maximum for any aircraft is restricted to what it could reach upon entering level flight. Thus the maximum altitude for these aircraft is significantly reduced and the region through which the aircraft must travel makes such impossible. Velocity variation could have created sufficient separation, however level profiles and constant accelerations tend to tighten the region of feasible velocities, thereby not making such possible either.

On top of the increased likelihood of choke points caused by the constant level and acceleration in ATD_{R2}, the constant accelerations in both ATD_{R1} and ATD_{R2} had a noticeable tendency of requiring additional fuel usage to be maintained. As such, there was sufficient reason to reintroduce variable velocity whilst keeping the constraints on altitude, and this was done when ATD_{R3} was created. While the re-inclusion of velocity variables does decrease the efficiency of ATD_{R3} as an optimizer variable, the benefits, as shown in Figure 67 and Table 15, gained from having velocity variability may make it worthwhile. The first thing to note in Figure 67 is that ideal unseparated aircraft velocities can effectively reach their maximum and plateau; like altitude, forcing a constant acceleration in ATD_{R2} meant the initial velocity for the middle portion could only be linearly varied to the final

velocity of the same portion, despite the restrictive limit due to aircraft weight disappearing much earlier. Also, because of the freedom in velocity, maximum attainable altitudes are increased; the vertical range of separation positions during the intersection is therefore also increased. More importantly, it was also possible for AC 4 and 5 to perform a concerted manoeuvre that created sufficient time separation between them so as to allow them to maintain the same altitude and still be conflict free. The last benefit of the velocity variability is that fuel usage is noticeably reduced, as confirmed in Table 15; without the constant acceleration, velocities can be picked that produce lower fuel usages.

It is important to note that the 80nm used to define the initial climb and final descent phases for these control nodes was an arbitrary number chosen to facilitate ease of programming whilst including the impact of the initial climb and final descent on the middle portion cruise. In programming terms it is possible to have during a flight multiple constant climb angles and acceleration portions of any length separated by any number of variable altitude and velocity portions of any length; the results shown here would then be indicative guides for a single variable-constant-variable sequence that such a flight would have. Further, the rationale behind the distribution and length of these sequences could be based on ATC, airline or pilot preferences, or it could be controlled according to data in the NMD store; air traffic densities, sector definitions, and other surface orientated data can be stored using NMD then brought out to autonomously or automatically define a sequence of constant and variable portions of a trajectory. The main point being that the application of these customized control nodes can be controlled in such a way as to suit a near infinite variety of trajectory form and preference combinations.

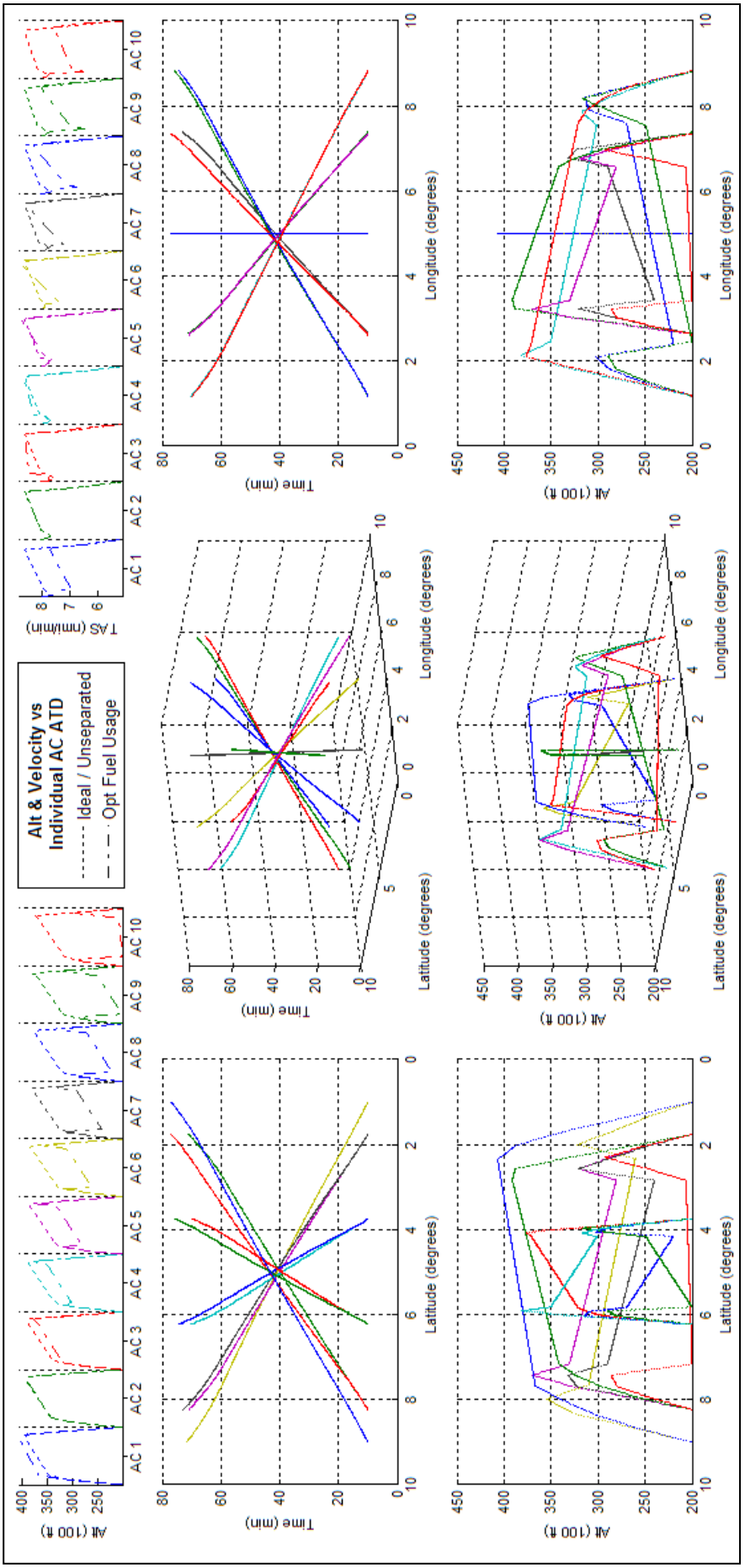

Figure 65 - BFO result for 10acCO using ATD_{R1}.

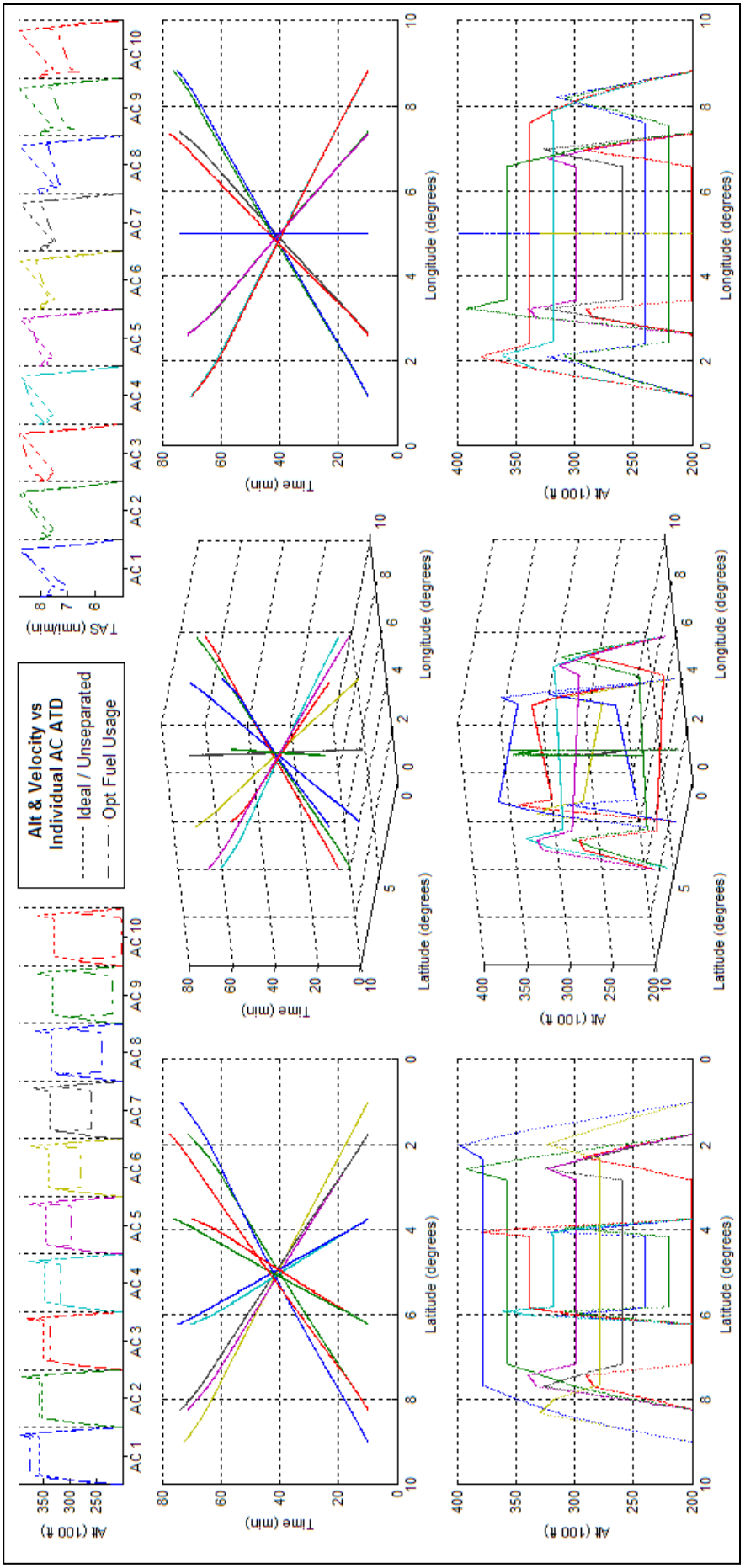

Figure 66 - BFO result for 10acCO using ATD_{R2}.

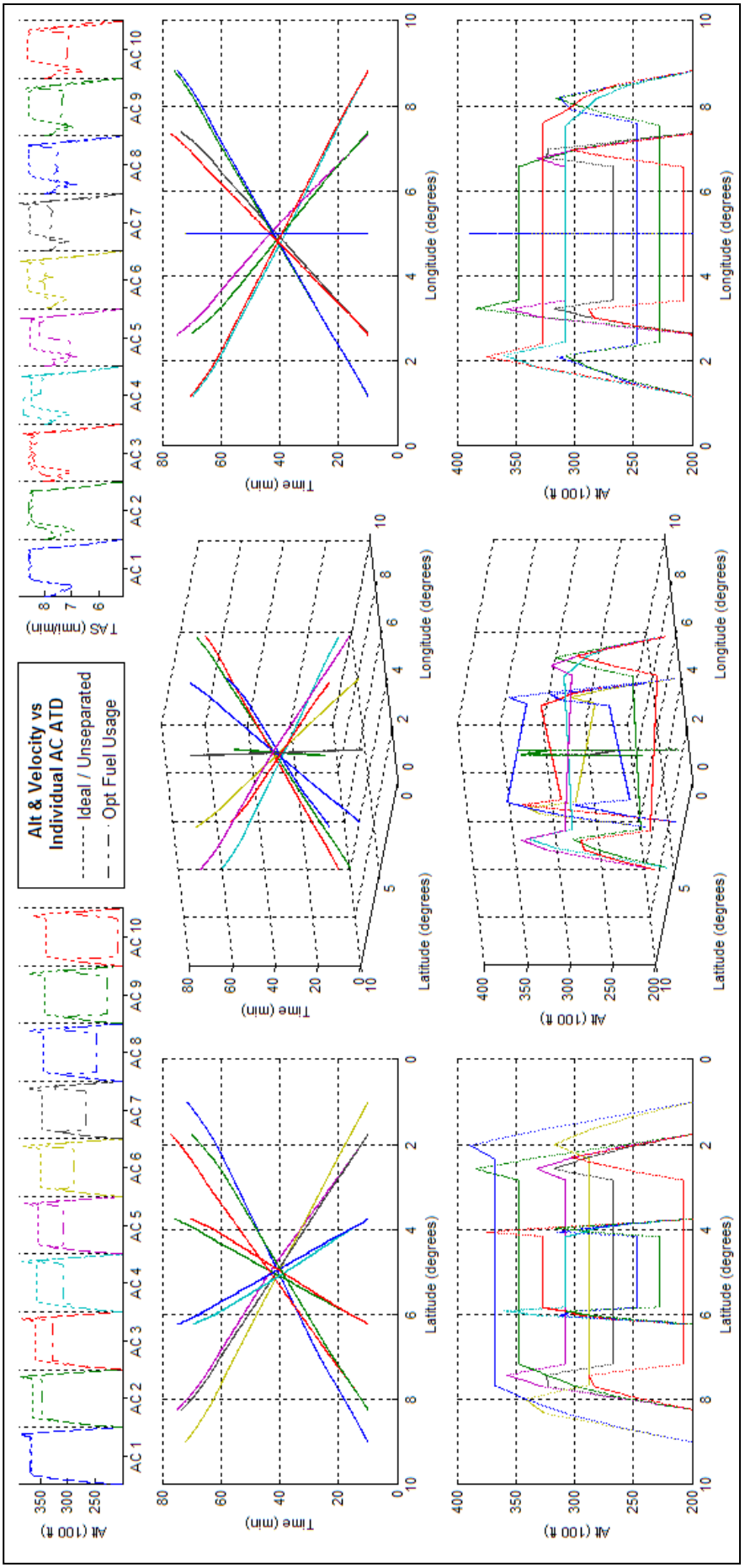

Figure 67 - BFO result for 10acCO using ATD_{R3}.

6.1.1 Collective Data on Static Usage of Customized control nodes:

The assertions made of ATD_{R1}, ATD_{R2}, and ATD_{R3}, using Figure 65, Figure 66, and Figure 67, are indicative of their usages in other scenarios. For the sake of comparison, the results of the three customized control node lists when using the same scenarios in Table 8 yields the success and number of runs for each combination in Table 14, the ATFU for each combination relative to its ATD_N counterpart in Table 15, and their assorted computational run times in Table 16. The range of optimizer runs a scenario can experience is between zero and two. Zero runs occur if no actual conflicts were found and Separation Optimization was sidestepped entirely. One run occurs if Separation Optimization reached a successful optimum that maintained 1e-2 accuracy on its constraints. Two runs occur if the first Separation Optimization failed or did not finish, or succeeded but with only 1e-1 accuracy; in each case the second run was made using the final result as an initial value and with 1e-2 accuracy on constraints. The optimization for a scenario was only considered as having failed if the last Separation Optimization failed; there have been cases where an optimization will fail its first run, but succeed in its second. With the exception of the failure for the BSO and ATD_{R3} attempt of '4acPH2H', the cause of which is still unknown and being sought after, the results were as expected. The first thing to note is the prevalence of one run only being sufficient enough for optimization; even with a 1e-1 constraint accuracy limit, most optimizations still reach 1e-2. Whether or not this is due to the BADA creation methods is unconfirmed, however the quality, depth and coverage of the BADA coefficients would suggest that this is the case.

Table 14 - Number of Optimizer Runs (absolute value) and Success/Failure (+/-) of Table 8 Scenarios under various Optimizer and Control Node settings

Control Node List	ATD_{R1}		ATD_{R2}		ATD_{R3}	
Scenario \ Optimizer	BFO	BSO	BFO	BSO	BFO	BSO
'2acPSd'	1	1	2	1	0	0
'4acPSd'	1	1	1	1	0	0
'10acPSd'	0	0	0	0	0	0
'2acCO'	1	1	1	1	1	1
'4acCO'	1	1	1	1	1	1
'10acCO'	1	1	-2	-2	1	1
'4acCH'	1	1	2	1	1	1
'10acCH'	1	1	1	1	1	2
'2acPH2H'	1	1	1	1	1	1
'4acPH2H'	1	1	1	1	1	-2
'10acPH2H'	1	2	-2	-2	-2	-2

The next thing to note is those that did not require Separation Optimization. While aircraft on the same route with the same heading with sufficient time separation between them can still influence each other, if constant climb angles and accelerations are adopted, velocity variation is often reduced, thereby causing conflicts to occur less often. In theory the customized control node list optimizations of '4acPSd' and '10acPSd' should be similar, however the same linear distribution of initial fuel capacities resulted in higher weight differences in '4acPSd', thereby causing higher velocity variations and therefore greater chance of conflict. The last things to note are the expected failures. The '10acCO' failures have been explained in 6.1; insufficient room for separation caused by customized control node list exacerbating constraints. '10acPH2H' is '10acCO' compacted on to one route; the failure of ATD_{R2} was expected as it could not handle '10acCO', in the case of ATD_{R3} the time separation enabled by velocity variation is irrelevant as such in a head on conflict, with no allowable cross track deviation and a

severely tightened vertical range of separation, would only change when and where the conflict occurs and does nothing to avoid it.

Table 15 - Relative ATFU (% against non-reduced) of Table 14 Runs (failures in parenthesis)

Control Node	ATD_{R1}		ATD_{R2}		ATD_{R3}	
Comparison / Scenario	BFO vs. ATD_N BFO	BSO vs. BFO	BFO vs. ATD_N BFO	BSO vs. BFO	BFO vs. ATD_N BFO	BSO vs. BFO
'2acPSd'	3.0%	0.6%	5.5%	0.7%	4.0%	0.0%
'4acPSd'	3.2%	0.0%	6.3%	2.1%	4.5%	0.0%
'10acPSd'	2.5%	0.0%	5.6%	0.0%	3.8%	0.0%
'2acCO'	2.8%	0.0%	6.0%	0.0%	4.1%	0.9%
'4acCO'	3.3%	1.5%	5.4%	1.7%	4.7%	1.9%
'10acCO'	8.2%	2.5%	(9.1%)	(2.6%)	8.6%	2.6%
'4acCH'	0.8%	4.3%	2.0%	3.1%	1.5%	4.9%
'10acCH'	2.2%	3.9%	5.4%	3.8%	4.3%	2.5%
'2acPH2H'	2.8%	1.4%	5.9%	0.1%	4.1%	0.5%
'4acPH2H'	4.0%	2.8%	6.7%	1.8%	5.8%	(-0.1%)
'10acPH2H'	11.4%	1.4%	(13.5%)	(1.9%)	(2.8%)	(3.1%)

For the purpose of comparison between ATFU, it is important to note that a failure to find an optimum that satisfies constraints usually obtains even lower fuel usages than the optimum if it exists; given the objective function of ATFU and the individually ideal initial value, satisfying constraints almost always comes at the cost of additional fuel. With this consideration, the first thing to note in Table 15 is that the results comparing the BFO results for all customized control node lists against ATD_N all show increases in ATFU, i.e. BFO using ATD_N always led to lower ATFU; this is expected as ATD_N is not reduced in terms of allowable variability and BFO seeks the lowest ATFU. Next, the BSO vs. BFO comparisons show that all valid BSO results use more fuel than their valid BFO counterparts, which is not unexpected; however the variation between BFO and BSO ATFU, when using the customized control nodes, is usually less than when the non-customized list is being used; the only situation that does not experience a greater BFO and BSO variation is '4acCH' wherein most conflict occurs just after entry and just before exit, i.e. where fully variable nodes exist. This suggests firstly that, due to conflict occurring during the middle portion, the customized control nodes are largely responsible for the increased ATFU. Secondly, given the '4acCH' result, increased fuel savings are only possible with more freedom in trajectory change. In terms of ATFU comparisons between the customized control node lists, ATD_{R1} uses the least; being able to reach higher altitudes over time equates to lower ATFU, however this does come at the cost of requiring the ability to maintain a constant climb angle. From there ATD_{R3} uses the next lowest; being able to control velocity in greater detail enabling it to reach better ATFU, however again this should come at the cost of increased computational effort. ATD_{R2} uses the most fuel and requires the ability to maintain constant acceleration, but its computational requirements should be similar to ATD_{R1} while maintaining the constant level provided by ATD_{R3}.

Table 16 - Relative Computational Time of Table 14 Runs (failures in parenthesis)

Comparison / Scenario	ATD_N BFO (hours)	ATD_{R1} BFO vs. ATD_N BFO (%Diff)	ATD_{R2} BFO vs. ATD_N BFO (%Diff)	ATD_{R3} BFO vs. ATD_N BFO (%Diff)
'2acPSd'	0.13	904%	-41%	-51%
'4acPSd'	1.23	-64%	-80%	-80%
'10acPSd'	21.82	-98%	-98%	-97%
'2acCO'	0.04	242%	-67%	305%
'4acCO'	0.08	-22%	614%	-3%
'10acCO'	2.41	278%	(231%)	398%
'4acCH'	0.31	-82%	132%	-79%

'10acCH'	1.33	-67%	-32%	22%
'2acPH2H'	0.14	-42%	-64%	-7%
'4acPH2H'	1.09	-2%	160%	-30%
'10acPH2H'	68.26	37%	(100%)	(421%)

As in section 4.3.2 the times shown in Table 16 were of single runs using 4 cores, with each core being one from an AMD Quad Core Opteron™ 2.3ghz processor with each core having 4GB of RAM, 160GB of scratch space, and the possibility of being on up to four different processors within an Infiniband Interconnect and CentOS 5 Linux based network; this implies that significant variation in computation times can occur. However it could still be possible to define some general trends and give possible explanations for certain times; but scenario and control node specific statements would require more detailed investigation. It should also be known that the program uses MatLab R2009b with 'fmincon' being the only high level function used; there is a significant possibility of time savings if a purpose built interior based optimizer function was created. With all this, the key queries would ask if the general trends in time differences between the three control node lists merit the fuel increases caused by the customized control nodes, as well as what could cause deviation from the general trends. Unfortunately the variation in computation times due to the reduction in control nodes had a greater impact from the way the optimization problem could change due to such, than from any reduction in the data size of the problem. This comes from the fact that even though more than half of the scenarios experienced a noticeable time reduction, the variation in computation times does not coincide with the original thought that ATD_{R1} and ATD_{R2} would have similar times and ATD_{R3} be comparatively slower.

Scenario and control node pairs with higher computation times do however compare well when the restrictions mentioned in 4.2.3 are considered in conjunction with the level of complexity of the scenario. Consider '10acCO', '10acCH', '2acPh2H', and '10acPH2H' as normative results that can all be seen to roughly match the original thought. '10acCO' and '10acPH2H' are extremely restricted due to airspace limits and the added complexity due to the customized control nodes noticeably exacerbates the computational time. In contrast, the significantly less restricted scenarios of '2acPH2H' and '10acCH' instead mostly experience significant drops in computation time. For all other scenarios the original thought was most likely affected by existing complexity in the problem. For example in '4acCH', ATD_{R2} is more likely to take longer as the restrictions on its middle portion allow changes to one aircraft's middle portion to cause constraint violations on the entirety of the middle portions of all other aircraft; this is due to conflict being focused on the start and ends of all the middle portions in '4acCH'. Barring computational uncertainty, this interaction between existing and control node complexity, is the reason for inconsistency in run times.

6.1.2 The Impact of Increasing Step Size on ATFU Optimization

Where a sensitivity analysis is performed in the literature, it is assumed that an optimal trajectory step length, or sets of, can be found by balancing between computational cost and solution quality [31][35][39]. However the research in this thesis assert that trajectory step length, along with other trajectory discretisation parameters, is a user defined input influenced by flight location, and consequently not a parameter the optimizer can vary at will. Discussion of solution quality must therefore include the impact and interaction of all trajectory discretisation parameters. This occurs in section 6.1.1 where the impact of different trajectory discretisation methods can be seen in different scenarios. While each scenario type utilizes different trajectory step lengths, it is the scenario

type, and the presence or lack of the other discretisation parameters that dominates solution quality, and is thus presented that way. However further insight can be gained from viewing the results in terms of the step lengths required to facilitate the various customization types.

Figure 64 shows the distribution of control nodes used in each of the scenarios mentioned in Table 14, however to apply it to each scenario, the middle portion had to be extended such that total distance of the control node customization matched the distances of the flights in each scenario. Consequently the length of the middle portion varies between scenarios and thus allows the impact of step length to be analysed. The graphical results of analysing Table 15 in this way, are presented in Figure 68; to facilitate comparison of results, the fuel usage for each scenario and customization combination were calculated as percentage increase of their ATD_N counterpart which use a constant 20nim step length in their optimization.

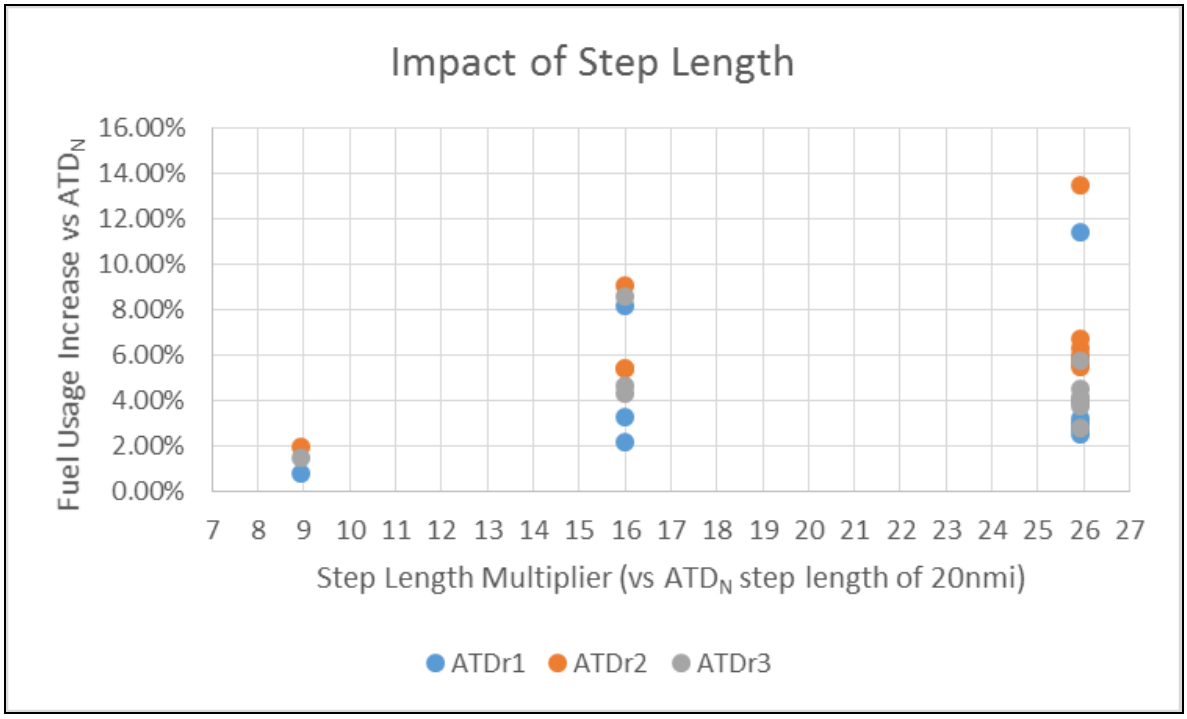

Figure 68 - The Impact of Step Length and Control Node Customization on Fuel Usage Minimization

The first piece of information provided by a sensitivity analysis based on step length is the relative size of the middle trajectory section with the step length used by ATD_N; .the minimum is 180nmi and the max is 520nim, thus these step lengths are respectively 9~26 times greater than the 20nmi used by ATD_N. However the range of additional fuel caused by the customations is limited to 0.8% and 13.5%; while the maximum additional fuel usage incurred suggests that part of this range would make control node customization economically unfeasible due to additional fuel cost alone, the minimum suggests the complete opposite and gives credence towards the possibility of economically justified utilization of the customizations to simplify trajectories. The concept gains further credence when it is recognized that the periods of constant altitude, climb angle or speed can be customized by a user for a portion or entirety of their trajectory; i.e. a user can use results similar to those shown in Figure 68 to modify and guage how much additional fuel usage they may spend in a customized trajectory.

The next piece of information gained from the sensitivity analysis is that the spread of results does conform to the notion that smaller steps in trajectory discretization do result in less additional fuel usage. Given that the smallest increase of 0.8% occurs at 9 times the size of the step length used by ATD_N, a sensitive analysis would

suggest that a) a 20nmi step length would be an inefficient use of computer power in ATFU optimizations, and that b) an optimal step length for ATD_N optimization exists between 20 and 180 nim. However the purpose of this analysis is to see the trends created by the various customizations and scenarios, and viewing Figure 68 from this perspective offers several insights. The first trend to notice is similar to that mentioned in the discussion of Table 15; within the same scenario, ATD_{R2} optimizations require more fuel than ATD_{R3} optimizations which require more fuel than ATD_{R1} optimizations. This trend is also observed in Figure 68 and can be used to identify 5 separate groupings each of which contain the orange-gray-blue sequence of dots that represent this trend. The first grouping has already been discussed and refers to the three results at 180nim; this grouping is of 4acCH which contains short trajectories with maximum number of intersecting aircraft at any point being two. The other four groupings are defined by the other 10-aircraft scenarios. The 10acCO scenario occurs at the top of the 320nmi set of results, while the 10acCH results sit at the bottom. The 10acPH2H occurs at the top of the 520nmi set of results, and the 10acPSd results occur at the bottom. The remaining 4 and 2 aircraft scenarios sits vertically between one of these two pairs. The key difference between and top and bottom of these pairs is in the complexity of the scenario. In the 320nmi column, the 10acCO scenario features a conflict group comprising of ten aircraft, whereas the same value for 10acCH is two aircraft. In the 520nmi column, the same values for the 10acPH2H and 10acPSd are respectively ten and four simultaneous aircraft. These values are reflected in their relative placement in Figure 68. One last thing to note about Figure 68 is that it does show that 10acCO optimization results does exceed the proportional fuel gain of optimizations using a 520nmi step size; this reconfirms results and discussions from section 6.1.1 that it is the scenario type that has a significant impact on optimizational result.

6.2 Interaction between PDO and Customized control nodes

It was mentioned previously that when using a PDO, most of the data in resultant trajectory portions yet to be flown is lost due to later, more updated, optimizer results overwriting them. While that is still technically true when using any of the customized control node lists, the resulting simplicity and ease of replication of the to-be-deleted trajectory portions should mean that the losses in terms of data, and computation time required in recreating it, are considerably reduced. However, as the biggest difference between the PDO and the static BFO is that the PDO periodically encounters new events that each force a re-optimization to occur at that time, further fuel savings can be gained using customized control nodes; the reason for this is twofold.

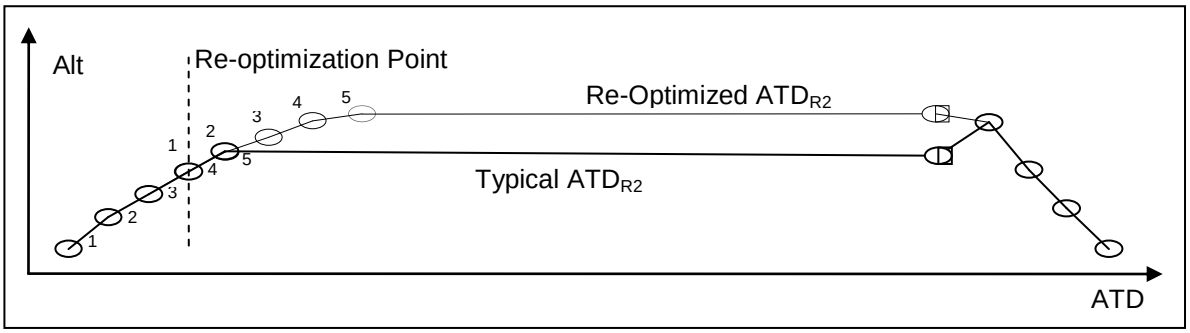

Figure 69 - Re-creation of Initial Control Nodes due to Re-Optimization.

The first is that in all customized control node lists, the properties of the middle portion are largely defined by the still variable trajectory portion that precedes it. The second stems from the fact that if a re-optimization occurs, the customized control node list has to be remapped against the remaining trajectory to prepare for necessary trajectory changes, i.e. as required by new aircraft entrants. Together it effectively means that, in a re-optimization using a customized list, a section of the middle portion effectively becomes the new variable trajectory portion that precedes the remainder of the middle portion, thereby allowing the trajectory to be re-optimized against a slightly different set of conditions. While this effectively means that customized control node properties relating to ease of supervision are lost when combining a PDO with a customized list, the reintroduction of variability allows access to trajectory shapes that were previously denied due to using the customized control nodes in a static scenario; this implies it is distinctly possible to attain ATD_N like results using the PDO and any of the customized control node lists. To test if the PDO can attain ATD_N like results two different minimalist perspectives of '10acPH2H' were trialled; the first using a simple minimalistic perspective and the second using a refined minimalistic perspective developed from lessons gained from the first trial.

6.2.1 Initial PDO and Customized control node results for '10acPH2H'

These were the first effective trials combining PDO with customized control nodes. There were no prior expectations on the results; it was easy to perceive how multiple re-optimizations over time would allow effective optimization of an increasingly larger portion of an initially customized list defined trajectory, but in terms of what that required as an optimum or actually implied as a result, nothing was known for certain. Thus the simple minimalistic perspective defined '10acPH2H' as a five event scenario; each event being synchronized against the entry of each successive pair of aircraft thereby creating a re-optimization frequency of once every eleven minutes. This matches the initial '10acPH2H' PDO scenario trialled in Figure 62 but using the customized

control nodes defined previously. While all three customized control node lists were initiated for trial, the result for ATD_{R2} had never reached completion, however from the two remaining results, it was clear that something was wrong. The two results, i.e. from using ATD_{R1} and ATD_{R3}, are shown in Figure 70 and Figure 71.

The two immediately apparent features of Figure 70 and Figure 71 are the inclusion of height oscillations, and the formation of aircraft clusters that share similar preferences for conflict resolution. In contrast the ATD_N PDO result of '10acPH2H', as shown in Figure 62, resulted in significantly smoother variation in altitude, as well as aircraft conflict being resolved via the sequencing of aircraft in time and altitude to support fuel minimization via minimal interruption to their ideal trajectory. Thus the main concern regarding these results was the cause the altitude oscilliations given their lack in the ATD_N PDO result. If these were BFO results, i.e. single stage optimization, an assessment of the traffic would correlate the aircraft clustering as a side effect of the appearance of height oscillations. These would be indicative of gridlocked air traffic; aircraft forced to slow down drastically to the extent of increasing effective distance covered via aggressive climb angle changes. The source cause would then be tracked through the sequence of aggressive climb angle changes in time to whatever caused the earliest aircraft to perform such aggressive manoeuvres; and, assuming no other issues, this source cause would be highlight as having caused the extreme result. From this assessment the source cause would have involved aircraft five in Figure 70, and aircraft nine in Figure 71, as these apparently held aircraft two, four, and six, in both cases, in a relative position where the climb angle changes were necessary; however neither aircraft five or nine showed any restrictions that would have prevented the optimizer from controlling them so as to lessen the fuel usage of aircraft two, four and six. This suggests that the aggressive climb angle changes were artificially induced via another method, which indicates that the PDO process was somehow to be blamed.

Looking at the altitude peaks, i.e. altitudes that experienced significant negative climb angle change, experienced by aircraft two, four and six, both cases showed that they respectively experienced five, four and three such peaks. These correlate to the number of optimization phases that the respective aircraft has actually been present for. Further, looking at aircraft two, in both cases it had experienced periods of initial speed and altitude variation, significantly longer than its final period of variation; this would indicate that its period of initial variation grew over time. It then became apparent that the aggressive climb angle changes were not performed to slow down aircraft, but were remnants of the aircraft's previous attempts at utilizing altitude freedom prior to the constant middle portion. Figure 65 and Figure 67 do show their respective customized control nodes performing similar manoeuvres prior to the middle portion; these were merely replicated in the PDO for each part of the middle portion that was granted variability. Further, as the PDO consistently maintained the separation mode set by prior entrants, it resulted in the clustering of the aircraft along similar altitudes.

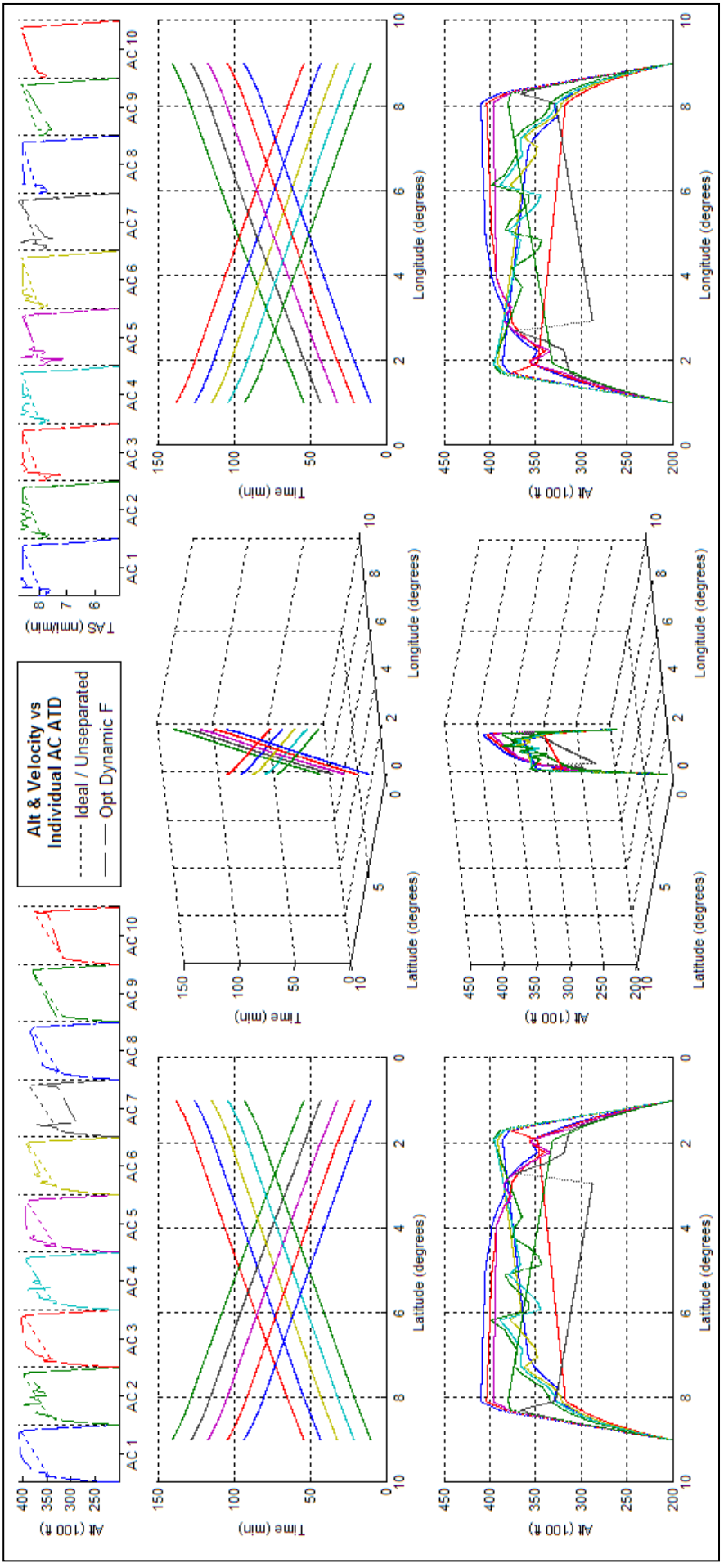

Figure 70 - PDO result for 10acPH2H using ATD_{R1} and synchronized to aircraft entry.

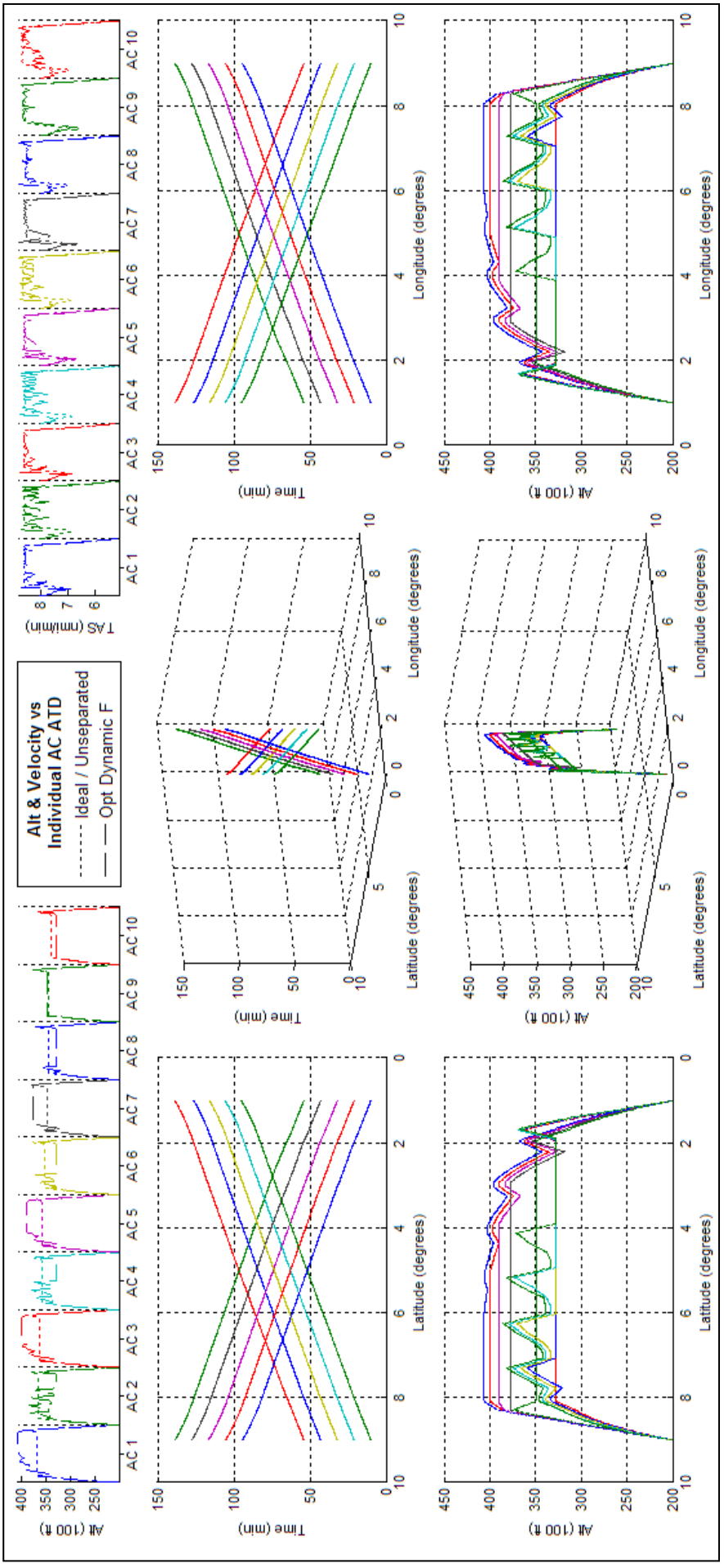

Figure 71 - PDO result for 10acPH2H using ATD_{R3} and synchronized to aircraft entry.

6.2.2 Refined PDO and Customized control node results for '10acPH2H'

While the results in 6.2.1 were not visually desirable, they did show how the PDO does reintroduce variability to trajectories over time; the undesired aggressive climb angle changes representative of the optimizer ability to attain better ATFU values, thus the PDO process itself is likely to be functioning acceptably. What is perceivably incorrect is how and when the process is actually being applied, i.e. the minimalist interpretation may not be correct. With an 11 minute interval between optimizations, it's clear that aircraft do have sufficient time to rise to a higher altitude, but rather than maintaining it, must descend to maintain separation as per the same PDO result that allowed it to rise. Making the PDO directly prevent the return to separation altitude would be unwise; doing so effectively destroys any the ability the BFO has of creating trajectories that are fully separated until they leave optimized airspace. The only other apparent options thus stem from altering either the minimalist perspective interpretation, or the customized control nodes themselves. The solution in both cases requires that the initial variable climb portion be long enough or the update interval short enough, such that the re-optimization occurs prior to the aircraft returning to its safe separation altitude. Altering the customized list would therefore require the initial climb portion to be made longer. Considering a maximum speed of 9nmi/min, a maximum descent distance of 40nmi, and buffer region of 20nmi, the initial climb distance would have to be doubled. In contrast, altering the update interval would require increasing its frequency; as aircraft seem to reach their peak just after the middle of the remapped initial climb portion, the original re-optimization interval would have to be halved. While the two options are equally valid, the frequency alteration has more appeal; alteration of the customized list may put even further restrictions on its intended specialization in the future, whereas reduction in time interval is already necessary for scenarios that have large number of aircraft entering at random times. Thus to test the impact of reducing the re-optimization time interval, pseudo new events were placed in '10acPH2H' halfway between currently existing new event triggers and run using the PDO and the various customized control node lists. The results are shown in Figure 72, Figure 73, and Figure 74.

Compared to Figure 70 and Figure 71, Figure 72 and Figure 74 show considerable improvement, while Figure 73 does confirm that the ATD_{R2} PDO implementation does work. As re-optimization stages only occurred until the last aircraft entered optimized airspace, the three results still do show typical elements of their customized control node list in their trajectory portions that had not yet experienced variability. However in the portions that did, there is considerable similarity between them, the ATD_N PDO result, and even the ATD_N BFO result for '10acPH2H'; nearly smooth cruise climbs, almost similar separation modes considering customized list influence, and most importantly the lack of successive aggressive climb angle changes and aircraft clustering effects. Some of the climb angle changes still seem to contain some height oscillations but it is likely that slightly further reduction of the re-optimization interval would be enough to cause an even smoother cruise climb. From another perspective, it is interesting that both variable and non-variable trajectory portions can coexist; it emphasizes the possibility that re-optimizations can be triggered depending on the perceived situation, and that using one does not prevent later use of the other. For example, a controller with sole discretion of the re-optimization trigger could, if highly efficient trajectories are desired, trigger re-optimizations fairly frequently, allowing aircraft to maintain ideal altitudes as long as possible. However, if sometime later an unexpected surge in traffic caused the controller to become dangerously busy, the controller could trigger re-optimizations only when a new aircraft entered optimized airspace; thereby gaining the complexity reducing benefits of the customized control nodes.

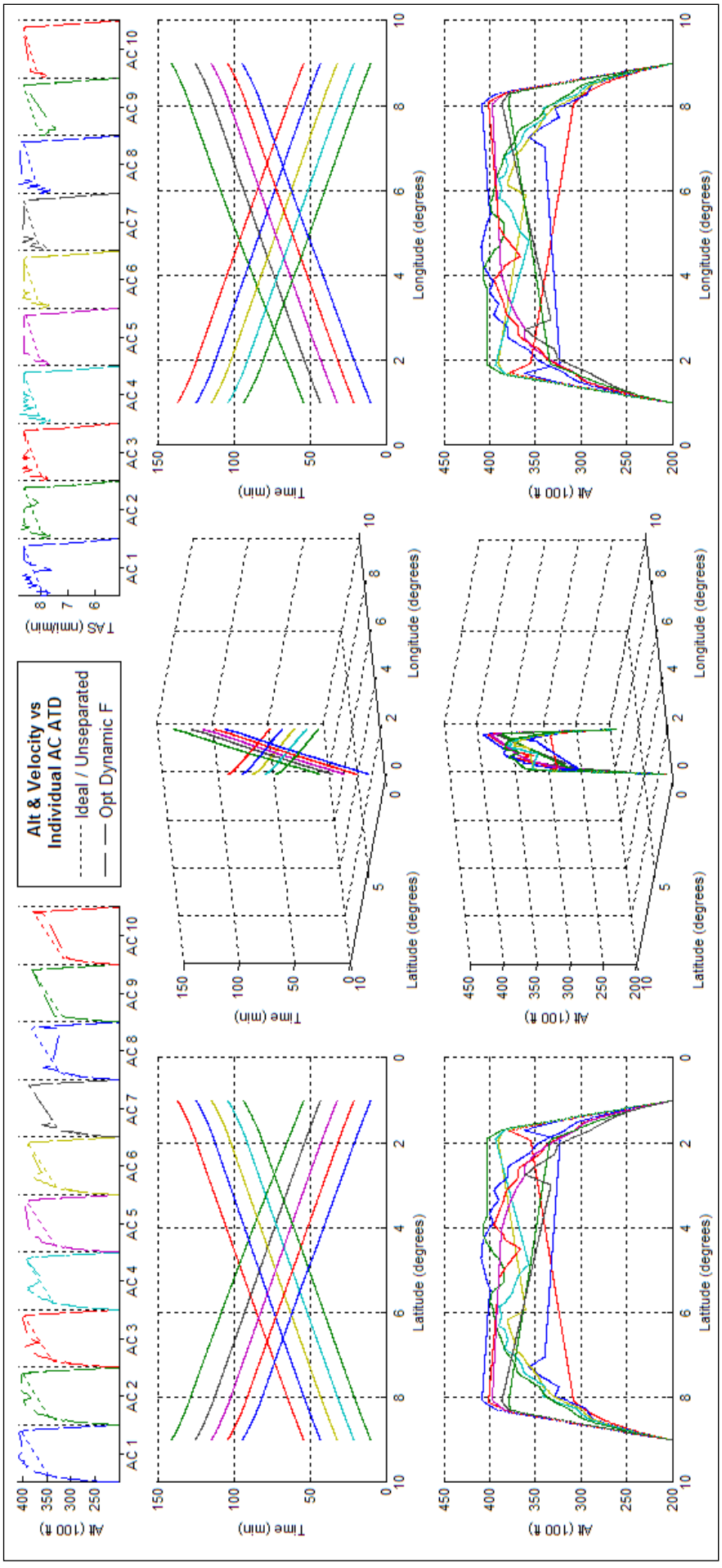

Figure 72 - PDO result for 10acPH2H using ATD_{RI} and event interval of 5.5 minutes.

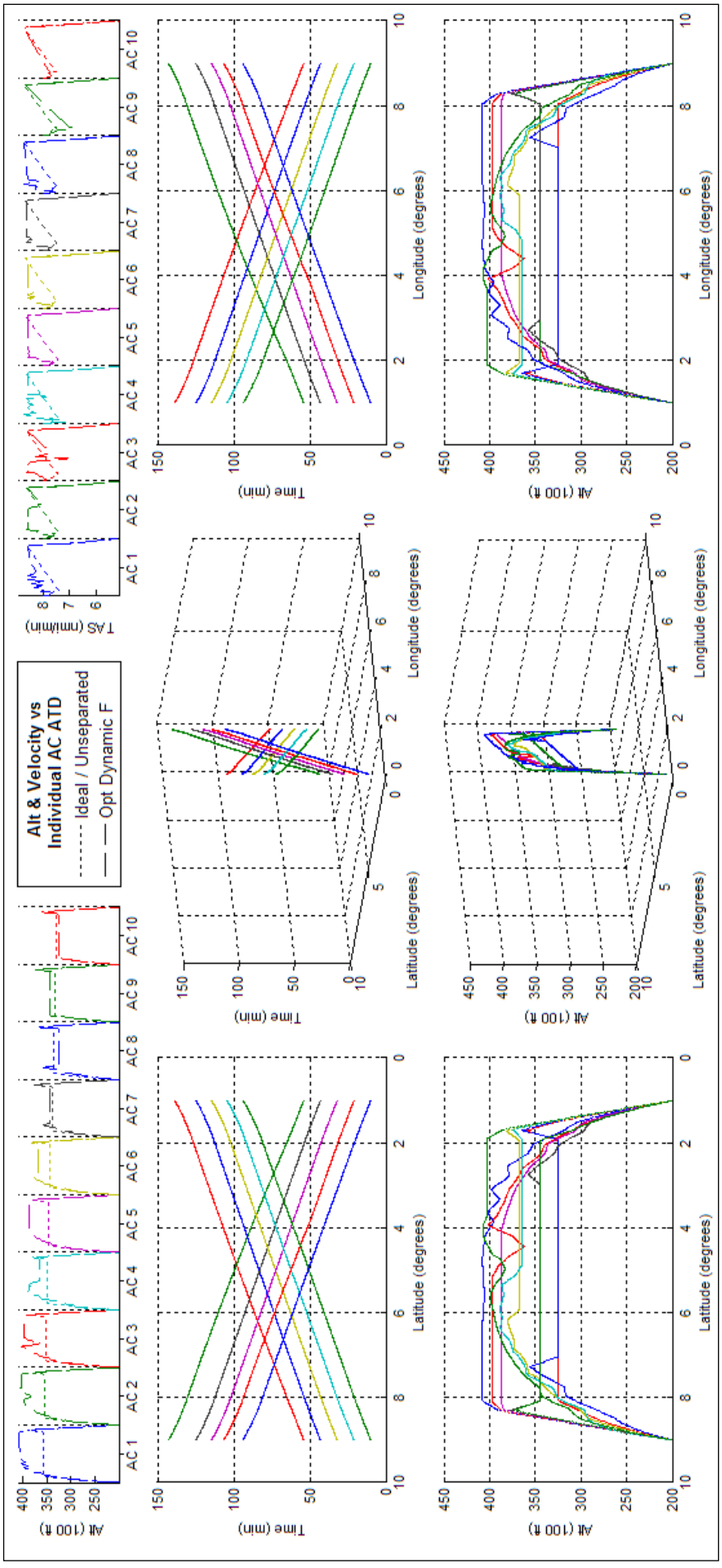

Figure 73 - PDO result for 10acPH2H using ATD_{R2} and event interval of 5.5 minutes.

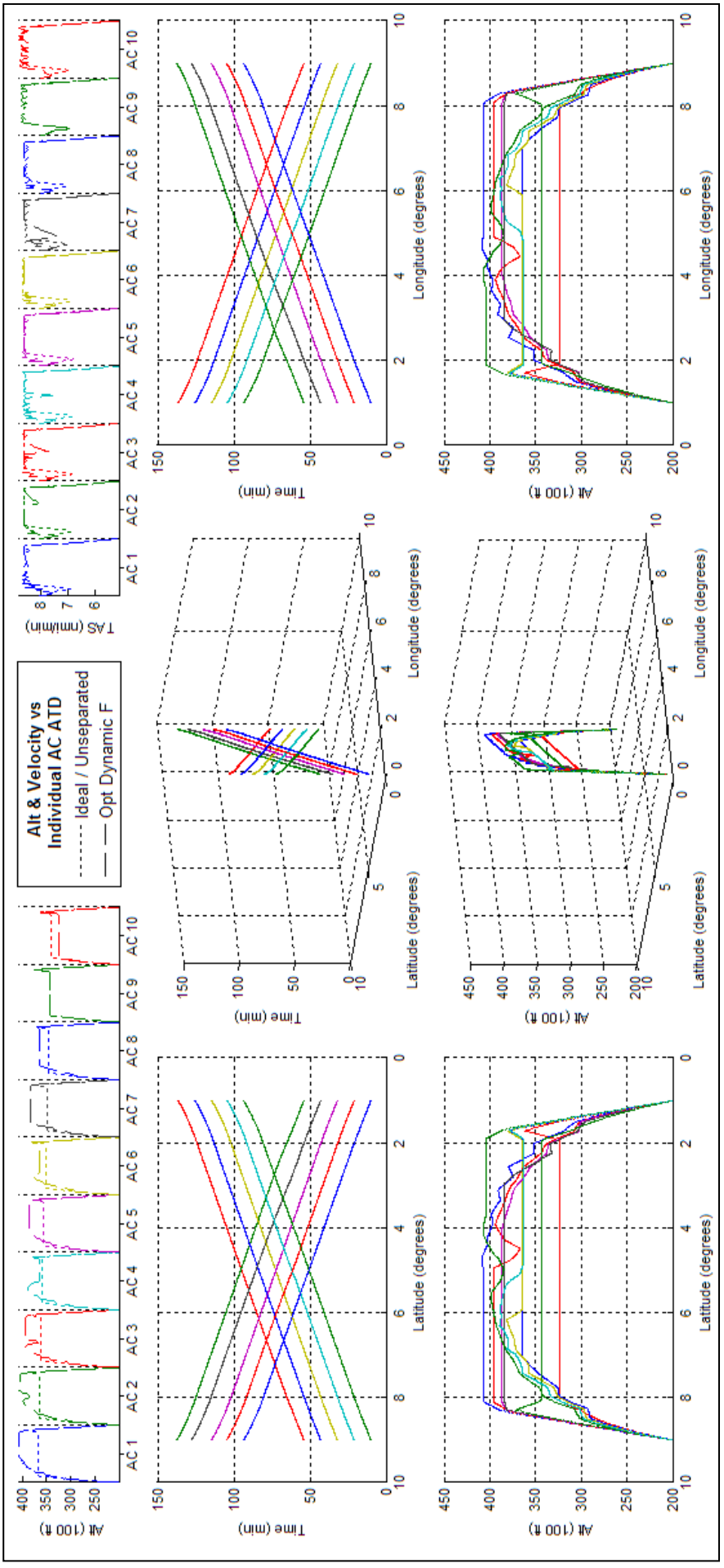

Figure 74 - PDO result for 10acPH2H using ATD_{R3} and event interval of 5.5 minutes.

6.2.3 Comparative PDO and Customized control nodes results for '10acPH2H'

Given the similarities between the PDO and Customized control node results for '10acPH2H', some of the details of their optimization need to be shown to allow comparison of their capabilities. For this reason the number of actual optimization runs used, the ATFU, and the computation times, of all optimizations, are shown respectively in Table 17, Table 18 , and Table 19, for each customized list including ATD_N, and each run of '10acPH2H' including its BFO result.

Table 17 - Number of Single (S) & Double (D) Stage Optimizations of '10acPH2H', failures marked as '-'.

Control Node List	ATD_N		ATD_{R1}		ATD_{R2}		ATD_{R3}	
Scenario \ Optimization Run Type	S	D	S	D	S	D	S	D
'10acPH2H' - BFO Result	1	0	1	0	0	-1	0	-1
'10acPH2H' - Initial PDO Result	5	0	5	0	??	??	4	1
'10acPH2H' - Refined PDO Result	9	0	9	0	9	0	8	1

As previously mentioned, the initial PDO ATD_{R2} result had still not finished the PDO process at the time of publication; the lack of numeric data for such in Table 17, Table 18, and Table 19 reflects that. The stereotypical components of the BFO run requirements are still present in Table 17; most re-optimization stages were single optimizations that satisfied 1e-2 accuracy despite the limit of 1e-1. The total number, i.e. single and double combined, of runs reflects the number of separate optimizations that had to be run during the course of the PDO. Also as previously mentioned in 6.1.1, the BFO result under ATD_{R2} and ATD_{R3} did actually fail; this is particular interest considering the PDO versions did not, it also serves as a reminder that the static applications of the customized control nodes do incur significant costs, in terms of fuel and trajectory freedom, that can easily be reduced with constant attention and re-optimizations.

Table 18 - Relative ATFU of '10acPH2H' Trials (failures in parenthesis)

Control Node List / Scenario	%Diff vs. ATD_N BFO fuel mass of 137.92 tonne			
	ATD_N	ATD_{R1}	ATD_{R2}	ATD_{R3}
'10acPH2H' - BFO Result	0.0%	11.4%	(13.5%)	(2.8%)
'10acPH2H' - Initial PDO Result	-0.7%	1.0%	??%	2.4%
'10acPH2H' - Refined PDO Result	-0.8%	0.5%	1.6%	0.3%

The most pertinent results regarding the combination of PDO and customized control nodes can be found in Table 18. Firstly, it shows the excessive amounts of fuel required by the BFO results; even though failed optimizations generally create significantly lower AFTU, the ATFU from the BFO using ATD_{R2} and ATD_{R3} still showed significantly higher ATFU amounts than the ATD_N BFO result. The ATFU from the BFO using ATD_{R1} confirmed this would occur for successful optimizations as well. However, when these were combined with the PDO and the initial interpretation of the scenario, ATFU values dropped significantly; showing quite well how frequent updates and re-optimizations can improve fuel usage optimization of customized control node lists. Finally, the most important results stems from the fact that it was originally suggested that combining the PDO with a customized control node list could create results containing trajectories similar to those created by using ATD_N; while this was visually shown to be the case in 6.2.2, Table 18 shows the same but in terms of actual fuel used. It shows the refined PDO result using two of the three customized control node lists came within 1% of the total fuel used by the BFO ATD_N result; which from the perspective of the BADA fuel calculation methodologies makes them the same. The one result that did not come within 1% was the result that used ATD_{R2}, which to be

fair has the highest fuel costs among the customized control node lists; however it did come to within 2%, which is still fairly close considering the complexity. It also has to be said that a fair amount of trajectory still had not been granted variability since re-optimization stopped after the last aircraft had entered optimized airspace; this likely means that further fuel savings could have been made if the re-optimizations were allowed to continue till the entirety of all trajectories had been allowed to be variable.

Table 19 - Relative Computation Time of '10acPH2H' Trials (failures in parenthesis)

Control Node List / Scenario	%Diff vs. ATD_N BFO time of 68.26 hours			
	ATD_N	ATD_{R1}	ATD_{R2}	ATD_{R3}
'10acPH2H' - BFO Result	0%	37%	(100%)	(421%)
'10acPH2H' - Initial PDO Result	-40%	-60%	??%	-53%
'10acPH2H' - Refined PDO Result	-49%	-66%	-56%	116%

While the concerns regarding Table 16 do still bear emphasis on the results for Table 19, the general trend for such suggests that the customized control nodes do reduce further the computational time required to run a dynamically varying situation. Further the relative computation times between refined PDO results does match the likely distribution of impact on computational times due to the customized control nodes. The refined PDO ATD_{R3} result is worrying, but is explained via the significant increase encountered by the BFO ATD_{R3} result. While the initial PDO ATD_{R3} result was out of sync with its BFO and refined PDO counterparts, concern over its occurrence is mitigated by the fact that the initial PDO results were grossly undesirable in the first place.

6.3 PDO Capacity Tests using Customized control nodes

The creation of the PDO allowed significantly large scenarios to be split into smaller chunks through the use of potential conflict group assessments. Using customized control nodes with the PDO provided results similar to that of a static application of the BFO, yet with noticeably lesser computation times; the cause stemming largely from the reduction of the number of control variables. A suitable test then would be to try and optimize a continental region's worth of air traffic; say for instance the Australian Domestic scenario as put forward in 5.2.2; it should be noted that this scenario is not an actual list of aircraft departure times and is just an even distribution of statistical data. However, as the scale of aircraft numbers was taken from [57], the set of air traffic created by this distribution should still be representative of continental scale air traffic. This type of scenario would ordinarily be avoided in testing due to the sheer volume of both air traffic and air space that would have to be considered; the BFO and PCO assume holistic and highly detailed knowledge, so their attempt at doing so would cause them to optimize a day's worth of traffic over the entire continent due to no apparent means of dividing air traffic being present. In terms of the optimizer this means hundreds of aircraft each with a requisite control variable hundreds of elements in length. The optimizer hessian alone would be billions of elements in size, and the impact of the 400 or so ATD_i per aircraft still has not been considered. In summary the possibility of an unaltered BFO or PCO performing a complete optimization process is highly unlikely due to the software and hardware it requires. However with the PDO, the combined minimalist perspective would only require less than 50 aircraft to be considered every five minutes, and the potential conflict group assessment would divide this group even further such that no individual group would contain more than 30 aircraft. When combined with the impact of the customized control nodes, which reduced the number of control variables per aircraft to 20 variables (10 altitudes and 10 velocities), the problem was made considerably simpler to handle. However as the optimizer has currently been setup to store all trajectories that were created in their NMD format, there's still a limitation on the number of intervals that can be assessed before no more RAM is available. Further, to avoid aircraft starting at potentially conflicted initial points, the optimizer can only begin when no aircraft are present. In consideration of the above issues a scenario consisting of the first two hours of the Australian Domestic Air Traffic shown in 5.2.2 was given to the PDO for optimization using MatLab® 64 bit on a single core of a 2.46GHz Quad Core Opteron™ with 32GB of RAM and 1.2TB of swap space made available to it. The PDO was tasked to run the problem using each of the three customized control node lists.

Of the three, only ATD_{R2} ran to completion; ATD_{R1} and ATD_{R3} stopped due to mainframe and software handling issues not directly caused by the PDO. ATD_{R2} ran for 678 hours; graphics displaying the results can be seen in Figure 75 with Table 20 giving a breakdown on the times that tasks, as categorized in 5.1, took to be completed. Unfortunately a large number of the mutually exclusive groups were not successfully optimized due to an unforeseen issue of the scenario; apparently airports that required aircraft to takeoff every five minutes fundamentally prevented any aircraft to land at that airport. Aircraft trying to land at such an airport would try to cooperative with departing aircraft to form a window in time to let them land; however at a five minute separation time between almost all departing aircraft and all landing aircraft needing a similar amount of time separation, there was no way of collecting enough time to allow aircraft to land. However, the optimizer did eventually find the scenario to be infeasible and using the result continued optimization till completion anyway; for this reason the capacity test was still a success as it did show that clustered traffic over a continental region could be handled by the optimizer. Further, as failed optimizations do take considerably longer, there is

confidence in a feasible scenario taking much shorter. Also, given the run was entirely sequential due to a single core being used, the use of parallel computing and more cores should reduce computation time significantly as well.

To prove that it could be faster under similar conditions but with a feasible scenario, the excessive take off rate fixes mentioned in 5.2.2 were inverted and applied on the arrival end of all flights; all aircraft were tasked to exit upper level airspace at a point 30 nautical miles prior to their previous exit. This effectively isolated all departing aircraft from all arriving aircraft and prevented the infeasibility that occurred previously. While such may not be ideal in practice, it is assumed that the knowledge of already present regions of descent and takeoff that are usually defined for airports would have a similar effect in reality. As only ATD_{R2} ran previously, this altered scenario was also run using ATD_{R2} to allow comparison. The optimization finished in 90 hours with all sub-scenario optimizations adhering to constraints, and all but two reaching an optimum. The time outs experienced for those two cases are still being assessed, but were expected to be due to interactions between immutable and non-immutable trajectories. The scenario's equivalent of Figure 75 and Table 20 are found in Figure 76 and Table 21. The biggest difference are the smoothness of trajectories involved, as well as the decreases in both the number of aircraft optimizations, and number of mutually exclusive groups that were experienced; these could easily be explained by aircraft being allowed to feasibly optimize their trajectories and therefore avoiding the massive delays they were experiencing previously.

As a final check on the capability of the optimizer, another trial with exactly the same scenario and conditions was run, but using a mix of A320 and 737 in place of the 747; the two aircraft were evenly distributed amongst the trips scheduled sorted according to time. The BADA details for these aircraft can be found in Table 11 and Table 12. The scenario's equivalent of Figure 76 and Table 21 are found in Figure 77 and Table 22. While the trial proved just as successful, optimization wise, as the 747 trial just previous, it experienced the same issues that the trials in 4.3.3 did; i.e. a lack of fuel caused increased complexity in the optimization problem. In order to compensate for the likely problems that setting a fixed initial fuel weight would have on a scenario this size, as well as to ensure that aircraft do have a realistic amount of fuel to carry out their flight, an aspect of the dynamic optimizer component mentioned in 5.1.3 ensured that aircraft entering optimized airspace would have at least 6% more fuel than that required to fly their optimum trajectory uninterrupted. This 6% buffer would ensure that when it came to catering for potential conflicts, that the aircraft would still have sufficient fuel to carry out their trip. However because the A320 and 737 have comparatively smaller total fuel capacities, this 6% does not give the same amount of trajectory flexibility that it does give to a 747; this consequently reduces the size of the potential trajectory of the aircraft and therefore makes their optimization more difficult to achieve. In terms of the Australian Domestic trial, this resulted in a significant increase in computation time; 350 hrs compared to the 90 hrs required when only using 747s. While there may be better ways of ensuring that aircraft have equal and sufficient flexibility to alter their trajectories, this would likely require far more detailed understanding of the policies and requirements of the ANSP as applied in reality. Nevertheless, the optimization trial was successful, and as a consequence of the success of this and the last trial it is possible to say that the optimizer can be used effectively even on a continental scale of air traffic.

6.3.1 Results with Infeasible Domestic Air Traffic

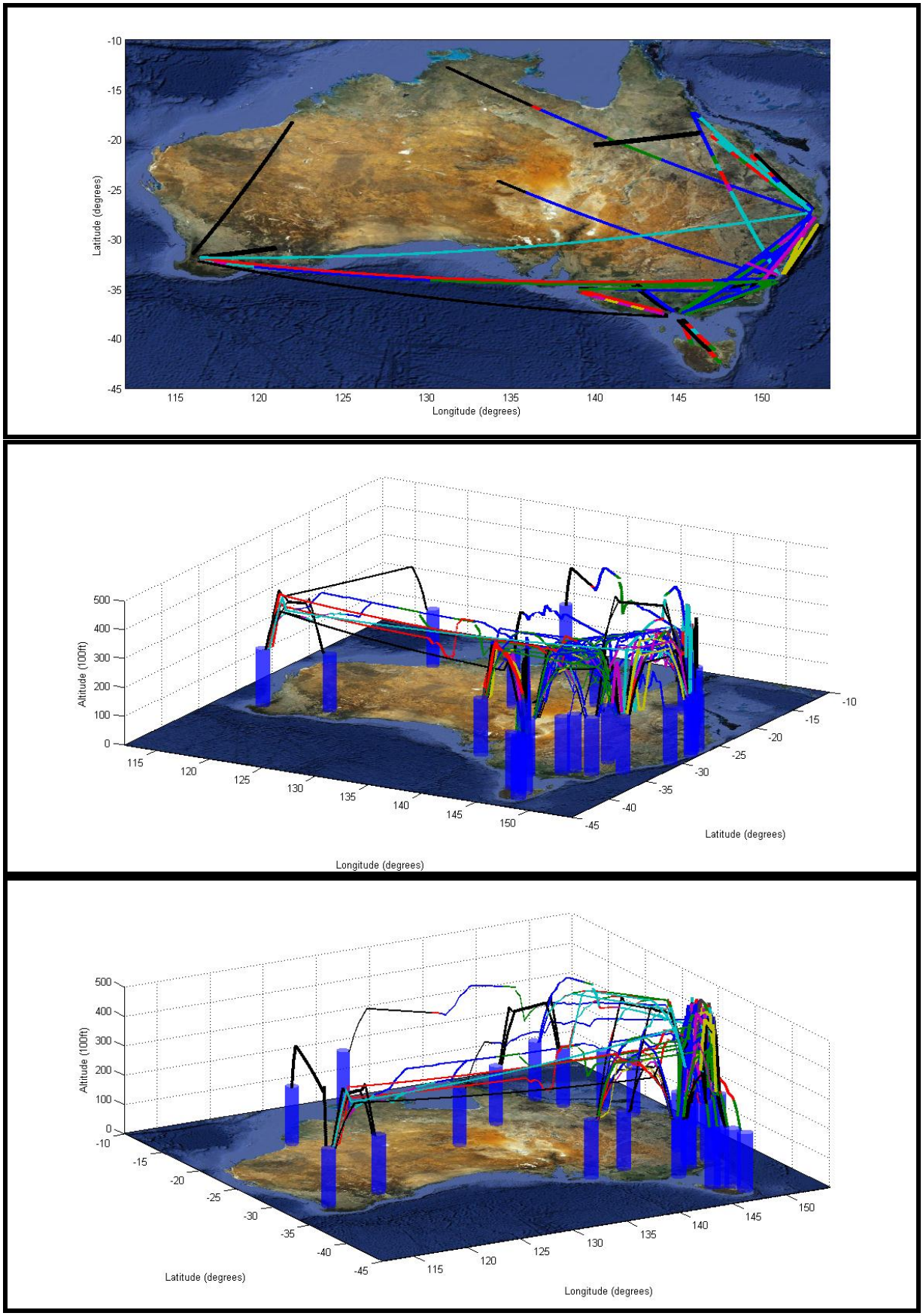

Figure 75 - PDO ATD_{R2} result for 2 hours' worth of Infeasible Australian Domestic Air Traffic, as seen from above (top), the South East (middle), and the South West (bottom).

Table 20 - PDO ATD_{R2} Infeasible Australian Domestic Optimization Details

Detail / Time Step	5.1.1 (s)	5.1.2 (µs)	5.1.3 (s)	5.1.4 (s)	5.1.5 (hr)	5.1.6 (s)	#New Entrants	#Aircraft Optimized	#Mutually Exclusive Groups
0	0.05	2.06	206.72	25.72	1.98	0.10	26	26	3
5	3.05	0.24	10.27	29.91	3.15	0.72	2	28	3
10	4.74	0.26	15.74	38.26	2.45	1.05	3	31	4
15	6.49	0.29	4.45	33.46	1.24	1.45	1	32	4
20	7.95	0.24	24.57	34.41	2.84	1.78	4	36	5
25	9.50	0.25	10.16	28.84	35.37	2.13	2	36	5
30	11.17	0.21	50.49	62.30	8.22	2.49	3	37	7
35	13.45	0.46	11.65	59.75	40.70	3.02	2	35	6
40	21.85	0.26	26.08	77.98	79.85	3.33	4	37	6
45	17.38	0.30	14.70	69.25	22.58	3.81	3	38	8
50	18.62	0.34	8.75	61.32	25.47	4.06	3	39	9
55	23.01	0.22	18.83	56.09	15.21	4.51	2	37	10
60	22.91	0.24	24.10	66.99	38.37	4.78	3	37	5
65	25.49	0.23	7.36	62.60	61.25	5.21	2	34	7
70	26.33	0.24	15.40	71.89	58.45	5.54	4	35	5
75	27.89	0.81	15.64	60.41	36.06	5.93	2	35	8
80	29.63	0.30	42.51	101.64	43.44	6.22	5	39	8
90	31.84	0.44	21.89	71.50	30.74	6.69	3	35	7
95	33.28	0.23	27.70	76.78	36.09	6.86	4	37	8
100	35.71	4.41	15.03	79.53	30.29	7.57	3	39	7
105	37.47	0.39	15.81	75.47	70.50	7.97	3	39	4
110	39.21	0.23	21.51	86.01	8.64	8.80	5	40	9
115	41.42	0.28	6.07	72.55	9.68	9.14	1	36	9
120	44.44	0.35	48.35	80.27	13.96	9.07	4	36	11
Total	532.90	13.27	663.80	1482.93	676.52	112.24	94	854	158

6.3.2 Results with Feasible Domestic Air Traffic

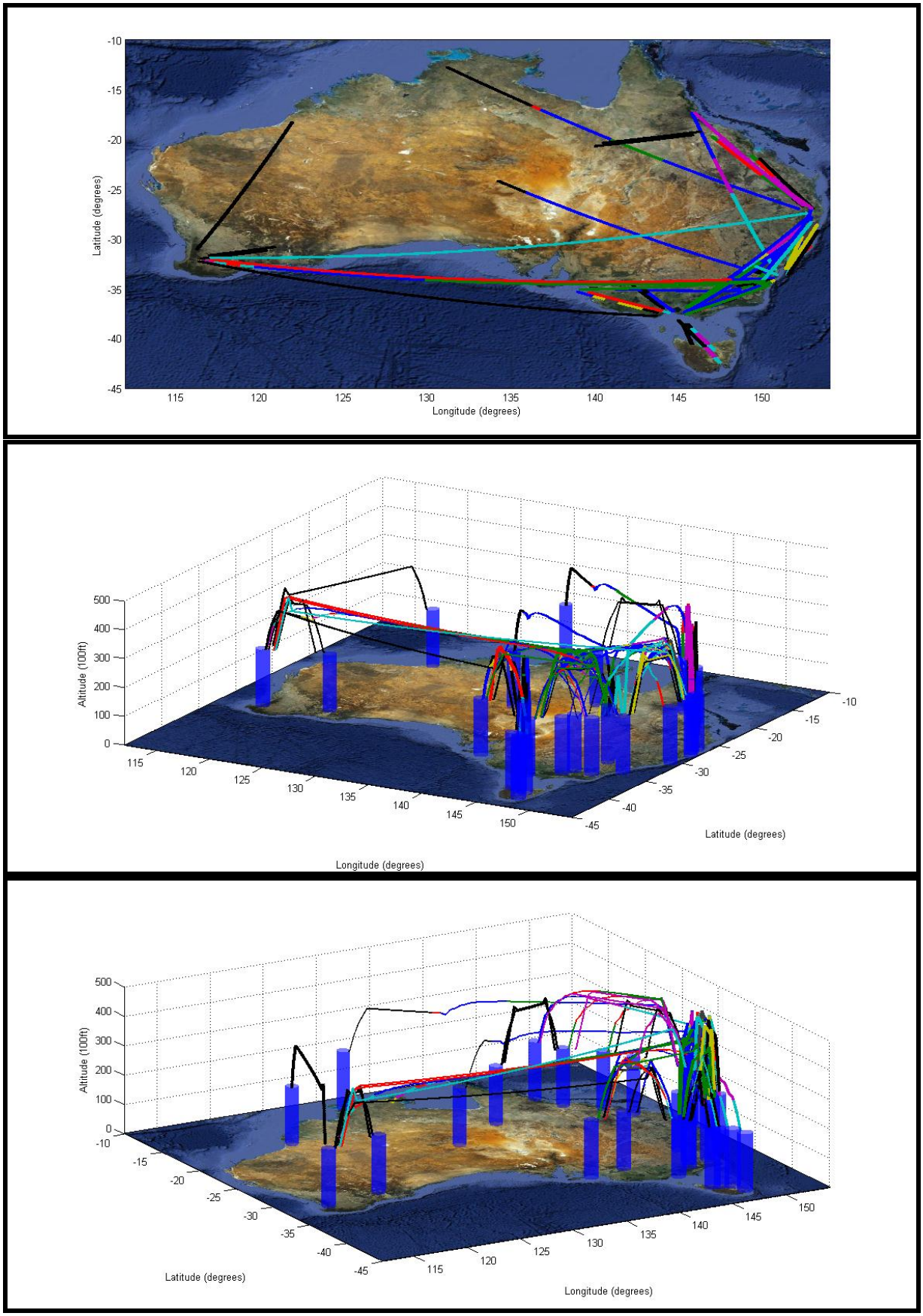

Figure 76 - PDO ATD_{R2} result for 2 hours' worth of Feasible Australian Domestic Air Traffic, as seen from above (top), the South East (middle), and the South West (bottom).

Table 21 - PDO ATD_{R2} Feasible Australian Domestic Optimization Details

Detail / Time Step	5.1.1 (s)	5.1.2 (µs)	5.1.3 (s)	5.1.4 (s)	5.1.5 (hr)	5.1.6 (s)	#New Entrants	#Aircraft Optimized	#Mutually Exclusive Groups
0	0.37	1.98	133.01	20.65	3.06	0.10	26	26	3
5	2.89	0.24	13.41	25.65	0.43	0.67	2	28	4
10	4.49	0.27	24.07	31.37	1.63	1.00	3	31	5
15	6.33	0.49	1.11	27.06	0.38	1.37	1	32	6
20	7.66	0.27	23.07	26.83	0.43	1.70	4	35	7
25	10.39	0.50	16.41	23.10	2.05	2.01	2	34	7
30	10.37	0.75	28.03	55.46	3.94	2.36	3	33	9
35	12.39	0.26	15.04	54.28	3.84	2.81	2	33	9
40	14.34	0.21	23.86	64.67	3.17	3.12	4	35	9
45	16.00	0.34	6.32	59.13	0.80	3.52	3	37	9
50	17.51	0.23	10.79	53.37	1.46	3.84	3	36	8
55	19.25	0.24	30.85	48.21	2.73	4.19	2	34	8
60	21.21	0.22	23.39	57.85	6.16	4.49	3	32	6
65	23.50	0.37	5.79	56.31	8.06	4.93	2	32	8
70	24.26	0.40	30.75	63.51	5.35	5.19	4	34	7
75	26.09	0.26	8.06	58.07	8.38	5.52	2	35	8
80	27.74	0.29	31.21	92.97	6.66	5.92	5	39	6
90	29.47	0.44	18.89	71.22	4.74	6.23	3	33	5
95	31.14	0.59	73.80	77.82	6.46	6.58	4	37	10
100	33.04	0.24	15.38	77.90	8.61	6.93	3	39	8
105	34.59	0.26	12.63	71.72	1.04	7.32	3	38	9
110	36.67	0.25	21.56	79.62	1.04	7.97	5	38	11
115	38.21	0.34	5.71	69.78	1.51	8.49	1	33	12
120	39.47	0.32	21.00	74.70	0.69	9.21	4	36	12
Total	487.37	9.74	594.14	1341.25	82.63	105.46	94	820	186

6.3.3 Results with Feasible Domestic Air Traffic Using a mix of A320 and B747

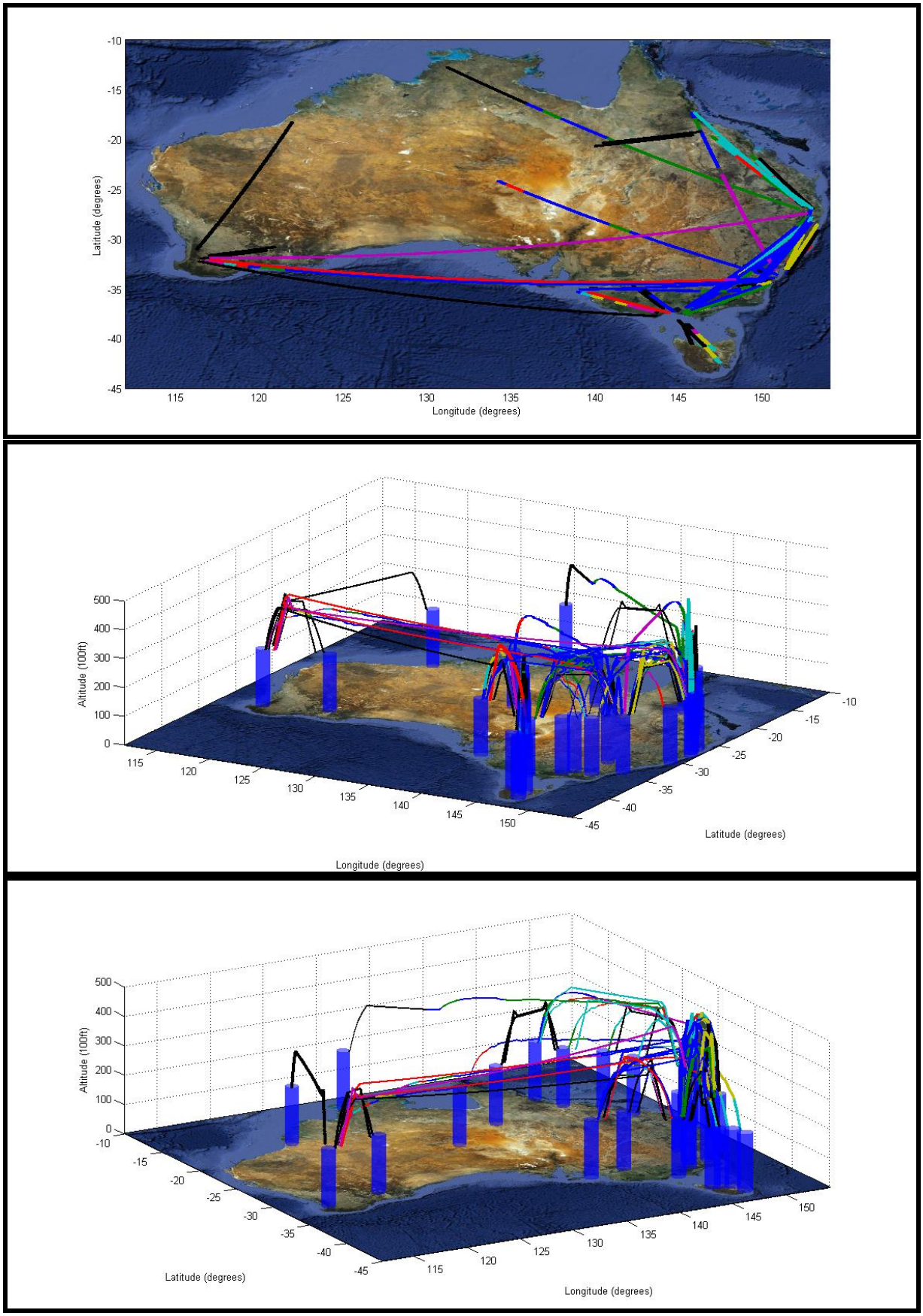

Figure 77 - PDO ATD_{R2} result for 2 hours' worth of Feasible Australian Domestic Air Traffic, as seen from above (top), the South East (middle), and the South West (bottom), using A320 and 737.

Table 22 - Details for the PDO ATD_{R2} Feasible Australian Domestic Optimization using A320 and 737

Detail / Time Step	5.1.1 (s)	5.1.2 (µs)	5.1.3 (s)	5.1.4 (s)	5.1.5 (hr)	5.1.6 (s)	#New Entrants	#Aircraft Optimized	#Mutually Exclusive Groups
0	0.09	1.96	368.05	20.57	6.82	0.09	26	26	3
5	2.91	0.22	44.47	23.59	0.62	0.63	2	28	4
10	4.53	0.30	162.27	31.46	0.57	0.97	3	31	6
15	6.16	0.21	62.11	27.42	0.59	1.37	1	32	6
20	7.43	0.22	24.27	29.03	0.47	1.65	4	35	7
25	9.24	0.27	6.23	24.95	3.93	1.97	2	35	7
30	10.24	0.23	86.01	59.05	1.33	2.35	3	36	9
35	12.38	0.26	73.44	58.33	15.02	2.82	2	35	9
40	14.09	0.21	436.12	69.53	3.52	3.17	4	37	9
45	15.90	0.32	15.17	64.61	1.57	3.49	3	38	10
50	17.86	0.29	446.41	63.15	8.09	3.78	3	40	9
55	19.60	0.33	101.49	58.63	2.37	4.16	2	39	8
60	21.09	0.29	49.28	64.36	21.89	4.52	3	37	6
65	23.53	0.48	53.53	61.17	18.37	5.03	2	34	8
70	25.03	0.27	307.92	72.70	49.06	5.30	4	36	7
75	26.25	0.20	13.88	67.77	45.76	5.64	2	37	6
80	28.25	0.21	39.77	104.85	73.32	6.00	5	41	7
90	30.11	0.20	24.87	86.28	11.96	6.47	3	40	4
95	32.04	0.49	45.95	89.78	52.91	6.78	4	39	6
100	33.74	0.44	77.66	92.33	19.75	7.01	3	40	8
105	35.24	0.26	25.17	85.38	2.03	7.43	3	41	9
110	37.59	0.28	90.81	94.52	1.64	7.97	5	43	11
115	40.16	0.25	18.21	86.88	1.18	8.35	1	40	11
120	43.29	0.26	252.96	91.46	2.55	8.85	4	38	11
Total	496.75	8.43	2826.06	1527.81	345.31	105.81	94	878	181

6.4 Conclusions

The purpose of this section is twofold. The first purpose is to give a summary of the research contributions performed in this chapter and this is performed in section 6.4.1. The second purpose is to highlight the impact the work had on the Research Questions mentioned in section 2.4.2 and this is discussed for each research question in section 6.4.2.

6.4.1 Chapter Summary of Research Contributions

Building up the capability of the PDO as well as dealing with several shortcomings of the BFO and PCO, the optimizer control nodes were customized to better reflect the desired properties of a trajectory; when these customizations were used in a static BFO, they yielded improvements in computational time as well as reduced separation complexity that would allow ease of ATC supervision and guidance, but largely at the cost of increased fuel usage. When the customized control nodes were used in the PDO with an appropriately small and therefore frequent re-optimization interval, the increases in ATFU were significantly decreased and became similar to both the static BFO and PDO results; essentially creating a potentially computationally efficient alternative to the two since the computational requirements were still lessened. Further, while it was initially expected that the complexity reducing properties of the customized control nodes would disappear if used in a PDO, it appears that if re-optimizations are held back to the bare minimum, i.e. only for new entrants, the complexity reducing properties are reasserted and provide ease of supervision till the next re-optimization is required; thereby allowing users to easily switch between high fuel efficiency and safer separation supervision. Lastly, to show that a combination of the PDO and customized control nodes can grant significant computational savings, a capacity test using a time sliced portion of a day's worth of Australian Domestic Air Traffic was successfully completed.

6.4.2 Current State of Research

6.4.2.1 Q1: Can a co-operative and sufficiently informed air traffic optimisation methodology achieve a reduction in total fuel usage compared to current ATM?

In chapter 3 Q1 was partially answered by showing that the PCO could minimize ATFU. However, the PCO was based on flight mechanic derivations of fuel consumption and could not be compared to current ATM. In chapter 4, the BFO had improved upon the representation of the air traffic model by using more accurate data, i.e. BADA, to define optimum trajectories, and also included the creation of the BSO which simulated current ATM methods for scheduling aircraft. These two inclusions allowed the BFO to be more realistic and to allow comparison with current ATM; the consequence was that chapter 4 did show that it was possible for a cooperative air traffic optimization methodology to reduce ATFU. In section 5.3.2.1 the PDO improved upon the air traffic model by enabling the model to change in a dynamic manner and thereby be representative of unforeseen changes to air traffic; this consequently improved the "informed" state of the air traffic optimization methodology, and could allow reduction of ATFU even in dynamic situations. However it also recognized that a reduction in ATFU compared to current ATM requires the application of the PDO in real time. Thus the contribution of Chapter 6 to answering Q1 is to show that the PDO can be used in real time. This does require

considerable computational hardware, however the scale of tests in Chapter 6, and the parallelability of the PDO, do indicate it is possible. Thus this chapter finalizes the answere to Q1: a cooperative and sufficiently informed air traffic optimization methodology can achieve a reduction ATFU compared to current ATM.

6.4.2.2 Q2: What information is required to achieve such an optimisation methodology and how sensitive are the results to the accuracy of the input information.

The information required for a customized decrease in the number and position of the trajectory change points is merely where the airline, aircrew or ANSP, desire those points to be. However it should be remembered that its introduction was caused by the optimizer being overly sensitive to trajectory constraints by moulding around them rather than distributing the necessary deviation across the trajectory. Therefore, as the customized control nodes do desensitize the optimizer into distributing necessary deviation across the entire trajectory, it has performed its role successfully.

6.4.2.3 Q3: How can constraints such as aircraft performance limitations, minimum separation and on-time arrival be incorporated into an optimizable UPT, and how do these affect total fuel usage?

While the majority of the optimizer's capability in these constraints are defined in chapters 3 and 4, the avenues created by having customizable control node points does mean various stakeholders can have another way of influencing some of these constraints whilst still achieving fuel reduction. For example trajectories can have trajectory control node distributions that cater for passenger service, or avoid chaotic conflict resolution in heavy traffic, or prevent uncomfortable accelerations when an ETA needs to be met; the fact that control node customization allows a user to pre-specify these areas additional ability to facilitate UPT.

6.4.2.4 Q4: How can a dynamic environment, such as deviation from or in-flight changes to the flight plan, airspace closure, and emergency diversion, be accommodated in an optimisation methodology?

The research in chapter 5 developed the means of carrying out optimization in a dynamic system; however it was the research in chapter 6 that enabled it to become more feasible from a user and computational perspective. From a user perspective, the chapter 5 results were representative of the best results achievable in an unpredictable scenario, however the resulting variability of the optimum trajectories did indicate potential issues if pilots or airlines could not handle the frequently re-optimized trajectories. Thus the research in chapter 6 investigated a means of making trajectories more user-friendly by selectively choosing where in the trajectory that climb angles and accelerations could change. Further research into how this method interacted with the iterative nature of the PDO showed that it could provide either highly variable or user friendly trajectories by varying the frequency of the PDO's reiterations; given that both did not diminish the computational efficiency of having less control nodes, it effectively created a computational efficient means of highly variable trajectories as well, to the point where even optimization of a continent's worth of air traffic can become feasible.

7. CONCLUSIONS AND RECOMMENDATIONS

The desired outcome of this research was the modelling of trajectories of air traffic in a continental sized region that were cooperatively optimized for minimum fuel consumption. In order to do this four research questions were created and answered over the course of this thesis. The following sections, firstly, lists the conclusions of the research in terms of the research questions, and secondly, defines the impact of the research and its subsequent recommendations.

7.1 Conclusions of the Research Questions

Q1: Can a co-operative and sufficiently informed air traffic optimisation methodology achieve a reduction in total fuel usage compared to current ATM?

In chapter 3 Q1 was partially answered by showing that the PCO could minimize ATFU. However, the PCO was based on flight mechanic derivations of fuel consumption and could not be compared to current ATM. In chapter 4, the BFO had improved upon the representation of the air traffic model by using more accurate data, i.e. BADA, to define optimum trajectories, and also included the creation of the BSO which simulated current ATM methods for scheduling aircraft. These two inclusions allowed the BFO to be more realistic and to allow comparison with current ATM; the consequence was that chapter 4 did show that it was possible for a cooperative air traffic optimization methodology to reduce ATFU. In chapter 5 the PDO improved upon the air traffic model by enabling the model to change in a dynamic manner and thereby be representative of unforeseen changes to air traffic; this consequently improved the "informed" state of the air traffic optimization methodology, and could allow reduction of ATFU even in dynamic situations. However it also recognized that a reduction in ATFU compared to current ATM requires the application of the PDO in real time. The contribution of Chapter 6 to answering Q1 was in showing that the issues outlined in Chapter 5 could be handled; it showed that the PDO can be used in real time. It did require considerable computational hardware, however the scale of tests in Chapter 6, and the parallelability of the PDO, do indicate it is possible. Thus this chapter finalizes the answere to Q1: a cooperative and sufficiently informed air traffic optimization methodology can achieve a reduction ATFU compared to current ATM.

Q2: What information is required to achieve such an optimisation methodology and how sensitive are the results to the accuracy of the input information?

In chapter 3, the requisite input information that was assessed was the information carried by the optimizer's air traffic model. Concern was placed on whether or not the PCO could precisely model smooth cooperation of air traffic; it was possible for the discretization of air traffic and its constraints to shape trajectories and include deviations from optimal trajectories that were not necessary. However, chapter 3 was successful in this regard, and cooperative trajectories created by the PCO, and later BFO, mould tightly to each other and do require cooperation between them.

In chapter 4, the requisite input information was the variety of aircraft flight models, and their corresponding flight mechanics, that were made available by incorporating BADA into the PCO to create the BFO. Concern was placed on the PCO only being able to handle certain flight models; given that the PCO was developed using

a fuel consumption model using that only had assumptions on coefficient of lift, thrust, and constant specific fuel consumption, the concern was justified. However, the BFO was re-tested using three more models; the B747-400, the A320, and the B737. Previous scenarios were re-tested with single and mixed aircraft models. Most optimizations were successful; the scenarios that failed did so because the scenario was impossible i.e. there was insufficient airspace to allow the aircraft models to fly to their destination without running out of fuel. Further, the resulting trajectories did show properties that correlated with the optimal trajectory of the aircraft model being used to define air traffic; consequently the BFO was sufficiently sensitive in its utilization of different BADA models to ensure aircraft specific data does show through to the optimization results. .

In chapter 5, the new input information under assessment was that required to enable dynamic optimization; i.e. knowledge of when, where, and which, new events occur in the future. To assess the sensitivity of the optimizer to variation in this information, the PDO was used to optimize several dynamic scenarios. When the scenario featured re-optimization events where nothing had actually changed, the PDO was capable of slightly improving the result; i.e. as allowed by the optimizer having an effectively increased number of control nodes. However, when faced with scenarios featuring frequent re-optimization events, the optimizer was capable of being over sensitive. Firstly, the optimizer could not distinguish between trajectories that were not affected by an unforeseen event and those that were; consequently every new event re-optimized air traffic in its entirety. To limit its effectiveness in this area, a means of isolating mutually exclusive air traffic was developed and applied; re-optimization scenarios thus first separated air traffic into mutually exclusive groups, then optimized each group separately with groups not requiring re-optimization being left alone. The addition of the isolation tool directly improved the optimizer's sensitivity to already optimal trajectories. The second way that the PDO was oversensitive was that its effectiveness in finding optimums in a static situation enabled the optimizer to pursue a variety of similarly fuel efficient, but differently shaped, trajectories; as unforeseen events can change a scenario enough to change the fuel efficiency of these trajectories, the optimizer was found to switch between these differently shaped trajectories and create a final trajectory that contains many changes in speed and altitude. While this trajectory would be fuel efficient, it was argued that a trajectory with less speed and altitude variation may be more fuel efficient.

In chapter 6, an approach to handling the oversensitivity of both the PDO and BFO was created. This approach introduced UPT elements for the purpose of simplifying air traffic complexity and providing an avenue for user preferences to be facilitated, however it had the side effect of limiting the optimizer's ability to switch between similarly fuel efficient trajectories with different shapes. This side effect was caused by control node customizations controlling where in the trajectory that portions of constant altitude, speed, or climb angle, would occur; if the aircraft was within a trajectory portion of constant parameter, trajectory changes in altitude and speed could only occur afterwards and consequently limited trajectories to those preferred by the user.

The combined results from the above chapters allow Q2 to be answered. The cooperative minimization of ATFU requires input information from a) an air traffic model for the purposes of separation, b) aircraft performance models for the purpose of fuel usage and performance limit calculation, c) the ATS for the purpose of defining changes in the air traffic scenario, and d) the trajectories' UPT for the purpose of including non fuel related trajectory properties. While each of these is capable of being over or under sensitive, this thesis has performed an assessment of their sensitivity, and created functions to limit or improve their sensitivity so as to provide effective and accurate cooperative minimization of ATFU.

Q3: How can constraints such as aircraft performance limitations, minimum separation and on-time arrival be incorporated into an optimizable UPT, and how do these affect total fuel usage?

Chapter 3 showed how aircraft performance limitations and minimum separation were necessary constraints of the system; this is due to their failure leading to an ATS breaking down and destroying all assumptions used in the optimizer. However in terms of minimizing ATFU, chapter 3 recognized that the most optimal trajectories involve violating these constraints. Consequently, the satisfaction of these constraints always requires an increase in total ATFU from that infeasible optimum. Chapter 3 also shows how to incorporate on-time arrival as part of an optimizable UPT. With aircraft specific constraints on arrival time, aircraft can be made to travel faster or slower so as to reach their destinations at their scheduled time. The provision of on-time arrival as part of the UPT almost always increases ATFU; the only instance it does not is when an aircraft's scheduled arrival time exactly matches the arrival time the optimizer determined for it without the arrival time constraint. However as interaction with other aircraft causes aircraft to deviate away from their optimal trajectory, they must spend additional fuel to return to the optimal trajectory; hence why on-time arrivals cause increases to ATFU.

Chapter 4 shows the incorportation of BADA into fuel usage and aircraft performance calculation. Its incorporation into the PCO was possible as the derived flight mechanics used in the PCO is similar to the HEM used by BADA. Consequently, BADA's incorporation increased the variety of aircraft performance limitations that could be controlled by the optimizer. The result was improved definition of aircraft trajectories. While these additional constraints did also increase ATFU, the real change was in how similar to real commercial air traffic the BADA models were; their closeness gave the optimizer the potential the ability to simulate minimization of ATFU in a realistic setting.

Chapter 6 incorporated the ability for users to customize their UPT to include trajectory portions that had constant altitude, climb angle or speed; this allowed users to pursue a fuel inefficient trajectory if they had reason to do so, such as the non-fuel related costs mentioned in section 2.2.3. It was the division of the optimizer variable from the baseline of fuel usage calculation that facilitated constant trajectory portions; a user could apply a variety of constant parameter sections throughout their trajectory and it would not affect how fuel usage was calculated. Further, this did not prevent the minimization of ATFU; while the trajectory portions had constant parameters, the optimizer still had control over what altitudes and speeds those portions would be flown at. Consequently UPT constaining constant parameter portions would still be optimized for fuel usage; however as the constant parameters do act as constraints, it is likely for the aircraft to experience increased fuel usage for as compared to having no constant parameter portions.

Q4: How can a dynamic environment, such as deviation from or in-flight changes to the flight plan, airspace closure, and emergency diversion, be accommodated in an optimisation methodology?

Chapter 5 was specifically performed to investigate how to answer Q4. The core issue that this research has tried to deal with, and the common facet of the events mentioned in Q4, is that they can be unforeseen; hence the development of a dynamic optimizer in the form of the PDO. Chapter 5 does show, in detail, how these events are accommodated for. However while the PDO effectively succeeds in handling new events, it was apparent from the optimization trials in section 5.2 that the optimization can be a bit oversensitive by requiring trajectory

changes directly after a new event has been recognized, which can be ideal but only if no other unexpected events occur afterwards. This suggests that the PDO could become more robust, and be more computationally efficient, by somehow decreasing the optimizer's ability to react quickly to new events.

It was due to the research in chapter 6 that enabled the PDO to become more feasible from a user and computational perspective. From a user perspective, the chapter 5 results were representative of the best results achievable in an unpredictable scenario, however the resulting variability of the optimum trajectories did indicate potential issues if pilots or airlines could not handle the frequently re-optimized trajectories. Thus the research in chapter 6 investigated a means of making trajectories more user-friendly by selectively choosing where in the trajectory that climb angles and accelerations could change. Further research into how this method interacted with the iterative nature of the PDO showed that it could provide either highly variable or user friendly trajectories by varying the frequency of the PDO's reiterations; given that both did not diminish the computational efficiency of having less control nodes, it effectively created a computational efficient means of highly variable trajectories as well, to the point where even optimization of a continent's worth of air traffic can become feasible.

7.1 Research Impact and Recommendations

There are significant impacts to end users, i.e. aircrew, airlines, ATC, and ANSP, due to the confirmation that the above research results led to real time Continental Co-operative Air Traffic Optimization via Fuel Usage Minimization. It was shown that aircrew and ATC would be able to facilitate fuel efficient trajectories more frequently and effectively by using the tool as a centralized aircraft scheduler that has access to flight plans, performance information and current flight data of all aircraft in a potentially continental sized airspace. The optimization tool's ability to not require a look-ahead time limit was confirmed and was shown to allow aircrew and ATC to adhere to an optimized trajectory throughout an entire flight, or until the occurrence of an unforeseen event that could impact the flight, e.g. weather or aircraft failure. However, in these events, the tool did show a seamless ability to re-optimize air traffic, and ensure ATC and aircrew could still facilitate continued minimum fuel usage. For ANSP and airlines, the key impacts were due to the confirmation that the tool only used deterministic optimization techniques and commercially available information and communications technology. The deterministic techniques ensure the process is predictable and can be replicated, and thus verifiable by either airlines, ANSP, or both. The commercially available technology ensures the process can be performed now, provided computational power proportional to air traffic density at the time is made available; it was confirmed that the computational power can be provided via distributed computing due to the tool's ability to divide airspace and air traffic without significantly affecting optimization. Together, these methods allow flexible implementation of the tool's computational resources by allowing ANSP or airline owned computational power to compute, verify, or integrate optimization results, in a shared or separate manner. There are no hard requirements or reliances on specific hardware, such as on-board or ATC systems, from the tool at this point in time, therefore airlines and ANSP of a region would need to define how to best separate the computational load between airline and ANSP assets, or whether or not to delegate the task entirely to ANSP.

There are other technical and industry issues that prevent this tool from being implemented. Due to the holistic development of the tool, purely technical issues are region specific; regions that allow non-standard routes will need further research on route optimization, and regions that cannot facilitate computational power proportional to the level of air traffic they experience may have to research more efficient optimization algorithms. Industry issues stem from how fuel usage, predicted and actual, still constitutes sensitive corporate information; agreements and procedures would have to be prepared to ensure that any information that can affect fuel usage of air traffic is actually distributed among the computational resources of the tool, irrespective of who owns the resource. It is expected that how these agreements and procedures are created for a region will have a significant impact on how the computational resources of the tool will be distributed in that region.

8. REFERENCES

A list of published documents that have influenced the research, but have not been directly referenced in the thesis can be found in Appendix M: Bibliography.

[1] Radio Technical Commission for Aeronautics, 1995. *Final Report of the RTCA Task Force 3: Free Flight Implementation*, RTCA Inc., Washington DC.

[2] Advisory Council for Aeronautics Research in Europe, 2002. *Strategic Research Agenda: Volume 1, Advisory Council for Aeronautics Research in Europe*, Advisory Council for Aeronautics Research in Europe. Viewed on 25 February 2012 at <http://www.acare4europe.org/docs/es-volume1-2/volume1.pdf >.

[3] Joint Planning and Development Office, 2007. *Concept of Operations for the Next Generation Air Transportation System*, Version 2.0, Joint Planning and Development Office, United States. Viewed on 25 February 2012 at <http://www.jpdo.gov/library/NextGen_v2.0.pdf>

[4] Single European Sky ATM Research, 2007. *SESAR Definition Phase D3 - The ATM Target Concept*, SESAR Consortium. Viewed on 10 July 2008 at < https://www.atmmasterplan.eu/http://prisme-oas.atmmasterplan.eu/atmmasterplan/faces/public/infoLibrary/structInfoLibrary.jspx>

[5] Advisory Council for Aeronautics Research in Europe, 2002. *Strategic Research Agenda: Volume 2 The Challenge of the Environment*, Advisory Council for Aeronautics Research in Europe. Viewed on 25 February 2012 at <http://www.acare4europe.org/docs/es-volume1-2/volume2-03-environment.pdf>.

[6] Civil Aviation Safety Authority, 2006. *Automatic Dependant Surveillance - Broadcast*, Civil Aviation Safety Authority of Australia. Viewed on 6 March 2012 at <http://www.casa.gov.au/wcmswr/_assets/main/pilots/download/ads-b.pdf>

[7] Eurocontrol, 2009. *Eurocontrol Specification for the application of the Flexible Use of Airspace (FUA)*. Eurocontrol. Viewed on 6 March 2012 at <http://www.eurocontrol.int/mil/gallery/content/public/milgallery/documents/fua_spec_1%201.pdf >

[8] Smolensky, M.W., Stein, E.S., 1998. *Human factors in air traffic control*, San Diego Academic Press, San Diego.

[9] Ruigrok, R.C.J., Hoekstra, J.M., 2007. "Human factors evaluations of Free Flight: Issues solved and issues remaining", *Applied Ergonomics*, Vol. 38(4), pp. 437.

[10] Grimaud, I., Hoffman, E., & Zeghal, K., 2001. "Limited delegation of separation assurance to the flight crew", *Air & Space Europe*, Vol. 3(3), pp. 285-287.

[11] Bonnemaison, B., Casaux, F., & Miquel, T., 1998. "Operational assessment of co-operative ASAS applications", USA/Europe Air Traffic Management R&D Seminar.

[12] Bayen, A.M., Raffard, R.L., & Tomlin, C.J., 2006. "Adjoint-Based Control of a New Eulerian Network Model of Air Traffic Flow", *IEEE Transactions on Control Systems Technology*, Institute of Electrical and Electronics Engineers, New York City, Vol. 14, No. 5.

[13] Federal Aviation Administration, 2012. *Air Traffic Organization Policy - Section 18. Route Advisories*, Order JO 7210.3X, U.S. Department of Transportation, USA.

[14] Single European Sky ATM Research, 2007. *SESAR Definition Phase D2 - The Performance Target*, SESAR Consortium. Viewed on 10 July 2008 at < https://www.atmmasterplan.eu/http://prisme-oas.atmmasterplan.eu/atmmasterplan/faces/public/infoLibrary/structInfoLibrary.jspx>

[15] Australian Strategic Air Traffic Management Group, 2003. "Australia ATM Strategic Plan - Volume 2", ASTRA, Viewed on 10 July 2008 at < http://astra.aero/strategicplan/docs/OZSTPLAN_Vol2.pdf >

[16] Kuchar, J. K., and Yang, L. C., 2000. "A Review of Conflict Detection and Resolution Modeling Methods", *IEEE Transactions on Intelligent Transportation Systems*, Institute of Electrical and Electronics Engineers, New York City, Vol. 1, No. 4.

[17] Yang, X., 2010. *Engineering Optimization: An Introduction with Metaheuristic Applications*, John Wiley & Sons, Inc., Hoboken.

[18] Amdahl, G., 1967. "Validity of the Single Processor Approach to Achieving Large-Scale Computing Capabilities", *AFIPS Conference Proceedings*, AFIPS Press, Reston, VA, Vol. 30, pp. 483-485.

[19] Duboc, L., Rosenblum, D.S., & Wicks, T., 2006. "A framework for modelling and analysis of software systems scalability", *Proceedings of the 28th International Conference on Software Engineering*, ACM New York, New York, pp. 949 - 952.

[20] Ruijgrok, G.J.J. 1990. *Elements of airplane performance*, Delft University Press, Delft.

[21] Anderson, J.D., 1999. *Aircraft Performance and Design*, WCB/McGraw-Hill, New York.

[22] Niedringhaus, W.P., 1995. "Stream option manager (SOM): Automated integration of aircraft separation, merging, stream management, and other air traffic control functions," *IEEE Transactions on Systems, Man, and Cybernetics*, Institute of Electrical and Electronics Engineers, New York City, Vol. 25, pp. 1269-1280.

[23] Frazzoli, E., Mao, Z.H., Oh, J.H., & Feron, E., 1999. "Resolution of conflicts involving many aircraft via semidefinite programming," *AIAA Journal on Guidance, Control, and Dynamics*, to be published.

[24] Tomlin, C., Pappas, G., & Sastry, S., 1998. "Conflict resolution for air traffic management: A study in multi-agent hybrid systems," *IEEE Transactions on Automatic Control*, Institute of Electrical and Electronics Engineers, New York City, Vol. 43, pp. 509-521.

[25] International Civil Aviation Organization, 2007. *Procedures for Air Navigation Services in Air Traffic Management*, 15th Edition, International Civil Aviation Organization.

[26] Durand, N., Alliot, J., & Chansou, O., 1995. “Optimal resolution of en route conflicts,” *Air Traffic Control Quarterly*, Air Traffic Control Association Institute, Vol. 3, No. 3, pp. 139-161.

[27] Ota, T., Nagati, M., & Lee, D.C., 1998. “Aircraft collision avoidance trajectory generation”, *Proceedings of the 1998 AIAA Guidance, Navigation and Control Conference*, AIAA, pp. 828-837.

[28] Wangermann, J.P., & Stengel, R.F., 1996. “Optimization and coordination of multi-agent systems using principled negotiation,” *Proceedings of the 1996 AIAA Guidance, Navigation and Control Conference*, AIAA, pp. 43-50.

[29] Harper, K., Mulgund, S., Guarino, S., Mehta, A. & Zacharias, G., 1999. “Air traffic controller agent model for free flight,” *Proceedings of the 1999 AIAA Guidance, Navigation and Control Conference*, AIAA, pp. 288-301.

[30] Chao, W., Jing, G., & Xiaohao, X., 2009. "Analysis of Air Traffic Flow Control through Agent-Based Modeling and Simulation", *Proceedings of the 2009 International Conference on Computer Modeling and Simulation*, Institute of Electrical and Electronics Engineers, New York City.

[31] Sridhar, B., Grabbe, S.R., & Mukherjee, A., 2008. "Modeling and Optimization in Traffic Flow Management", *Proceedings of the IEEE*, Institute of Electrical and Electronics Engineers, New York City, Vol. 96, No. 12.

[32] Menon, P.K., Sweriduk, G.D., & Sridhar, B., 1999. “Optimal strategies for free-flight air traffic conflict resolution,” *AIAA Journal on Guidance, Control, and Dynamics*, AIAA, Vol. 22, No. 2, pp. 202-211.

[33] Nuic, A., Poinsot, C., Iagaru, M.G., Gallo, E., & Navarro F.A., 2005. "Advanced Aircraft Performance Modelling for ATM: Enhancements to the BADA Model." *Proceedings of the 24th Digital Avionics System Conference*, DASC 2005.

[34] Menon, P.K., Sweriduk, G.D., & Bilimoria, K.D., 2004. "New Approach for Modeling, Analysis, and Control of Air Traffic Flow", *AIAA Journal on Guidance, Control, and Dynamics*, AIAA, Vol. 27, No. 5.

[35] Vela, A., Solak, S., Singhose, W., & Clarke, J.P., 2009. "A Mixed Integer Program for Flight-Level Assignment and Speed Control for Conflict Resolution", *Proceedings of the Joint 48th IEEE Conference on Decision and Control and 28th Chinese Control Conference Shanghai*, Institute of Electrical and Electronics Engineers, New York City.

[36] Alam, S., Abbass, H.A., & Barlow, M., 2008. "ATOMS: Air Traffic Operations and Management Simulator", *IEEE Transactions on Intelligent Transportation Systems*, Institute of Electrical and Electronics Engineers, New York City.

[37] Vilaplana, M.A., Goodchild, C., & Elefante, S., 2001. "Co-operative Optimal Airborne Separation Assurance in Free Flight Airspace", *Air Transportation Systems Engineering*, American Institute for Aeronautics and Astronautics, USA.

[38] Eurocontrol, 2004. *User Manual for the Base of Aircraft Data (BADA)*, Revision 3.6, Eurocontrol, France.

[39] Air Transport Association, 2004. ATA quarterly airline cost index: first quarter 2004, Air Transport World, Nov, 2004, Vol. 41(12), p.76(1)

[40] Pham, V.V., 2010. Australian Aviation Emission Inventory Development and Analysis, Environmental Modelling & Software, *Elsevier*, Vol. 25(12), pp. 1738-1753

[41] Goldberg, D.E., 1989. *Genetic Algorithms in Search, Optimization & Machine Learning*, Addison-Wesley.

[42] Wolsey, L.A., 1998. *Integer Programming*, John Wiley & Sons.

[43] Nemhauser, G.L., & Wolsey, L.A., 1988. *Integer and Combinatorial Optimization*, John Wiley & Sons.

[44] Dantzig, G.B., Orden, A, & Wolfe, P., 1955. "Generalized Simplex Method for Minimizing a Linear from Under Linear Inequality Constraints", *Pacific Journal of Mathematics*, Vol. 5, pp. 183-195.

[45] Waltz, R.A., Morales, J.L., Nocedal, J., & Orban, D., 2006. "An Interior Algorithm for Nonlinear Optimization that combines line search and trust region steps," *Mathematical Programming*, Vol. 107, No. 3, pp. 391-408.

[46] Yokota, T., Gen, M., & Li, Y.X., 1996. "Genetic algorithm for non-linear mixed integer programming problems and its applications" *Computers & Industrial Engineering*, Vol. 30, Iss. 4.

[47] Gill, P.E., Murray, W., & Wright, M.H., 1991. *Numerical Linear Algebra and Optimization*, Vol. 1, Addison Wesley.

[48] International Civil Aviation Organization, 2003. *European Region Area Navigation Guidance Material*, 5th Edition, European and North Atlantic Office of ICAO.

[49] Raghunathan, A.U., Gopal, V., Subramanian, D., Biegler, L.T., & Samad, T., 2003. "3D Conflict Resolution of Multiple Aircraft via Dynamic Optimization", *Proceedings of the 2003 AIAA Guidance, Navigation and Control Conference*, AIAA.

[50] Boeing, 2005. *747 Family: Technical Specifications - 747 Classics*, Boeing, Last Retrieved on 22 March 2012 at < http://www.boeing.com/commercial/747family/pf/pf_classics.html#300 >.

[51] ASTM International, 2009. *ASTM Standard D1655-09 Standard Specification for Aviation Turbine Fuels*, ASTM International, West Conshohocken, PA, DOI: 10.1520/D1655-09, Viewed on 1 April 2009 at < www.astm.org >.

[52] Ilan, K., Shevell, R., 1997. *Aircraft Design: Synthesis and Analysis*, Aircraft Aerodynamics and Design Group, Stanford University, Viewed on 22 March 2012 at < http://adg.stanford.edu/aa241/propulsion/largefan.html >.

[53] Scott, J., 2004. *Drag Coefficient & Lifting Line Theory*, Aerospaceweb.org, Viewed on 22 March 2012 at < http://www.aerospaceweb.org/question/aerodynamics/q0184.shtml >.

[54] Obert, E. 2009. "Pressure Distributions on Components which are not intended to generate Aerodynamic Forces", *Aerodynamic Design of Transport Aircraft*, Delft University of Technology, Delft.

[55] GE Aviation, 2009. *Model Cf6-80C2: Power Specifications*, GE Aviation. Viewed on 22 March 2012 at < http://www.geaviation.com/engines/commercial/cf6/cf6-80c2.html >.

[56] Eurocontrol, 2003. "B743_.opf", *Aircraft Performance Operational File*, BADA Revision 3.6, Eurcontrol, France, 2003.

[57] Bureau of Infrastructure Transport and Regional Economics, 2009. *Aviation Statistics: Australian Airline Domestic Activity 2008*, Domestic Annual 153, Bureau of Infrastructure Transport and Regional Economics, Australia.

APPENDIX A Technological Overview

The main portion of the thesis goes into the details of the trajectory optimization process as required, largely, by the defined problem of trajectory control and the issues experienced in modelling it for the purposes of optimization. However a distinct requirement of defining trajectory control comes from understanding the technological limitations that could prevent or inhibit potential methods of defining actual or potential trajectories. The main question asked by this section is "Where exactly is the air traffic industry in improving the flight profile of any individual aircraft?" and answers this by giving a summary of technological changes that lead to the current level of technological implementation in air traffic. However, as pointed out in the main thesis, there were no real technological limitations beyond sufficiently accurate trajectory predictions, which were assumed to be inherent in the externally created, and therefore invariable, aircraft performance models that were used.

A.1 Trajectory Control Prior to NextGen and SESAR

A large number of sources cover the development and introduction of the current ATM system from various view points, however the following statements [A1] seem to be the most common. When civilian air travel was first introduced, air traffic control did not exist and pilots were relied upon to maintain the safety of their passengers; i.e. "see and avoid" procedures were in effect. Separation had not been an issue given the small number of aircraft, their low flight ceiling, and their ability to use short and unprepared runways. As the number and size of aircraft increased, the requirement to use a developed airfield began to cause congestion, and therefore the need to plan and coordinate aircraft arrivals and departures became apparent. At nearly the same time, there came recognition of the destructive possibilities of flying close to other aircraft, especially between the larger and smaller aircraft types, such that air traffic controllers had to ensure sufficient space existed between aircraft. Later on, as aircraft speed and altitude ceiling increased, visibility diminished and the need for beyond the horizon control was further established.

At the beginning of civilian air travel the intended flight profile, i.e. the aircraft's trajectory with respect to altitude, was at its, theoretically, most efficient form; a plane takes off at an airport, reaches cruise (which it was allowed to optimally maintain, i.e. rising as fuel weight decreased), then lands as soon as it gets to its point of arrival. Admittedly, there were occasional interactions with the local environment, usually mountains and severe weather, which caused flight routes, i.e. the aircraft's trajectory with respect to earth surface location, to deviate wildly, however the ability to fly, at the pilot's discretion, the most efficient flight profile was there. As each of the aforementioned developments in ATM history occurred, a corresponding inefficiency was introduced to the then requisite flight profile, further decreasing the chances of the most efficient flight profile from occurring. Airfield congestion created the need for holding patterns, additions of loop patterns of infinite length to the flight profile, to allow air traffic control to safely coordinate aircraft landings. Separation requirements on approach further increased time required to land, and therefore also the use of holding patterns. When separation requirements were necessarily extended beyond the horizon, separation by altitude was introduced, and thus the ability to rise while cruising was severely reduced. Additionally, as each safety requirement was introduced, flight control moved slowly away from the pilot towards on ground controllers.

To be fair, the ability to fly higher than dangerous terrain, then eventually over severe weather, had a positive effect on the possibility of carrying out the most efficient flight profile. The same could be said of the ever advancing geological and meteorological prediction and detection technology that allowed this to occur. Unfortunately, they only act as a subsidiary effect to the measures mentioned above, never fully bringing out the most efficient flight profile.

A.2 Trajectory Control Introduced during NextGen and SESAR

At this point the air traffic industry had been limited by the safety requirements mentioned above for about half a century [A1], staying mostly constant whilst other technologies had to be rigorously developed and tested before being allowed to be applied in standard use (examples of which were codifying written data and various controller station upgrades [A1]). While the reasons for NextGen and SESAR being started are fairly numerous [A1], [A2], [A3], the core of it stems from the ever increasing gap between useful technology available in the world and their cumbersome counterparts that had to be used, and the inefficiencies caused by the current traffic monitoring and handling system compared to the most efficient flight profile that all aircraft are capable of when alone. Thus with the introduction of NextGen and SESAR there is a staggered application of verifiably safe products and software that had a clear and valued application within the current ATM systems in place. In other words, all the inefficiencies that have been brought to our attention thus far have a corresponding upgrade or alteration that severely diminishes that inefficiency.

It should be mentioned that NextGen and SESAR are not the only programmes that support ATC and ATM modernization; a considerable number of countries around the globe have their own programmes or government backed departments responsible for modernizing air traffic in their region, and some are even responsible for previous development of technologies and concepts highlighted by the two programmes. However, the relative size and publicity of the two programmes does force other programmes and departments to heavily define themselves from the perspectives of the two programmes in terms of where they align and where they differ; the two programmes acting as a useful standard for comparison of a country's state of air traffic modernization for the purposes of interoperability with other countries. Thus as timescale for the modernization of air traffic, the reference of NextGen and SESAR implementation is apt. Further, while NextGen and SESAR have an aim in allowing the most efficient (i.e. the most fuel saving, and therefore least costly, flight profile) flight profile to occur, their goals and actions extend past that to cater for the entire air travel industry, thus some technologies of seemingly unimportant relevance may have considerable impact on any air traffic optimization methods developed here. For the purposes of this thesis, the resultant NextGen and SESAR minimization of inefficiencies caused by ATM systems can be summarized via attempts at satisfying three main requirements; timely and accurate information regarding all relevant entities and conditions in the environment, the precise prediction of changes of entities and conditions within the environment, and a throughput load less than the theoretical limit imposed by the handling/processing capabilities of any stationary entity within the environment.

A.3 Timely and Accurate Information

The ability to know as much as possible about the environment and whatever is unfolding within it is a well-established limitation to the capabilities of those controlling entities within the environment. To improve such capabilities, the solution would be to improve technologies that assist detection, infrastructure for transfer of data, or data management. Both programmes are developing technologies, replacements or improvements in all

three categories to ensure consistency with current technological capability. However, of these technologies, two particular ones, present in both programmes, are also introducing new functionality to ATM systems; Automatic Dependent Surveillance Broadcast (ADS-B) [A4] and System Wide Information Management (SWIM) [A5].

SWIM is merely the cohesive management system that draws information from all sources within the ATM system network then collates it in such a manner as to be useful for whoever calls for the information [A6]. Its optimal shape and form are currently debatable due to its necessary property of mirroring ATC methods of application; however it is most likely where continental scale controls would take place so it has significant importance as a centralizing concept. On the other hand, ADS-B is a verified method of information exchange that gives information, not just about pilots with reference to their departure/arrival points, but also about any aircraft within range that is also fitted with ADS-B technology [A7]. ADS-B is the key technology for allowing pilots to interact with each other, and therefore allow them to handle the separation aspect of flight rule requirements. The main form to be used in the two programmes is '1090 MHz Mode S Extended Squitter' or 1090ES [A8], [A9]. Other variations (e.g. Universal Access Transceiver, UAT) were trialled and some may be used for specific niches of aviation [A8], [A9]. As an example of the data transfer capability of ADS-B, details on the 112Bit (excluding preamble) long 1090ES are displayed in Table 23. Currently 1090ES is capable of using sixteen registers, variations of the 56 of the 112bits of data reserved for ADS-B operations of a particular nature (each one defined by a 5bit Format Type Code). The remaining 56 bits handle aircraft/data identification and error detection issues [A10]. Registers of importance, Table 23a) to c), and the entire 1090ES sequence, Table 23d), are shown therein.

Table 23 - Bit Sequences for the BDS 05h Ext. Squitter for Airborne Position (a) and Airborne Velocity (b), the BDS 62h Target State & Status per DO-260A (c), and 1090ES as a whole (d).

a)		b)		c)		d)	
Bits	Contents	Bits	Contents	Bits	Contents	Bits	Contents
5	Format Type Code	5	Format Type Code	5	Format Type	5	Format Type
2	Surveillance Status	3	Subtype (Ground /Air Speed)	2	Subtype	2	Subtype
1	Single Antenna Flag	1	Intent change flag	18	Target Altitude and Flags	18	Target Altitude and Flags
12	Altitude	1	IFR capability flag	14	Target Heading/Track	14	Target Heading/Track
1	Time	3	Velocity Uncertainty	7	Position Accuracy and Integrity	7	Position Accuracy and Integrity
1	CPR Format	10+1	East-West Velocity + sign	5	Reserved	5	Reserved

17	CPR encoded latitude	10+1	North-South Velocity + sign	2	ACAS status and RA status
17	CPR encoded longitude	9+1+1	Vertical rate + sign + source	3	A/C emergency and priority status
		2	Turn indicator		
		7+1	Diff. geo & baro height + sign		

The data formats above are defined by ICAO standards for "Mode S Specific Services" and while likely to change given the ongoing research into ADS-B technology, are considered standards for such development. ADS-B effectively extends the timely availability of important knowledge within the region to all pilots, allowing pilots to move more effectively around entities within their region.

A.3.1 Precise Prediction of Change

The ability to correctly and timely predict all change in the environment is the necessary complement to knowing everything about the environment. Even if it was possible to timely and accurately verify any occurring event within an environment, any predictions regarding what would happen next, could well be incorrect. That said, the introduction of technologies like ADS-B, the Integrated Terminal Weather System of NextGen [A11], the Meteorological Information Service of SESAR [A5], BADA, NextGen Equivalent of BADA, and other technologies that allows 4 dimensional (4D, space and time) trajectory prediction [A12], are making creation of aircraft routes easier and much less susceptible to deviations.

ITWS [A13] and MET [A6]are similar systems that more precisely predict the localized effect of weather on any aircraft within its network, further decreasing the deviation caused by weather. The effect of ADS-B on flight planning is that it gives increased confidence on data regarding plane to plane distances, therefore decreasing reliance on fairly robust horizontal and vertical separation minima and allowing the use of what were considered complex (due to the coupling of horizontal and vertical movement) 4D routes. The overall effect of these is the reintroduction of parts of the most efficient flight profile; a continuous climb departure (CCD) and a continuous descent arrival (CDA).

A.3.2 Throughput Limits

A noticeable limit to the ATM system was defined by how many aircraft an ATC or an airport could possibly handle. During the en-route or cruise phase of an aircraft's flight profile, the straightest route was mitigated by the positioning of on ground detection sites [A13] and that guiding ATC, due to the repetitious activities they have to perform for each flight they guide, can only guide so many aircraft at any one time [A1]. During the departure (less so for arrival) portion of the flight, the most efficient route (i.e. a CCD or CDA) would be lengthened by how long it would take to get landing/takeoff clearance, which, due to the extra time required to safely cover error in landing/takeoff time for previous aircraft, could cause further delay.

With the introduction of automation and augmentation of various ATC roles via implementation of projects and technologies such as the Advanced Technologies & Oceanic Procedures (ATOP) [A13], En Route Automation Modernization (ERAM) [A13], Terminal Automation and Replacement (TAMR) [A13], Arrival Management (AMAN) [A6], Departure Management (DMAN) [A6], etc., the actual on ground time to process aircraft has become significantly shorter. Also with the installation of new detection sites and spot coverage systems, like the Wide Area Augmentation System (WAAS) [A13], the straightest CDA or CCD is becoming more frequently possible. As for the issue of runway congestion, a combined use of 4D planning [A14], Self-Separation (SSEP) and Airborne Separation Assistance Systems (ASAS) [A15] allow for the scheduling of arrivals far in advance and as soon as the issue arises [A16], effectively using pilot driven sequencing, merging and separation techniques [A17] to position themselves a set distance and time behind those landing before them.

These separation systems, in particular, are significantly relevant to the development of optimization capability that could rely on, or otherwise affect, them. The technologies and procedures [A18] that make up such would therefore become key considerations. As per ADS-B influence on NextGen and SESAR, the technologies used are usually dependant on ADS-B in some way. ADS-B ground surveillance applications include the use of Airport Surface Surveillance, Radar, Non-Radar, and Aircraft Derived Data, based technologies. Further, Airborne Traffic Separation Assurance technologies, i.e. those used on-board aircraft; allow the use of Airborne Flight Operation, Airport Surface, In Trail Procedure (ITP), and Visual Separation on Approach, based applications. These technologies and applications then allow applications and procedures to be used elsewhere for the purposes of spacing and separation. Airborne Spacing applications give aircraft the ability to maintain a fixed distance from other aircraft and can include applications for Sequencing and Merging (S&M) and Crossing and Passing (C&P), as well as further support for ITP. Airborne Separation applications give aircraft the ability to ensure separation from other aircraft and include Lateral and Vertical C&P, Follow and Merge operations in ITP, and further support for S&M. It was hoped that eventually these would facilitate applications that grant Airborne Self Separation [A19], i.e. the ability to ensure separation from other aircraft without ATC involvement, i.e. applications that manage Free Flight Airspace, Managed Airspace, and Free Flight Tracks. However these are currently unsupported future capabilities; discussions of S&M, C&P and ITP modes of separation bear more importance to the efforts outlined in this thesis.

S&M is the ATC enforcement and control of aircraft adherence to predefined routes that leads to, and is significantly far from, an airport or high traffic junction. The aim of which is to reduce time and fuel spent in holding patterns above an airport. S&M is significantly similar to the methods already put to use at high traffic airport departure and arrivals and is thus historically safe [A20]. Since it is effectively a coordinating measure for landing and takeoff, it will require ATC intervention and control therefore gaining significant data redundancies. Obviously control is centralized so risks due to interaction and negotiation are minimal. Given that high traffic scenarios are expected, and thus planned for, compound issues due to erroneous commands are also limited.

C&P was the most noticeable issue for implementing Free Flight, and it was this particular aircraft-aircraft interaction that NLR solved via simulations and testing to validate the concept [A21]. It is essentially the resolution of a scenario where an aircraft is at risk of entering the wake field of, or colliding with, another aircraft. With ATC involvement, data redundancies are gained, and risks due to interaction, negotiation, and compound errors are limited; the scenario is simplified to route restriction akin to legacy separation methods.

Without ATC involvement, data sources are limited to on-board systems, pilots are reliant on standard flight rules/programs to negotiate and determine changed intent, and the issue of interfering with other oncoming aircraft exists after performing the change; essentially requiring significant investment and research in enforced standard flight rules, negotiation programs, and enhanced ACAS with accurate intent detection capability. Even now, the technology requirements for VC&P are still considered to be a significant challenge to ensuring C&P safety with ATC involvement [A9].

ITP appears to be developed from including pilot assistance in S&M procedures. Where traffic density is not high, aircraft positions can be controlled via combined references to a known route or track, and an aircraft already on that track. The interesting fact about ITP is its safety. Even without ATC intervention the method can use both on-board systems and pilot visual capability to ensure data correctness, responsibility of scenario is left mostly with the following plane thereby significantly reducing risk due to interaction and negotiation, and the adherence to a known track limits the effect of compounding error after a procedure is performed.

It should be noted that the main additional capability that S&M, C&P, and ITP, provide is in procedural safety hence their inclusion as throughput limits. They pose varying levels of safety in terms of data redundancy, aircraft-to-aircraft interaction and negotiation risks, and post procedure area or compound effect. Any future air traffic optimization capability would thus have to consider interoperability issues.

A.3.3 The Effect of NextGen and SESAR

The last three sections imply that much of the ATM system development planned by NextGen and SESAR surrounds the new additions to their ATM system; changes to any processes currently existing were clearly only to adapt to these additions. No innovative changes were intended to be applied to the structure of processes that allow the system to work, as defined 50 years ago. In other words this is mostly a technological improvement, making a bureaucratic type industry even more mechanistic, and therefore benefits in terms of increased efficiency should be fairly clear.

A.4 Trajectory Control Post NextGen and SESAR

There are currently two noticeable lines of thought regarding methods of trajectory control post NextGen and SESAR. The first consists of those considered or developed prior to the two programmes; and the second consists of those that were created by the introduction of NextGen and SESAR. Due to the significant technological jump that NextGen and SESAR present, the first lot are comparatively more conceptual, and therefore more ideal than the second.

A.4.1 Advanced Trajectory Control Concepts Prior to NextGen and SESAR

Trajectory control concepts developed prior to NextGen and SESAR largely consists of concepts like those mentioned in Free Flight, ideas that were deemed commercially unviable (either too high a cost for too little gain or at too high a risk) at the time by the two programmes. This lack of acceptance does not invalidate them as means of trajectory control, just that applying such in the current circumstances would mean a drop in capability or safety. In fact true Free Flight is still considered by some as one of the bright possible futures for ATM systems affected by NextGen and SESAR.

"The basic notion of free flight is that aircrews obtain the freedom to select their trajectory including the responsibility of resolving conflicts with other aircraft" [A22], and whilst simplistic in terms can be considered as a number of separate and idealistic concepts all applied simultaneously; willingness and ability to move as wanted and not as planned, pilots having the ability to work closely and in real time with each other, and, most important of all, having accurate situational certainty at all times by all entities involved. All of these must be present for true free flight to occur.

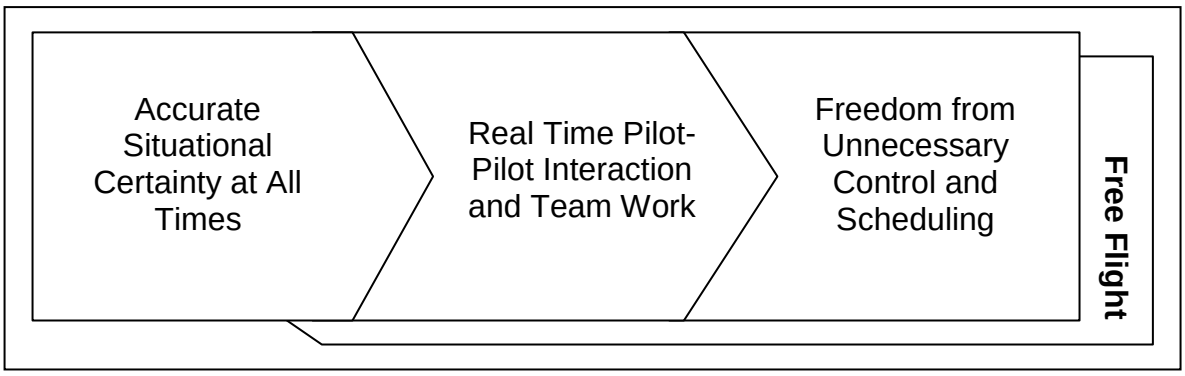

Figure 78 - Figure A1: Free Flight Concepts and Ideals in Order of Development

Figure 78 implies the requirement of each concept on a lower one; the lowest one being the need to have accurate situational certainty at all times. Matching this graph with work done by NextGen and SESAR, their work is consists mostly with performing the lowest concept. Making current and projected environmental knowledge and its distribution as timely and as accurate as possible, goes a long way to ensuring that actions made at any given moment are as safe and as efficient as possible. Any optimisations granted in this step are likely to occur as a part of these two programmes, or as optimisation concepts created from applying those two programmes, and therefore have already been mentioned or will be mentioned later.

The next ideal past accurate situational certainty is for pilots to have the ability to work closely and in real time with each other. In practical terms, it meant the ability of pilots to navigate, via interactions with other pilots alone, through a number of other aircraft in the same vicinity [A23]. In one of its earlier conceptual forms, the ability for a pilot to coordinate himself through a randomly filled environment was considered a direct solution of free flight ideals due to its ability to create flight profiles very similar to the most efficient one possible. The theory was that inefficiencies caused by having separation enforced at all times via altitude were likely to be significantly more than inefficiencies caused by having separation enforced only at times when separation minima (due only to wake vortices) was likely to be breached.

Such work was proven mathematically possible for scenarios where the entities of concern were only aircraft [A23] or where such had to be routed past a restricted area [A24]. The concept stumbled when an airfield was introduced into the scenario; while theoretically possible, it required a one sided responsibility on the part of the landing airplane as the airfield, once permission to attempt landing had been given (which given the concept would begin when the aircraft descended from cruise), would have no control over the landing craft. As this presented a liability with no safety countermeasures, there was little interest in developing the last portion much further. There was an initial attempt to have the introduction of some capability as a part of the two current programmes [A25], but this was weighed out due to the cost of the required equipment and the noticeable lack of tests that could verify its full use. The two programmes settled for limited versions in the form of new ATC

directed pilot commands that required a pilot to act on the presence of another pilot; self-separation and merging as they are currently known and as mentioned earlier.

The willingness and ability to move as wanted and not as planned, when reworded implies the wish of pilots to have all control decisions made by joint discussion of only entities in the air. Or as supporters of free flight put it, a common set of rules and codes which all aircraft can follow to determine how one acts in the presence of others, without the aid of ground based air traffic control [A26]. A suitable analogy would be the comparison of trains, monorails and trams (current situation) to trucks, buses and taxis (free flight). The former has to move on rails previously set down and which are altered by an external source, the latter following road rules and regulations to use a pathway shared by many others.

It is hard to see how this would affect flight profile optimisation, and for similar reasons some have considered this aspect of free flight only a "pilot's dream", however it is possible, but the optimisation would go towards changing an individual flight profile's size, not its shape. Using the previous analogy as a base, there are commercial scenarios where the use of trucks, buses and taxis are proven to be more profitable than trains or trams. In such scenarios, the key decisive elements are the existence of numerous stops or drop off points around a central location, or simply the lack of rails to reach the intended destination. Similar scenarios could exist in the air traffic industry when an international airport has incoming passengers going to various surrounding areas that are a flight's distance away, or when passengers have to get from an international airport to a much smaller and less frequented domestic one. It is a necessary assumption that the plane types that would fill such roles are much smaller than ones used at international airport hubs. Some have argued that this state is already possible considering the ramifications of increasing use of small business jets and light aircraft [A27], exactly the type of plane size that would benefit most from the willingness and ability to move freely.

A.4.2 Advanced Trajectory Control Concepts due to NextGen and SESAR

The second lot of possible control methods stem as a direct result of the introduction of new technologies and processes by NextGen and SESAR. However, first consider the state of the flight profile as affected by these new technologies and processes; holding patterns have been mitigated significantly except for those with really severe and constant congestion, and separation minima is only defined by wake vortices and, overall, there is no reason not to maintain a highly efficient flight profile shape. The only real deviations in the flight profile are those caused by the physical limitations presented by other aircraft and severe weather conditions in the vicinity. Thus the only way to improve this flight profile, other than the further improvement of the technologies mentioned, lies in the fact that any future controls have to consider the effect of the entirety of a flight's profile on its surrounding air traffic, as well as the effect that traffic could have on that flight's profile, to determine what is the optimum flight profile for that aircraft.

Advancing this thought even further creates the possibility of altering the trajectories of all air traffic, in essence manipulating likely flight profiles with respect to other neighbouring likely flight profiles. The issue with doing this beforehand, i.e. in a time period during which a planned flight schedule could be developed for a specific area, is the variation introduced by weather and the corresponding redundancies such entail. If the flight process could be calculated in real time, as defined by complete and accurate situational certainty, then there could be room for increasing efficiencies for flight profiles within that area. Theoretically this concept was always possible under free flight; however, the main distinction between free flight and the developing ATM systems is

that for the latter control is being handled by a centralized or coordinated on-ground source, which is currently a foregone necessity of this level of control detail and cohesion.

A.5 Conclusion

While technological integration and development, even to currently, was largely a case of meeting perceived needs and ideals, the actual technology involved could always be categorized via the need to receive timely and accurate information, have the ability to precisely predict trajectories, and the ability to define ATC or regional throughput limits. Or in other words, technology that better enable the timely prediction of when the actions of air traffic breach the limitations of those that control it. However, as can be seen in the review of technology that currently exist, the first and third categories are significantly well developed with limitations only in terms of how much they can consider, and how fast they can do so, which in themselves can be readily handled via providing more computational power; the accurate prediction of trajectories still needs work apparently, however until such pops up, a combined use of already appropriately buffered ATC separation methods and performance models that are currently as accurately as possible, should be sufficient for now.

A.6 References

[A1] Smolensky, MW., Stein, ES. Human factors in air traffic control, San Diego Academic Press, San Diego. 1998.

[A2] RTCA, Final Report of RTCA TF3: Free Flight Implementation, RTCA TF3, RTCA Inc., Washington, 1995.

[A3] SESAR Consortium, "SESAR Air Transport Framework: The Current Situation", SESAR Definition Phase - Milestone Deliverable 1, SESAR Consortium, July 2006.

[A4] RTCA. (2002) Minimum Aviation System Performance Standards for Automatic Dependent Surveillance-Broadcast, RTCA Inc., Washington.

[A5] SESAR Consortium. (2008) "SESAR Master Plan", SESAR Definition Phase - Milestone Deliverable 5, SESAR Consortium, April.

[A6] SESAR Consortium, "SESAR Master Plan", SESAR Definition Phase - Milestone Deliverable 5, SESAR Consortium, April 2008.

[A7] RTCA, Minimum Aviation System Performance Standards for Automatic Dependent Surveillance-Broadcast, RTCA Inc., June 25, Washington, 2002.

[A8] Askew, P. (2002) ADS-B Surface Surveillance Trails 2002, National Air Traffic Services Ltd, Analysis & Research Department - Research & Innovation Group, UK.

[A9] SESAR Consortium. (2008) "SESAR ATM Deployment Sequence", SESAR Definition Phase - Milestone Deliverable 4, SESAR Consortium, January.

[A10] EUROCONTROL. (2007) ADS-B for Dummies, European Organisation for the Safety of Air Navigation, EUROCONTROL Experimental Centre, Bretigny-sur-Orge, France.

[A11] FAA. (2008) NextGen Implementation Plan, U.S. Department of Transportation, Federal Aviation Administration, Washington.

[A12] Mayer, R.H. & Sprong, K. (2007) Improving Terminal Operations - Benefits of RNAV Departure Procedures at Dallas-Fort Worth and Hartsfield-Jackson Atlanta International Airports, Center for Advanced Aviation System Development, The MITRE Corporation, McLean, Virginia.

[A13] Federal Aviation Administration, NextGen Implementation Plan, U.S. Department of Transportation, Federal Aviation Administration, Washington, 2008.

[A14] Mayer, R.H. and Sprong, K., Improving Terminal Operations - Benefits of RNAV Departure Procedures at Dallas-Forworth and Hartsfield-Jackson Atlanta International Airports, Center for Advanced Aviation System Development, The MITRE Corporation, McLean, Virginia, January 2007.

[A15] Hoffman, E. Martin, P. Pütz, T. Trzmiel, A. and Zeghal, K., Airborne Spacing: Flight Deck View of Compatibility with Continuous Descent Approach (CDA), European Organisation for the Safety of Air Navigation, EUROCONTROL Experimental Centre, Bretigny-sur-Orge, France, September 2007.

[A16] Wanke, C. and Greenbaum, D., Incremental, Probablistic Decision Making for En Route Traffic Management, The MITRE Corporation, McLean, Virginia, October 2007.

[A17] MacWilliams, P. and Porter, D., An Assessment of a Controller Aid for Merging and Sequencing Traffic on Performance-Based Arrival Routes, The MITRE Corporation, McLean, Virginia, October 2007.

[A18] Shaw, C. (2008) "ASAS-TN2: ASAS Applications Maturity Assessment", ASAS-TN2 Seminar Paris, April.

[A19] Hoffman, E; Martin, P; Pütz, T; Trzmiel, A; & Zeghal, K. (2007) Airborne Spacing: Flight Deck View of Compatibility with Continuous Descent Approach (CDA), European Organisation for the Safety of Air Navigation, EUROCONTROL Experimental Centre, Bretigny-sur-Orge, France.

[A20] MacWilliams, P. & Porter, D. (2007) An Assessment of a Controller Aid for Merging and Sequencing Traffic on Performance-Based Arrival Routes, The MITRE Corporation, McLean, Virginia.

[A21] Hoekstra, J.M; Ruigrok, R.C.J; and van Gent, R.N.H.W. (2000) "Free Flight in a Crowded Airspace?", 3rd USA/Europe Air Traffic Management R&D Seminar, June 2000.

[A22] Blom, H.A.P. Bakker, G.J. Obbink, B.K. and Klompstra, M.B., "Free flight safety risk modelling and simulation", 2nd International Conference on Research in Air Transportation ICRAT 2006, Beograd, Serbia, June 24-28, 2006.

[A23] Hoekstra, J.M. Ruigrok, R.C.J. and van Gent, R.N.H.W., "Free Flight in a Crowded Airspace?", 3rd USA/Europe Air Traffic Management R&D Seminar, Napoli, 13-16 June 2000.

[A24] Van Balen, K. and Bil, C. "Optimal Re-Routing of Aircraft around Closed Airspace in Free Flight", 12th Australian International Aerospace Congress, Melbourne, 19-21 March 2007.

[A25] Herndon, A.A. Cramer, M. Sprong, K. and Mayer, R.H., Analysis of advanced flight management systems (FMSs), flight management computer (FMC) field observations trials, vertical path, Center for Advanced Aviation System Development, The MITRE Corporation, McLean, Virginia, August 2008.

[A26] Ruigrok, RCJ., Hoekstra, JM. Human factors evaluations of Free Flight: Issues solved and issues remaining, Applied Ergonomics 38(4): 437, 2007.

[A27] Lebourg, S., “ASAS Self Separation and Cruise Climb for Business Jets”, Presentations of the Final Airborne Separation Assistance System Thematic Network 2 (ASAS-TN2) Seminar, Paris, France, April 14-15, 2008.

APPENDIX B Air Traffic Modelling Development

The biggest concern in developing a means of modelling air traffic was in finding a means that could cater for the array of possible traffic control and optimization methods available; failure to do so meant the inability to use potentially useful technology and methods in the future. Unfortunately this was not restricted to methods of minor relevance as two primary airspace calculation methodologies used to understand and manipulate air traffic, i.e. conflict detection and sectorisation, initially displayed significant difficulty in allowing bi-directional correlation of their data; conflicts could easily gather relevant sector data for their resolution, however the means and data required to accurately show conflict and traffic density within a sector had not been publicly developed to a useful level. Further, the same was true for any other type of data that was defined in terms of earth surface boundaries; quantifying such for the use of trajectory prediction and control was easily possible, however manipulating that data using trajectory information was not.

B.1 Nautical Minute Discretisation

The solution adopted in this thesis came about by handling the two core issues behind the incompatibility of conflict detection and sectorisation; a lack of useful interpretative methods, and a lack of detail fidelity. Conflict detection was defined via the collocation of different aircraft trajectories, i.e. the relative longitude, latitude, and altitude position of the aircrafts with respect to the same time; given dimensional limits that define actual conflict, it was thus a situational state that varied across a region defined by the trajectories of its constituents. In contrast sectors and their data are constants across a region defined via the aggregation of historically preferred routes. In order to allow ease of correlation, it must be at least possible to interpret one as a component of the other; however despite existing in the same dimensions, doing so is difficult. It would involve using geodesic mathematics to create an earth surface polygon with edges defined by the overlap of the two regions, and that is if only longitude and latitude are considered; the involvement of time and altitudinal conflict limits complicates matters significantly. To avoid potential dimensional misinterpretation, as well as the significantly complex data management required of it, finite element methodology was utilized to introduce data uniformity and ease of correlation. Further, with increased maturity of finite element methods, there was some potential in discretising four dimensional volumes, and using the properties gained from doing so to assist in speeding up computational calculations [B1] and avoiding the computational limitations as experienced by ATC [B2].

For most earth surface defined data, the discretisation was simple and largely already in place. As shown in A.3.1, equally spaced linear intervals could easily be allocated for all four dimensions; longitude and latitude in terms of either degrees or minutes, and altitude and time respectively in terms of appropriate distance and time intervals. However for any route type data, i.e. any data based on great-circles or defined via singular, or irregular, lines along the earth surface, other information was necessary for it to be transposed into its equivalent longitude and latitude dimensions; once that had been done it could be used to transfer time and altitude data, with their discretisation decided by the function required. Foremost of the information required to perform route conversion were simple definitions defined using the haversine formula; i.e. the accurate distance and relative bearing between two points on the earth's surface. This formula is most frequently used here to determine Along Track Distance, or ATD, and Cross Track Distance, or CTD. Imagine a great circle path between a start and finish point as well as a third point anywhere on the earth's surface. The ATD defines the distance between the start point and the point on the great circle path closest to the third point. It has a maximum value of one half the

earth's circumference, and can easily be made to be negative or positive to indicate if it's on the smallest arc or not. Its equation is:

$$\left|\overrightarrow{AB}\right| = GCD formula \qquad \textbf{(42)}$$

The CTD defines the distance between the third point and a point on the great circle path closest to the third point. It is negative when the point is to the 'left' of the path from the perspective of the starting point, and positive to the 'right'. It has a maximum absolute value of one quarter the earth's circumference. Its equation is:

$$\left|\overrightarrow{AB}\right| = GCD formula \qquad \textbf{(43)}$$

Another necessary assumption used here is that a region of unit longitude interval width and unit latitude interval height can be represented by its centre point. For a sector, or any convex shaped enclosure of lines, if a centre point maintains a consistent CTD sign whilst using the sector edges as a path, then its associated unit region could be considered part of that enclosure. For a route, or any singular line defining a region with an allowable cross track deviation, if a centre point's absolute CTD value is less than the allowable cross track deviation, and its ATD values place it between the start and end of its route, then the centre point's associated region could be considered part of that route.

With a means of correlating unit regions with trajectories, sectors, and earth surface defined data, and vice versa, the next important consideration was the unit region's size. As the smallest distance likely to be encountered in upper level airspace, i.e. the amount of cross track deviation allowed for an aircraft, is measured in nautical miles, a single nautical mile as the longitudinal and altitudinal interval would have made sense. However, it was previously shown that meteorological and other earth surface based data were defined in the degrees and minutes of latitude and longitude; it was thus necessary to consider the nautical minute as an alternate interval. While nautical mile discretisation presented less variation in the size of the unit region, it presented more variation in its orientation among neighbouring unit regions, which would have limited potential data indexing methods. In contrast, while Nautical Minute Discretisation, or NMD, varied in size between the equator and the poles, its orientation among neighbouring unit regions remained constant; this made data control interesting as it allowed a wider range of data indexing methods. This, and the data consistency it affords with other meteorological and earth surface based data, made NMD the preferred starting point as a means of understanding and modelling air traffic in this research.

B.2 Hastening NMD of Trajectories

While NMD was great at defining trajectories in the longitude and latitude domain, doing so required a fair amount of time and memory; this was due to the large number of operations that had to be performed. Imagine a FIR about 2000 minutes high and 3000 minutes wide; to define the component unit regions for each trajectory being considered, at least one operation each of (42) and (43) would be required of each of the six million unit regions within the FIR. With limited airports in existence, it would be expected that a considerable number of routes are repeated frequently; this suggested a potential time saver would be to calculate each unique trajectory once, and then reapply the same for each reoccurrence. Unfortunately, as the optimization tool is designed towards a mode of flight that does not necessarily cater for static air space structures or routes, it is highly possible the number of unique trajectories could vastly outweigh the number of repeated trajectories; therefore

rendering the prior point moot. Instead the actual process had to be improved in some way so as to allow fast conversion of a trajectory into NMD data; the use of the fast indexing properties mentioned previously highlighted a particular avenue under which this could occur, particularly if used in conjunction with a code execution method that supported NMD. After going through various different methods, all of which had issues in terms of using too much memory, having holes in the path, or having inappropriate ends, an appropriate method was defined using MatLab R2009a code.

B.2.1 Route Region Recognition

An alternative way to think of the processes outlined here is that instead of checking the already existent list of square minutes defined within a FIR by NMD, the required list of 'nodes' are instead calculated. An apt analogy is in the definition of the potential intersection of two orbits; such is performed by forming an equation representing minimum distance between the two then resolving for the necessary 4D that represent that point, not by discretising the orbits with respect to time and calculating all such distances to find the minimum. The necessary information to calculate the nodes that would represent a particular trajectory are: the start and end point in terms of longitude and latitude, the maximum allowable deviation of the route in terms of CTD, as per [B3] this is denoted as S_y, and, as the haversine formula is being used, the locally accepted Earth radius. With these the limits of the route region can be defined.

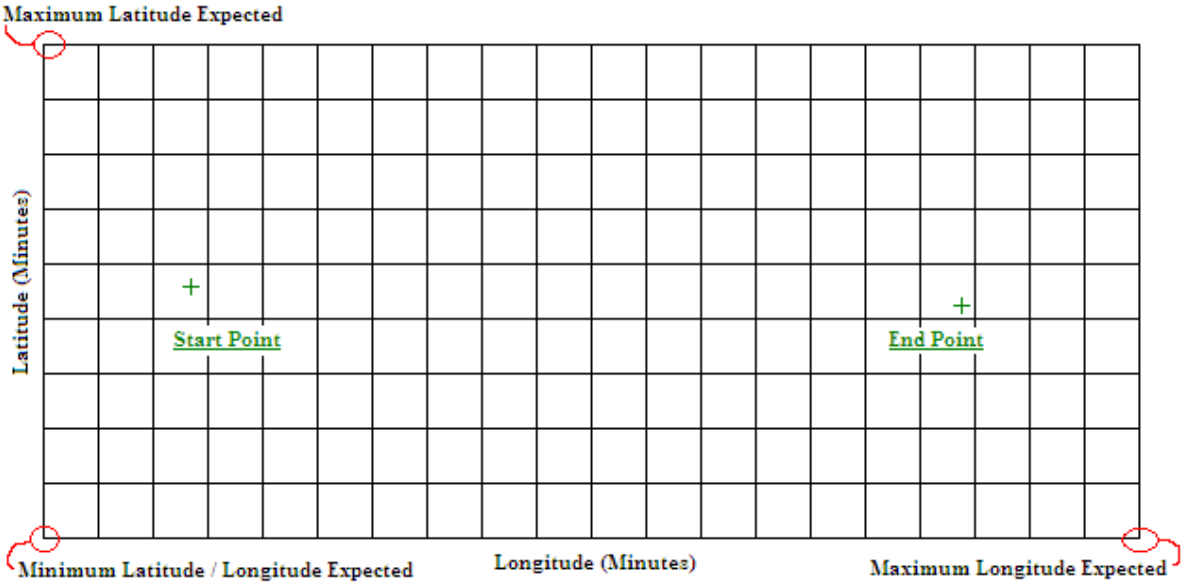

Figure 79 - Recognition of Route Region Limits

The range of latitudes is defined first. The latitudes of the start and end point are first sorted for minimum and maximum, which are then expanded directly using S_y on both limits; distances along a meridian not requiring great circle formulae to cater for distance warp due to earth curvature. These limits are then rounded towards the nearest outlying minute to allow correlation to the latitude index of the NMD nodes. In the situation that these values exceed the maximum and or minimum of the FIR itself, the minute defining the breeched border is taken instead of the breeching value. The range of longitudes is defined in a similar manner, however great circle formulae are required to find the maximum and minimum S_y expansion; such values may note correlate simply with the longitudinal limits so four potential values are checked and two chosen. At this point only four resultant values are created, however with these it becomes easy to imagine a grid defined using these values and the

discrete minutes between them; the points in this grid, as shown in Figure 79, correlates exactly with already existing NMD nodes.

B.2.2 Defining Latitude Limits per Minute Longitude

This next step hastens route definition by again taking advantage of the simplicity of determining distances along meridians. First, the longitude values of the start and end point are expanded outwards to the nearest minute of longitudes; these two values are then used to create a vector array, *i*, defining the minutes of longitude between and including them. Next, the bearings of the route are defined for both longitudinal edges of each of these minutes, i.e. $\theta_{i-.5}$ and $\theta_{i+.5}$. Then for each *i*, the maximum distance of the lateral separation point from the intersection between the route and the polar path going through either $\theta_{i-.5}$ or $\theta_{i+.5}$, is calculated as l_i:

$$l_i = \max\left[\frac{2\times S_y}{\sin\theta_{i-.5}}, \frac{2\times S_y}{\sin\theta_{i+.5}}\right] \quad \textbf{(44)}$$

The accepted form [8] of calculating *l* uses a S_y coefficient of one, and $\Delta\theta$, the difference between the bearings of the two tracks, instead of a maximum based on $\theta_{i-.5}$ and $\theta_{i+.5}$. The lack of $\Delta\theta$ is due to one track being the north polar track, which is already zero. The S_y coefficient of two is due to the possibility of intentional variation in the aircraft's CTD dimension, whereas the accepted form only catered for travel along the centre line; *l* had to cater for travel along the maximum allowed CTD. The maximum function ensures that the largest distance is taken, no matter the orientation of the route. In the event that only one or a few minutes of longitude are present, i.e. the longitude limits were the same or close together, the calculated l_i will reach infinity as θ becomes zero.

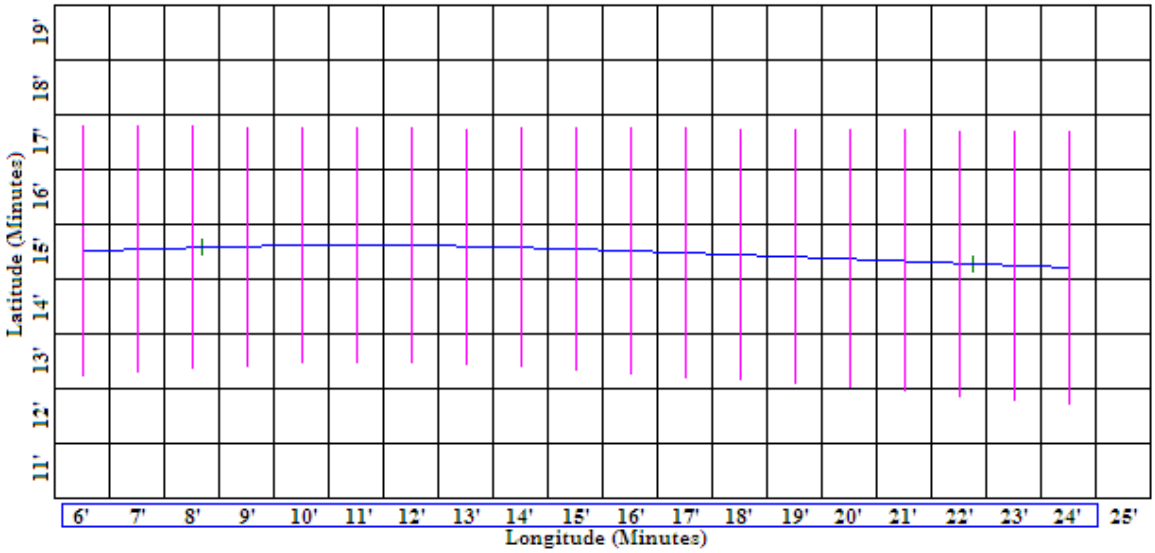

Figure 80 - Unrounded Latitude Limits per Minute Longitude

The next step calculates the latitudes, *j*, defining the intersection between the route and all minutes of longitude, within and including the longitude limits set out in B.2.1. Their respective l_i are then added and subtracted to *j*, and rounded outwards to the nearest minute, to determine the maximum and minimum latitudes that could be encountered when passing each *i*. For the minutes present in the longitude limits, but not included in *i*, the nearest value of l_i is used to avoid indeterminacy; this usually means non *i* near the minimum longitude limit use l_{imin}, while the rest use l_{imax}. If l_i is infinite, or some value that would breach the latitude limits set out in B.2.1, the breeched limit is used in place of the breeching value; such is a frequent occurrence for near polar routes, as

well as intercontinental routes that exit or enter outside the FIR. The blue line in Figure 80 defines j, while the pink lines define range defined by the minimum and maximum latitudes for each longitude minute.

B.2.3 Collection and Refinement of Indices

With the latitude limits per minute longitude rounded outwards to the nearest latitude minute, it is computationally cheap to create vector arrays containing latitude minutes for each longitude minute. It is similarly cheap to then combine all such minutes, and their corresponding longitude, into a two column matrix showing the longitude and latitude of each NMD node that could represent the route, as in Figure 81. However to cater for potential errors from the indeterminacy avoidance measure used above, nodes must satisfy one of two checks; failure results in their removal from the list.

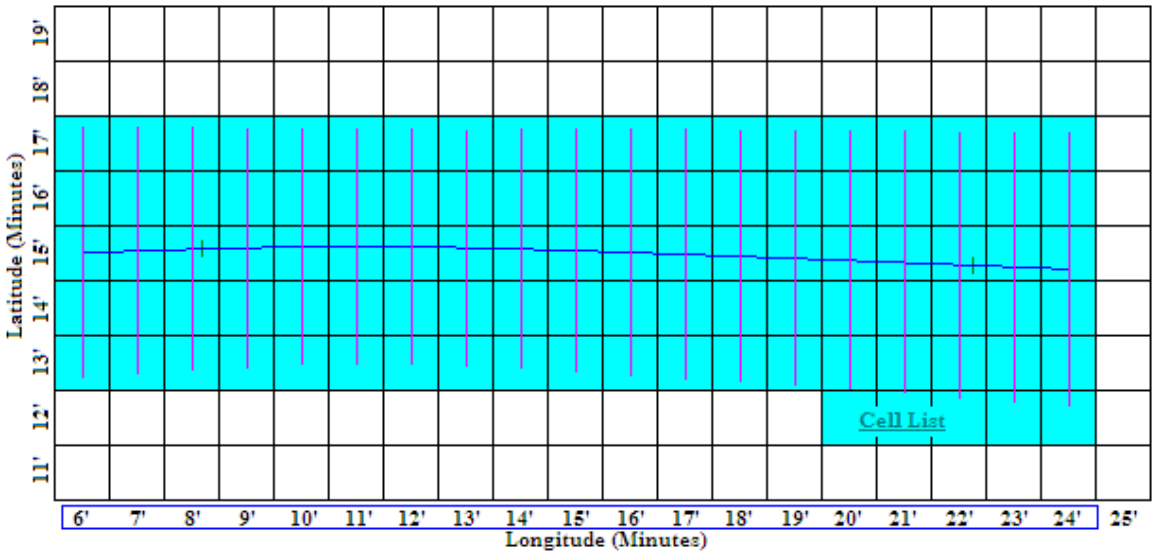

Figure 81 - Collection of Nodes that represent the route.

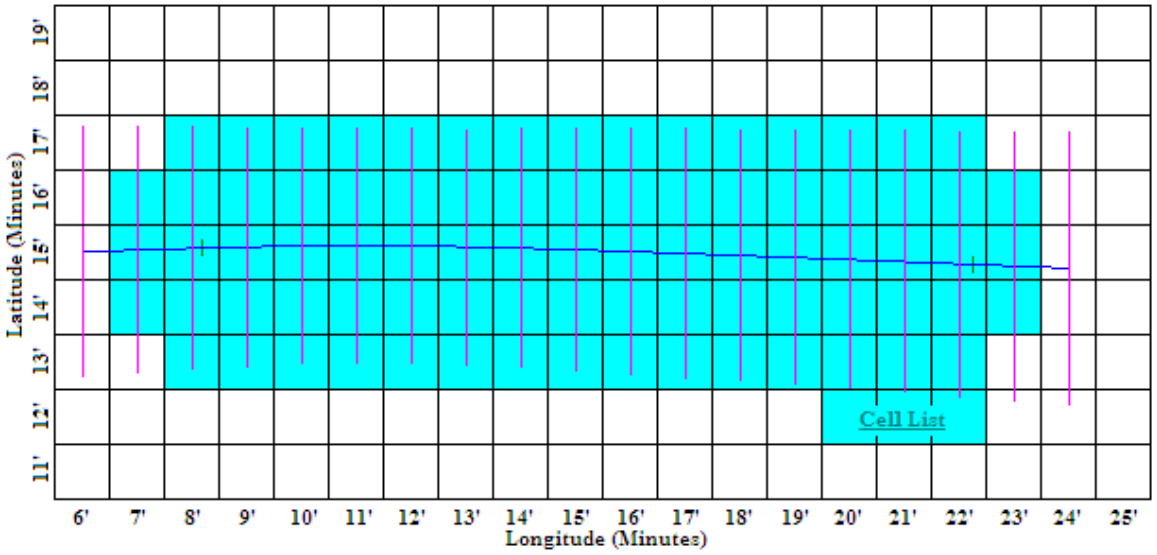

Figure 82 - Refined NMD Node List for Accurate Route Definition

The distances used in these checks also includes a buffer equal to half the longest diagonal at the checked node's latitude; this buffer caters for the possibility that a distance check reaches into a node's area, but not far enough so as to include the node's representative longitude and latitude. The overall impact of these checks usually causes the typical route definition shown in Figure 82. The first check governs nodes that exist between or on the

exit and entry points; it requires that nodes must have a CTD of less than S_y plus buffer, as well as an ATD value that is greater than or equal to zero for the route as is, as well as backwards. Nodes representing aircraft presence at the entry and exit points usually fail the ATD checks; while nodes closer to the equator when considering polar routes, usually fail the CTD check. The second check governs the start and end points, and assumes a circular region to define the presence of an aircraft entering or exiting airspace; this check requires a node to be within a great circle distance less than S_y plus buffer. It keeps nodes that would usually fail the first check, but are required to effectively represent airspace entry and exit.

B.2.4 Hastening Effectiveness

The first important point to note is that this method only creates and checks the indices of nodes that could be used to define a route; it is therefore not checking all nodes within a FIR. The creation of the nodes themselves consists of merely address indexing and pre-allocation of data; the crux of computation time for a route would be in the checks used to define initial latitude limits per longitude, as well as to eliminate unwanted nodes later. Given a constant S_y, computation time is therefore largely proportional to the route's length within the FIR. Actual tests on computation speed are carried out later.

B.3 References

[B1] Massink M, and DeFrancesco N. "Modelling Free Flight with Collision Avoidance." Proceedings for the Seventh IEEE International Conference on Engineering of Complex Computer Systems, 2001.

[B2] Lope, J, Vilaplana M, Bayraktutar I, Klooster J, Asensio JM, McDonald G, Kappertz P. "Towards an open test bed for the study of trajectory synchronization in the future ATM system: The ASIS initiative." Integrated Communications, Navigation and Surveillance Conference, ICNS '09, 2009

[B3] International Civil Aviation Organization. Procedures for Air Navigation Services in Air Traffic Management, 15th Edition, International Civil Aviation Organization, 2007.

APPENDIX C US Air Traffic Modelling

With the ability to model air traffic using route definitions detailed to the nearest nautical mile in both CTD and ATD, it was possible to simulate air traffic and gather knowledge on general airspace properties and phenomena that could be needed later. In particular there was a desire to see how the route shape preferences between aircrew, ATC, and ATM would interact with each other over time and in the face of increasing air traffic density. There was also a fear that flying direct routes could be made inefficient over time due to increasing traffic. Gathering information on these phenomena would assist in defining limits and requirements in later tools. Normally such a task would be an extremely difficult to carry out if a high level of accuracy was required; for every potential route, routes showing preferred alterations by both ATC and ATM would have to be defined and compared against each other. However as a cursory investigation, several potentially wrong assumptions could be made to create sufficiently similar airspace properties and phenomena.

The assumptions used here cover aircrew, ATC, and ATM preferences on route shape, as well as a simple means of comparison between the three. For aircrew it was assumed that an Unaltered Air Trip, or UAT, represented by a simple great circle arc between departure and destination was desired as it represented basically the minimum needed to perform a flight. For ATC their route preference was assumed to be UAT locally distorted to resolve conflict and minimize deviation; this reflecting essentially what they do in practice. As a Radial distortion of UAT was intended to minimize deviation due to conflict, these were called Radial Air Trips or RAT. For ATM, given their proficiency of setting up useful route structures that alleviate air traffic via their planned distribution over a wider area, a continental sized 'high way' system of routes was developed to replicate their preferences; a single route that was altered to suit this system was called a High Way Trip, or HWT. The simple means of comparison involves calculating the fuel usage of an approximately correct average aircraft, flown on a schedule of routes approximating likely to be travelled routes in the future, with momentary increases in fuel approximated from likely interactions incurred from all such aircraft routes being flown according to either UAT, RAT, or HWT.

C.1 Fabricating Route Preferences

To facilitate this comparison, the assumptions need to be developed to allow appropriate simulacrum of them. To that end the specifics behind each of the assumptions are stated with details of their application with visual examples. The approximate average aircraft used to define aircraft presence has an optimum cruise at 8 nmi per minute and 40kft altitude, with a fuel burn rate of 100 kg per minute that increases by 1kg per minute for the duration of every aircraft encountered on the route; this last point being an approximation of increased fuel usage associated to the altitudinal deviations required to resolve conflict. An approximation of a realistic schedule of routes is derived from RITA data regarding T-100 air routes in the US for the month of January, 2008[C1]; the approximated FIR thus being the continental US. Increases in route occurrences are calculated using the 4.72% a year increase that SESAR mentioned may happen till 2025 [C2].

C.1.1 UAT Route Structure

UAT are simple point-point great circle arcs representing a particular route. For ease of traffic maintenance, its structure caters for one main lane for each direction on a path, and two smaller lanes for each main. UAT are the

most basic route form, best used in light traffic; in such they become the most efficient and easily controlled route form, and thus the most likely to be used in free flight. Figure 83 and Figure 84 show the distribution of airspace traffic densities that are created if a purely UAT based airspace structure is likely to cause.

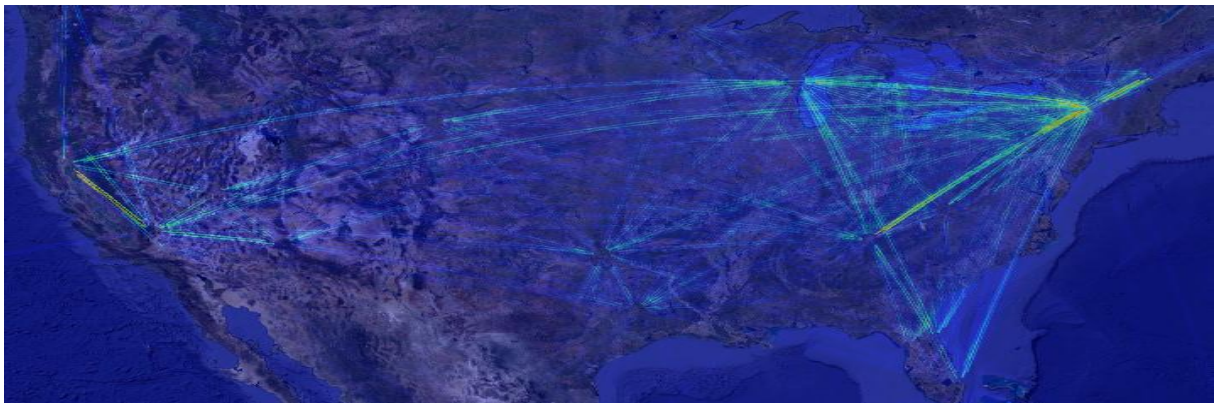

Figure 83 - UAT: Air Traffic Density Distribution

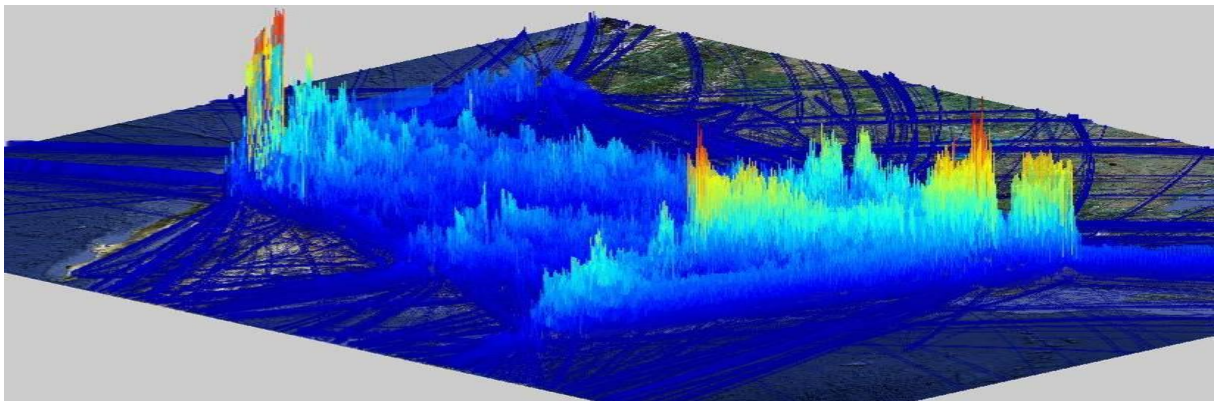

Figure 84 - UAT: Current Relative Local Average Deviation Map

Note the peak areas being generated at airports and regions where traffic from fairly close airports interacts with each other; as the increase in fuel usage is being made directly proportional to this density, this distribution of peaks will significantly increase fuel usage for aircraft travelling through.

C.1.2 RAT Route Structure

RAT is effectively UAT that are altered using a horizontally radial deviation, to manoeuvre a plane away from areas with high traffic concentration; as would be defined using a UAT airspace structure. The distortion is intended to allow, in a fairly simple manner, aircraft to fly through areas of lower traffic, more often, allowing optimum altitudes (and thus lower fuel burn rates) to be gained in a much greater proportion. Figure 85 shows an example distortion for one aircraft. For the purposes of this test this distortion is forced on all scheduled routes leading to less fuel being used. Using Figure D6 as an example, this could lead to a maximum fuel burn rate increase of 1kg/minute, as opposed to a maximum fuel burn rate increase of 3kg/minute as in the left frame. All other attributes are similar to UAT, and examples of its density distribution and the deviation such causes can be seen in Figure 86 and Figure 87.

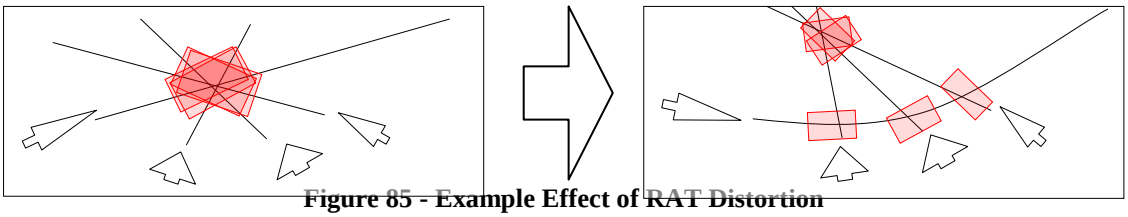

Figure 85 - Example Effect of RAT Distortion

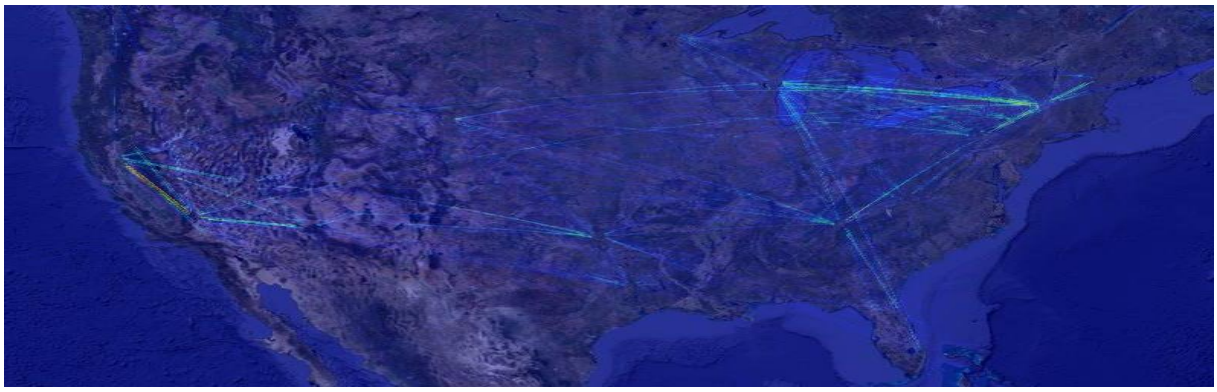

Figure 86 - RAT: Air Traffic Density Distribution

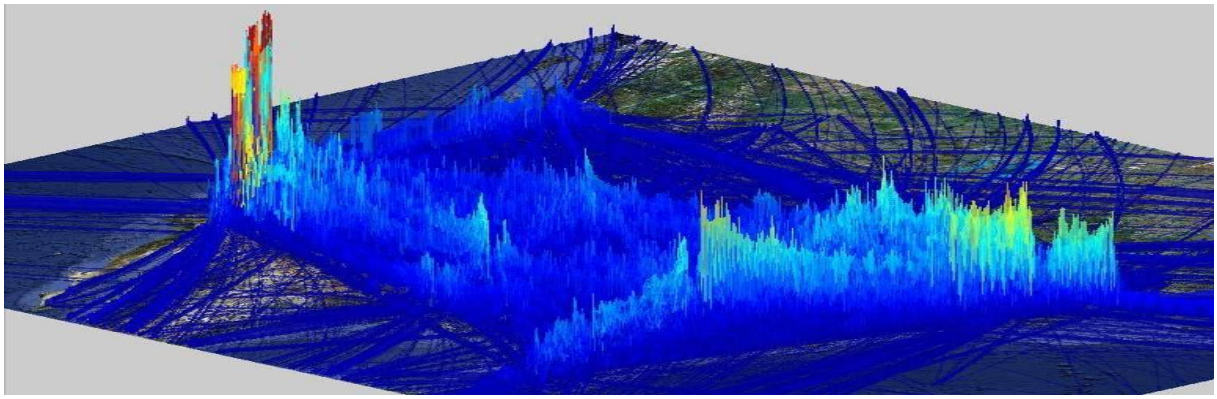

Figure 87 - RAT: Current Relative Local Average Deviation Map

It should be mentioned that since RAT air structures change according to the UAT traffic data given to it, it is by definition a form of adaptive airspace structure. There is also some discussion over whether or not RAT could resemble a true Free Flight, but that would imply that pilots could disseminate traffic in a similar manner and manoeuvre accordingly, which is possible.

C.1.3 HWT Route Structures

HWT is literally a large static pre-defined route structure; a simplistic means of simulating air structures currently used because of their ability to simplify conflict and improve throughput. In this paper, the highest three flight levels (from 37kft to 40kft) are saved for a horizontally spaced, non-crossing ‘highway', as seen in Figure 88, and assumes UAT for all flight levels below these three. In this highway, there is no need for outside of path collision avoidance as each four cornered “ring” of the highway has two lanes going in either direction around the centre, and are expandable to up to ten nautical miles on either side to accommodate aircraft also using that ring at that time. The highway’s altitude and lack of crossing routes ensures that aircraft have a constant optimum fuel burn rate throughout their time in the highway.

Figure 89 - HWT: Air Traffic Density Distribution (non-highway)

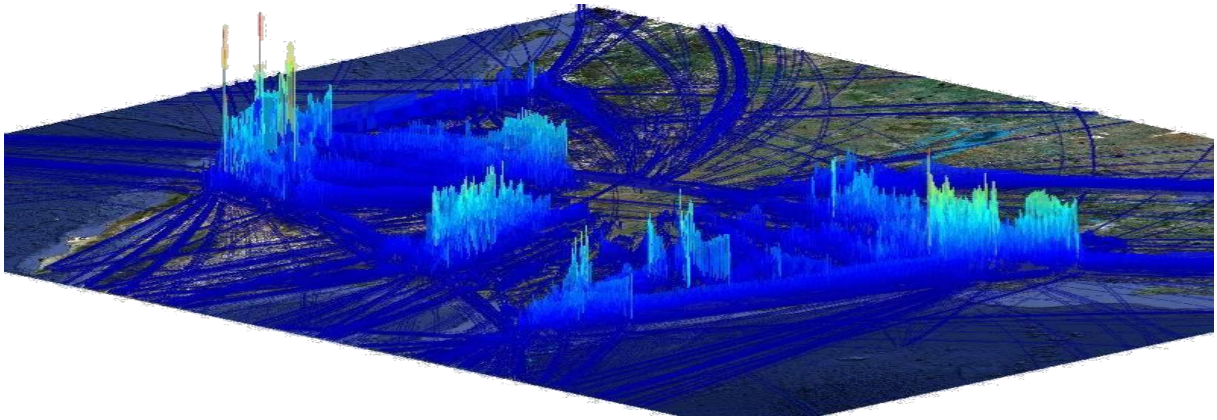

Figure 90 - HWT: Current Relative Local Average Deviation Map

The spatial cost of this structure is twofold: first is the increased length of the highway between points needed to ensure no crossing routes, and the second is the increased air traffic concentration due to limited access paths to the highway. The first cost is an inherent aspect of traffic and collision avoidance; the more time spent avoiding such, the more distance covered. Unless the ring is directly over both airports, the route length will be significantly longer than in UAT. The second cost is due to the limited amount of access points for using the highway. For this version of the HWT, only 72 equally spaced access points were created for each ring of the highway. It is possible to have even more access points on each ring and thereby spread traffic concentrations better, but the algorithms that were required to do so were not ready at the time of testing. Examples of its air

traffic density distribution and relative local average deviation map can be seen in Figure 88, Figure 89, and Figure 90. Regardless of the costs of using the highway, it was a necessary as it allowed a more efficient alternative to flying through dense traffic for continental flights. Also, the highway structure was designed to be of more assistance to the higher traffic routes; filling the role of an airspace structure that supports such.

C.1.4 Comparison of Preferences

Each of the airspace structures are simulated using the approximated aircraft and route schedule on the assumption that only that airspace structure is being used (except in the case of RAT, which requires UAT to calculate deviations). During these simulations, each structure takes the data for a particular air trip, converts it into route coordinate data indicating the square nautical minutes that would be affected by the route, and leaves the number of air trips that would be flown by that route as traffic data within the nautical minutes affected. This collection of data is simulated for the entirety of trips found within the RITA data for the month of January, 2008 (30422 of which are capable of choosing an airspace structure). When finished, a field comprising of individual nautical minute squares, and the amount of traffic to be flown through each of them, is created. This field of data is the basis of the Density Distribution and Relative Local Average Deviation graphs shown depicting the various airspace structures. The graphs shown all use 2008 unaltered data, and are thus considered "current" for the purposes of visualization.

Referring back to increased fuel usage due to encounters with other aircraft, an important assumption used is that average traffic (number of trips per month) within a nautical minute is directly indicative of average vertical deviation required to safely ensure collision avoidance, in the same nautical minute. For example, if within a square minute, three aircraft are noted as being present at the same height, within the same 5 minute period (the time it takes for a wake vortices to dissipate), there is a strong likelihood that one of the three aircraft will have to deviate two flight levels under its own optimum altitude to avoid causing or experiencing turbulence. Using appropriate factors, it becomes possible to find the average local traffic for a particular square, and thus infer from that the average deviation below optimum altitude for safe flight. This drop will have a direct effect on fuel usage, thus allowing the simulation to show the interrelationships between route deviation, fuel usage and pilot structure preference.

Using this assumption, and the same methods for placing traffic data, total traffic data experienced along a path is collected, and an average value for vertical deviation can be obtained. Once every route's length and average altitude deviation is known, it becomes possible to roughly calculate how much fuel an individual trip required under each airspace structure. As the process for each structure can be discretely performed for various stages in air traffic user growth, it then also becomes possible to define changes in airspace structure efficiency over time, and thus allowing the recognition of these trends by future air traffic control tools.

C.2 Results and Discussion

In this section, the results from the three simulations are gathered and compared to see if any was growing inefficient over time, and in so doing so, confirm that the likely cause of it from the interrelationships that the various airspace structures had with each other. For the purposes of determining fidelity of the simulation, it should be noted that the field of simulation was created for the area between the longitudes of 135~56.25º West,

and between the latitudes of 22.5~56.25 º North. As the base unit for holding traffic data was one square minute, this resulted in a field 4725 units wide and 2025 units high.

C.2.1 Summarized Results: Comparing All Structures.

A summarized form of the raw data retrieved from the simulations is shown as data in Table 24 and graphically in Figure 91. In Table 24 the columns respectively represent: year, number of routes that prefer UAT, number of routes that prefer RAT, number of routes that prefer HWT, and the number of flights that had equal preference between two or more of the airspace structures.

Table 24 - Route Pref. totals for each Airspace Structure assuming a time step of 16 years

Year	P-UAT	P-RAT	P-HWT	P>1
2008	3714	24188	2509	11
2024	3179	24552	2680	11
2040	2675	24809	2927	11
2056	2297	25027	3087	11
2072	1975	24864	3572	11
2088	1658	24757	3996	11
2104	1322	24595	4492	13
2120	1078	23991	5339	14
2136	884	23158	6366	14
2152	586	21852	7974	10
2168	445	19716	10251	10

As can be seen from Table 24 and Figure 91, the most pertinent detail is that RAT has the highest preference amongst pilots by fuel usage alone. It increased in percentage preference from 80% to 82% between 2008 and 2072, decreasing thereafter. UAT preference went from 12% to 1% over the 160 year period, and experienced a slight delay in drop between 2104 and 2120 when its value was 4% of the total. HWT steadily increased in percentage preference, parallel to RAT between 2008 and 2056, however when RAT percentage preference was beginning to drop in 2072, HWT preference began to increase at a faster rate.

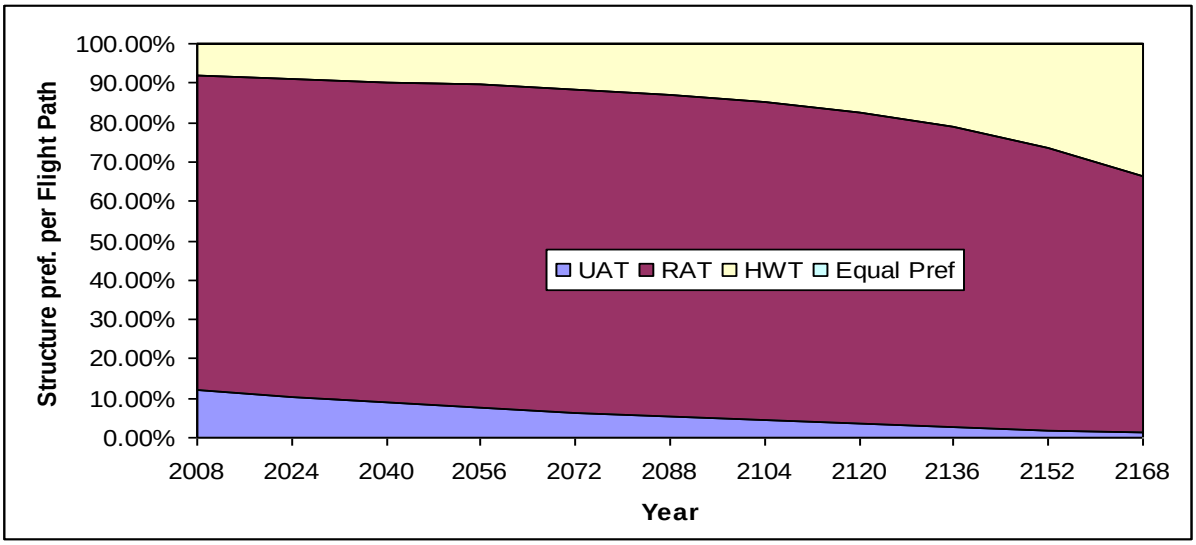

Figure 91 - Pilot Air Structure Preference between All Structures

For UAT, what is seen from the beginning is that UAT preference was decreasing quite rapidly, and given the shape of the drop implies that even some of the fundamental pathways, wherein UAT should be better than RAT or HWT, are beginning to prefer RAT or HWT. The most likely reason for this is that UAT does not allow unplanned horizontal deviation, and so even a route with no crossing traffic would eventually buckle under its own traffic. For RAT, the changes in percentage preference are quite clear and imply that it would both increase and decrease in preference when compared to HWT over time and increasing air traffic. The fact that it has both implies that any use of it would be a temporary measure and thus need a plan for its eventual obsolescence. For HWT, the changes seen in Table 24 and Figure 91 could agree with the concept of a complex airspace structure increasing in comparative preference via increasing comparative efficiency. However, for reasons outlined in 0, this may not be the case. Still, it is a strong indication that the trend may exist within the interrelationship of the airspace structures.

C.2.2 Summarized Results: Comparing Structure Pairs.

Data regarding airspace structure comparison between only two of the airspace structures is shown as data in Table 25 and graphically in Figure 92, Figure 93, and Figure 94. In Table 25 the columns respectively represent: year, number of routes that prefer UAT over RAT, number of routes that prefer RAT over HWT, and number of routes that prefer HWT over UAT. Essentially, Table 25, Figure 92, Figure 93, and Figure 94, show pilot preferences on the assumption that a third choice was not available. For any pair involving RAT, the results and implications mirror those obtained from Table 24 and Figure 91; eventual death when compared with HWT, eventual domination when compared with UAT. The more pertinent data is in the relationship between HWT and UAT, which further implies the likelihood of a trend wherein complex structures eventually gain dominance over other forms of air structure. Figure D15 shows how UAT and HWT experience a near constant relationship with each other until a certain point in time when HWT begins to dominate UAT for structure preference. A comparison between HWT and UAT is similar to comparing two sides of the airspace efficiency debate, more freedom to take more efficient routes against more control to enable more efficient routes to be taken. It is therefore indicative of the inherent cost associated with path avoidance of any kind on the assumption of increasing traffic load. Unfortunately again for reasons mentioned in 0, this result is not entirely acceptable, but still is a strong indication of HWT domination as a likely end form for air traffic.

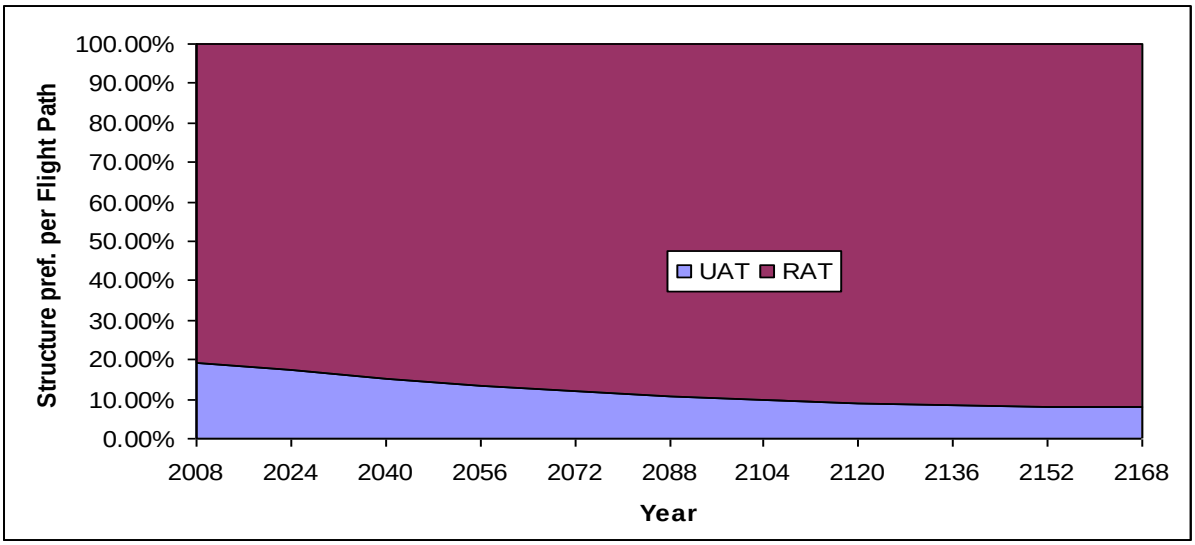

Figure 92 - Pilot Preference between UAT and RAT

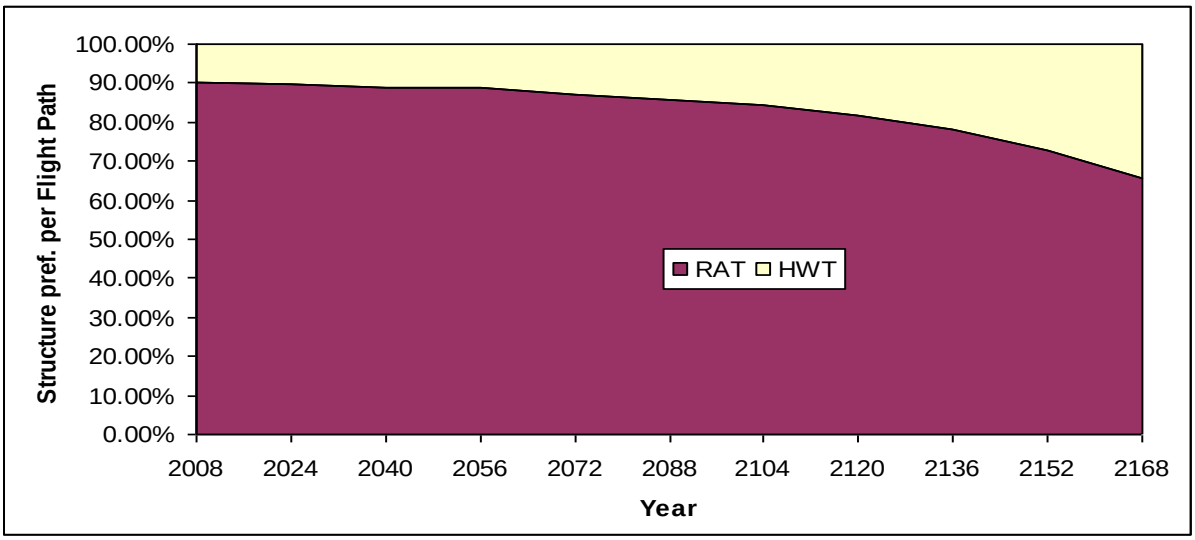

Figure 93 - Pilot Preference between RAT and HWT

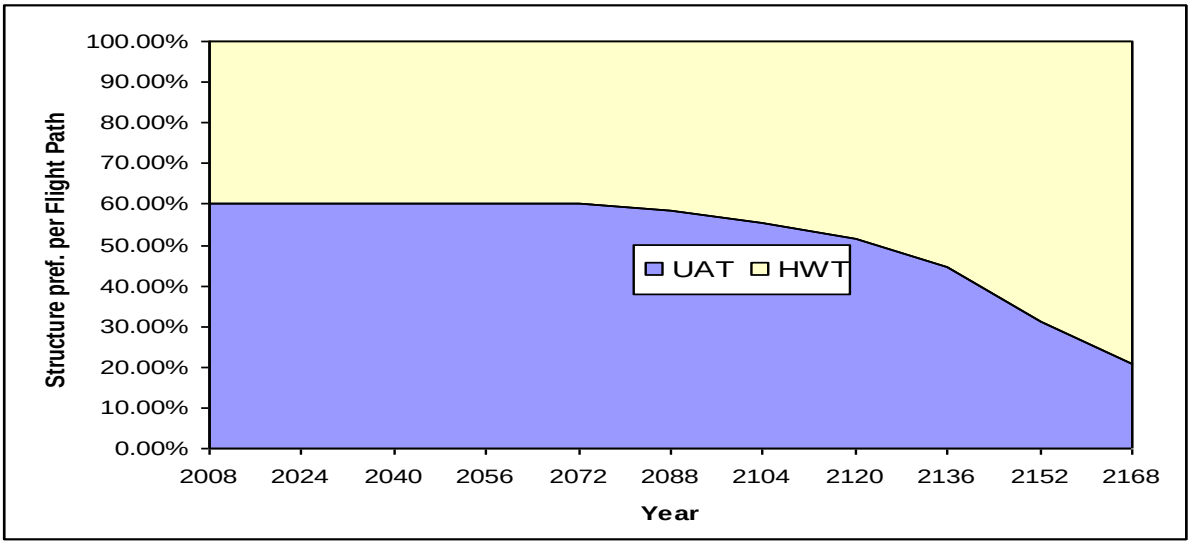

Figure 94 - Pilot Preference between HWT and UAT

Table 25 - Route Pref. totals between only two Airspace Structures assuming a time step of 16 years.

Year	UAT>RAT	RAT>HWT	HWT>UAT
2008	5855	27450	12080
2024	5261	27274	12074
2040	4581	27075	12075
2056	4027	26963	12076
2072	3609	26441	12173
2088	3271	26032	12652
2104	2931	25653	13500
2120	2711	24846	14722
2136	2557	23742	16794
2152	2471	22196	20924
2168	2455	19969	24134

C.2.3 Further Discussion

The favoured form of free flight style air structure, UAT, growing inefficient over time can be effectively seen in all relationships regarding UAT. However to ensure spatial relevance, and to understand the spatial situation within the data collected, data regarding maximum fuel usage, and maximum vertical flight deviation were also collected, and is shown in Table 26.

Table 26 - Fuel Usage and Flight Deviation data

Year	Max Fuel Used [Δkg]	Max Flight Deviation [ΔFlight Level or 1kft]
2008	112724	0
2024	112862	1
2040	113153	2
2056	113758	4
2072	115025	9
2088	117672	18
2104	123205	37
2120	134770	78
2136	158942	163
2152	209466	340
2168	315069	711

The formulas for calculating fuel usage appear to be sound, as spending 115 tonnes of fuel is likely, especially in current times for the longer flights. However, the increases in fuel used appear to become more dramatic after 2104. The reason for this, and unreliability of the results obtained earlier lies in the next column.

On the assumption of an aircraft with a maximum operating altitude of 40kft (12,192m), and wake profiles having a maximum drop height of 1kft (305m), the maximum number of aircraft that can be handled in a square nautical minute, every 5 minutes, and therefore the maximum vertical flight deviation allowed, would thus be 40. As can be seen table.3 for every year past 2104, the average maximum vertical flight deviation is higher than that. The fact that the numbers in the Max Flight Deviation column are maximums of average traffic deviations taken over an entire path, could imply that a) even in the later data collections, there would be regions that are not as heavily trafficked, and that b) even in the heavily loaded routes, traffic may not always be that bad. However it does mean that data past 2104 has to be treated with an amount of suspicion.

Fortunately all the trends shown thus far, except for the fall of RAT when compared to the other two, have their starting point occur before 2104. So while, the results are not as clear, the same conclusions could be drawn with regards to them. In the case of RAT' preference drop, more accurate simulations will have to be made to determine if that is the case.

C.3 Conclusions

Overall, over time, the simulations have shown the death of UAT as a preferred structure, the rise and possible fall of RAT as a preferred structure, and the eventual domination of HWT as the preferred structure. As each is inherently more complex and structured than the last, this does highly agree with the possibility of free flight style of air transport growing progressively more inefficient as more traffic was introduced. More importantly, the fact that this was shown using the three airspace structures indicates that it was the interrelationship between them that was causing the trend in the first place. Taken together, the conclusions map out the limits of various levels of airspace structure and do suggest that any potential form of air traffic control must be capable of evolving as each form of air structure is applied, in order to ensure its presence in it.

C.4 References

[C1] Bureau of Transportation Statistics, "Air Carrier Statistics (Form 41 Traffic): T-100 Market Data (All Carriers)" Research and Innovative Technology Administration, US Department of Transport, Washington DC, 2008.

[C2] SESAR Consortium, "SESAR Air Transport Framework: The Current Situation", SESAR Definition Phase - Milestone Deliverable 1, SESAR Consortium, July 2006.

APPENDIX D NMD Potential Usefulness

The US air traffic modelling trials gave two important lessons. The first was that NMD of airspace in conjunction with the NMD of aircraft routes could appropriately model air traffic. The second was that any air traffic control tool developed had to be designed to handle a mixed assortment of constraints; constraints that had effectively been defined using the NMD model of air traffic. The key question was therefore on the ability of this means of modelling to be developed further so as to become an air traffic control tool. It was highly plausible that this be the case, so effort was put into developing functions based on NMD that could effectively support air traffic control in the future. The capabilities that were developed are shown below and are grouped according to their relevance to trajectory mapping, conflict assessment, and conflict resolution; each of these being necessary for air traffic control.

D.1 Trajectory Mapping

This refers to the way the path of an aircraft is perceived in four dimensional (4D) space, i.e. longitude, latitude, altitude and time. The previous NMD work successfully conformed trajectory data to longitude and latitude; the key query here is how altitude and time, as well as other pertinent properties of the trajectory, fit within an NMD data framework. Given the longitude and latitude nature of NMD, the simple answer was to use the ATD of the trajectory as a baseline to transfer all trajectory data; this made sense as the ATD does allow correlation with changes in trajectory properties as an aircraft travels the route. Thus all that was needed to define an aircraft's complete trajectory in terms of NMD data was to define altitude, time, and assorted data with respect to the distance travelled while on the route. It should be mentioned that the possibility to discretise altitude and time data in a manner similar to longitude and latitude was available; however there has never been any particular reason to do so throughout the research.

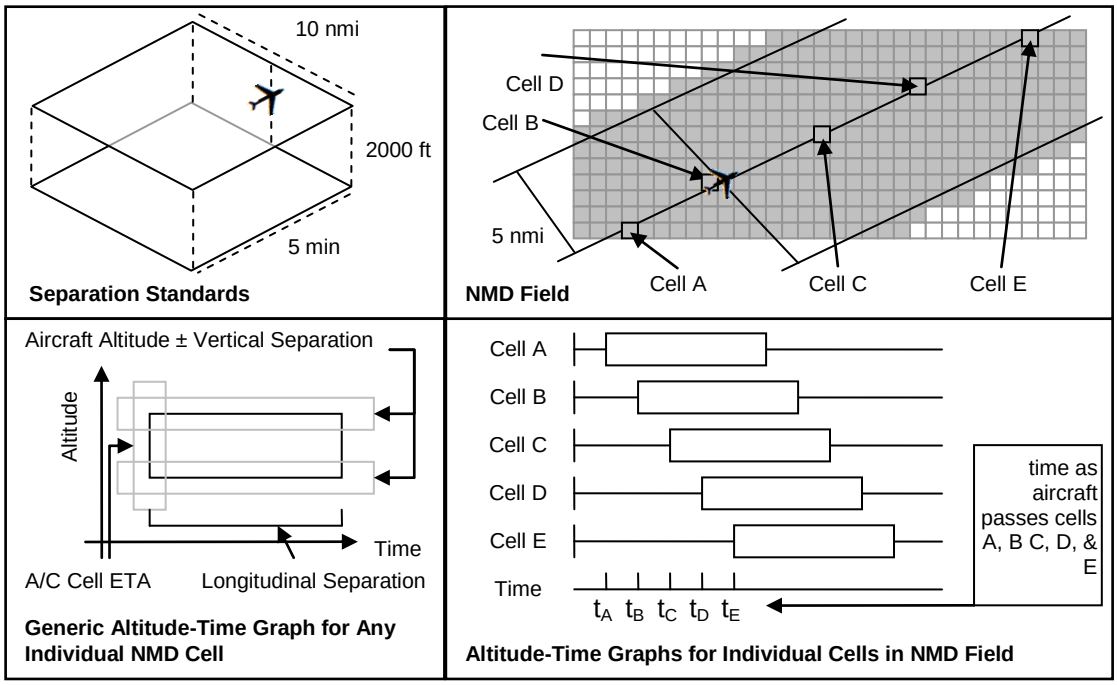

Figure 95 - Presence of an Aircraft on a NMD Field

For the purposes of conflict this definition is not sufficient; parameters defining separation limits in terms of altitude and time had to be included so that an aircraft's presence could be defined, and more importantly, not allowed to overlap with the equivalent presence of other aircraft. To include this data the altitude and time equivalents of allowable lateral deviation, i.e. vertical separation minima and longitudinal separation minima in terms of time, were used to expand upon the trajectory data to define an aircraft presence. The results of this yielded the presences defined in Figure 95.

The other query was how to transfer other pertinent data. In the case of data that varies along the route, the method just used to transfer trajectory altitudes and times is sufficient. In the case of data that varies across the earth surface, such as wind and environmental phenomena, then it needs to be interpolated against the NMD nodes within the FIR; provided it is defined using standard longitude and latitude intervals, the interpolation should be simple. In the case of sector data, provided the sector is a surface polygon with no corner greater than 180 degrees, a CTD check using the sectors edges in an anti-clockwise sequence assuming they were paths and using the node reference point as the off path point should be enough to determine if a node is inside a sector; in such a case the CTD would be positive for all edges, and will not be if otherwise. Sectors with corners greater than 180 need to be broken into smaller polygons to undergo the same process. The process of defining routes and sectors as NMD data, and how similar earth surface data can be incorporated into such, is seen in Figure 96.

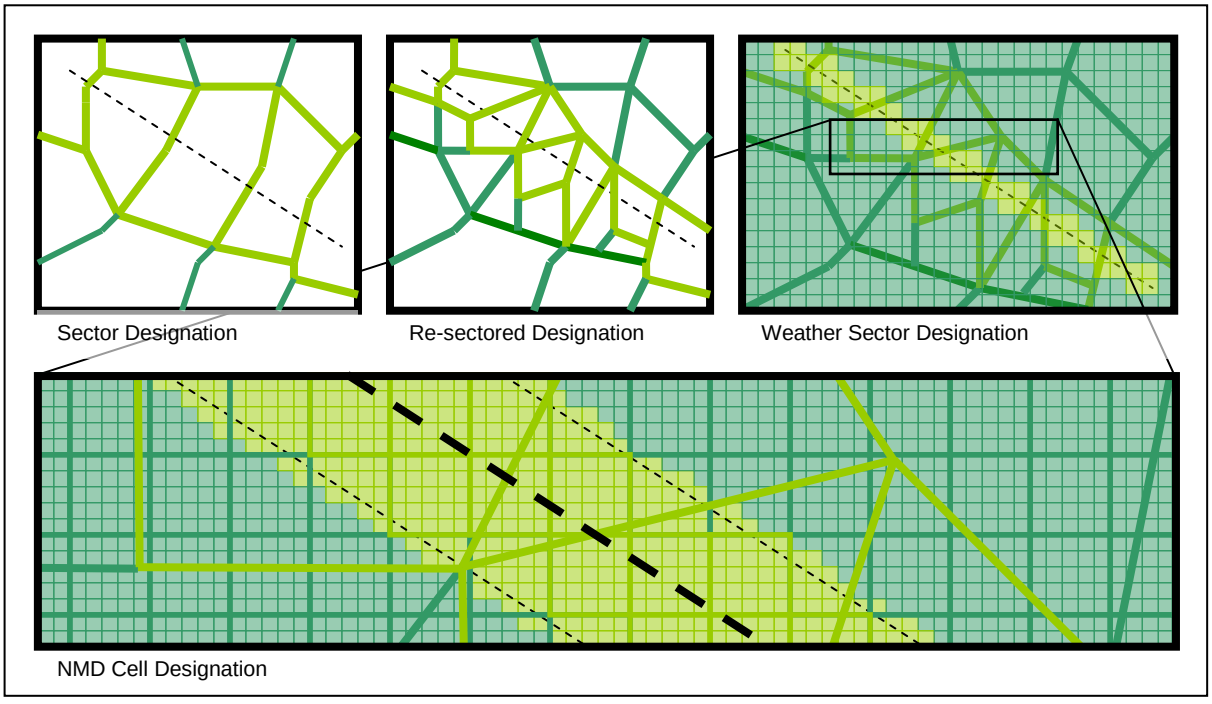

Figure 96 - Sector Designation as allocated for a flight - Current Sectors to NMD Cells

It should be mentioned that if such discretised data changes with time and is discretised to show such, e.g. wind, then it only requires that further NMD fields be created to store that data.

D.2 Conflict Detection

The means of conflict detection varies according to whom or what carries it out. For a human air traffic controller, a conflict is any situation where the applicable requisite minima are unlikely to be maintained. Most CDR methods mentioned in the literature review it is whenever an elliptical or 'puck' field of conflict of

multiple aircraft overlay each other. For NMD, it is whenever the height and time presence of multiple aircraft inside a single NMD cell overlay each other. Figure 12 compares these visually.

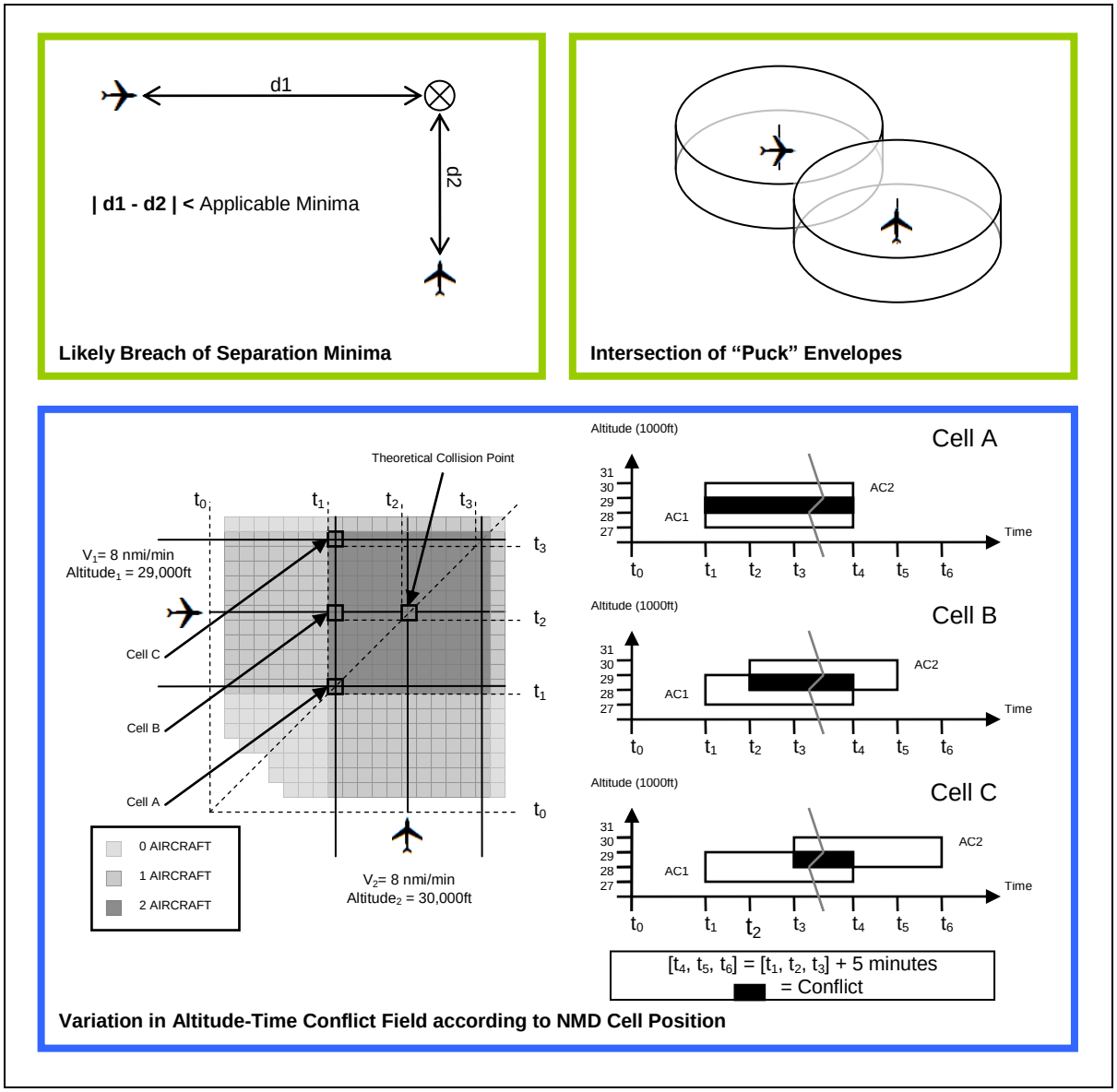

Figure 97 - Conflict Modelling and Detection

While Figure 12 suggests difference between the three, the differences are only effective in the minute details; both the 'puck' and NMD methods of conflict detection do cater for separation requirements that define if and how conflict occurs, and may in fact be reliant on such.

D.2.1 Conflict Modelling

With traffic modelling it was sufficient to know the variation in density of aircraft passing a cell over time. However in order to manipulate it, the exact time and details of their passage must be made known. NMD, due to its match with earth surface data, automatically caters for the possibility that any two aircraft defined for a particular NMD node have the ability to conflict with each other; thus conflict modelling can occur solely by comparison of aircraft data within a single NMD node. However, since trajectories cover many nodes it is likely that a significant number of nodes would catch details on the conflict. So much so that it becomes possible to model such conflict with significant detail in the earth surface domain. Figure 98 has a list of examples of this

model. It should be noted that even with many perspectives on the conflict it does change the fact they are all representations of conflict; when trajectory control occurs, the conflict in each node must be safely separated.

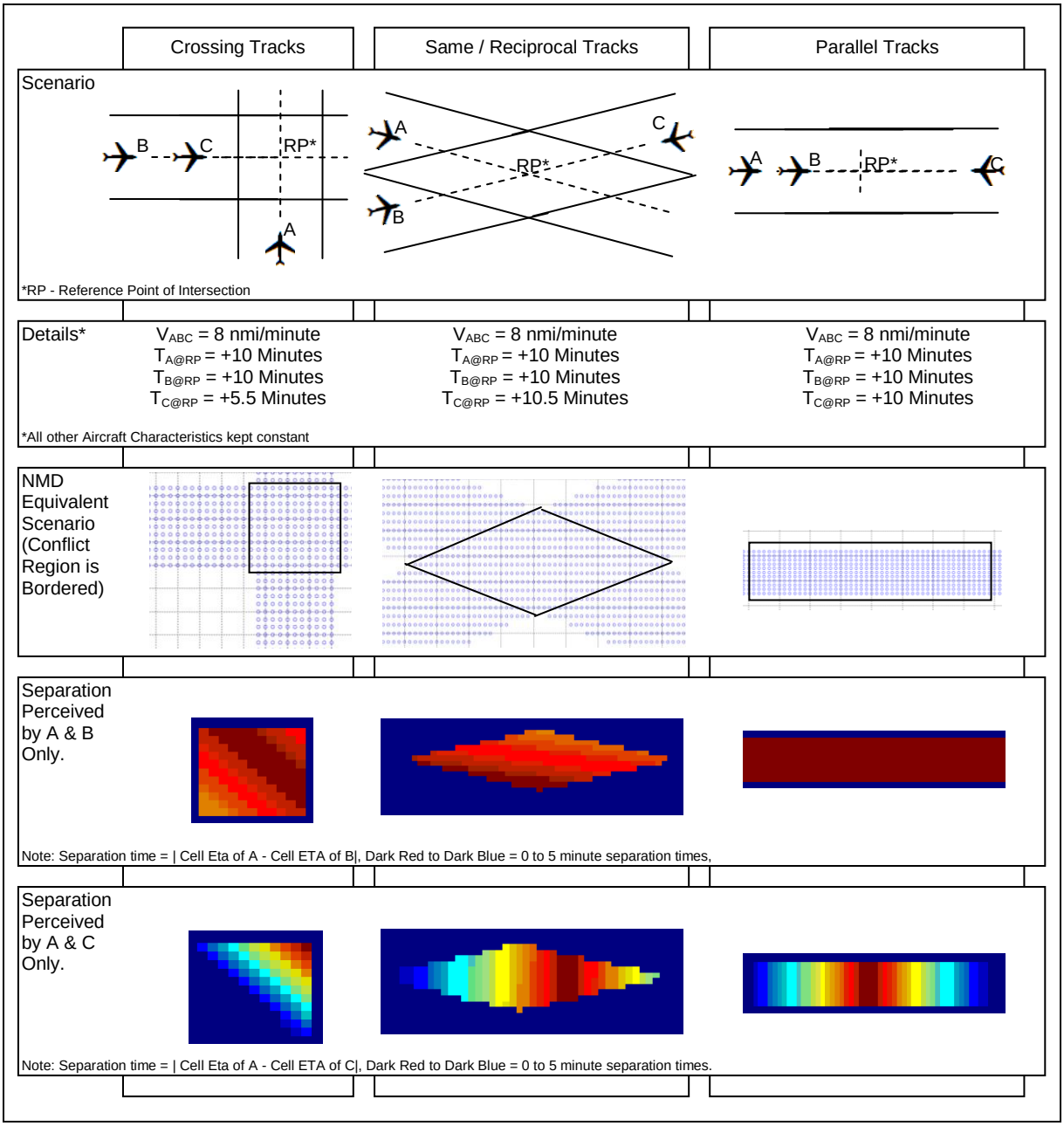

Figure 98 - Intersection Modelling via Distributed Variation in Separation Times

While this could be construed as complicating conflict, it does lend some benefits. First is that it does breaks down all conflict types into individually assessable portions of space; transferring relevant ATC data, even if the same conflict occurs in two different sectors, is easily performed. Second is that it allows various sized conflicts to be superimposed upon each other; if the parallel track scenario between A and B from Figure 98 were superimposed on the bottom half of the crossing track scenario between A and C from the same figure, because of the fidelity of the conflict modelling, the resulting resolution of conflict would incur far less deviation from optimum than what would be incurred if the parallel tracks were placed on the top half of the crossing tracks. The last point is that because NMD allows ease of conflict combination, finding critical points for resolution should be possible; consider Figure 99.

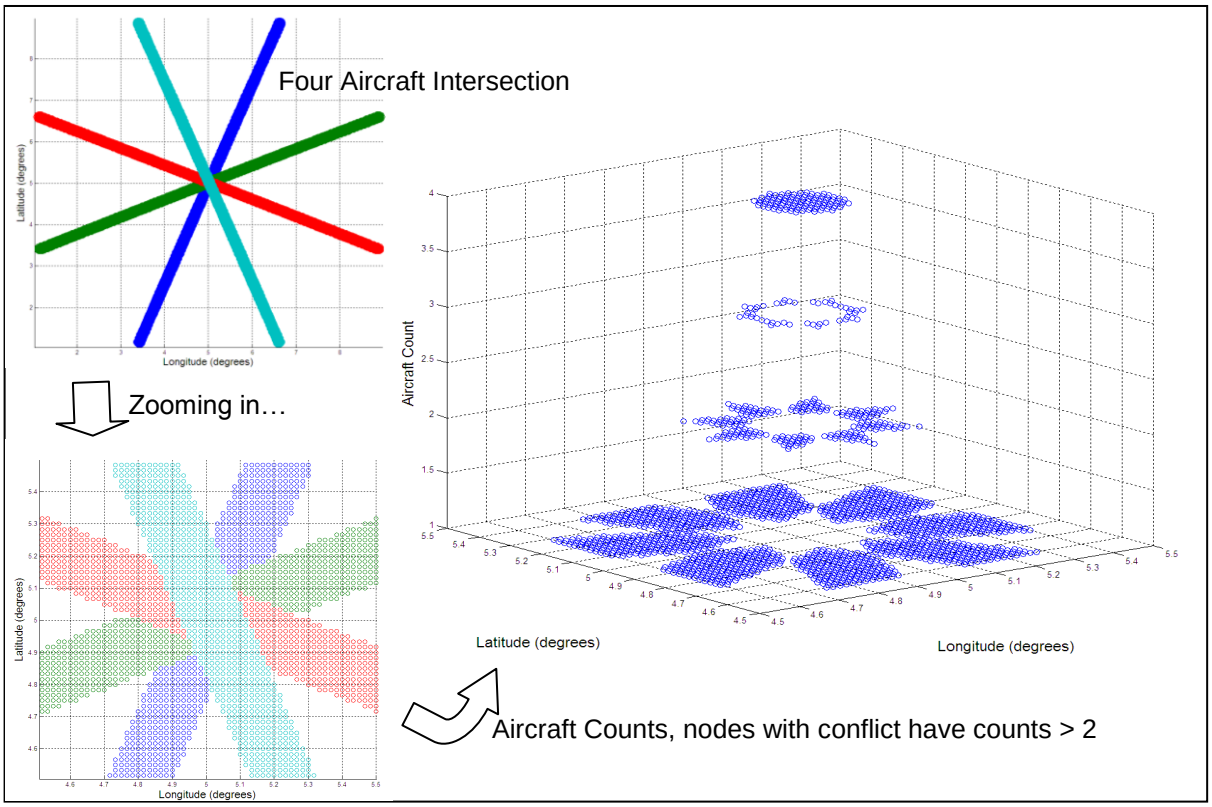

Figure 99 - Critical Conflict Point Definition

What is being suggested in Figure 99 is that conflicts can be ranked according to various data. For procedural application of control rules this ability is of particular usefulness as such rules could be sequentially applied based on some version of this ranking.

D.2.2 Computational Requirements

For the purpose of conflict detection the use of NMD is practically a brute force method. It can be done simpler by using the great circle theory with some assumptions on the proximity of involvement of intersections. However, as mentioned previously, accuracy of information required for resolution of highly complex conflict scenarios may be insufficient. As a brute force method, the pertinent interest would therefore be in terms of processing time. The costs in terms of additional processing time, or the equivalent hardware required to support it, has to be leveraged against the benefits it gives in terms of additional situational assessment and minimized data transfer. In order to facilitate such an assessment, computation time trials were run on two airspace scenarios. However as current performance properties of conflict detection and resolution software are only known to organizations that use such software, trying to define an industry standard for the sake of comparison is difficult. Furthermore, differences in airspace complexity, hardware, software, and code interpretation of great circle theory cause such software to vary in performance and would make comparisons difficult. Instead, the two airspace scenarios simply recorded times of computation, and numbers of expected computation sessions (ECS) for assessment. Two issues have to be mentioned regarding these tests. The first regards the validity of using MatLab as representative of actual computation times. The second regards how the computation times are interpreted.

The experiment assumes that MatLab is representative of actual computation speeds. MatLab is indeed representative of processing capability currently available, and particularly in the area of numerical computation

and use of parallel processors. Furthermore, it does use IEEE standards wherever applicable. Its use in time trials made sense and would be indicative of likely computation times in a crowded data environment. Just to make sure that any unintentional code was utilized in the program, the NMD program was written entirely without toolboxes, and should therefore be transferrable to other software platforms. There is the possibility that MatLab can cause unintended software acceleration, but that is indicative of current numerical computation methodology, and therefore a positive inclusion for testing on MatLab. In addition, the simulation times excluded time for graphics processing which is a negative consideration for potential real time use, however as the NMD data layers inside use a linear index indicative of the actual airspace field, creating an image representing the data therein is not as time consuming as using plot functions available in MatLab. Overall however, MatLab does adhere to the limitations of the computer system, so whatever computation times are achieved, should allow appropriate indication of computation times on other systems.

As no industrial comparison can be made with the computation times recorded, an internal measurement system was used to see if the NMD program was being processed faster or slower than expected. Computation times for MatLab functions are usually proportional to an aspect of the data the function handles. If what aspect therein is known, it can be used to define what can be called an expected computation session (ECS). As time should be directly proportional to the number of expected computation sessions, one can determine the state of the computation process from the way computation time per ECS changes as number of computations increases. If time per ECS is constant, it implies that significant variation will only occur at higher numbers of computations; further testing would still be required to ensure that Time per ECS is not increasing, however as an indicator of performance, time predictions, using it as a modifier on the predicted number of ECS, should yield relatively accurate results. If time per ECS is increasing it implies that unintended data processing is occurring and slowing the program down. It suggests that inefficient code is still present in the program and needs to be removed. Time modifiers calculated in this scenario should not be used for prediction of computation times. If time per ECS is decreasing, it implies that data acceleration is occurring and speeding the program up. While time modifiers gained in this scenario can successfully predict computation times, care should be taken to ensure that the values for ECS are correct.

Table 27 - Margins and Column Width

Function	Time Modifier (sec) (@ Max #ECS)	Time Per ECS Variation
NMD Cell Allocation	2.28E-06	Constant
Profile & Trajectory Determination	1.71E-04	Increasing
Profile to NMD Data Distribution	6.49E-04	Increasing
Conflict Assessment	3.34E-06	Decreasing

The results in Table F1 are the Time Modifiers, and Time per ECS trends for computation times achieved using MatLab R2009a (32 bit) on an Intel® Core™ i7 3.60 GHz computer running Windows Vista. Parallel Distribution requires a MatLab Toolbox, and was avoided in these trials; the times are indicative of the program run in sequence as opposed to parallel. As NMD Cell Allocation and Conflict Assessment experienced either constant or decreasing time per ECS values, their time modifiers can be used to predict computation times under other scenarios. For example: NMD Cell Allocation's ECS value was determined by the number of times a cell had been included as part of an aircraft's path. Therefore allocation of cells for a 600nmi journey with a 10nmi

allowable cross track deviation would take 13.7ms to calculate. Conflict Assessment's ECS value was determined by the number of aircraft in all cells that were checked for conflict. Conflict assessment for a continent with 6 million cells, averaging 7000 aircraft per cell, would take 38.97 hours for the lone computer to process, memory conditions permitting; given the potential for parallel processing, and a potential desire to split up based on sectors, this could end up being quite small in practice. Unfortunately, as the other two functions experienced increasing time per ECS values, they could not be used to predict other scenarios in their current form. Additional data processing was found in the profiling function with a save function that stores already made NMD profiles within a storage format (cell array) for later use. The cause in the distribution function was the growing data size of the NMD storage layers. In both cases a sufficiently sized predefined matrix would remove the increasing Time per ECS values; however the complexity for such would be significant and would require further assessment of likely data usage.

D.3 Conflict Resolution

The resolution of conflict is, at the simplest level, whatever action is needed to ensure that an apparent conflict does not occur. As mentioned previously in the main thesis, there are four ways of defining what this action is; manual assessment, proscribed procedures, force field distribution, or via optimization. The main body of the thesis shows how NMD was developed to support optimized resolution of conflict as that appeared to be the only path towards a provably optimum set of air traffic. However even before such was developed there was recognizable potential for NMD to carry out or support CDR via the other three methods using some of the innate properties provided by NMD.

When an aircraft is mapped against a set of NMD cells, information regarding the aircraft's state as it passes any cell is stored in that cell. Thus it is possible to perform basic deviations as a means of applying short term conflict resolution via NMD suggestion of alternative altitudes, speeds and lateral deviations to clear a conflict. The provision of alternative altitudes and speeds stems from an assessment of the cell's aircrafts' desired, minimum and maximum speeds and altitudes, and available times within the cell. Lateral deviation is determined by the relative bearing of conflicting aircraft within an NMD cell. Figure 100 shows the three deviations, as generated by a potential two aircraft conflict in a single cell, and the information required for each. In essence, NMD has the ability to create suggestions for manoeuvres in any dimension. There are three implications to this.

The first is that assessment of alternatives could occur at the conflict determination level, i.e. that existence of conflict automatically calls up solutions. This indicative of manual CDR and suggests synergy with an automatic re-optimization process in the event of a conflict that just appeared. Provided airspace complexity is low, and that aircraft therein usually fly an altered path, the automatic determination of a manoeuvre to an optimized trajectory would be appealing.

The second is that the selection of alternatives can be done in a holistic manner, using potential guides or desirables, such as reduced fuel emissions, to define control of the entire system. This is powered by the NMD ability to model conflict for the whole airspace, and should lend itself readily to conceptual flight rules that lack the ability to handle high density airspace complexity. It was this concept that led to the initially force field, and eventual optimization, methods used in the thesis.

The third is the ability of individual NMD nodes to perform assessments with respect to other NMD nodes. This initially came from a desire to cluster different NMD nodes together; thus allowing sector limitations to be collectively defined for the nodes in that sector. However, given the fidelity of NMD, it was recognized that such properties could be allowed to vary significantly such that nodes where such constraints did not have to be entirely true all the time were actively defined and exploited. This thereby led to the possibility of correlating NMD nodes since such definition required understanding of the state of other nodes. This concept therefore inherently supports proscribed procedures to be used as such require knowledge of either sector states or conflict states elsewhere from the current position of aircraft, to define an optimum action.

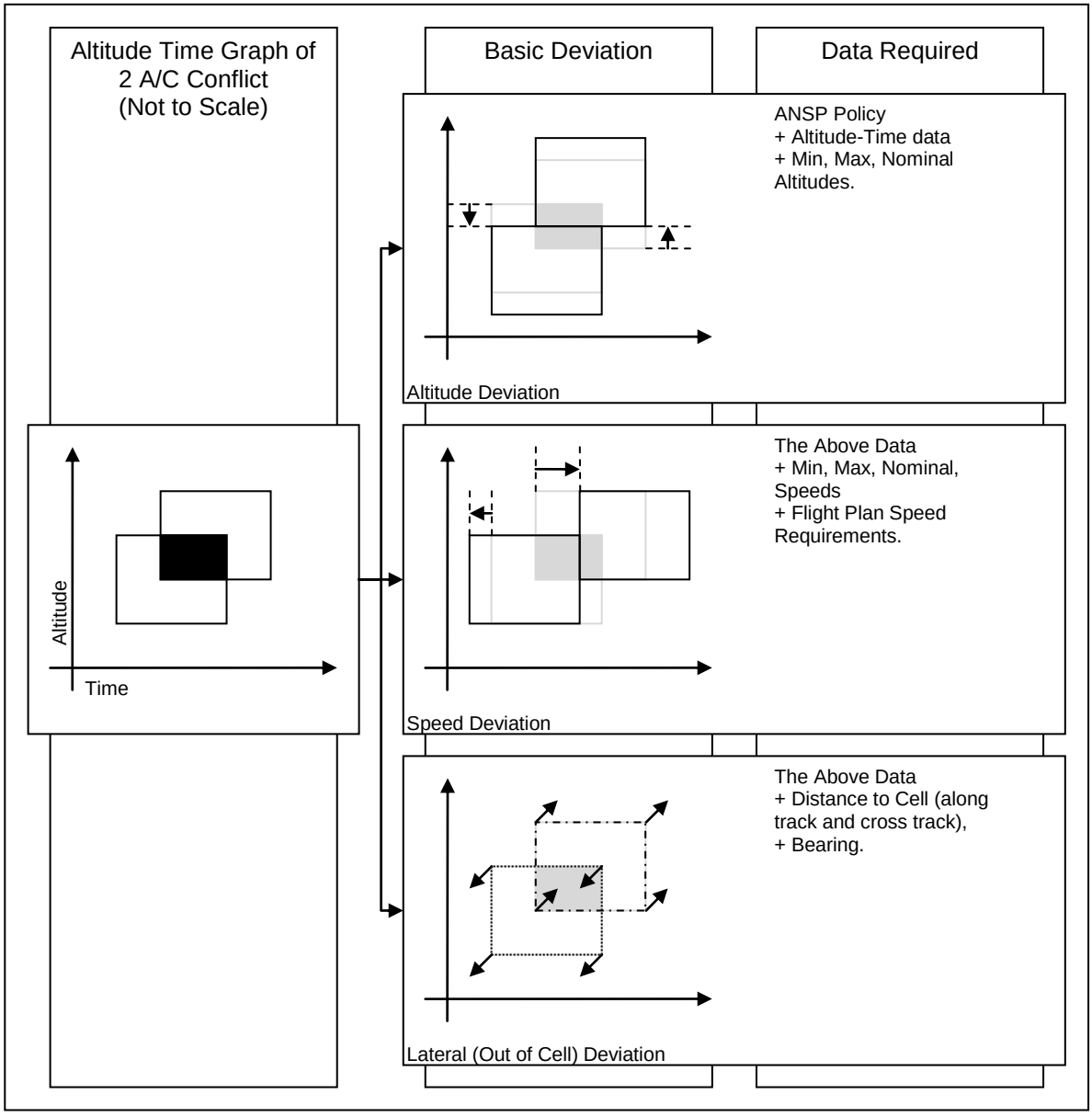

Figure 100 - Basic Deviations for Short Term Conflict Resolution

APPENDIX E Example Simulations

This appendix outlines the scenarios that are used to test the optimizer in all its forms. In all cases, the only real variation in optimizer input is the length and position of the aircraft trajectories; all other parameters are derived from these using consistently assumed formulas and values as outlined in Table 28 and Table 3 below. It should be noted that these are the same as those used in section 3.4 of the thesis, but for transparency, more information is shown here. Most of this additional information is merely clarification on trajectory positions, however the differences in the initial fuel available to aircraft warrant further explanation of its rationale which is twofold. The first reason is that given the max range of most jet aircraft and the size of the test area, aircraft with full fuel capacity were expected to not have issues with running out of fuel whilst inside the test area, i.e. the constraint of always having some fuel would never be tested. The second reason is that the optimization of completely similar aircraft would cause optimization results defined by rounding off error. To prevent these two issues the amount of fuel initially available to each aircraft was reduced to at least 45% of their total fuel capacity with more reductions further differentiating between aircraft in a scenario. More specifics on the distribution and calculation of this are shown in Table 3.

Table 28 - Optimizer Control and Fuel Calculation Node Spacing Assumptions for All Scenarios

Constant	Units	Value
S_{FLIGHT}	nmi	Distance Covered in the Flight.
$\Delta ATD_{N\ IDEAL}$	nmi	*20 nmi*
$\Delta ATD_{i\ IDEAL}$	nmi	*5 nmi*
ΔATD_N	nmi	S_{FLIGHT} / *ceil(* $S_{FLIGHT} / \Delta ATD_{N\ IDEAL}$ *)*
ΔATD_i	nmi	ΔATD_N / *ceil(*$\Delta ATD_N / \Delta ATD_{i\ IDEAL}$ *)*
$ATD_{i\ 1}$	nmi	ΔATD_i / *2*

Table 29 - Aircraft Weight Assumptions for All Scenarios

Constant	Units	Value
MTOW	N	Maximum Take-off Weight; assumes full payload and fuel capacity.
FC_T	N	Total Fuel Capacity; assumed to be MTOW less full payload.
$\%FC_1$	-	Initial % of FC_T that contains fuel; linearly varied between 15% and 45%
W_1	N	Initial Aircraft Weight*; (MTOW - (1 -* $\%FC_1/100$*) ** FC_T*)*

E.1 Parallel Same Direction (PSd) Scenarios

The Parallel Same Direction (PSd) scenarios were developed to represent the mundane occurrence of multiple aircraft following the same well known route in a safely time separated sequence. However, despite its simplicity, it is the most memory intensive of all the scenarios due to the consistent proximity of each aircraft to others in the sequence. This proximity ensures that the aircrafts' potential presence or trajectories always overlap and therefore cannot be taken out of optimization. Further, the more aircraft in the sequence, the more likely any single aircraft deviations will accumulate and cause bigger deviations in the optimized result.

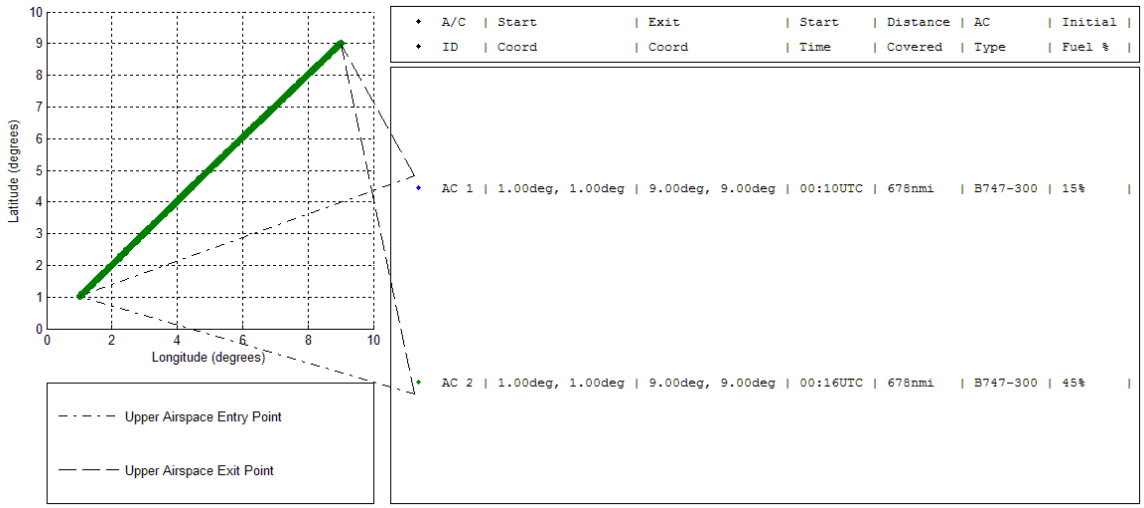

Figure 101 - Scenario 2acPSd

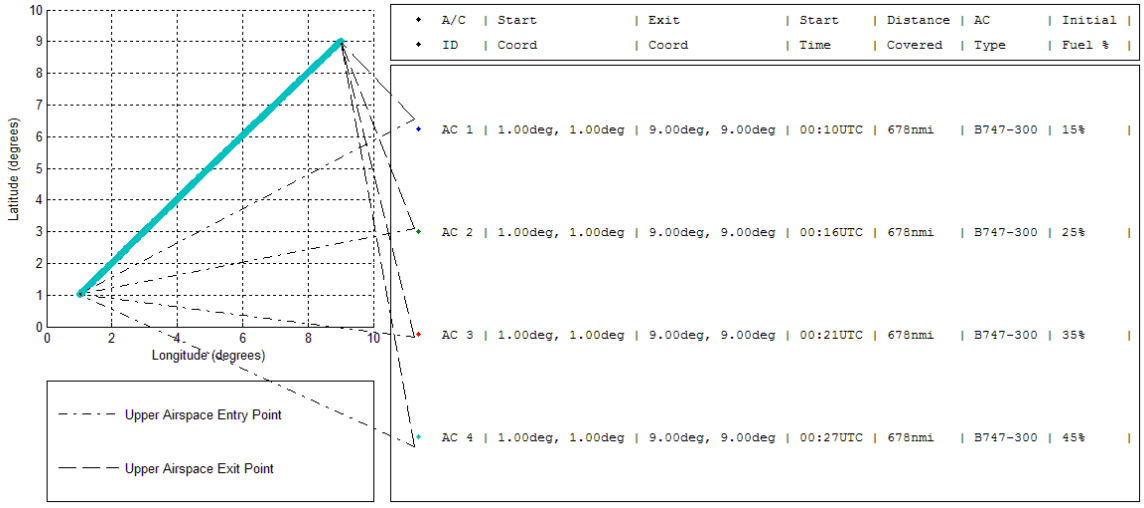

Figure 102 - Scenario 4acPSd

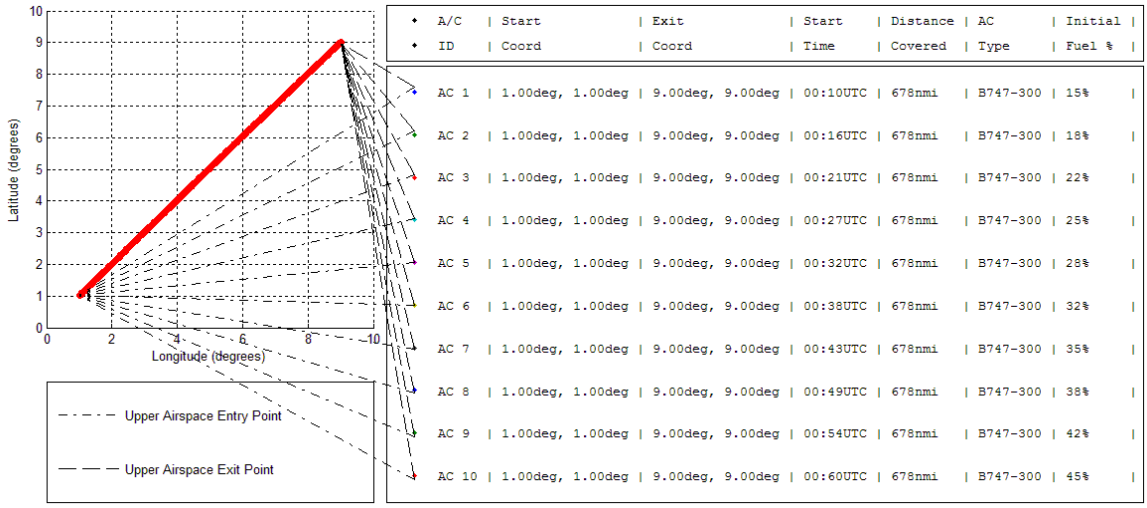

A/C ID	Start Coord	Exit Coord	Start Time	Distance Covered	AC Type	Initial Fuel %
AC 1	1.00deg, 1.00deg	9.00deg, 9.00deg	00:10UTC	678nmi	B747-300	15%
AC 2	1.00deg, 1.00deg	9.00deg, 9.00deg	00:16UTC	678nmi	B747-300	18%
AC 3	1.00deg, 1.00deg	9.00deg, 9.00deg	00:21UTC	678nmi	B747-300	22%
AC 4	1.00deg, 1.00deg	9.00deg, 9.00deg	00:27UTC	678nmi	B747-300	25%
AC 5	1.00deg, 1.00deg	9.00deg, 9.00deg	00:32UTC	678nmi	B747-300	28%
AC 6	1.00deg, 1.00deg	9.00deg, 9.00deg	00:38UTC	678nmi	B747-300	32%
AC 7	1.00deg, 1.00deg	9.00deg, 9.00deg	00:43UTC	678nmi	B747-300	35%
AC 8	1.00deg, 1.00deg	9.00deg, 9.00deg	00:49UTC	678nmi	B747-300	38%
AC 9	1.00deg, 1.00deg	9.00deg, 9.00deg	00:54UTC	678nmi	B747-300	42%
AC 10	1.00deg, 1.00deg	9.00deg, 9.00deg	00:60UTC	678nmi	B747-300	45%

Figure 103 - Scenario 10acPSd

E.2 Cross Over (CO) Scenarios

The Cross over (CO) scenarios were developed primarily due to influence from the literature; their generic form was used frequently as examples of CDR testing and development due to their effective representation of intersection points where CDR methods would be necessary for improving aircraft interaction. Due to the small surface area of conflict, the results for this scenario type are expected to be altitude dominated; the small time frame in which conflict occurs implying that more direct fuel savings would come from short altitude changes rather than the minor speed changes that would have to occur over a longer period of time. As the number of aircraft increases, the amount of available altitudinal space should decrease and cause other conflict resolution methods to occur.

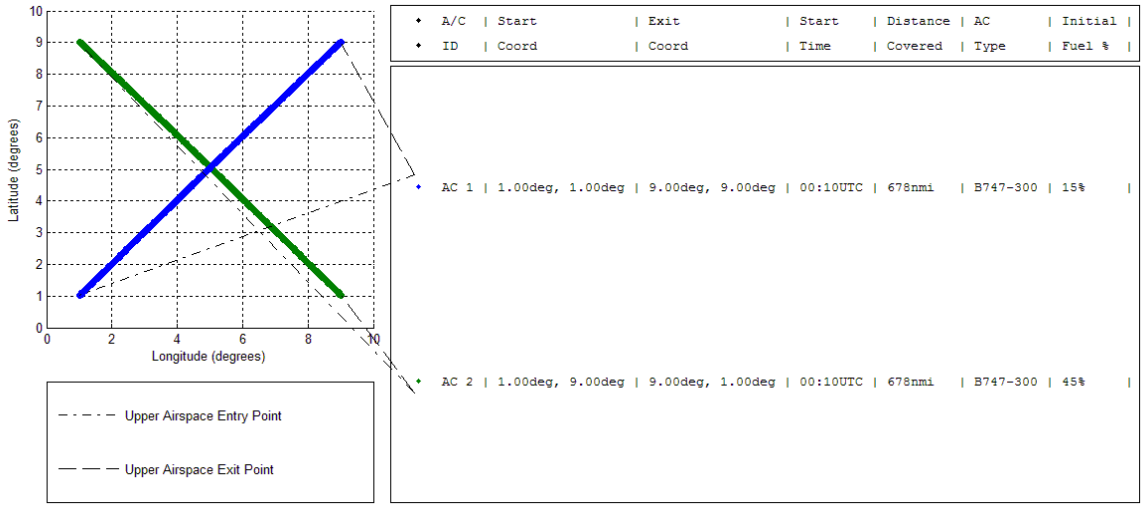

A/C ID	Start Coord	Exit Coord	Start Time	Distance Covered	AC Type	Initial Fuel %
AC 1	1.00deg, 1.00deg	9.00deg, 9.00deg	00:10UTC	678nmi	B747-300	15%
AC 2	1.00deg, 9.00deg	9.00deg, 1.00deg	00:10UTC	678nmi	B747-300	45%

Figure 104 - Scenario 2acCO

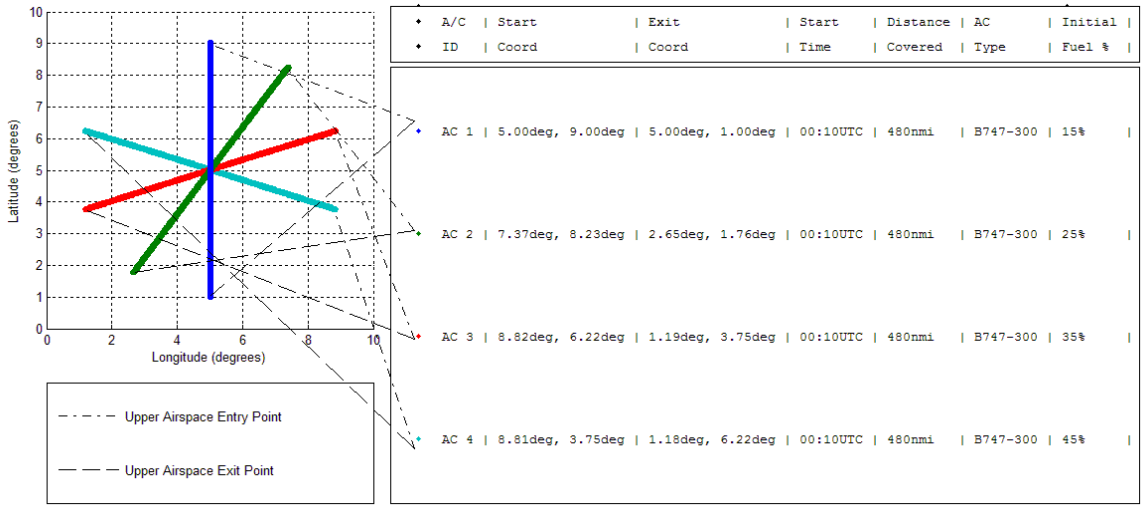

A/C ID	Start Coord	Exit Coord	Start Time	Distance Covered	AC Type	Initial Fuel %
AC 1	5.00deg, 9.00deg	5.00deg, 1.00deg	00:10UTC	480nmi	B747-300	15%
AC 2	7.37deg, 8.23deg	2.65deg, 1.76deg	00:10UTC	480nmi	B747-300	25%
AC 3	8.82deg, 6.22deg	1.19deg, 3.75deg	00:10UTC	480nmi	B747-300	35%
AC 4	8.81deg, 3.75deg	1.18deg, 6.22deg	00:10UTC	480nmi	B747-300	45%

Figure 105 - Scenario 4acCO

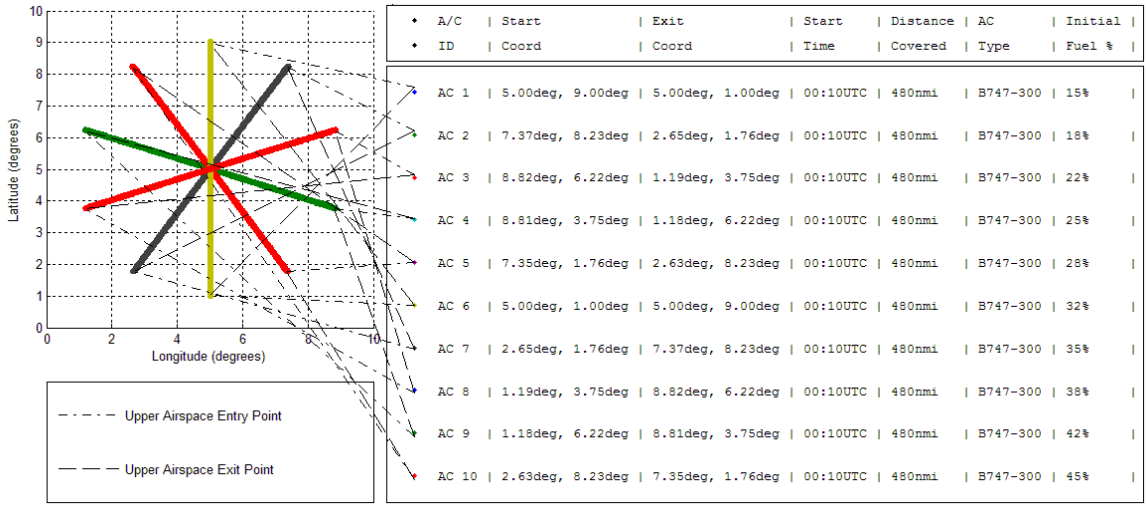

A/C ID	Start Coord	Exit Coord	Start Time	Distance Covered	AC Type	Initial Fuel %
AC 1	5.00deg, 9.00deg	5.00deg, 1.00deg	00:10UTC	480nmi	B747-300	15%
AC 2	7.37deg, 8.23deg	2.65deg, 1.76deg	00:10UTC	480nmi	B747-300	18%
AC 3	8.82deg, 6.22deg	1.19deg, 3.75deg	00:10UTC	480nmi	B747-300	22%
AC 4	8.81deg, 3.75deg	1.18deg, 6.22deg	00:10UTC	480nmi	B747-300	25%
AC 5	7.35deg, 1.76deg	2.63deg, 8.23deg	00:10UTC	480nmi	B747-300	28%
AC 6	5.00deg, 1.00deg	5.00deg, 9.00deg	00:10UTC	480nmi	B747-300	32%
AC 7	2.65deg, 1.76deg	7.37deg, 8.23deg	00:10UTC	480nmi	B747-300	35%
AC 8	1.19deg, 3.75deg	8.82deg, 6.22deg	00:10UTC	480nmi	B747-300	38%
AC 9	1.18deg, 6.22deg	8.81deg, 3.75deg	00:10UTC	480nmi	B747-300	42%
AC 10	2.63deg, 8.23deg	7.35deg, 1.76deg	00:10UTC	480nmi	B747-300	45%

Figure 106 - Scenario 10acCO

E.3 Cross Hatch (CH) Scenarios

The Cross Hatch (CH) scenarios were developed to define aircraft conflicts in an ATS that distributed aircraft going in the same direction among different but mostly parallel routes. In terms of the problem this meant conflict spanning a much larger area, but at significantly reduced density. These scenarios were therefore expected to be fairly mundane; the reduced aircraft density leading to minimal or non-existent trajectory deviations. The CH scenarios were also little different from the rest in that they do not have the geometrically shapely increase in aircraft that the other scenario types do. This is largely because of the lower expectations on their results as well as knowledge that the critical scenarios of this type would most likely require a number of aircraft that would exceed the allowable memory available during testing.

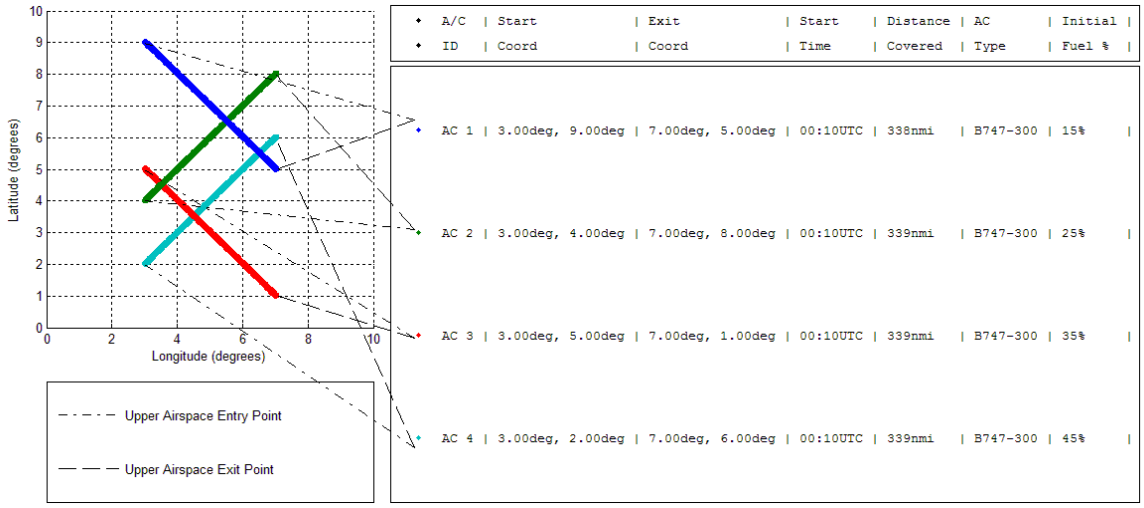

A/C ID	Start Coord	Exit Coord	Start Time	Distance Covered	AC Type	Initial Fuel %
AC 1	3.00deg, 9.00deg	7.00deg, 5.00deg	00:10UTC	338nmi	B747-300	15%
AC 2	3.00deg, 4.00deg	7.00deg, 8.00deg	00:10UTC	339nmi	B747-300	25%
AC 3	3.00deg, 5.00deg	7.00deg, 1.00deg	00:10UTC	339nmi	B747-300	35%
AC 4	3.00deg, 2.00deg	7.00deg, 6.00deg	00:10UTC	339nmi	B747-300	45%

Figure 107 - Scenario 4acCH

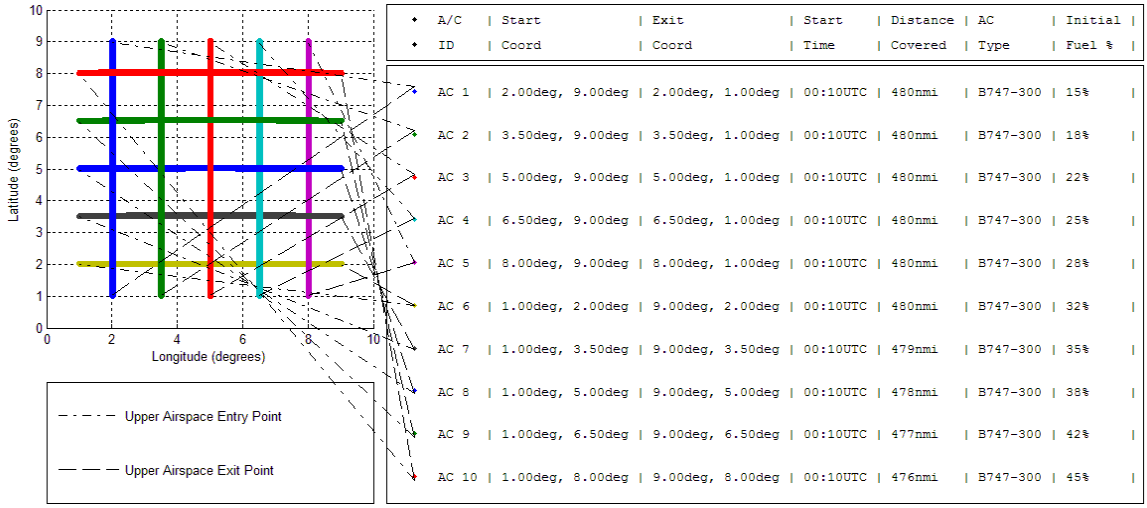

A/C ID	Start Coord	Exit Coord	Start Time	Distance Covered	AC Type	Initial Fuel %
AC 1	2.00deg, 9.00deg	2.00deg, 1.00deg	00:10UTC	480nmi	B747-300	15%
AC 2	3.50deg, 9.00deg	3.50deg, 1.00deg	00:10UTC	480nmi	B747-300	18%
AC 3	5.00deg, 9.00deg	5.00deg, 1.00deg	00:10UTC	480nmi	B747-300	22%
AC 4	6.50deg, 9.00deg	6.50deg, 1.00deg	00:10UTC	480nmi	B747-300	25%
AC 5	8.00deg, 9.00deg	8.00deg, 1.00deg	00:10UTC	480nmi	B747-300	28%
AC 6	1.00deg, 2.00deg	9.00deg, 2.00deg	00:10UTC	480nmi	B747-300	32%
AC 7	1.00deg, 3.50deg	9.00deg, 3.50deg	00:10UTC	479nmi	B747-300	35%
AC 8	1.00deg, 5.00deg	9.00deg, 5.00deg	00:10UTC	478nmi	B747-300	38%
AC 9	1.00deg, 6.50deg	9.00deg, 6.50deg	00:10UTC	477nmi	B747-300	42%
AC 10	1.00deg, 8.00deg	9.00deg, 8.00deg	00:10UTC	476nmi	B747-300	45%

Figure 108 - Scenario 10acCH

E.4 Parallel, Head - Head Collisions

The parallel, head to head (PH2H) collisions were intended to be the most critical, extreme, and indicative, scenarios of the lot. This was due to three reasons. The first is because of the larger potential region of conflict between aircraft pairs; while not quite as large as a PSd scenario, it is still noticeably larger than a CO or CH scenario. The second is due to the actual point of conflict avoidance having a small but significantly more variable position. In CO and CH scenarios the point of conflict avoidance was only two dimensional (altitude and time). In PSd scenarios the point of conflict avoidance could be described as three dimensional (altitude, time and ATD) however the consistent direction meant conflict avoidance occurred at all ATD and not a particular location. In PH2H the point of conflict avoidance could actually be anywhere in the region of conflict. The third reason came from combining the two previous; the enlarged region of conflict, and the singular but variable point of conflict avoidance, meant much greater freedom in the resulting shape of the interaction between aircraft and would therefore give greater indication of optimizer trajectory control.

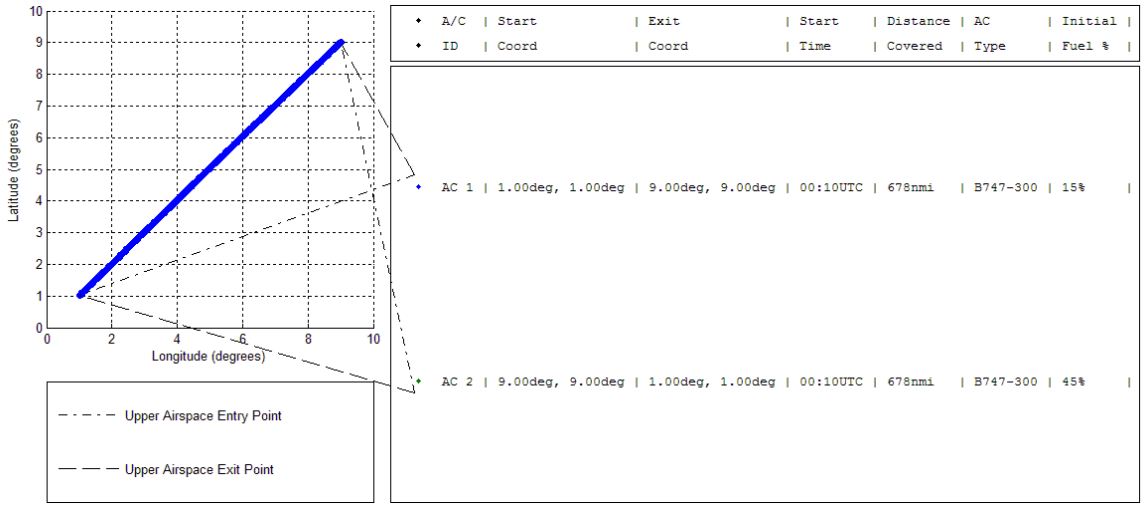

A/C ID	Start Coord	Exit Coord	Start Time	Distance Covered	AC Type	Initial Fuel %
AC 1	1.00deg, 1.00deg	9.00deg, 9.00deg	00:10UTC	678nmi	B747-300	15%
AC 2	9.00deg, 9.00deg	1.00deg, 1.00deg	00:10UTC	678nmi	B747-300	45%

Figure 109 - Scenario 2acPH2H

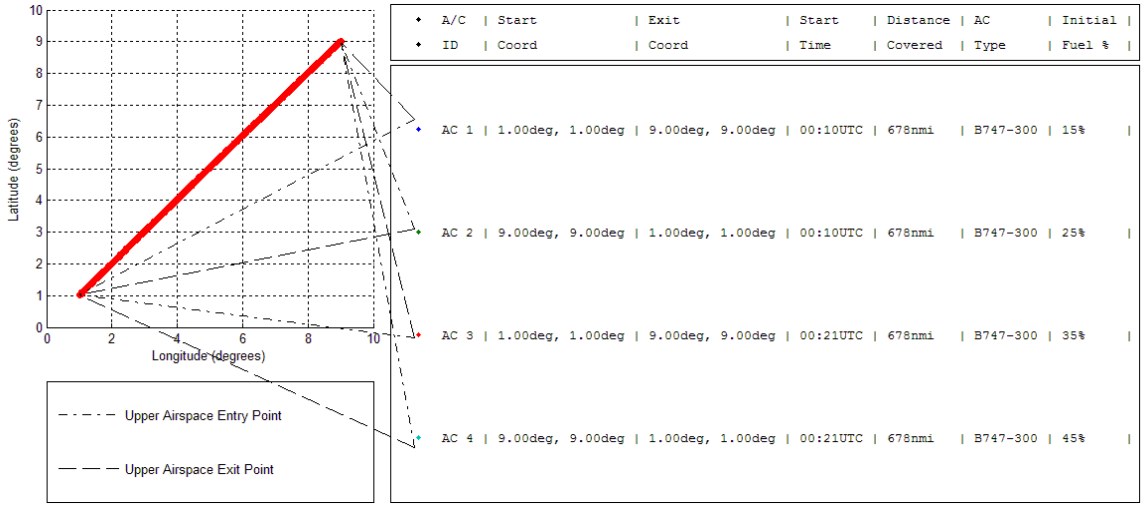

A/C ID	Start Coord	Exit Coord	Start Time	Distance Covered	AC Type	Initial Fuel %
AC 1	1.00deg, 1.00deg	9.00deg, 9.00deg	00:10UTC	678nmi	B747-300	15%
AC 2	9.00deg, 9.00deg	1.00deg, 1.00deg	00:10UTC	678nmi	B747-300	25%
AC 3	1.00deg, 1.00deg	9.00deg, 9.00deg	00:21UTC	678nmi	B747-300	35%
AC 4	9.00deg, 9.00deg	1.00deg, 1.00deg	00:21UTC	678nmi	B747-300	45%

Figure 110 - Scenario 4acPH2H

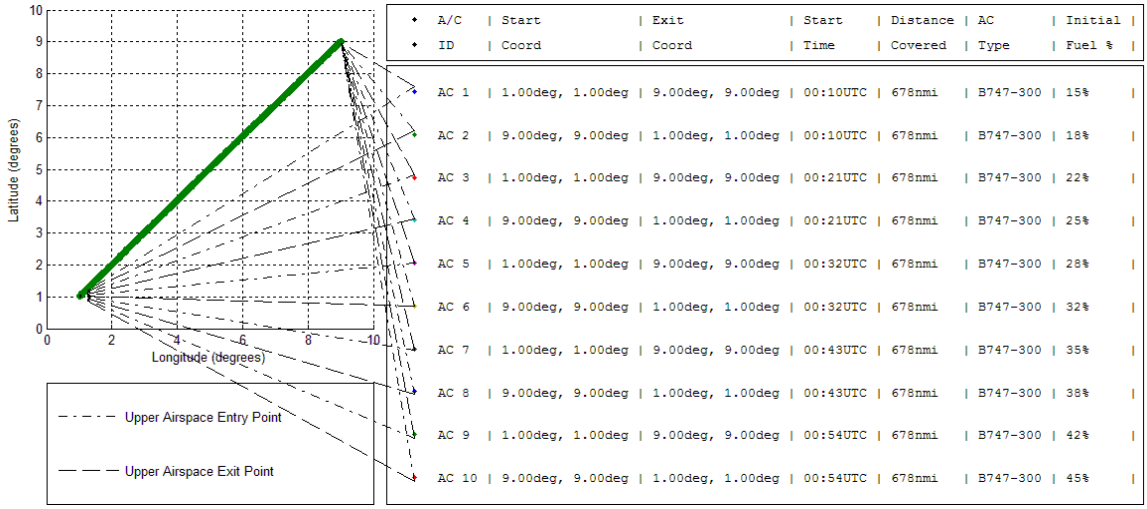

A/C ID	Start Coord	Exit Coord	Start Time	Distance Covered	AC Type	Initial Fuel %
AC 1	1.00deg, 1.00deg	9.00deg, 9.00deg	00:10UTC	678nmi	B747-300	15%
AC 2	9.00deg, 9.00deg	1.00deg, 1.00deg	00:10UTC	678nmi	B747-300	18%
AC 3	1.00deg, 1.00deg	9.00deg, 9.00deg	00:21UTC	678nmi	B747-300	22%
AC 4	9.00deg, 9.00deg	1.00deg, 1.00deg	00:21UTC	678nmi	B747-300	25%
AC 5	1.00deg, 1.00deg	9.00deg, 9.00deg	00:32UTC	678nmi	B747-300	28%
AC 6	9.00deg, 9.00deg	1.00deg, 1.00deg	00:32UTC	678nmi	B747-300	32%
AC 7	1.00deg, 1.00deg	9.00deg, 9.00deg	00:43UTC	678nmi	B747-300	35%
AC 8	9.00deg, 9.00deg	1.00deg, 1.00deg	00:43UTC	678nmi	B747-300	38%
AC 9	1.00deg, 1.00deg	9.00deg, 9.00deg	00:54UTC	678nmi	B747-300	42%
AC 10	9.00deg, 9.00deg	1.00deg, 1.00deg	00:54UTC	678nmi	B747-300	45%

Figure 111 - Scenario 10acPH2H

APPENDIX F Pre Control NODE Division Results

The following graphical results show the errors and issues that caused the control node division mentioned in section 3.3.5. For discussion of the results and impacts of these results, please refer to that section. For instructions on how to read the graphs, please refer to section 3.4.1. To recap, each section in this appendix shows three graphs:

- The first graphs shows optimization results of the scenario assuming fuel minimization with no constraint on ETA.
- The second graph shows is the same as the first, but with a constraint on ETA requiring aircraft to land at a time such that their average speed over the entire journey was 420kts. Please refer to section 3.4 for rationale.
- The third compares the trajectory shape, fuel usage and flight time of each aircraft between the results of the first and second graph

To be clear, the main difference between these results and the results in other appendices was that ATD_N was used as the baseline for the optimizer variable, and as the baseline for calculating aircraft fuel usage and performance; later results will use ATD_N as the baseline for the optimizer variable and ATD_i as the baseline for calculating aircraft fuel usage and performance.

F.1 Generic Boeing 747-300 - Scenario 2acPSd

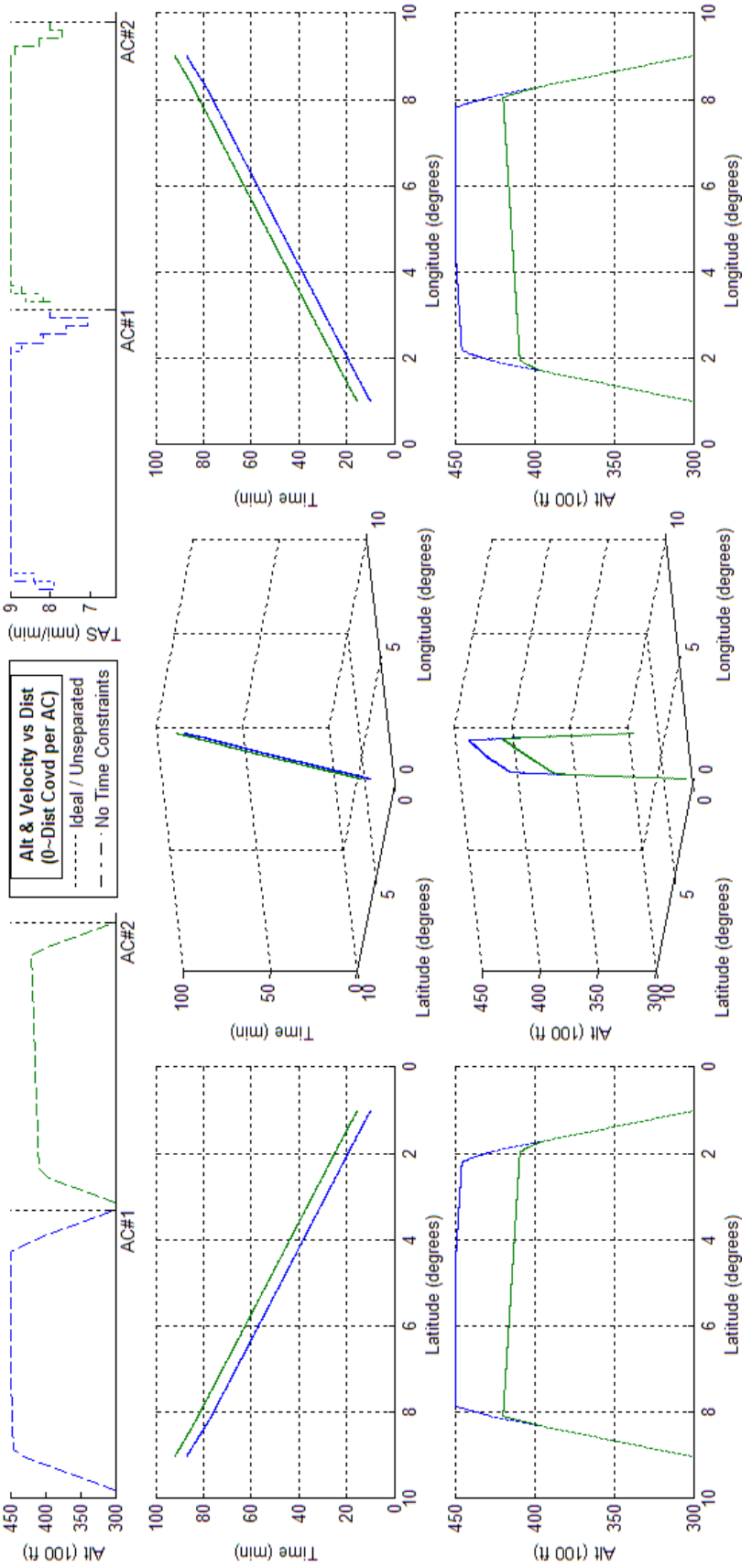

Figure 112 - Optimized 2acPSd assuming no arrival time constraints.

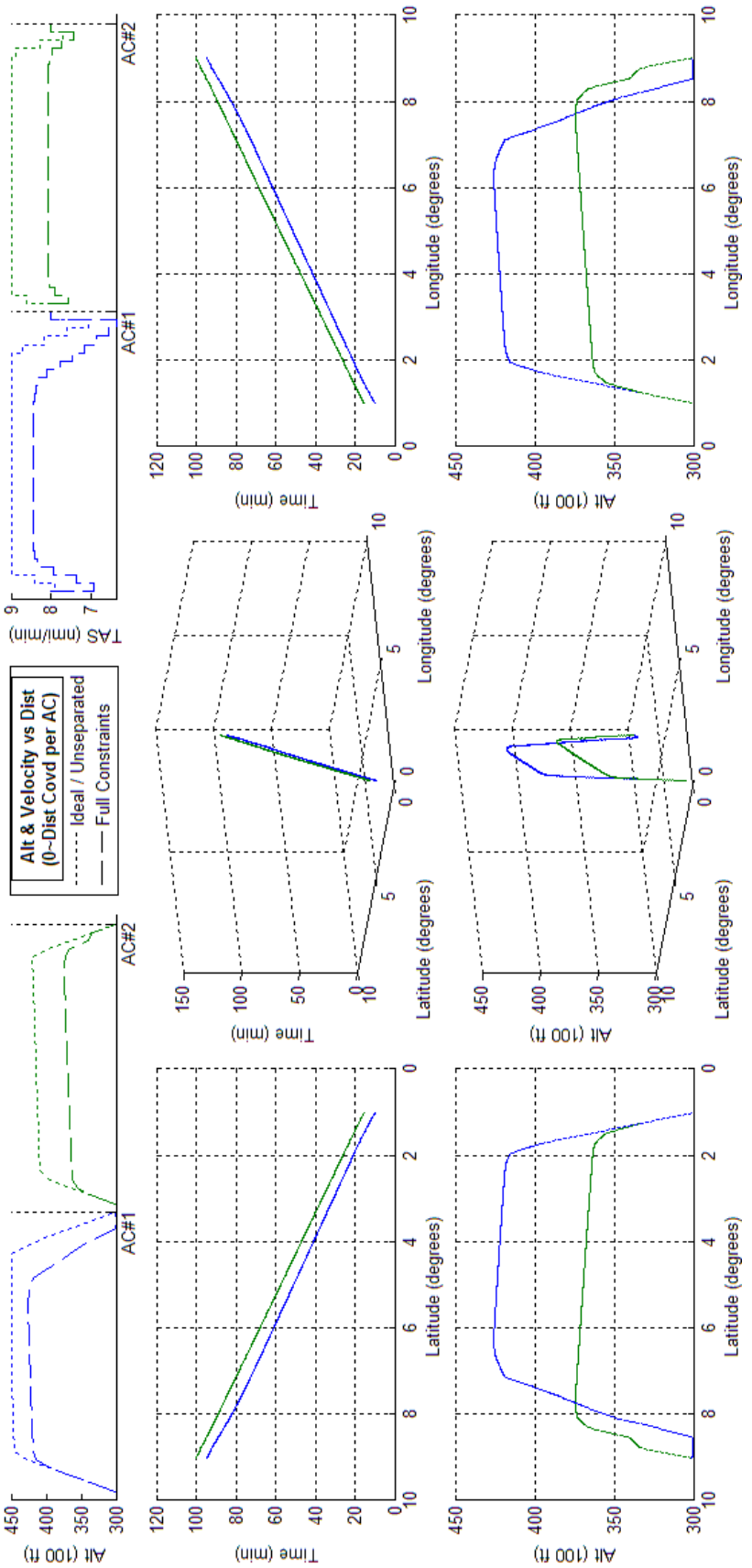

Figure 113 - Optimized 2acPSd assuming arrival time constraints.

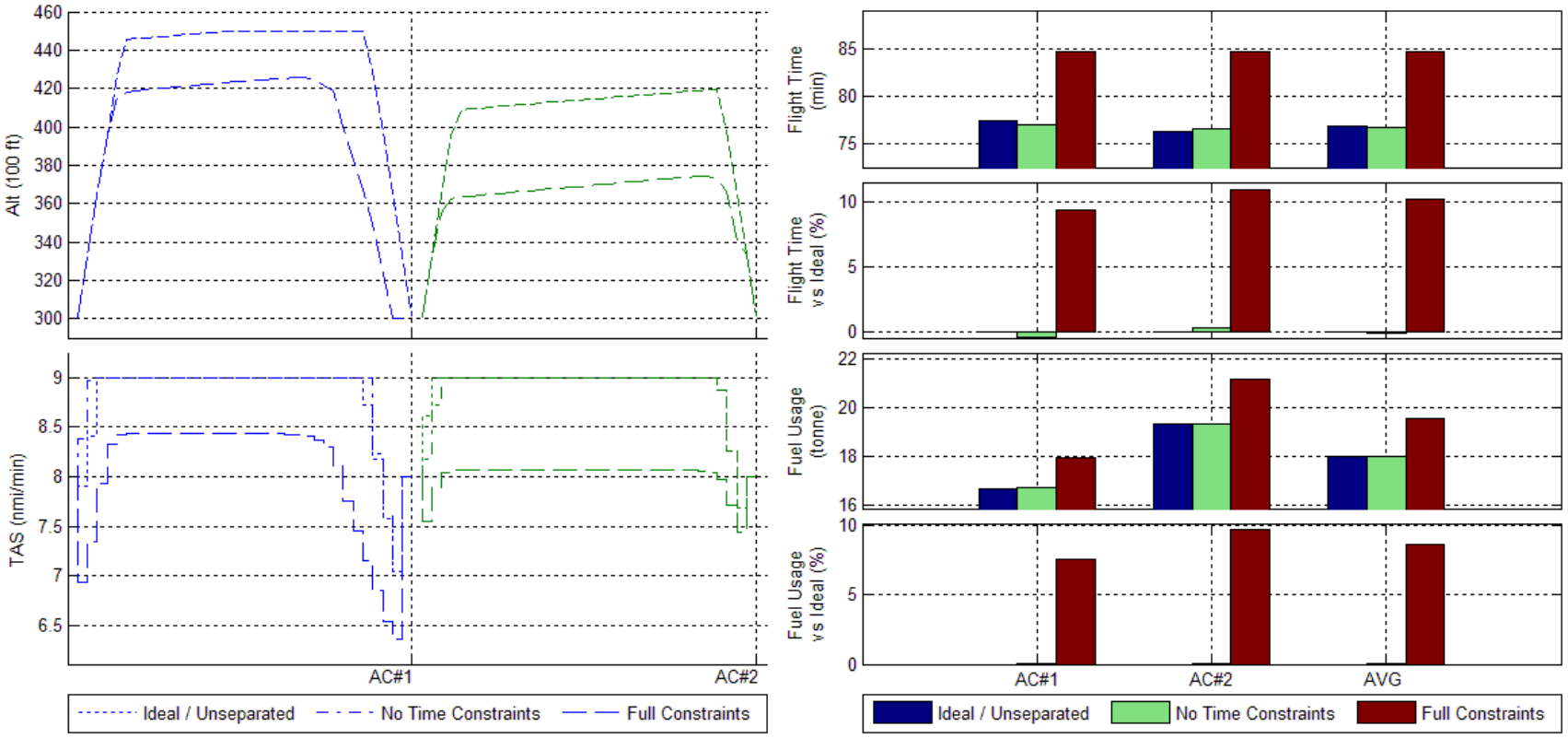

Figure 114 Trajectory Shape, Flight Time, and Fuel Consumption Comparisons of Optimized 2acPSd results with and without an arrival time constraint

F.2 Scenario 4acPSd

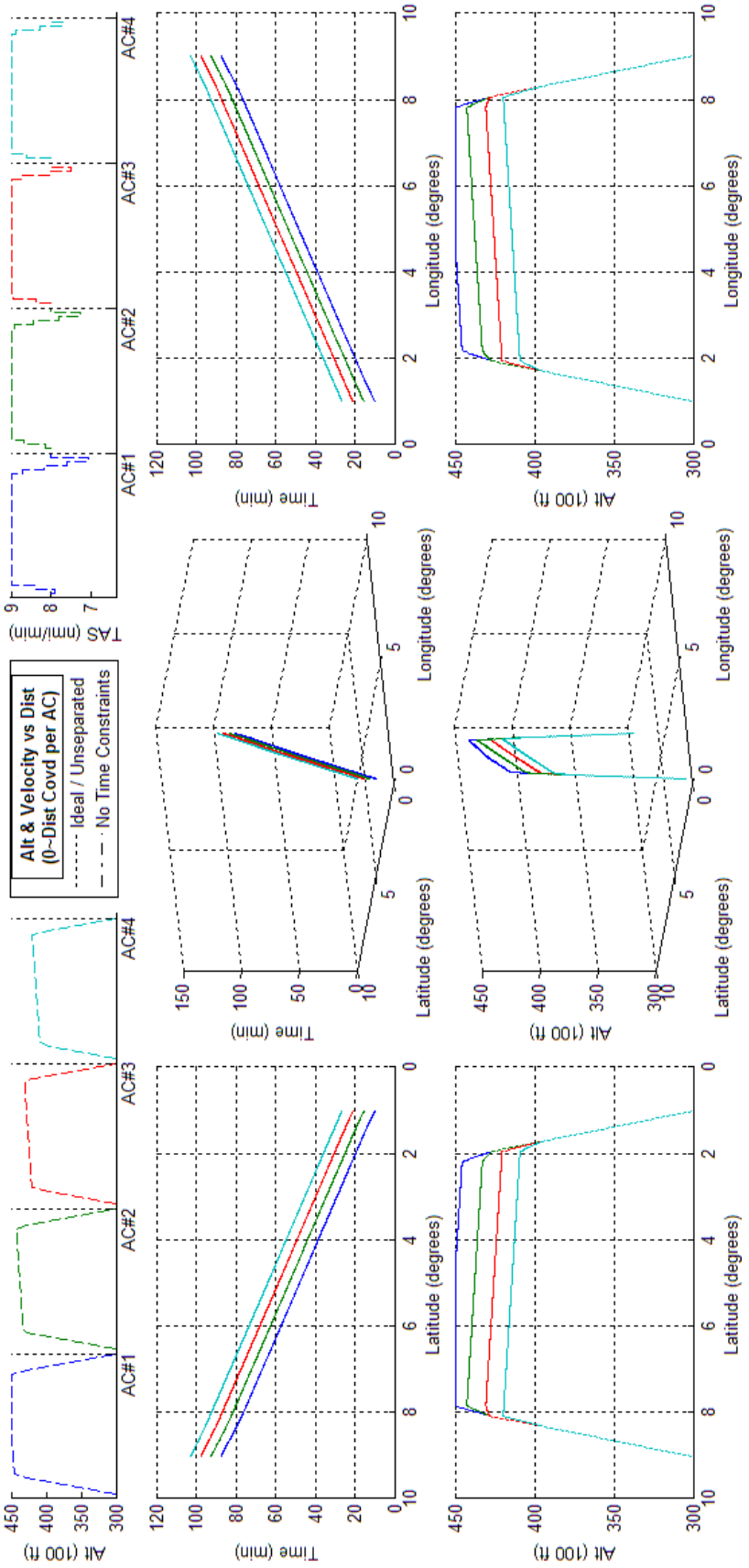

Figure 115 - Optimized 4acPSd assuming no arrival time constraints.

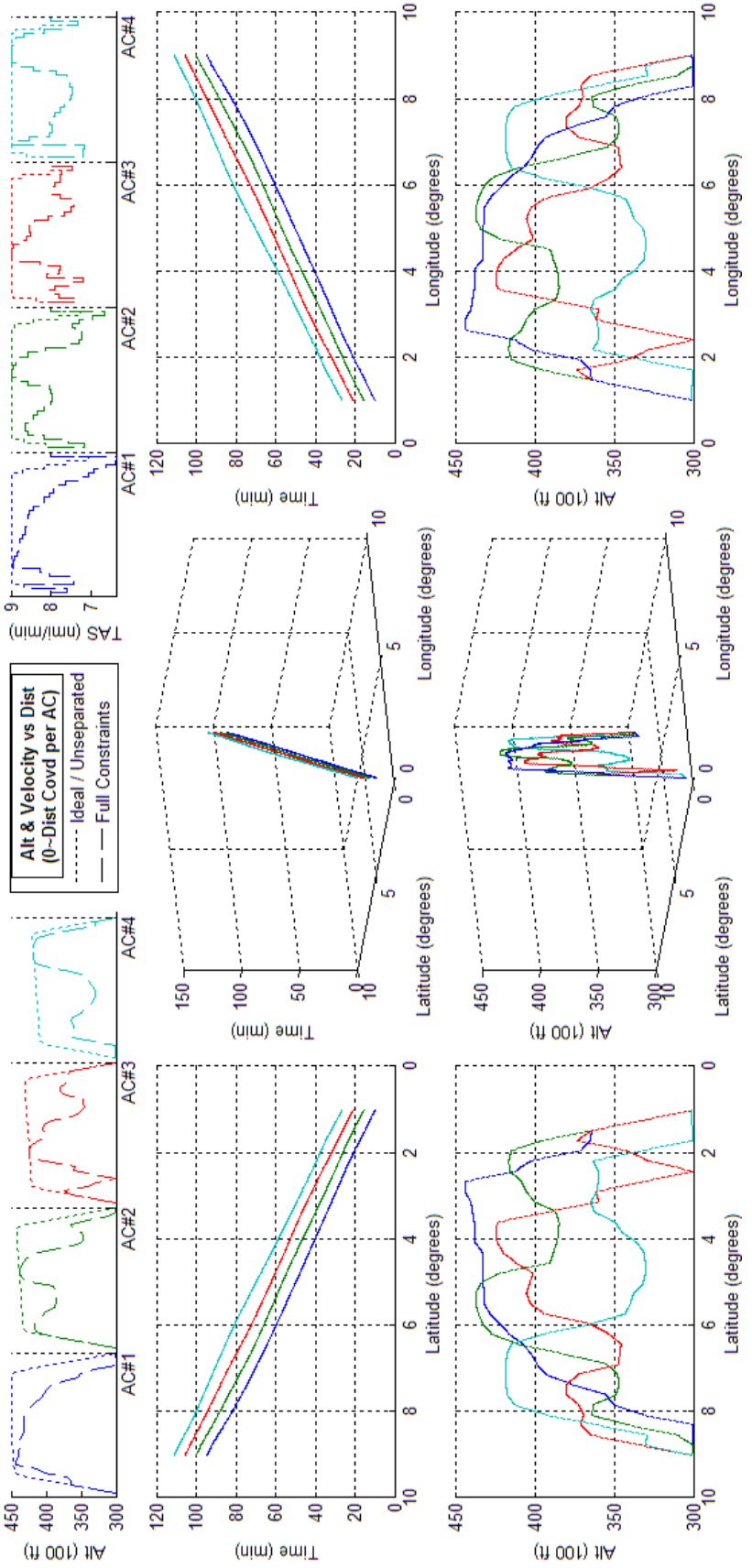

Figure 116 - Optimized 4acPSd assuming arrival time constraints.

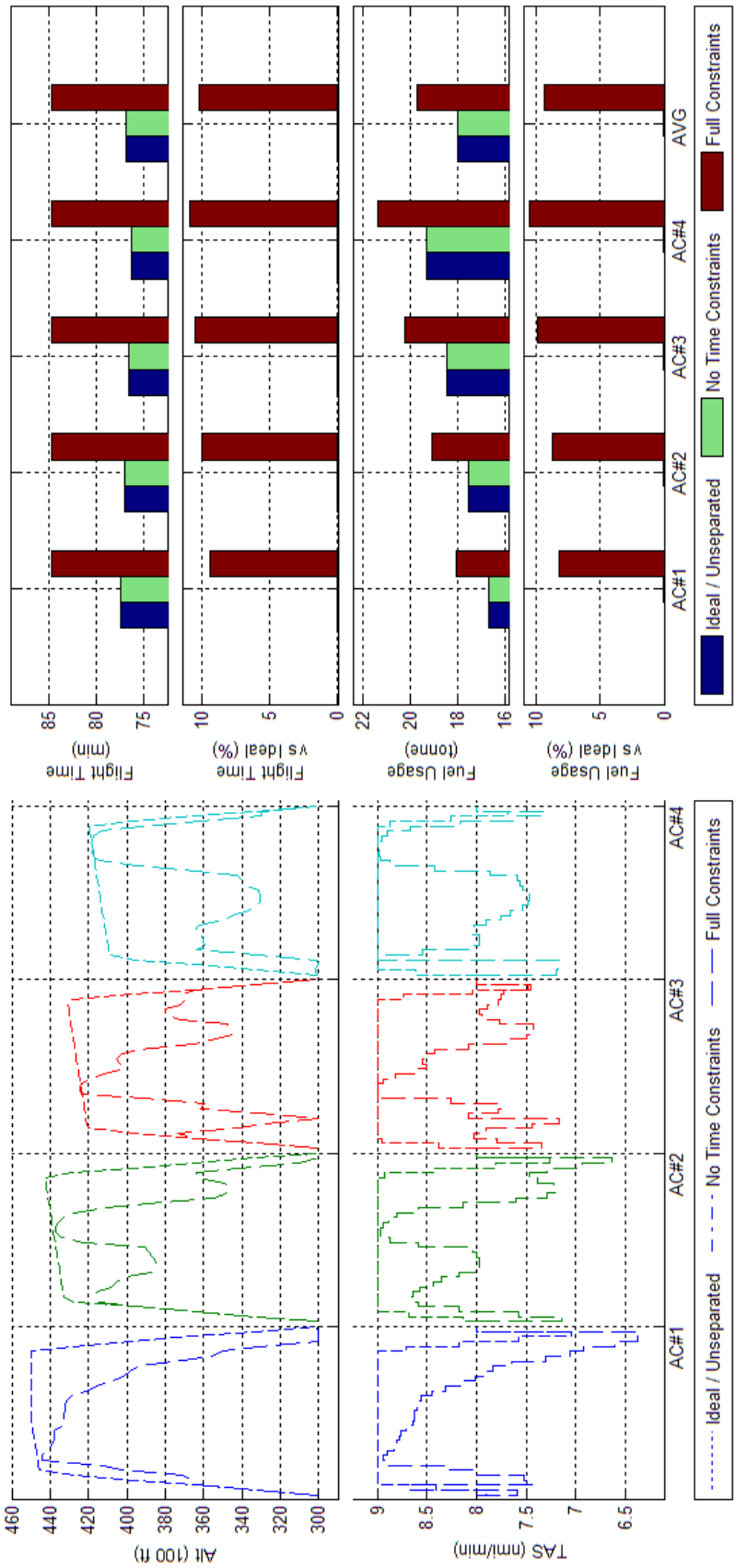

Figure 117 Trajectory Shape, Flight Time, and Fuel Consumption Comparisons of Optimized 4acPSd results with and without an arrival time constraint

F.3 Generic Boeing 747-300 - Scenario 10acPSd

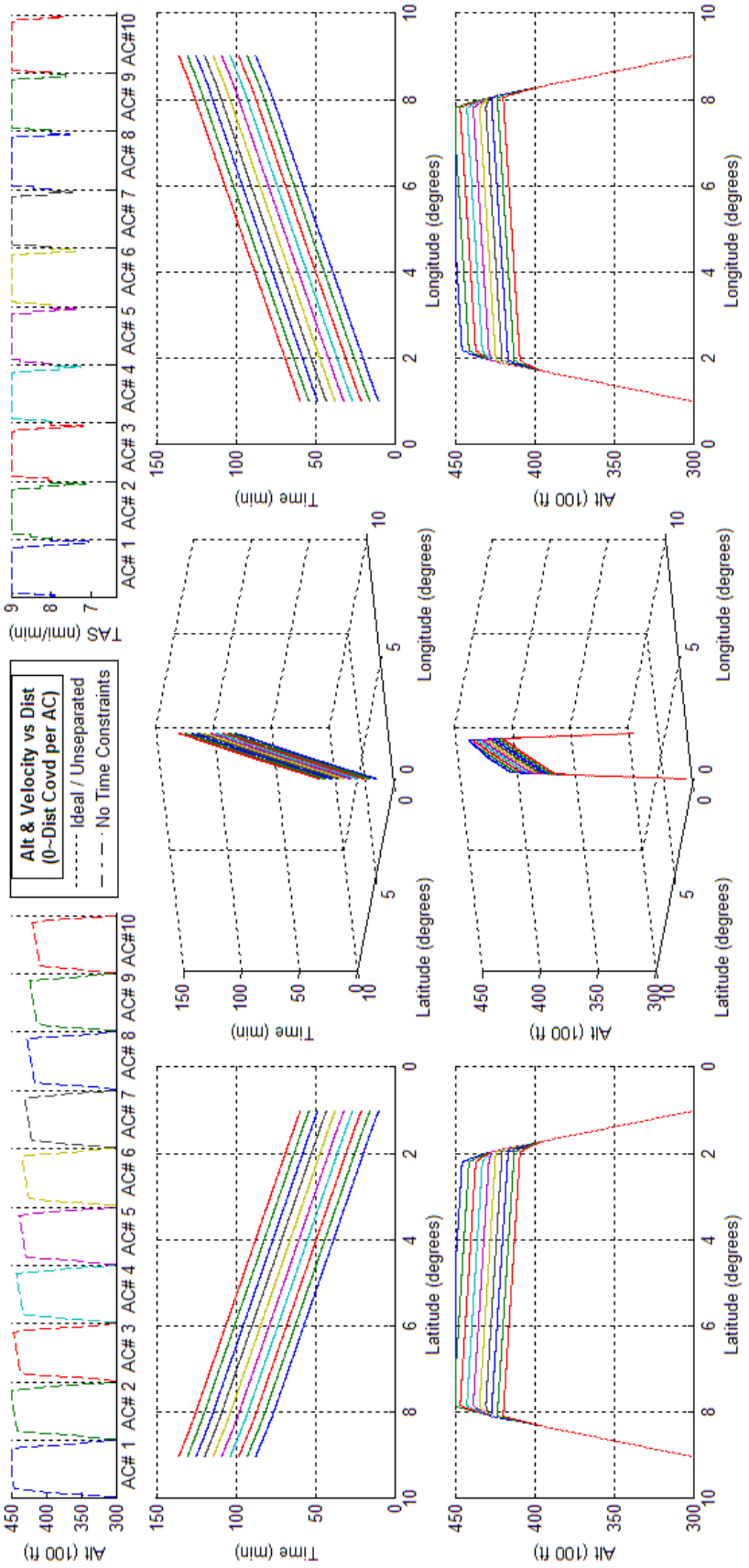

Figure 118 - Optimized 10acPSd assuming no arrival time constraints.

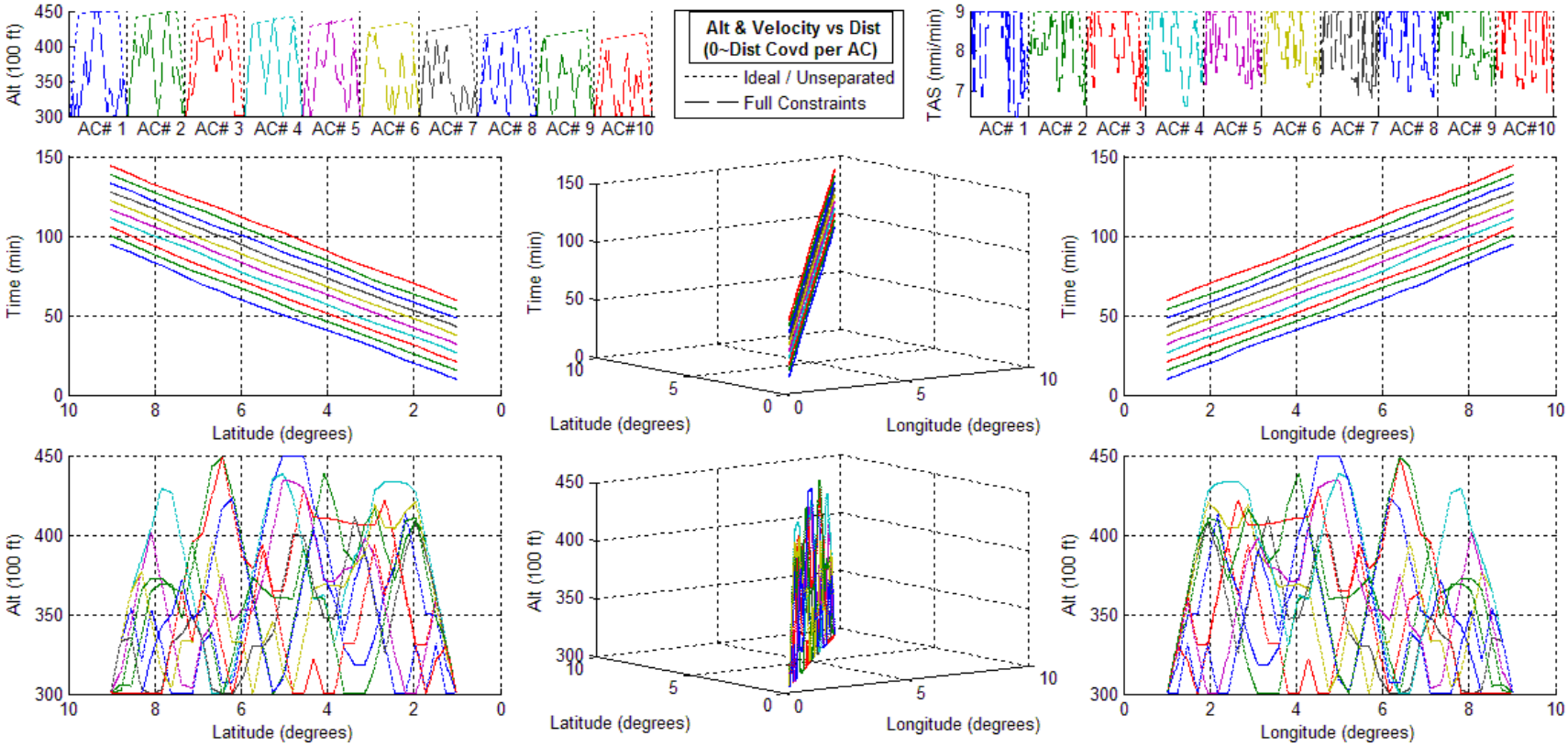

Figure 119 - Optimized 10acPSd assuming arrival time constraints.

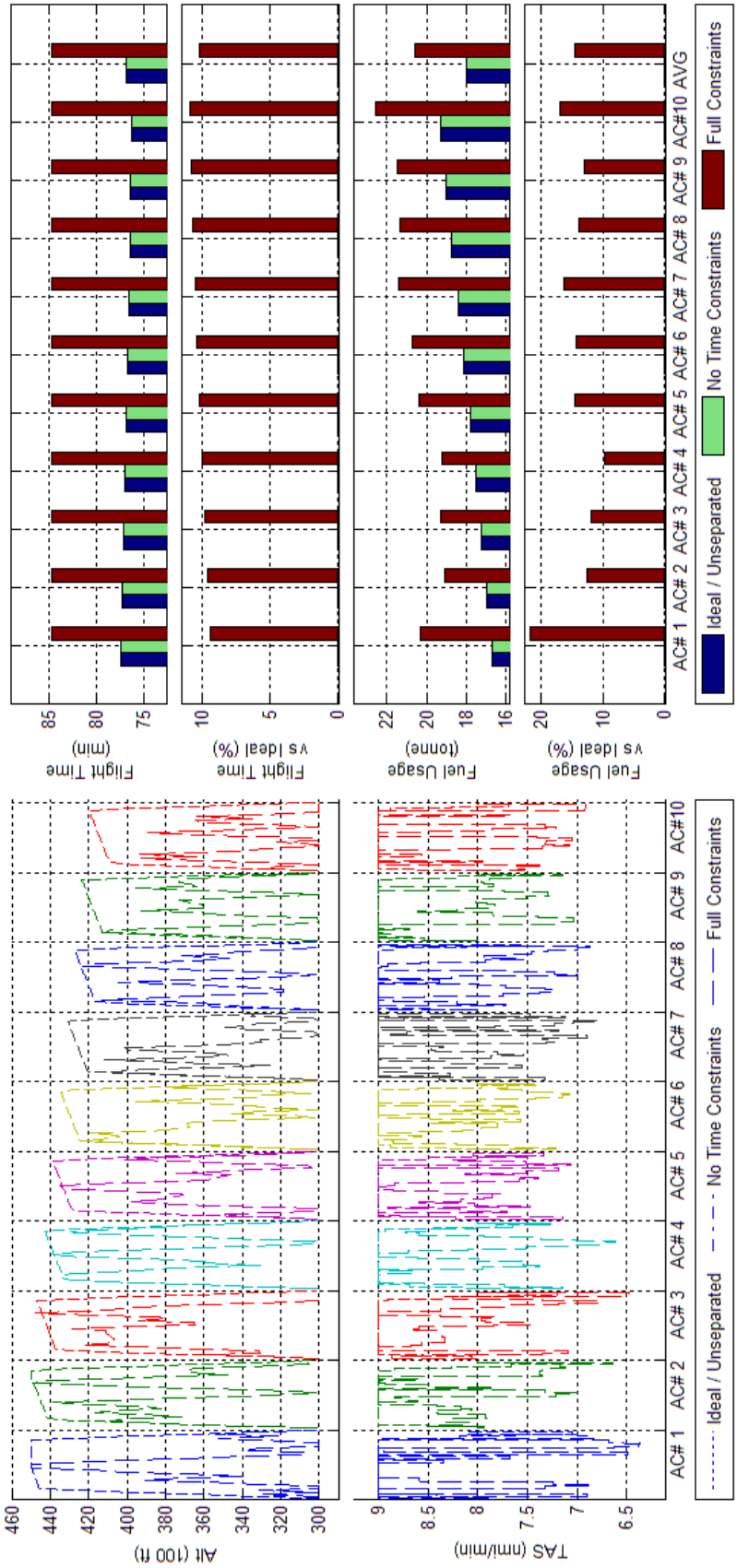

Figure 120 Trajectory Shape, Flight Time, and Fuel Consumption Comparisons of Optimized 10acPSd results with and without an arrival time constraint

F.4 Generic Boeing 747-300 - Scenario 2acCO

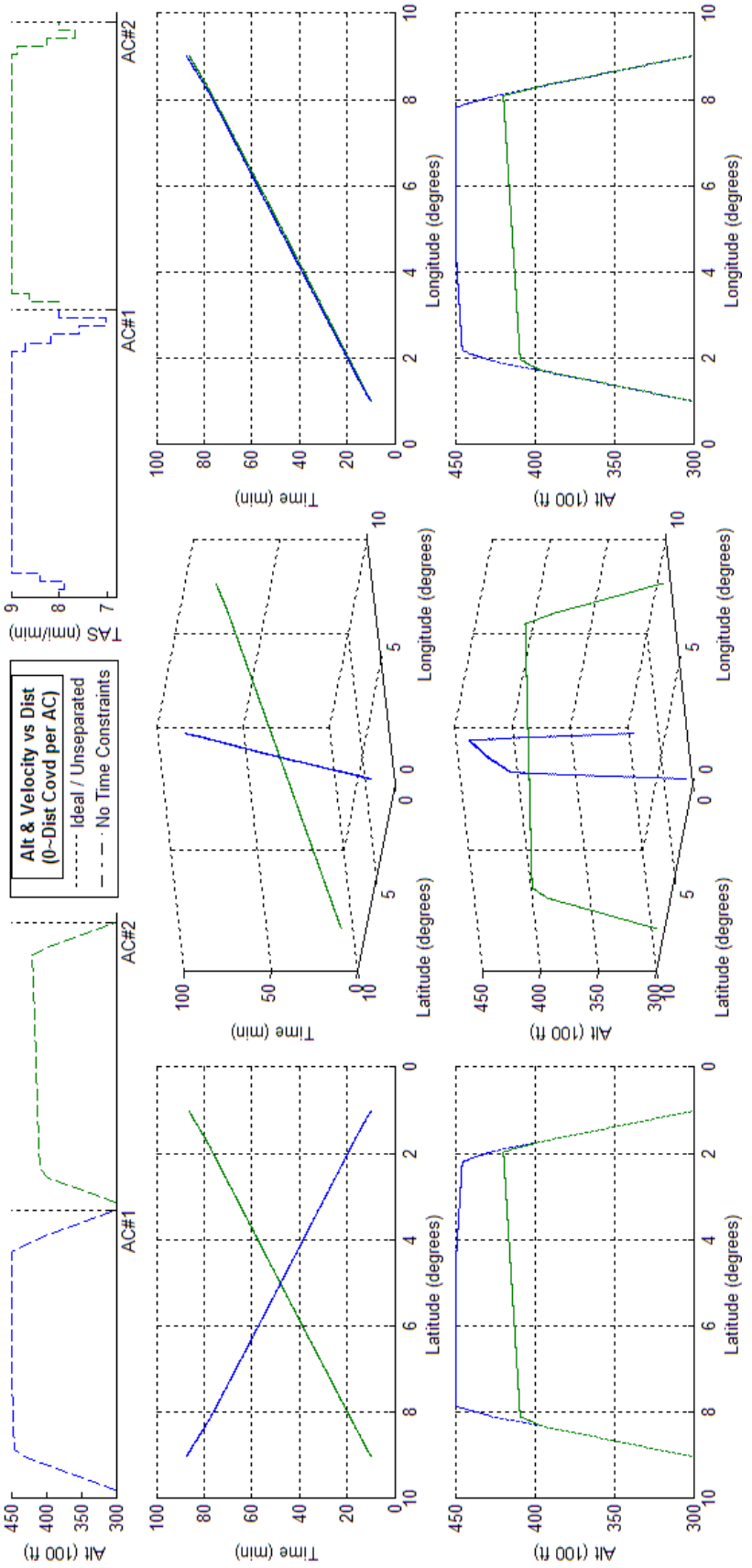

Figure 121 - Optimized 2acCO assuming no arrival time constraints.

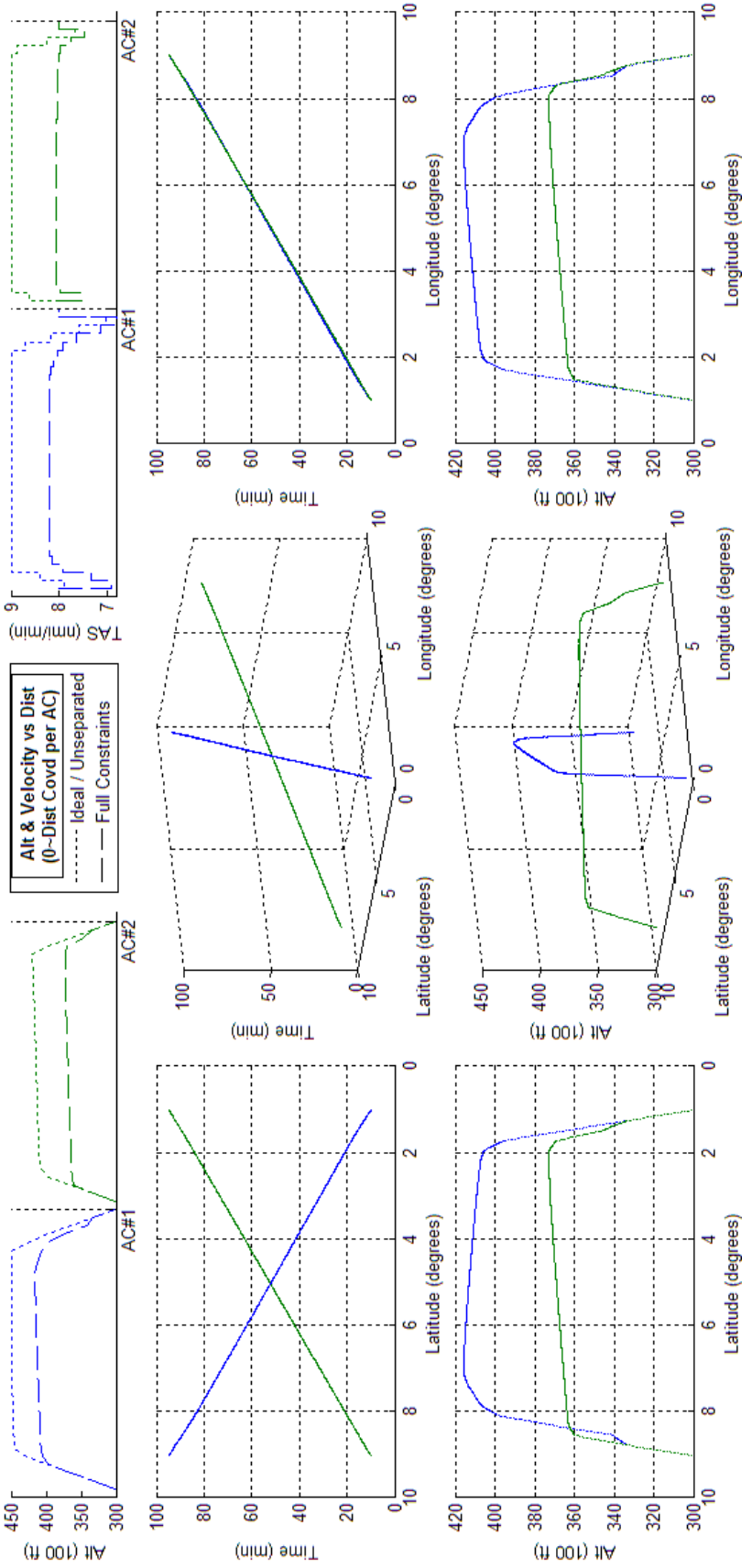

Figure 122 - Optimized 2acCO assuming arrival time constraints.

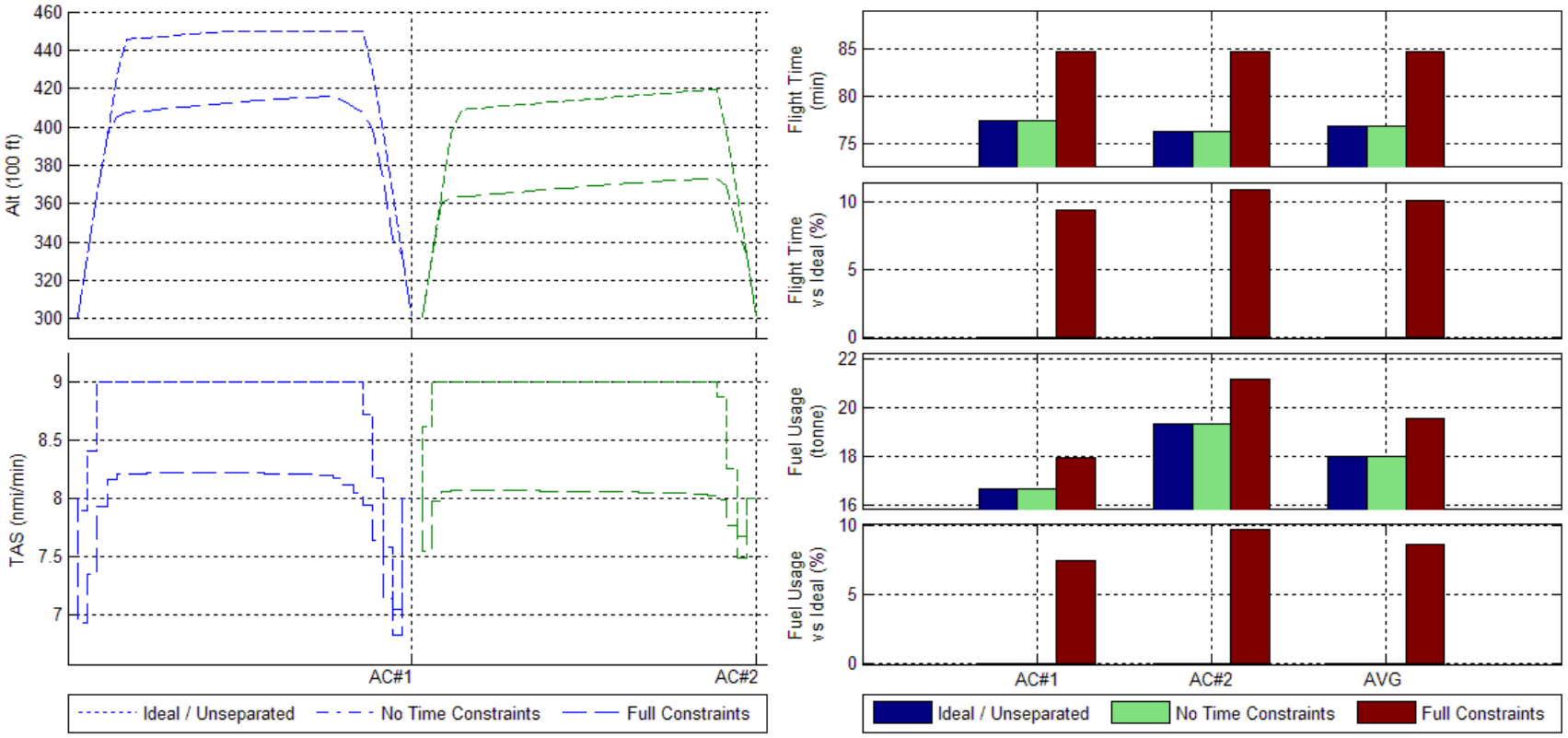

Figure 123 Trajectory Shape, Flight Time, and Fuel Consumption Comparisons of Optimized 2acCO results with and without an arrival time constraint

F.5 Generic Boeing 747-300 - Scenario 4acCO

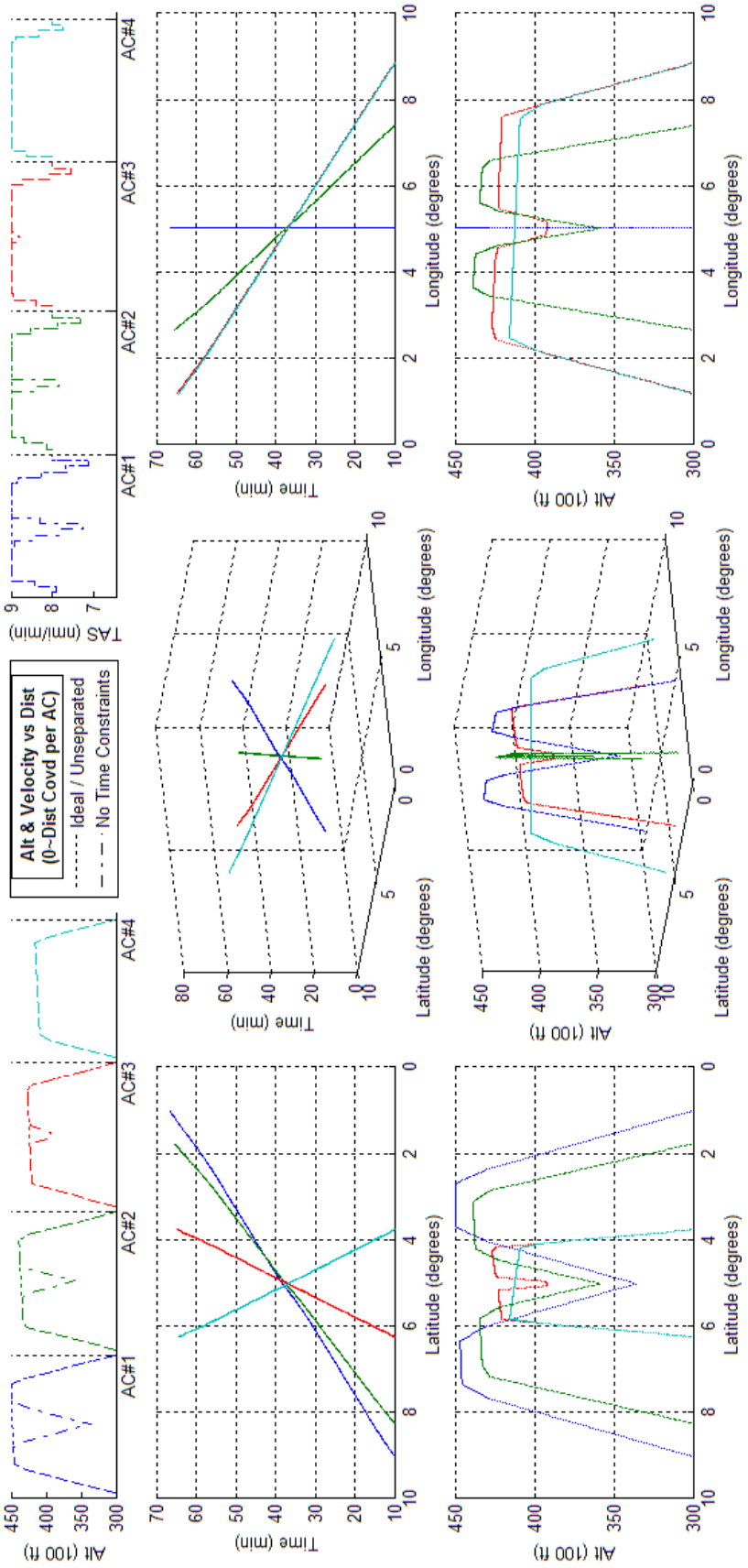

Figure 124 - Optimized 4acCO assuming no arrival time constraints.

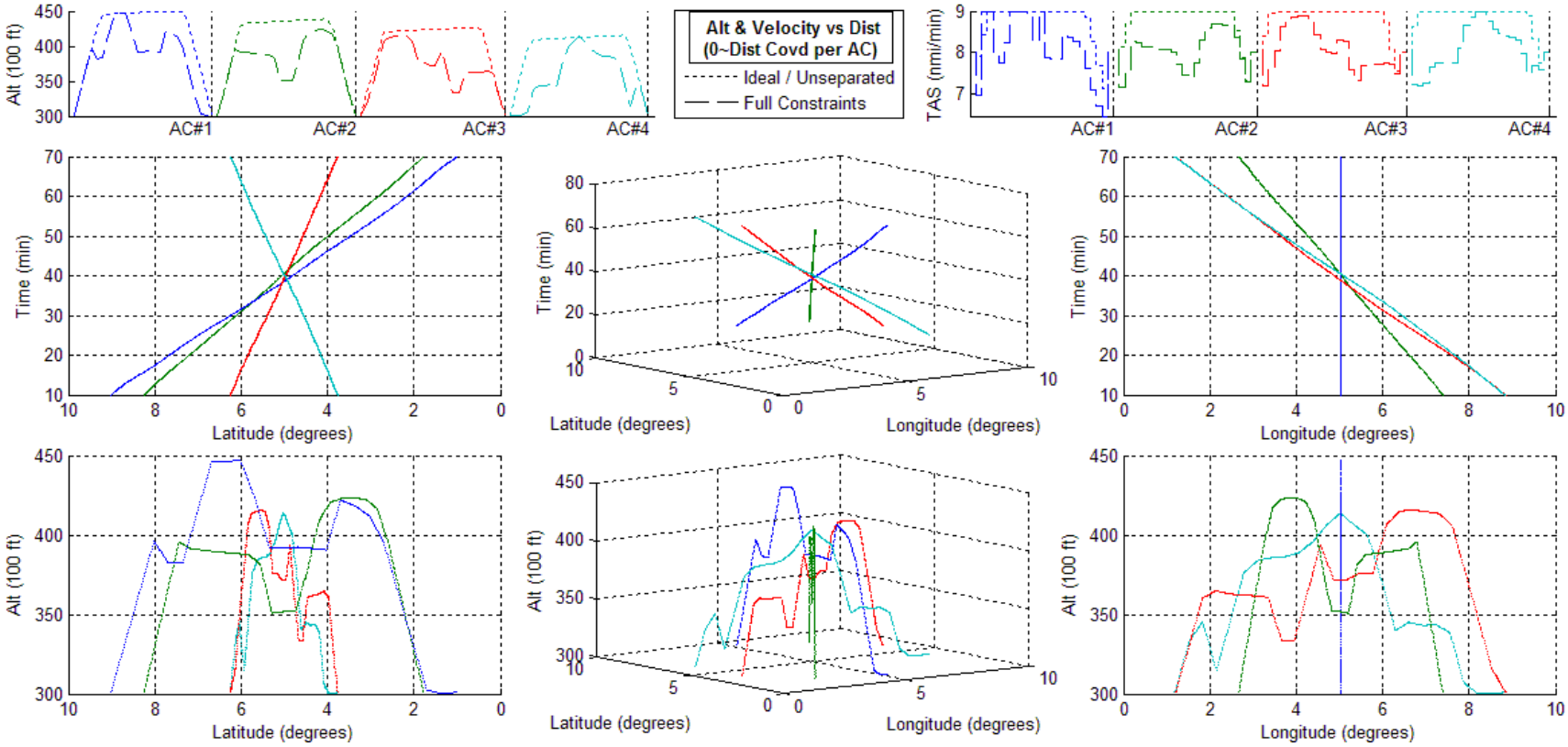

Figure 125 - Optimized 4acCO assuming arrival time constraints.

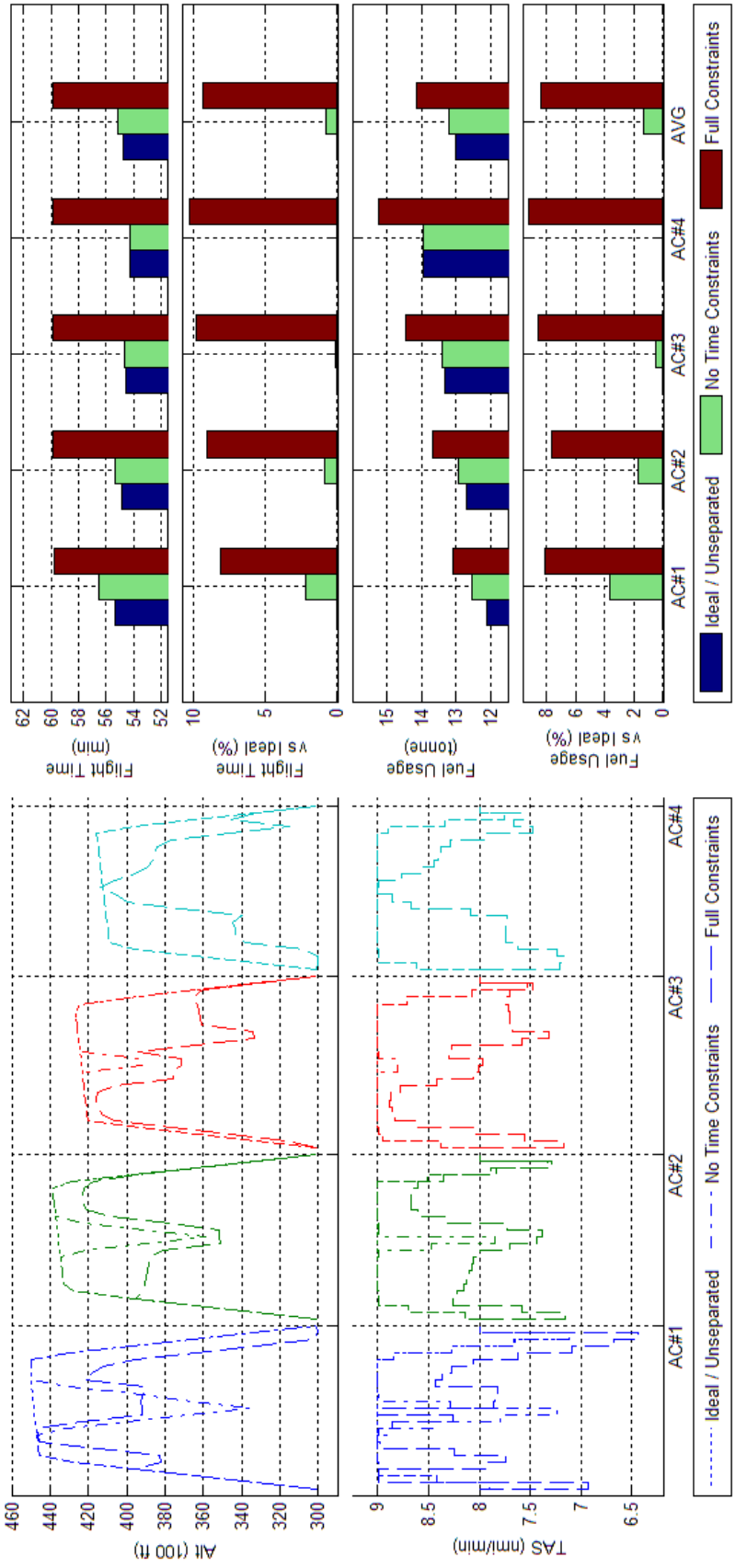

Figure 126 Trajectory Shape, Flight Time, and Fuel Consumption Comparisons of Optimized 4acCO results with and without an arrival time constraint

F.6 Generic Boeing 747-300 - Scenario 10acCO

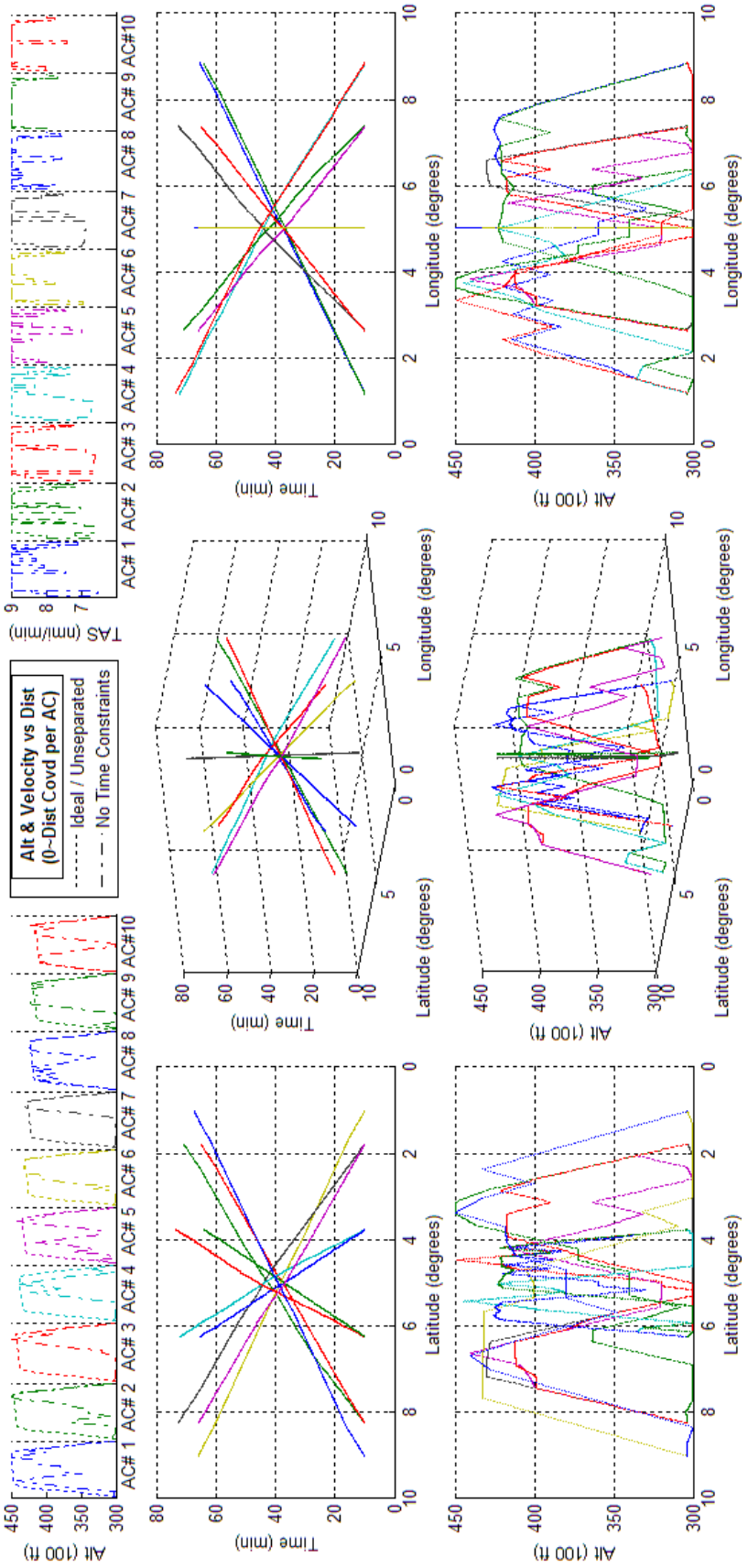

Figure 127 - Optimized 10acCO assuming no arrival time constraints.

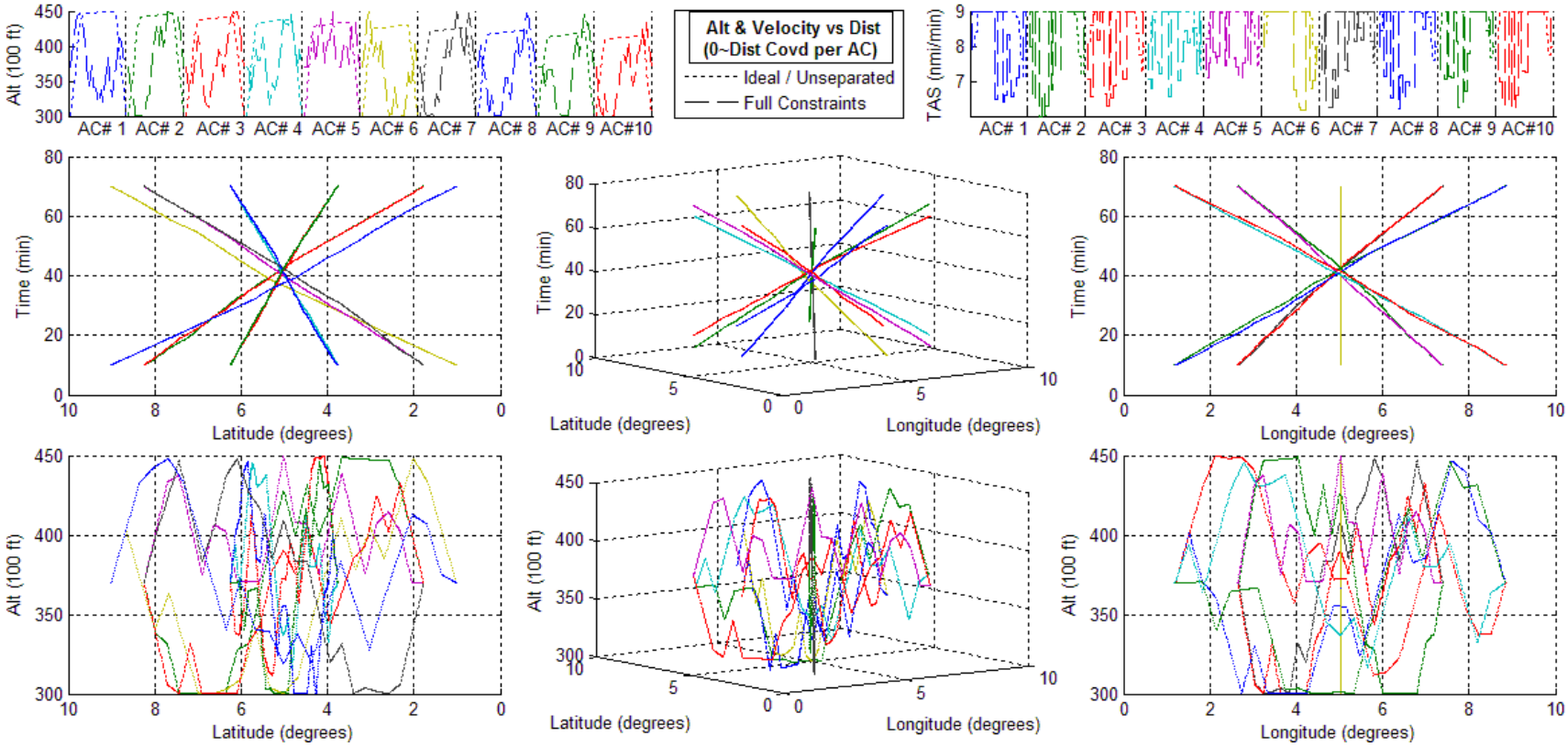

Figure 128 - Optimized 10acCO assuming arrival time constraints.

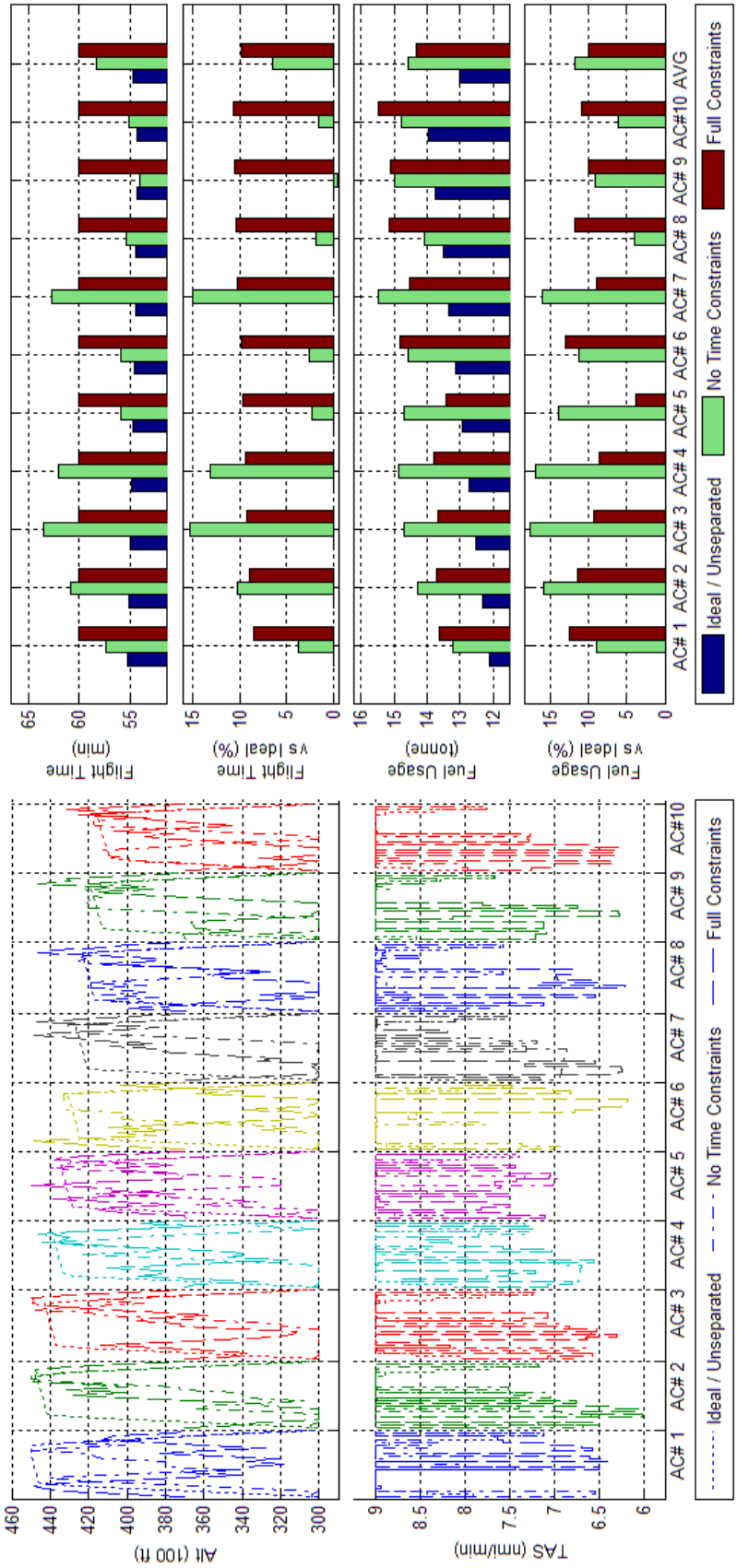

Figure 129 Trajectory Shape, Flight Time, and Fuel Consumption Comparisons of Optimized 10acCO results with and without an arrival time constraint

F.7 Generic Boeing 747-300 - Scenario 4acCH

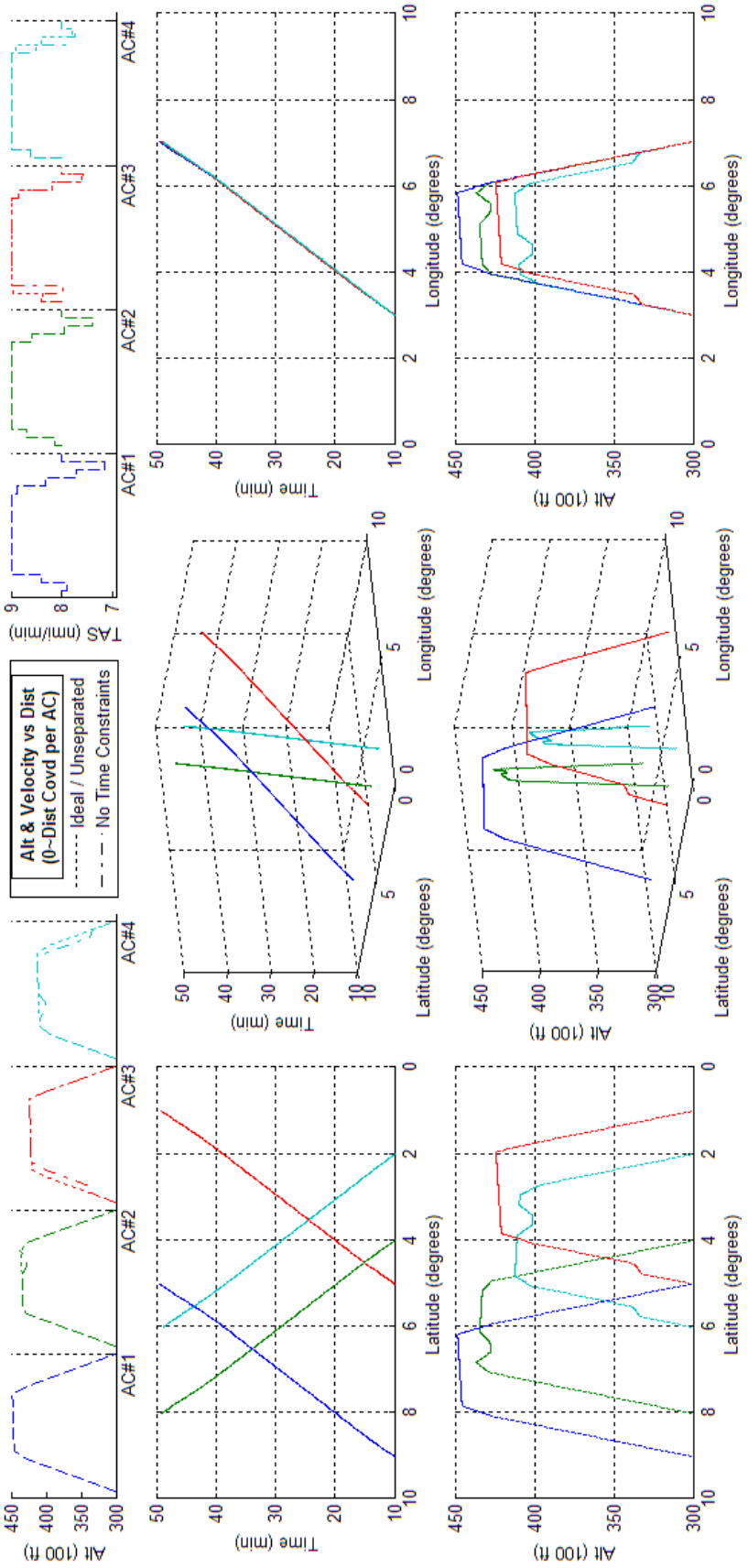

Figure 130 - Optimized 4acCH assuming no arrival time constraints.

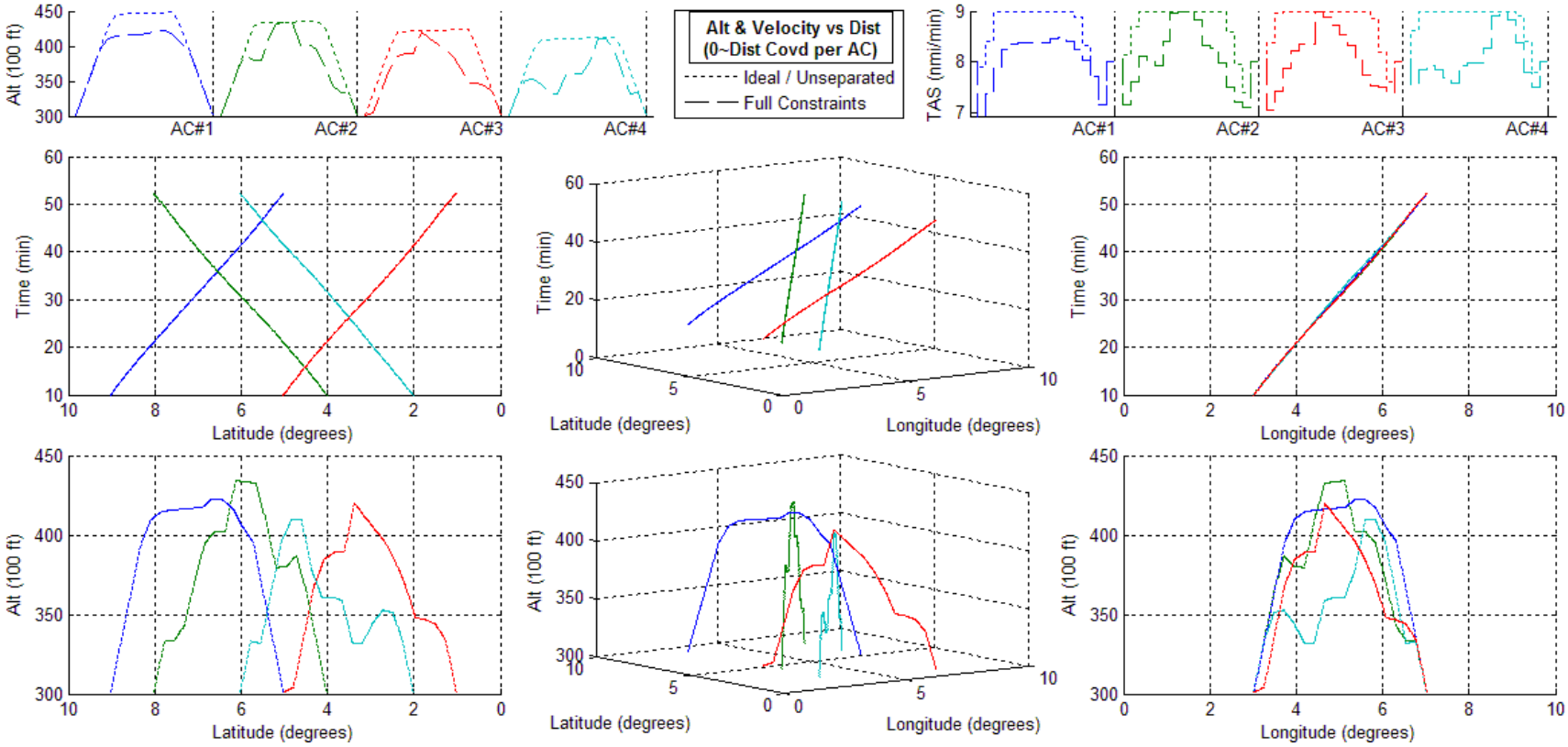

Figure 131 - Optimized 4acCH assuming arrival time constraints.

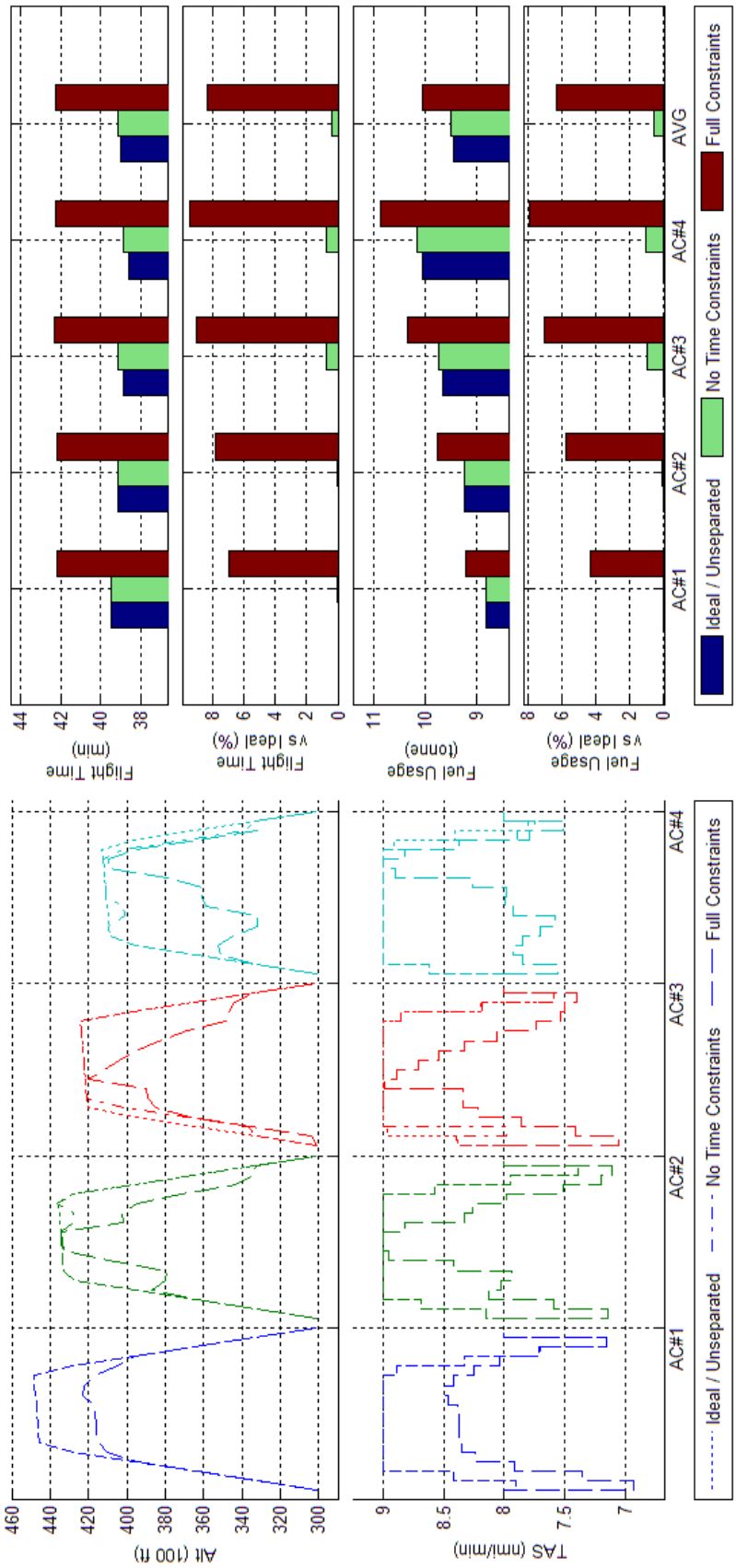

Figure 132 Trajectory Shape, Flight Time, and Fuel Consumption Comparisons of Optimized 4acCH results with and without an arrival time constraint

F.8 Generic Boeing 747-300 - Scenario 10acCH

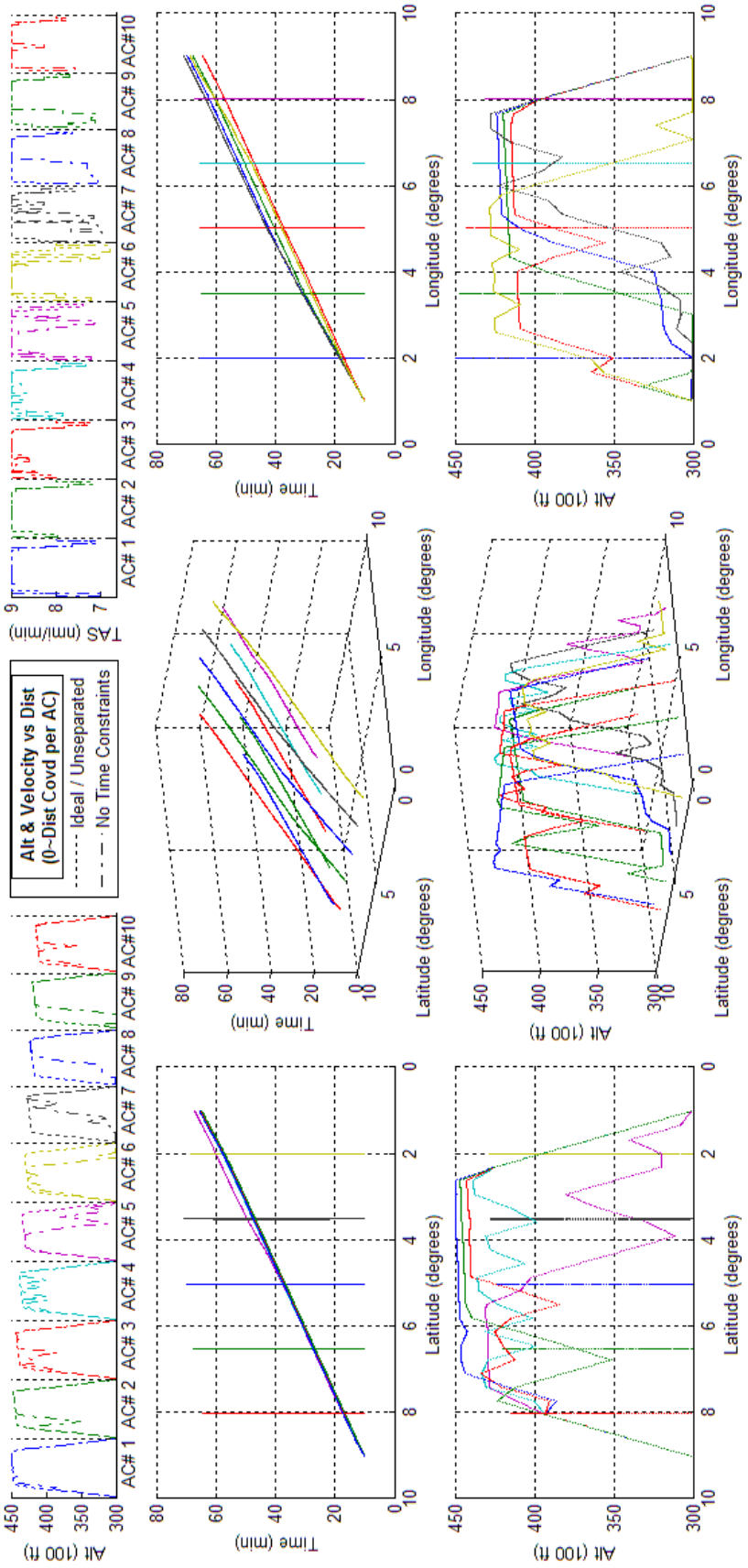

Figure 133 - Optimized 10acCH assuming no arrival time constraints.

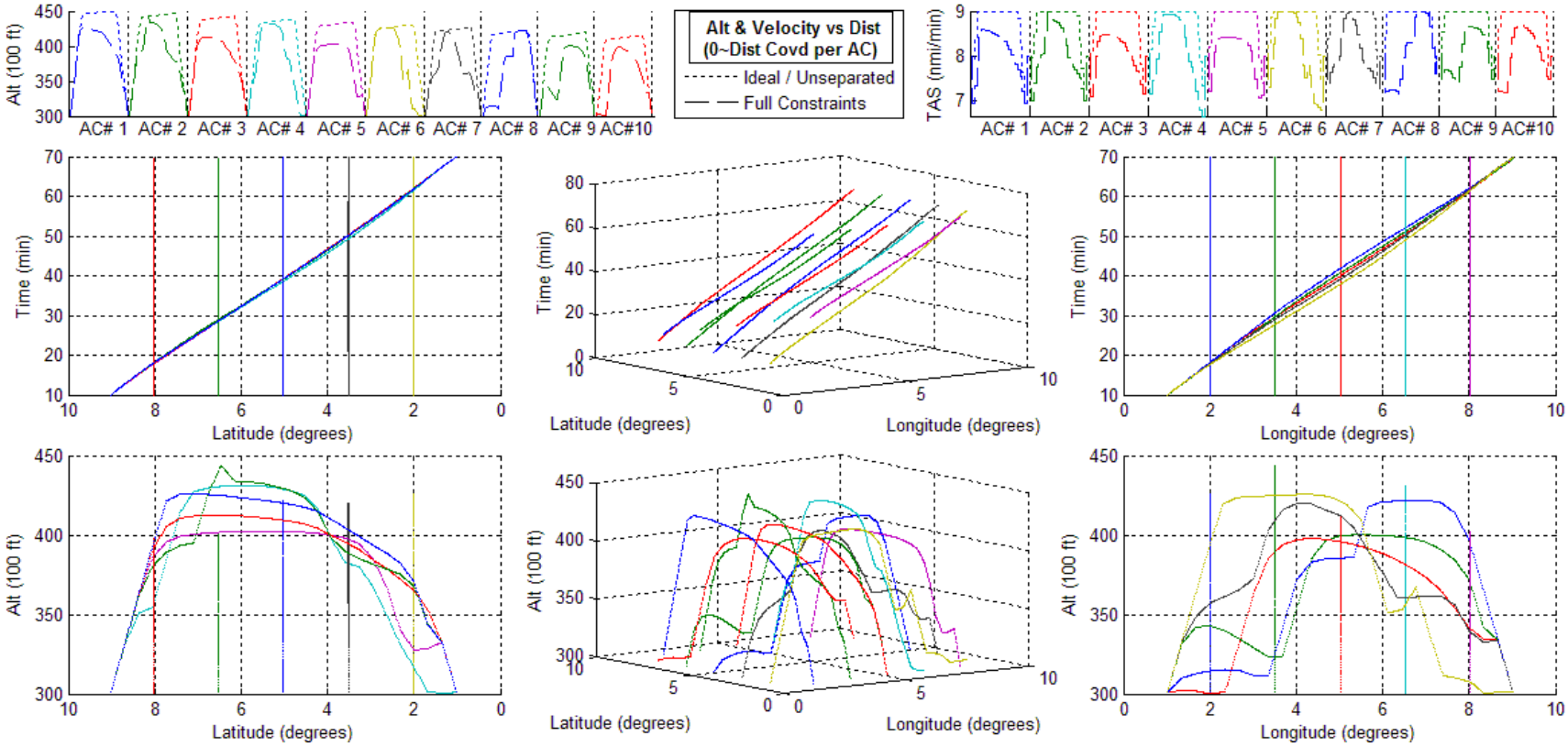

Figure 134 - Optimized 10acCH assuming arrival time constraints.

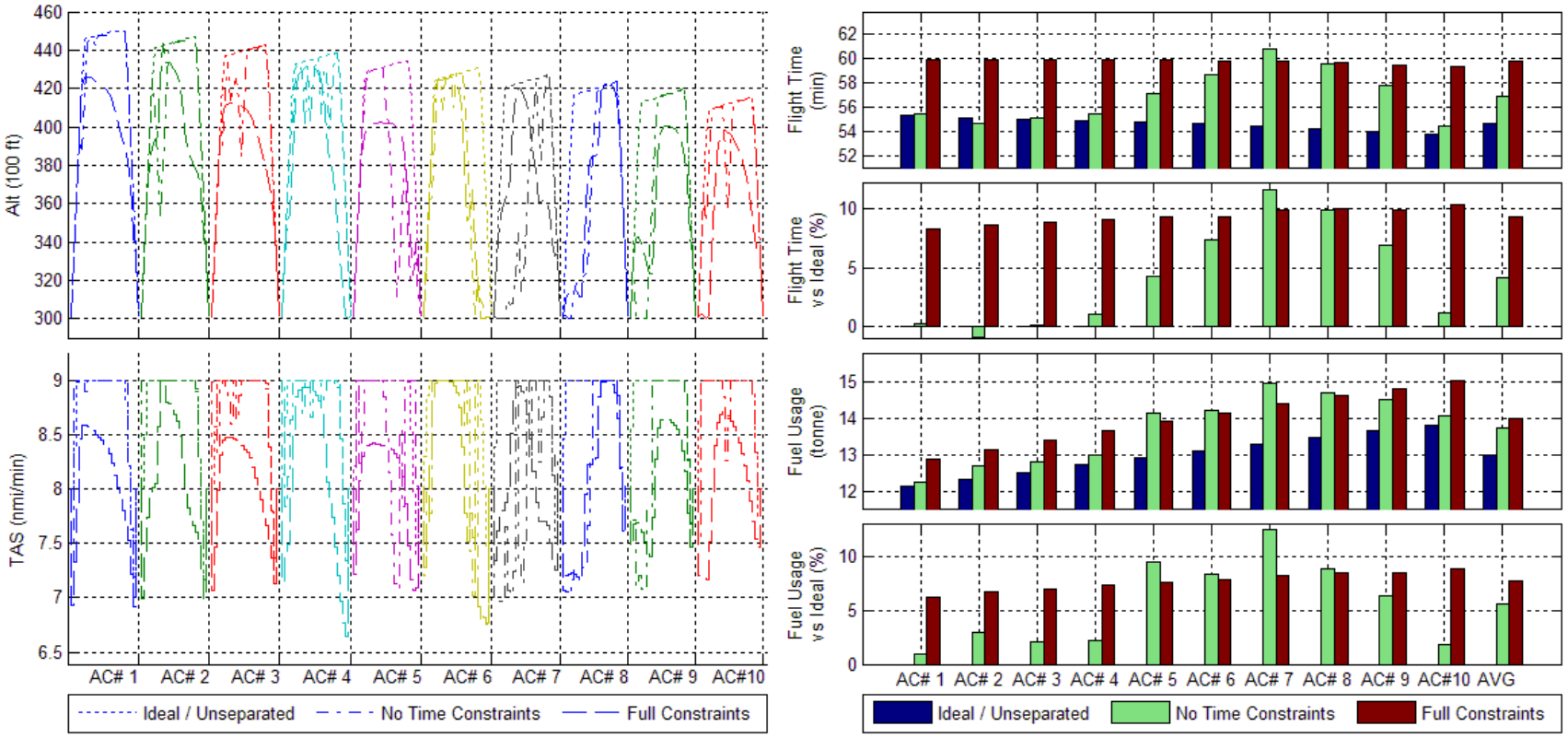

Figure 135 Trajectory Shape, Flight Time, and Fuel Consumption Comparisons of Optimized 10acCH results with and without an arrival time constraint

F.9 Generic Boeing 747-300 - Scenario 2acPH2H

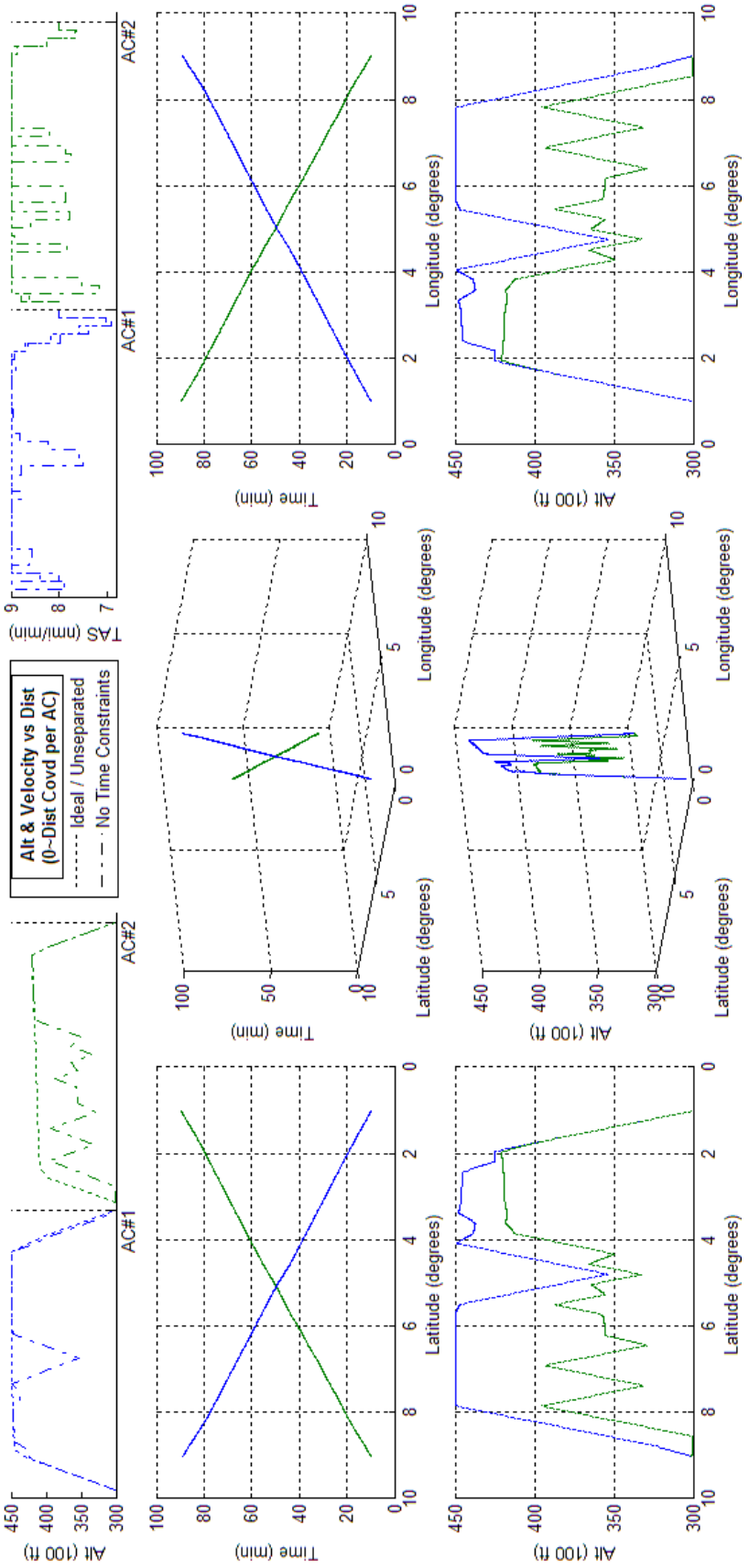

Figure 136 - Optimized 2acPH2H assuming no arrival time constraints.

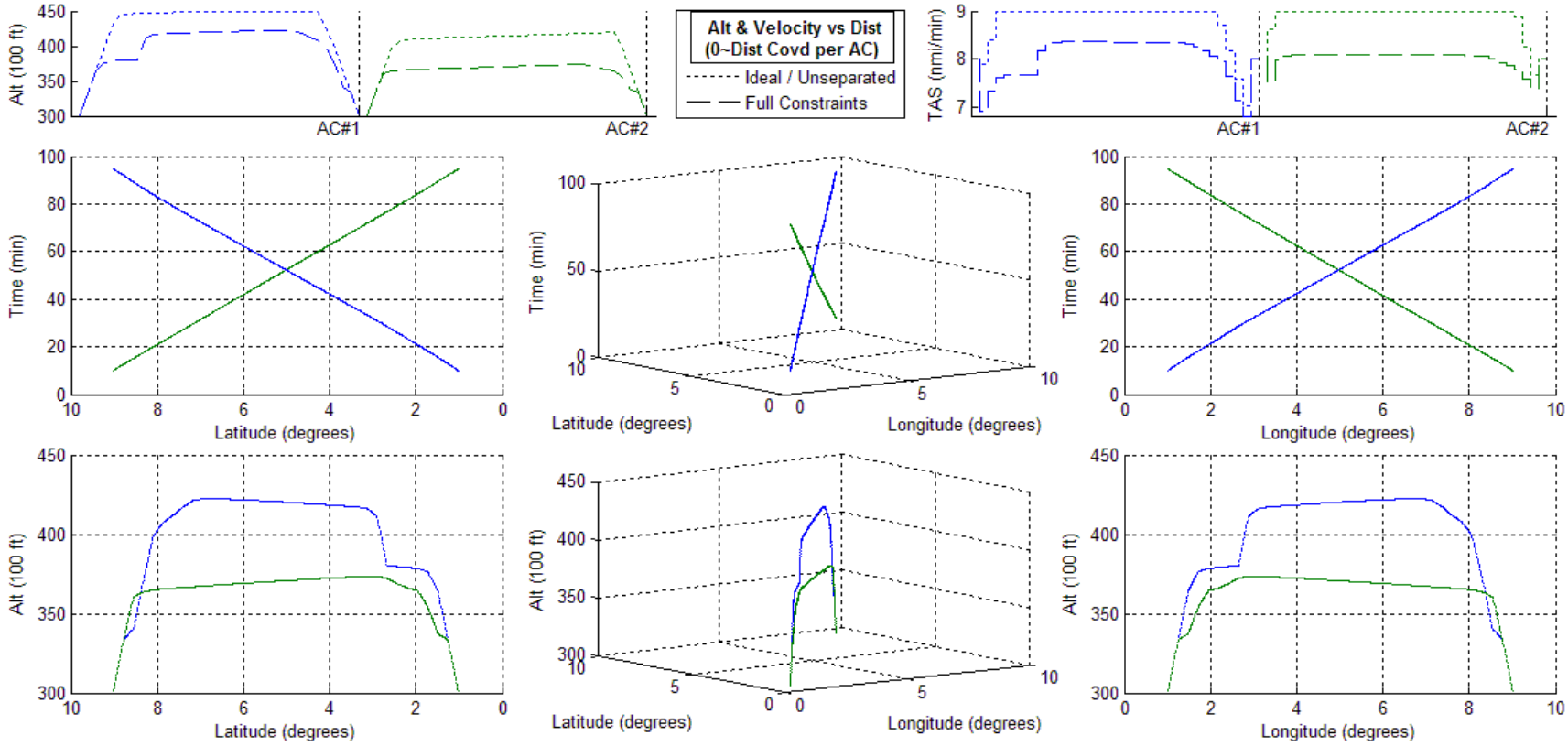

Figure 137 - Optimized 2acPH2H assuming arrival time constraints.

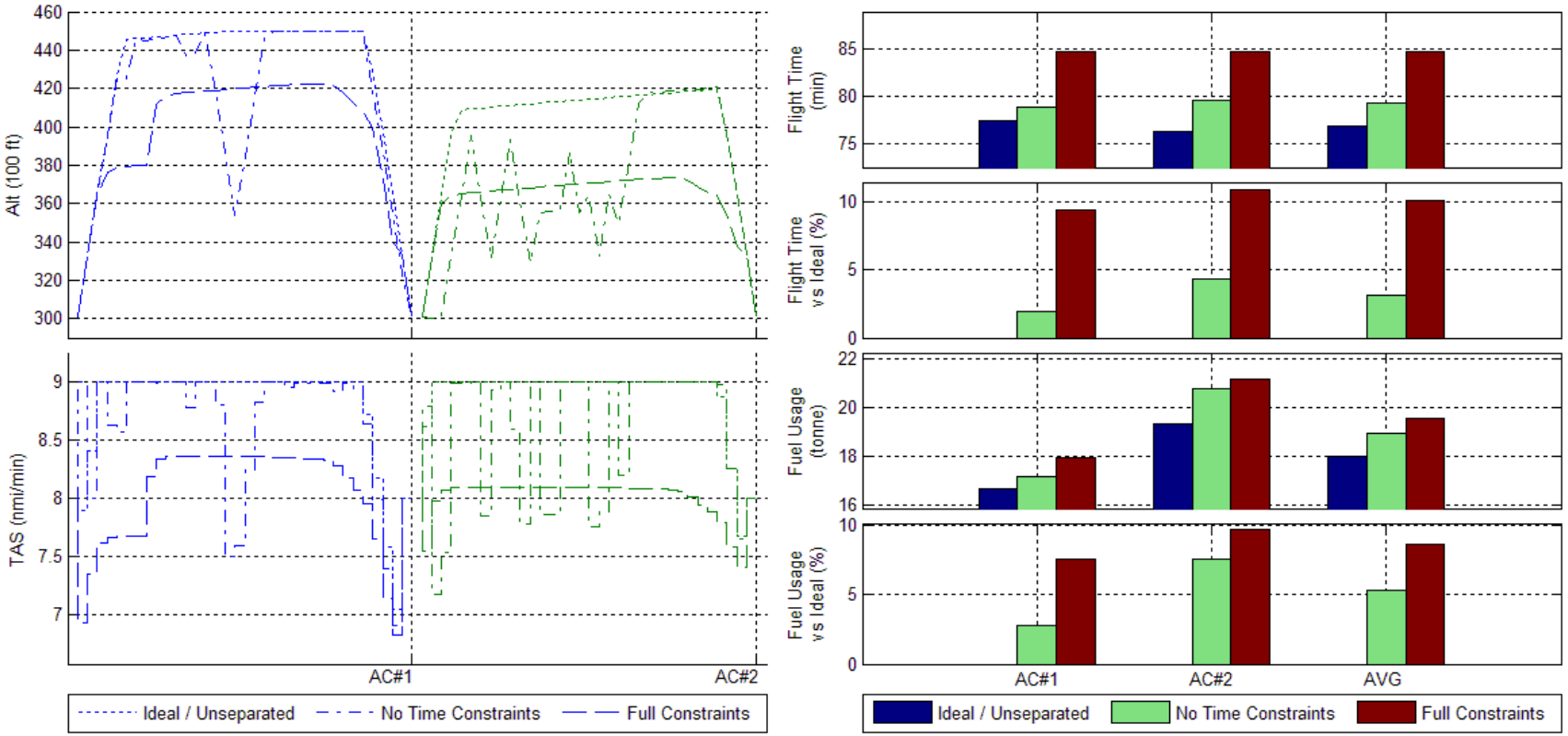

Figure 138 Trajectory Shape, Flight Time, and Fuel Consumption Comparisons of Optimized 2acPH2H results with and without an arrival time constraint

F.10 Generic Boeing 747-300 - Scenario 4acPH2H

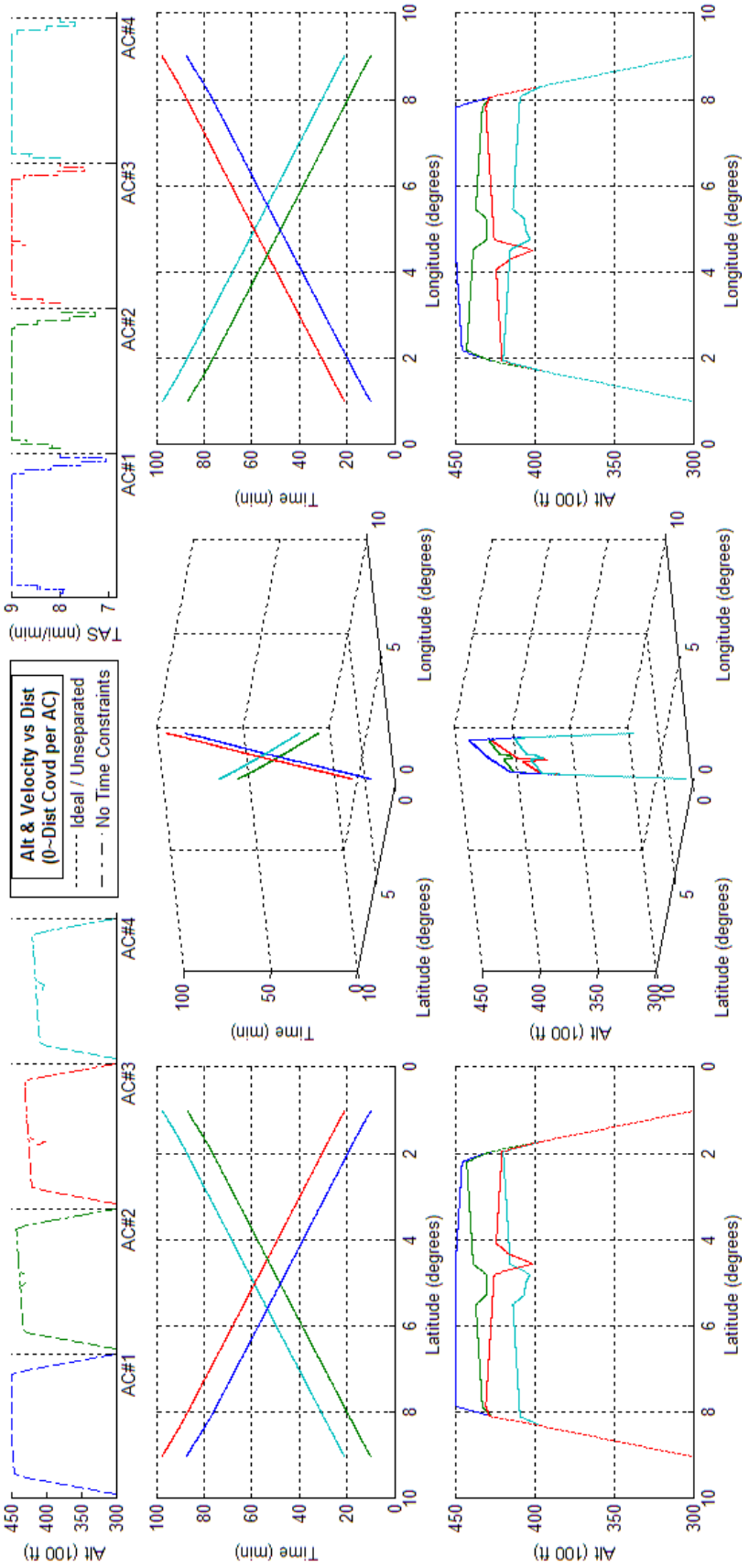

Figure 139 - Optimized 4acPH2H assuming no arrival time constraints.

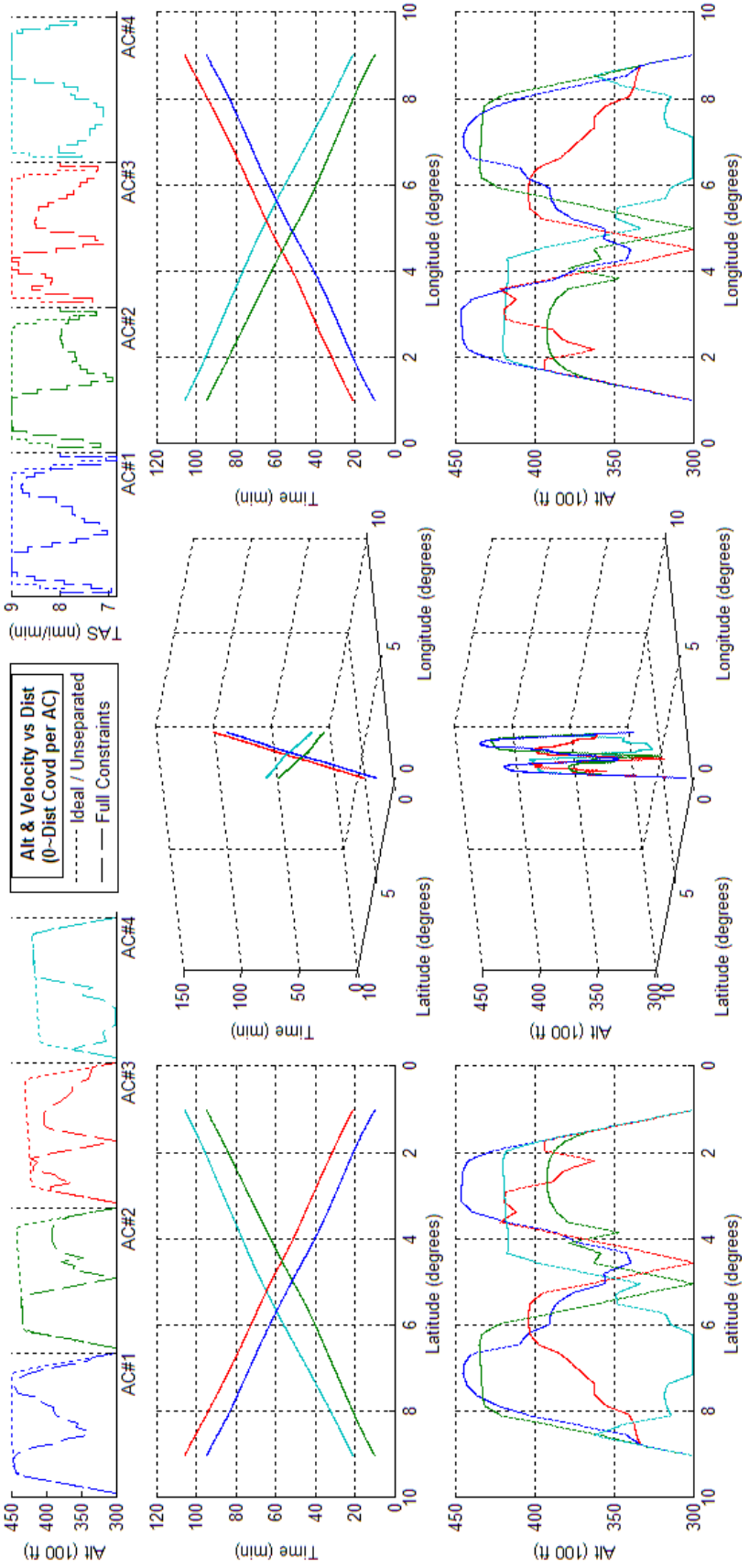

Figure 140 - Optimized 4acPH2H assuming arrival time constraints.

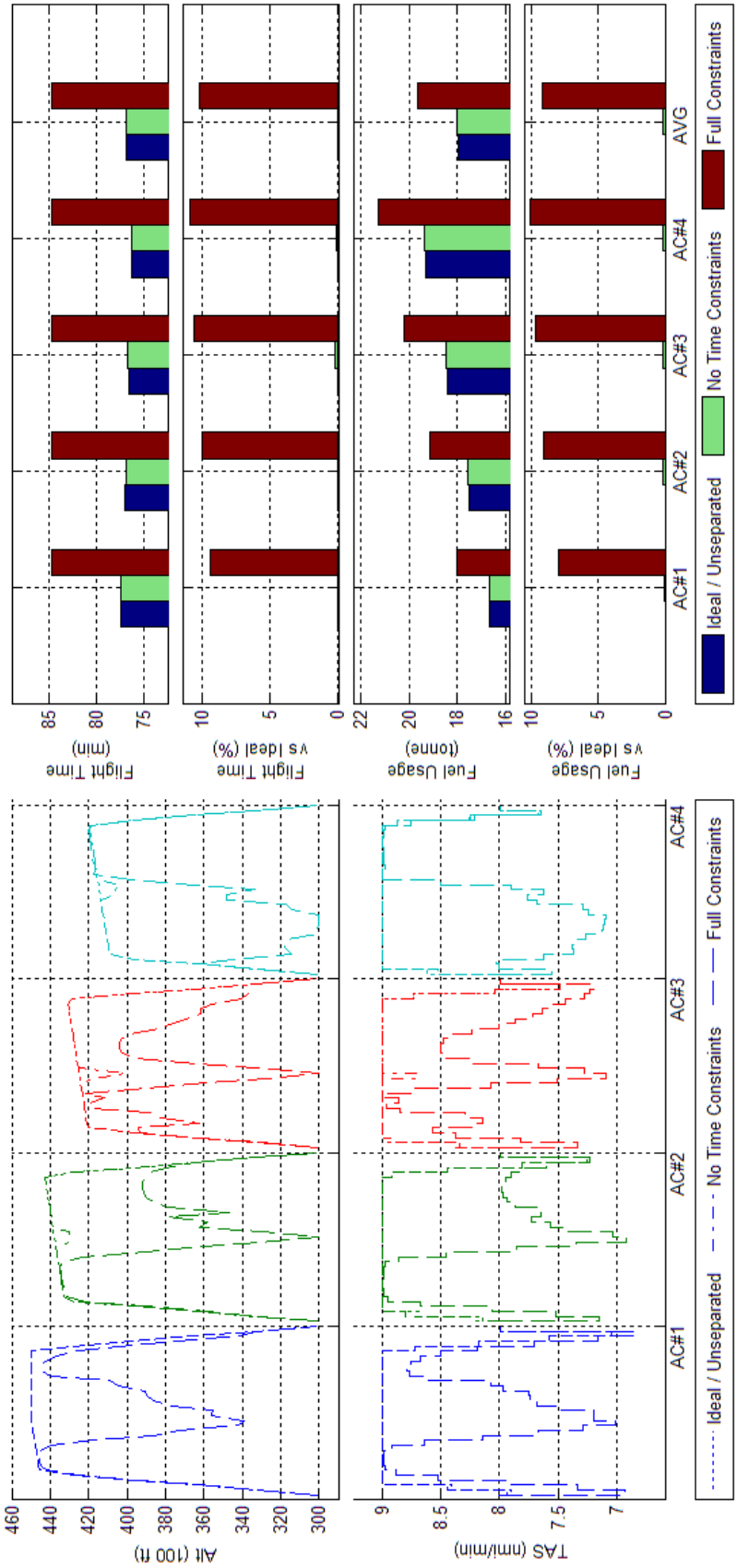

Figure 141 Trajectory Shape, Flight Time, and Fuel Consumption Comparisons of Optimized 4acPH2H results with and without an arrival time constraint

F.11 Generic Boeing 747-300 - Scenario 10acPH2H

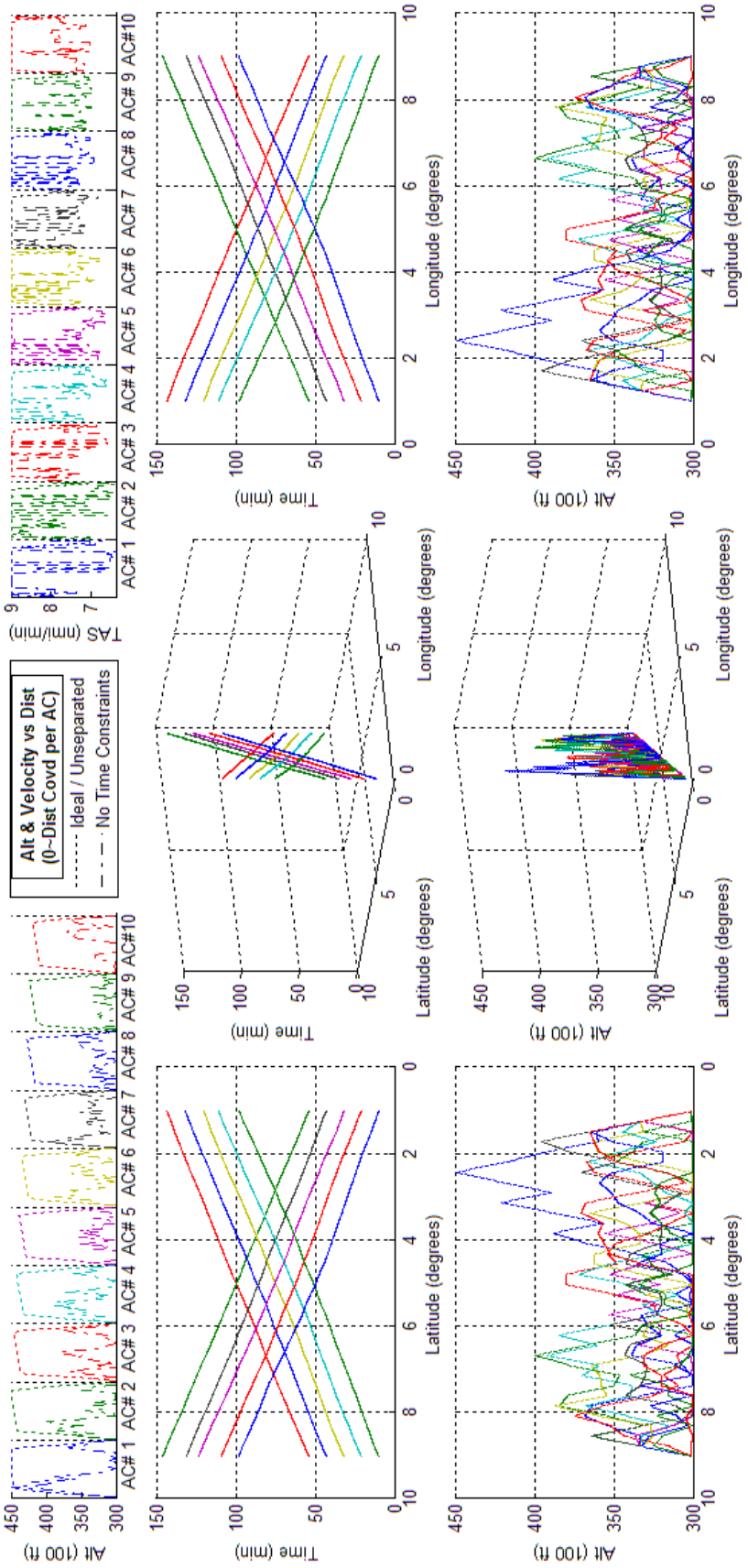

Figure 142 - Optimized 10acPH2H assuming no arrival time constraints.

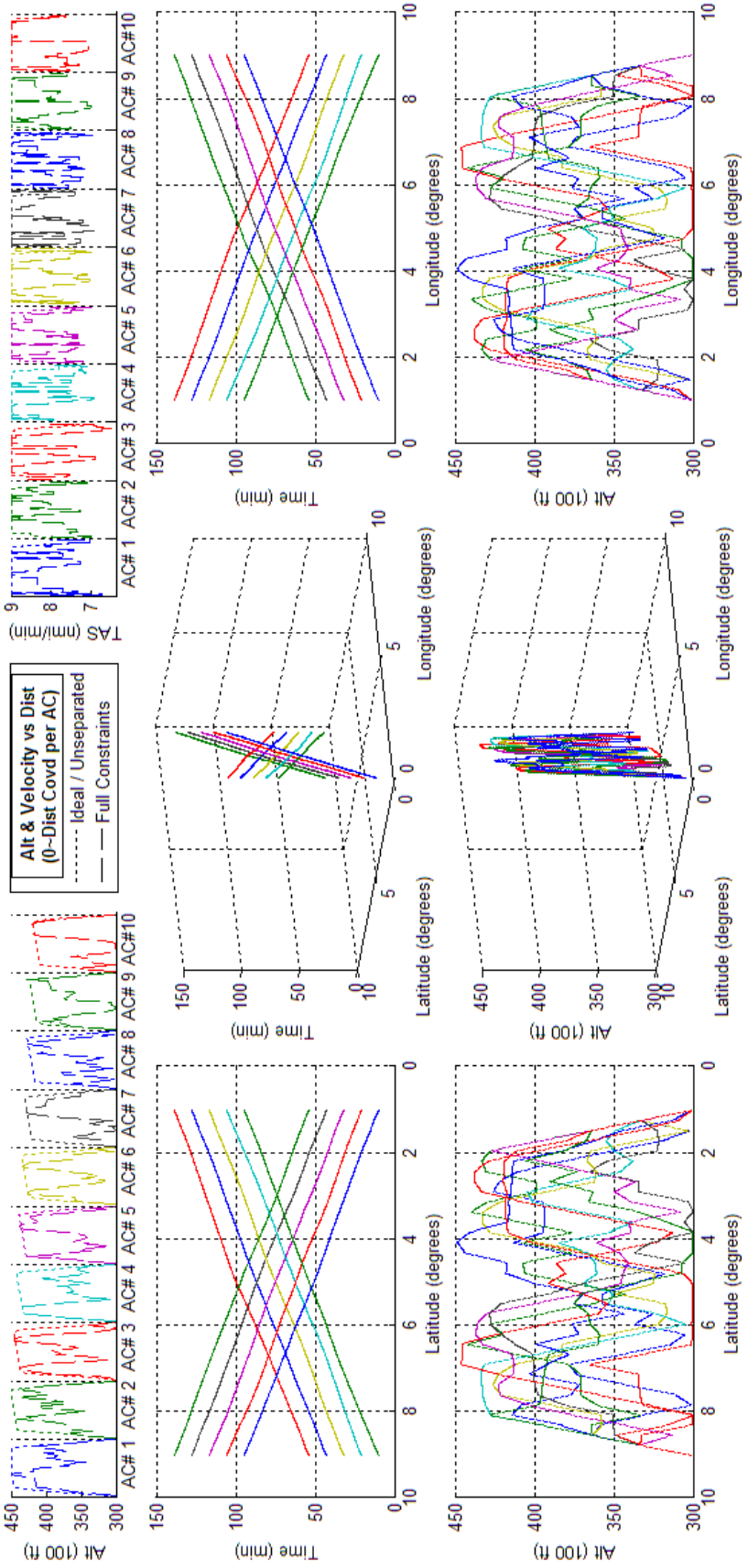

Figure 143 - Optimized 10acPH2H assuming arrival time constraints.

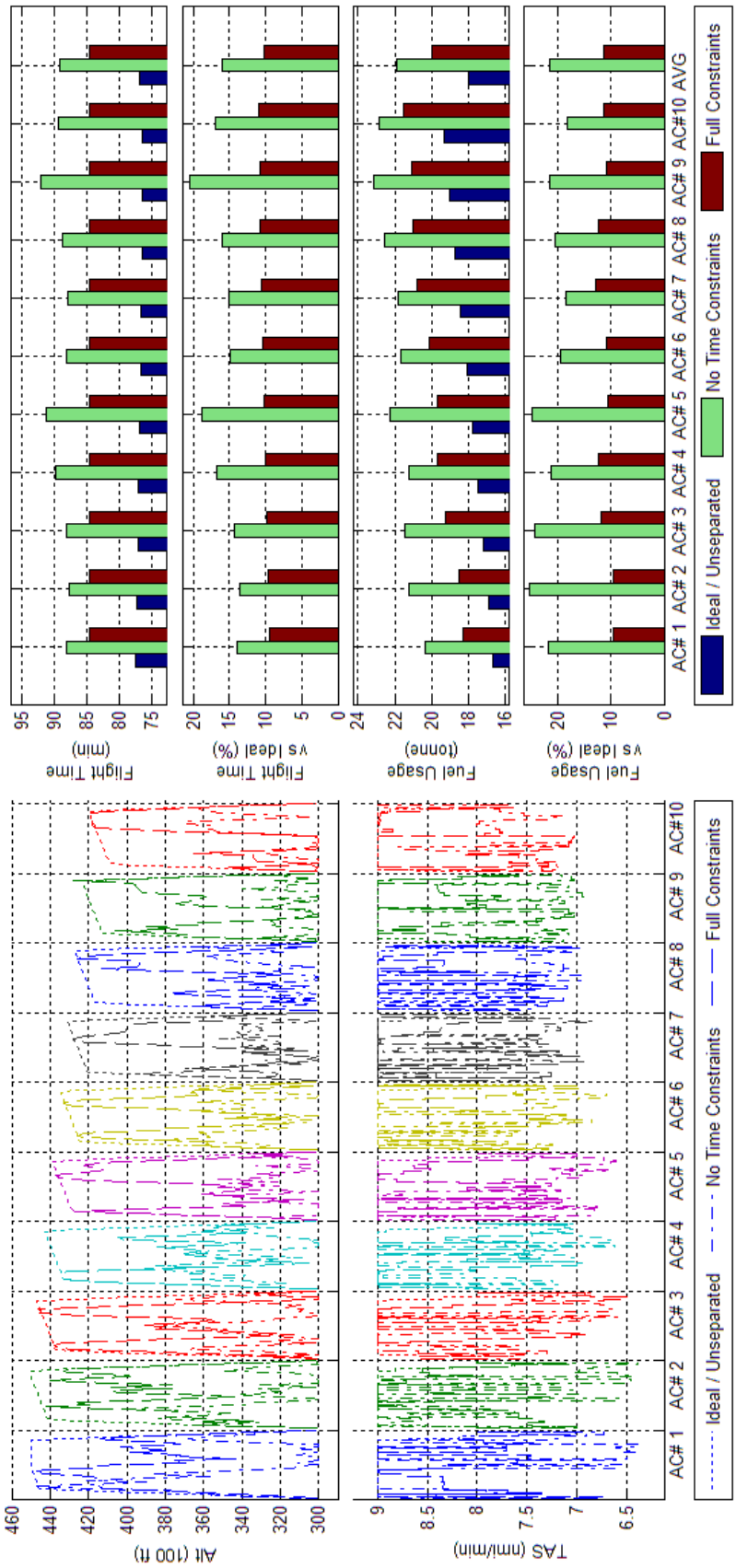

Figure 144 Trajectory Shape, Flight Time, and Fuel Consumption Comparisons of Optimized 10acPH2H results with and without an arrival time constraint

APPENDIX G Prototype Core Optimizer Results

The following graph show the results for the completed PCO mentioned in section 3.3. For discussion of the results and impacts of these results, please refer to section 3.4. For instructions on how to read the graphs, please refer to section 3.4.1. To recap, each section in this appendix shows three graphs:

- The first graphs shows optimization results of the scenario assuming fuel minimization with no constraint on ETA.
- The second graph shows is the same as the first, but with a constraint on ETA requiring aircraft to land at a time such that their average speed over the entire journey was 420kts. Please refer to section 3.4 for rationale.
- The third compares the trajectory shape, fuel usage and flight time of each aircraft between the results of the first and second graph

The main purpose of these results is that they were first time that consistent fuel minimization results had been achieved in the research. Later efforts will build on these results by improving upon where and how the method could be used when optimizing an ATS; either by using more detailed aircraft performance models or generalizing its usage in scenarios with unpredictable or heavy air traffic.

G.1 Generic Boeing 747-300 - Scenario 2acPSd

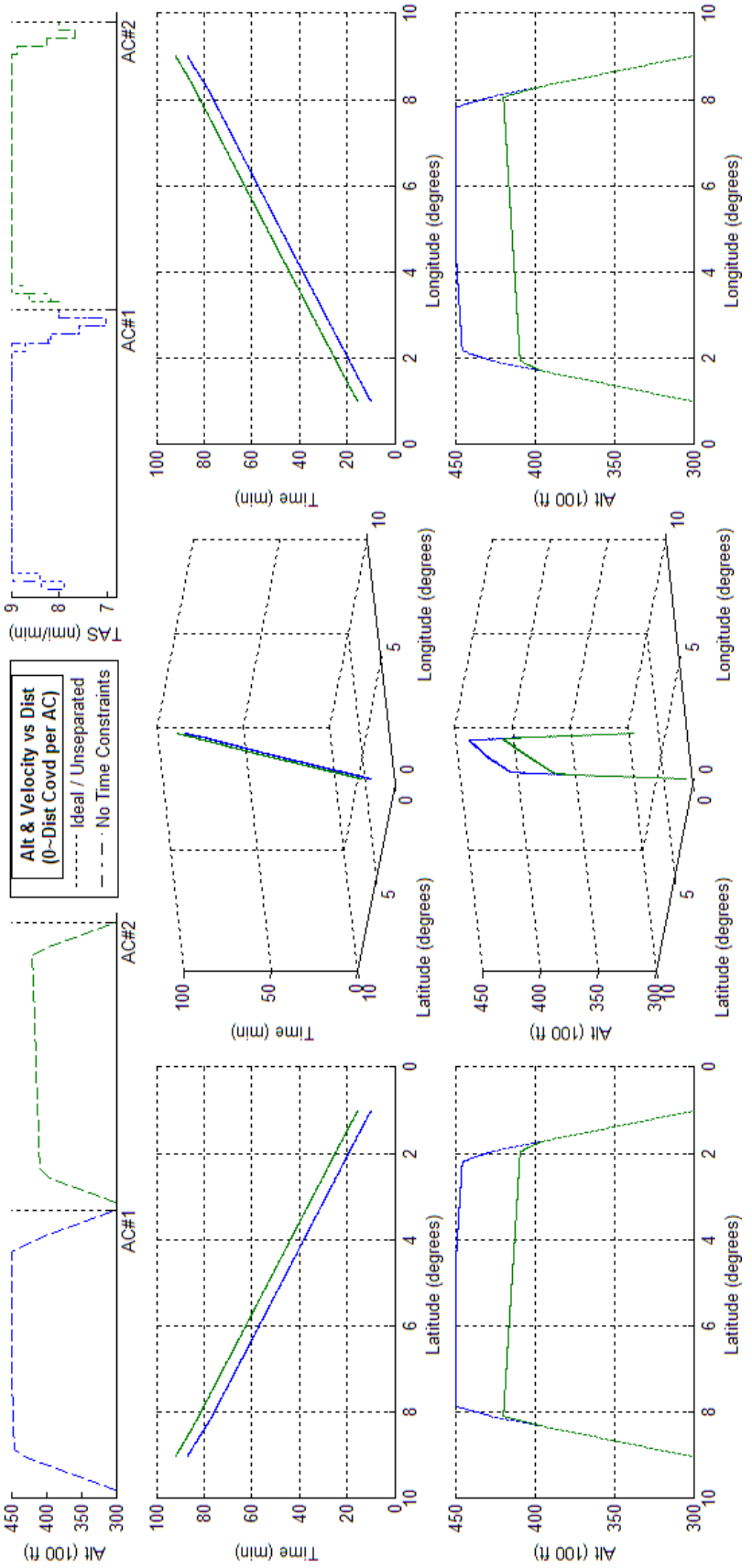

Figure 145 - Optimized 2acPSd assuming no arrival time constraints.

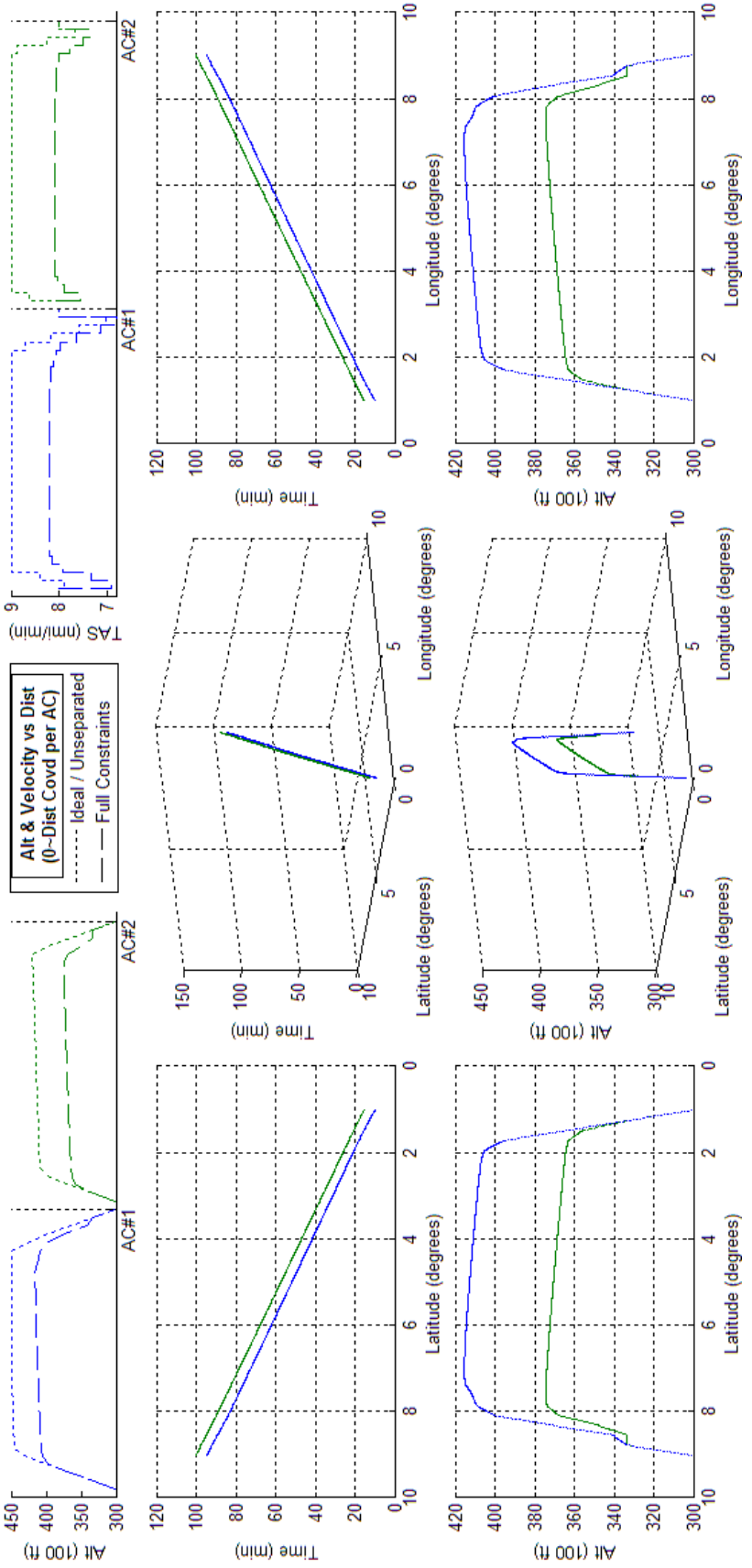

Figure 146 - Optimized 2acPSd assuming arrival time constraints.

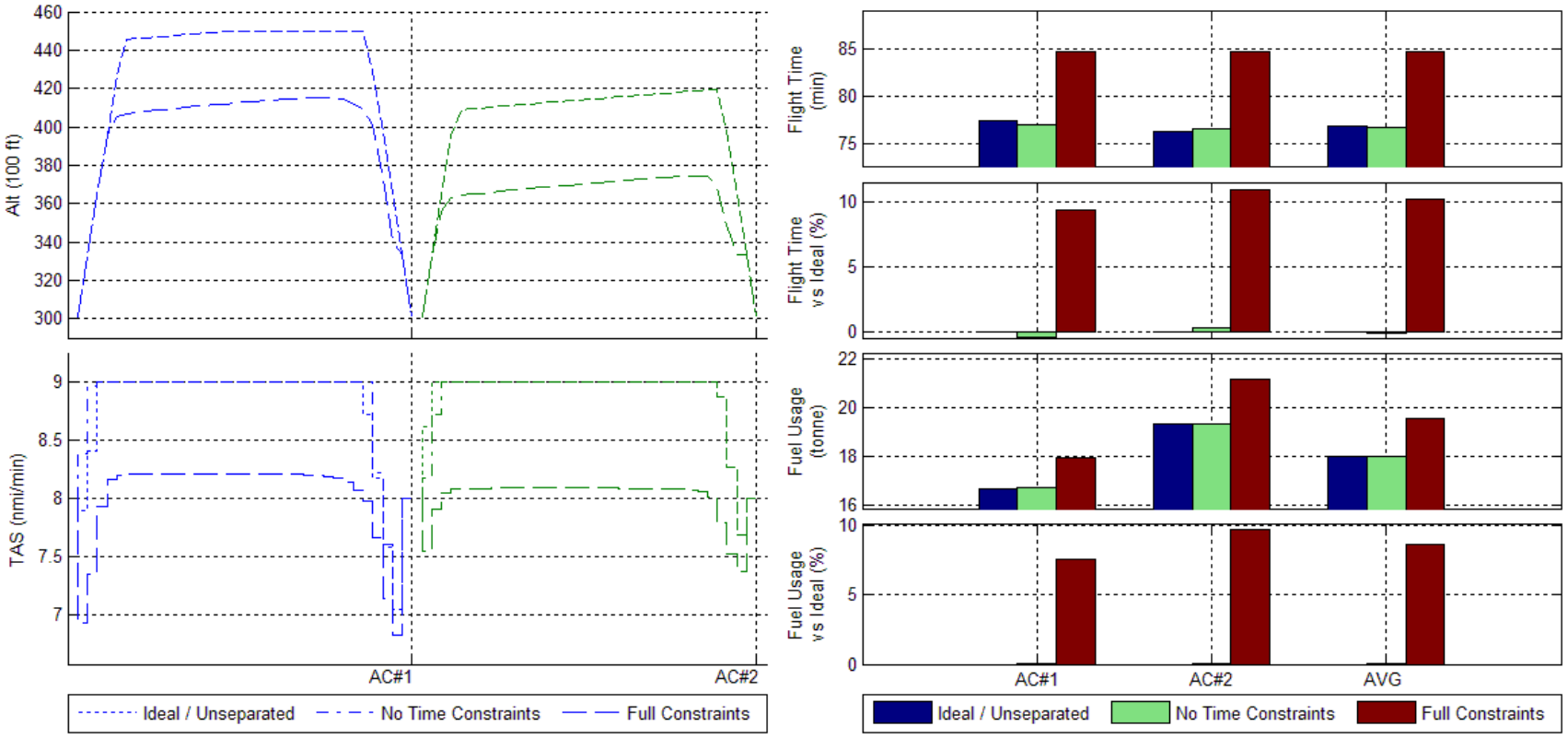

Figure 147 Trajectory Shape, Flight Time, and Fuel Consumption Comparisons of Optimized 2acPSd results with and without an arrival time constraint

G.2 Generic Boeing 747-300 - Scenario 4acPSd

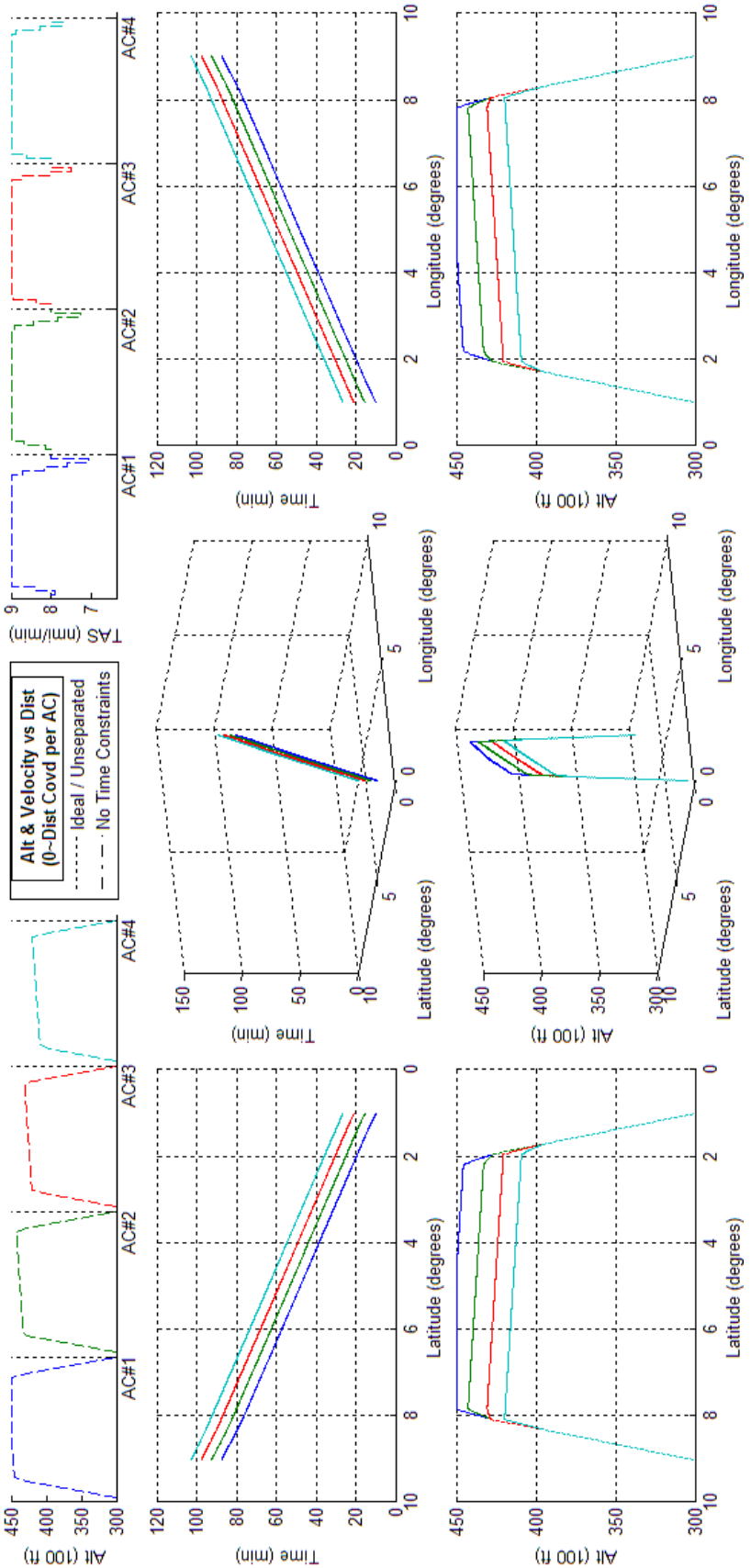

Figure 148 - Optimized 4acPSd assuming no arrival time constraints.

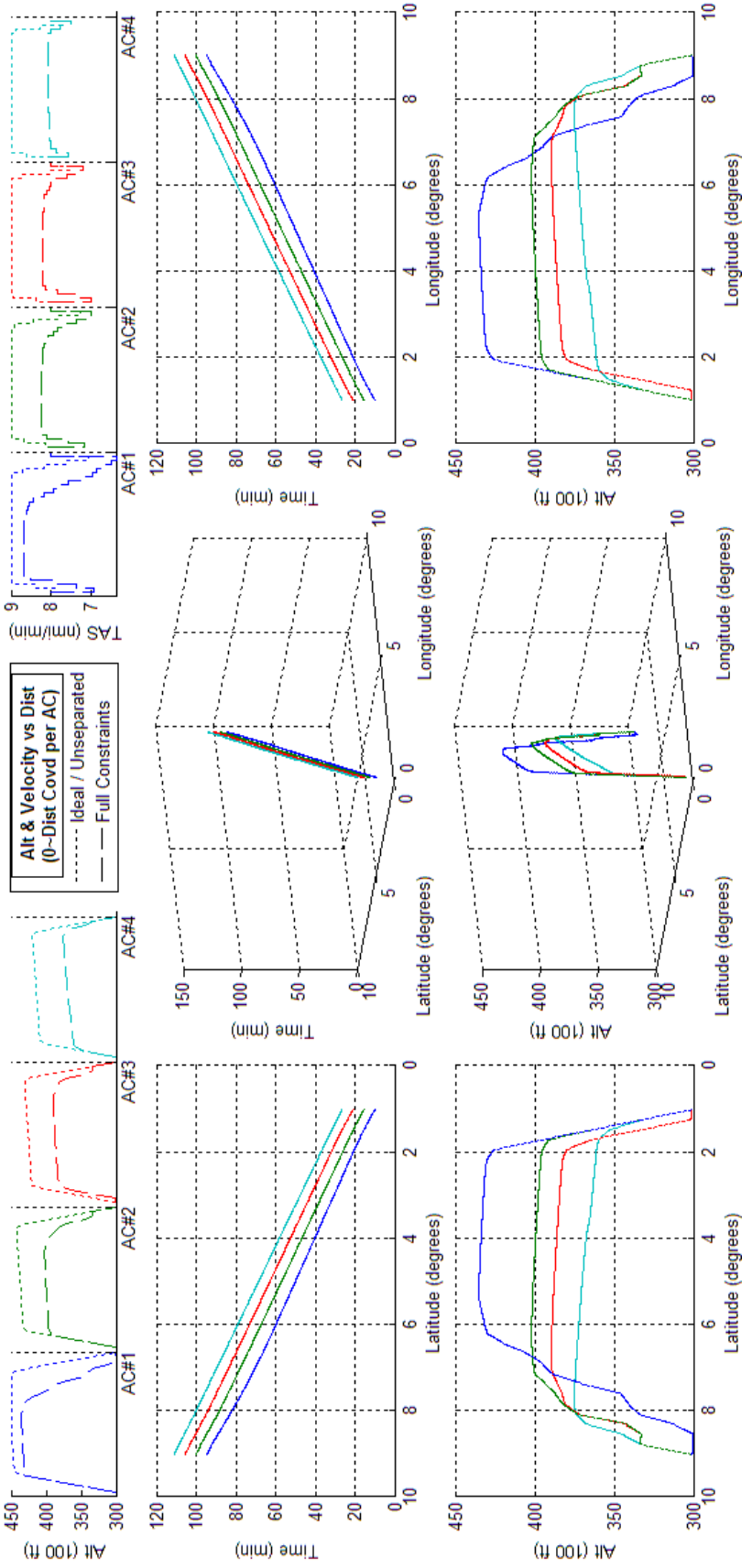

Figure 149 - Optimized 4acPSd assuming arrival time constraints.

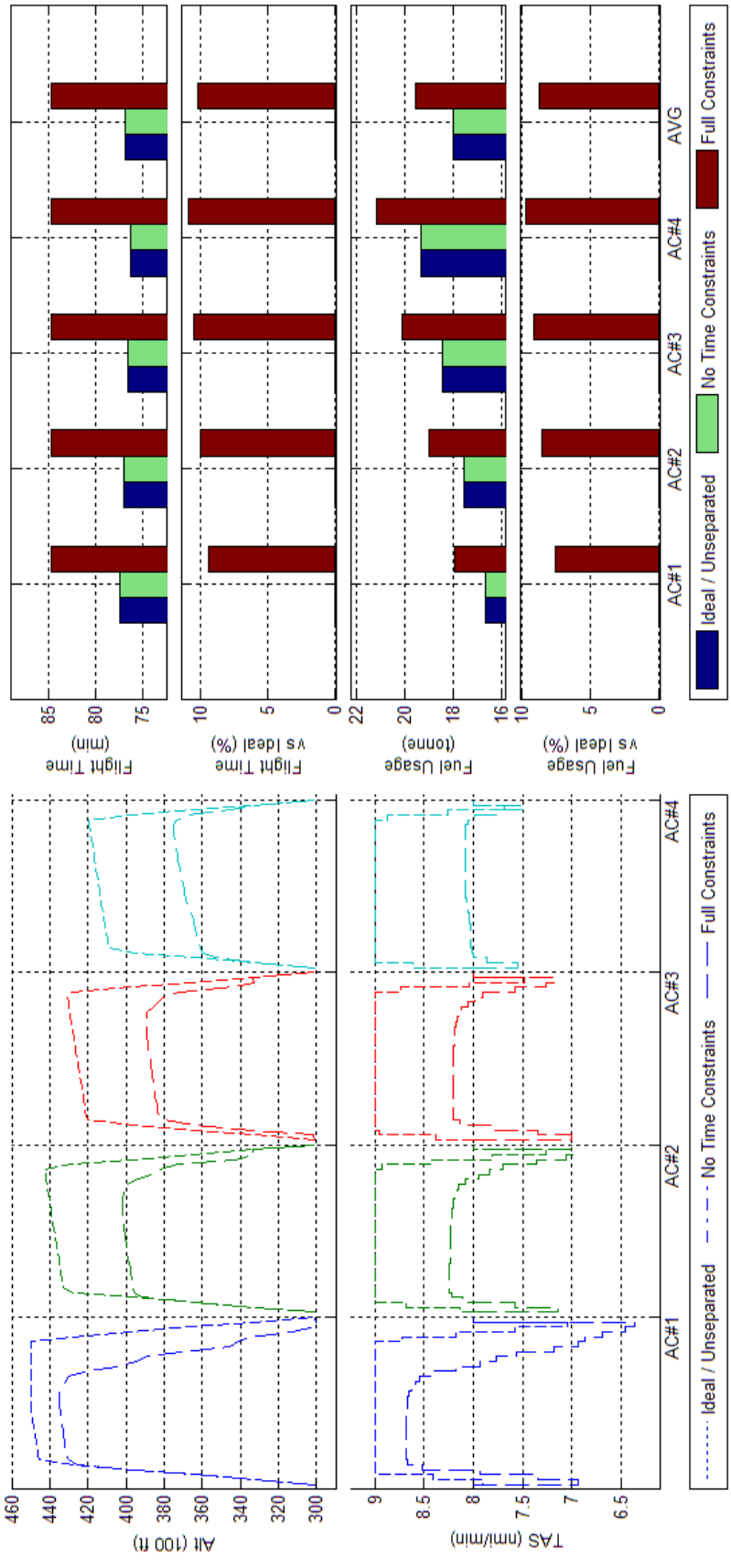

Figure 150 Trajectory Shape, Flight Time, and Fuel Consumption Comparisons of Optimized 4acPSd results with and without an arrival time constraint

G.3 Generic Boeing 747-300 - Scenario 10acPSd

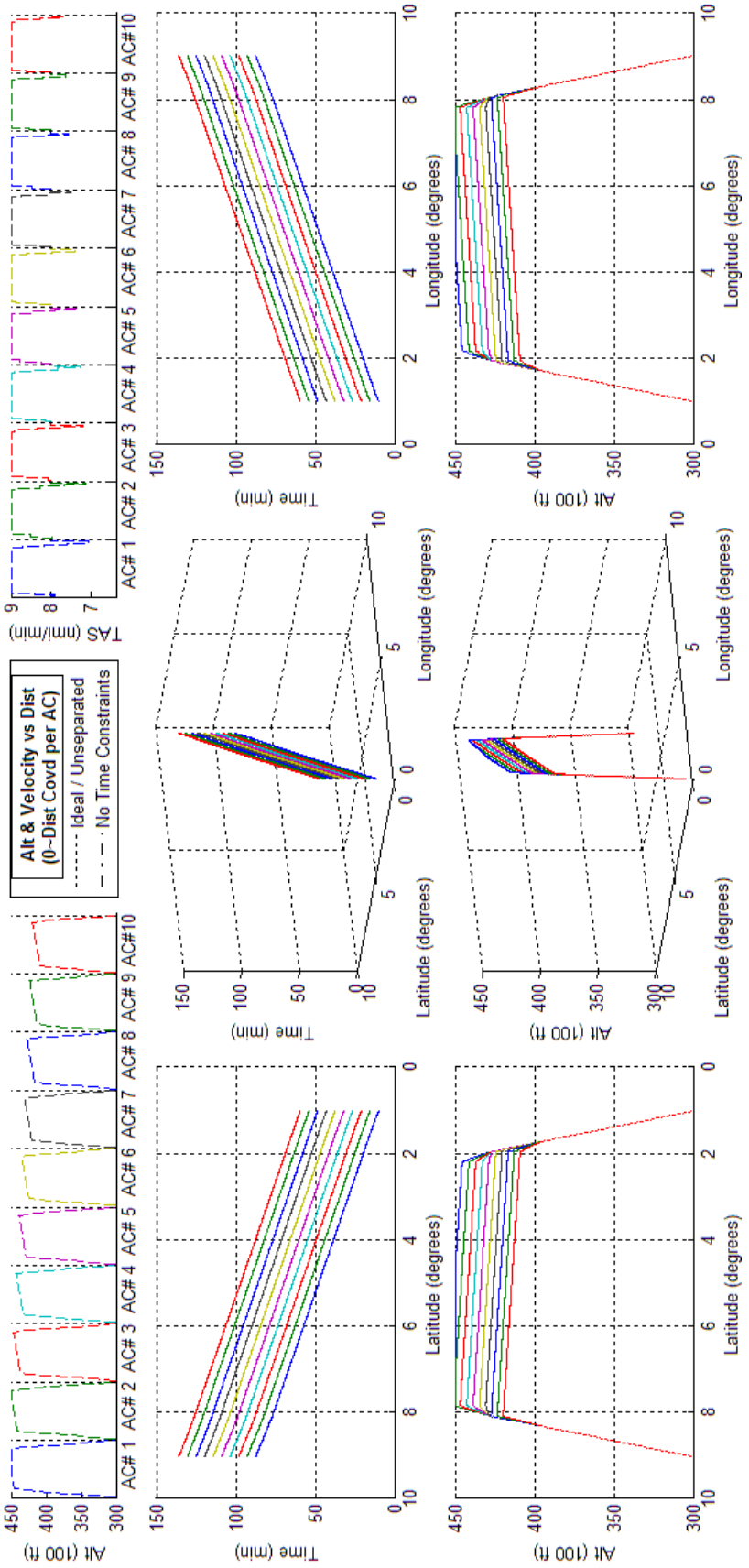

Figure 151 - Optimized 10acPSd assuming no arrival time constraints.

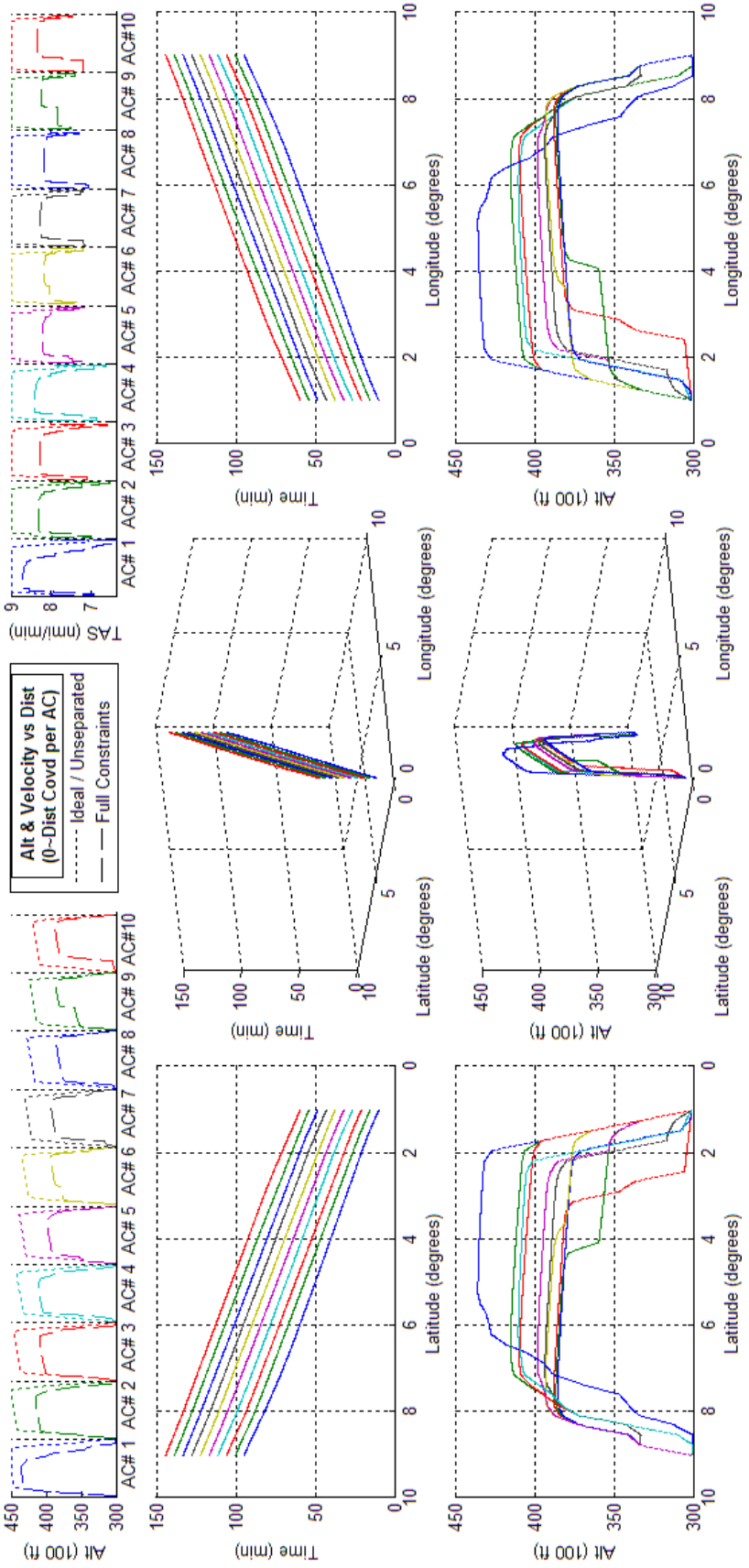

Figure 152 - Optimized 10acPSd assuming arrival time constraints.

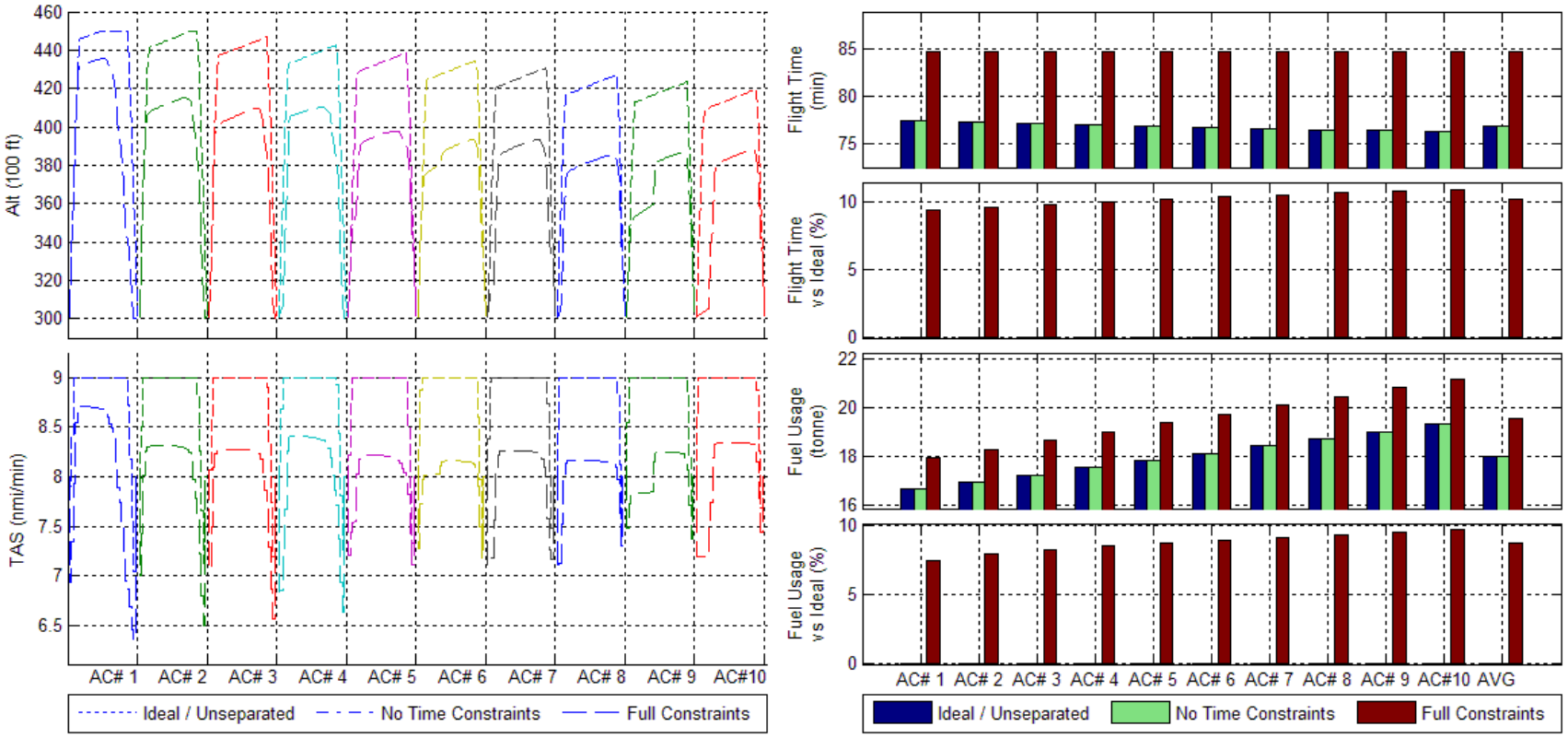

Figure 153 Trajectory Shape, Flight Time, and Fuel Consumption Comparisons of Optimized 10acPSd results with and without an arrival time constraint

G.4 Generic Boeing 747-300 - Scenario 2acCO

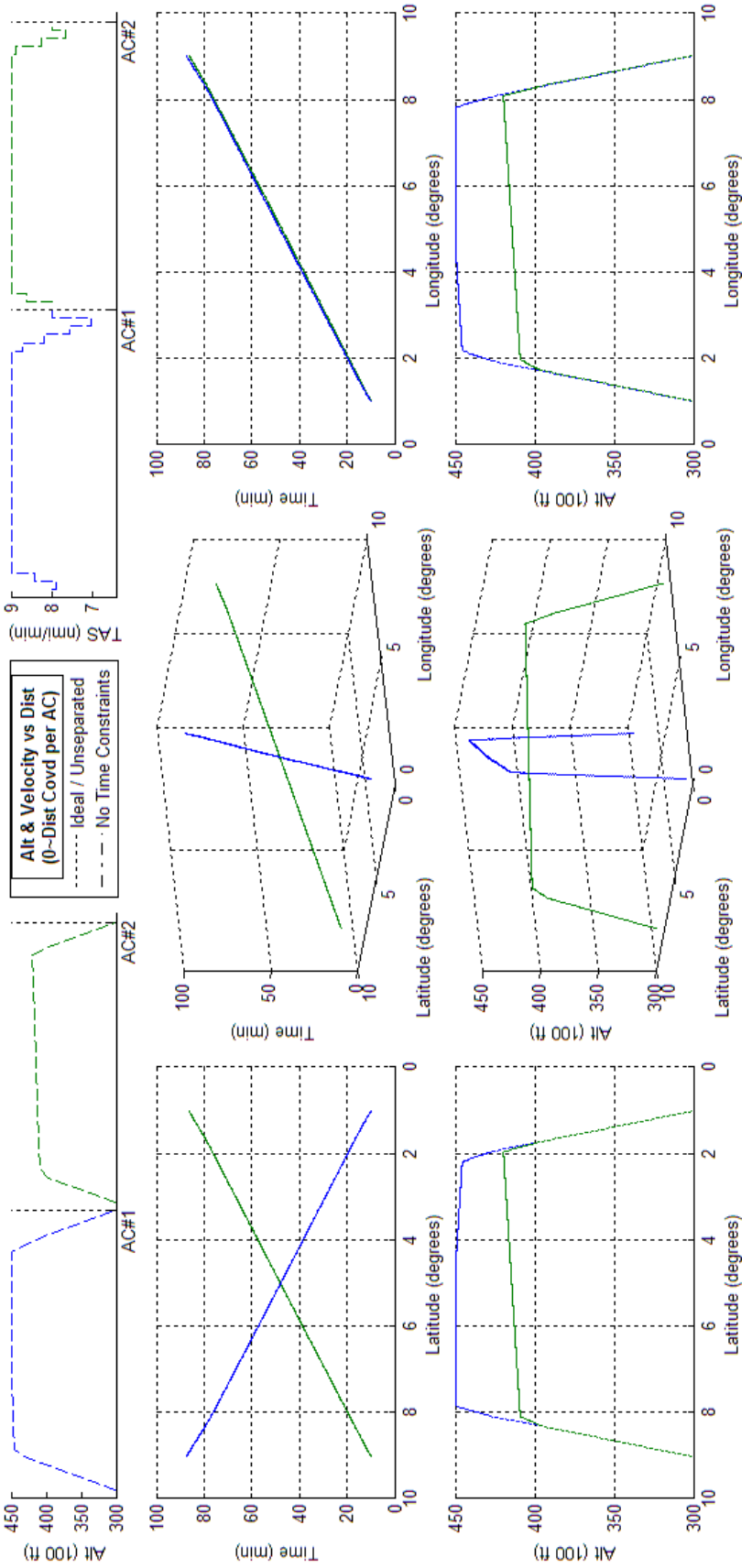

Figure 154 - Optimized 2acCO assuming no arrival time constraints.

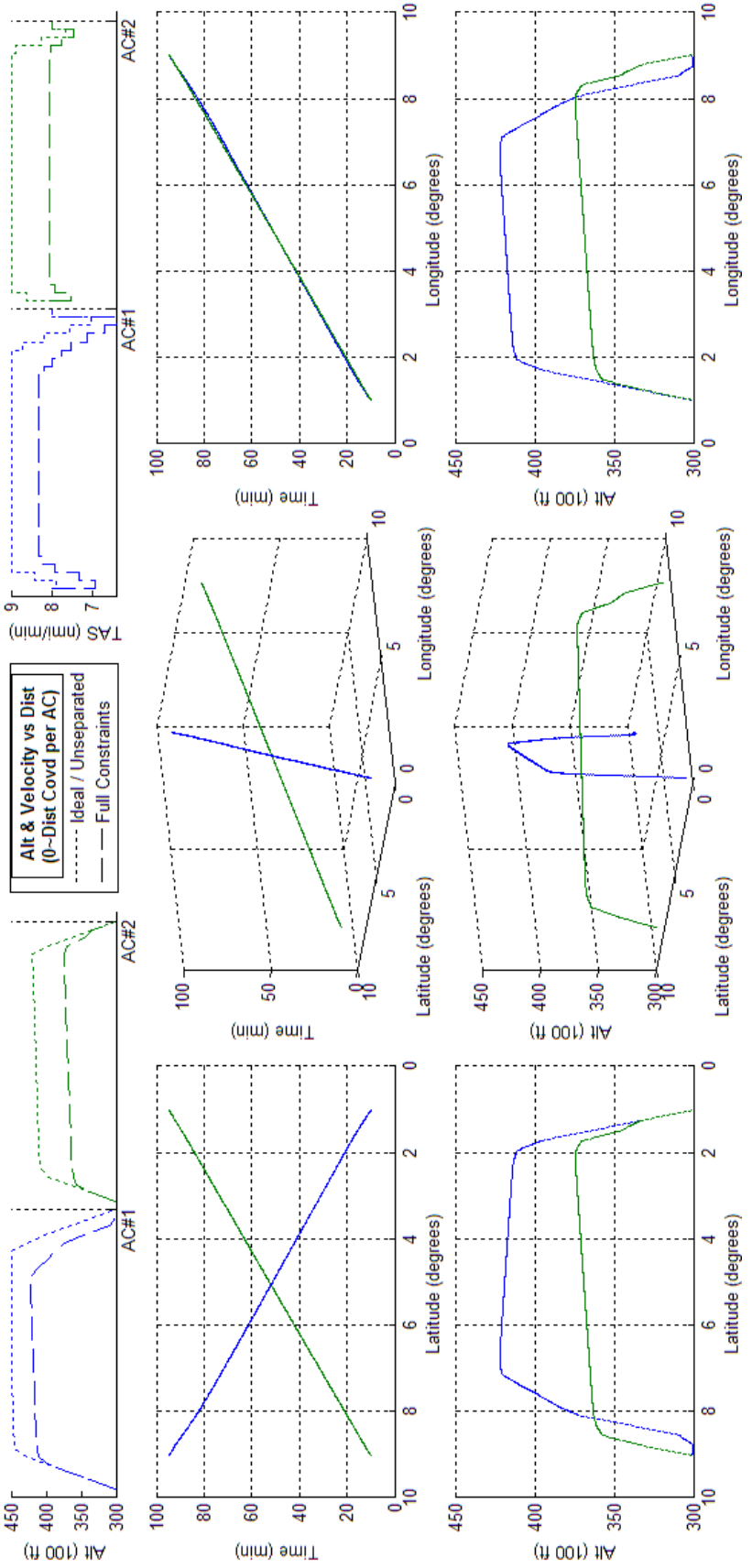

Figure 155 - Optimized 2acCO assuming arrival time constraints.

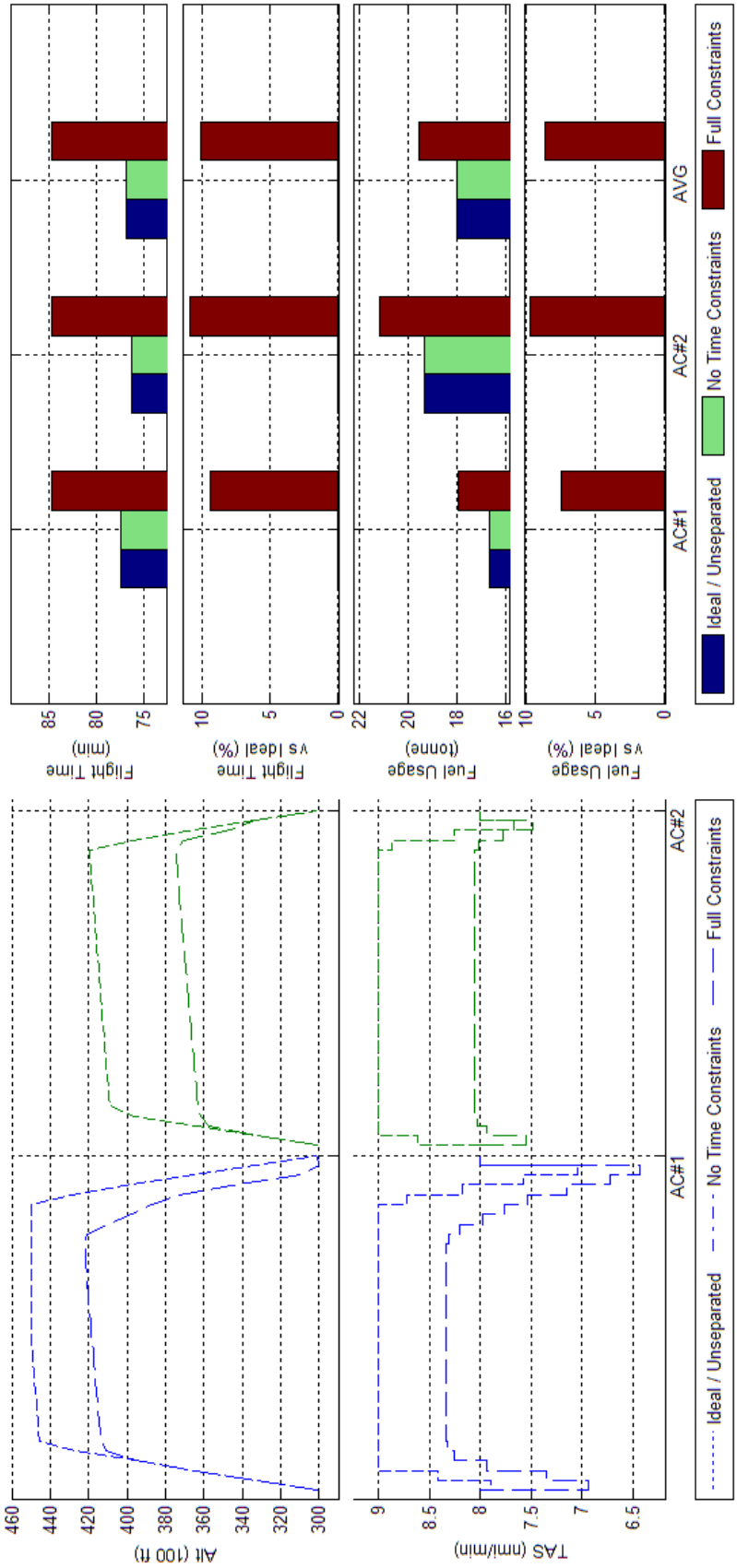

Figure 156 Trajectory Shape, Flight Time, and Fuel Consumption Comparisons of Optimized 2acCO results with and without an arrival time constraint

G.5 Generic Boeing 747-300 - Scenario 4acCO

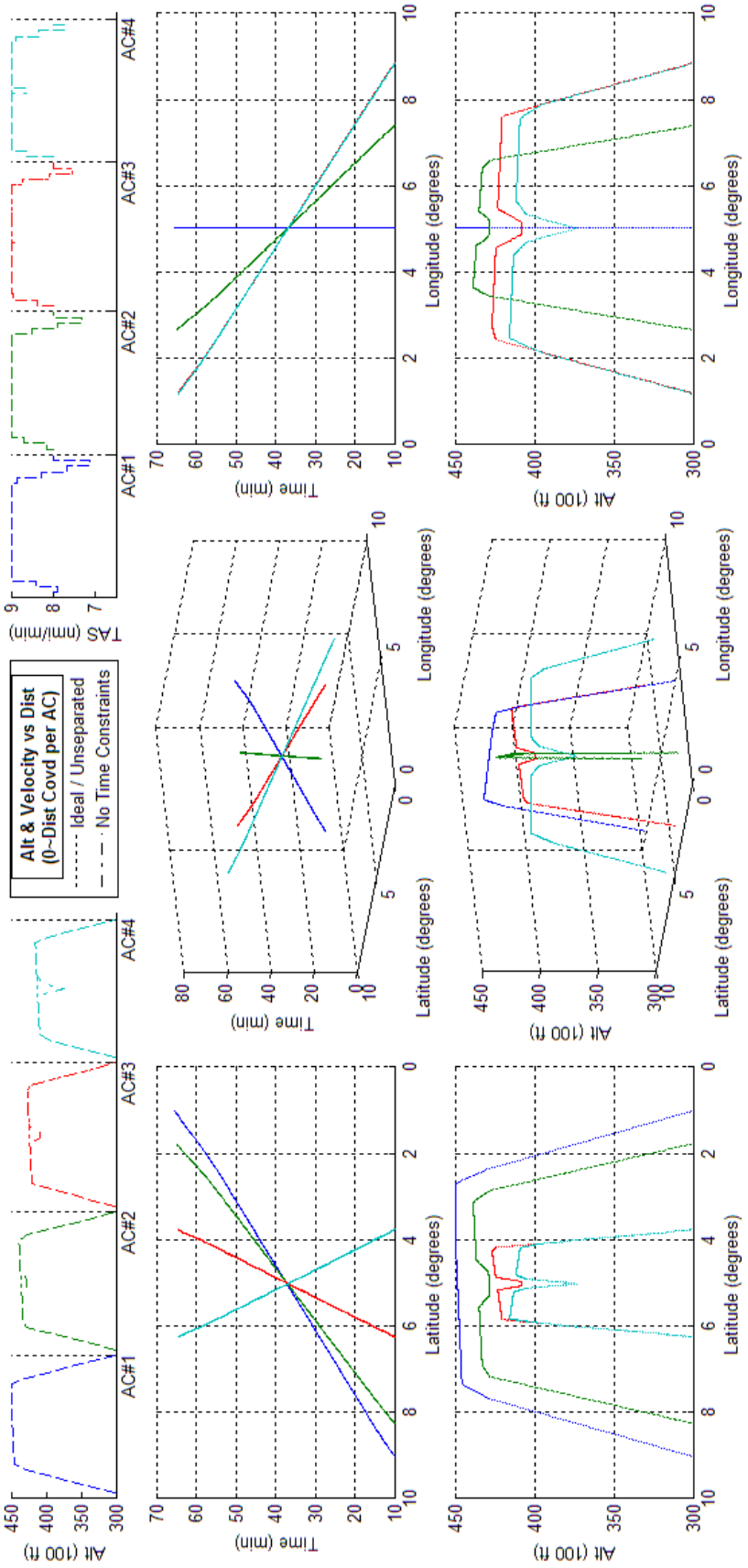

Figure 157 - Optimized 4acCO assuming no arrival time constraints.

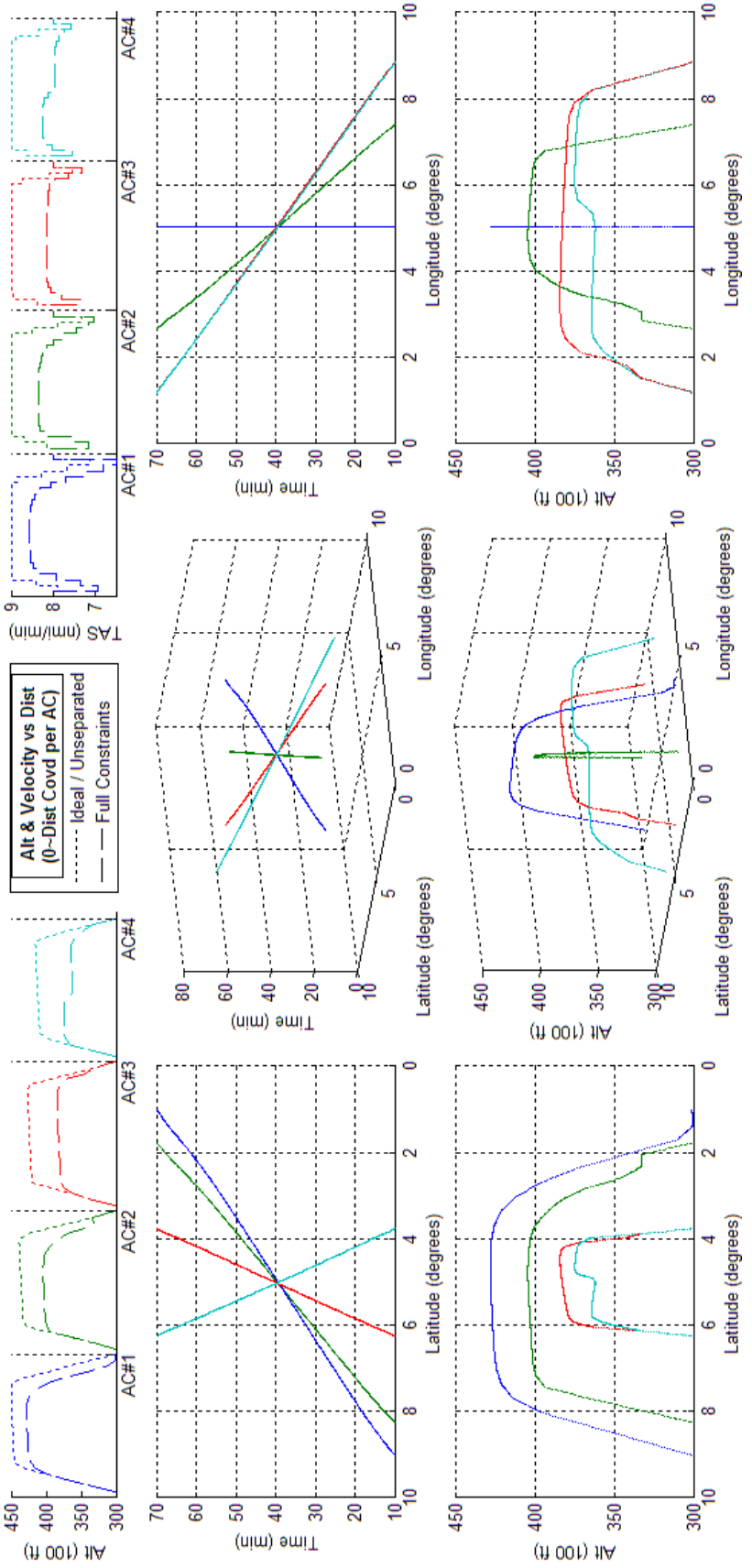

Figure 158 - Optimized 4acCO assuming arrival time constraints.

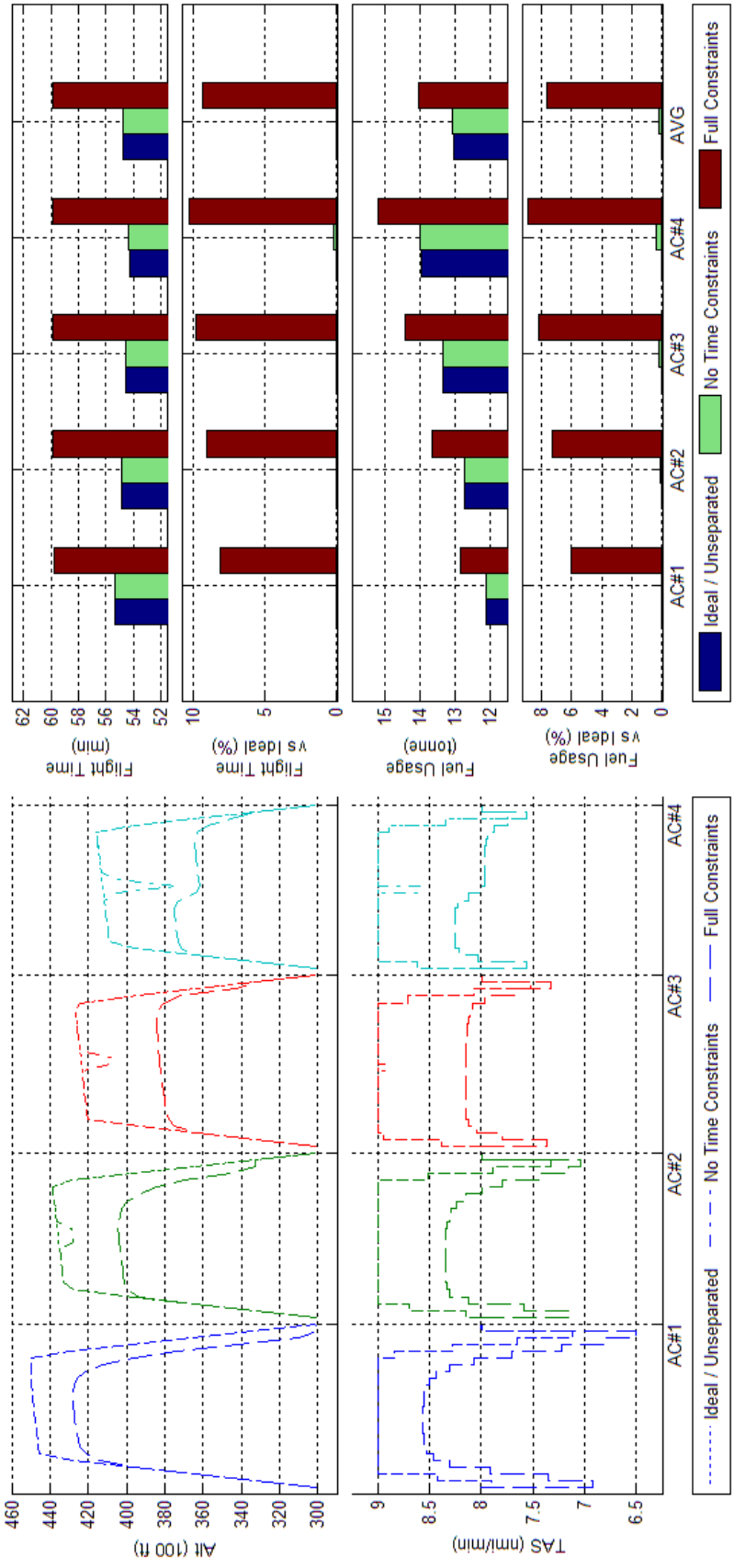

Figure 159 Trajectory Shape, Flight Time, and Fuel Consumption Comparisons of Optimized 4acCO results with and without an arrival time constraint

G.6 Generic Boeing 747-300 - Scenario 10acCO

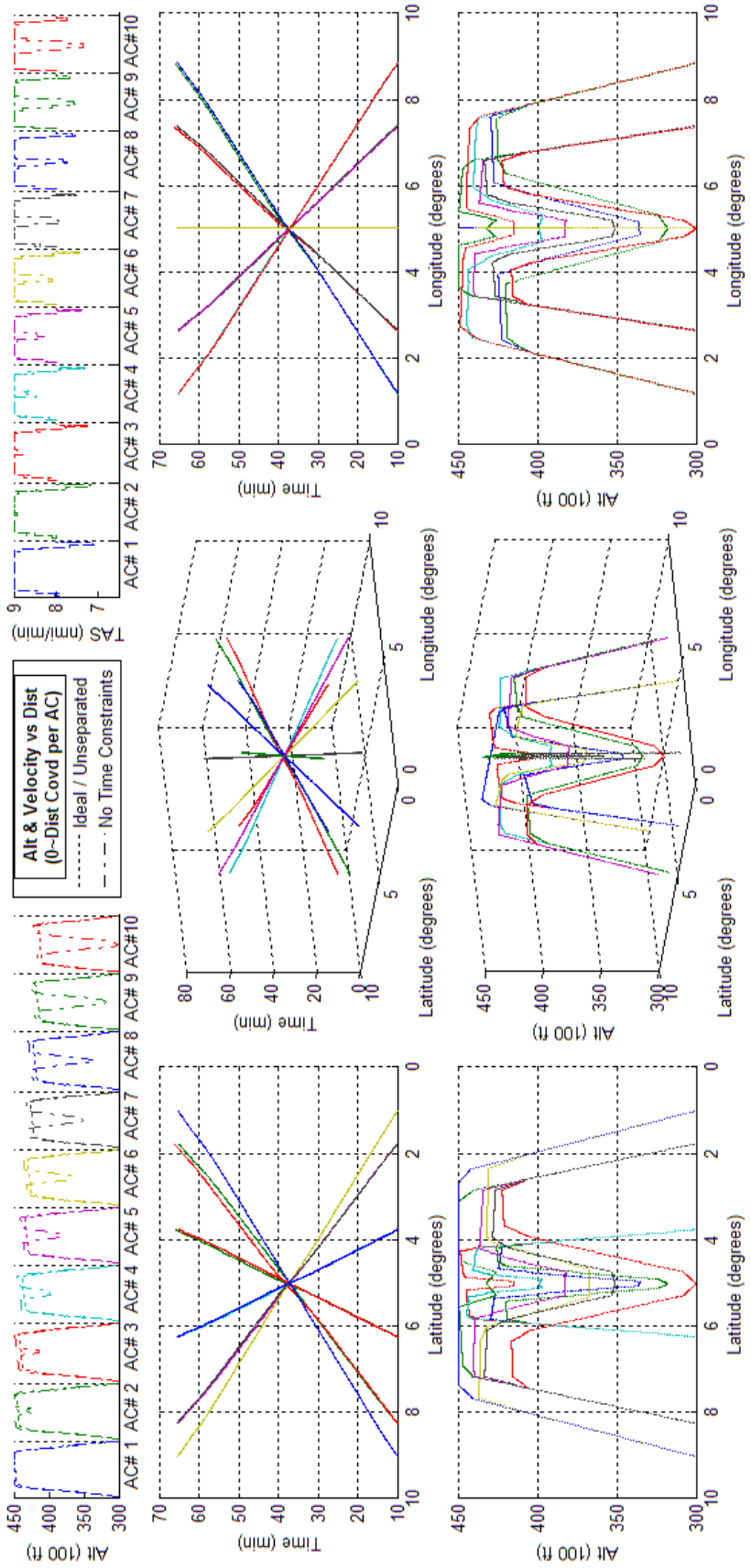

Figure 160 - Optimized 10acCO assuming no arrival time constraints.

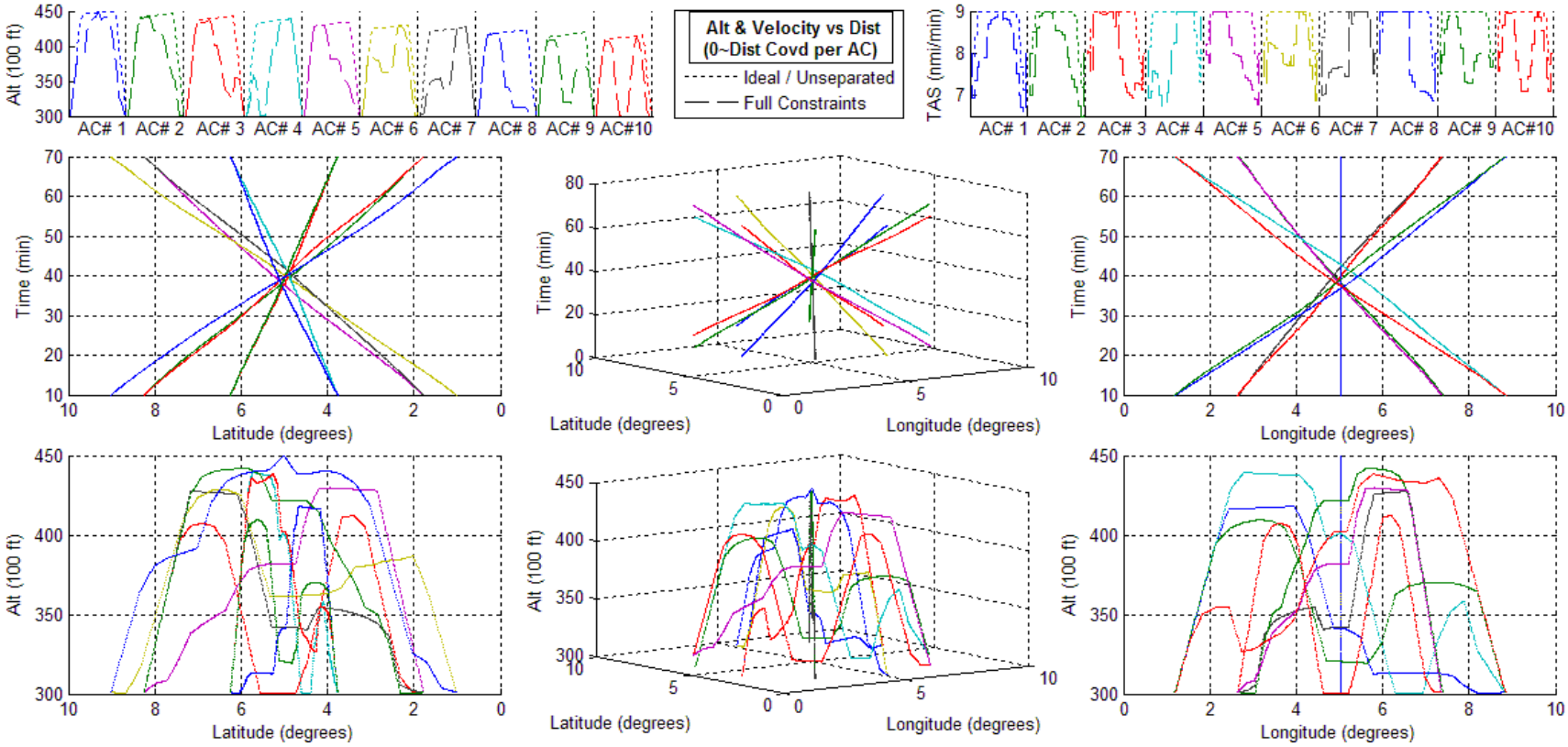

Figure 161 - Optimized 10acCO assuming arrival time constraints.

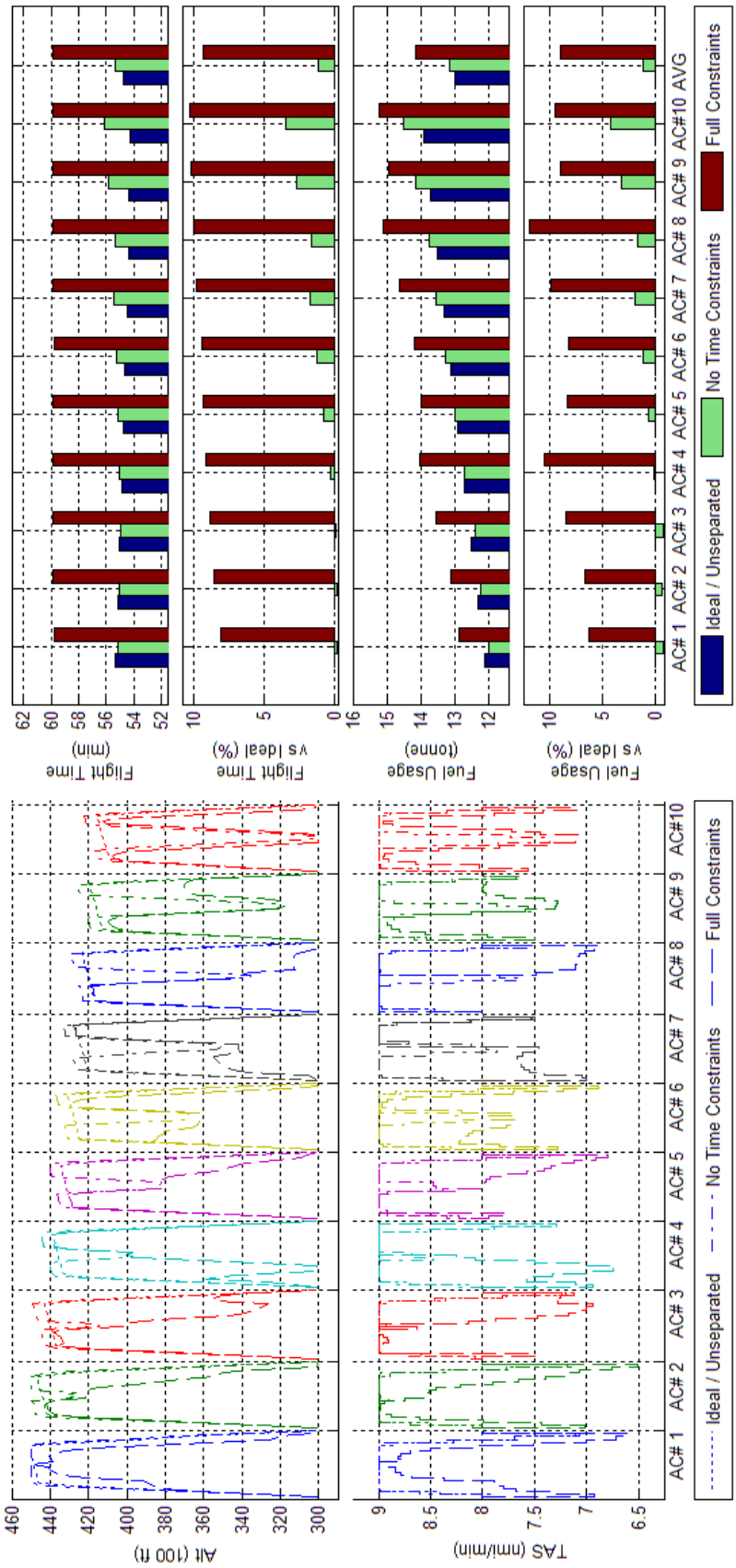

Figure 162 Trajectory Shape, Flight Time, and Fuel Consumption Comparisons of Optimized 10acCO results with and without an arrival time constraint

G.7 Generic Boeing 747-300 - Scenario 4acCH

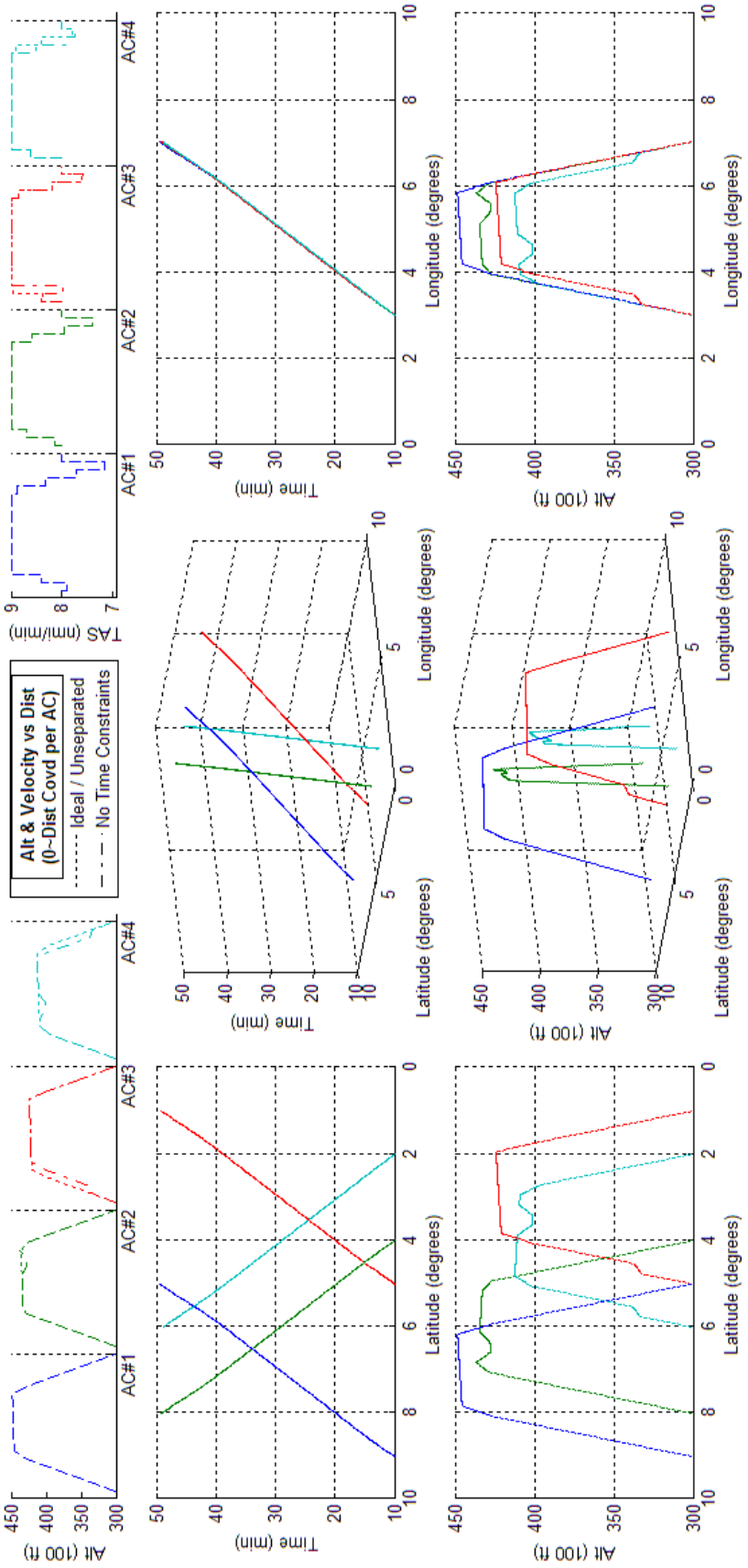

Figure 163 - Optimized 4acCH assuming no arrival time constraints.

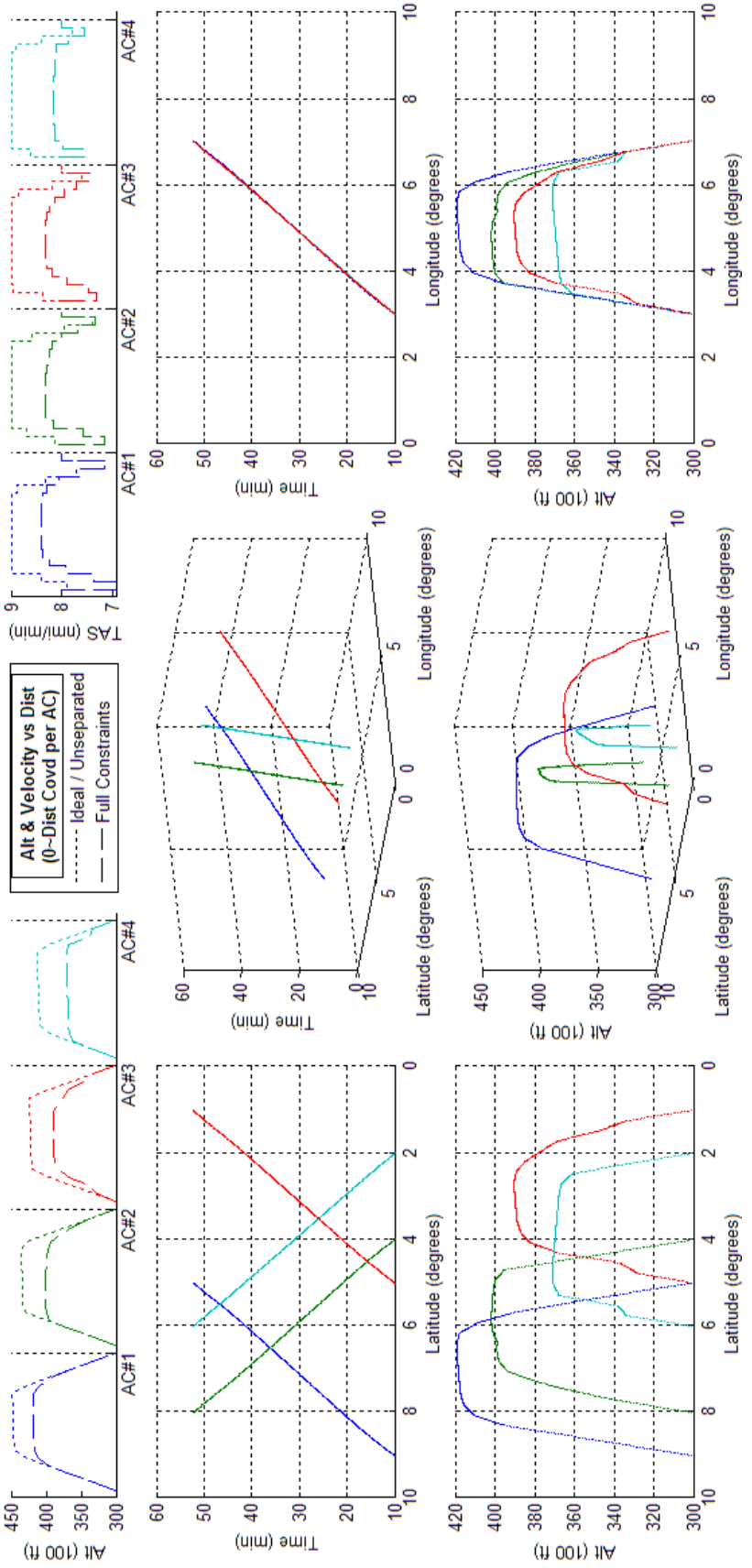

Figure 164 - Optimized 4acCH assuming arrival time constraints.

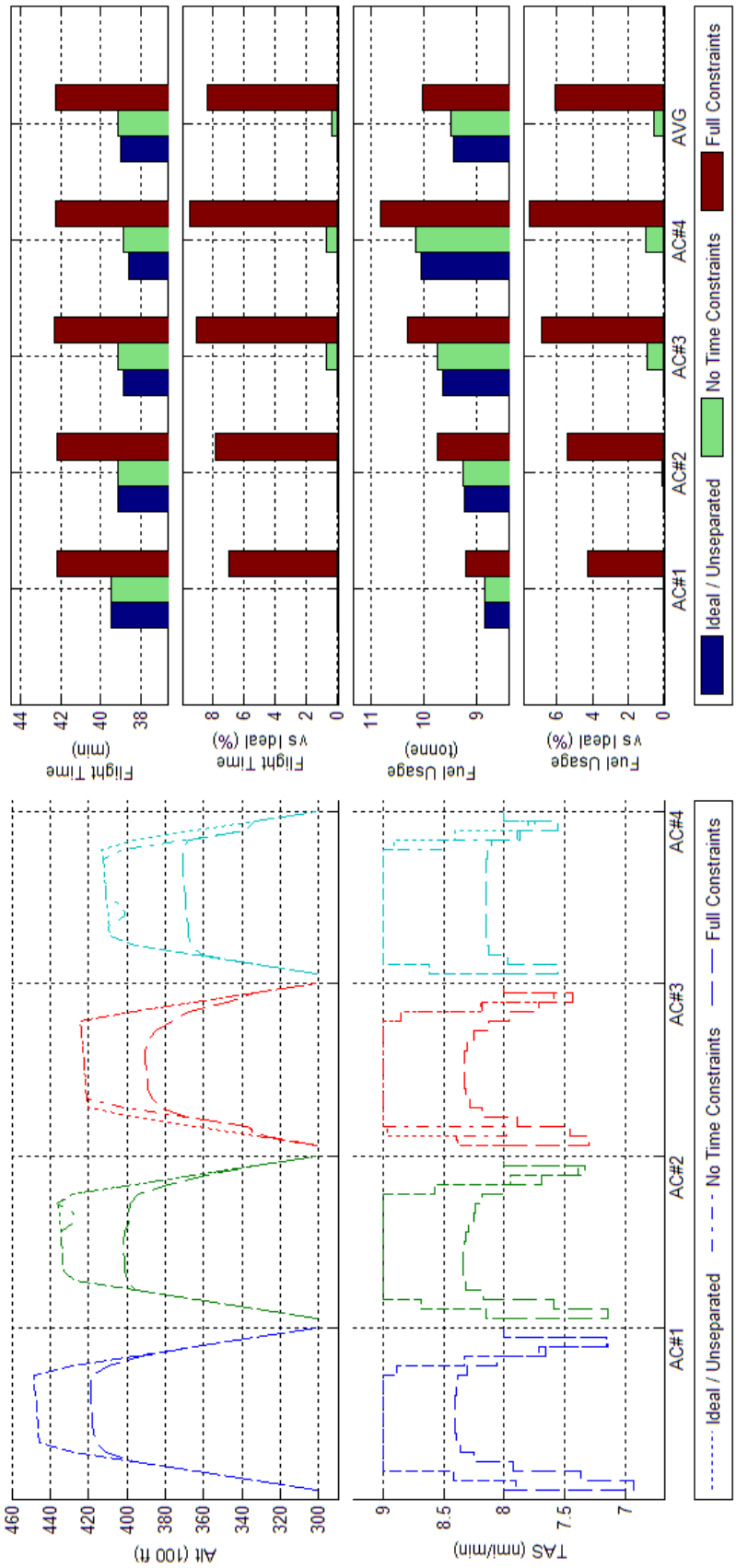

Figure 165 Trajectory Shape, Flight Time, and Fuel Consumption Comparisons of Optimized 4acCH results with and without an arrival time constraint

G.8 Generic Boeing 747-300 - Scenario 10acCH

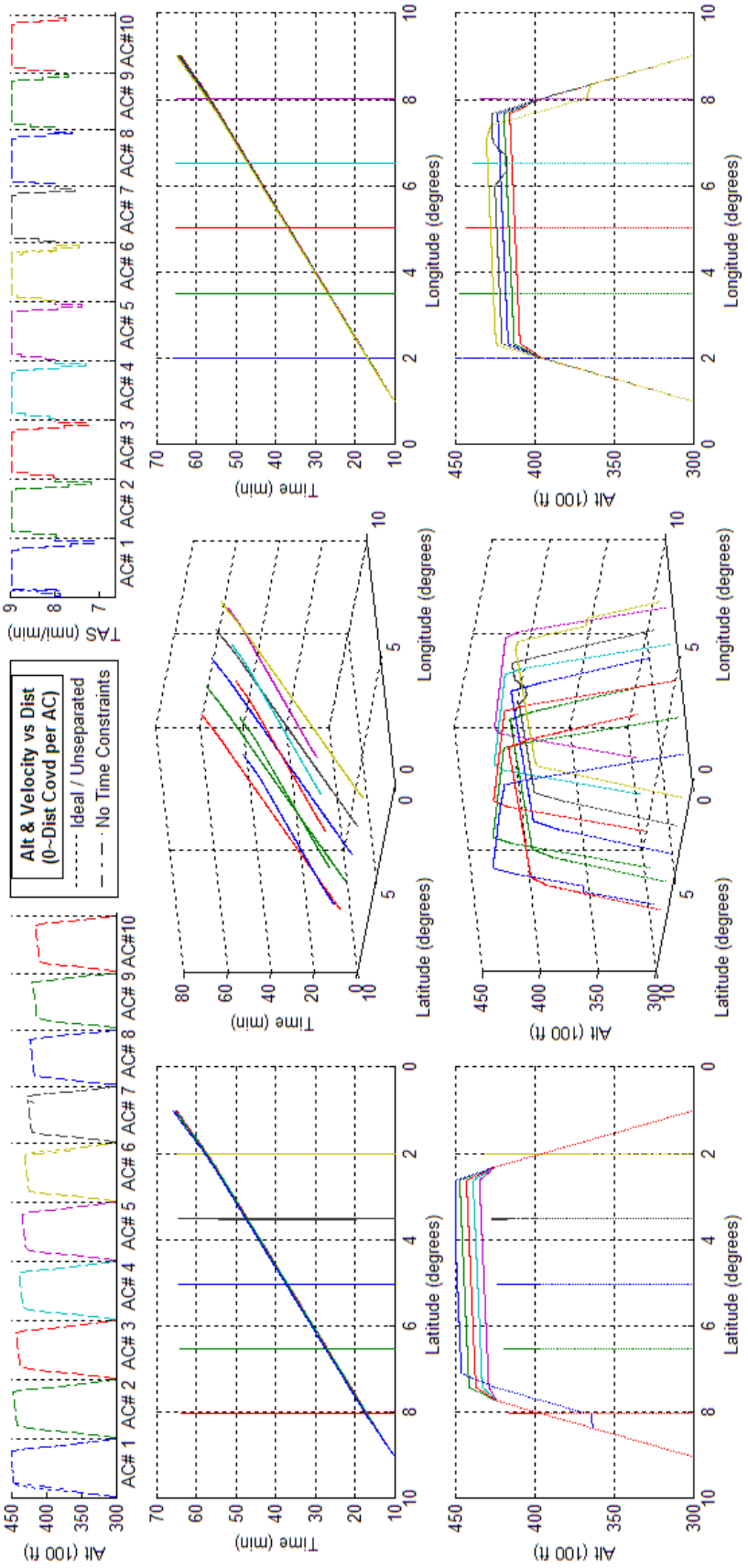

Figure 166 - Optimized 10acCH assuming no arrival time constraints.

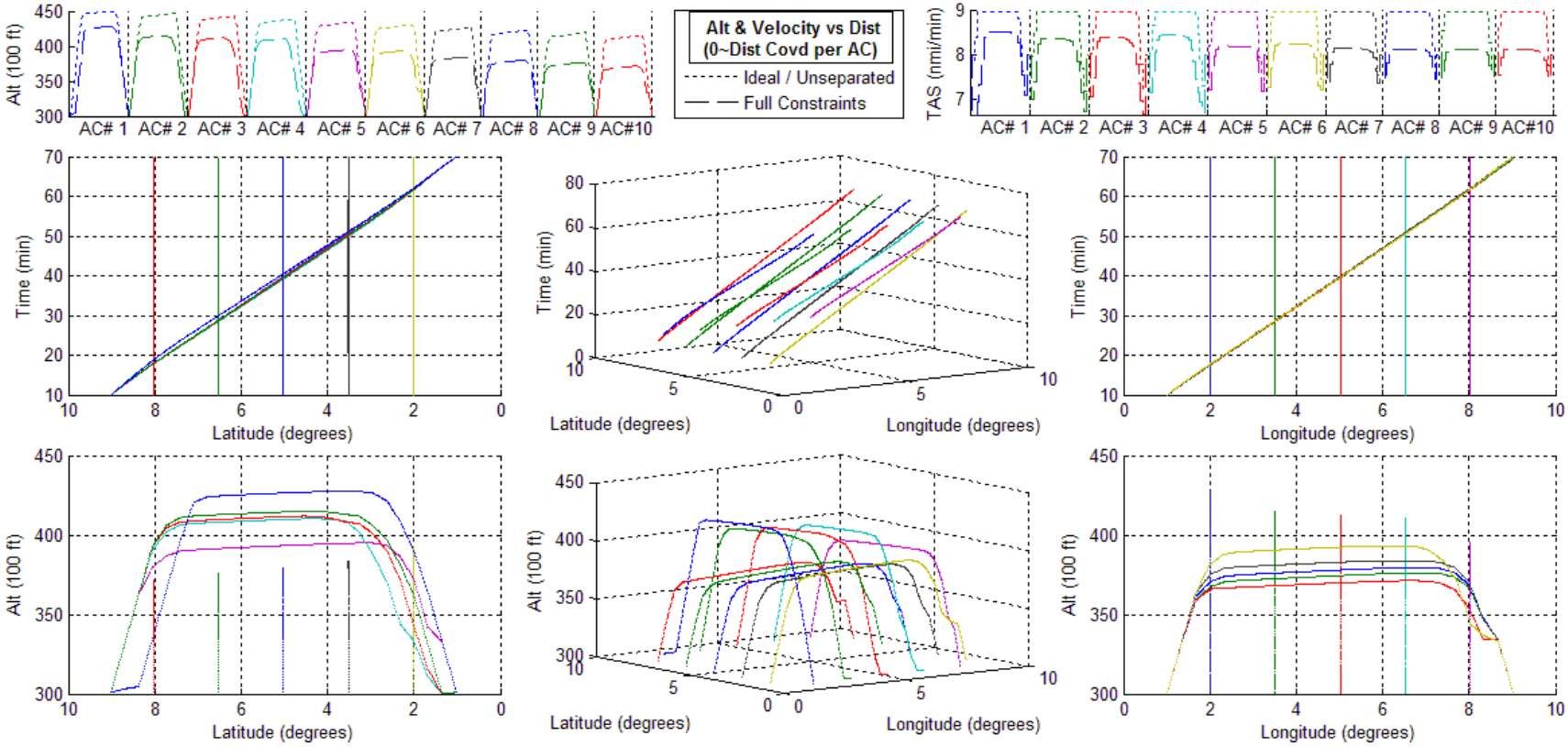

Figure 167 - Optimized 10acCH assuming arrival time constraints.

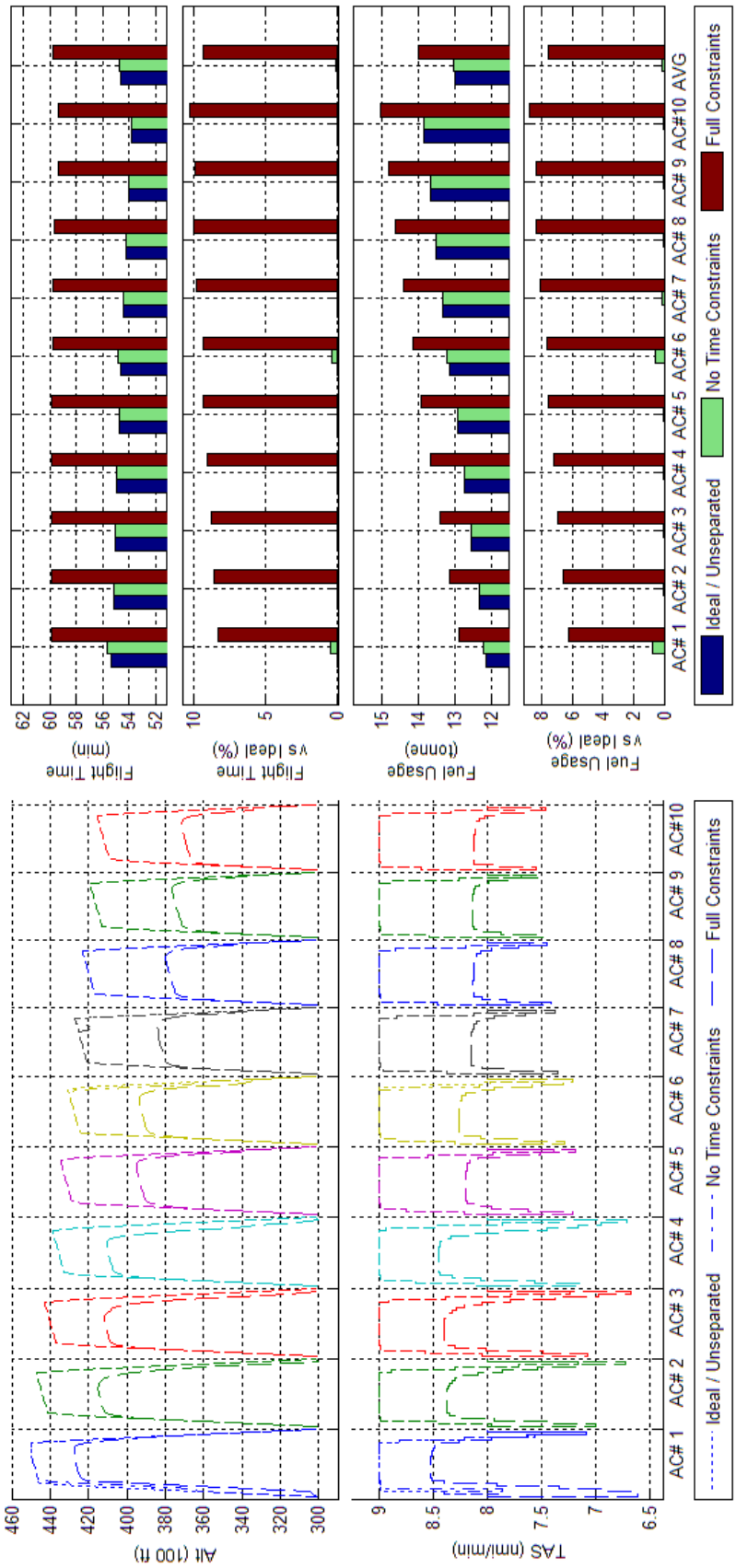

Figure 168 Trajectory Shape, Flight Time, and Fuel Consumption Comparisons of Optimized 10acCH results with and without an arrival time constraint

G.9 Generic Boeing 747-300 - Scenario 2acPH2H

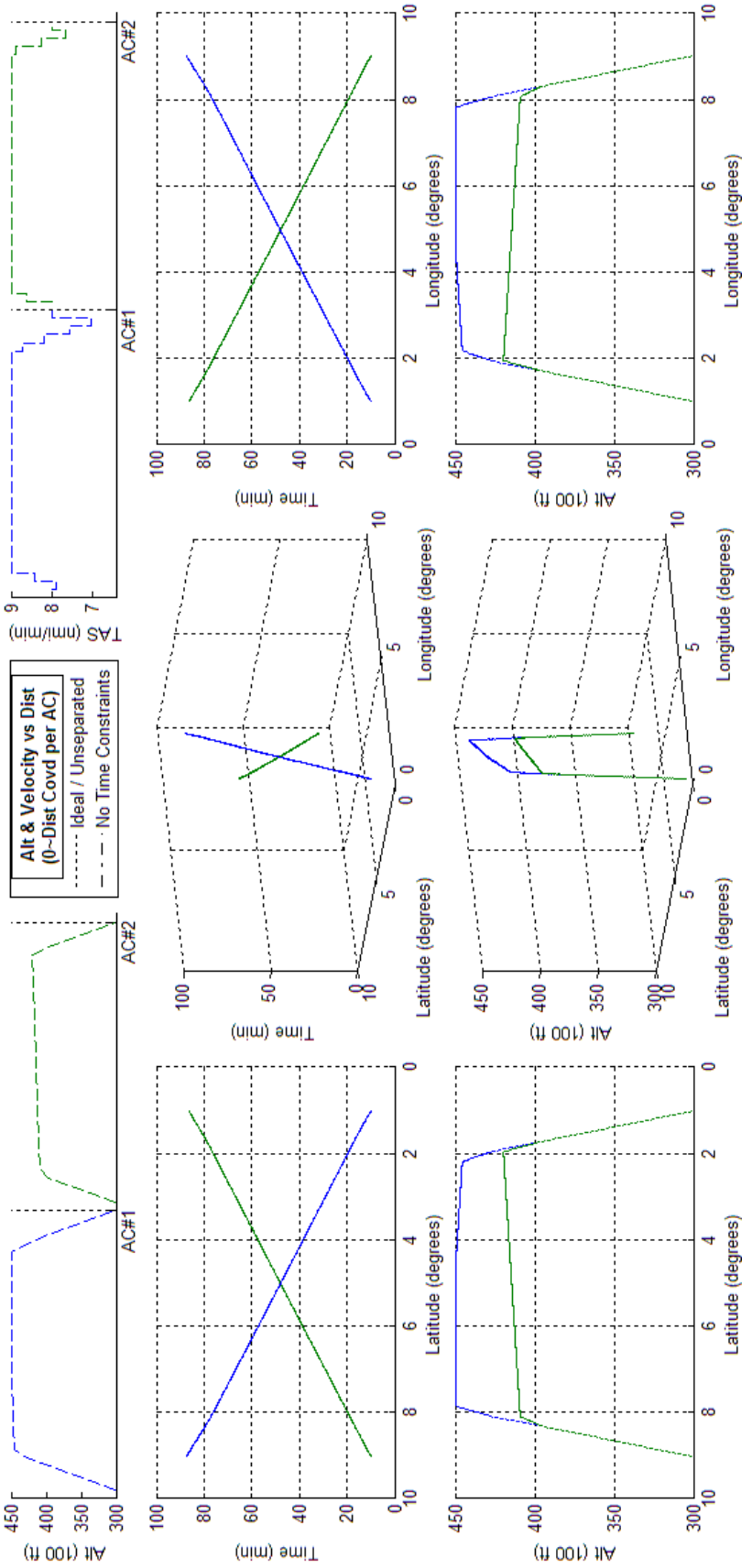

Figure 169 - Optimized 2acPH2H assuming no arrival time constraints.

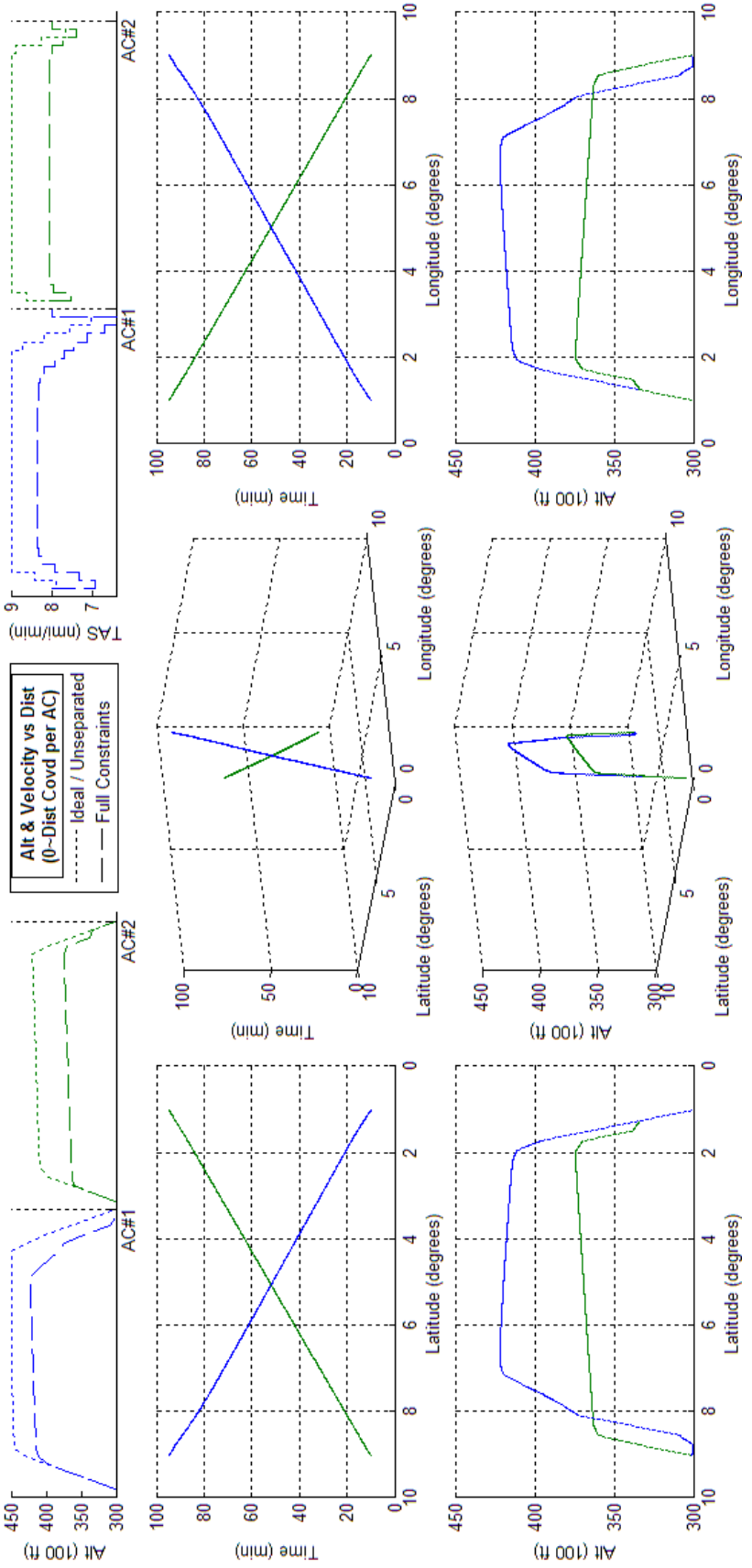

Figure 170 - Optimized 2acPH2H assuming arrival time constraints.

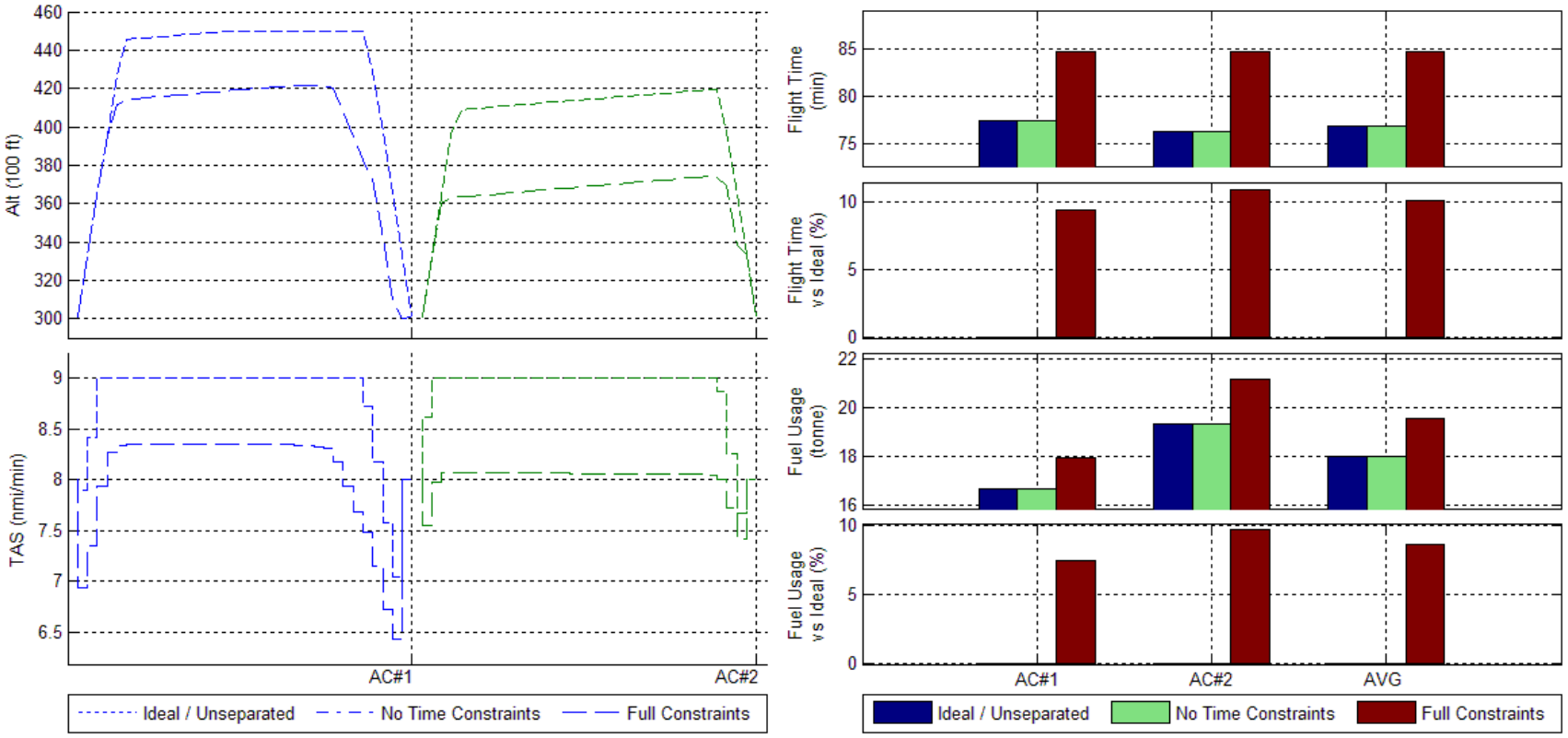

Figure 171 Trajectory Shape, Flight Time, and Fuel Consumption Comparisons of Optimized 2acPH2H results with and without an arrival time constraint

G.10 Generic Boeing 747-300 - Scenario 4acPH2H

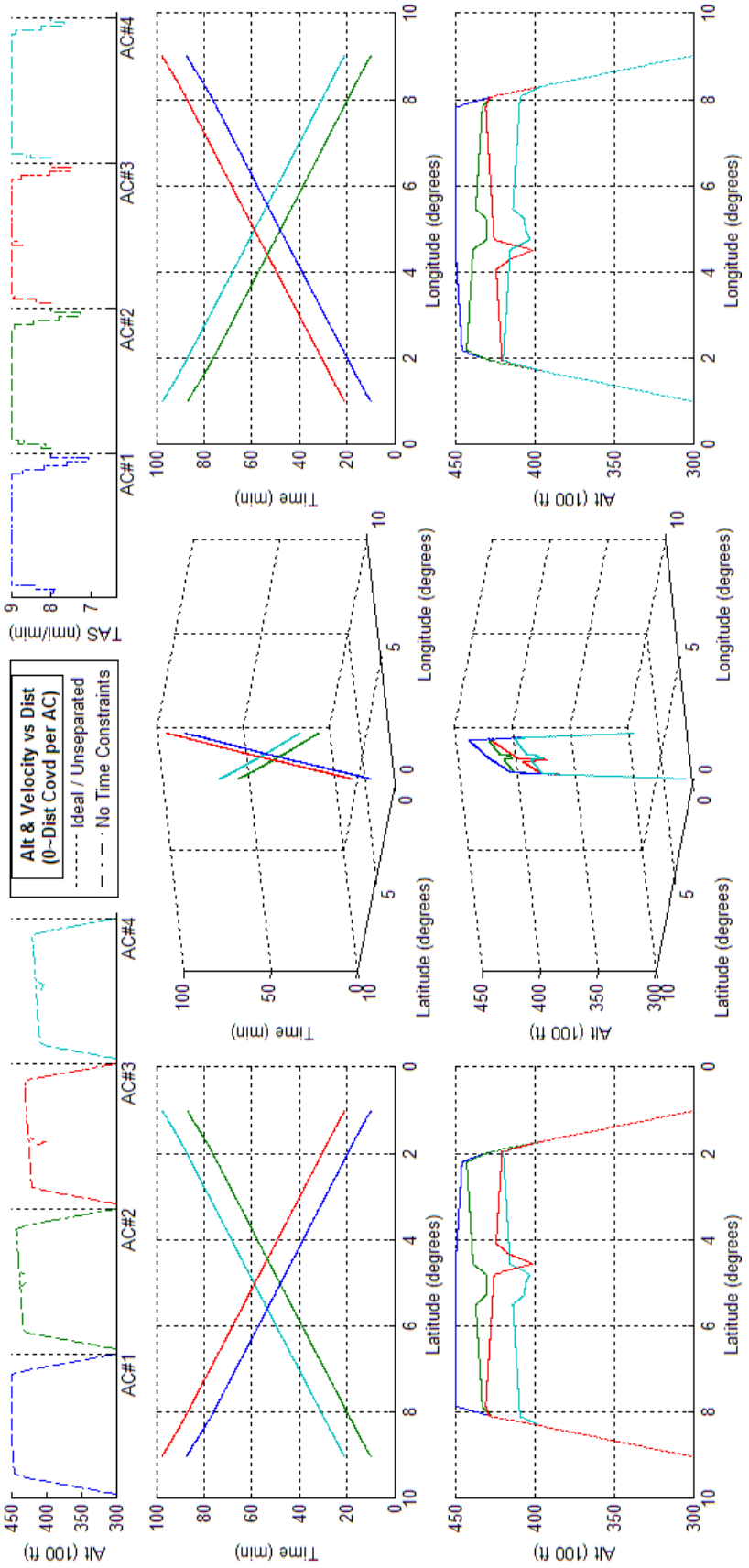

Figure 172 - Optimized 4acPH2H assuming no arrival time constraints.

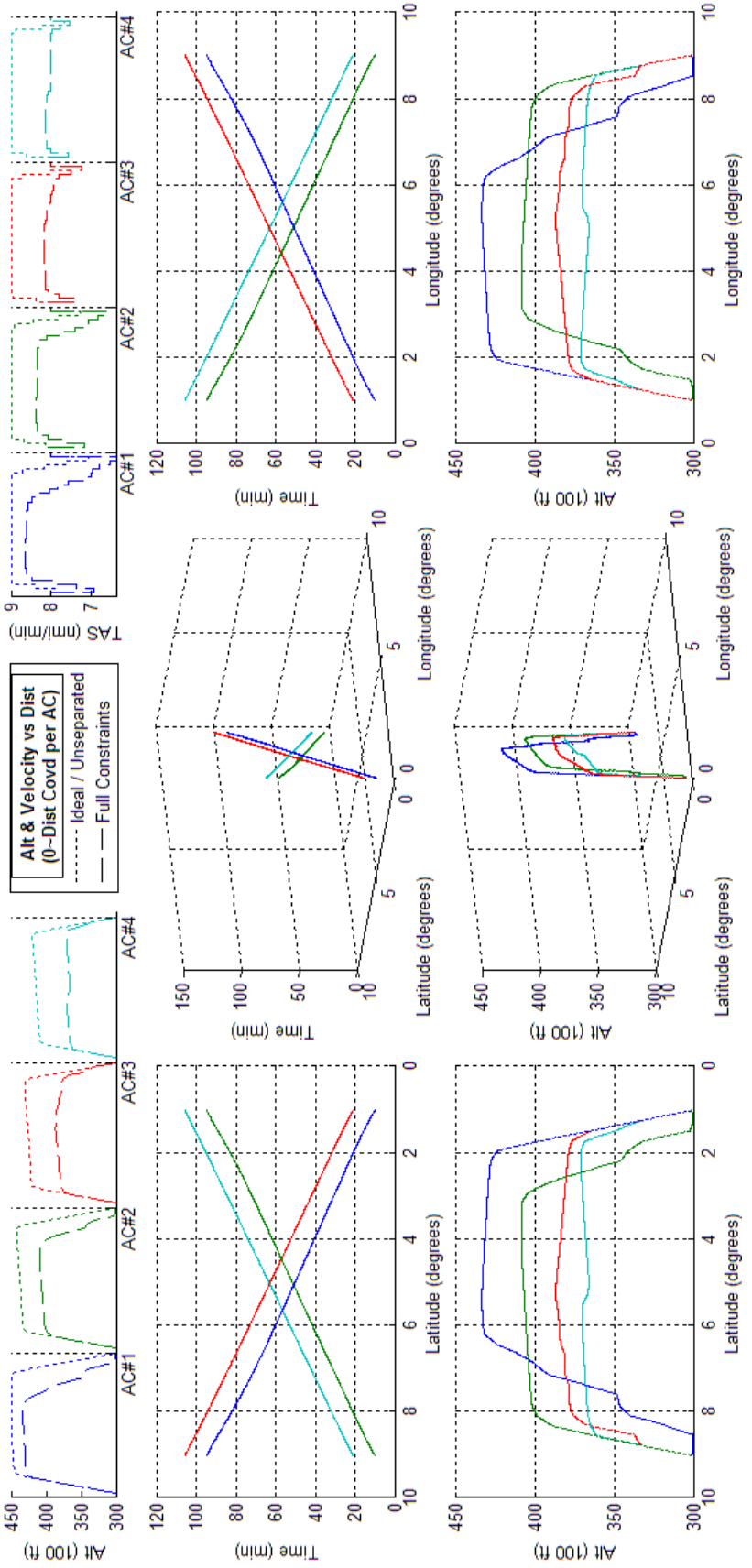

Figure 173 - Optimized 4acPH2H assuming arrival time constraints.

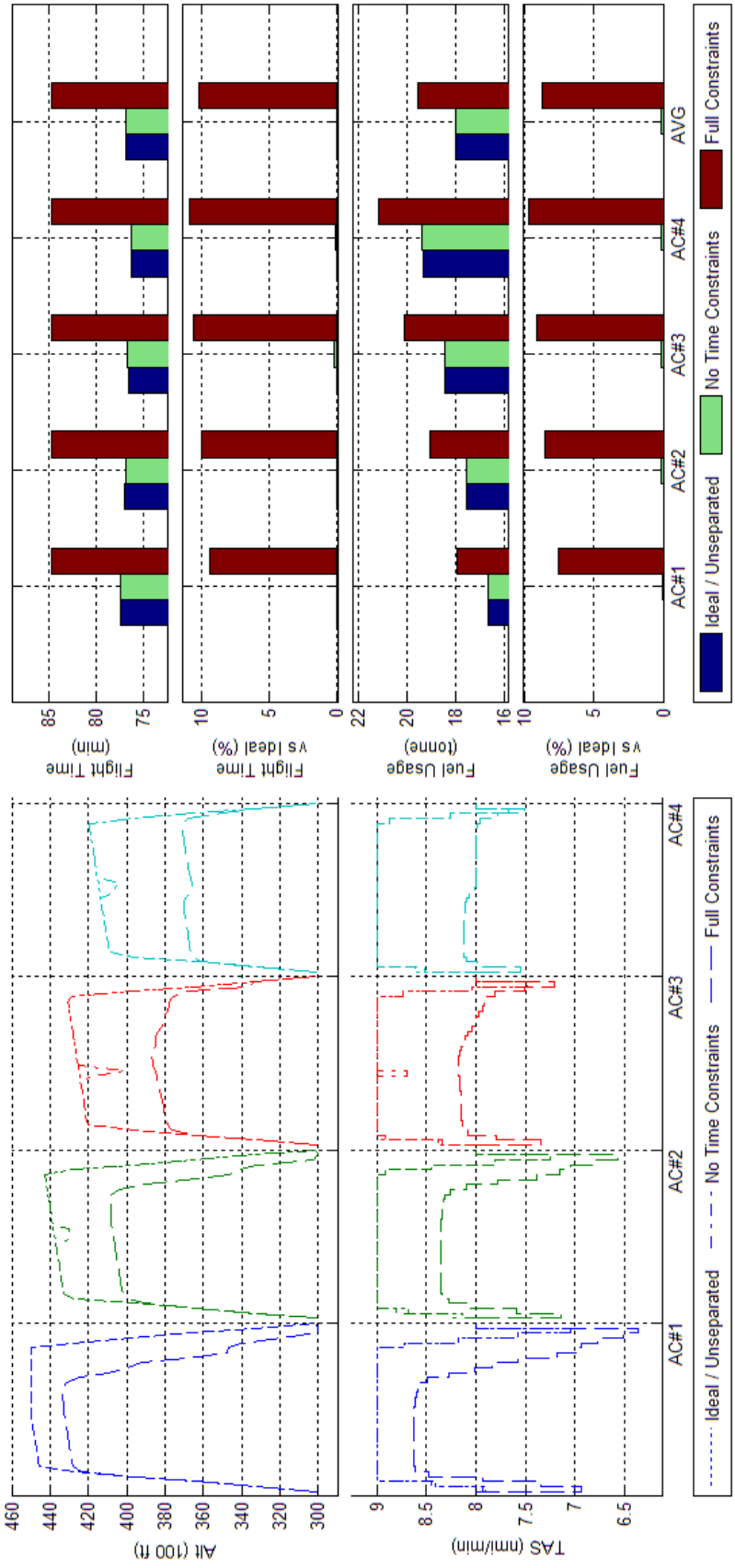

Figure 174 Trajectory Shape, Flight Time, and Fuel Consumption Comparisons of Optimized 4acPH2H results with and without an arrival time constraint

G.11 Generic Boeing 747-300 - Scenario 10acPH2H

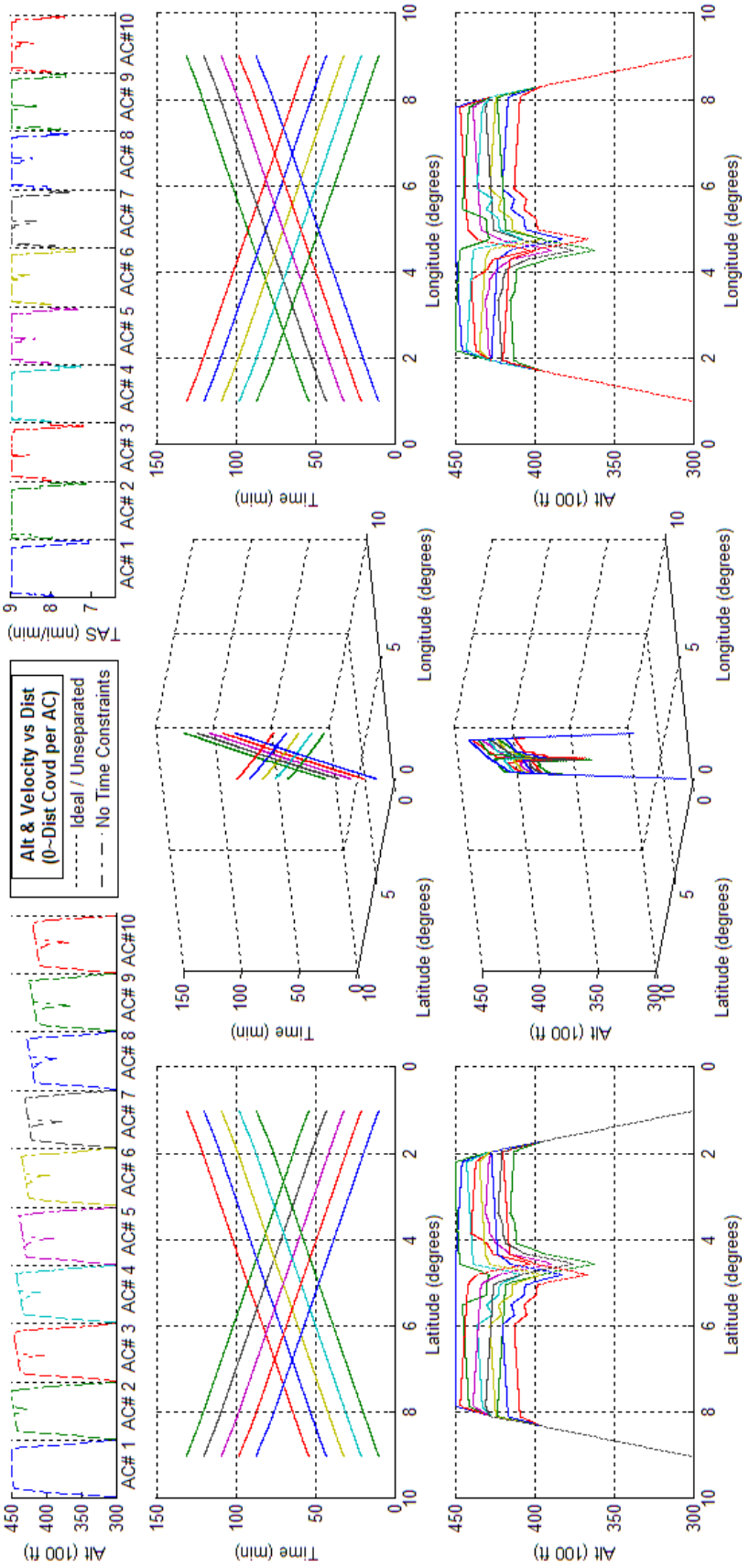

Figure 175 - Optimized 10acPH2H assuming no arrival time constraints.

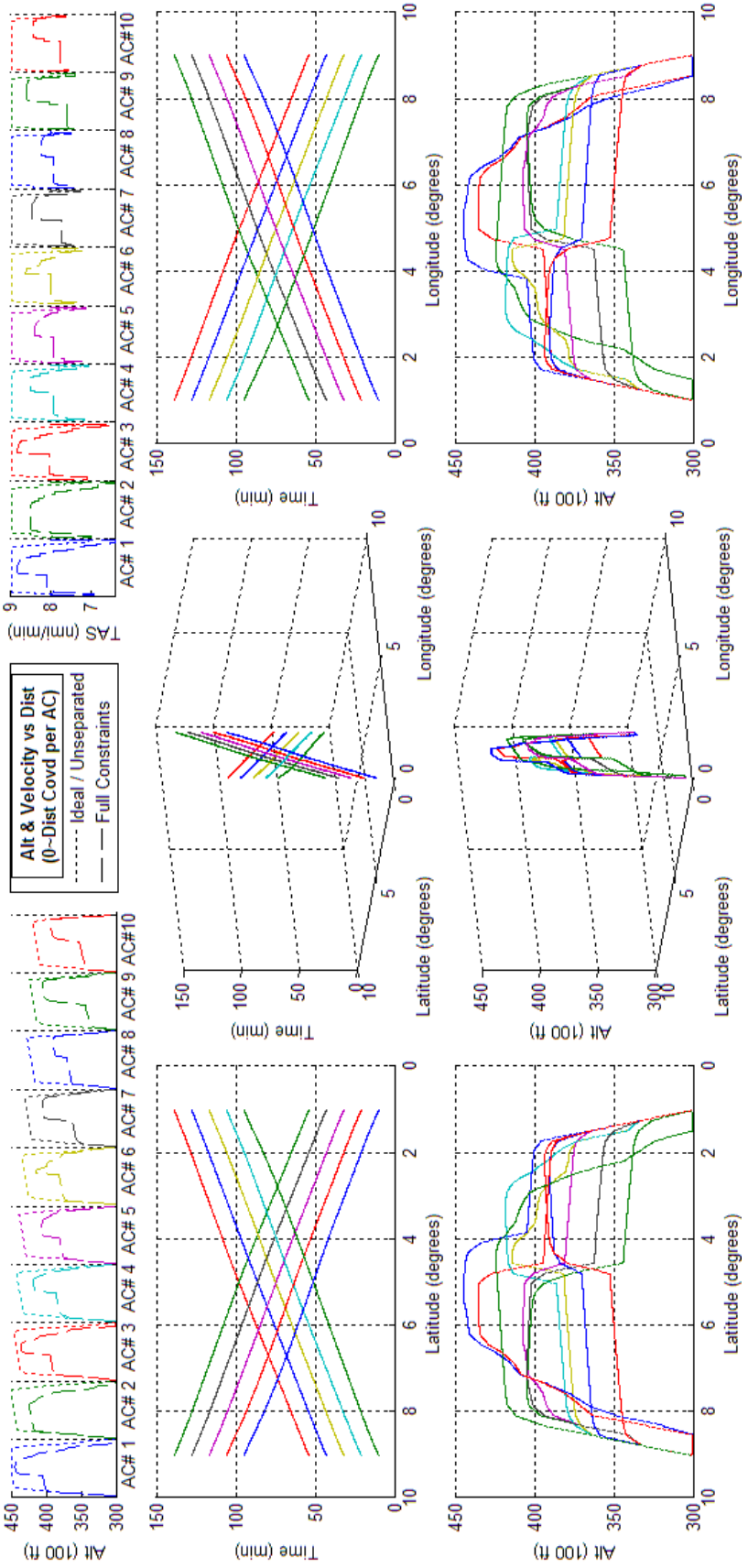

Figure 176 - Optimized 10acPH2H assuming arrival time constraints.

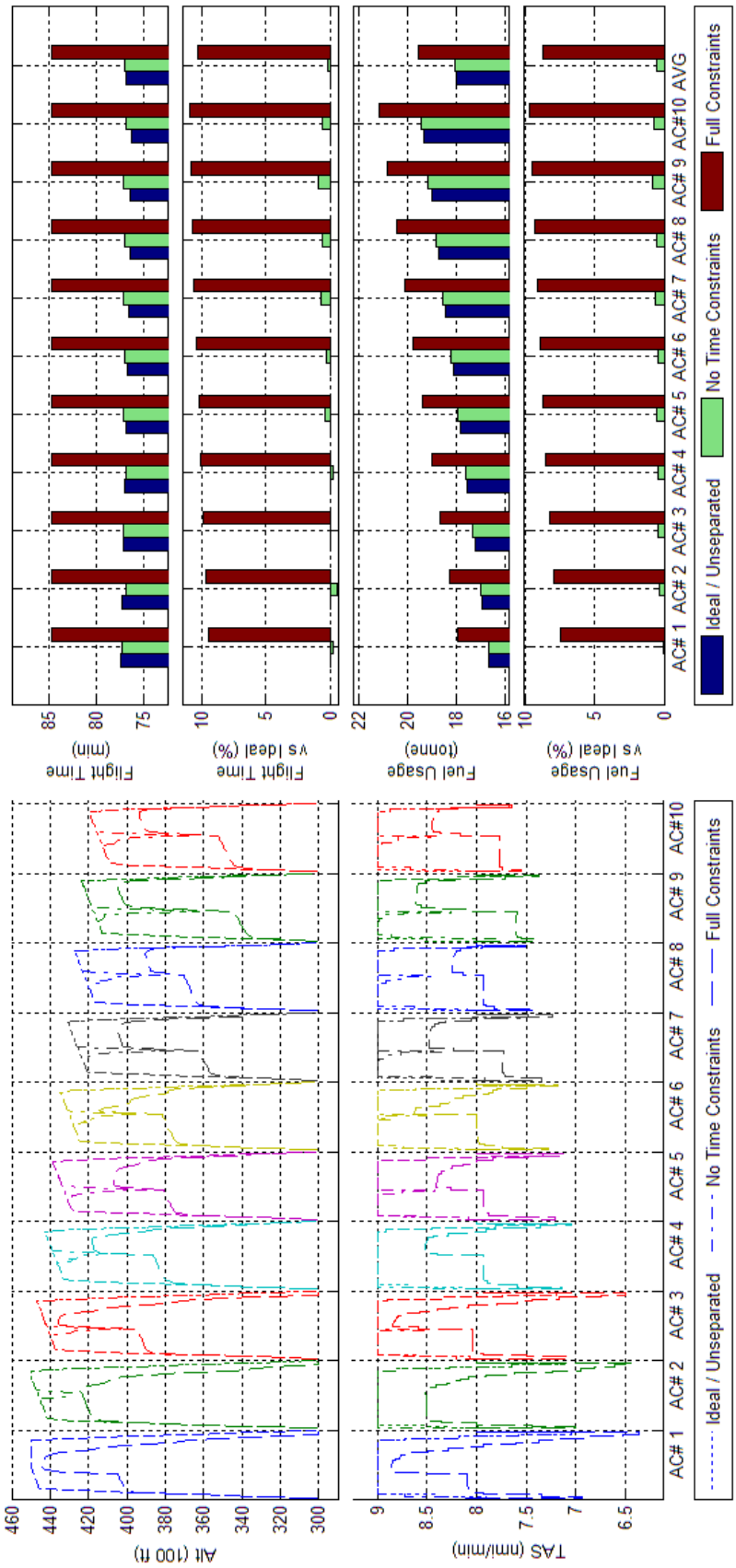

Figure 177 Trajectory Shape, Flight Time, and Fuel Consumption Comparisons of Optimized 10acPH2H results with and without an arrival time constraint

APPENDIX H BADA Equations

The following equations show the engine specific formula utilized in the BADA model smoothness tests.

H.1 Engine Specific Fuel Consumption Equations

For jets this was:

$$\mu = \frac{C_{f1}}{60 \times 1000} \times \left(1 + \frac{V_{TAS} \times 1.9438}{C_{f2}}\right) \times C_{fcr}$$

For Turboprops this is:

$$\mu = \frac{C_{f1}}{60 \times 1000} \times \left(1 - \frac{V_{TAS} \times 1.9438}{C_{f2}}\right) \times \frac{V_{TAS} \times 1.9438}{1000} \times C_{fcr}$$

For Piston engines this is constant and not based on *T*, thus cruise fuel flow, f_{cr}, skips μ and is:

$$f_{cr} = C_{f1} \times C_{fcr}$$

H.2 Engine Specific Thrust Constraint Equations

For Jets, the equation and optimizer friendly constraint were:

$$T_{req} \le C_{Tcr} \times C_{Tc1} \times \left(1 - \frac{h}{C_{Tc2}} + C_{Tc3} \times h^2\right)$$

$$\frac{T_{req}}{C_{Tcr} \times C_{Tc1}} - \left(1 - \frac{h}{C_{Tc2}} + C_{Tc3} \times h^2\right) \le 0$$

For Turboprops, the equation and optimizer friendly constraint were:

$$T_{req} \le \frac{C_{Tcr} \times C_{Tc1}}{V_{TAS} \times 1.9438} \times \left(1 - \frac{h}{C_{Tc2}}\right) + C_{Tcr} \times C_{Tc3}$$

$$\frac{T_{req}}{C_{Tcr} \times C_{Tc1}} - \frac{1}{V_{TAS} \times 1.9438}\left(1 - \frac{h}{C_{Tc2}}\right) - \frac{C_{Tc3}}{C_{Tc1}} \le 0$$

For Piston engines, the equation and optimizer friendly constraint were:

$$T_{req} \le C_{Tcr} \times C_{Tc1} \times \left(1 - \frac{h}{C_{Tc2}}\right) + \frac{C_{Tcr} \times C_{Tc3}}{V_{TAS} \times 1.9438}$$

$$\frac{T_{req}}{C_{Tcr} \times C_{Tc1}} - \left(1 - \frac{h}{C_{Tc2}}\right) - \frac{C_{Tc3}}{V_{TAS} \times 1.9438 \times C_{Tc1}} \le 0$$

APPENDIX I BADA Model Continuity Tests- B743

This appendix shows records for the BADA model smoothness testing for the Boeing 747-300 from BADA version 3.6. This data acted as validation that the model parameter variation defined by the application of BADA methods used here did result in fuel consumption functions that would provide useful results when used by the BFO. It should be noted that this is only the tests that were run for B743; further tests were run for all aircraft available in BADA 3.6, with no issues seen in models with complete aircraft performance data. There are eighteen specific graphs covered in the next four pages; among them are nine different aircraft 'situations', with each situation showing both the feasible variation in fuel usage, as well as the causes behind the shape of infeasible portions of said fuel usage. The nine 'situations' shown include; 1) zero acceleration and zero climb angle, 2) 0.015g acceleration and zero climb angle, 3) -0.015g acceleration and zero climb angle, 4) zero acceleration and 1.5° climb angle, and 5) zero acceleration and -1.5° climb angle, 6) 0.015g acceleration and 1.5° climb angle, 7) -0.015g acceleration and 1.5° climb angle, 8) 0.015g acceleration and -1.5° climb angle, and 9) -0.015g acceleration and -1.5° climb angle.

The first and third pages shows the aircraft's feasible fuel usage at various speeds, altitudes, and initial percentage fuel capacity. For clarity, slices of the fuel usage in terms of the three parameters were taken at 15% fuel capacity increments. Additionally, two perspectives of fuel usage data are provided to allow sight of potentially hidden portions of the data. The variation in colour in these graphs do indicate the variation in fuel usage as it changes between various speeds, altitudes and initial percentage fuel capacity; a numerical legend for such variation is shown on the left.

The second and fourth pages shows the aircraft's infeasible fuel usage under the same speeds, altitudes and fuel capacity, but correlates them according to which of the constraints caused that point to be infeasible. For the purpose of understanding and comparison, these have been placed directly behind their situational counterparts. Given that multiple constraints can be breached at any point, infeasible regions can and do overlap. Most of the constraints shown do correlate with those mentioned in the main body and do use the same nomenclature, however one constraint not discussed seriously enough to warrant mathematics was " $\%FC_f < {}^1/_6 * \%FC_i$ " which is merely a constraint breach representing situations where an aircraft had used up 5/6 of its spare fuel capacity; given that aircraft are supposed to have 30 minutes of spare flight time, breaching this requirement indicated that the aircraft would have less than 5 mins of fuel after landing which posed a significant hazard if it failed to land.

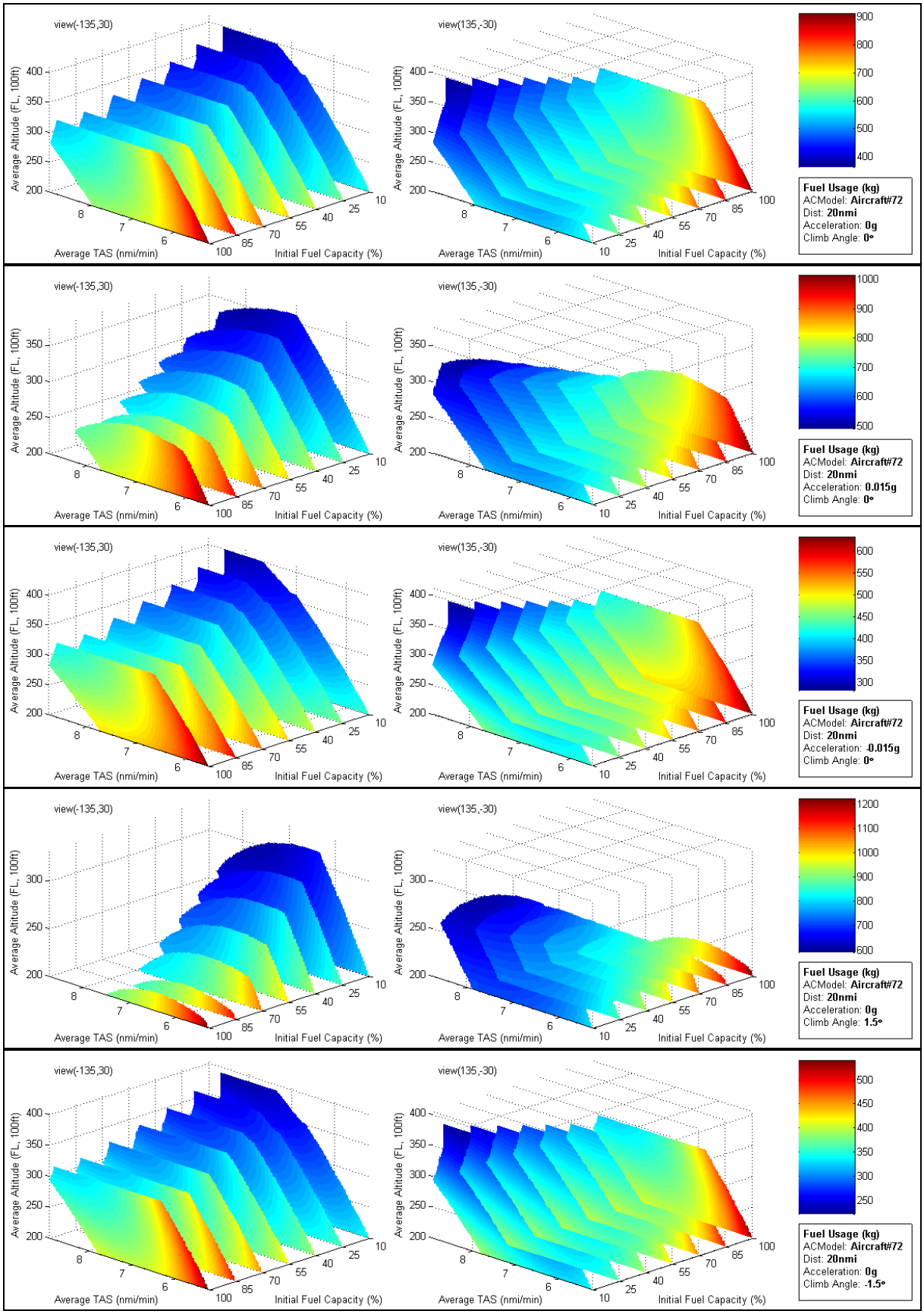

Figure 178 -Fuel Consumption at various *h*, *TAS*, and F_i, assuming various a_l and γ.

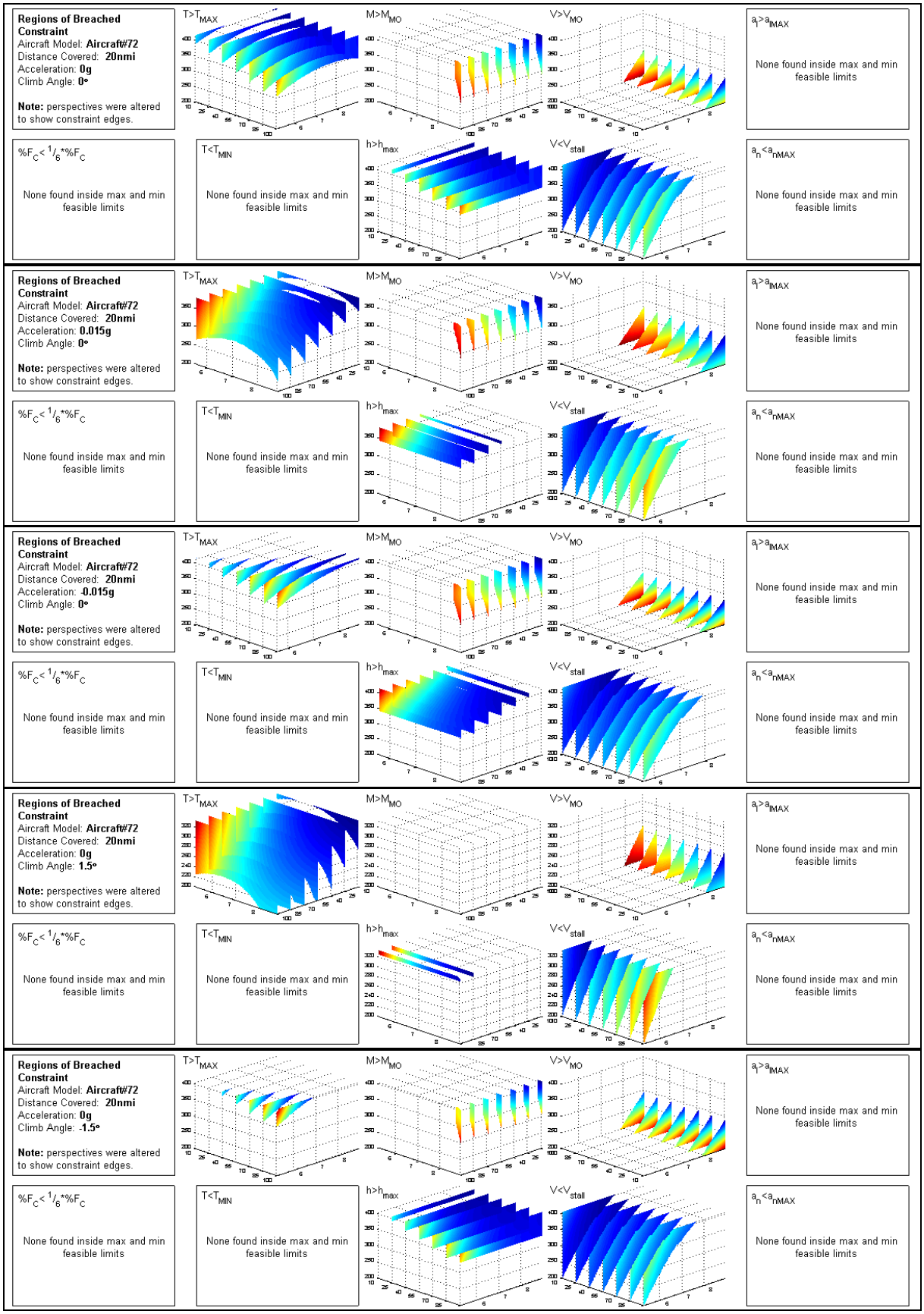

Figure 179 -Performance Constraints at various *h*, *TAS*, and F_i, assuming various a_l and γ.

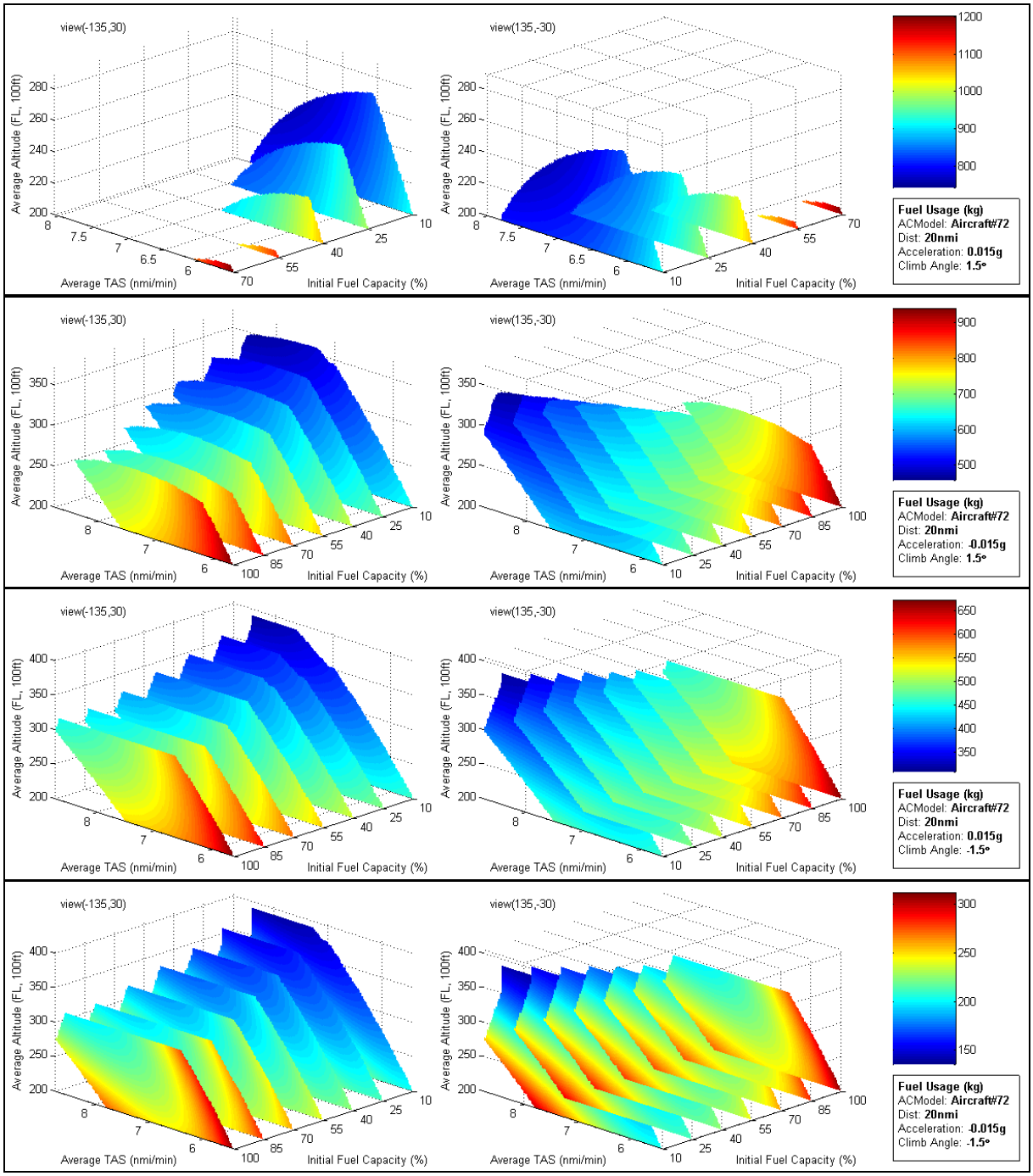

Figure 180 -Fuel Consumption at various *h*, *TAS*, and F_i, assuming combinations of nonzero a_l and γ.

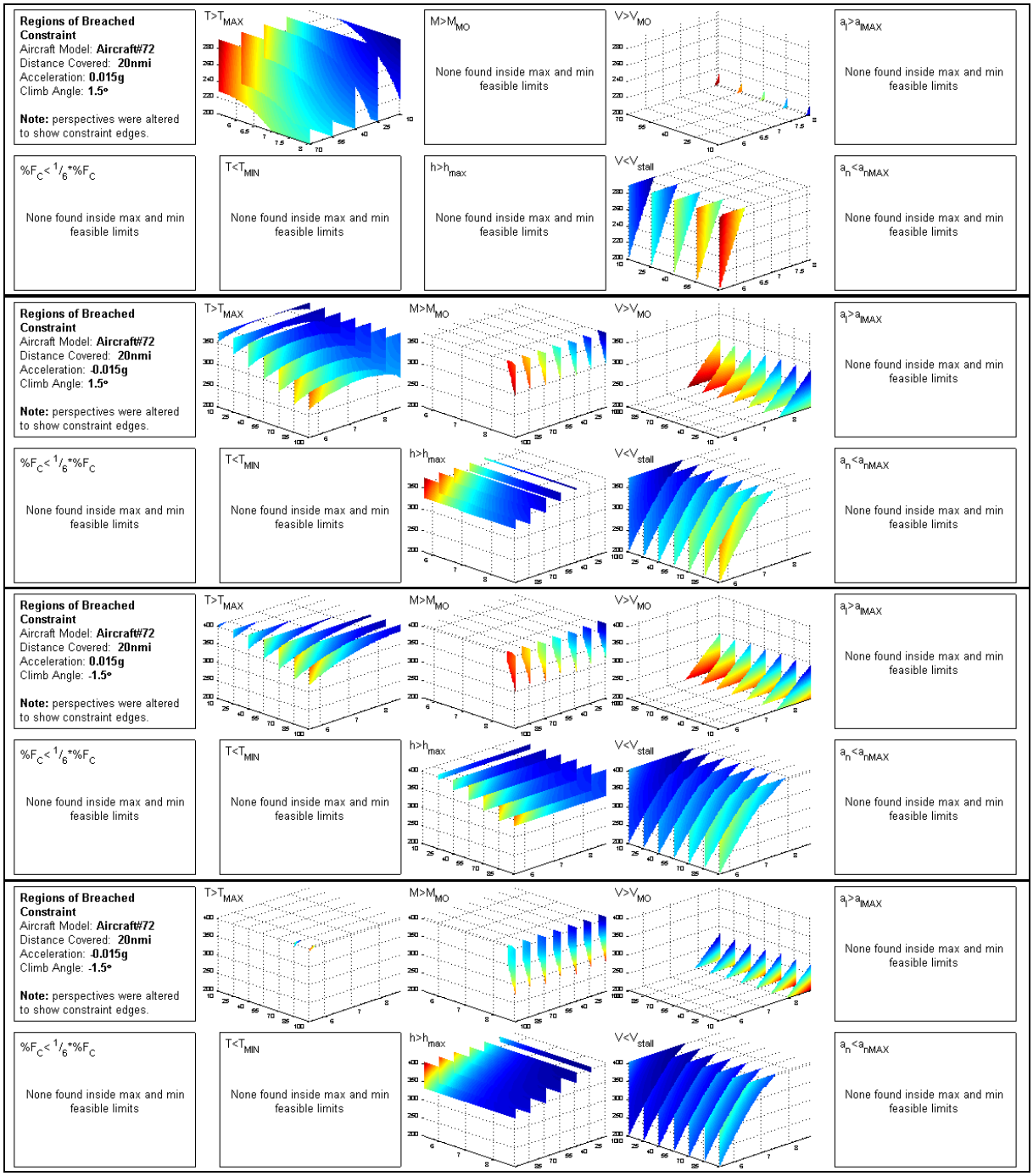

Figure 181 -Performance Constraints at various *h*, *TAS*, and F_i, assuming nonzero combinations a_l and γ.

APPENDIX J BADA Fuel Optimization Results

The following graphs show the results for the PCO when using BADA data, as mentioned in Chapter 4 of the thesis. For discussion of the results and impacts of these results, please refer to section 4.3.2. For instructions on how to read the graphs, please refer to section 3.4.1. Each section in this appendix shows five graphs:

- The first graph shows optimization results of the scenario assuming ATFU minimization and no ETA constraint.
- The second graph is the same as the first, but shows the impact of having an ETA constraint.
- The third graph compares the trajectory shape, fuel usage and flight time of each aircraft between the unconstrained and constrained ETA results.
- The fourth graph is the same as the first, but shows the impact of minimizing deviation from schedule instead of ATFU.
- The fifth graph is the same as the third, but comparing the results of the first and fourth graphs.

The main purpose of these results was twofold. The first was to show that the method developed for the PCO could be used with various forms of ATFU calculation. Consequently the first, second, and third graphs are equivalent to the three graphs shown for each scenario in Appendix G. The second was to show the potential improvement in ATFU minimization that actual ATFU minimization has when compared to merely reducing physical impact of having to deviate away from other aircraft, i.e. minimization of schedule deviation. The fourth and fifth graphs are the visual representation of this issue with summarized information shown in section 4.3.2.

J.1 BADA Boeing 747-300 - Scenario 2acPSd - ATD_N

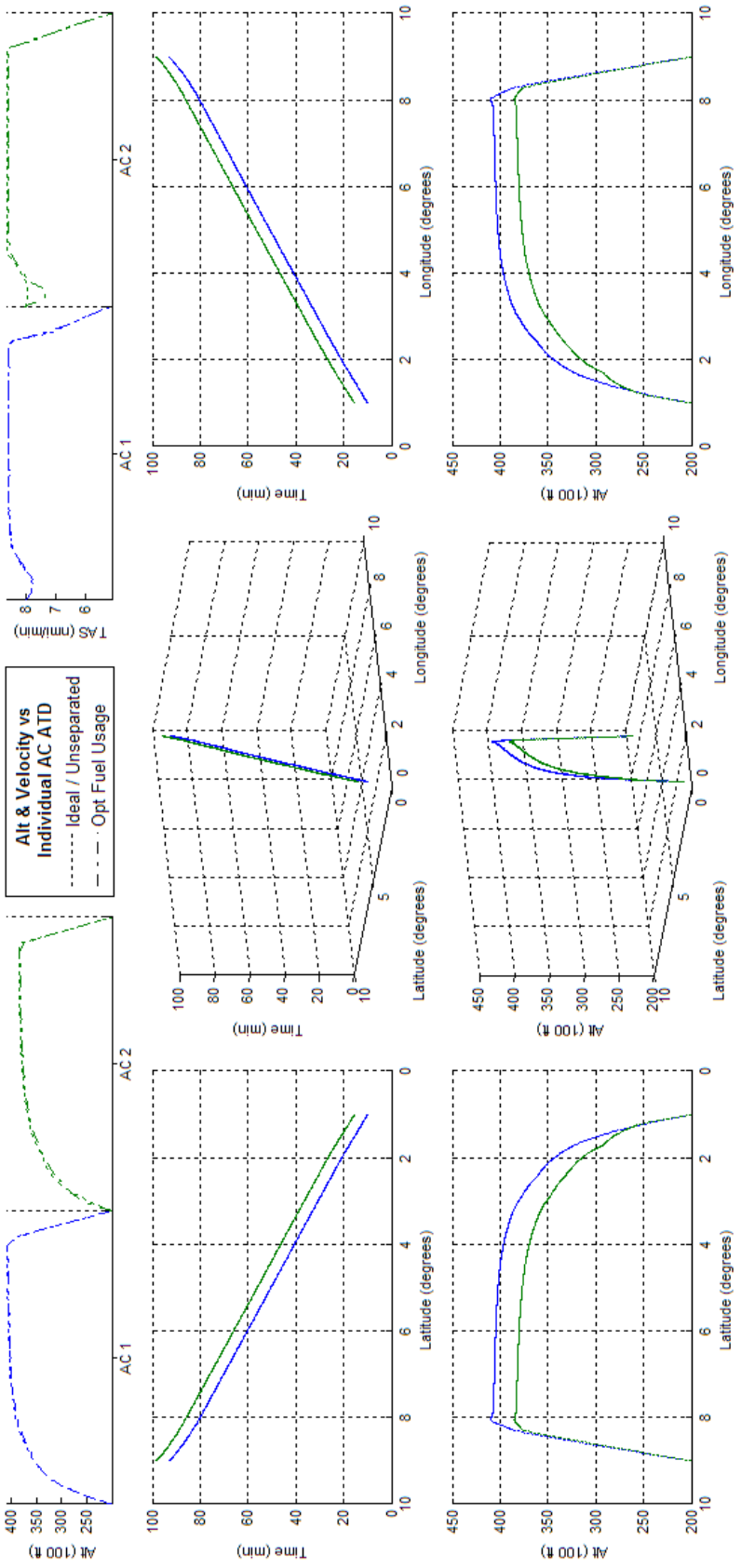

Figure 182 - Fuel Optimized 2acPSd ATD_N Results

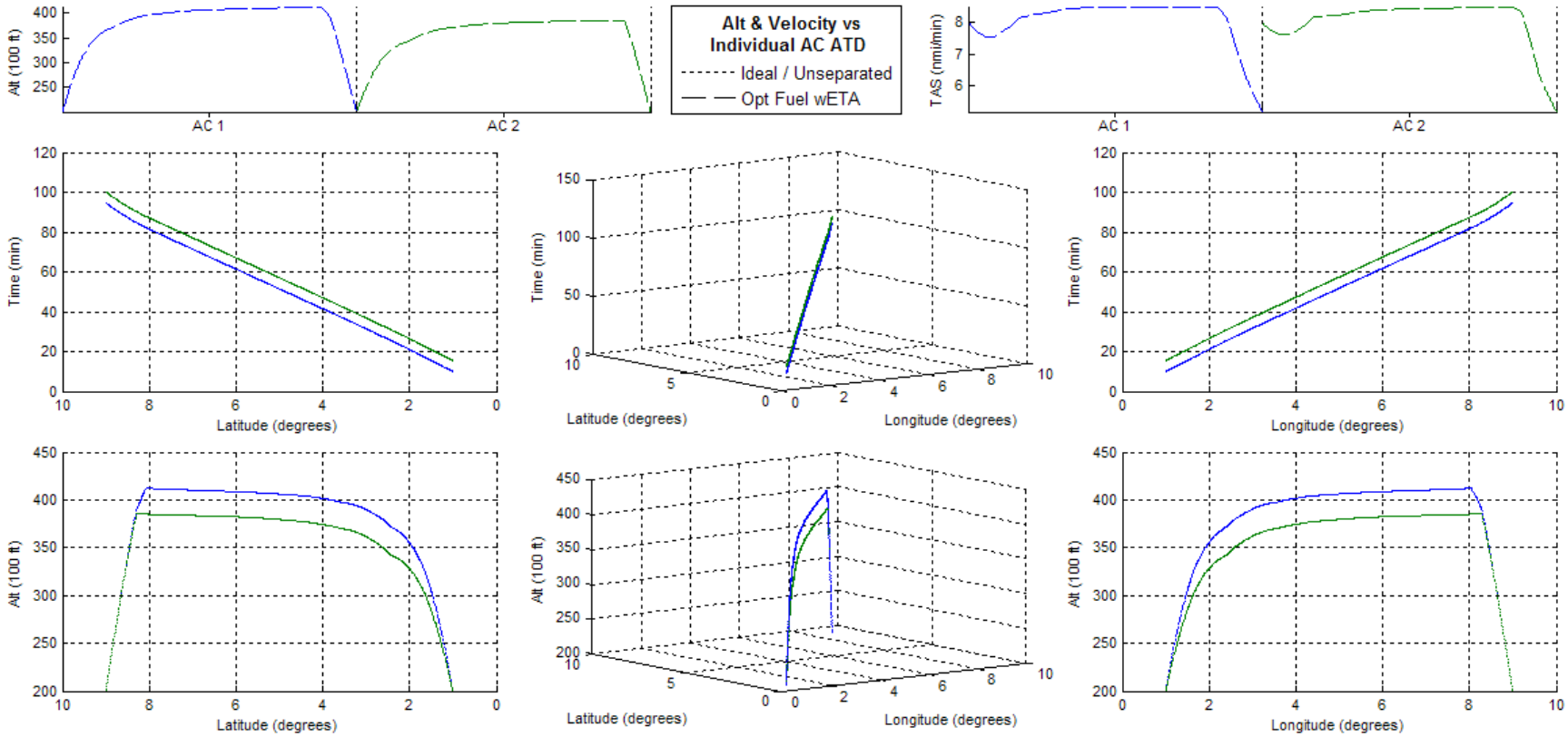

Figure 183 - Constrained ETA, Fuel Optimized 2acPSd ATD_N Results

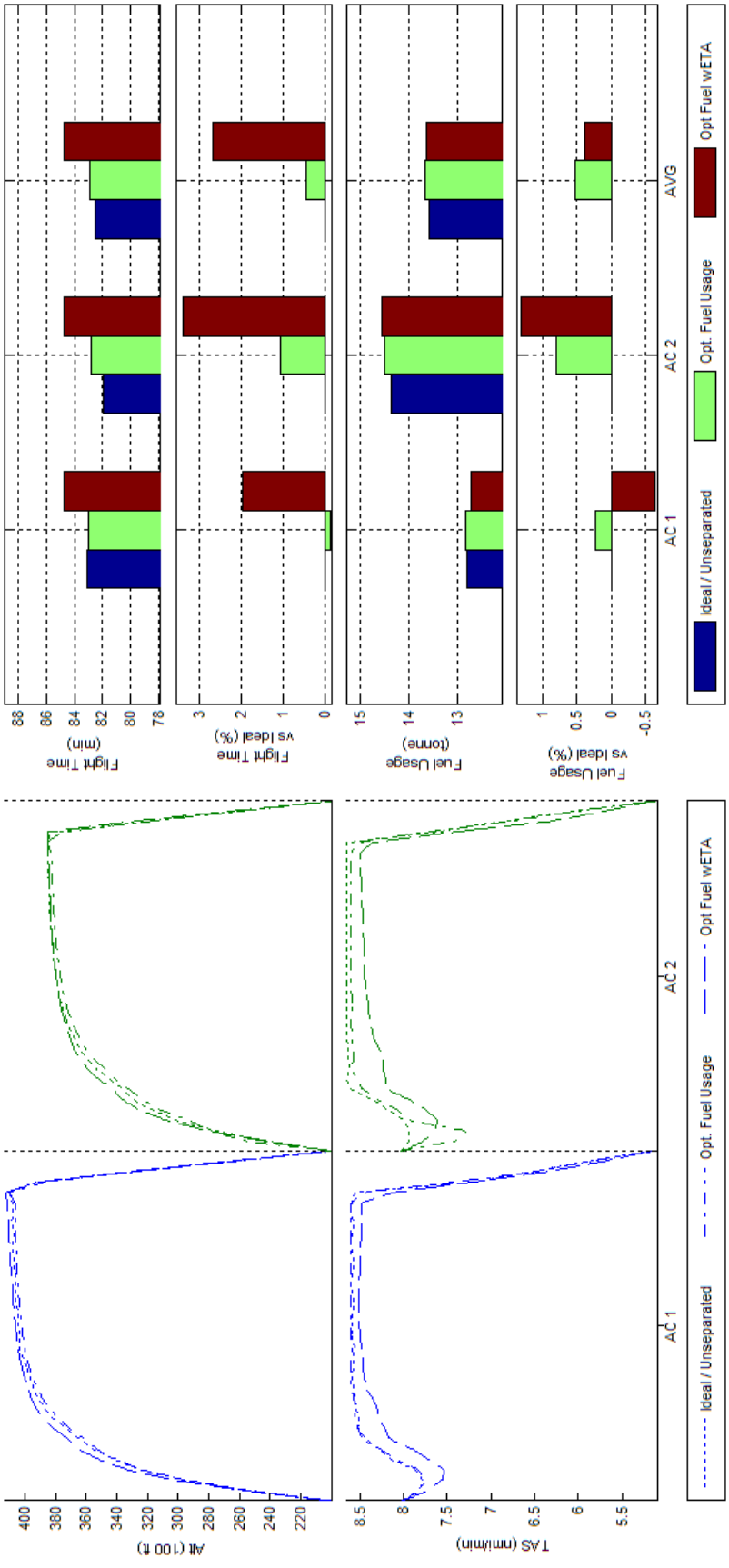

Figure 184 - Trajectory Shape, Flight Time, and Fuel Consumption Comparisons of Unconstrained and Constrained ETA, Fuel Optimized 2acPSd ATD_N Results

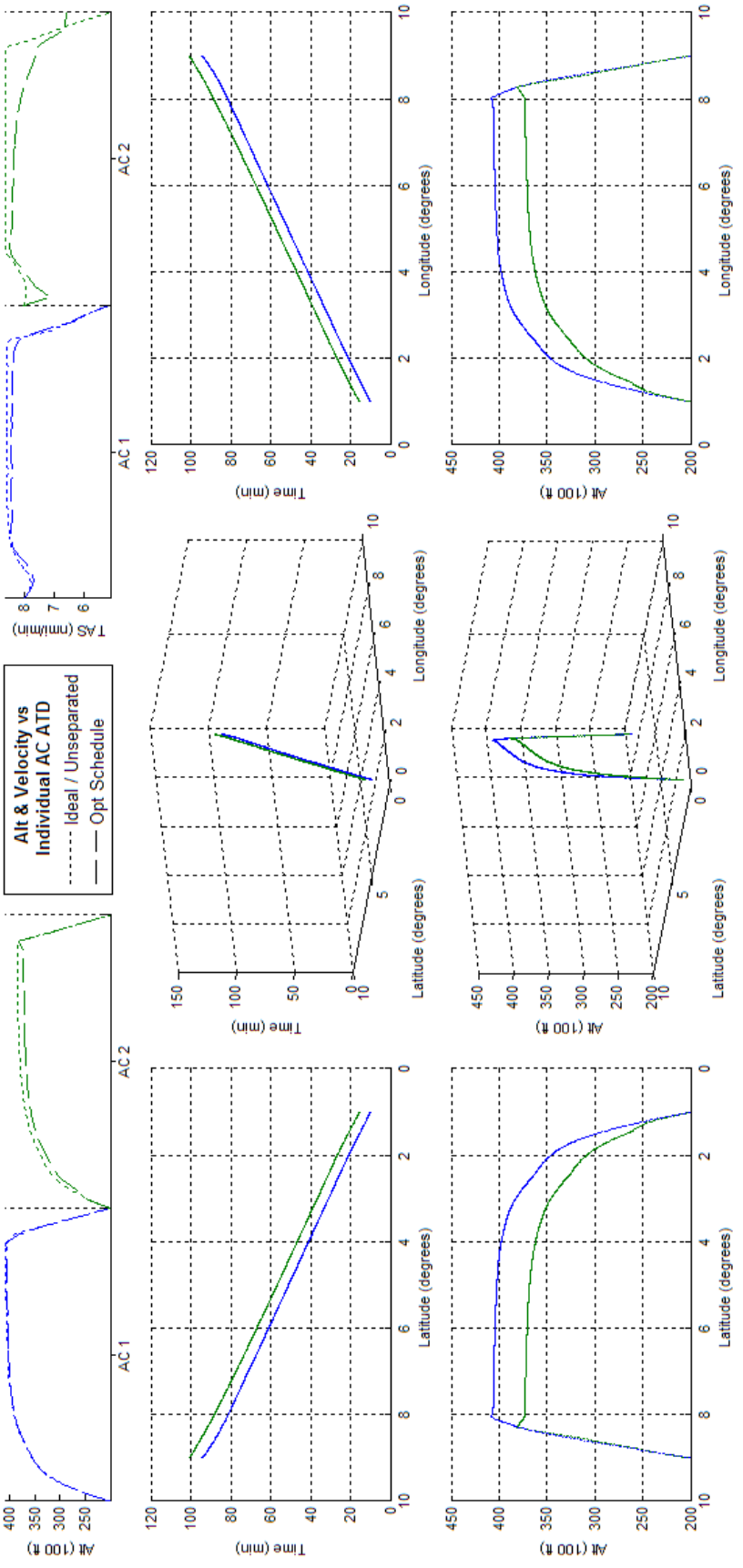

Figure 185 -Schedule Optimized 2acPSd ATD_N Results

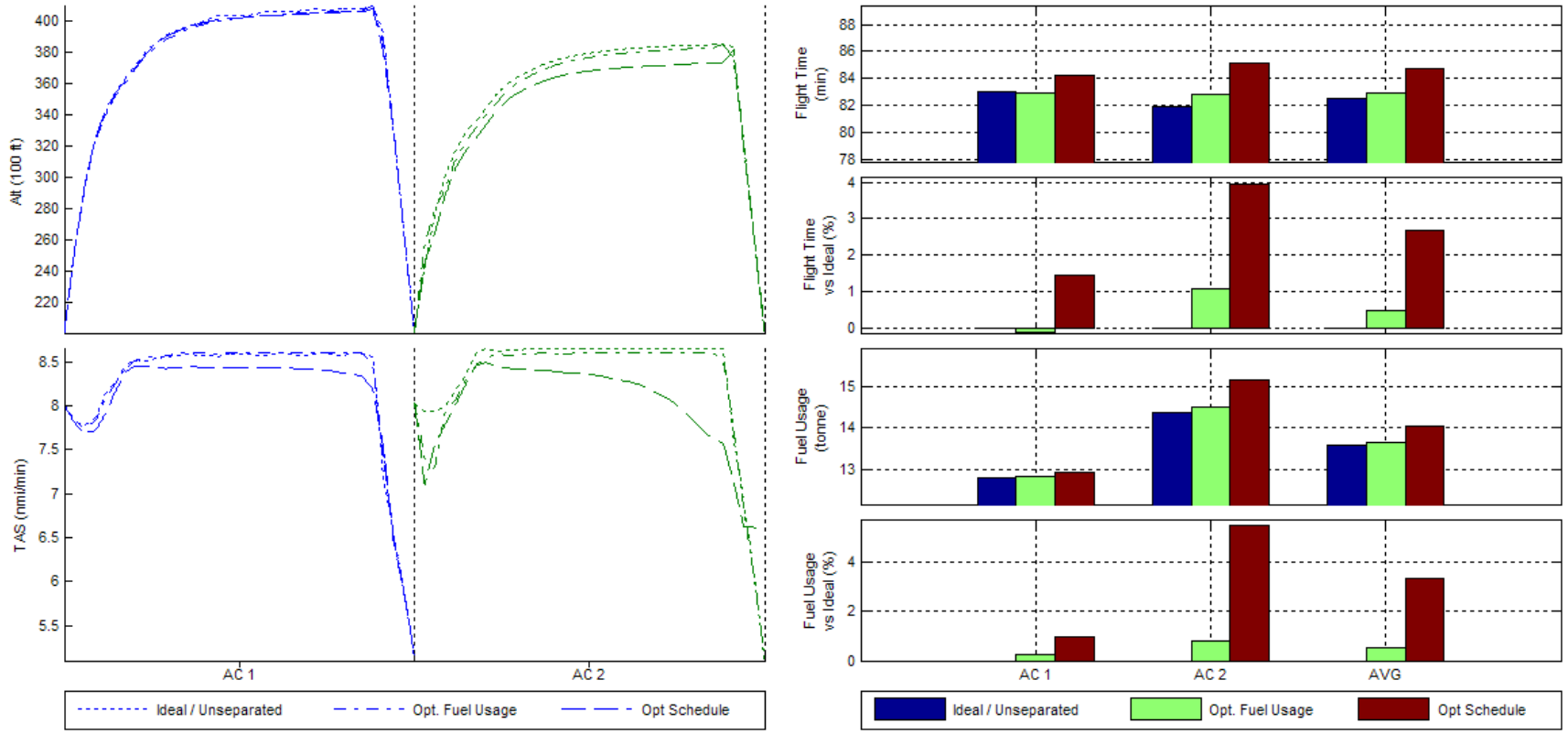

Figure 186 - Trajectory Shape, Flight Time, and Fuel Consumption Comparisons of Fuel and Schedule Optimized 2acPSd ATD_N Results

J.2 BADA Boeing 747-300 - Scenario 4acPSd - ATD_N

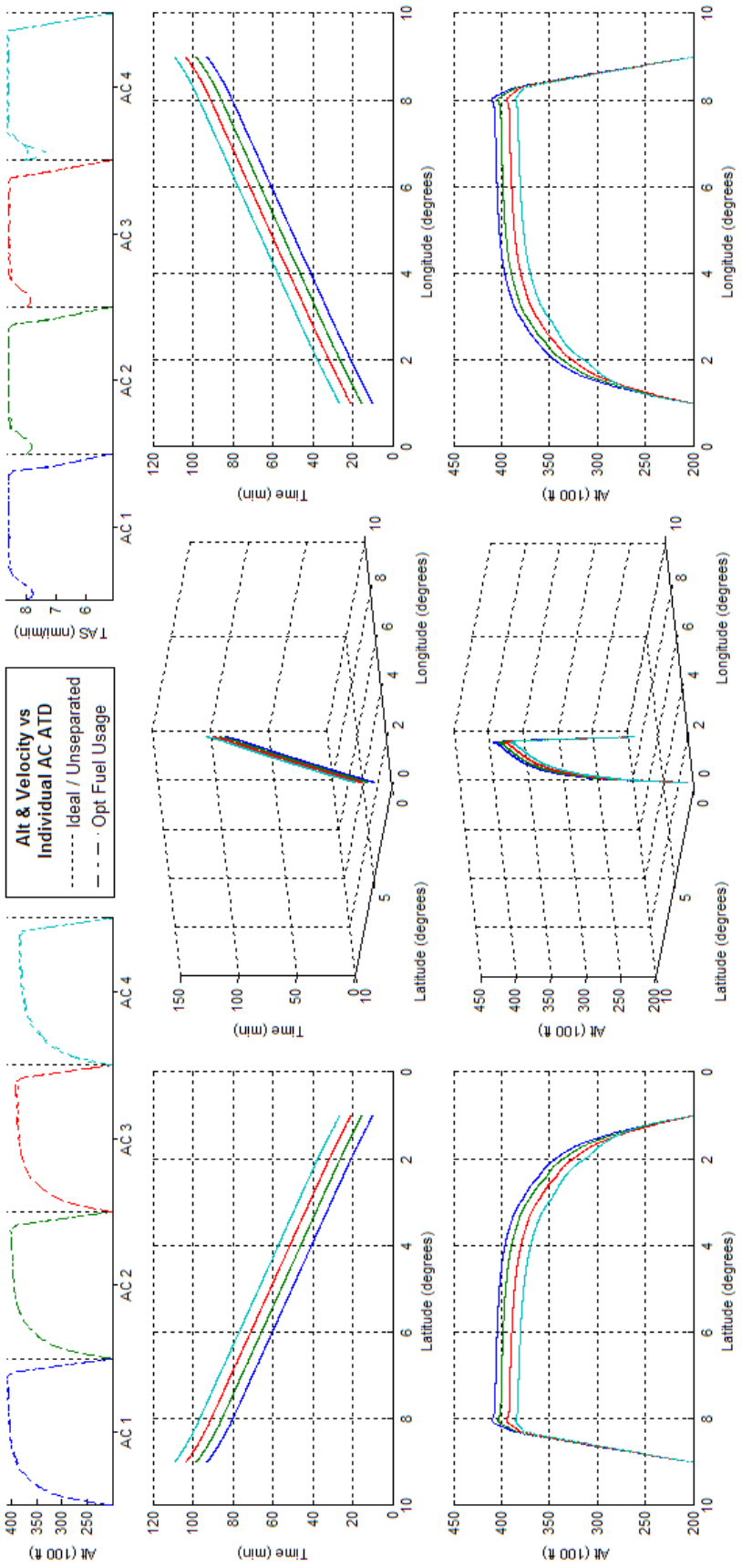

Figure 187 - Fuel Optimized 4acPSd ATD_N Results

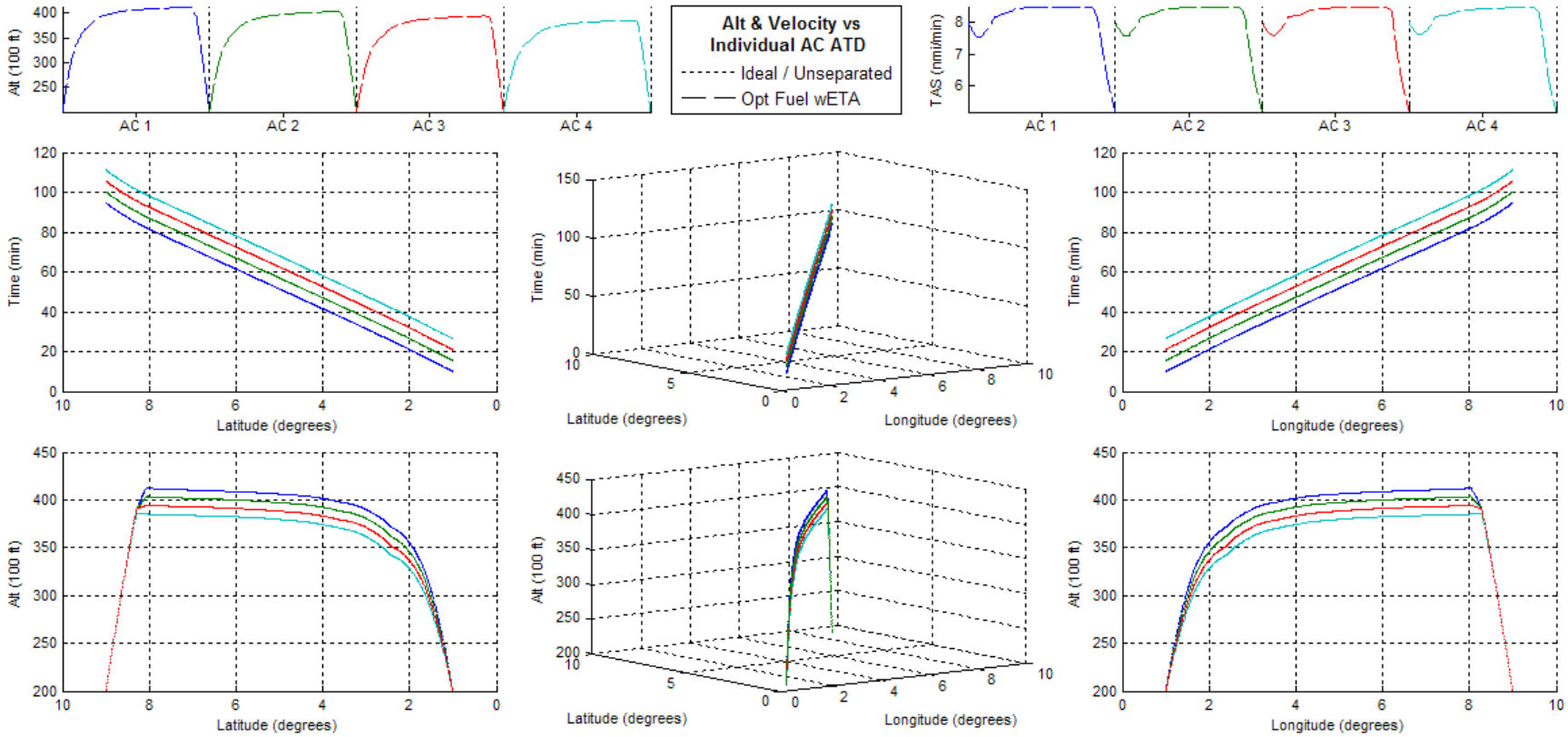

Figure 188 - Constrained ETA, Fuel Optimized 4acPSd ATD_N Results

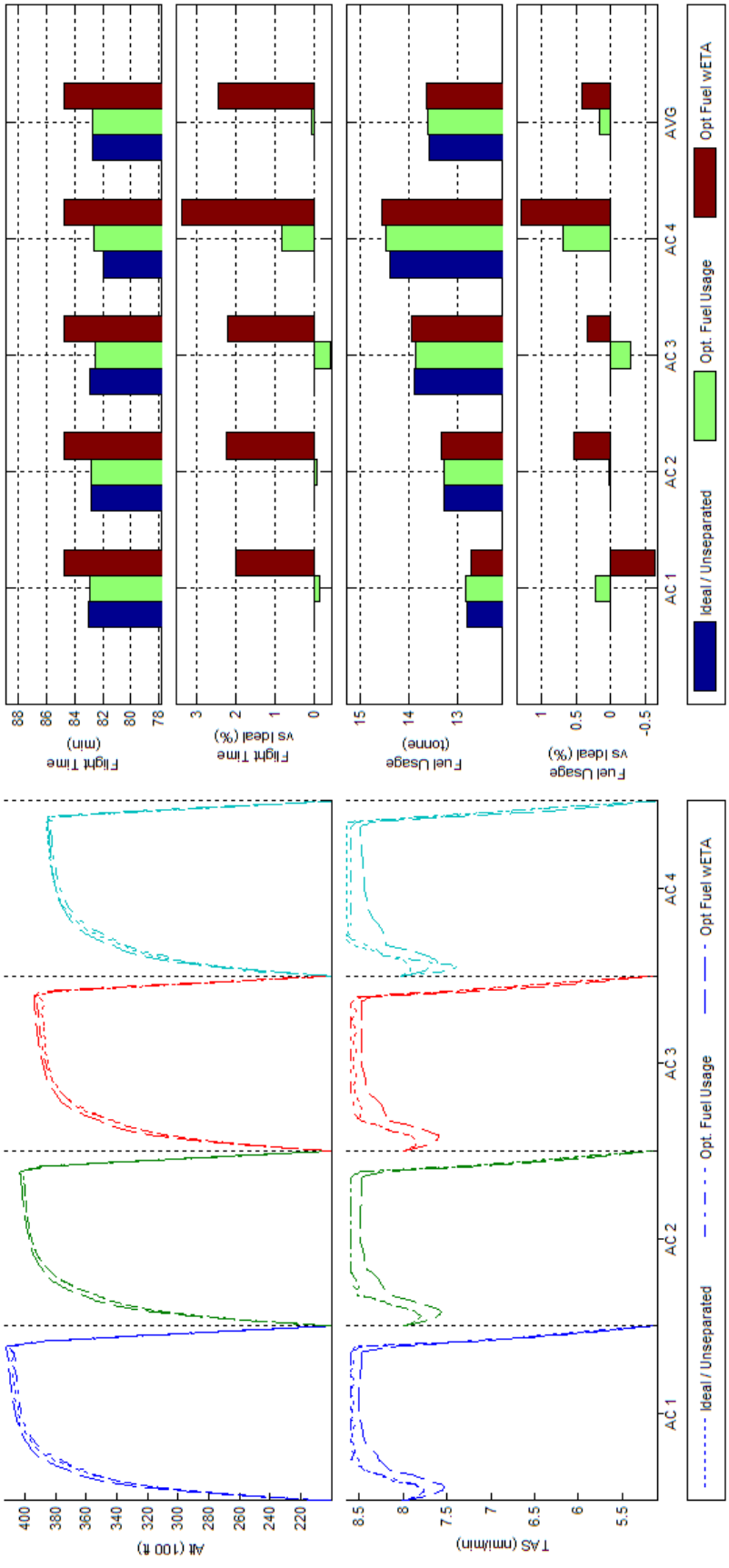

Figure 189 - Trajectory Shape, Flight Time, and Fuel Consumption Comparisons of Unconstrained and Constrained ETA, Fuel Optimized 4acPSd ATD_N Results

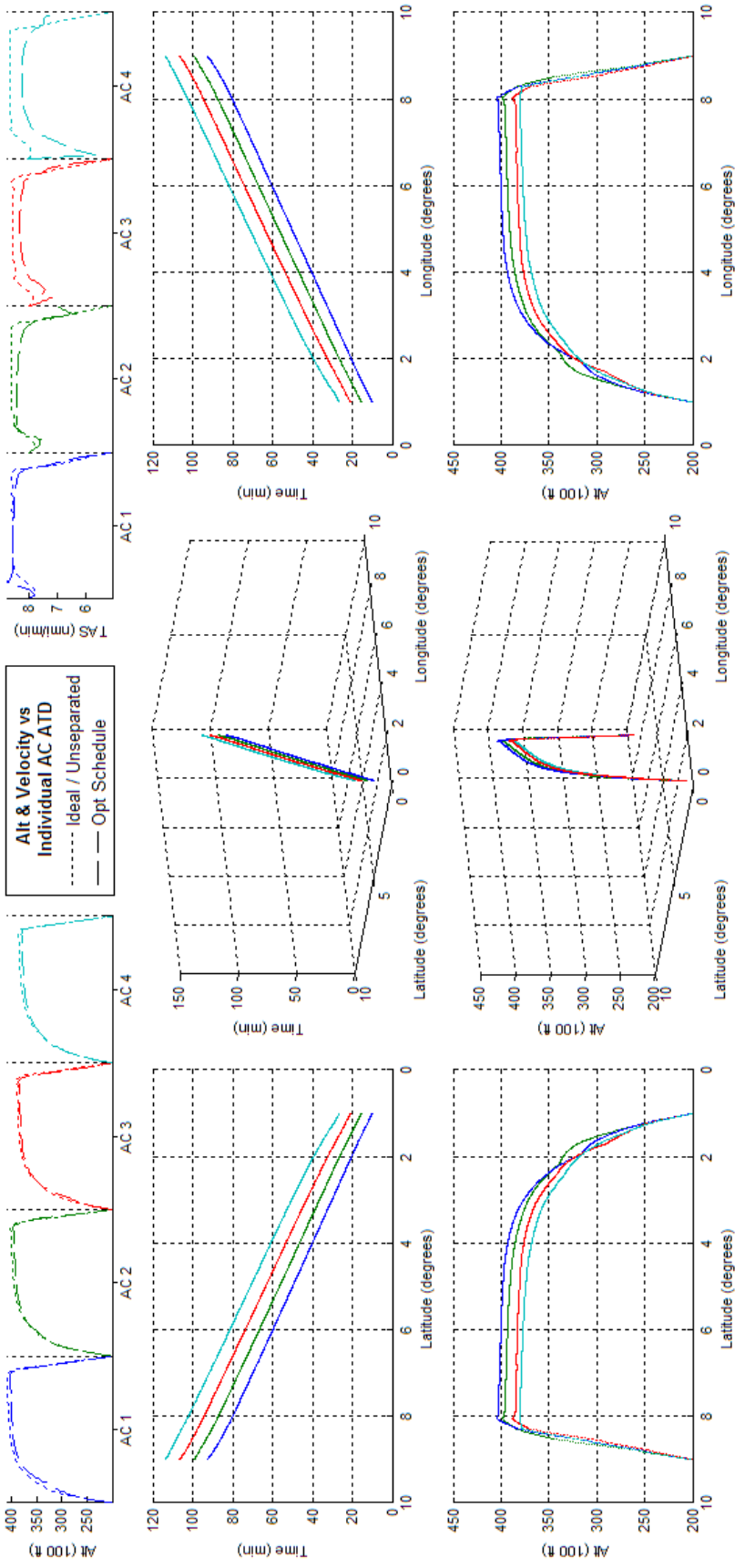

Figure 190 - Schedule Optimized 4acPSd ATD_N Results

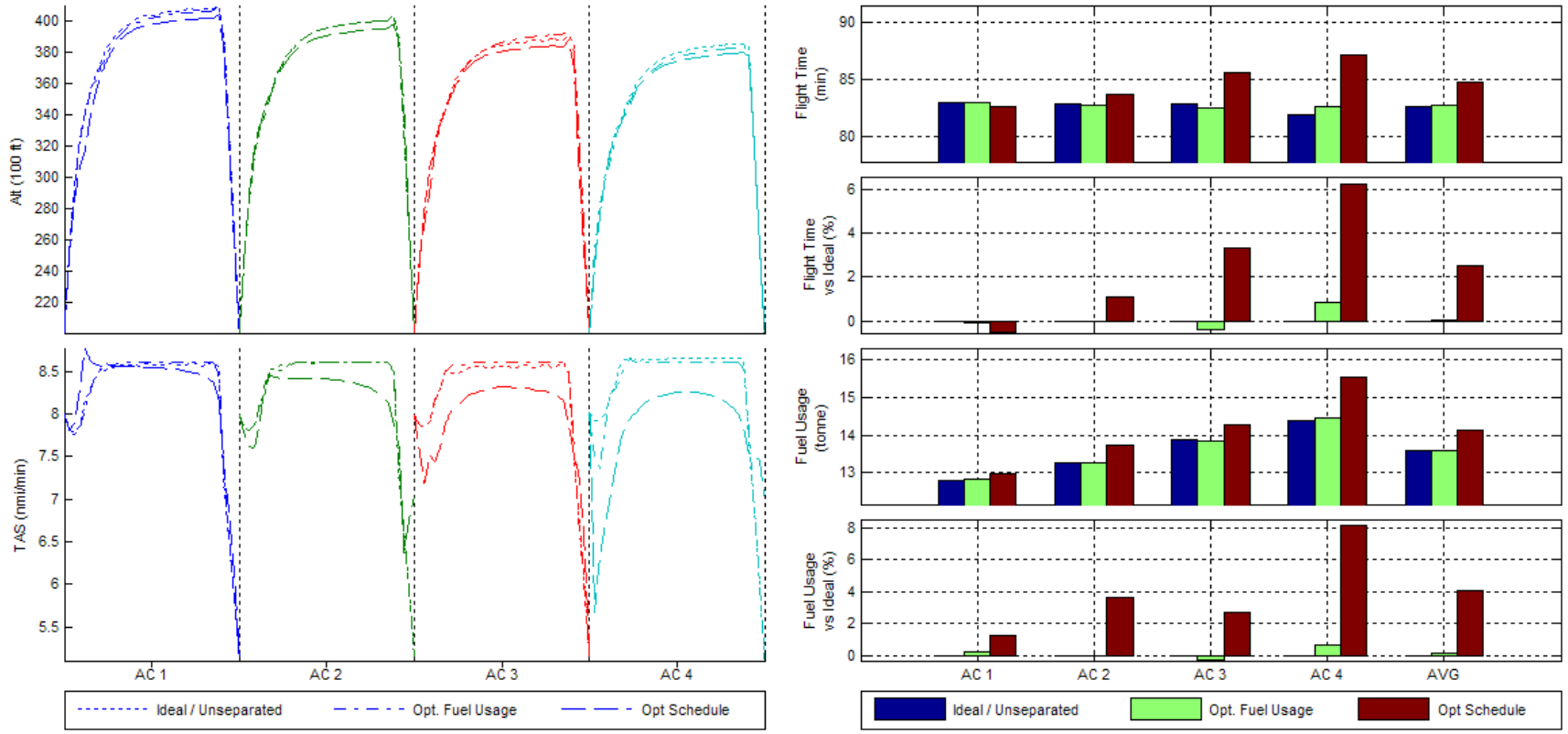

Figure 191 - Trajectory Shape, Flight Time, and Fuel Consumption Comparisons of Fuel and Schedule Optimized 4acPSd ATD_N Results

J.3 BADA Boeing 747-300 - Scenario 10acPSd - ATD_N

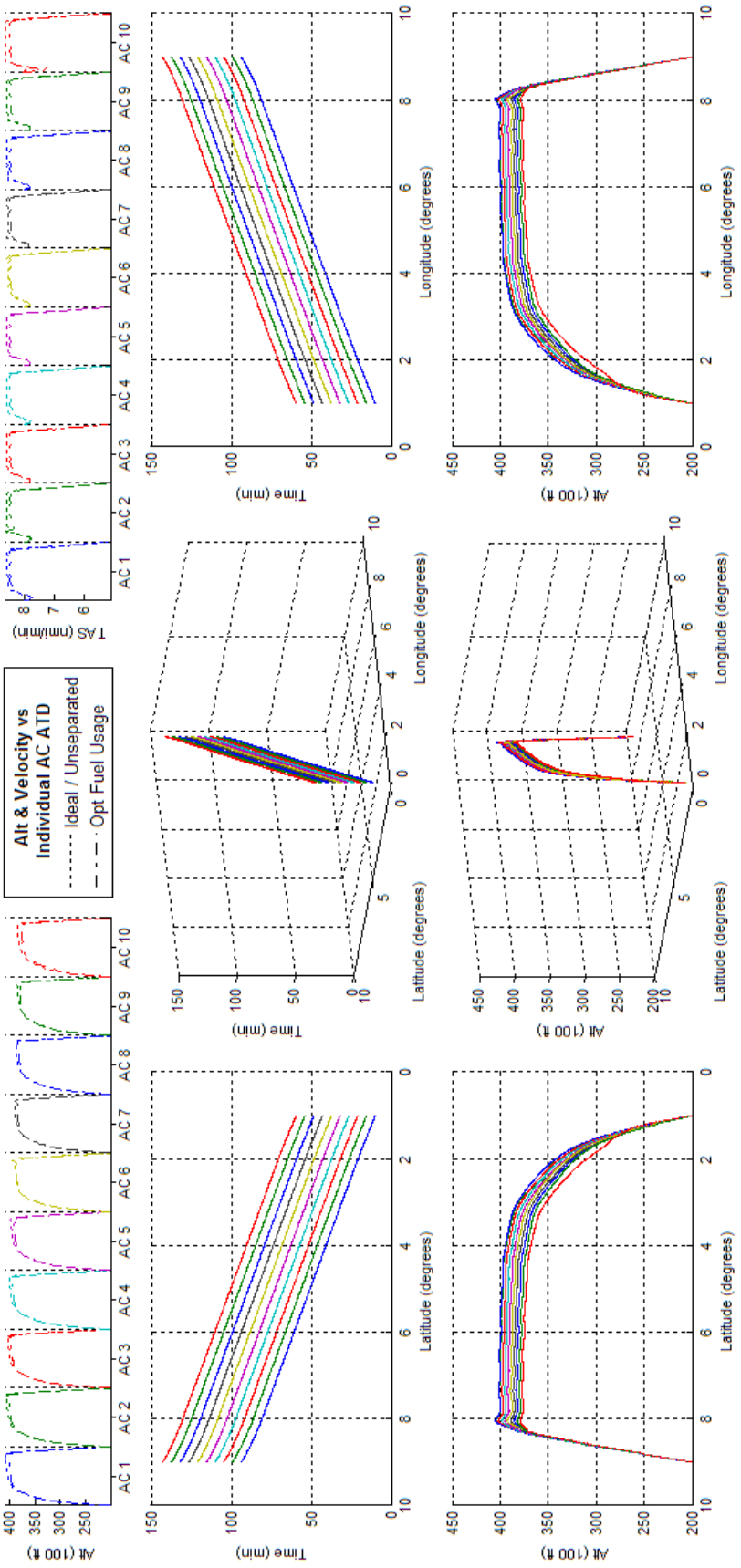

Figure 192 - Fuel Optimized 10acPSd ATD_N Results

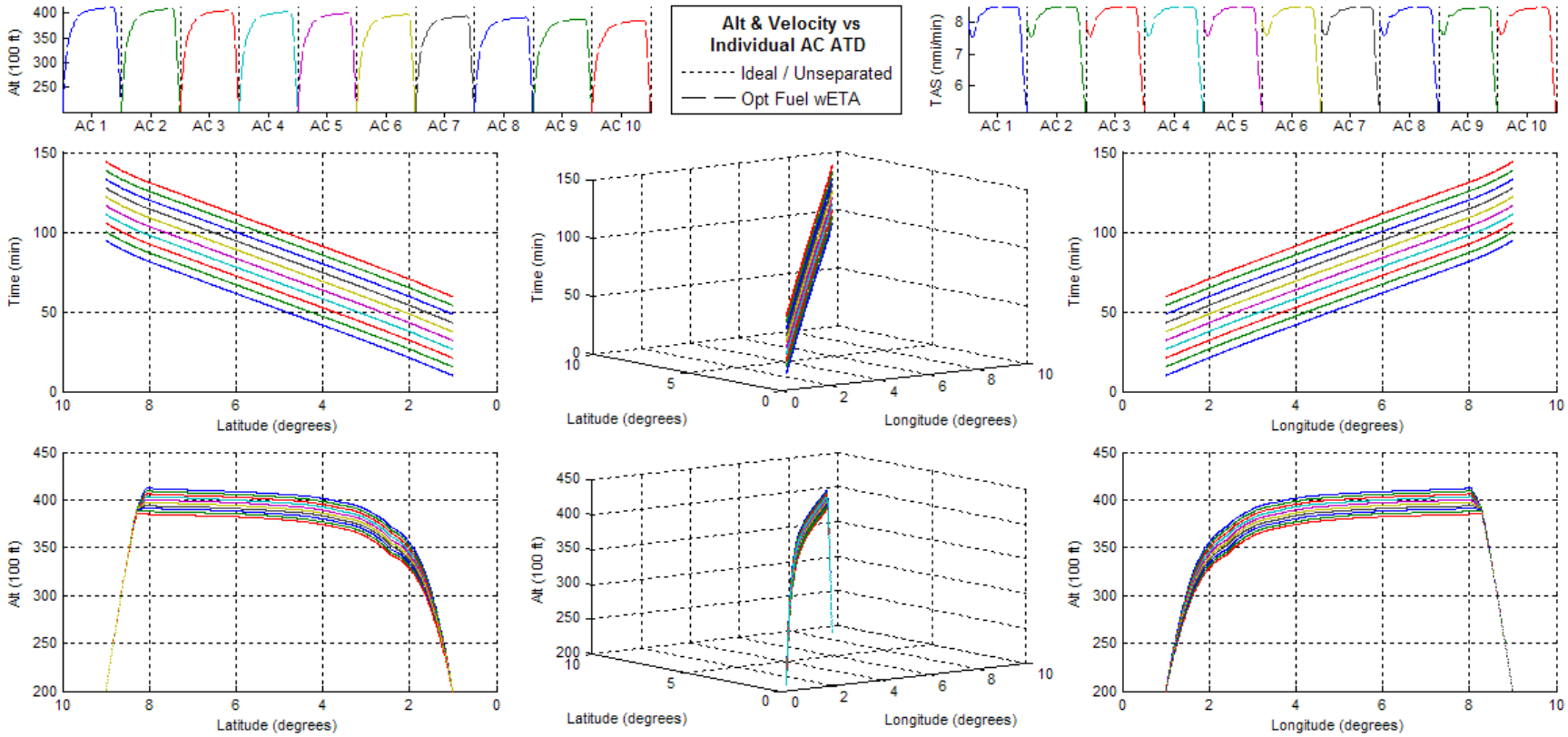

Figure 193 - Constrained ETA, Fuel Optimized 10acPSd ATD_N Results

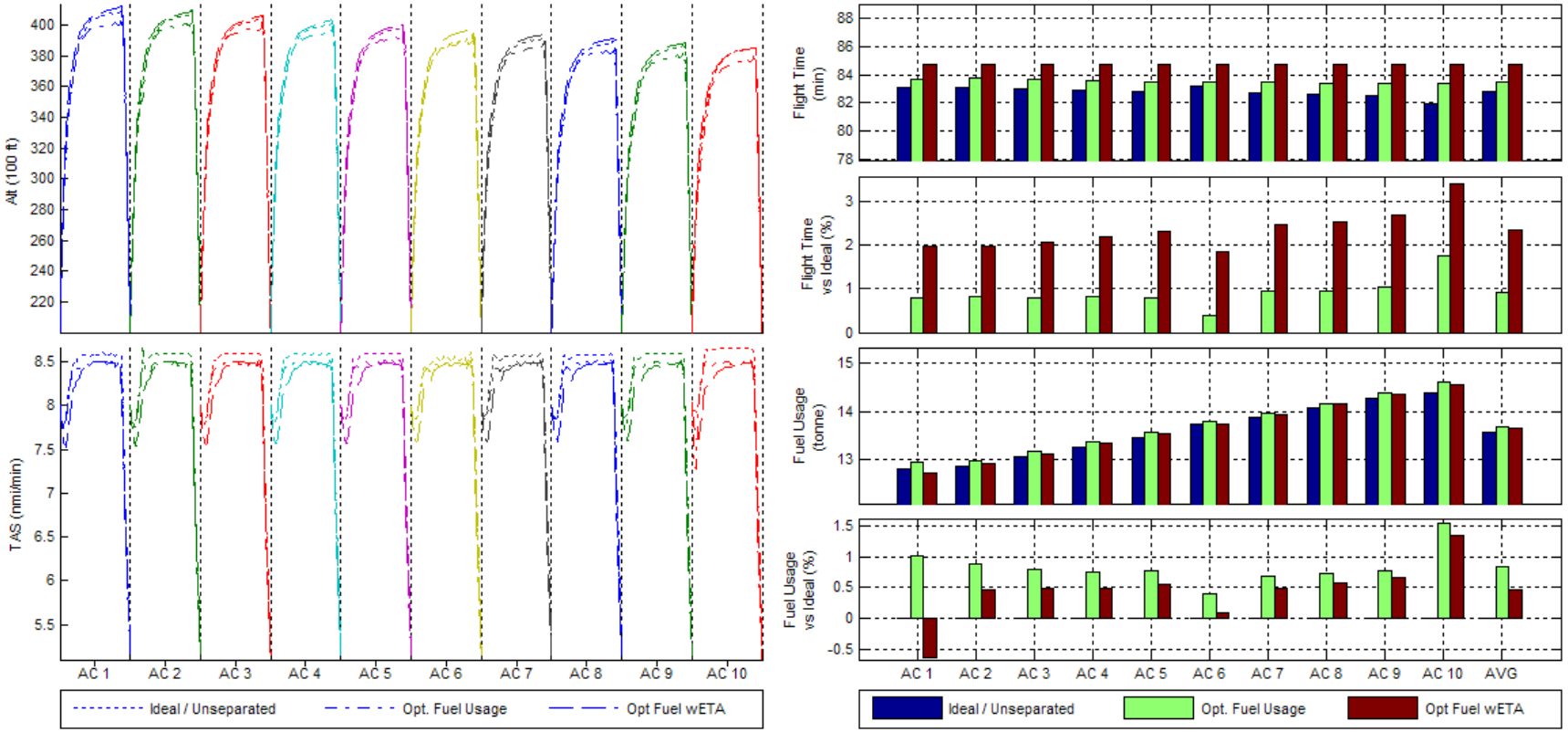

Figure 194 - Trajectory Shape, Flight Time, and Fuel Consumption Comparisons of Unconstrained and Constrained ETA, Fuel Optimized 10acPSd ATD_N Results

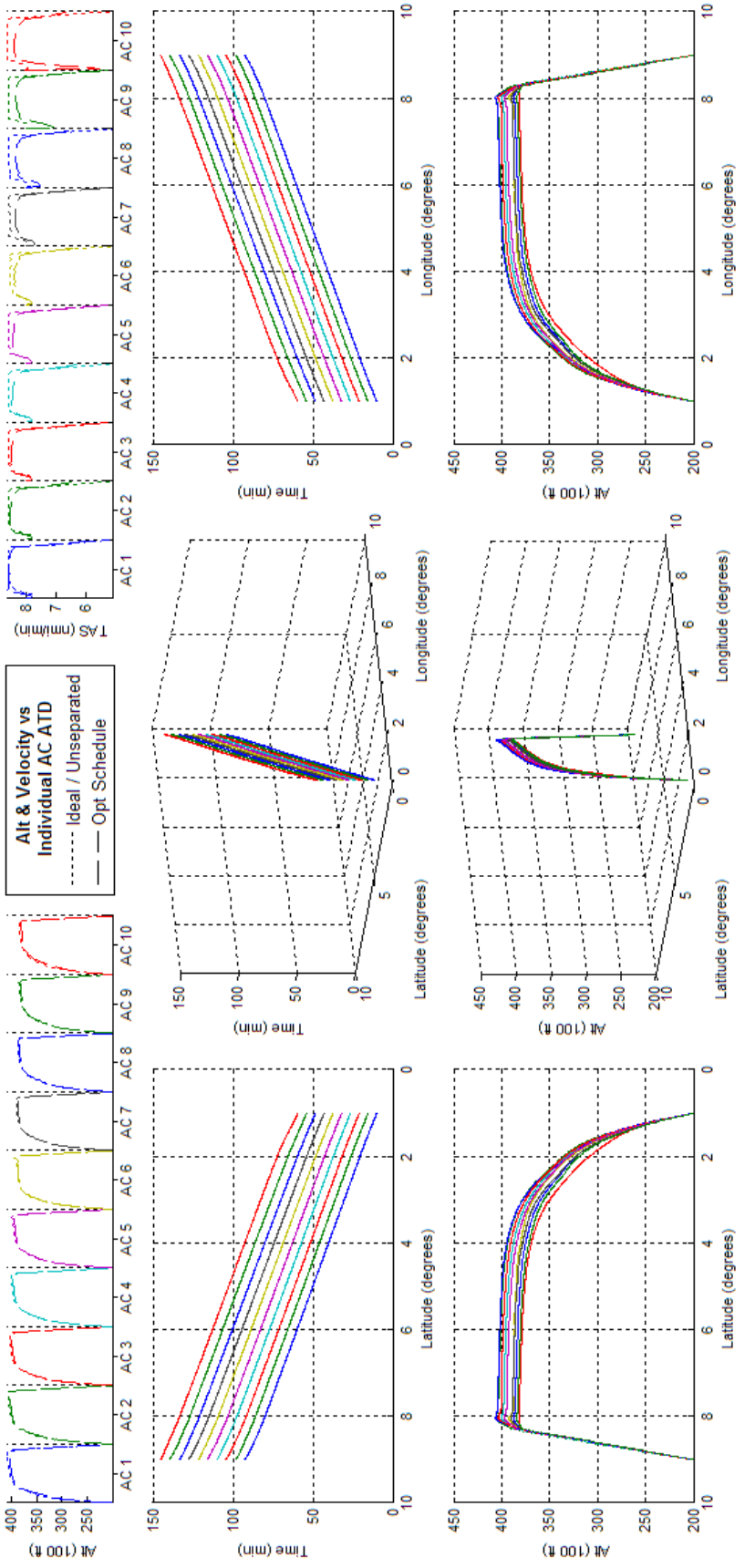

Figure 195 - Schedule Optimized 10acPSd ATD_N Results

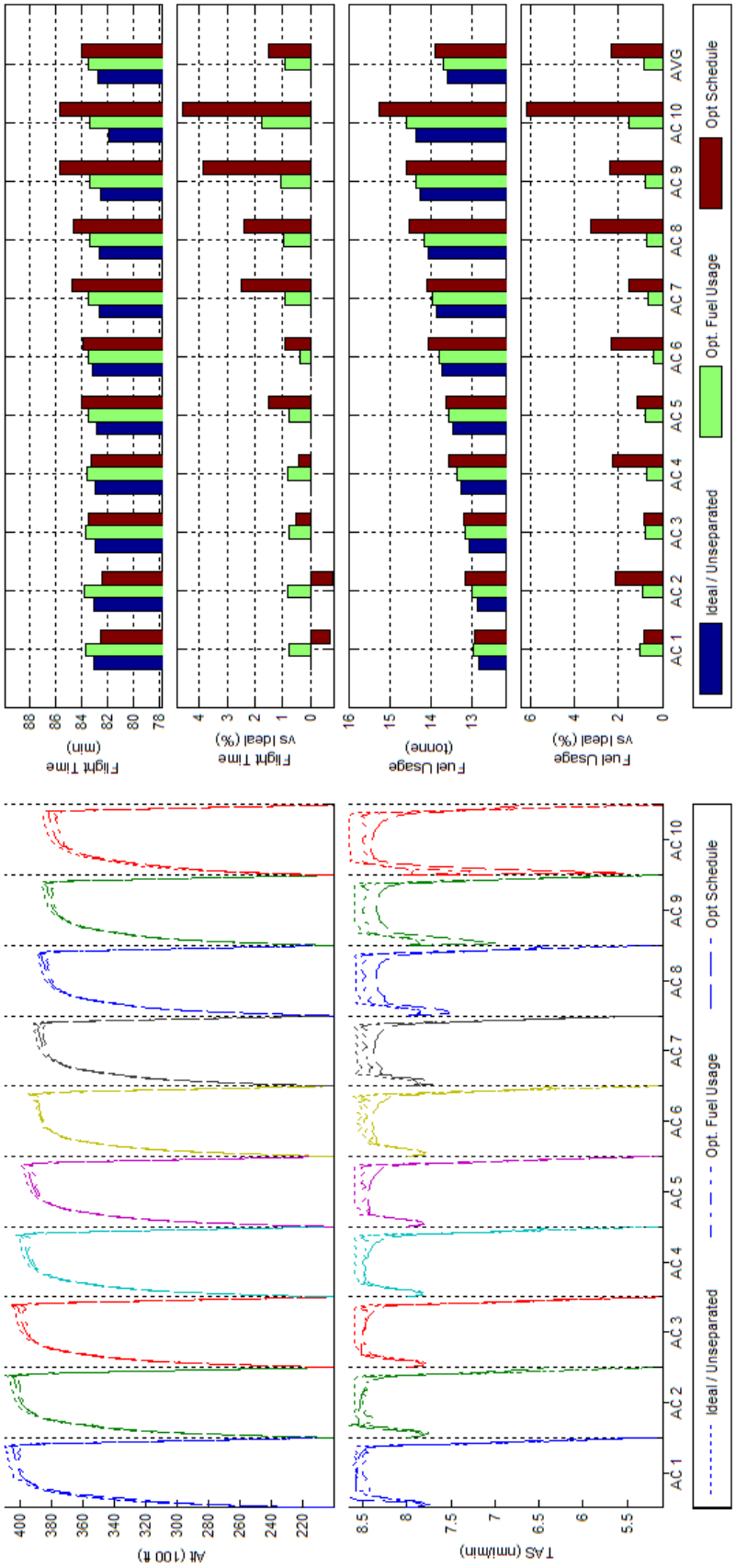

Figure 196 - Trajectory Shape, Flight Time, and Fuel Consumption Comparisons of Fuel and Schedule Optimized 10acPSd ATD_N Results

J.4 BADA Boeing 747-300 - Scenario 2acCO - ATD_N

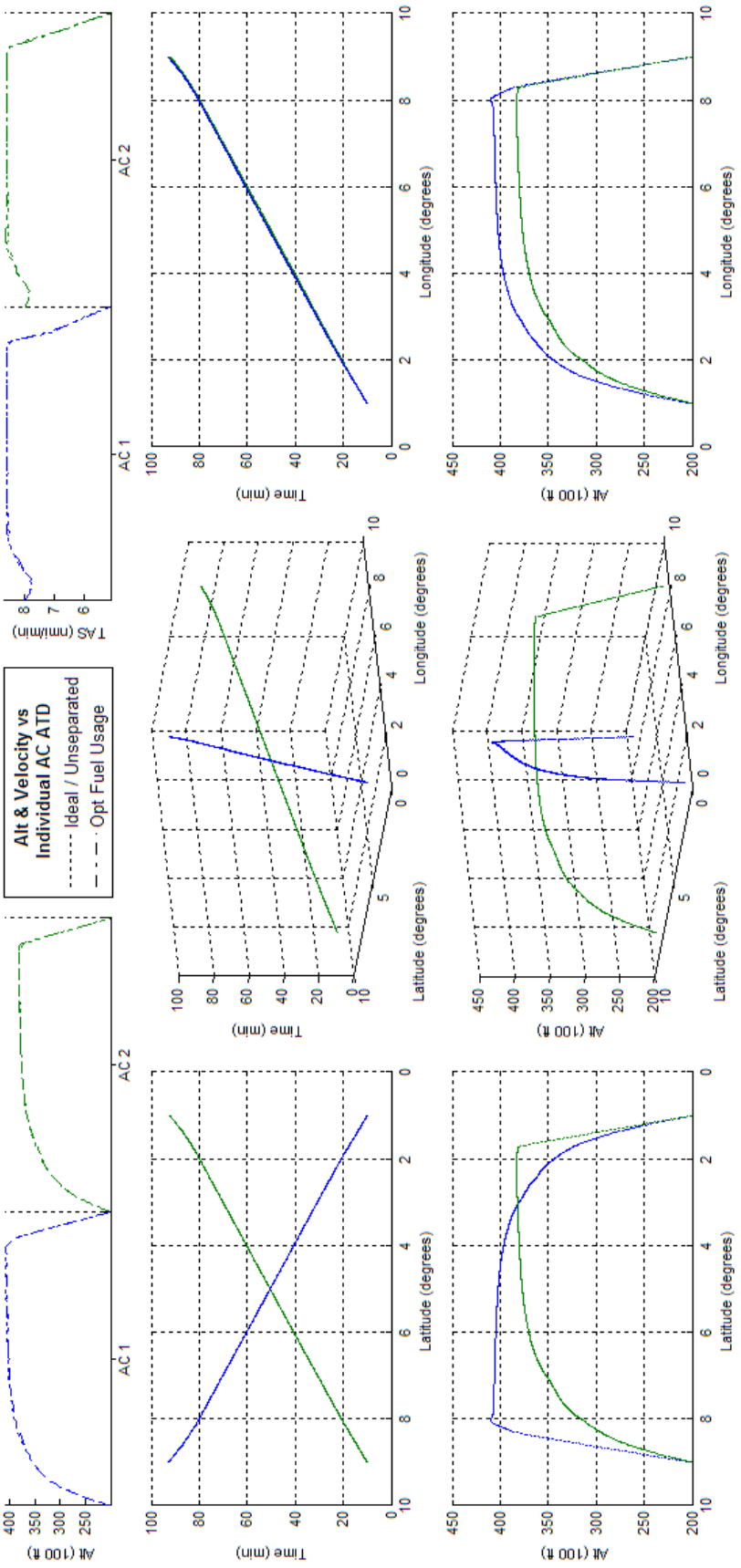

Figure 197 - Fuel Optimized 2acCO ATD_N Results

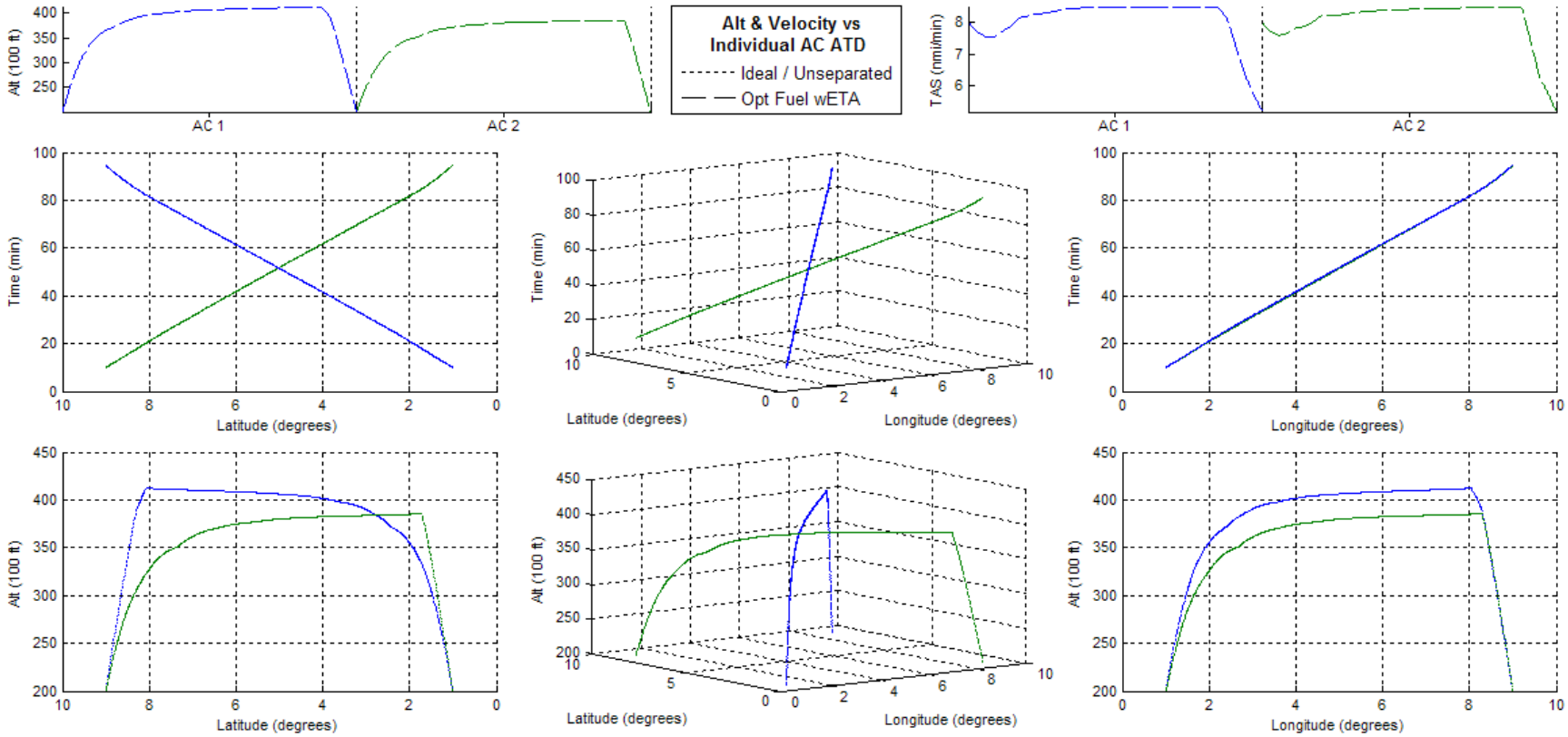

Figure 198 - Constrained ETA, Fuel Optimized 2acCO ATD_N Results

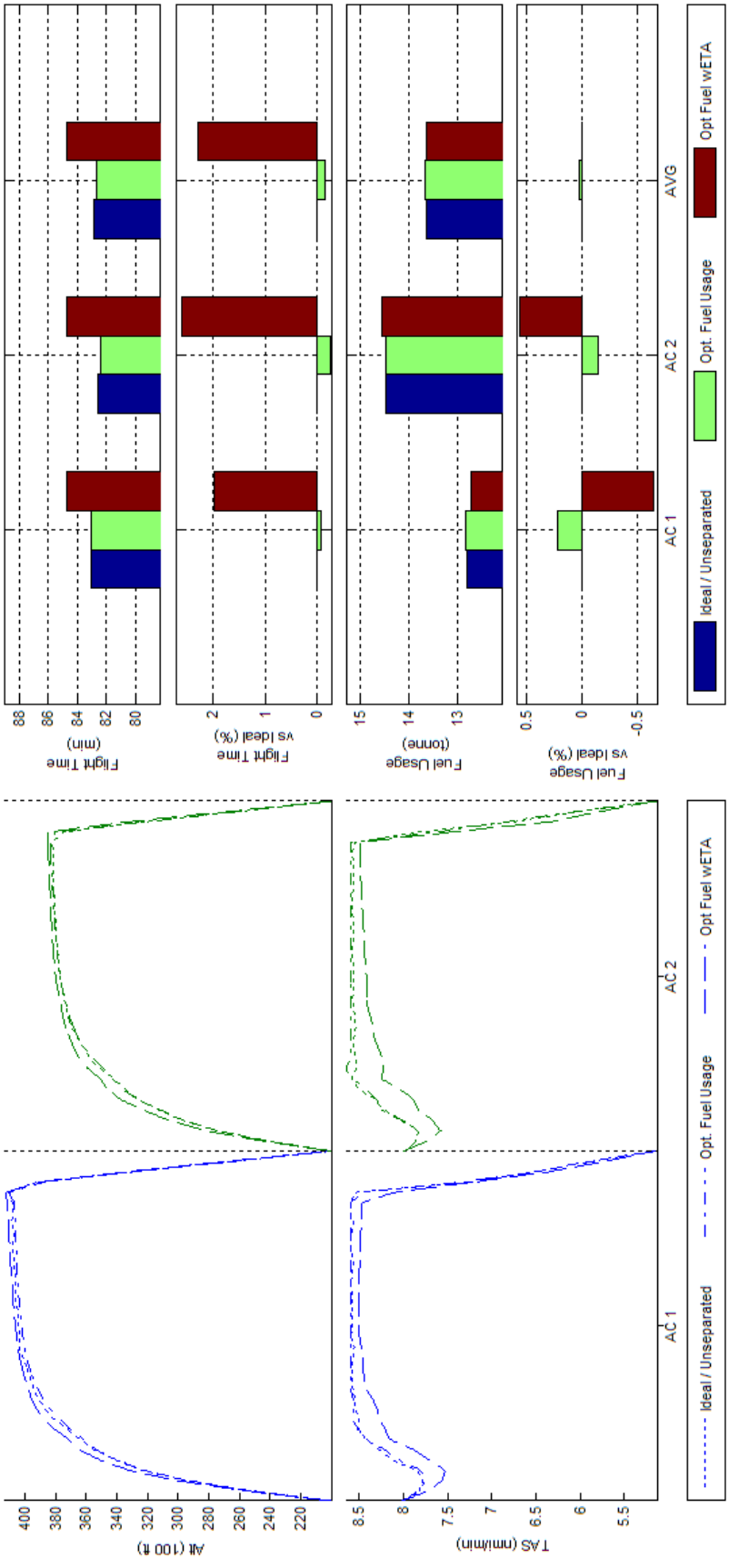

Figure 199 - Trajectory Shape, Flight Time, and Fuel Consumption Comparisons of Unconstrained and Constrained ETA, Fuel Optimized 2acCO ATD_N Results

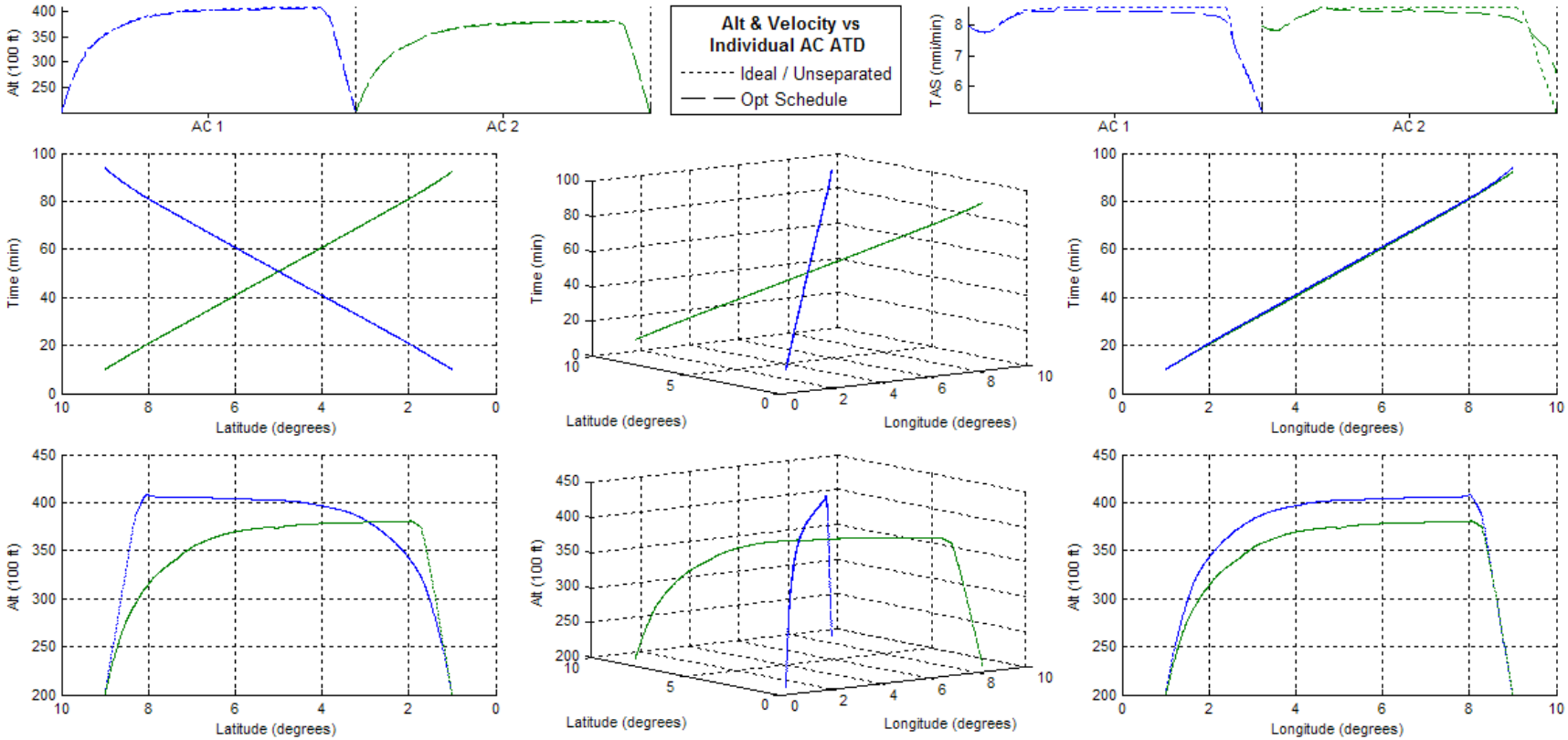

Figure 200 - Schedule Optimized 2acCO ATD_N Results

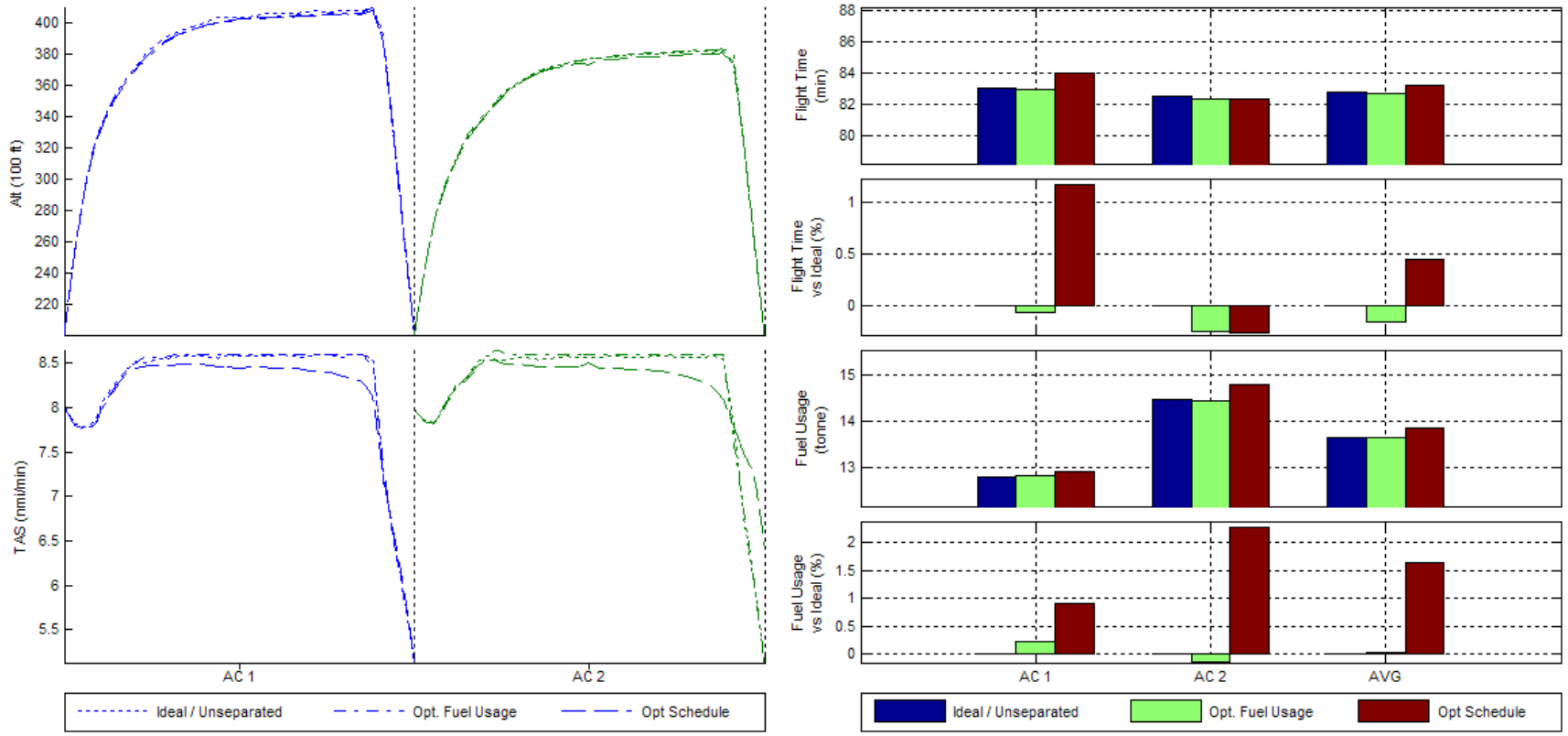

Figure 201 - Trajectory Shape, Flight Time, and Fuel Consumption Comparisons of Fuel and Schedule Optimized 2acCO ATD_N Results

J.5 BADA Boeing 747-300 - Scenario 4acCO - ATD_N

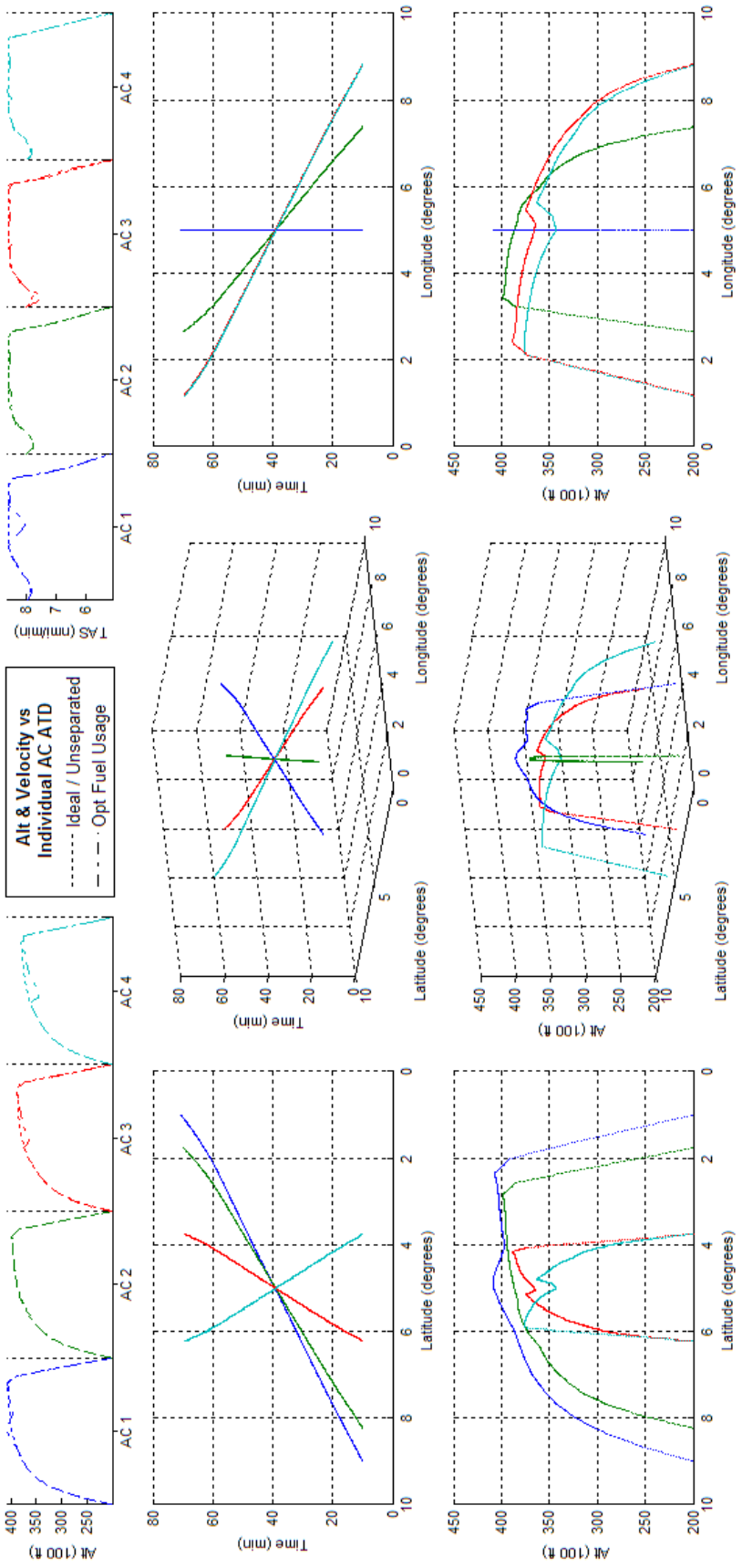

Figure 202 - Fuel Optimized 4acCO ATD_N Results

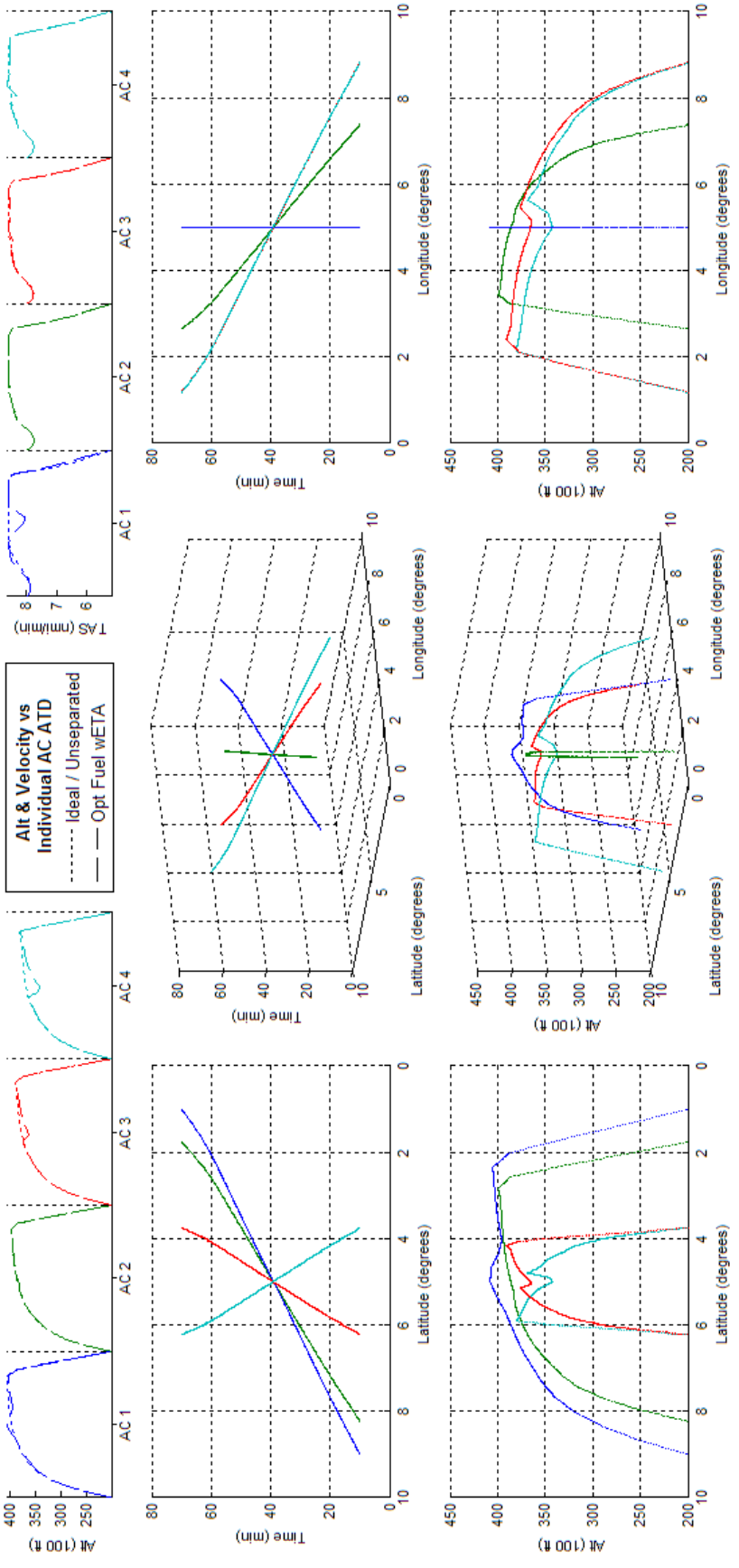

Figure 203 - Constrained ETA, Fuel Optimized 4acCO ATD_N Results

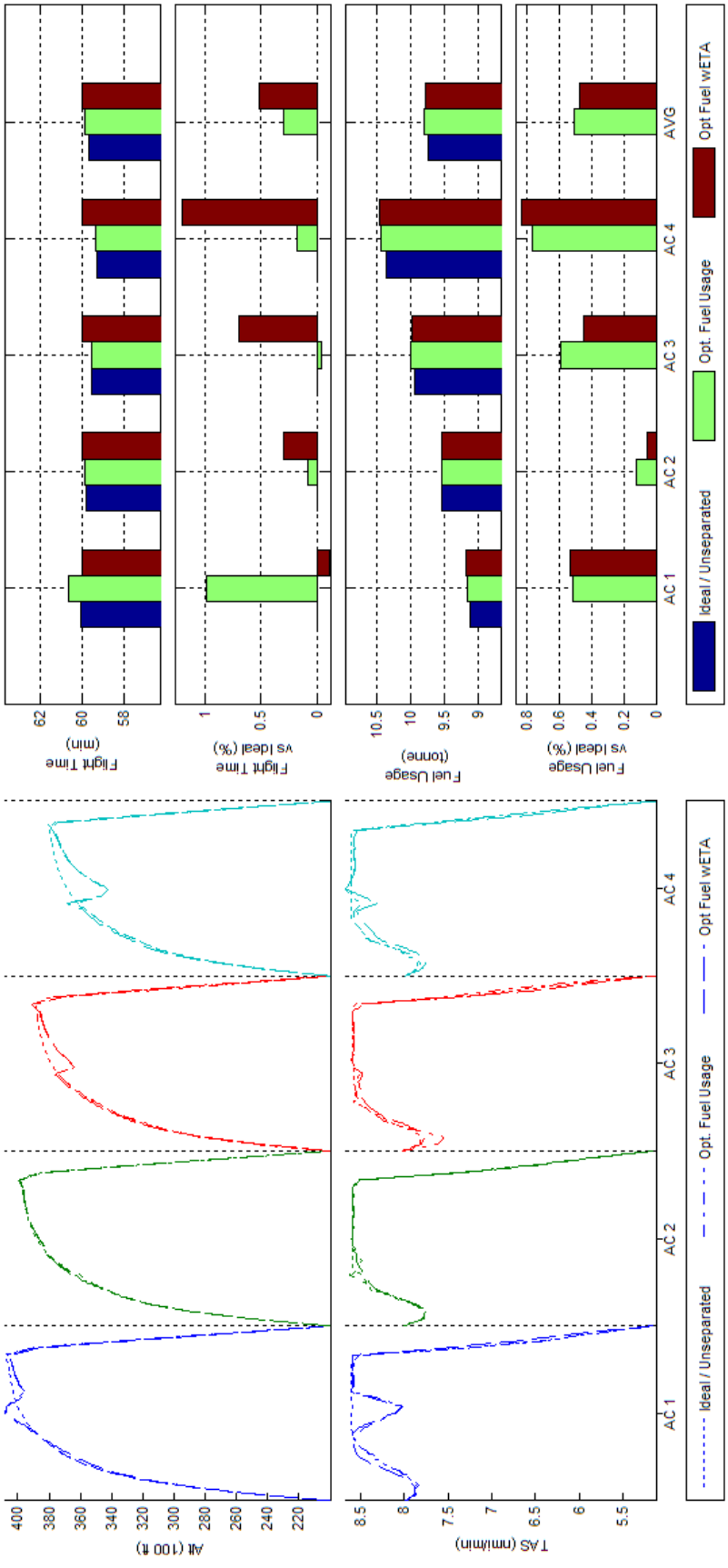

Figure 204 - Trajectory Shape, Flight Time, and Fuel Consumption Comparisons of Unconstrained and Constrained ETA, Fuel Optimized 4acCO ATD_N Results

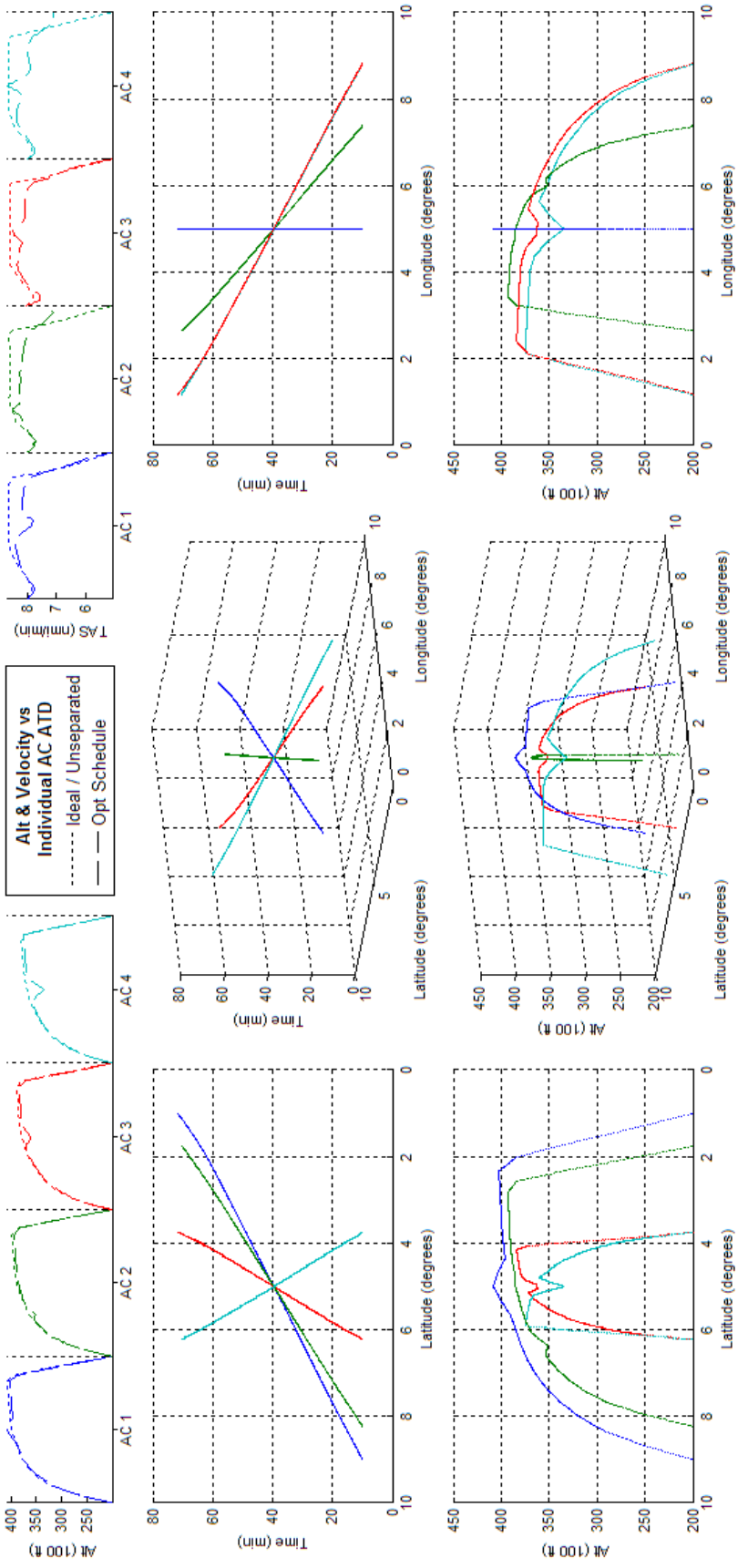

Figure 205 - Schedule Optimized 4acCO ATD_N Results

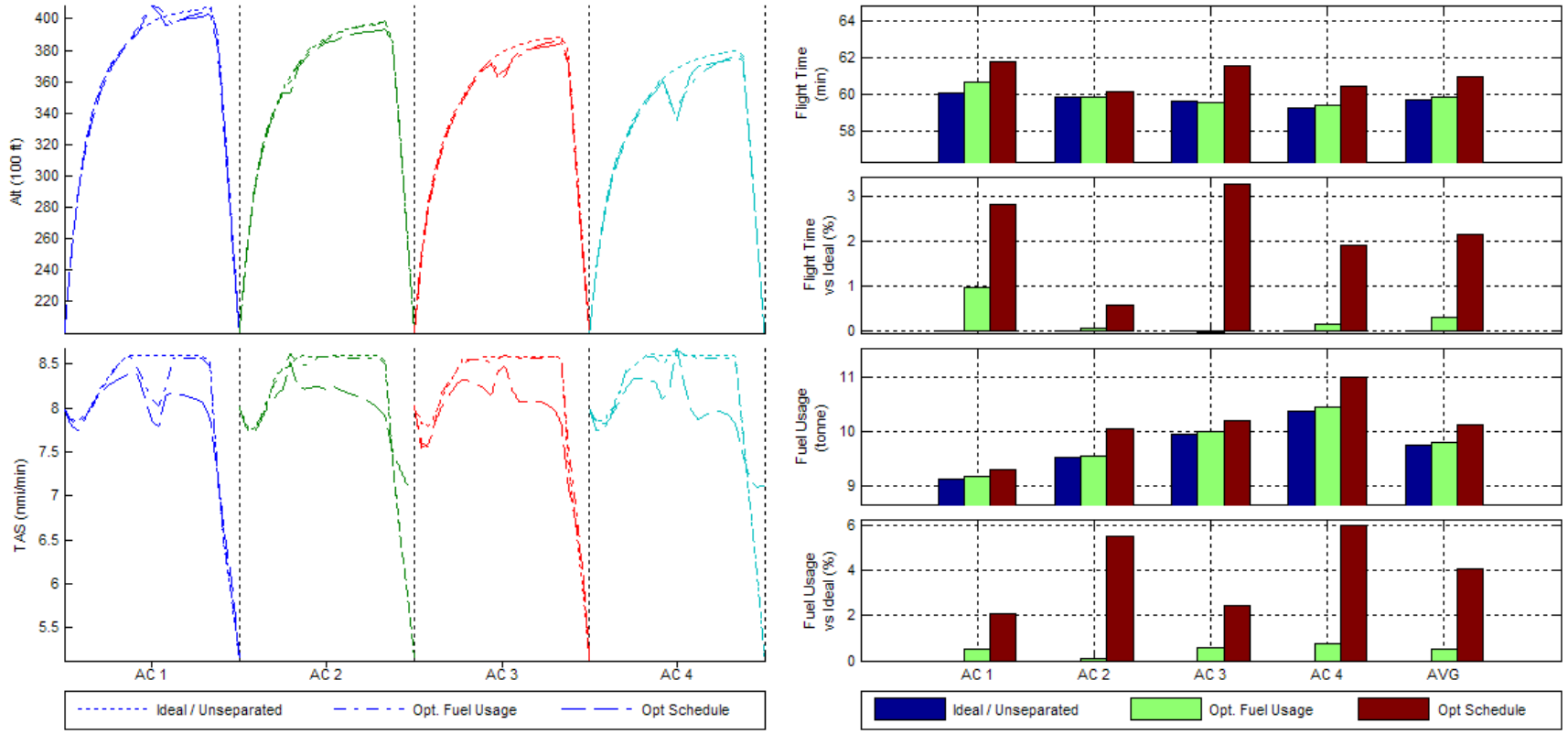

Figure 206 - Trajectory Shape, Flight Time, and Fuel Consumption Comparisons of Fuel and Schedule Optimized 4acCO ATD_N Results

J.6 BADA Boeing 747-300 - Scenario 10acCO - ATD_N

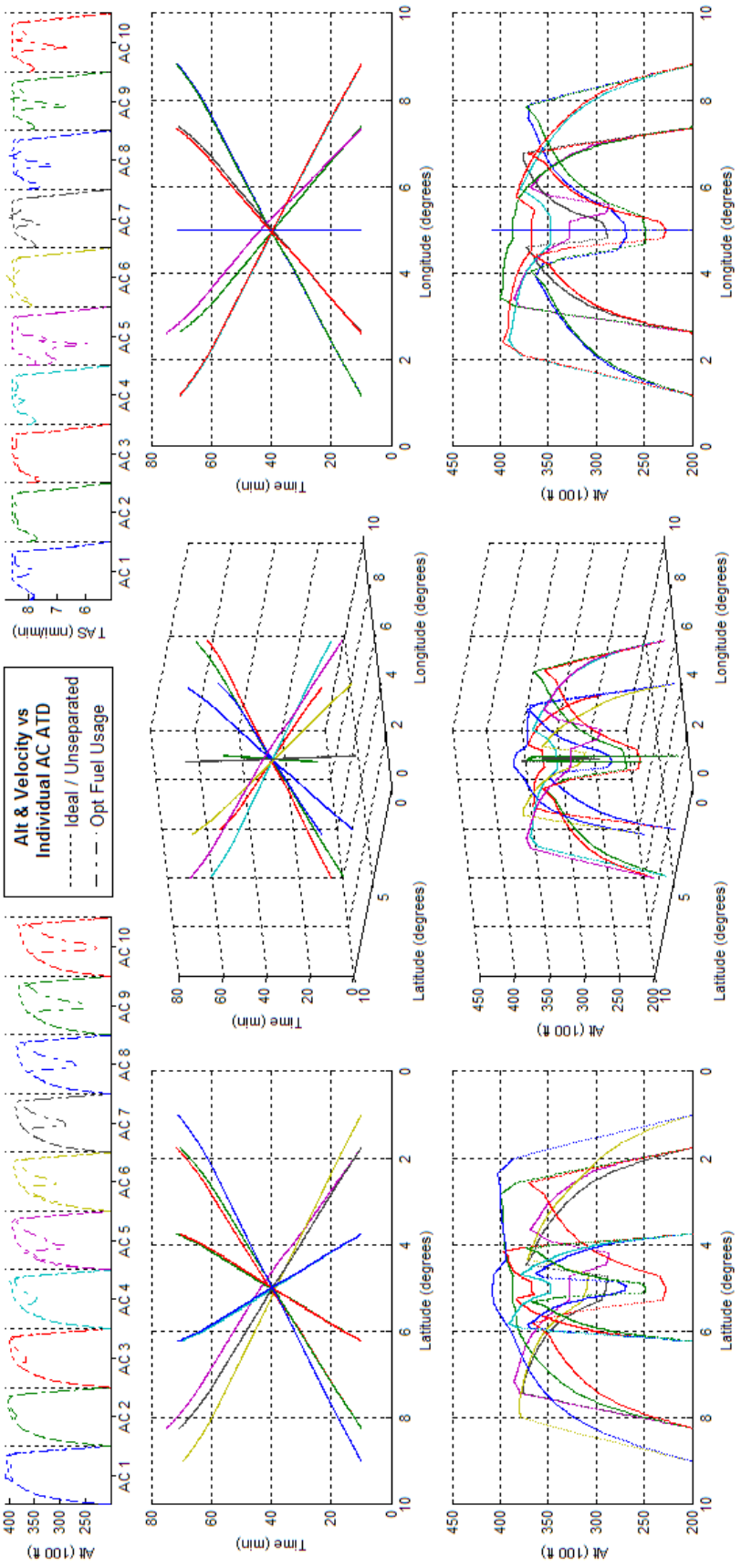

Figure 207 - Fuel Optimized 10acCO ATD_N Results

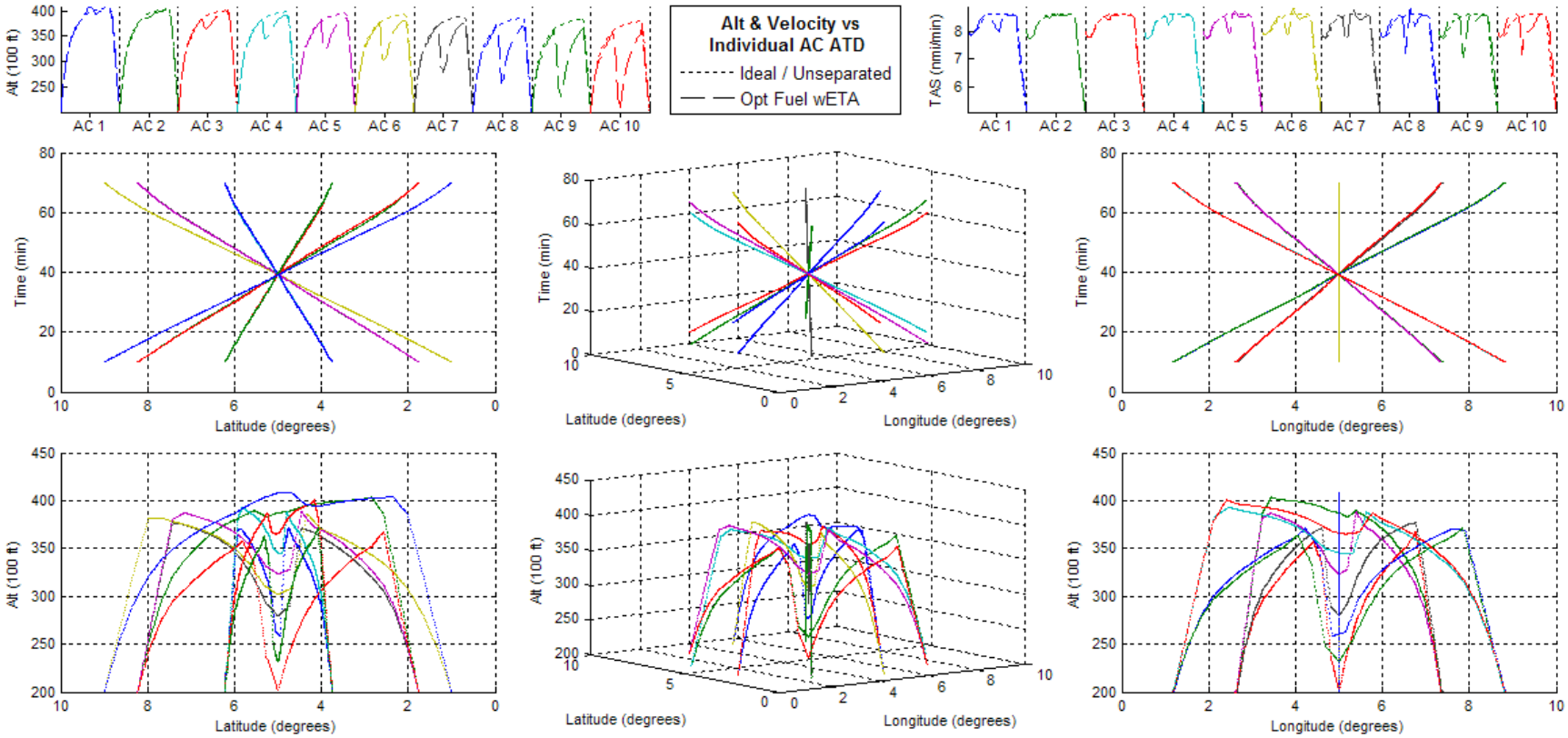

Figure 208 - Constrained ETA, Fuel Optimized 10acCO ATD_N Results

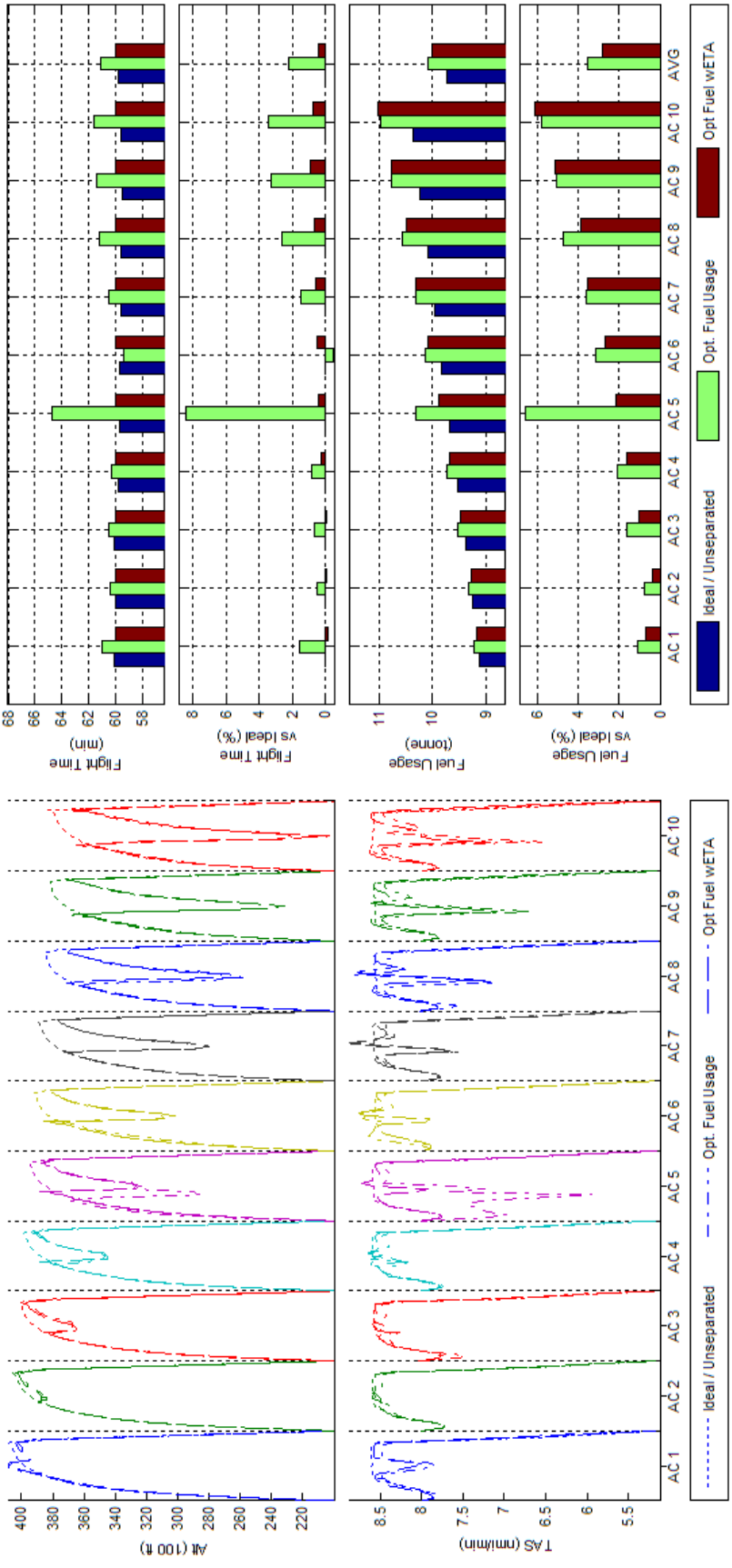

Figure 209 - Trajectory Shape, Flight Time, and Fuel Consumption Comparisons of Unconstrained and Constrained ETA, Fuel Optimized 10acCO ATD_N Results

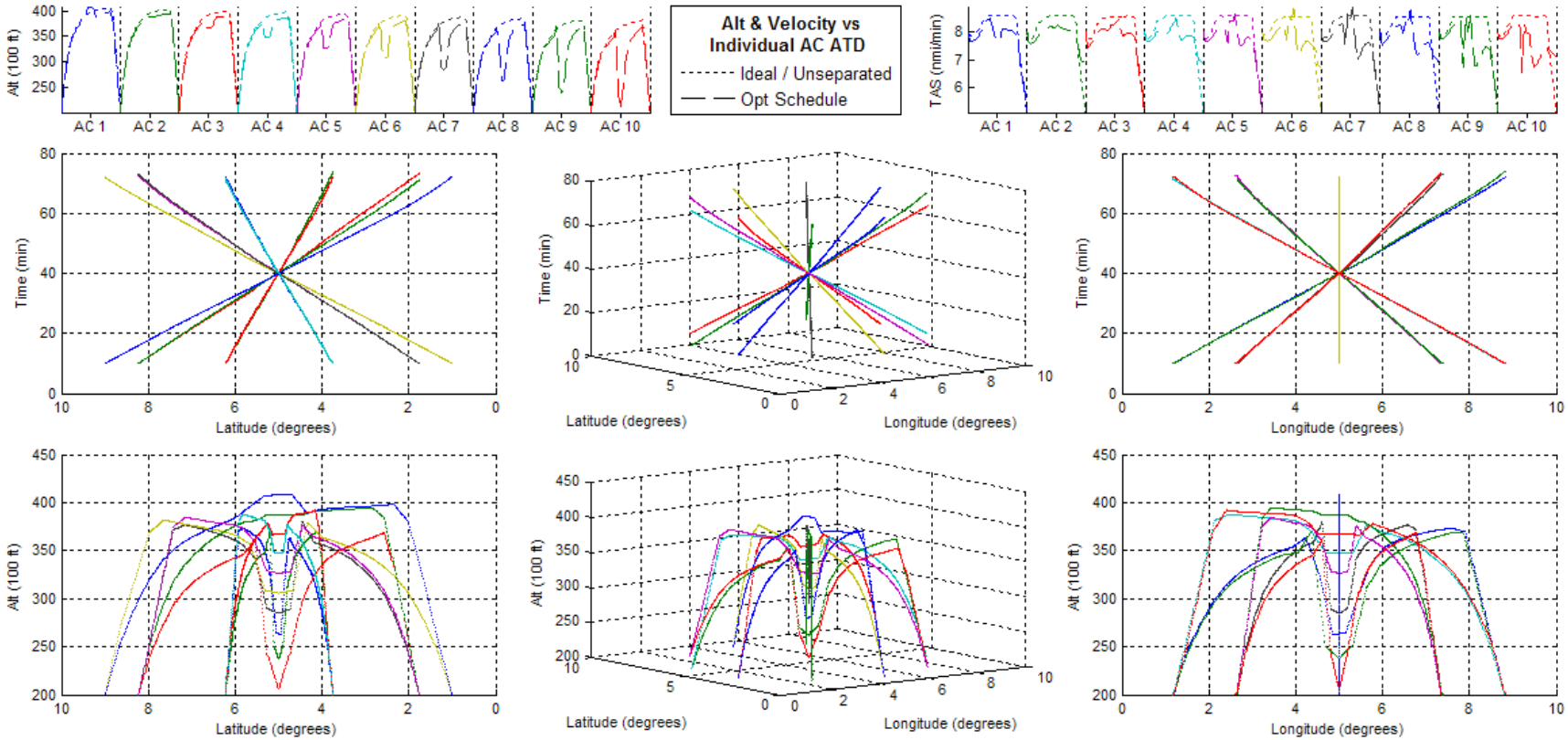

Figure 210 - Schedule Optimized 10acCO ATD_N Results

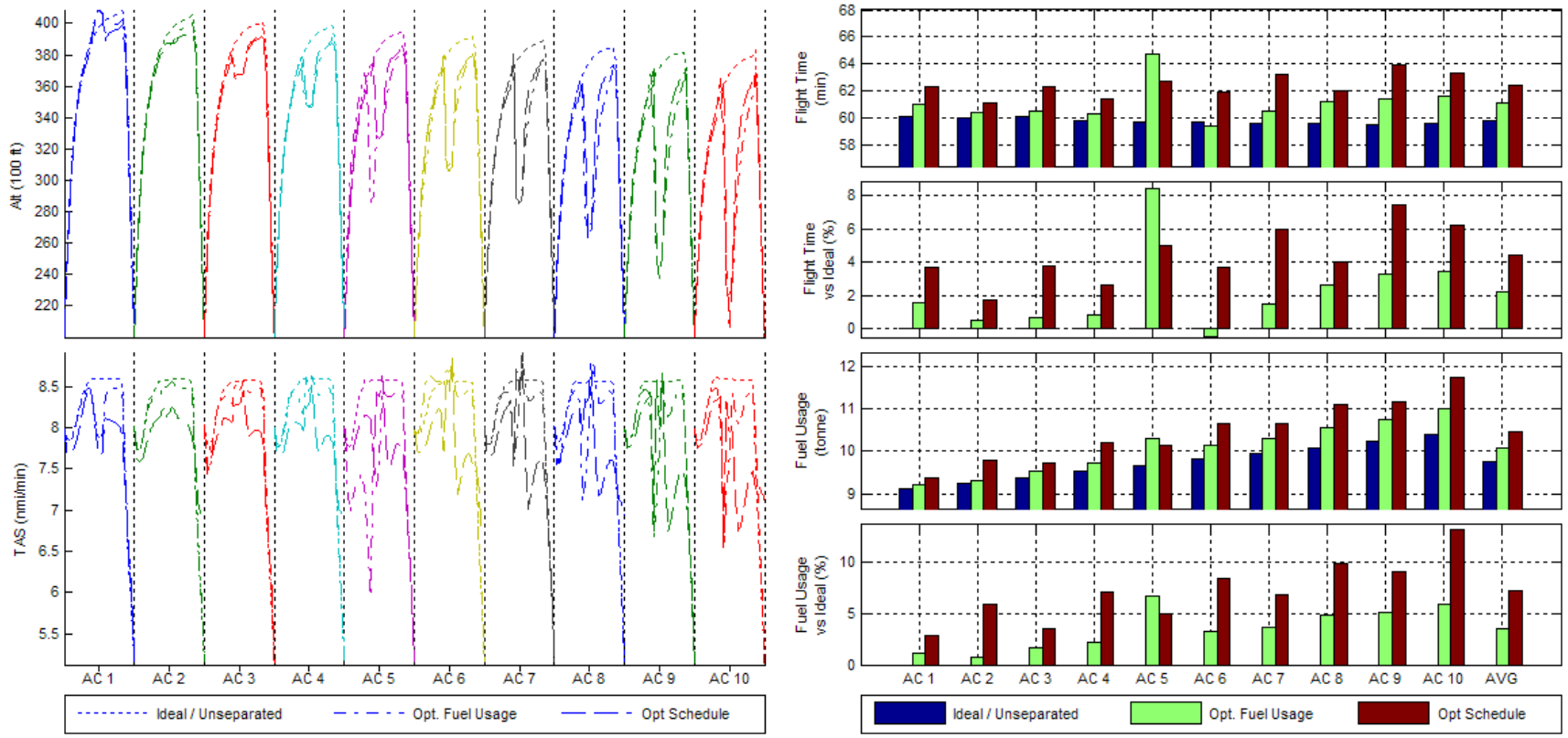

Figure 211 - Trajectory Shape, Flight Time, and Fuel Consumption Comparisons of Fuel and Schedule Optimized 10acCO ATD_N Results

J.7 BADA Boeing 747-300 - Scenario 4acCH - ATD_N

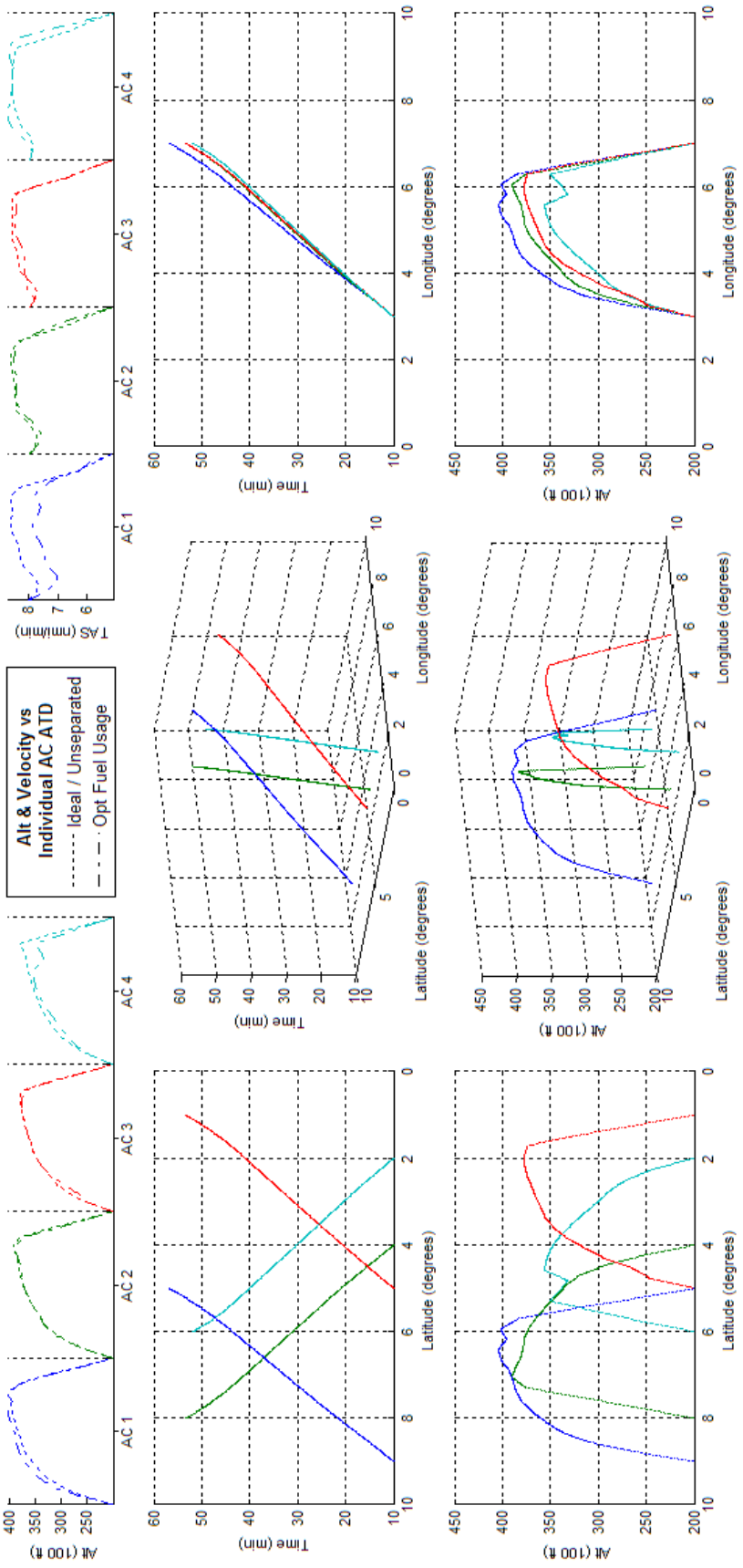

Figure 212 - Fuel Optimized 4acCH ATD_N Results

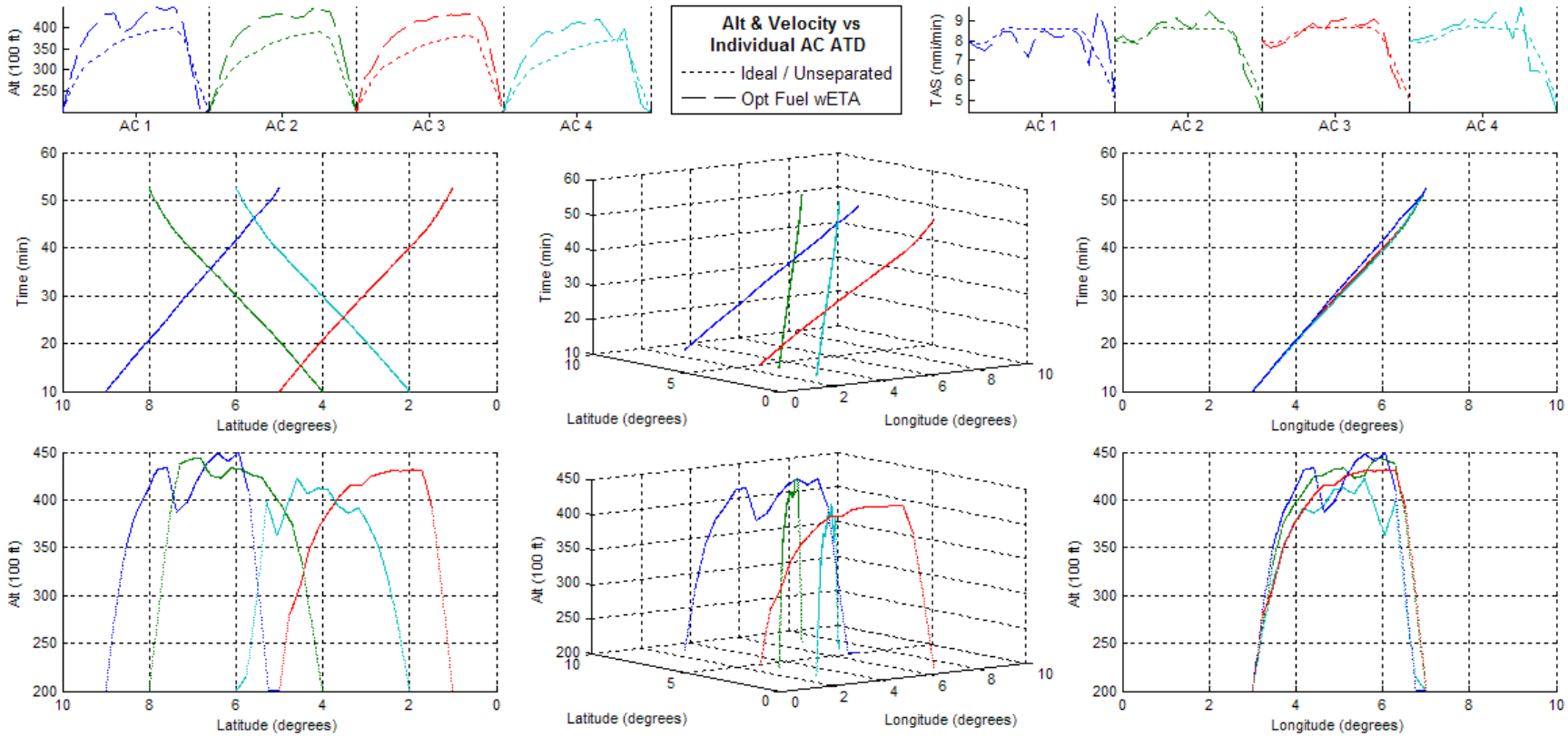

Figure 213 - Constrained ETA, Fuel Optimized 4acCH ATD_N Results

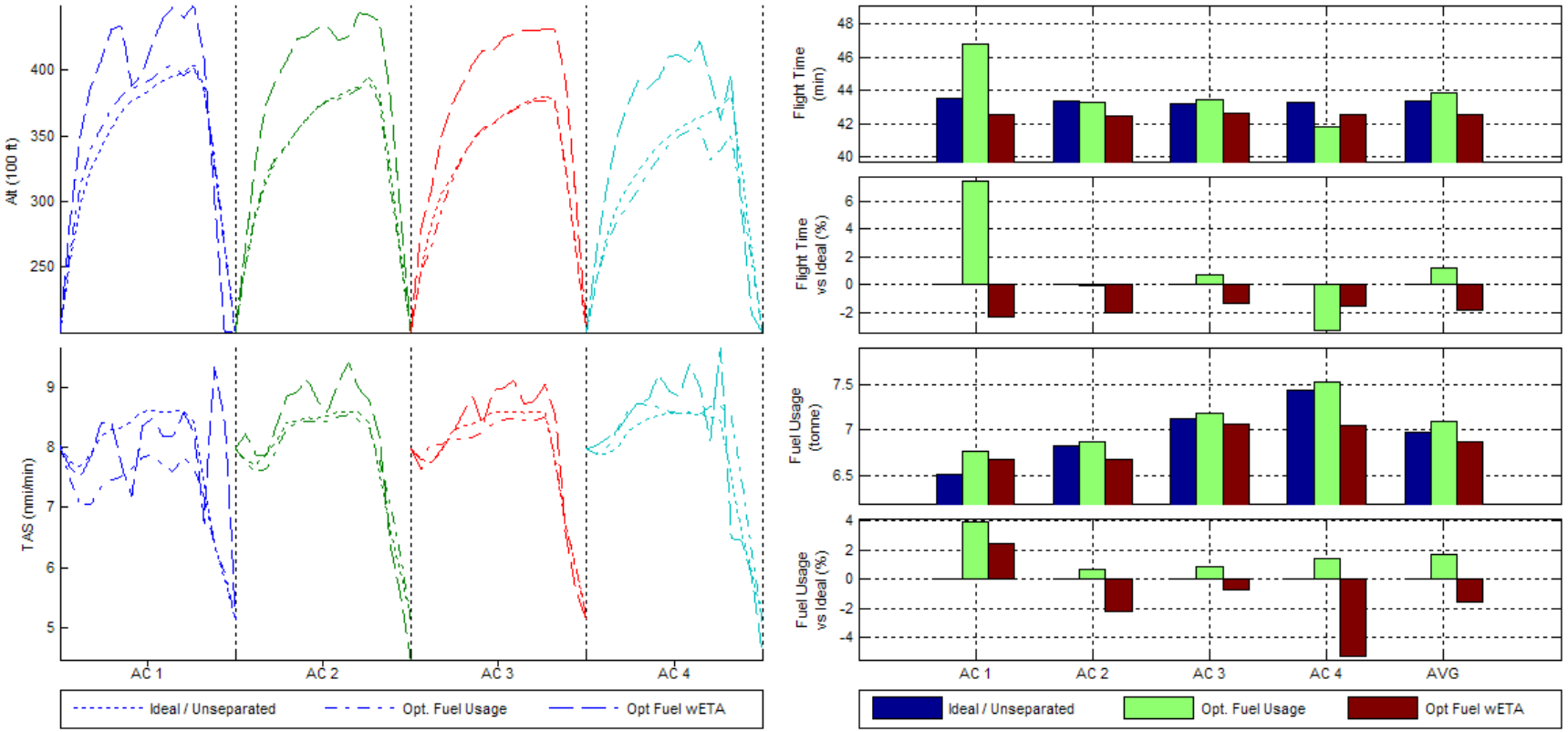

Figure 214 - Trajectory Shape, Flight Time, and Fuel Consumption Comparisons of Unconstrained and Constrained ETA, Fuel Optimized 4acCH ATD_N Results

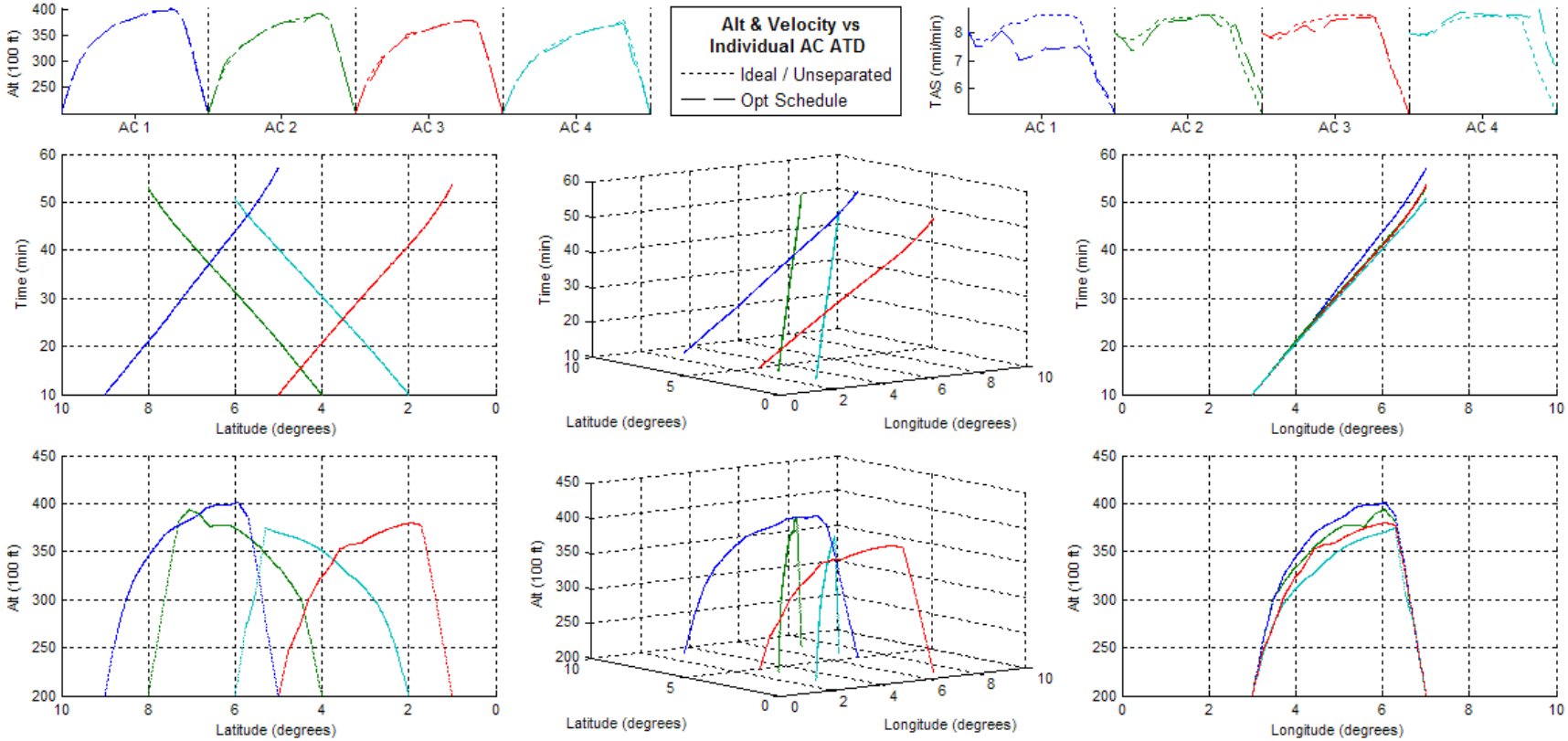

Figure 215 - Schedule Optimized 4acCH ATD_N Results

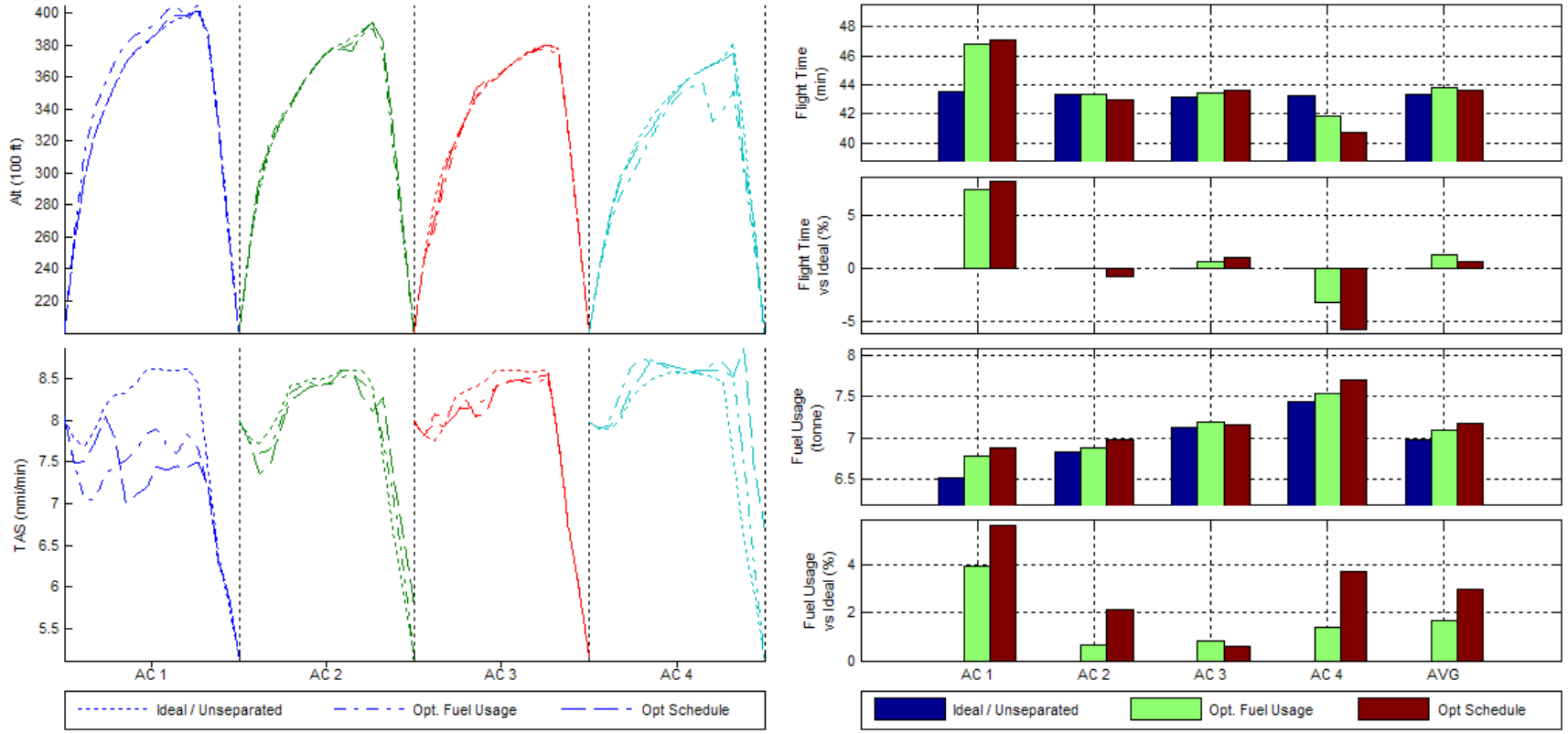

Figure 216 - Trajectory Shape, Flight Time, and Fuel Consumption Comparisons of Fuel and Schedule Optimized 4acCH ATD_N Results

J.8 BADA Boeing 747-300 - Scenario 10acCH - ATD_N

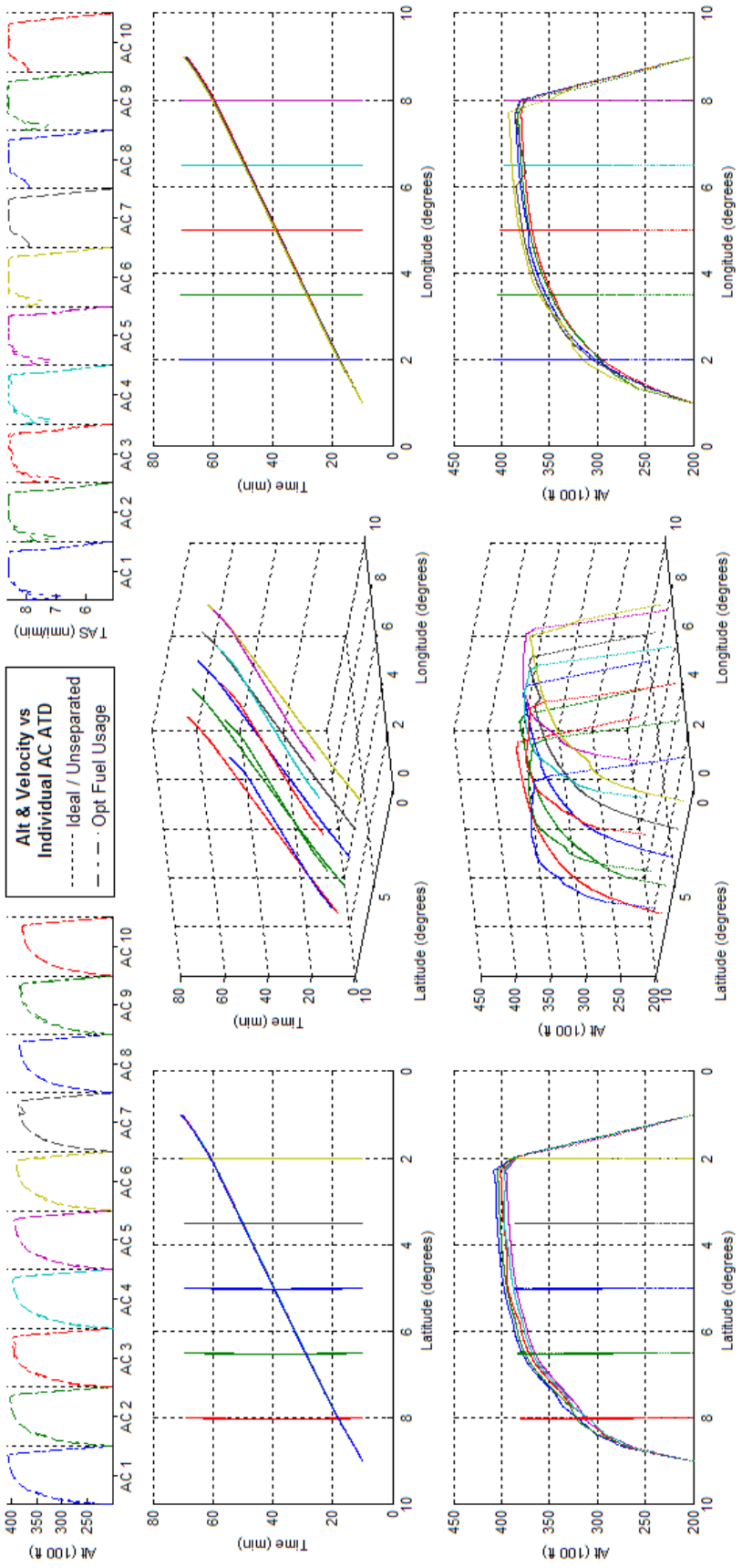

Figure 217 - Fuel Optimized 10acCH ATD_N Results

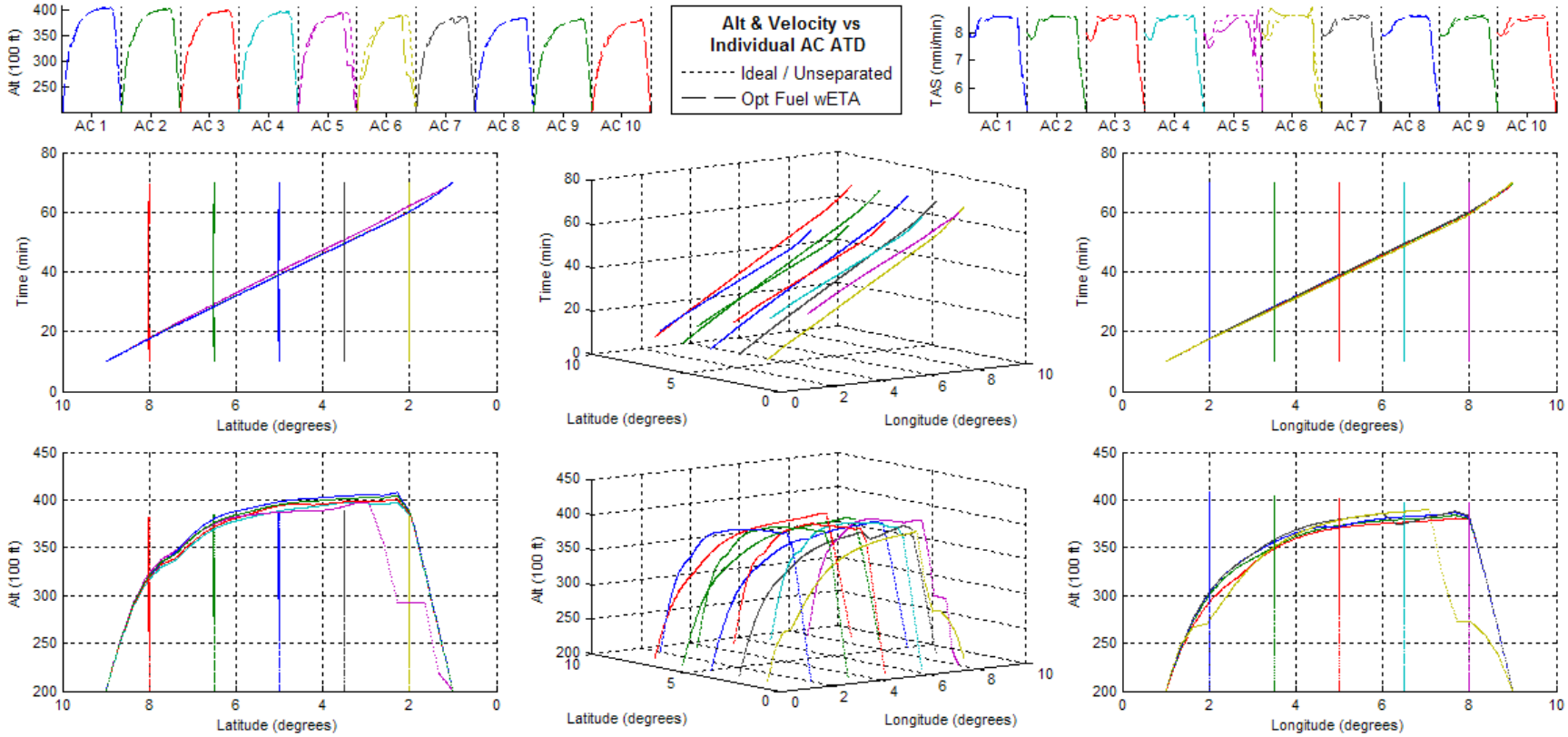

Figure 218 - Constrained ETA, Fuel Optimized 10acCH ATD_N Results

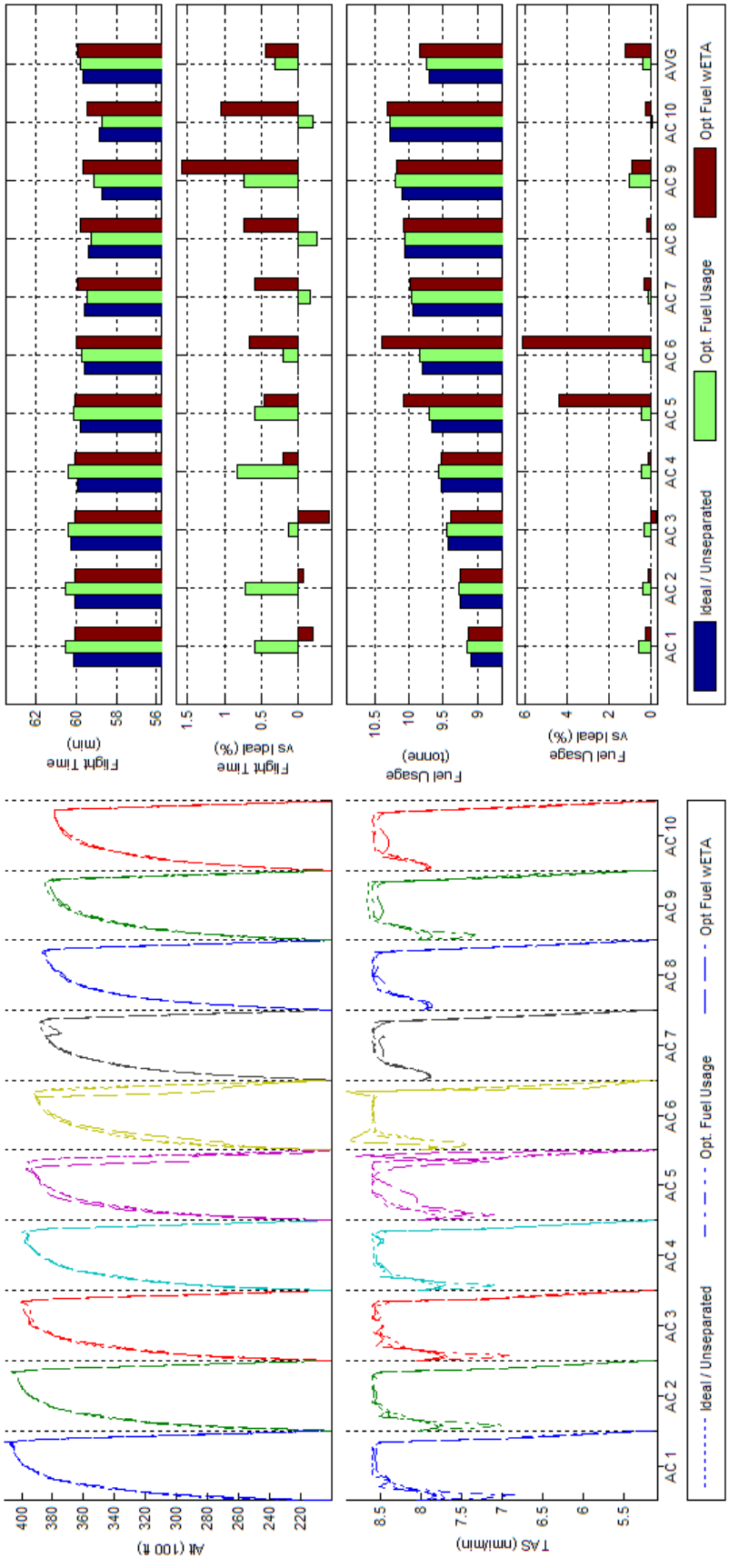

Figure 219 - Trajectory Shape, Flight Time, and Fuel Consumption Comparisons of Unconstrained and Constrained ETA, Fuel Optimized 10acCH ATD_N Results

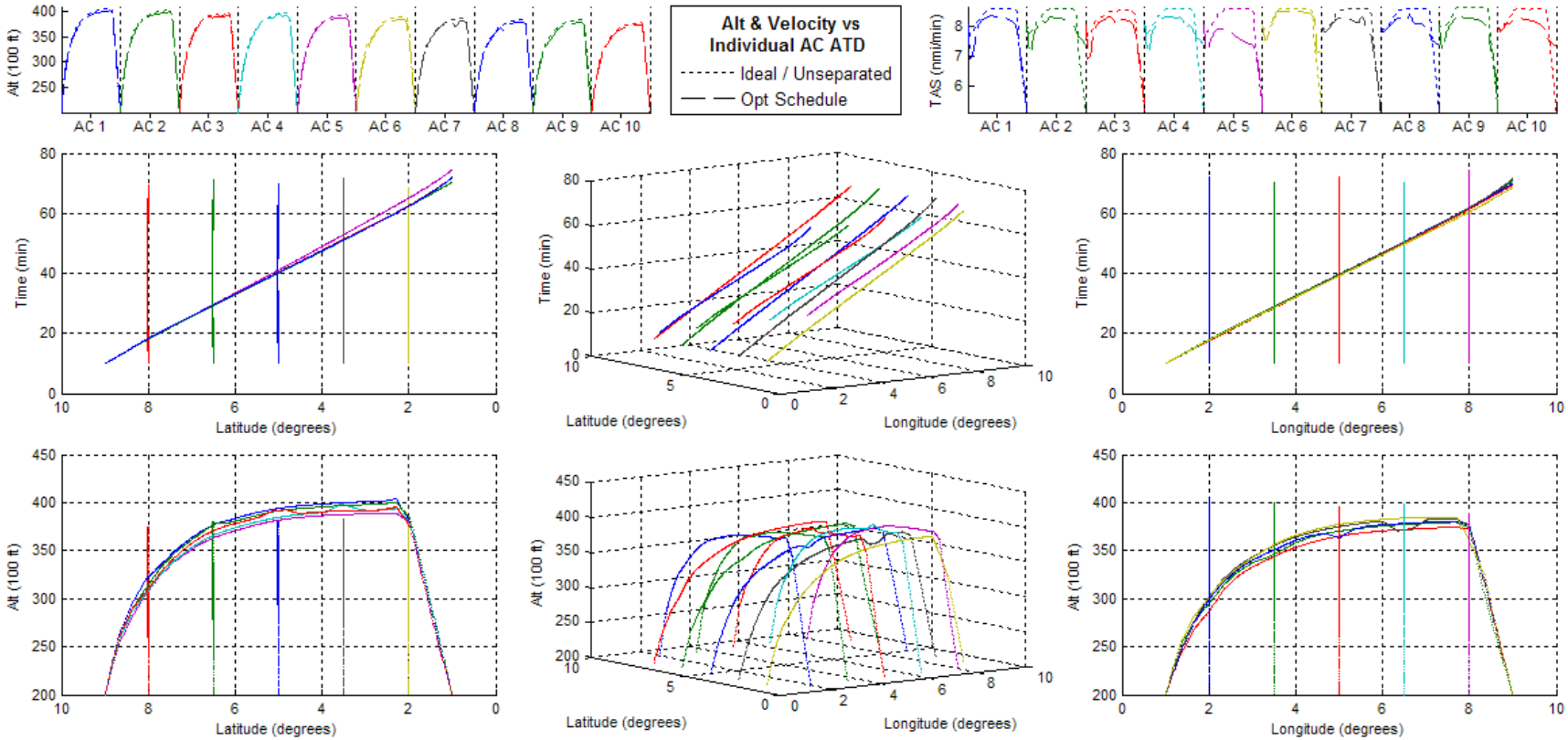

Figure 220 - Schedule Optimized 10acCH ATD_N Results

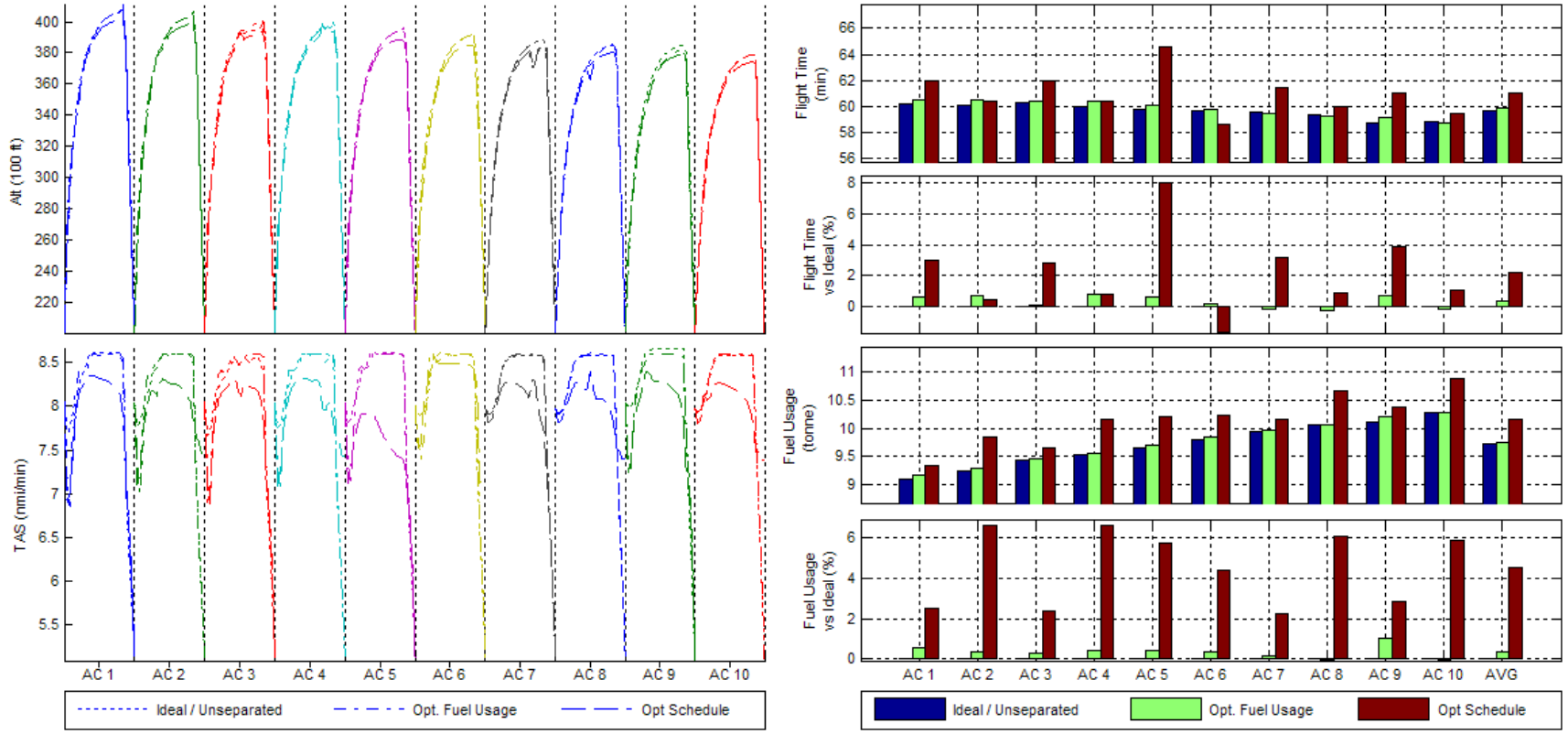

Figure 221 - Trajectory Shape, Flight Time, and Fuel Consumption Comparisons of Fuel and Schedule Optimized 10acCH ATD_N Results

J.9 BADA Boeing 747-300 - Scenario 2acPH2H - ATD_N

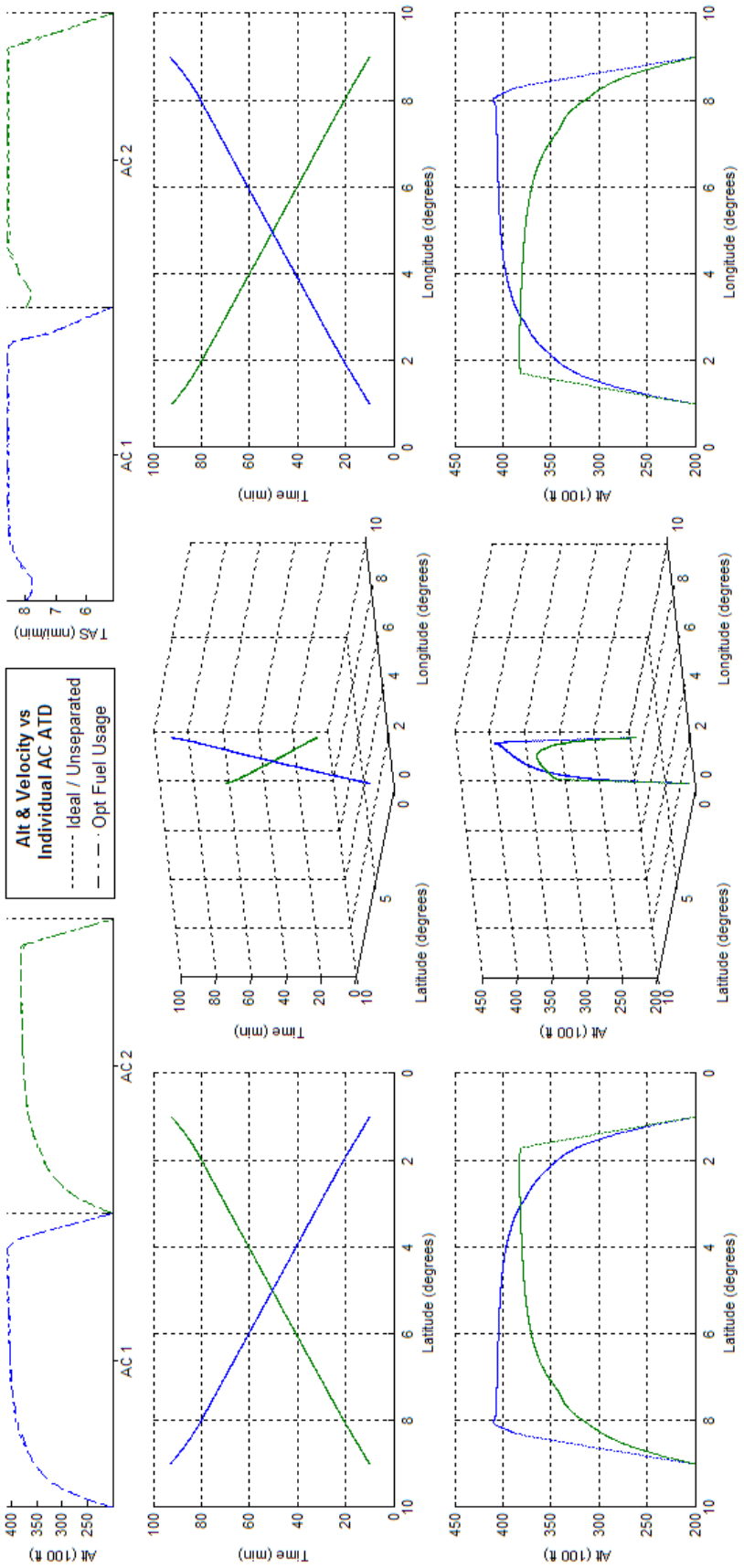

Figure 222 - Fuel Optimized 2acPH2H ATD_N Results

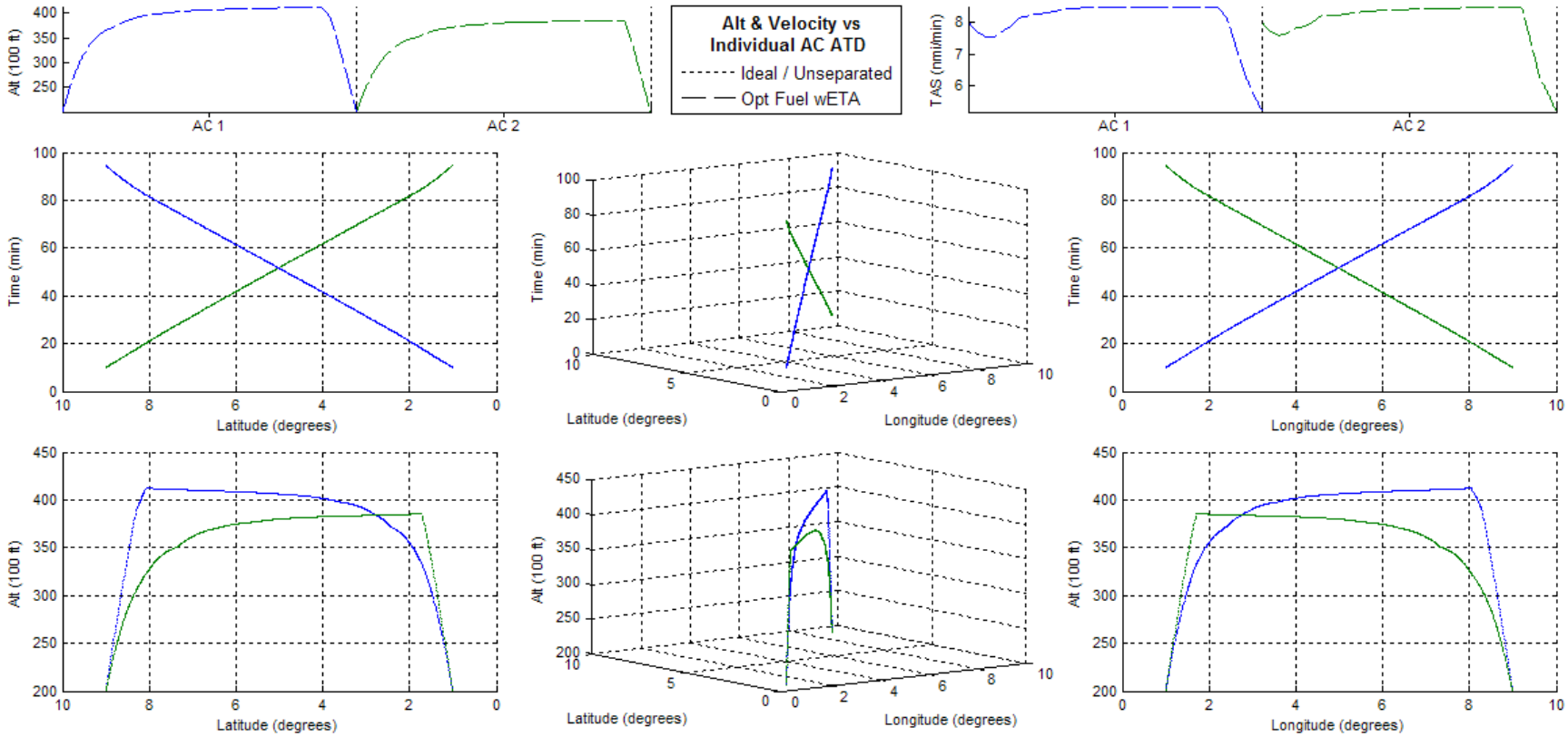

Figure 223 - Constrained ETA, Fuel Optimized 2acPH2H ATD_N Results

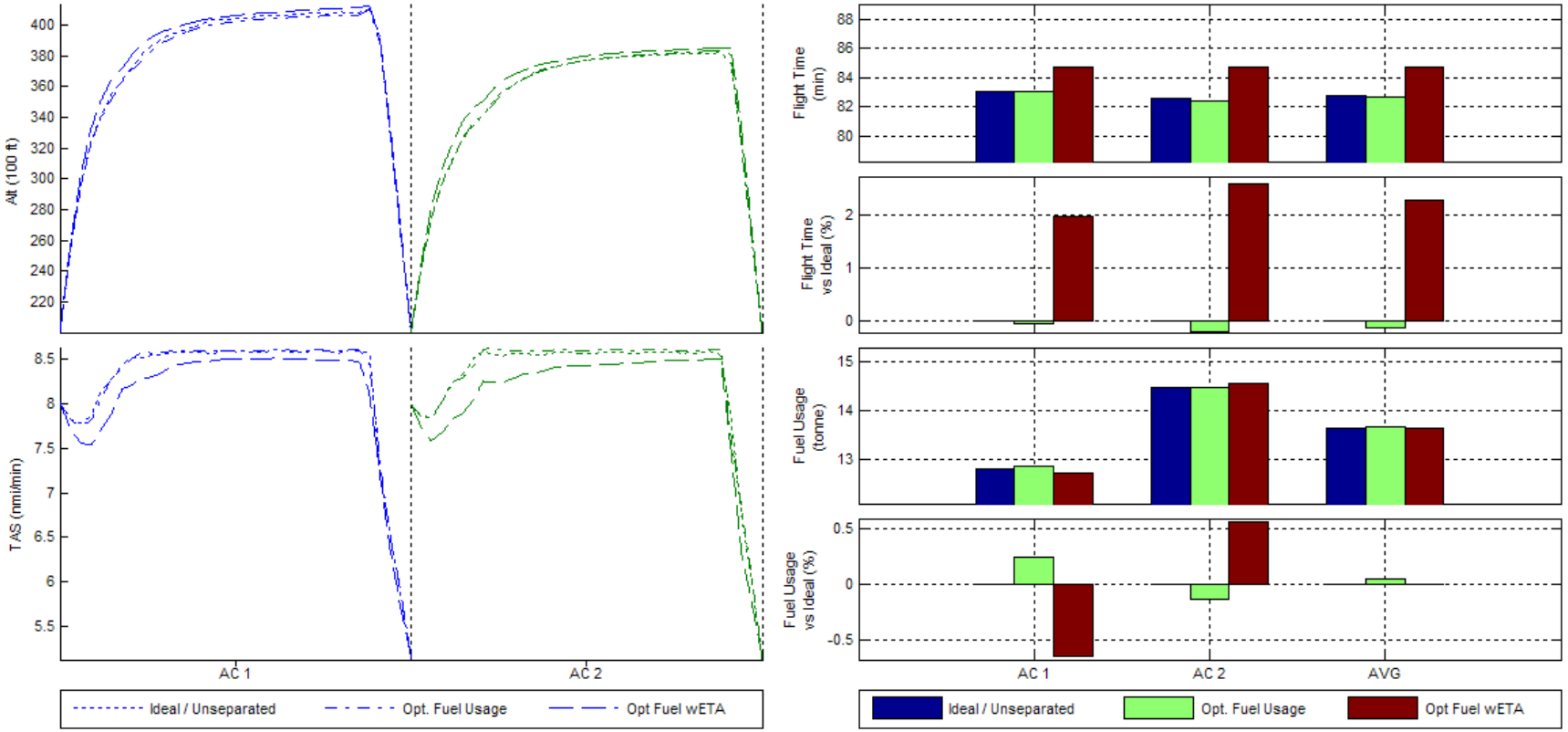

Figure 224 - Trajectory Shape, Flight Time, and Fuel Consumption Comparisons of Unconstrained and Constrained ETA, Fuel Optimized 2acPH2H ATD_N Results

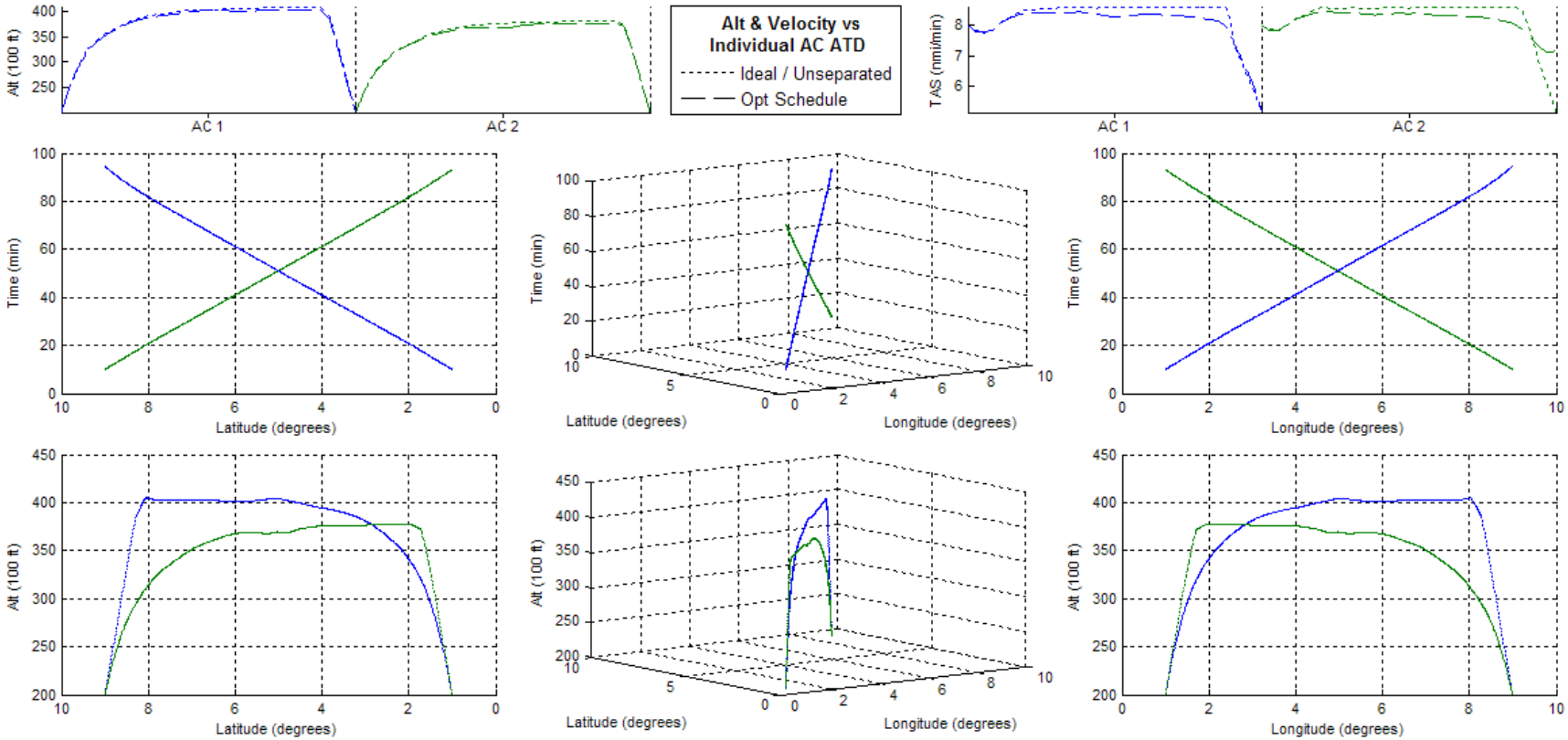

Figure 225 - Schedule Optimized 2acPH2H ATD_N Results

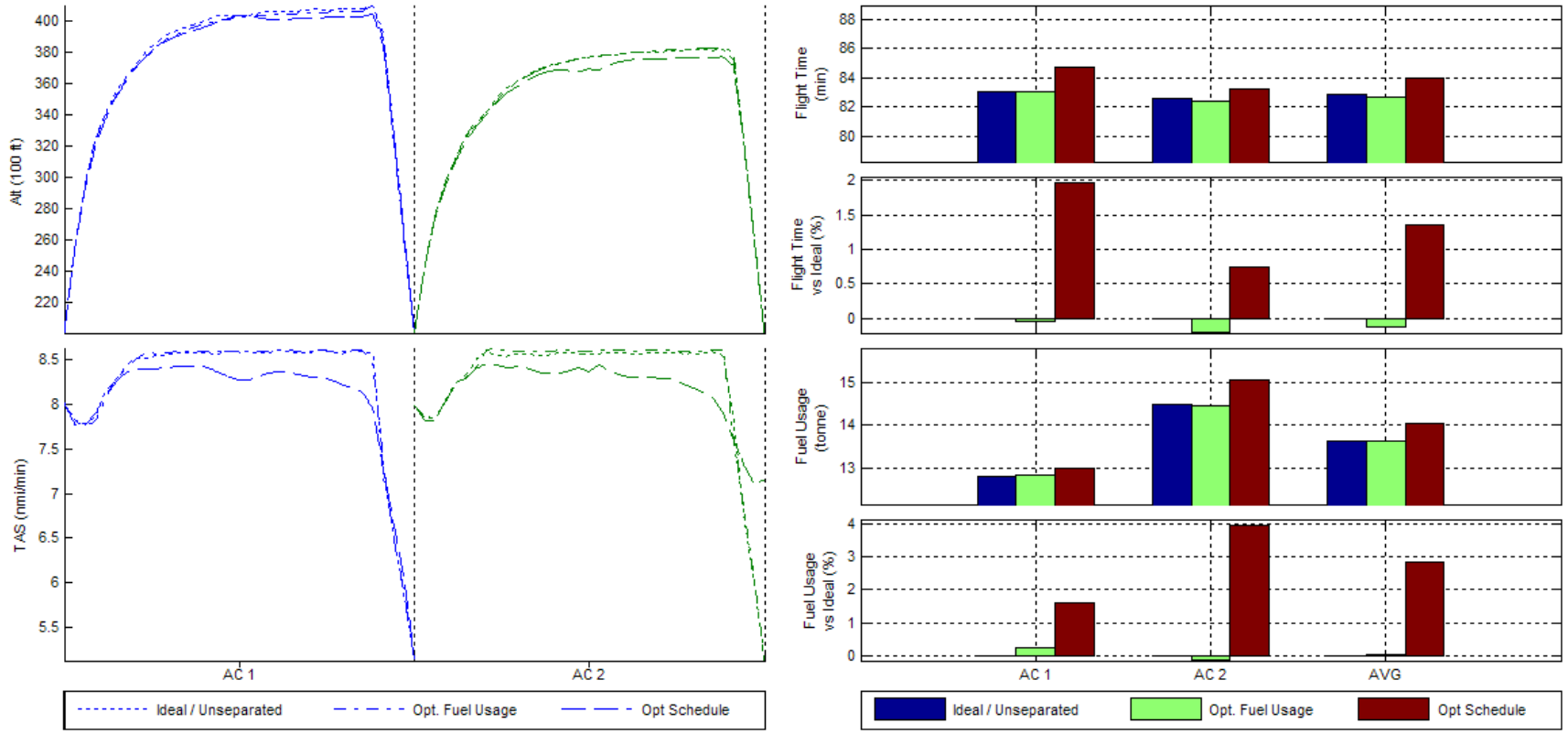

Figure 226 - Trajectory Shape, Flight Time, and Fuel Consumption Comparisons of Fuel and Schedule Optimized 2acPH2H ATD_N Results

J.10 BADA Boeing 747-300 - Scenario 4acPH2H - ATD_N

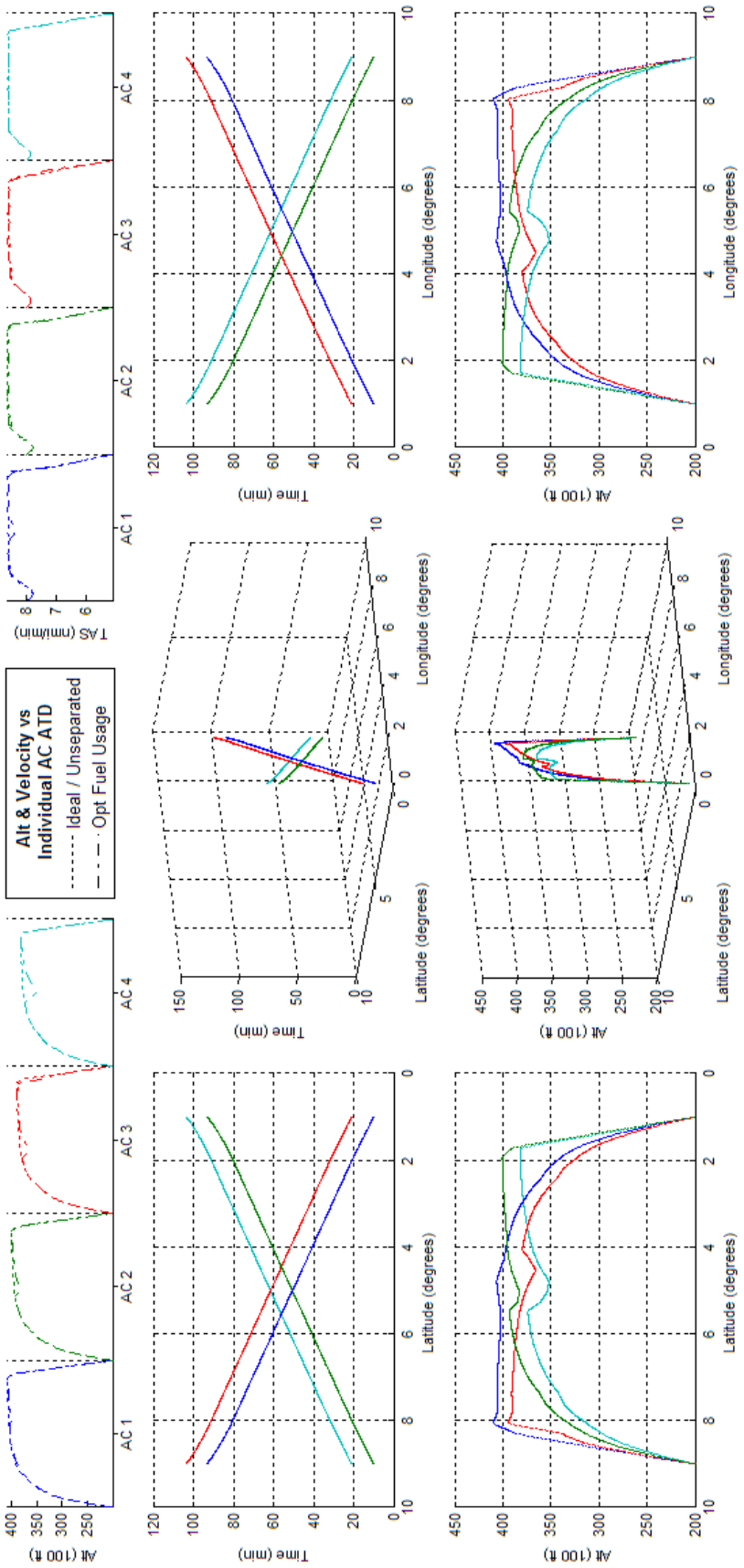

Figure 227 - Fuel Optimized 4acPH2H ATD_N Results

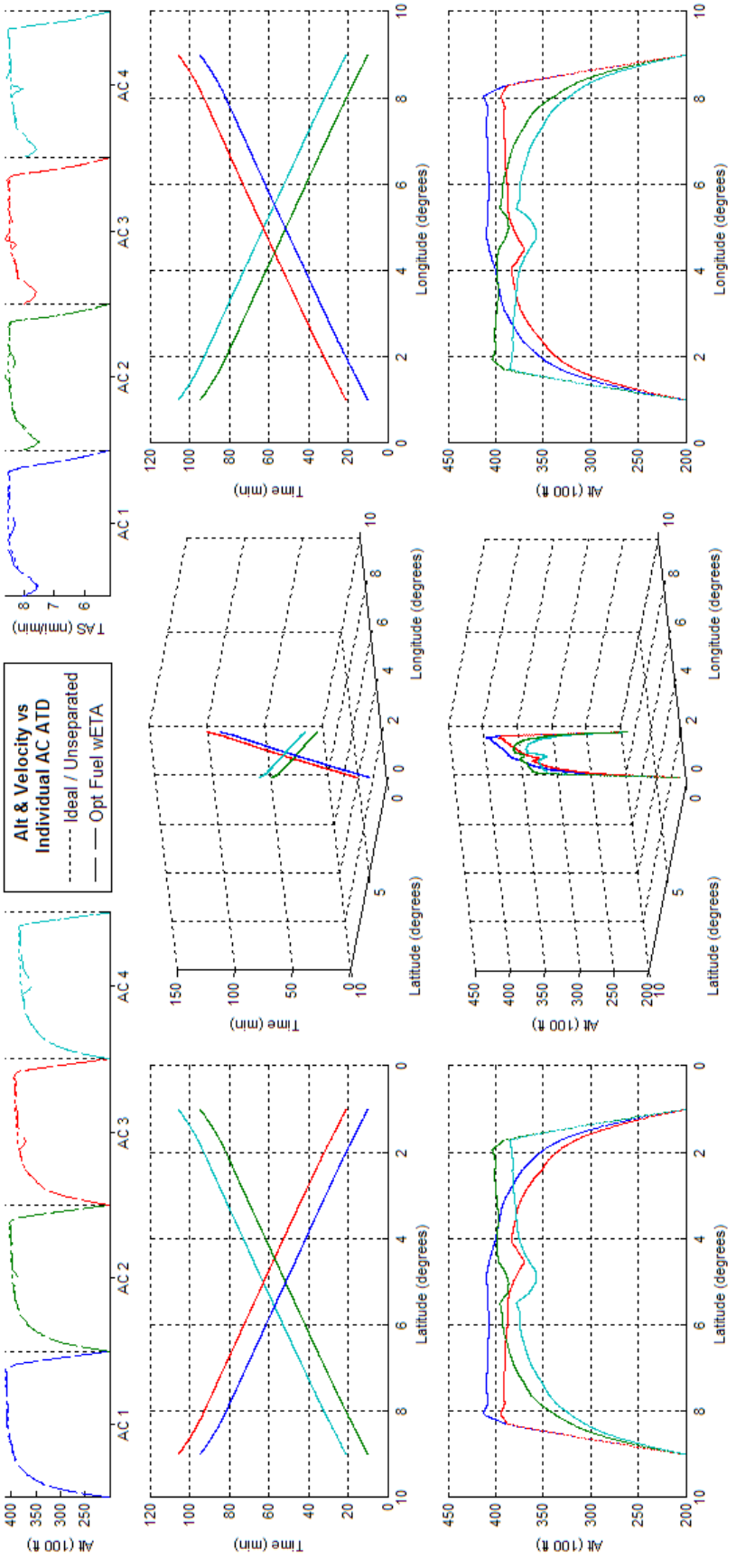

Figure 228 - Constrained ETA, Fuel Optimized 4acPH2H ATD_N Results

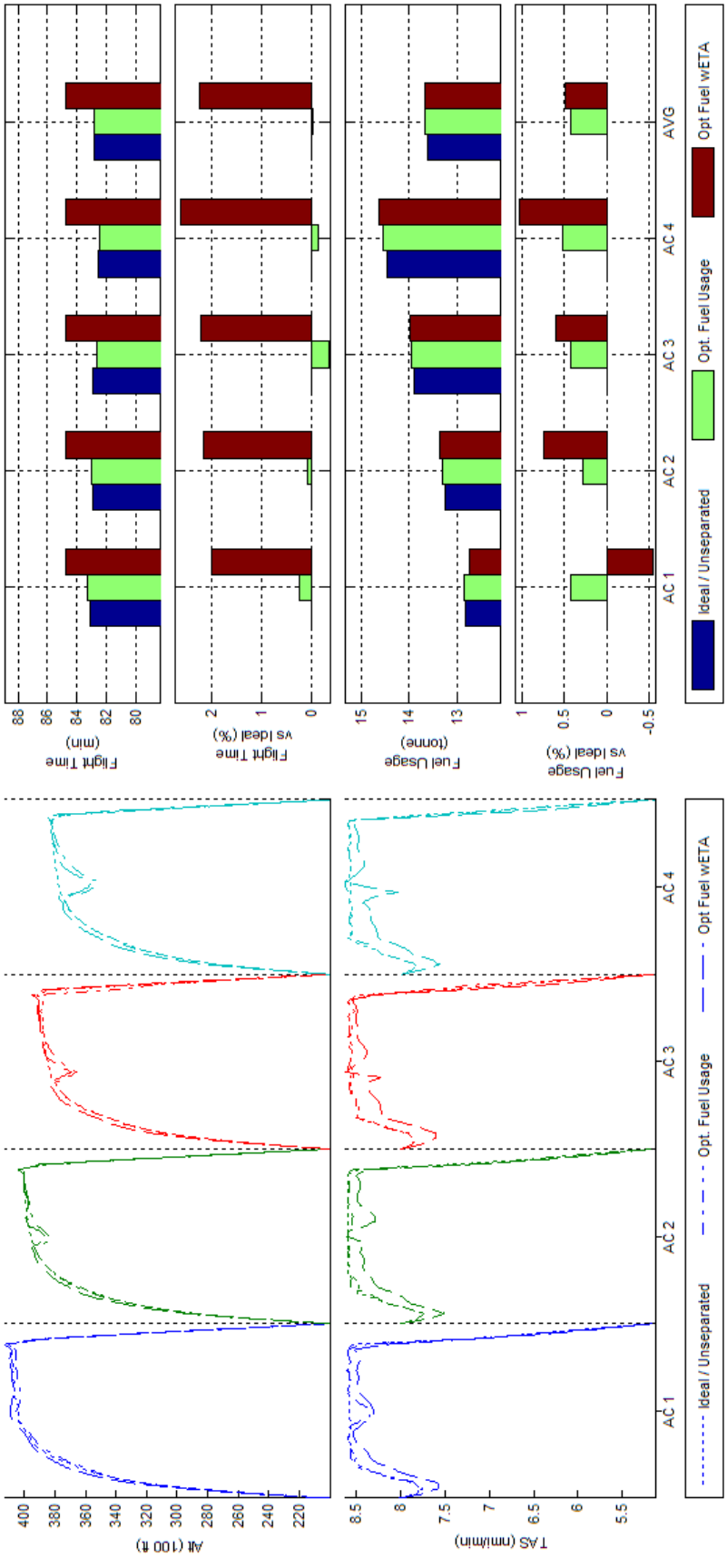

Figure 229 - Trajectory Shape, Flight Time, and Fuel Consumption Comparisons of Unconstrained and Constrained ETA, Fuel Optimized 4acPH2H ATD_N Results

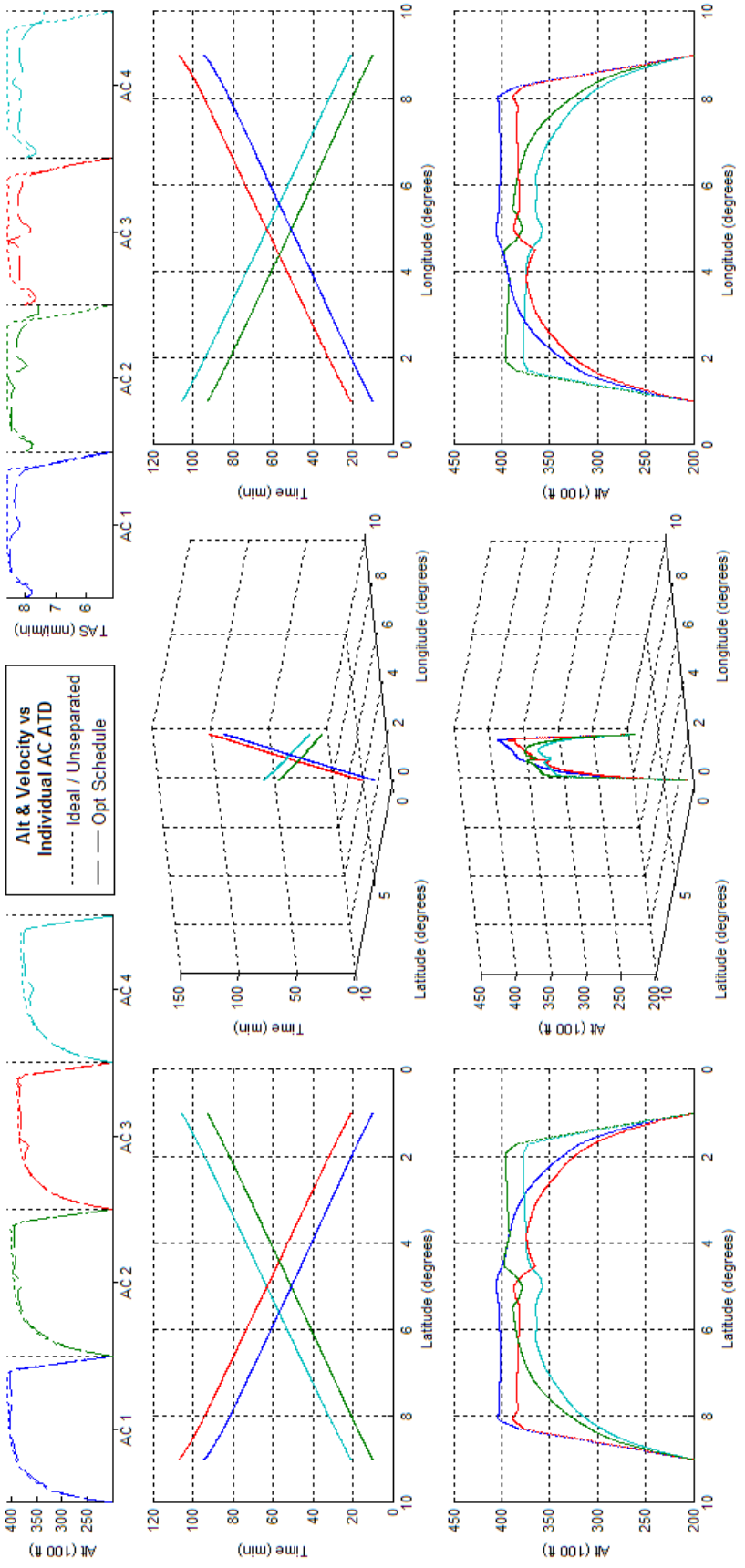

Figure 230 - Schedule Optimized 4acPH2H ATD_N Results

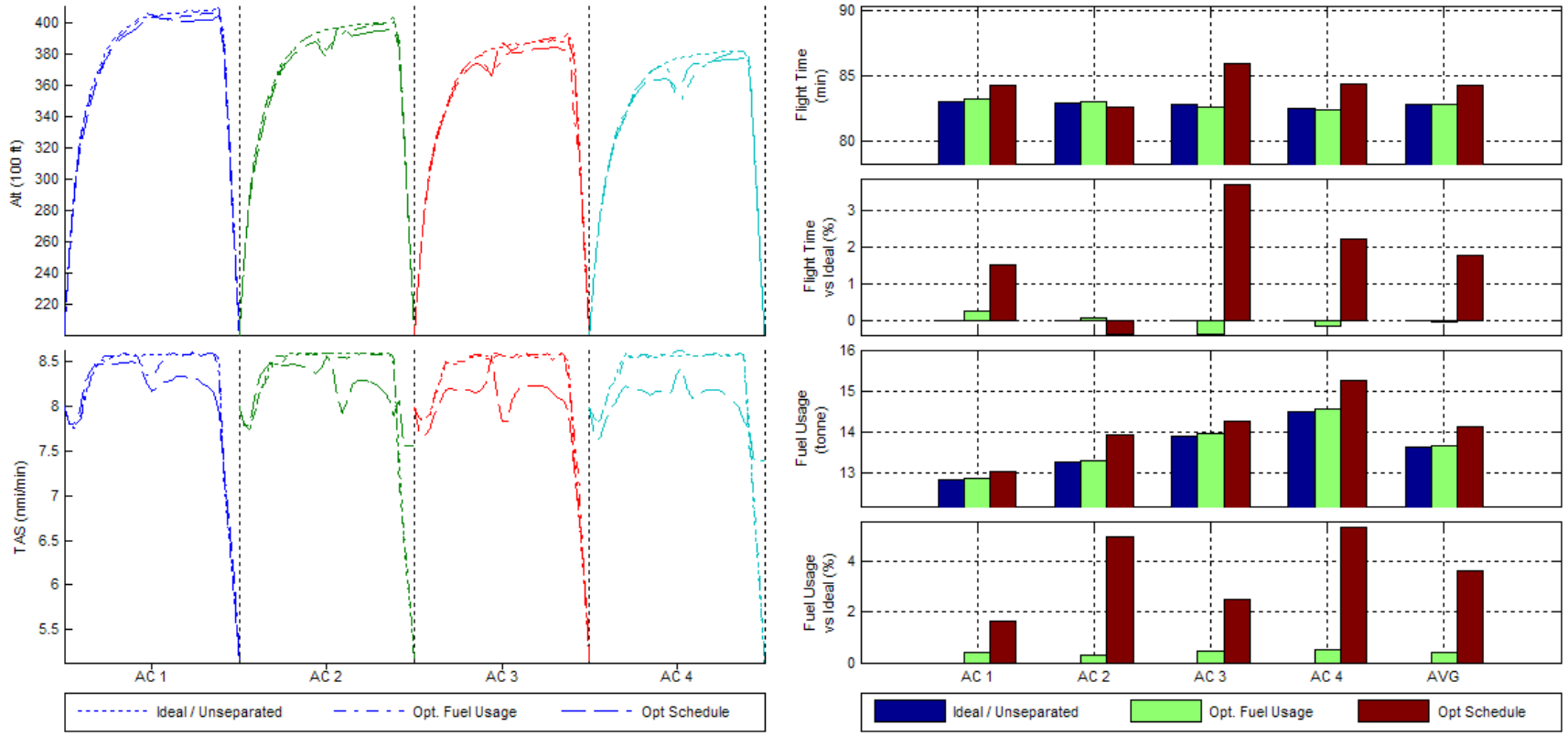

Figure 231 - Trajectory Shape, Flight Time, and Fuel Consumption Comparisons of Fuel and Schedule Optimized 4acPH2H ATD_N Results

J.11 BADA Boeing 747-300 - Scenario 10acPH2H - ATD_N

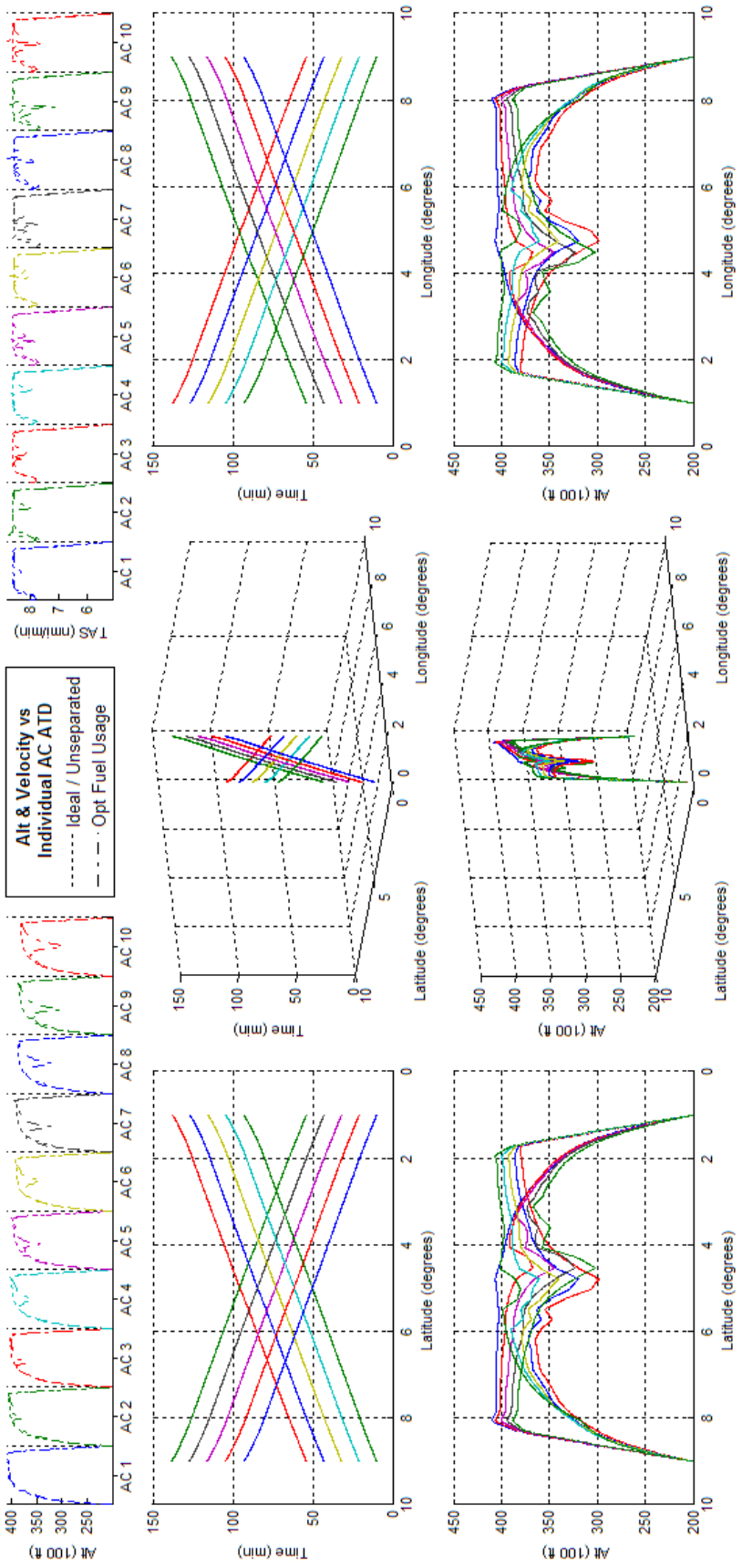

Figure 232 - Fuel Optimized 10acPH2H ATD_N Results

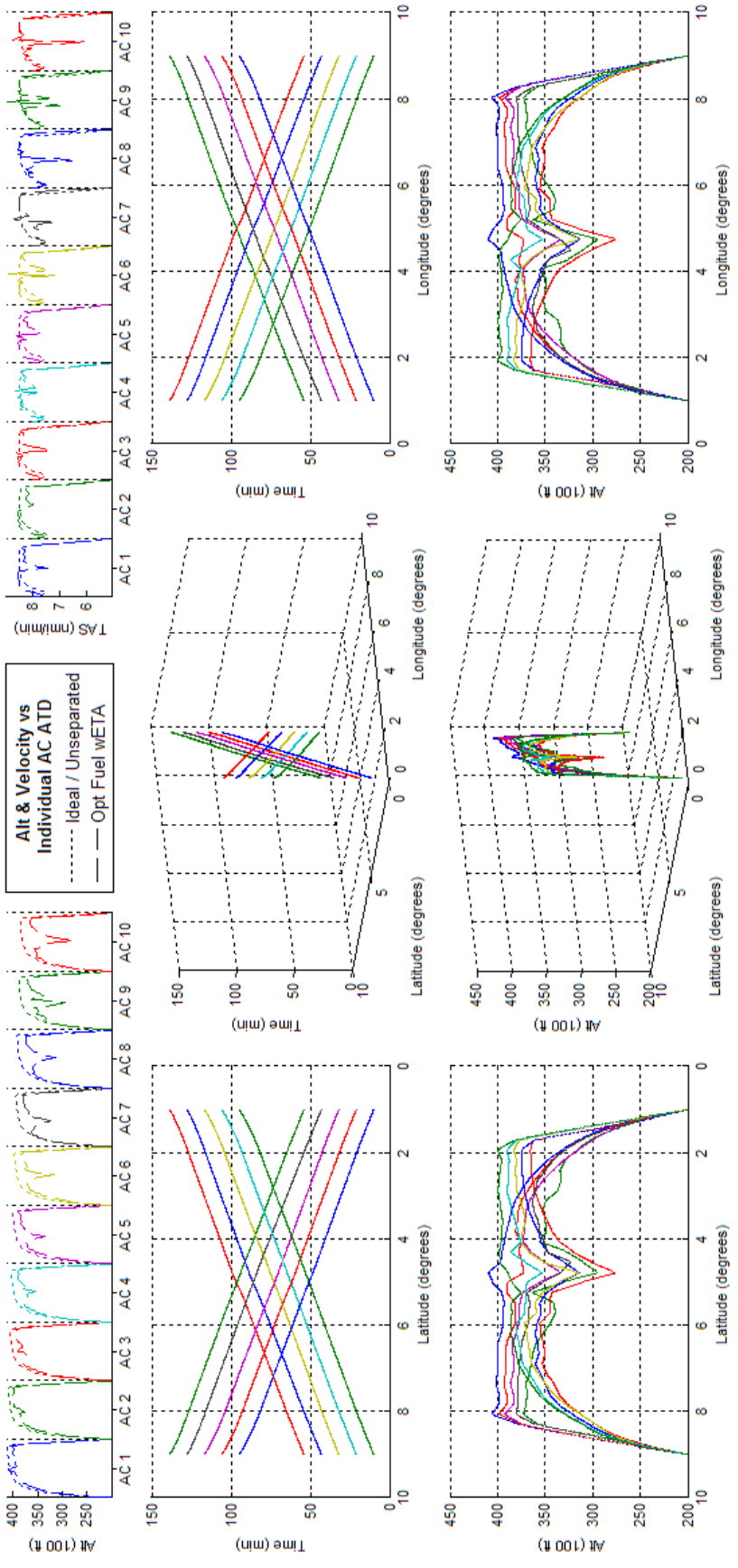

Figure 233 - Constrained ETA, Fuel Optimized 10acPH2H ATD_N Results

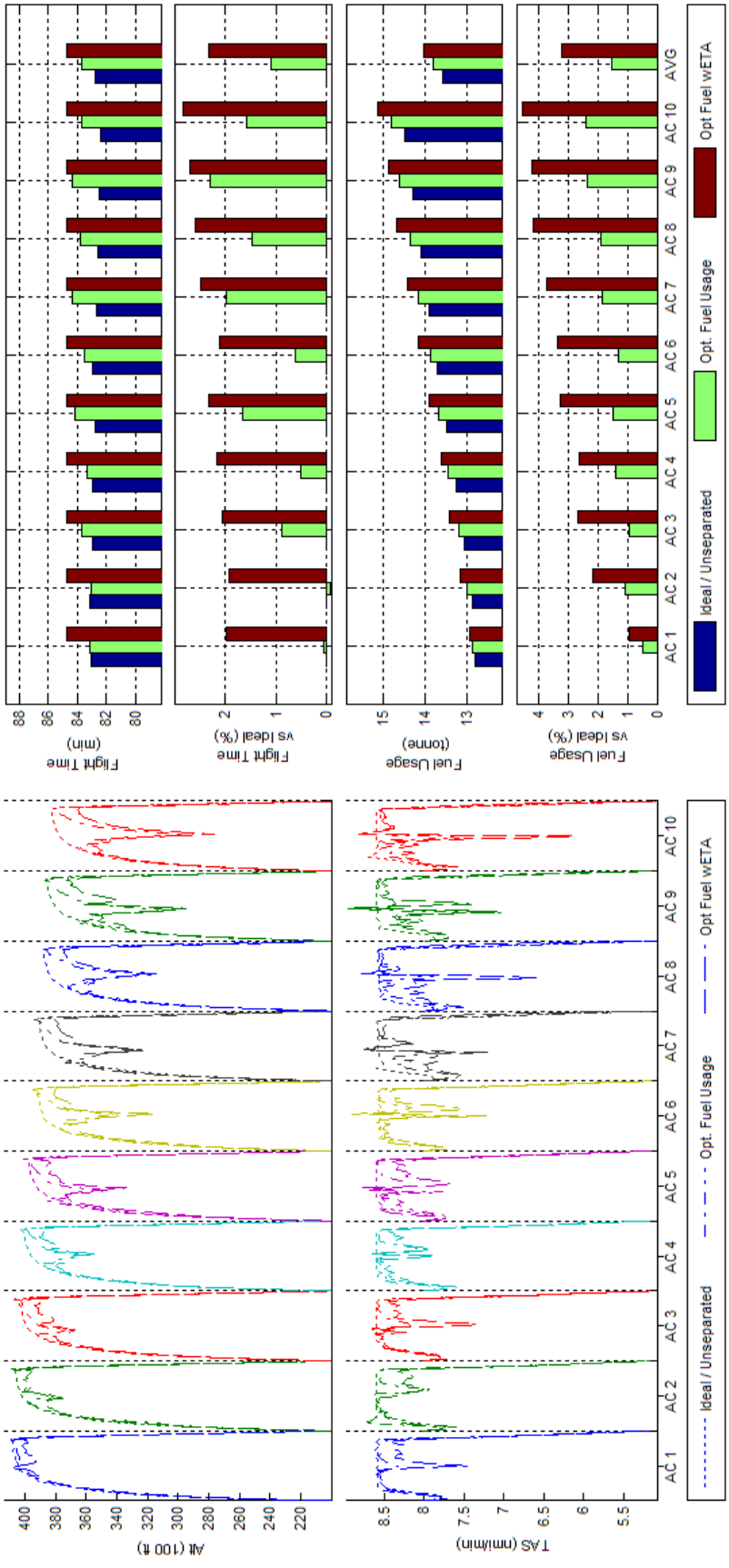

Figure 234 Trajectory Shape, Flight Time, and Fuel Consumption Comparisons of Unconstrained and Constrained ETA, Fuel Optimized 10acPH2H ATD_N Results

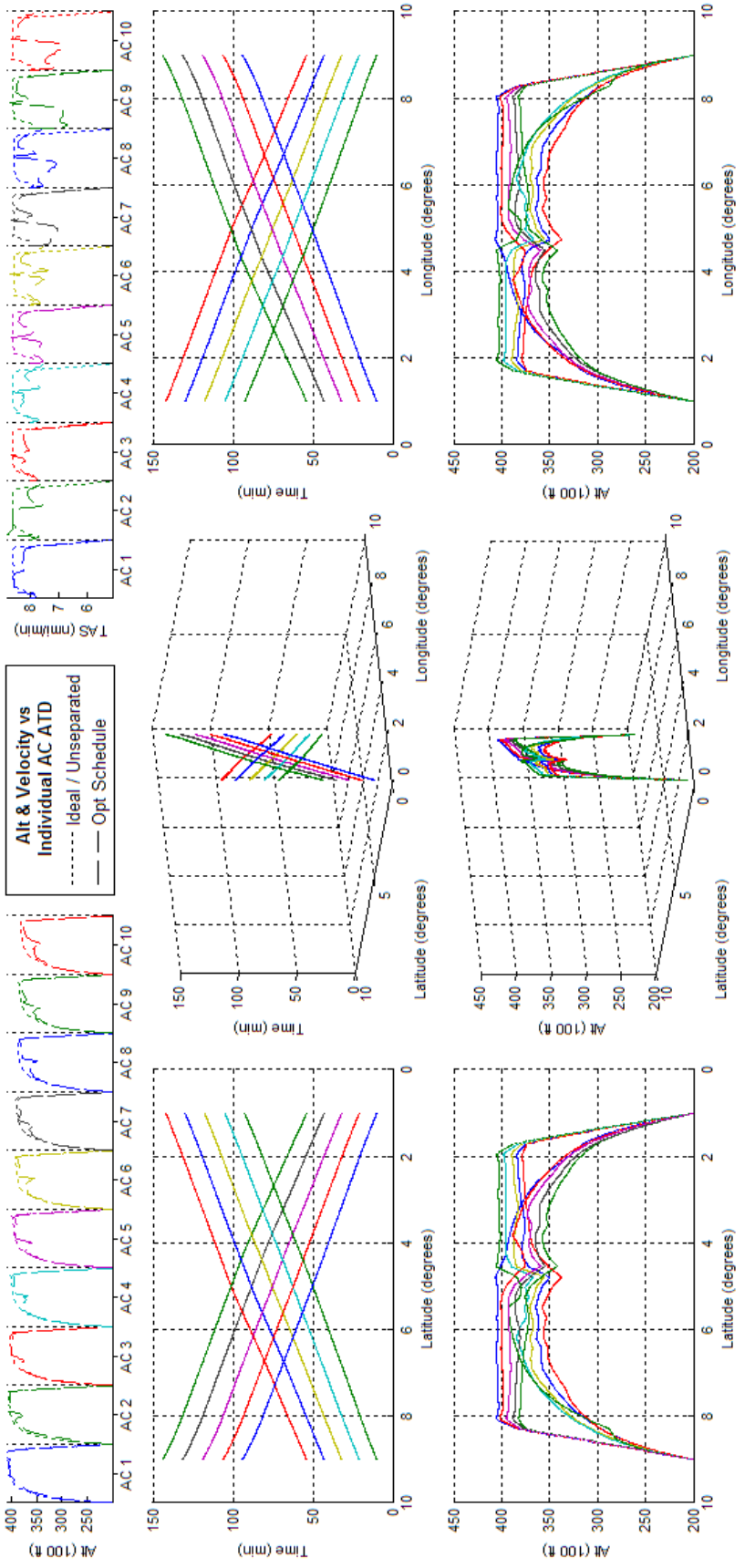

Figure 235 -Schedule Optimized 10acPH2H ATD_N Results

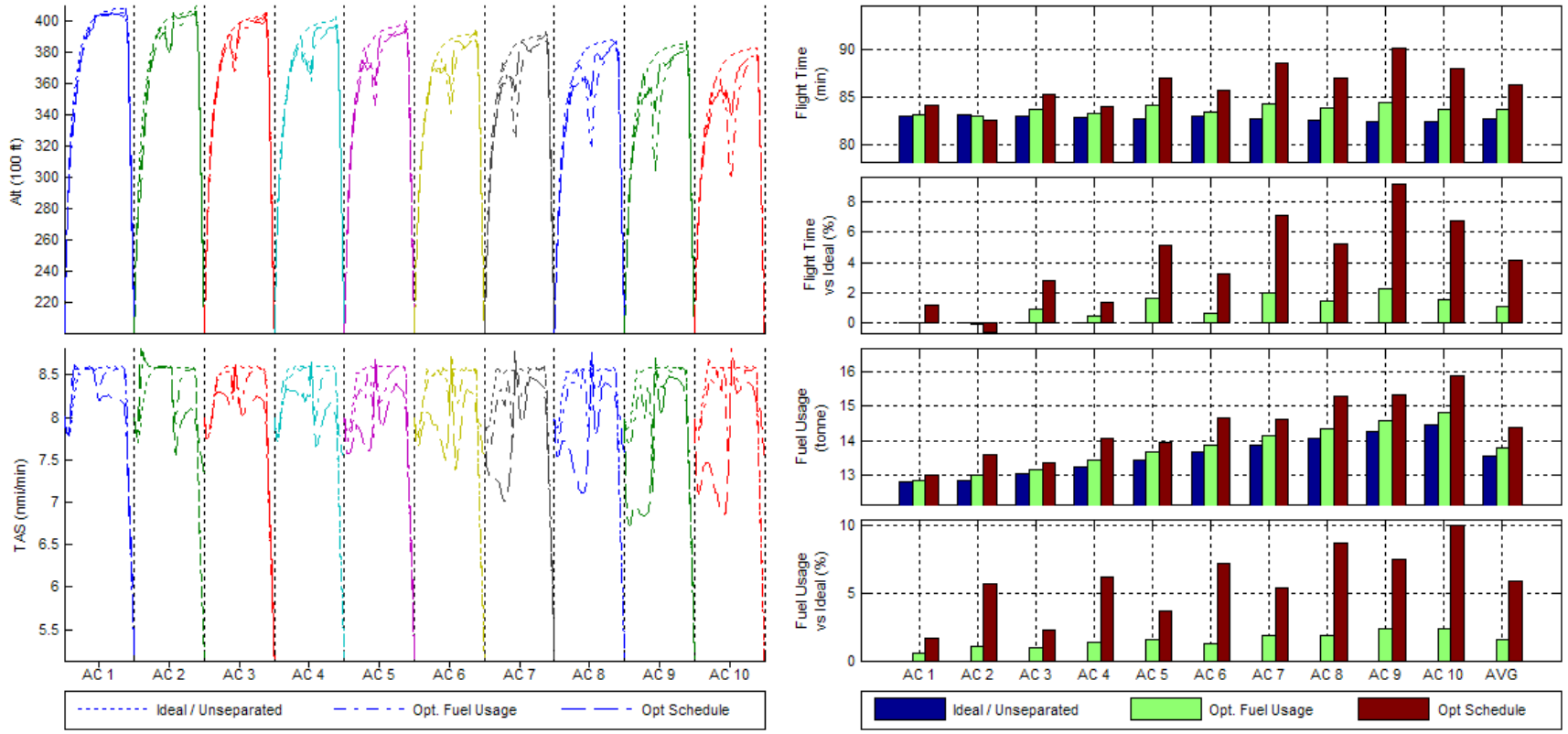

Figure 236 Trajectory Shape, Flight Time, and Fuel Consumption Comparisons of Fuel and Schedule Optimized 10acPH2H ATD_N Results

APPENDIX K BFO Multi-Model Results

The following graphs show the results for the PCO when using BADA data of different aircraft, individually and in a combined scenario, as mentioned in Chapter 4 of the thesis. For discussion and impacts of these results, please refer to section 4.3.3. For instructions on how to read the graphs, please refer to section 3.4.1. As a reminder, BADA Conditions of Use disallow public comparison of the fuel usage of different aircraft models; consequently this appendix only shows the optimization results in terms of the shapes and variation inside of the resulting optimizer variable and the optimized trajectory. Further, as optimizations of scenarios with unconstrained arrival times appeared to be severely constrained to the point of incomplete optimizations due to insufficient computation time for some scenarios, all schedule optimizations and fuel optimizations of scenarios with constrained arrival times were not attempted; hence only non-arrival time constrained results are displayed.

K.1 BADA Airbus A320 - Scenario 2acPSd - ATD_N

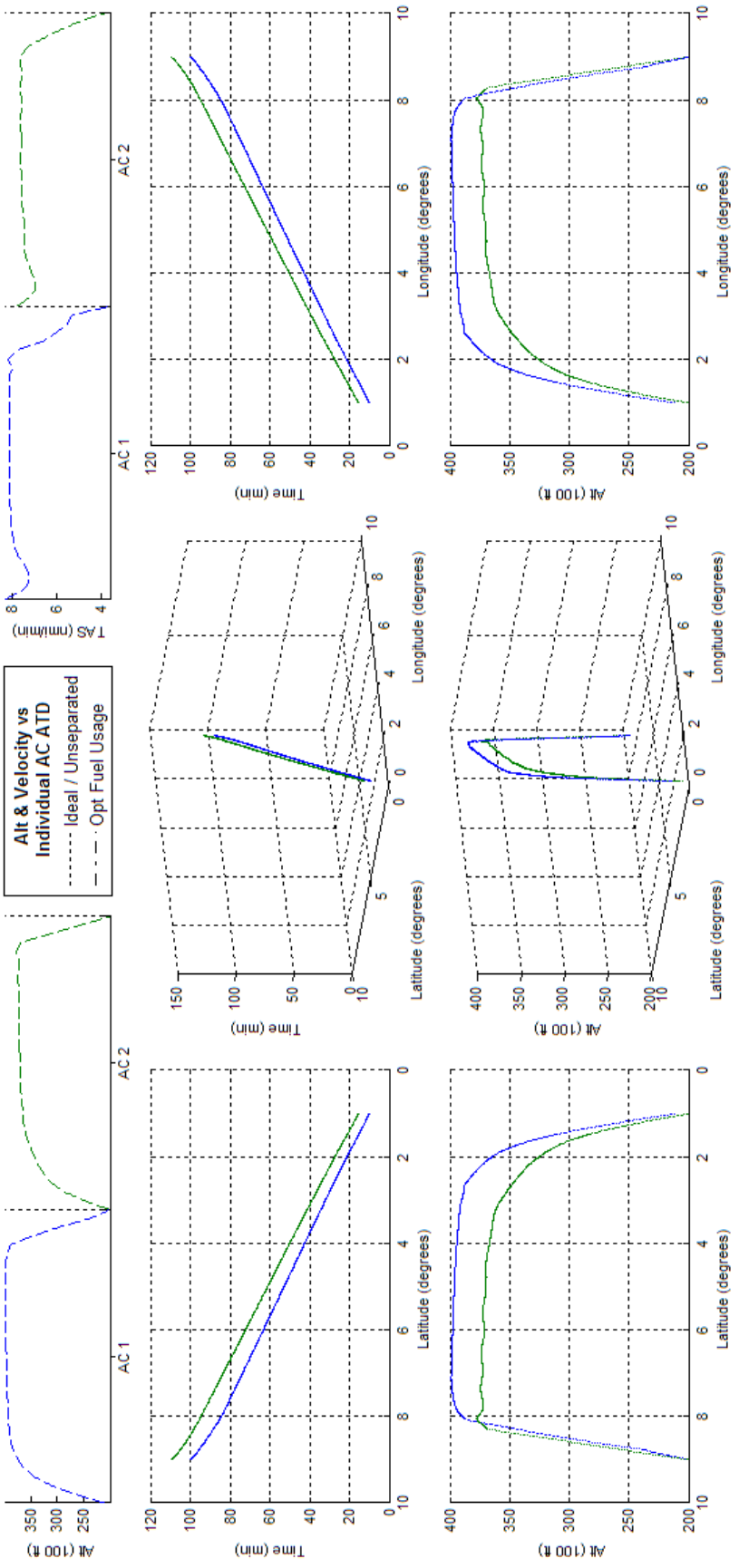

Figure 237 - Fuel Optimized 2acPSd ATD_N Results

K.2 BADA Airbus A320 - Scenario 4acPSd - ATD_N

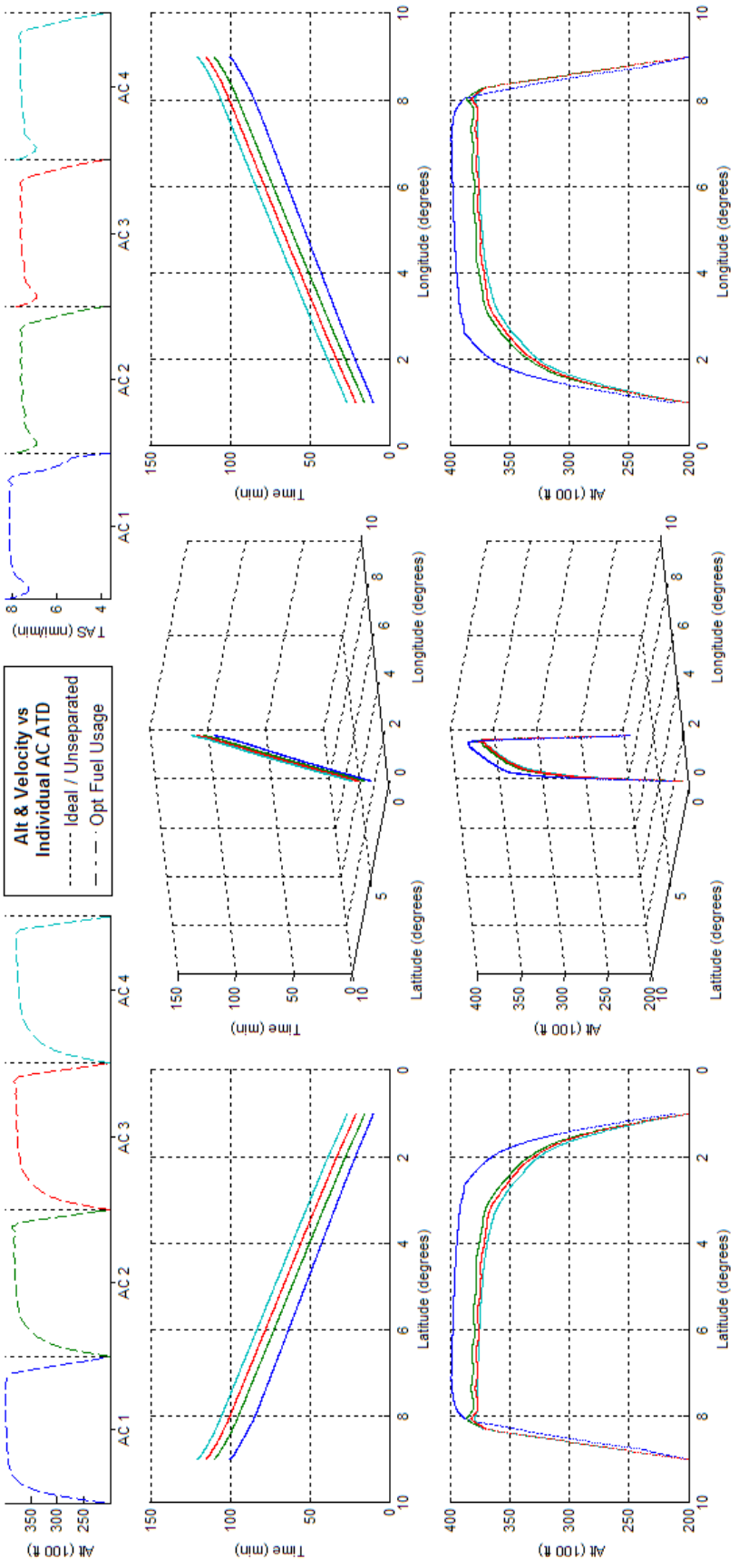

Figure 238 - Fuel Optimized 4acPSd ATD_N Results

K.3 BADA Airbus A320 - Scenario 2acCO - ATD_N

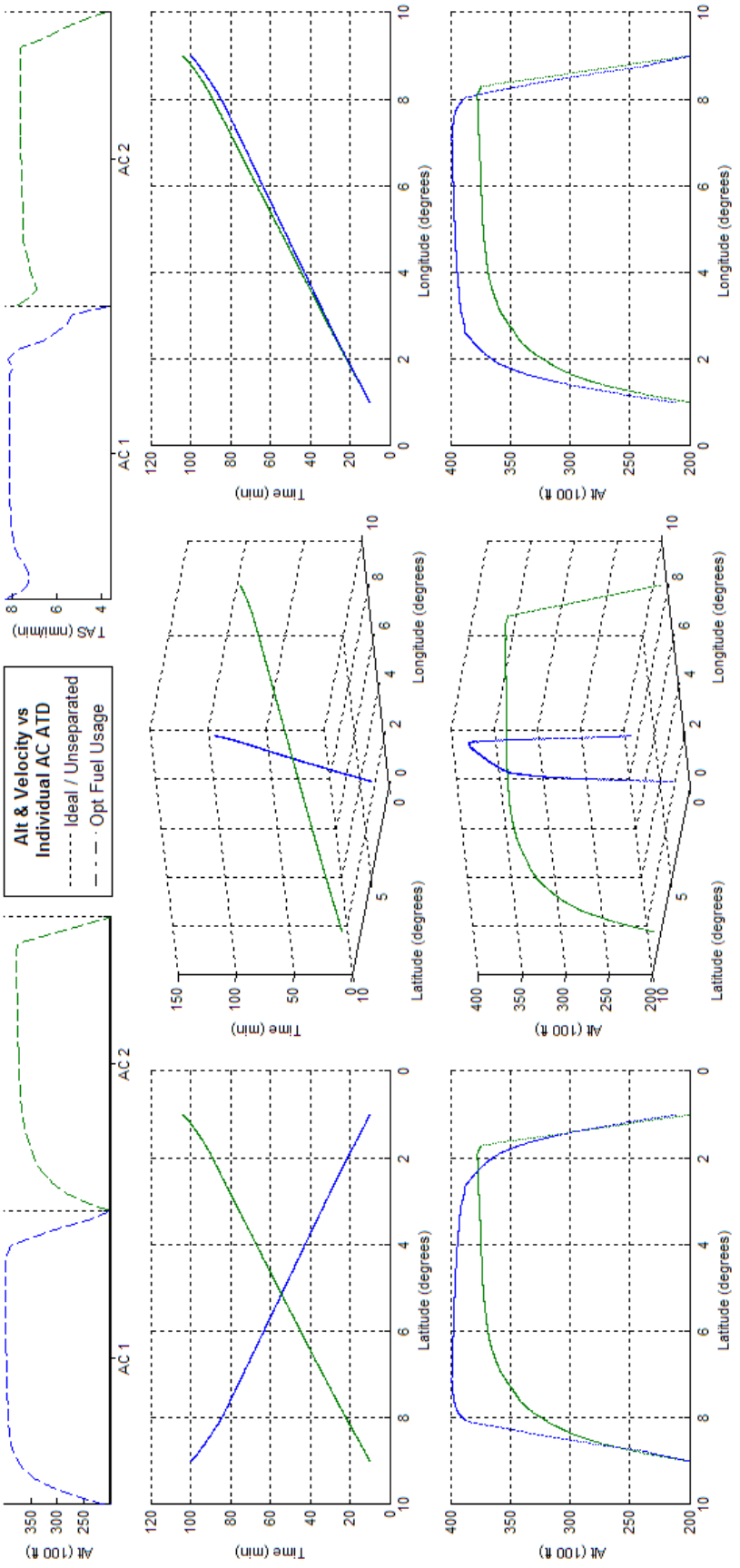

Figure 239 - Fuel Optimized 2acCO ATD_N Results

K.4 BADA Airbus A320 - Scenario 4acCO - ATD_N

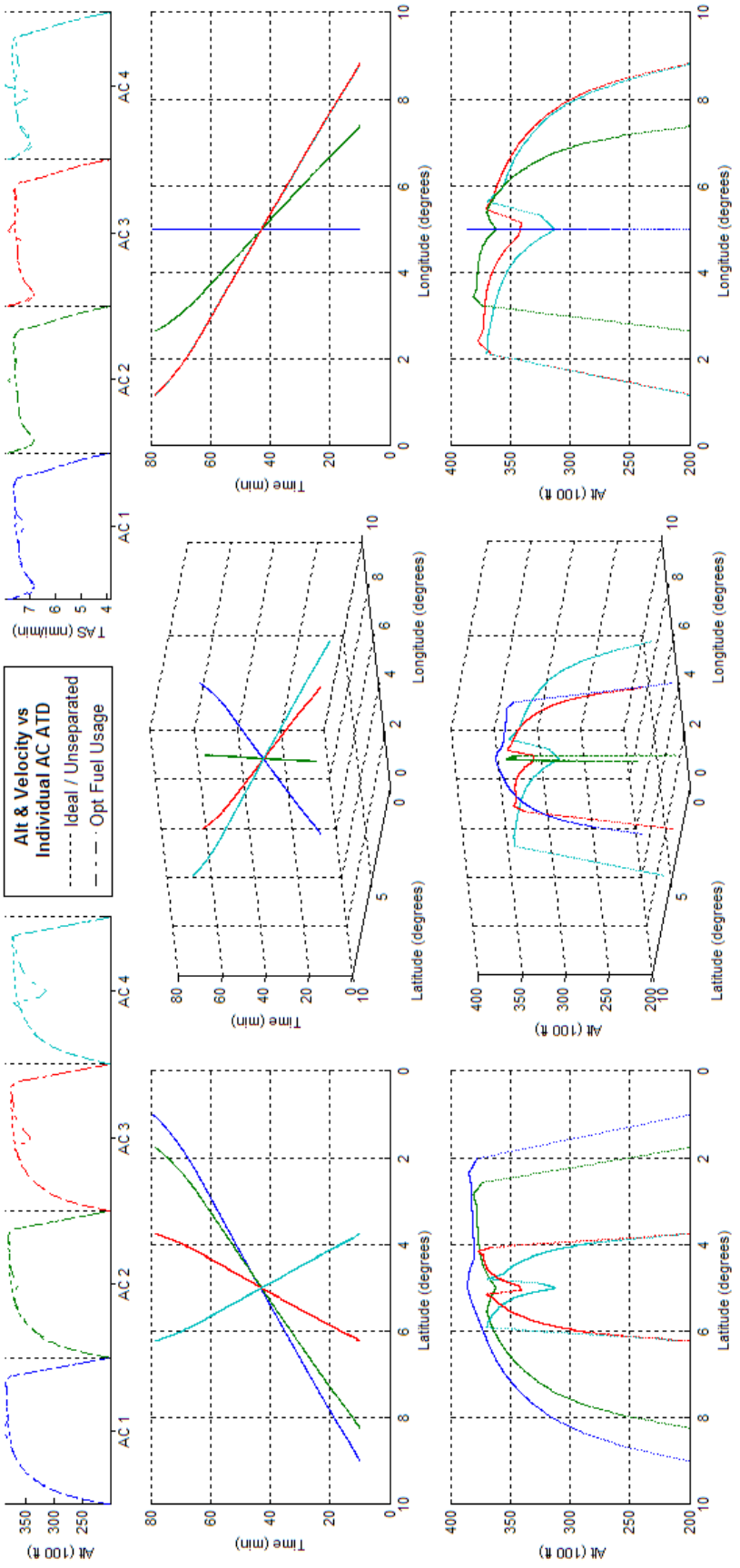

Figure 240 - Fuel Optimized 4acCO ATD_N Results

K.5 BADA Airbus A320 - Scenario 10acCO - ATD_N

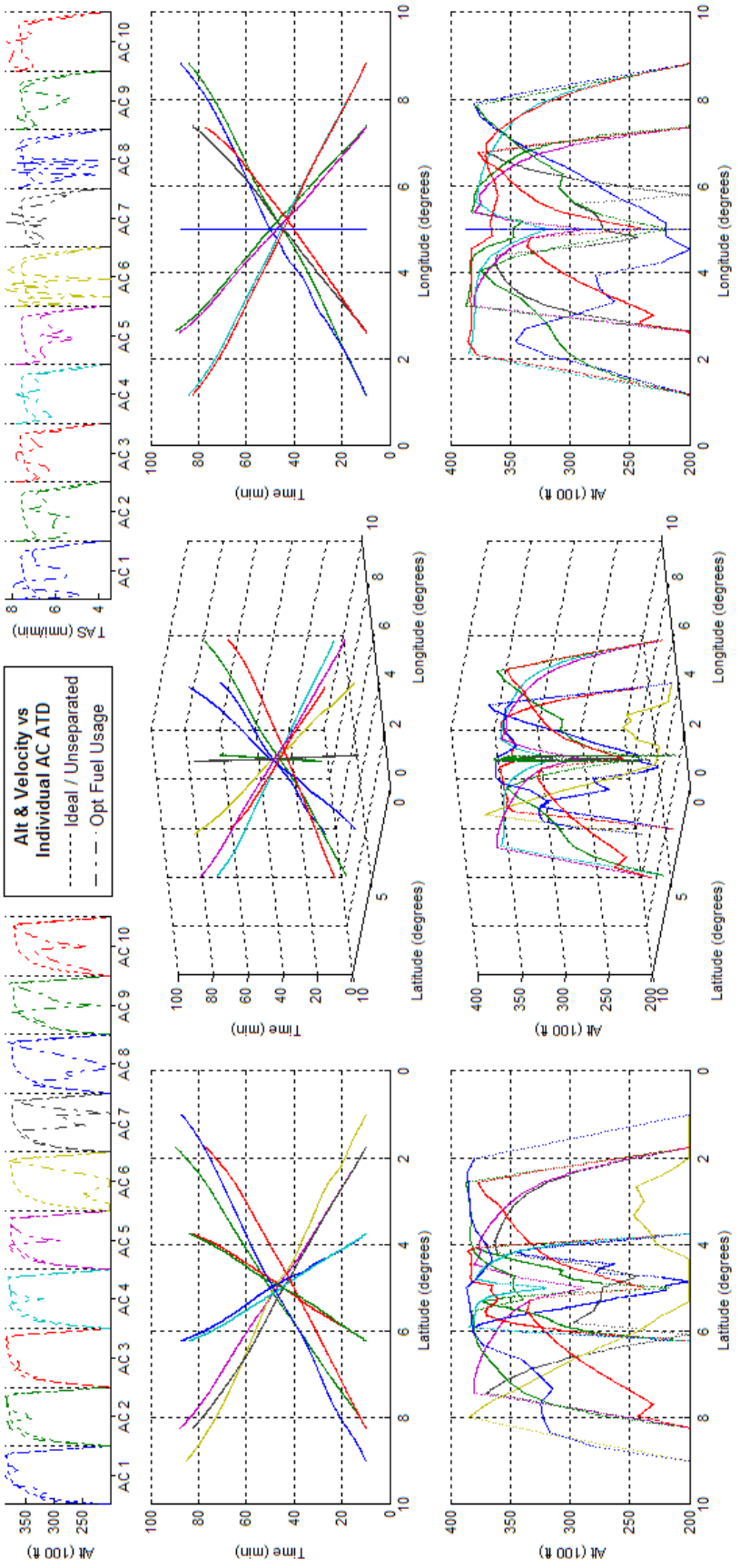

Figure 241 - Fuel Optimized 10acCO ATD_N Results

K.6 BADA Airbus A320 - Scenario 4acCH - ATD_N

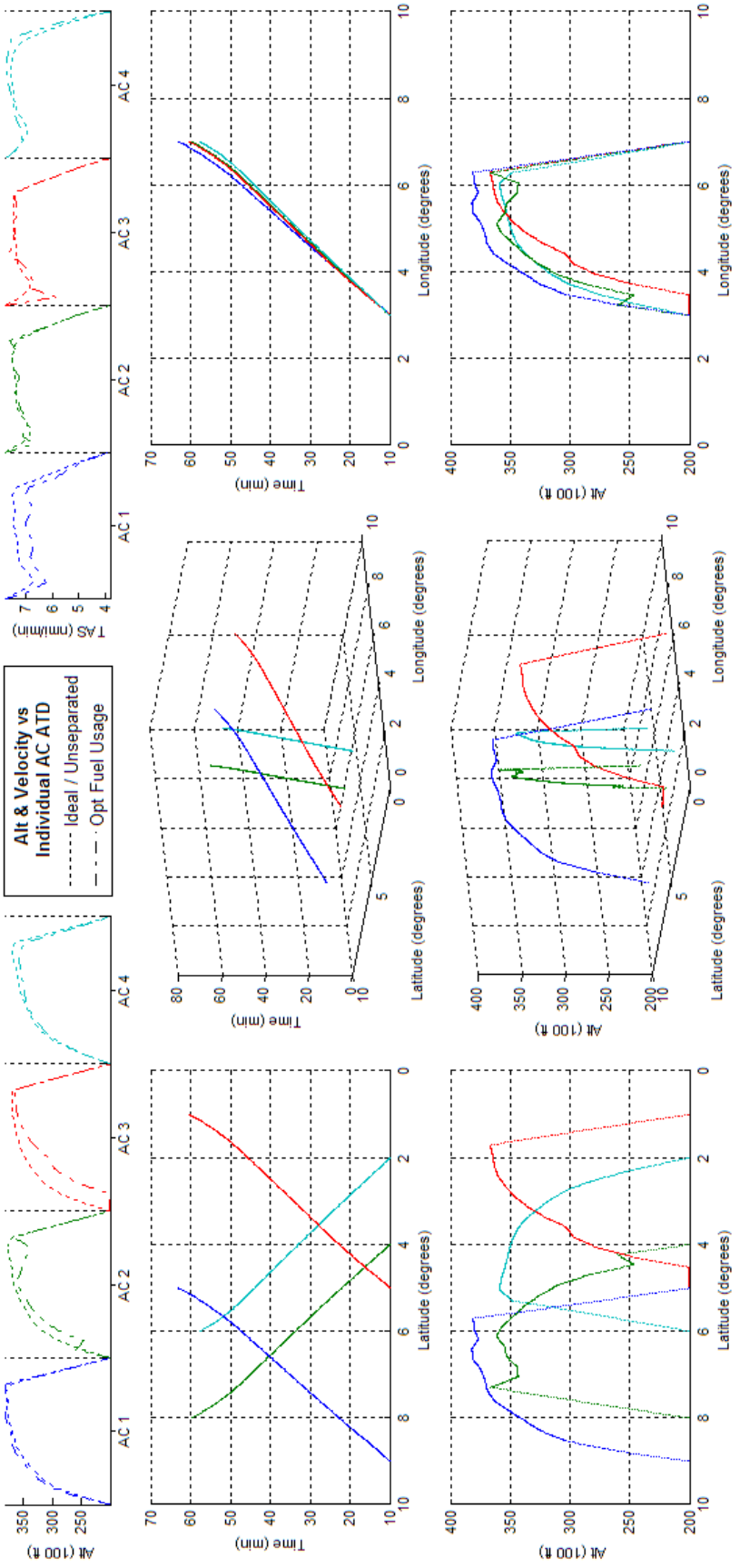

Figure 242 - Fuel Optimized 4acCH ATD_N Results

K.7 BADA Airbus A320 - Scenario 10acCH - ATD_N

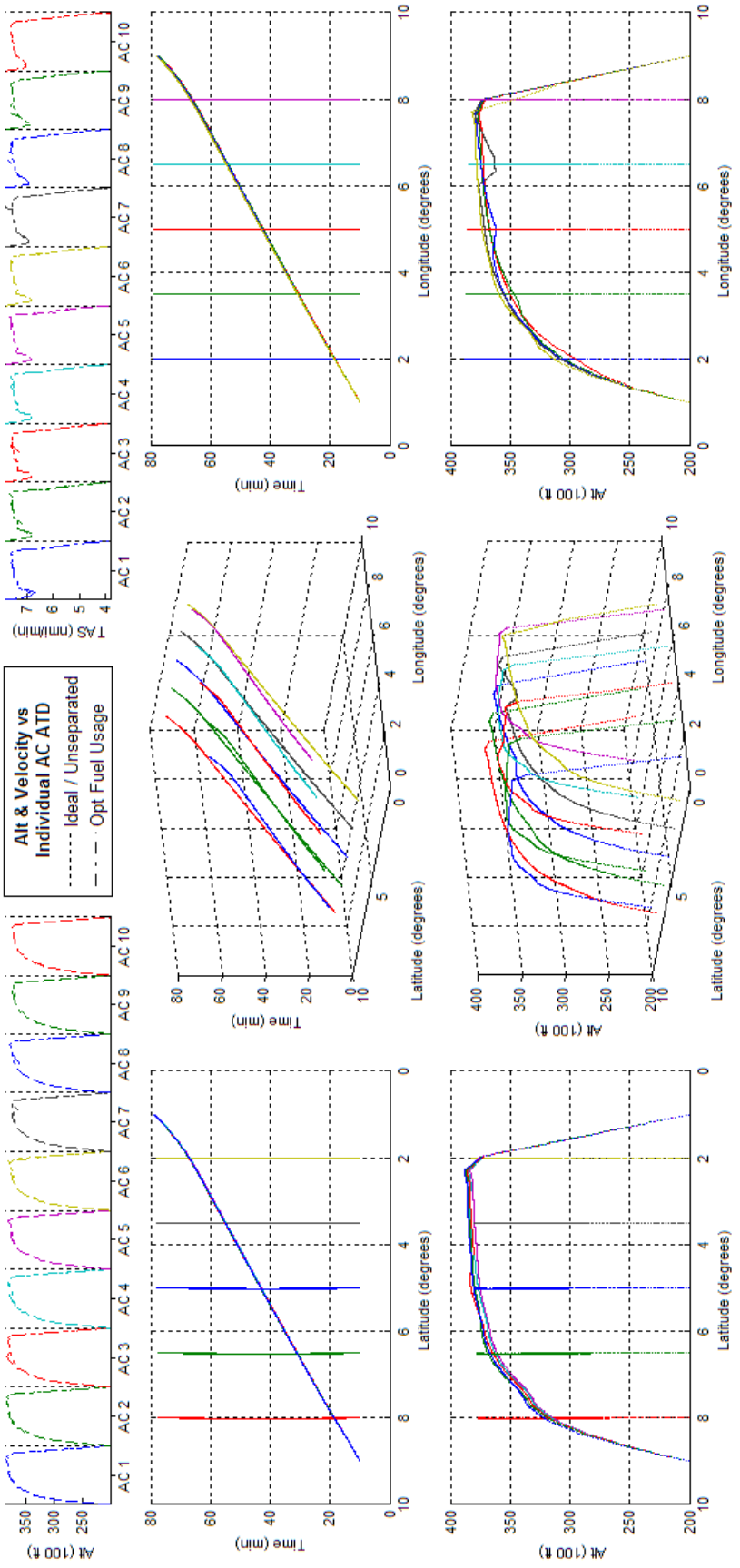

Figure 243 - Fuel Optimized 10acCH ATD_N Results

K.8 BADA Airbus A320 - Scenario 2acPH2H - ATD_N

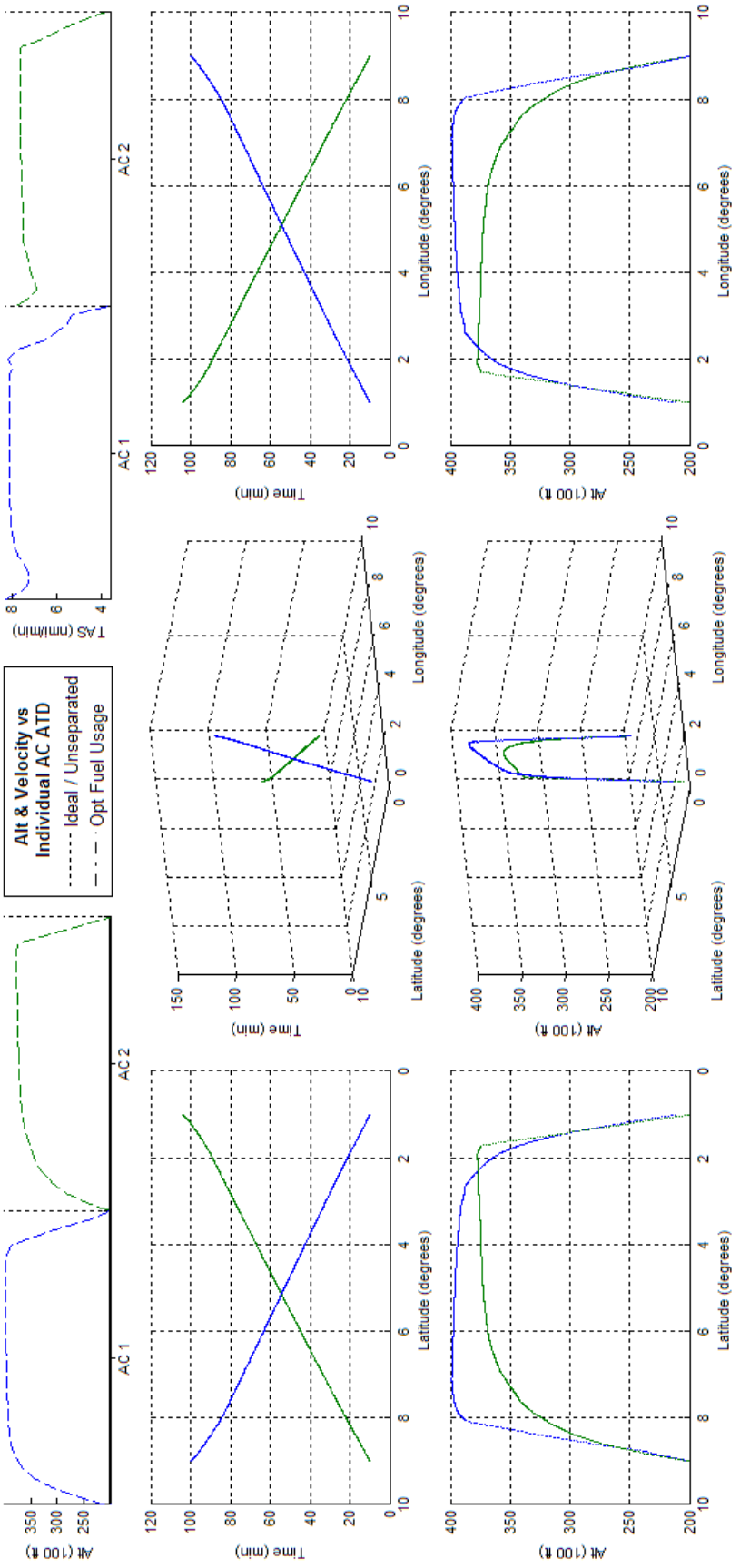

Figure 244 - Fuel Optimized 2acPH2H ATD_N Results

K.9 BADA Airbus A320 - Scenario 4acPH2H - ATD_N

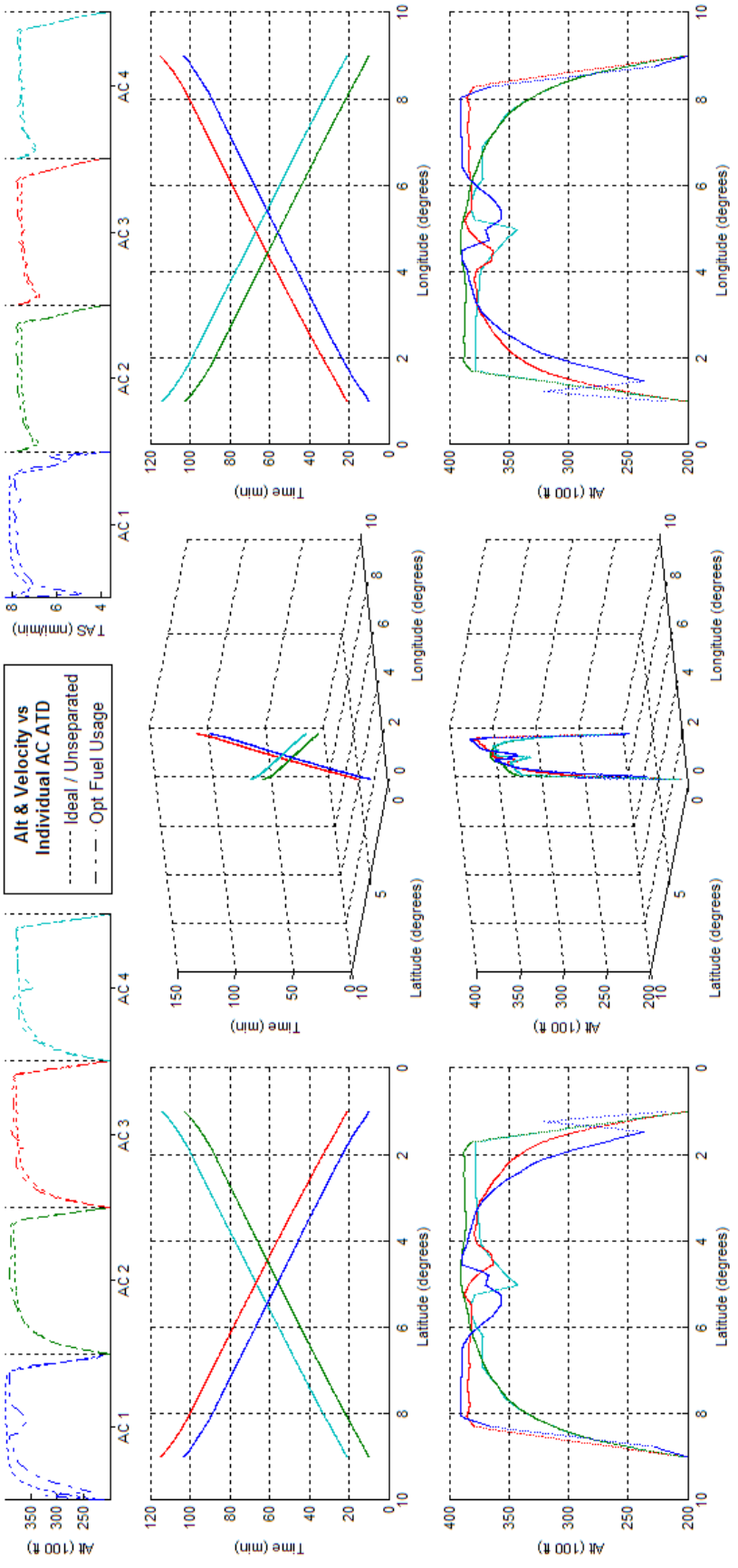

Figure 245 - Fuel Optimized 4acPH2H ATD_N Results

K.10 BADA Boeing 737-300 - Scenario 2acPSd - ATD_N

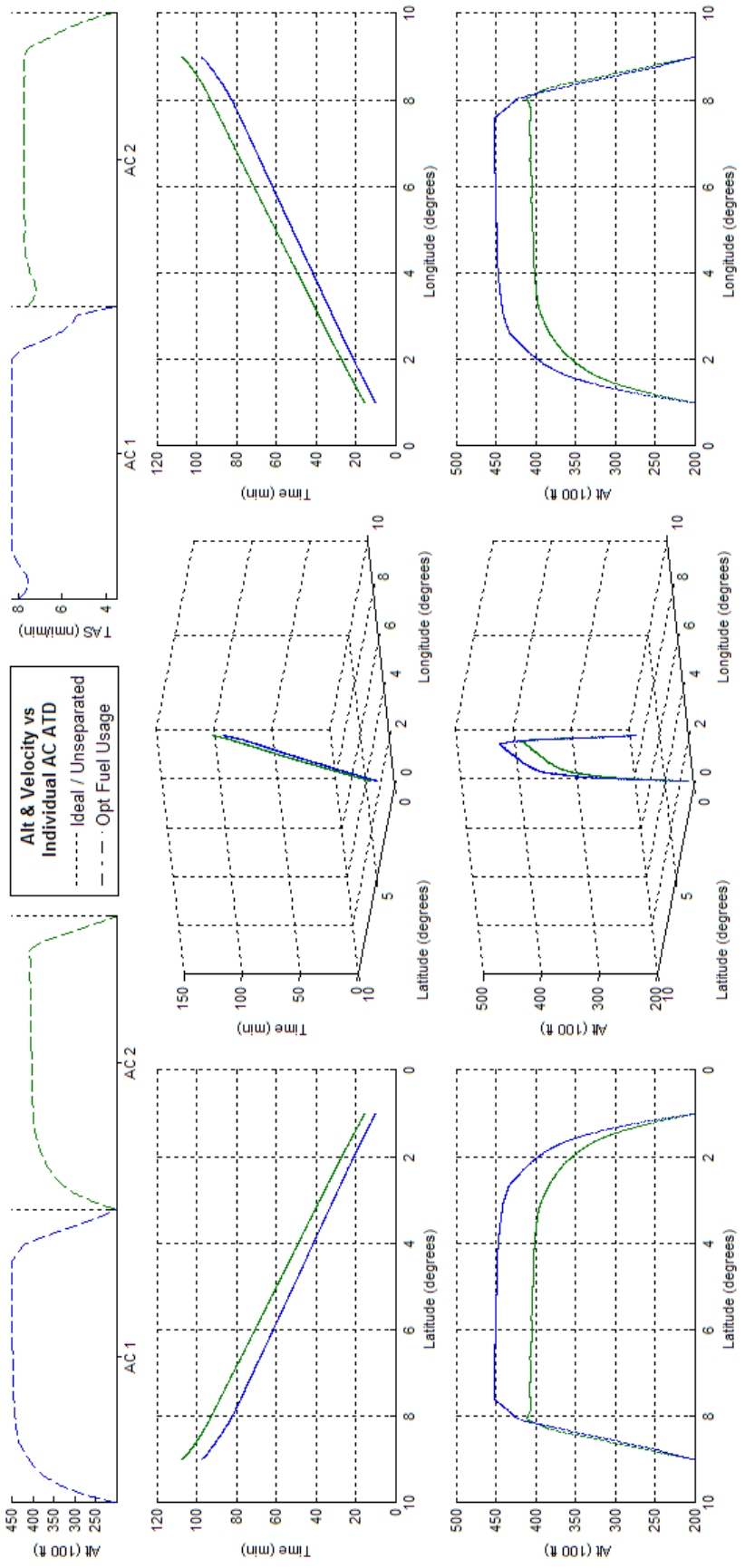

Figure 246 - Fuel Optimized 2acPSd ATD_N Results

K.11 BADA Boeing 737-300 - Scenario 4acPSd - ATD_N

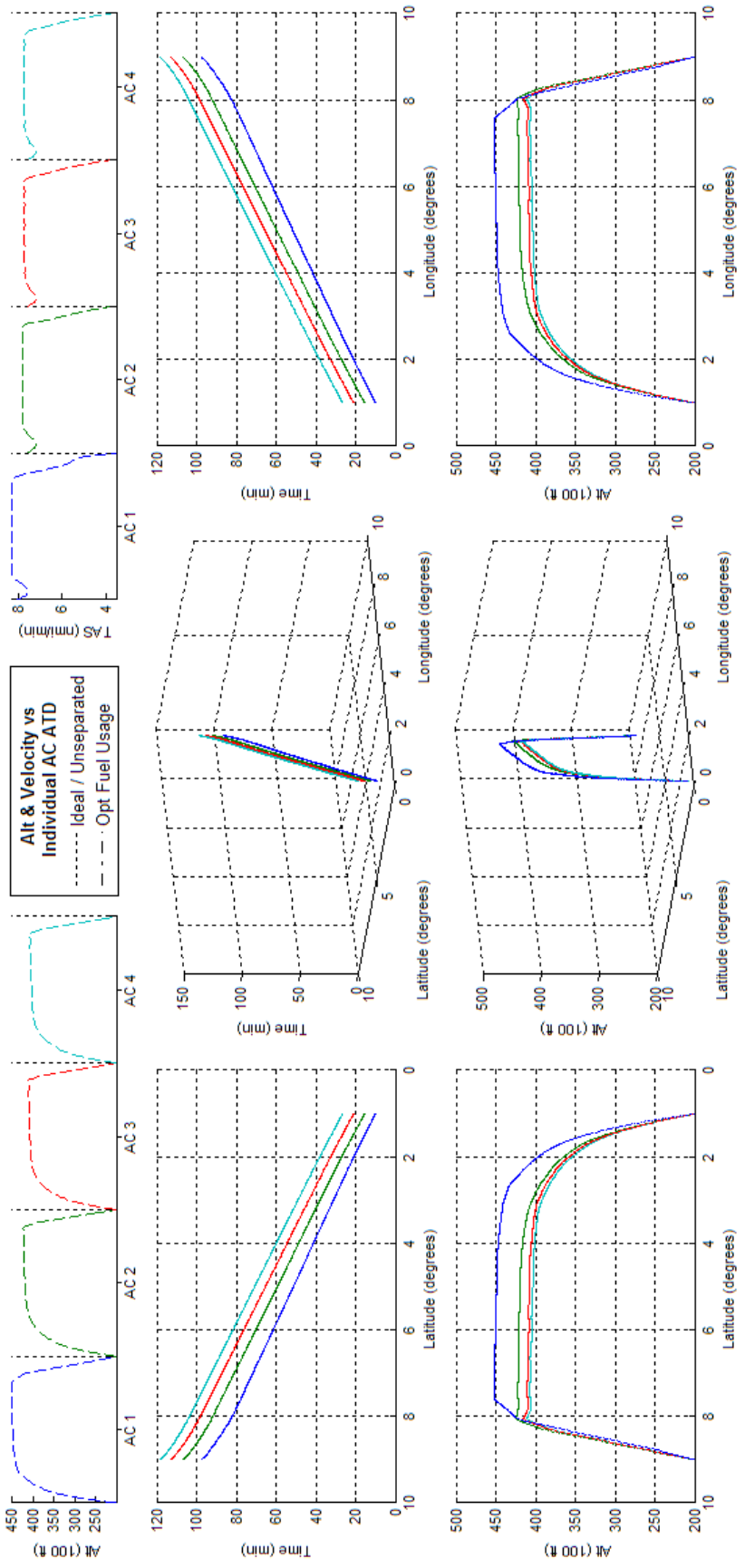

Figure 247 - Fuel Optimized 4acPSd ATD_N Results

K.12 BADA Boeing 737-300 - Scenario 2acCO - ATD_N

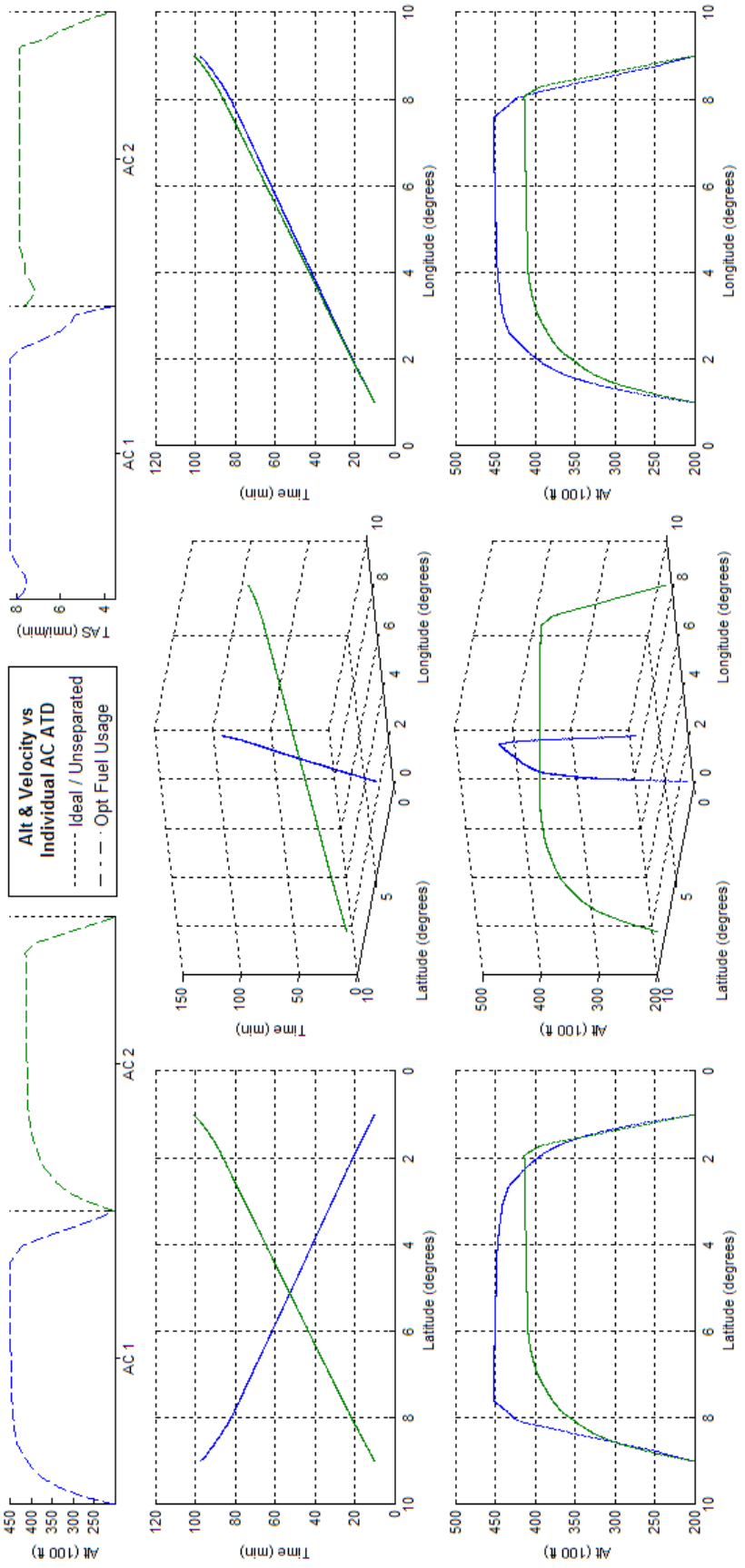

Figure 248 - Fuel Optimized 2acCO ATD_N Results

K.13 BADA Boeing 737-300 - Scenario 4acCO - ATD_N

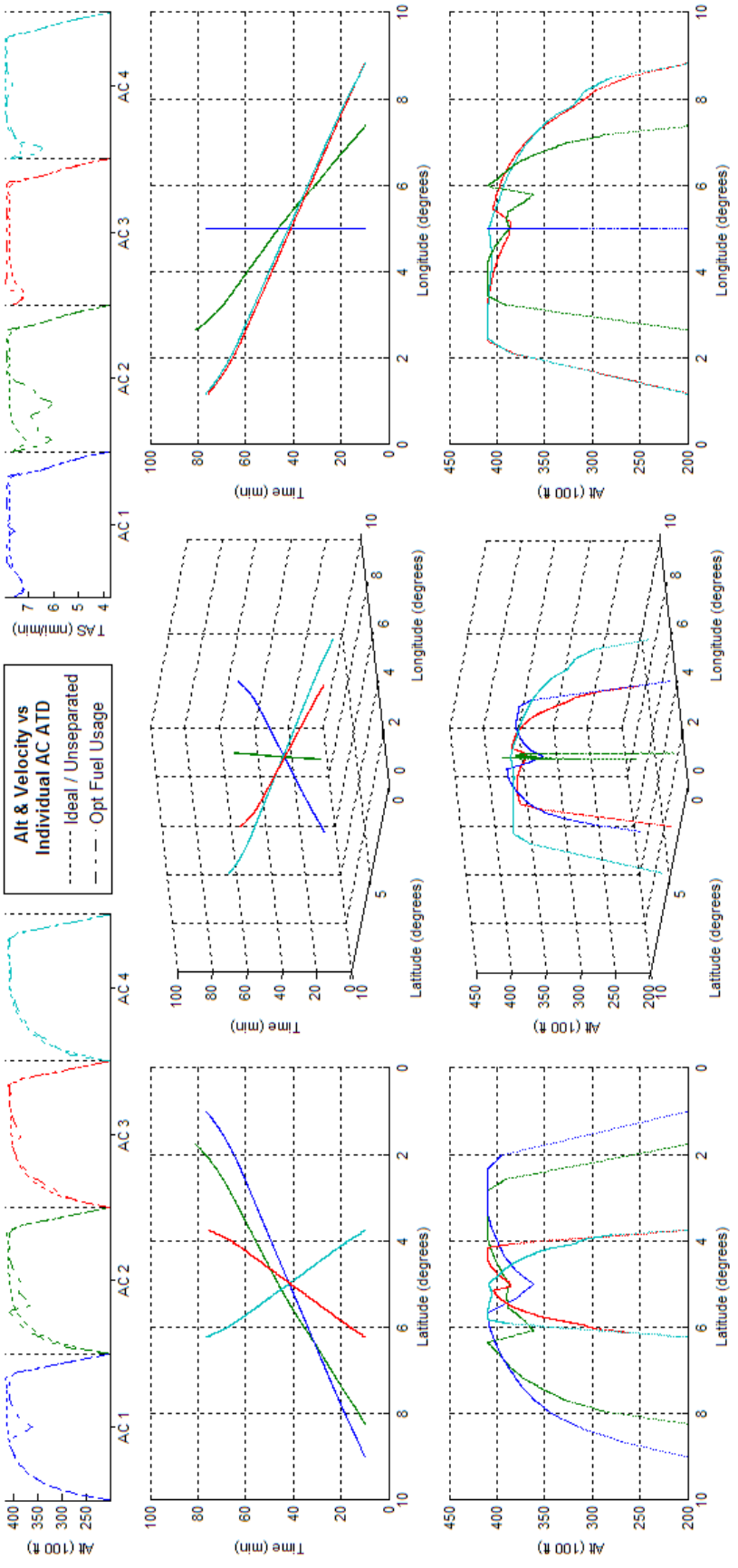

Figure 249 - Fuel Optimized 4acCO ATD_N Results

K.14 BADA Boeing 737-300 - Scenario 10acCO - ATD_N

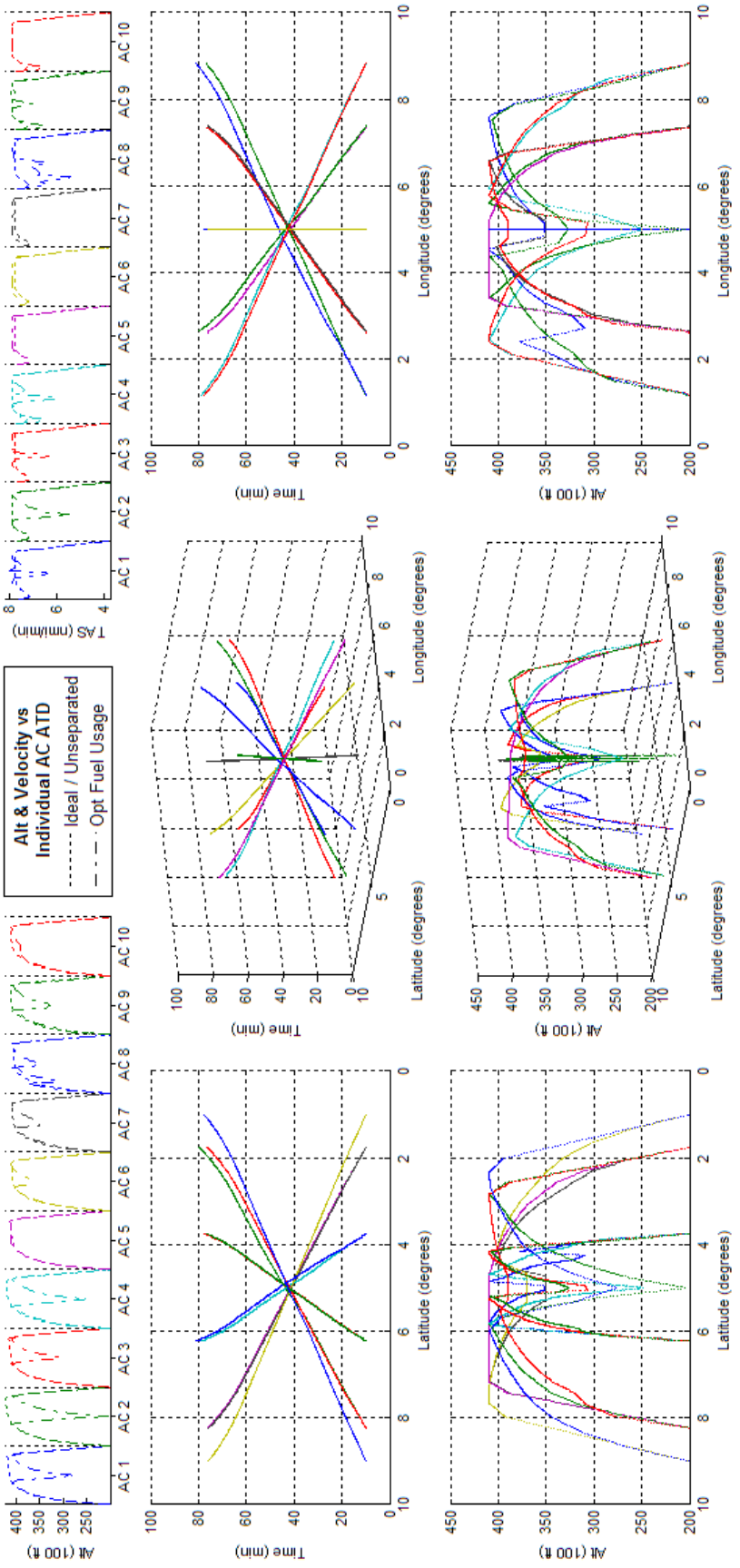

Figure 250 - Fuel Optimized 10acCO ATD_N Results

K.15 BADA Boeing 737-300 - Scenario 4acCH - ATD_N

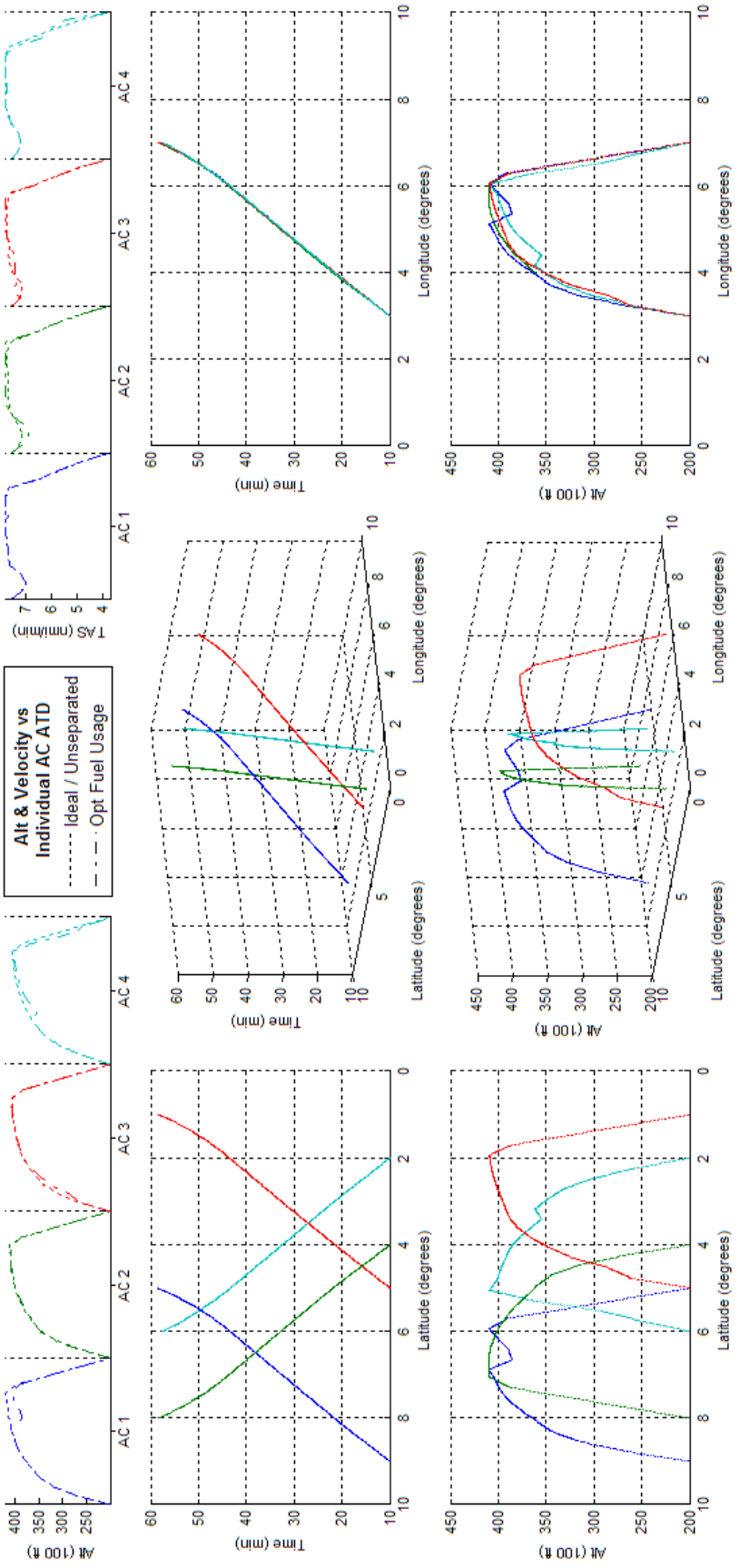

Figure 251 - Fuel Optimized 4acCH ATD_N Results

K.16 BADA Boeing 737-300 - Scenario 10acCH - ATD_N

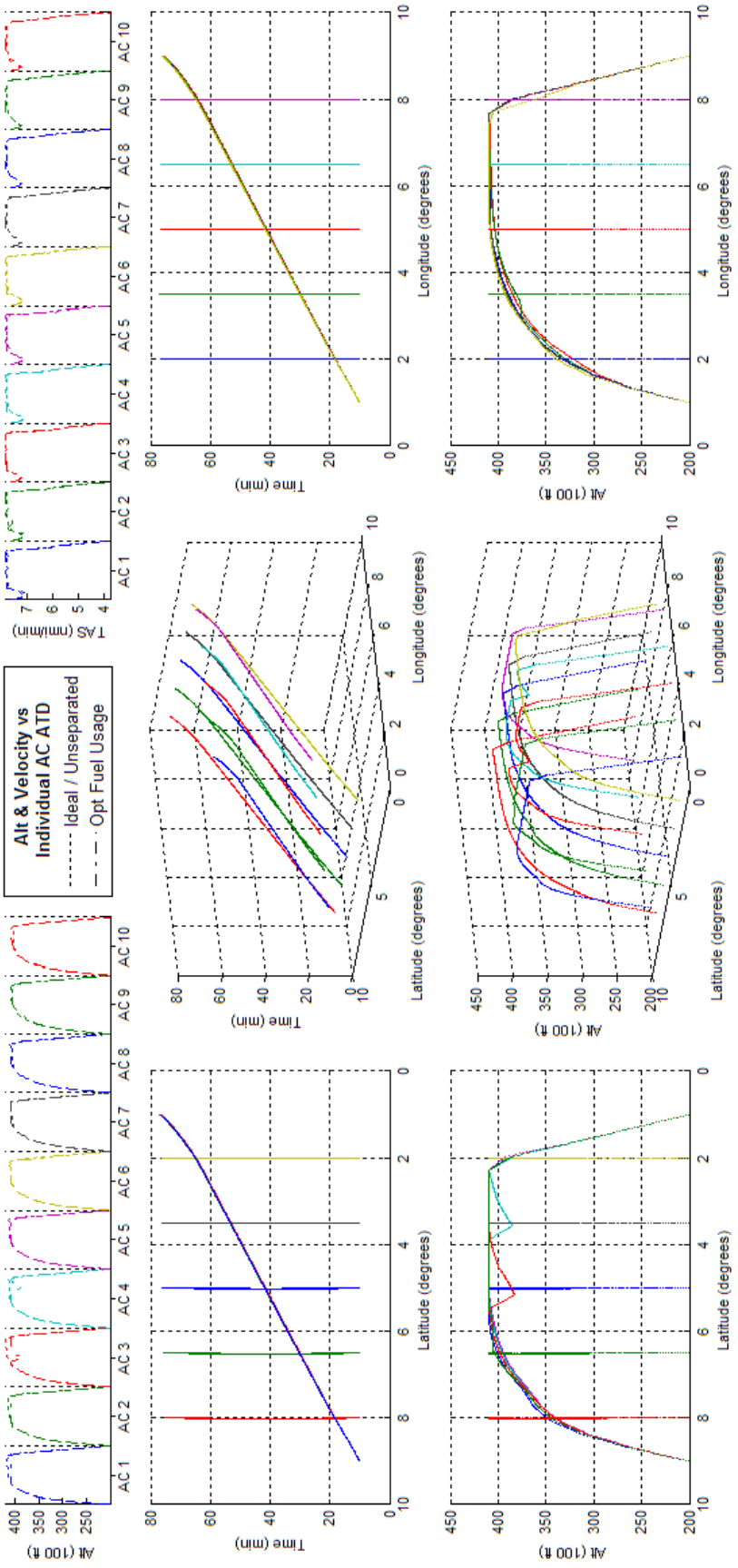

Figure 252 - Fuel Optimized 10acCH ATD_N Results

K.17 BADA Boeing 737-300 - Scenario 2acPH2H - ATD_N

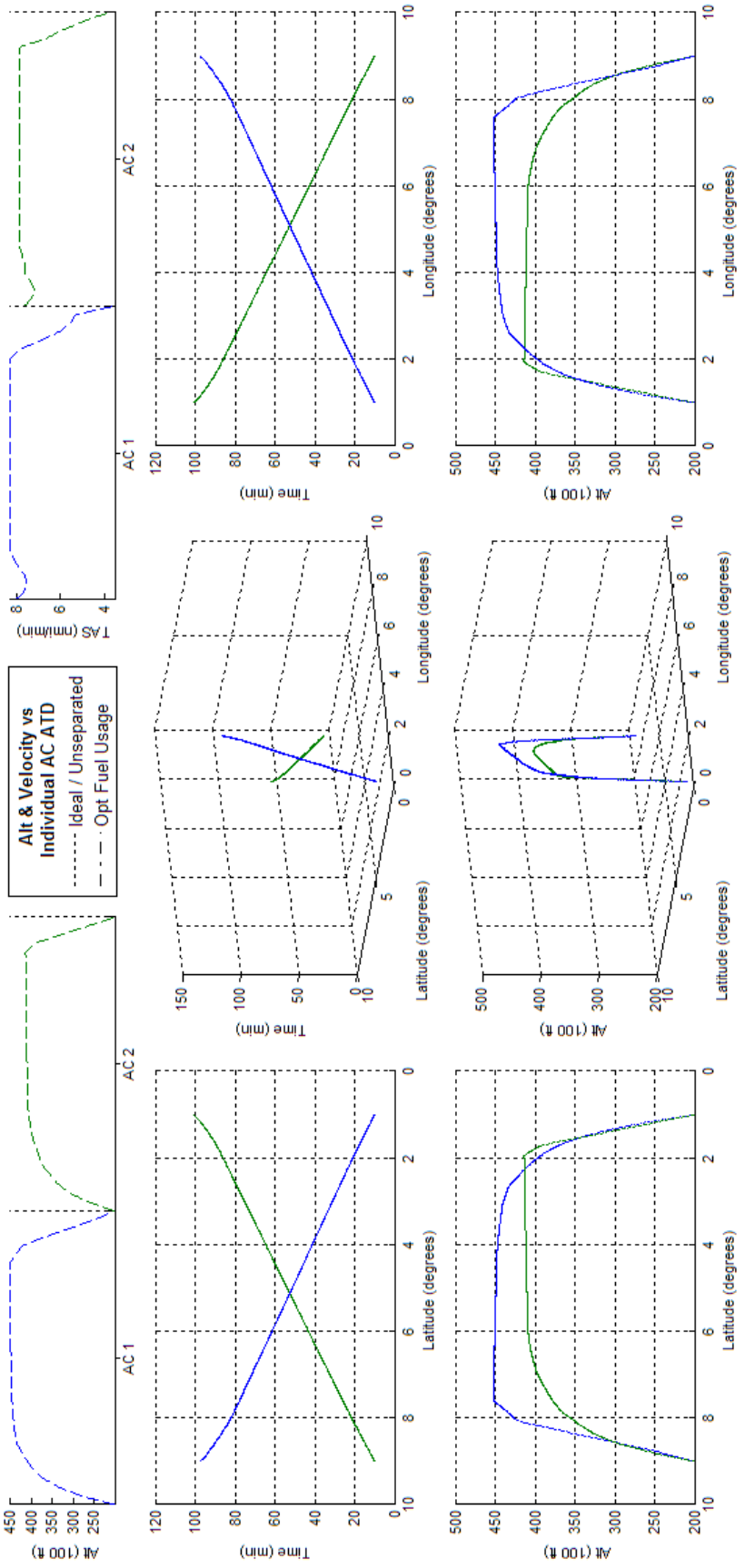

Figure 253 - Fuel Optimized 2acPH2H ATD_N Results

K.18 BADA Boeing 737-300 - Scenario 4acPH2H - ATD_N

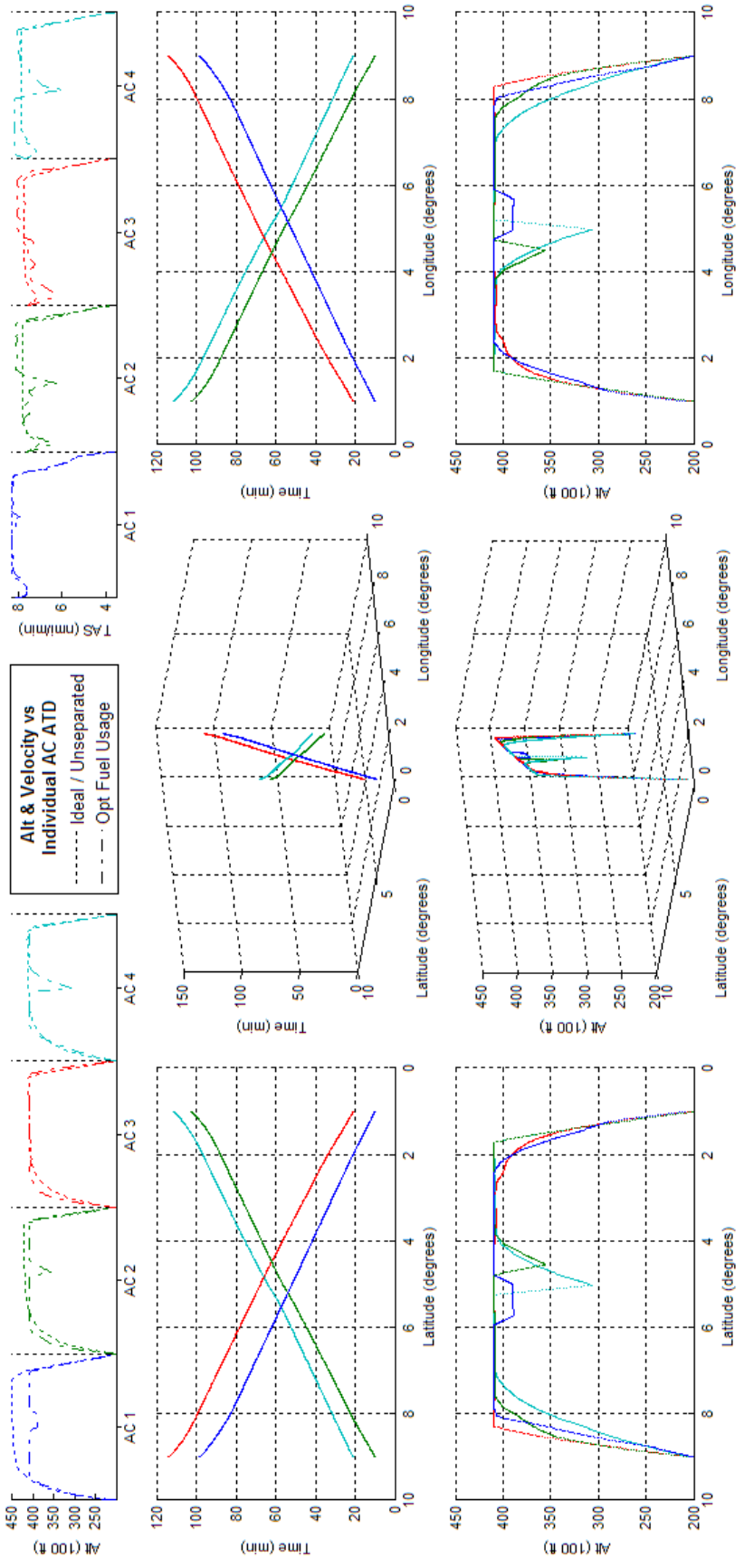

Figure 254 - Fuel Optimized 4acPH2H ATD_N Results

K.19 BADA Airbus A320 & Boeing 737-300 - Scenario 2acPSd - ATD_N

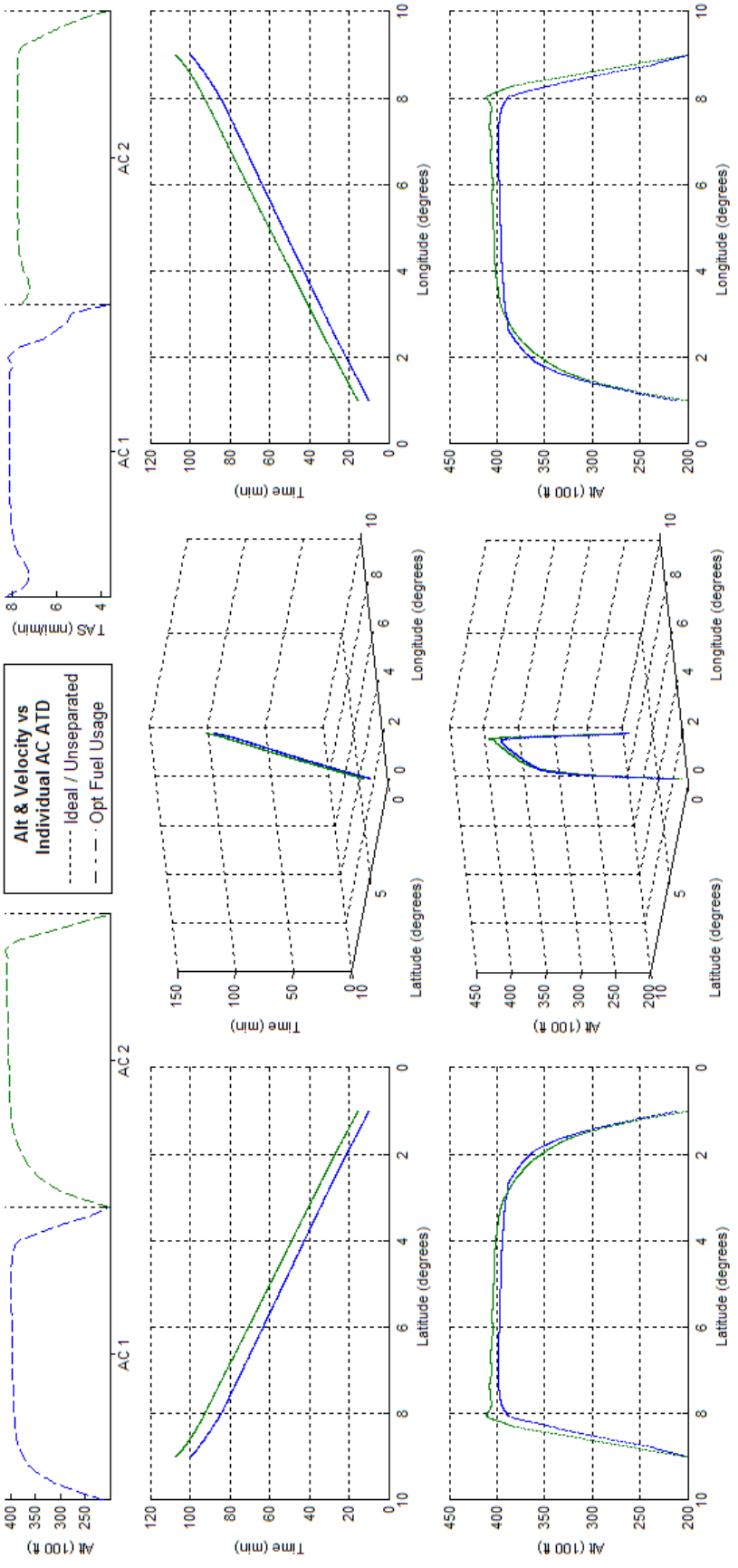

Figure 255 - Fuel Optimized 2acPSd ATD_N Results

K.20 BADA Airbus A320 & Boeing 737-300 - Scenario 4acPSd - ATD_N

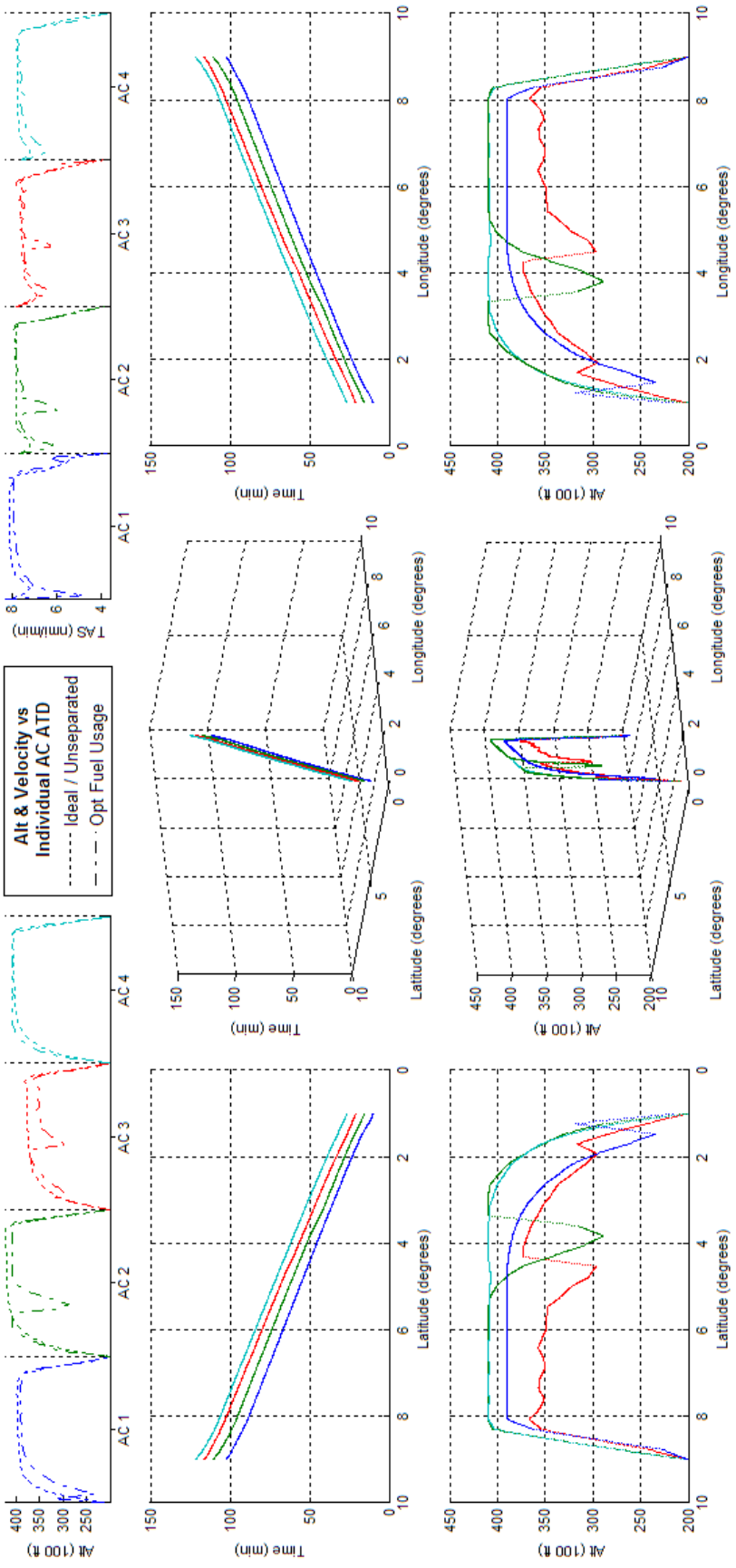

Figure 256 - Fuel Optimized 4acPSd ATD_N Results

K.21 BADA Airbus A320 & Boeing 737-300 - Scenario 2acCO - ATD_N

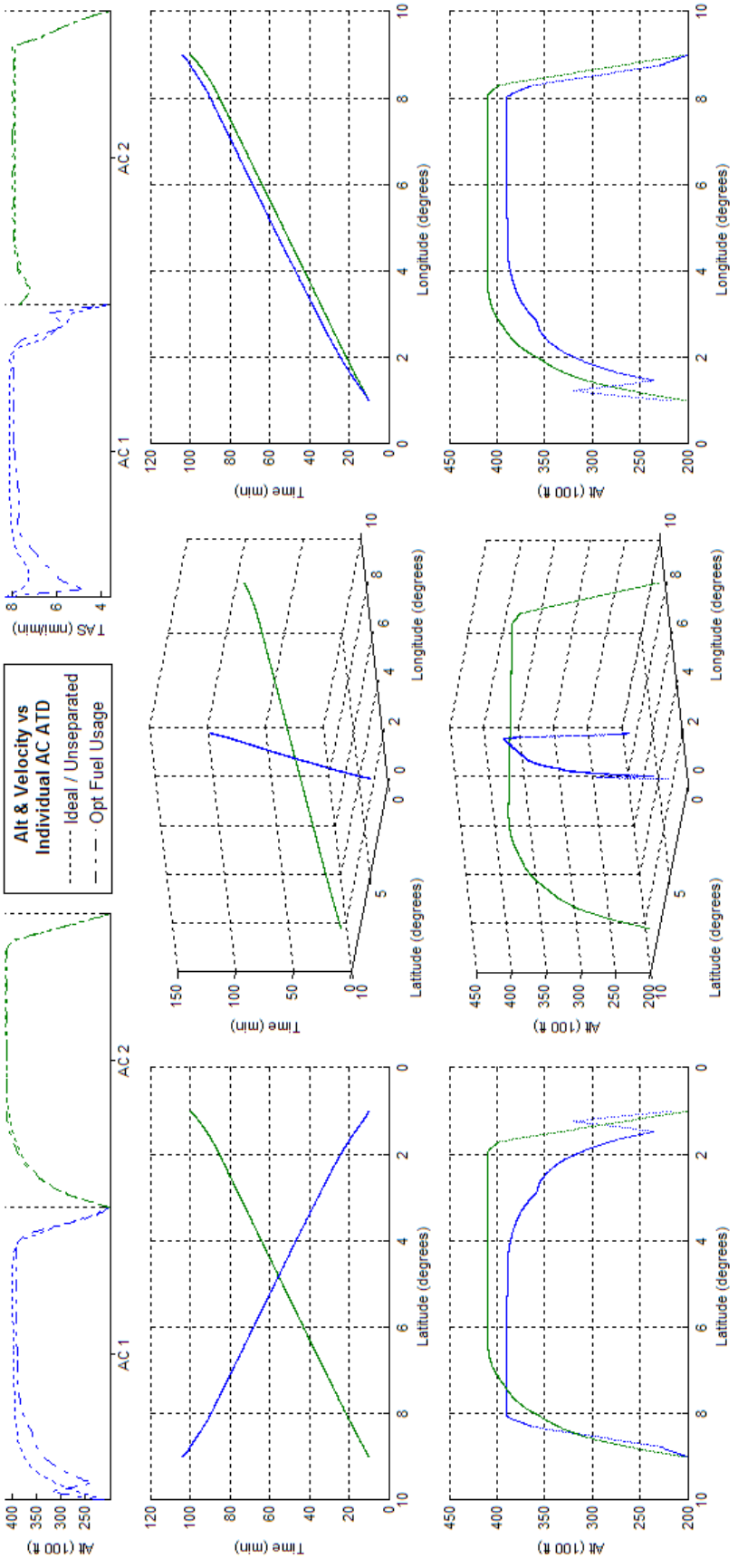

Figure 257 - Fuel Optimized 2acCO ATD_N Results

K.22 BADA Airbus A320 & Boeing 737-300 - Scenario 4acCO - ATD_N

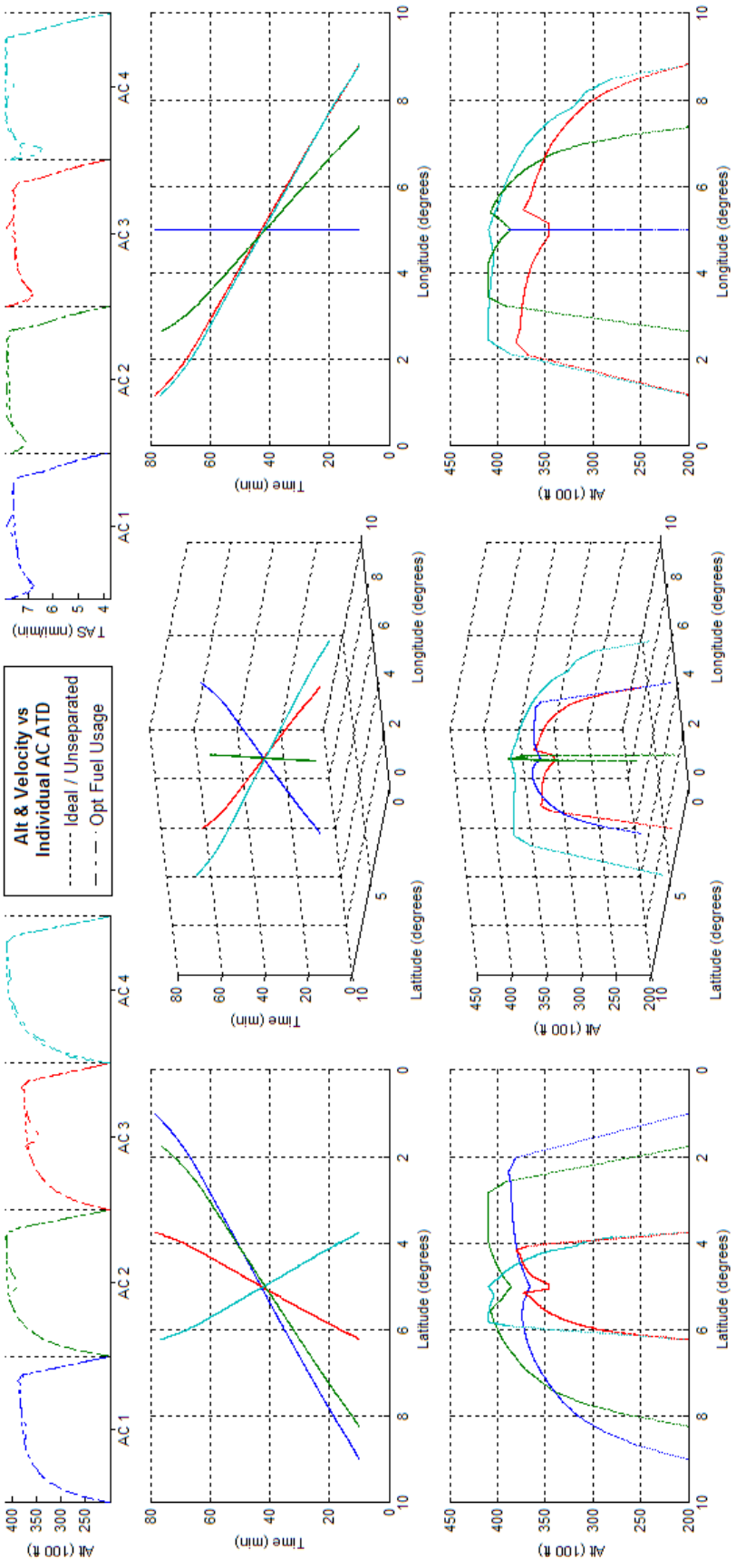

Figure 258 - Fuel Optimized 4acCO ATD_N Results

K.23 BADA Airbus A320 & Boeing 737-300 - Scenario 10acCO - ATD_N

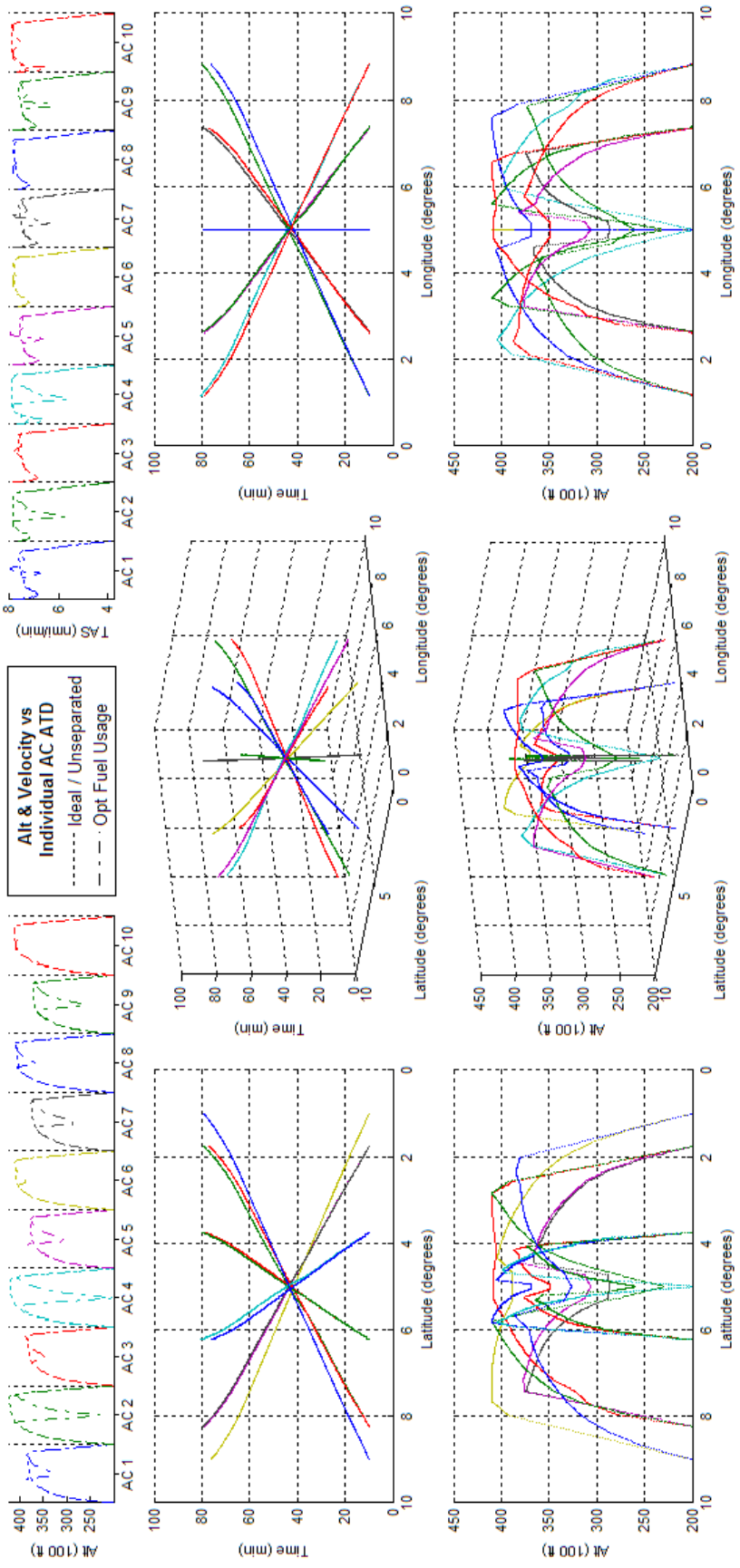

Figure 259 - Fuel Optimized 10acCO ATD_N Results

K.24 BADA Airbus A320 & Boeing 737-300 - Scenario 4acCH - ATD_N

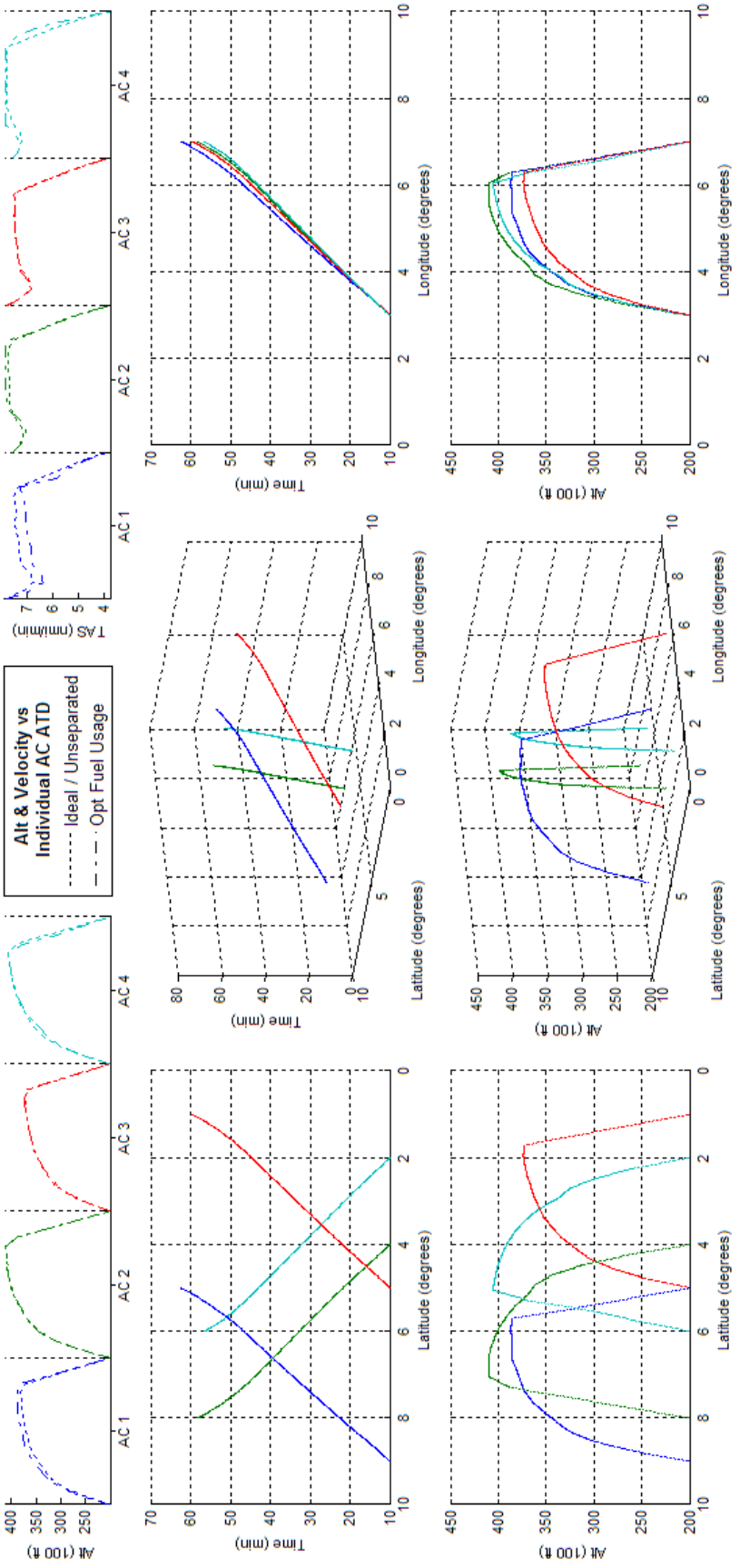

Figure 260 - Fuel Optimized 4acCH ATD_N Results

K.25 BADA Airbus A320 & Boeing 737-300 - Scenario 10acCH - ATD_N

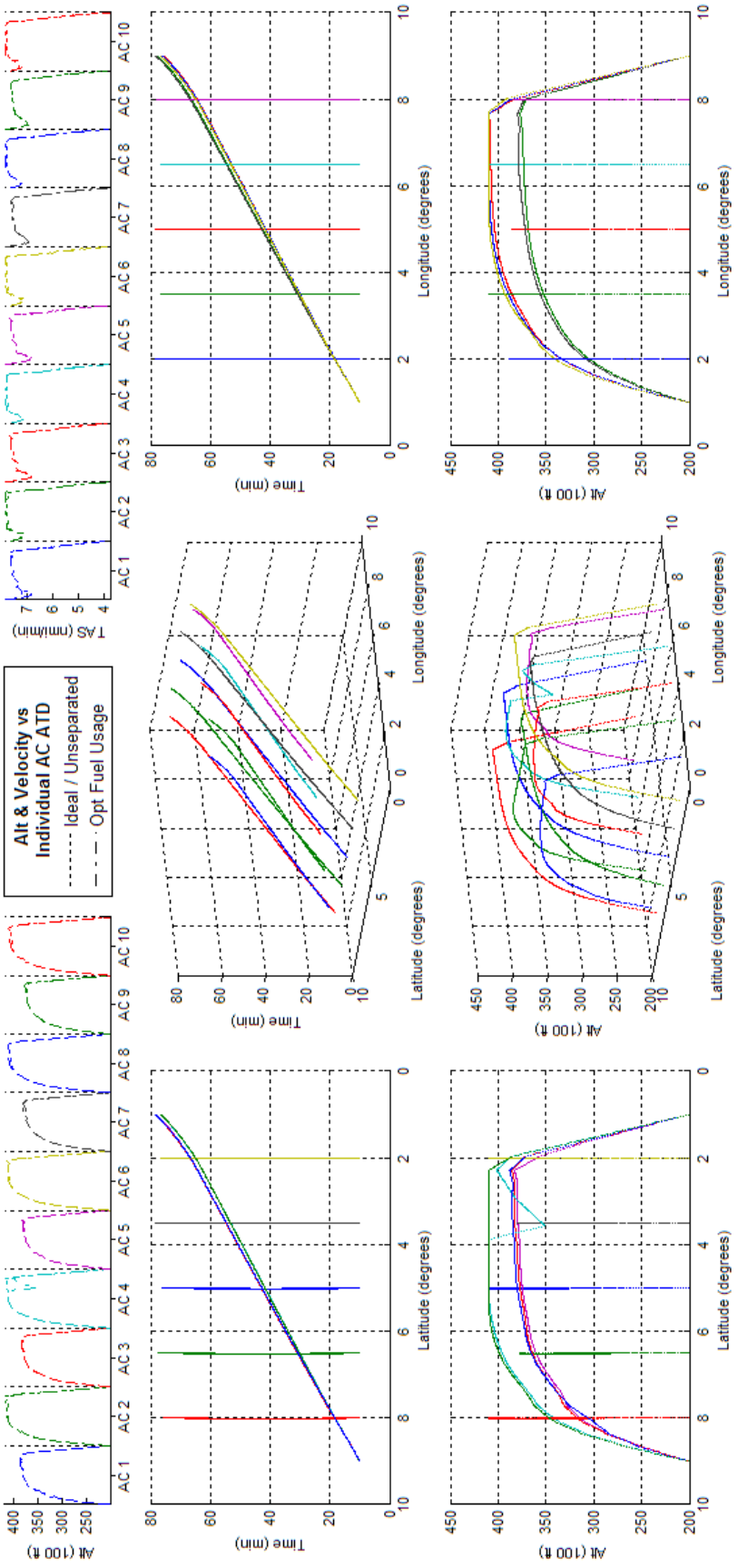

Figure 261 - Fuel Optimized 10acCH ATD_N Results

K.26 BADA Airbus A320 & Boeing 737-300 - Scenario 2acPH2H - ATD_N

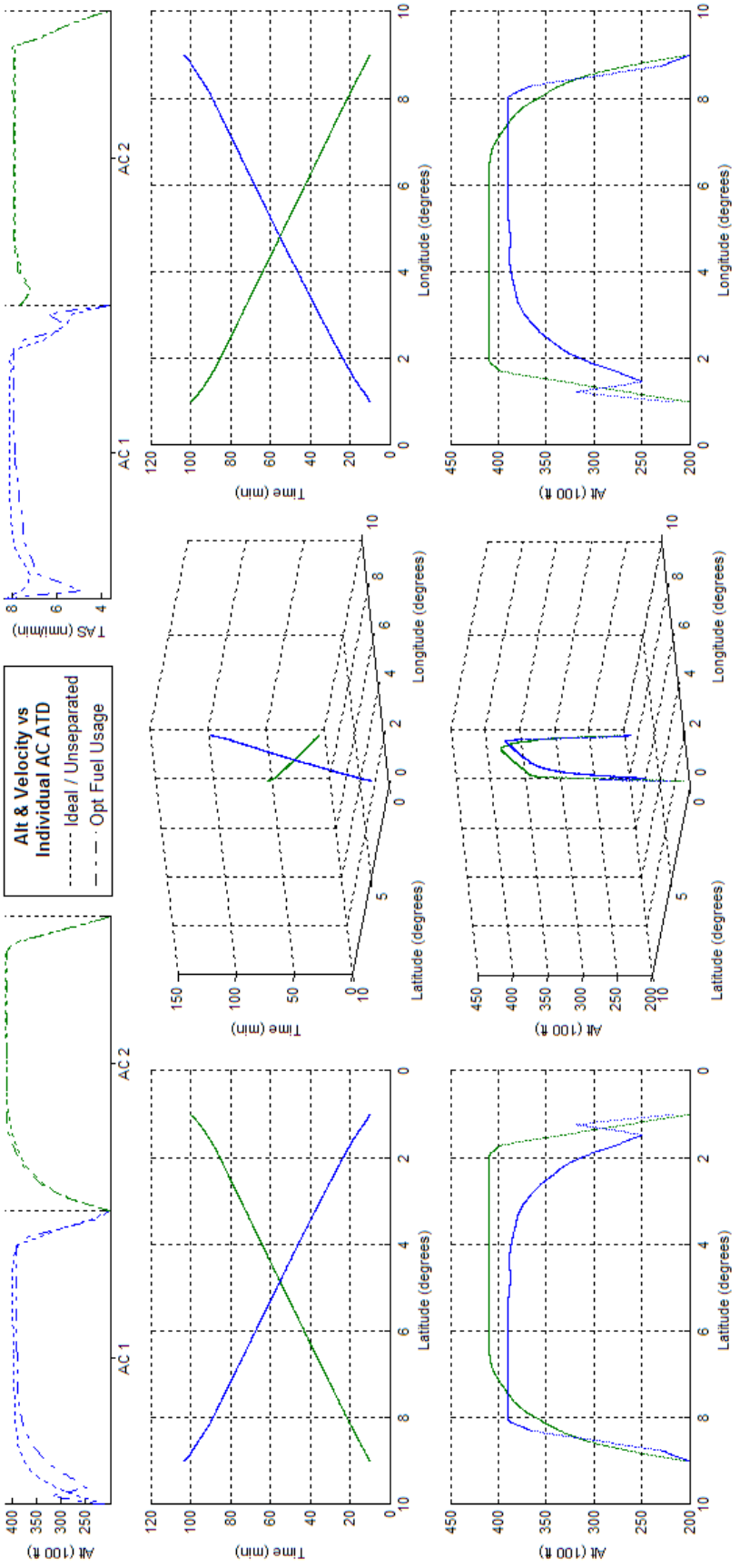

Figure 262 - Fuel Optimized 2acPH2H ATD_N Results

K.27 BADA Airbus A320 & Boeing 737-300 - Scenario 4acPH2H - ATD_N

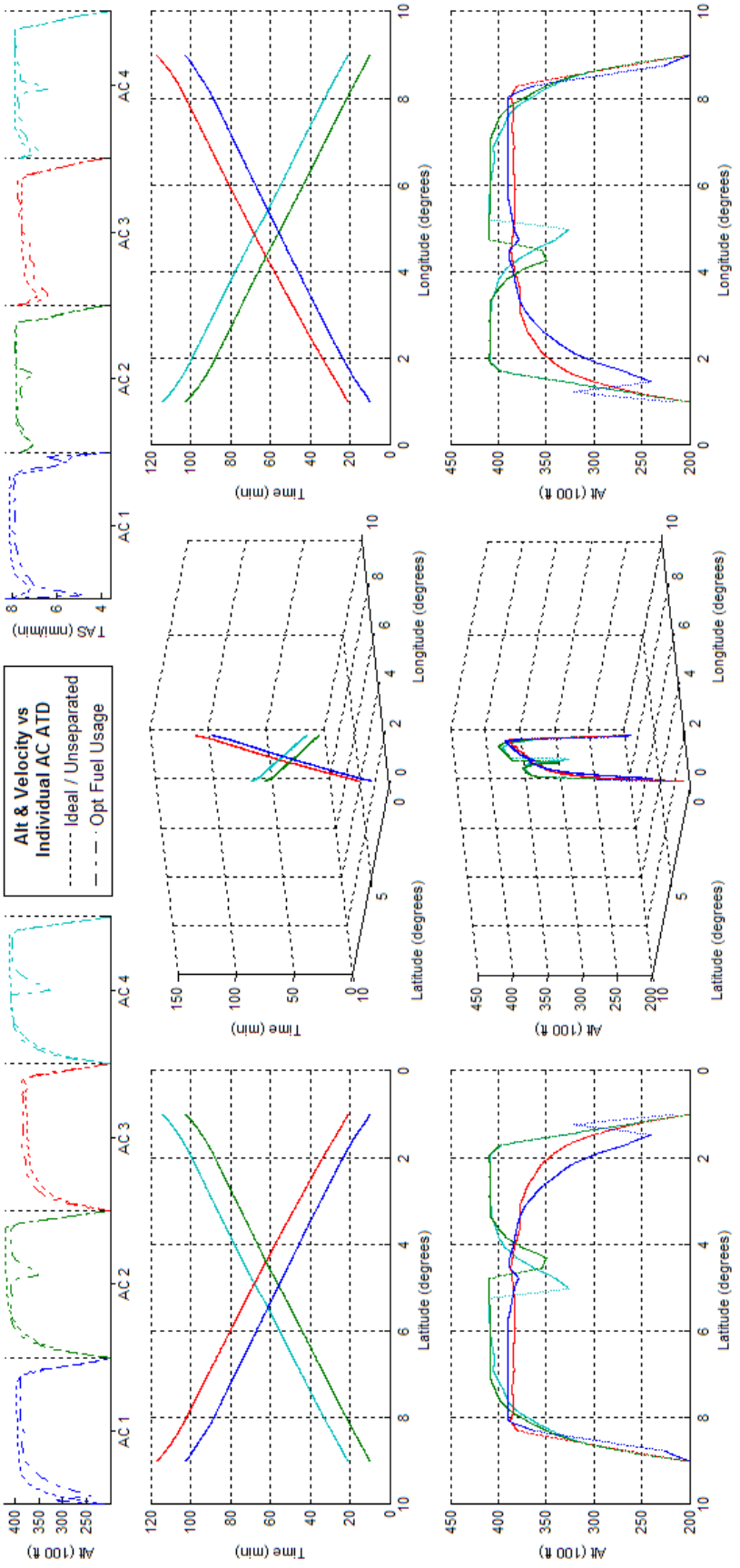

Figure 263 - Fuel Optimized 4acPH2H ATD_N Results

APPENDIX L Customized control node Results

The following graphs show the results for the optimization for the customized control node lists, as mentioned in Chapter 6 of the thesis. For discussion of the results and impacts of these results, please refer to section 6.1.1. For instructions on how to read the graphs, please refer to section 3.4.1 for the basic explanation of the graphs, then section 6.1 for the changes caused by having customized control nodes. Each section in this appendix shows three graphs:

- The first graph shows optimization results of the scenario assuming ATFU minimization and no ETA constraint.
- The second graph is the same as the first, but shows the impact of having an ETA constraint.
- The third graph compares the trajectory shape, fuel usage and flight time of each aircraft between the unconstrained and constrained ETA results.

It should be mentioned that since three customized control node lists were developed, each scenario defined in Appendix E was optimized using each customized control node list, then presented in this appendix and ordered according to scenario. Again to recap, the three customized control node lists were defined as ATD_{R1}, ATD_{R2}, and ATD_{R3}. ATD_{R1} kept the middle portion at a constant climb angle, ATD_{R2} kept the middle portion at a constant altitude, and ATD_{R3} did the same as ATD_{R2}, but allowed nonlinear velocity variation during the middle portion of the trajectory. More information on this can be found in section 6.1 of the thesis.

L.1 BADA Boeing 747-300 - Scenario 2acPSd - ATD_{R1}

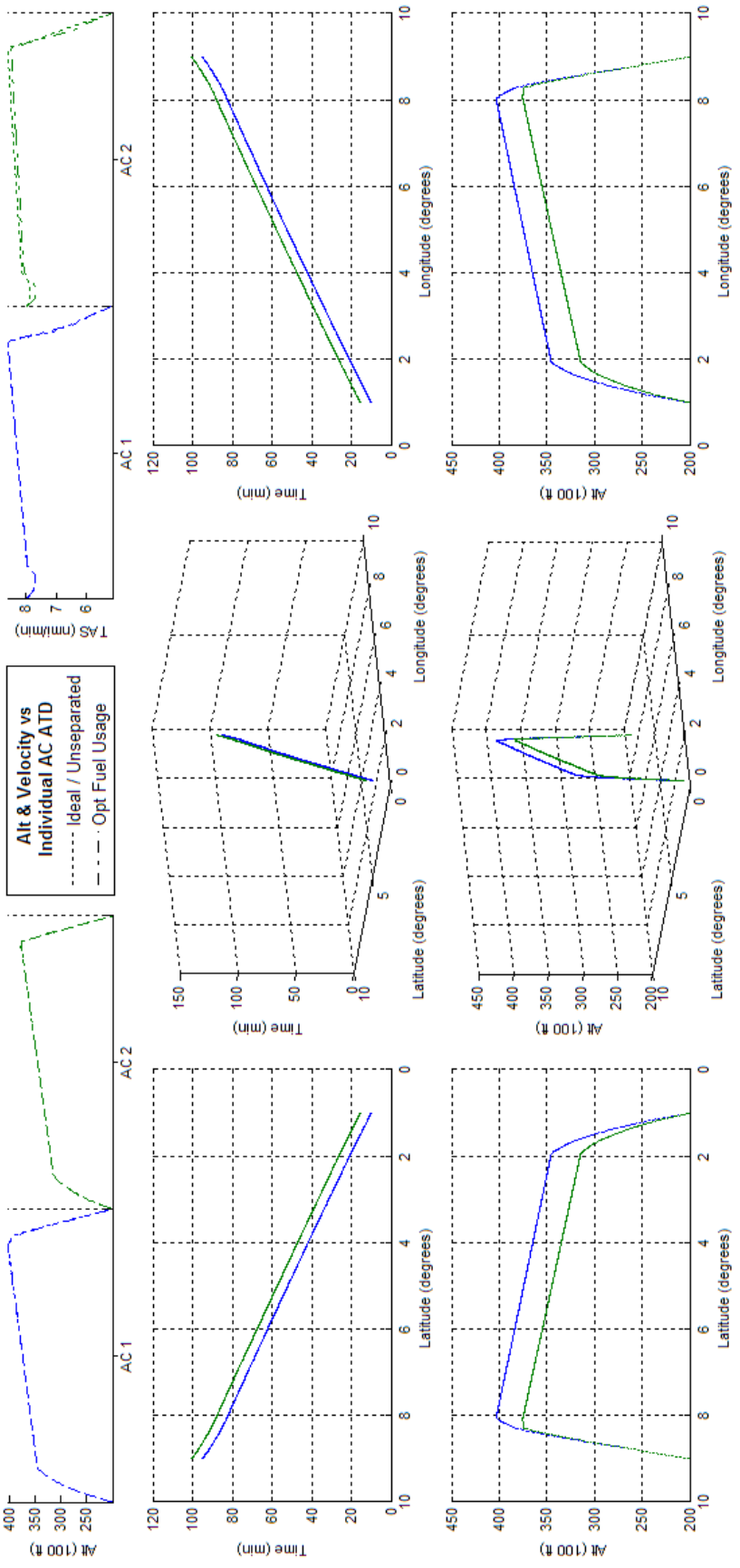

Figure 264 - Fuel Optimized 2acPSd ATD_{R1} Results

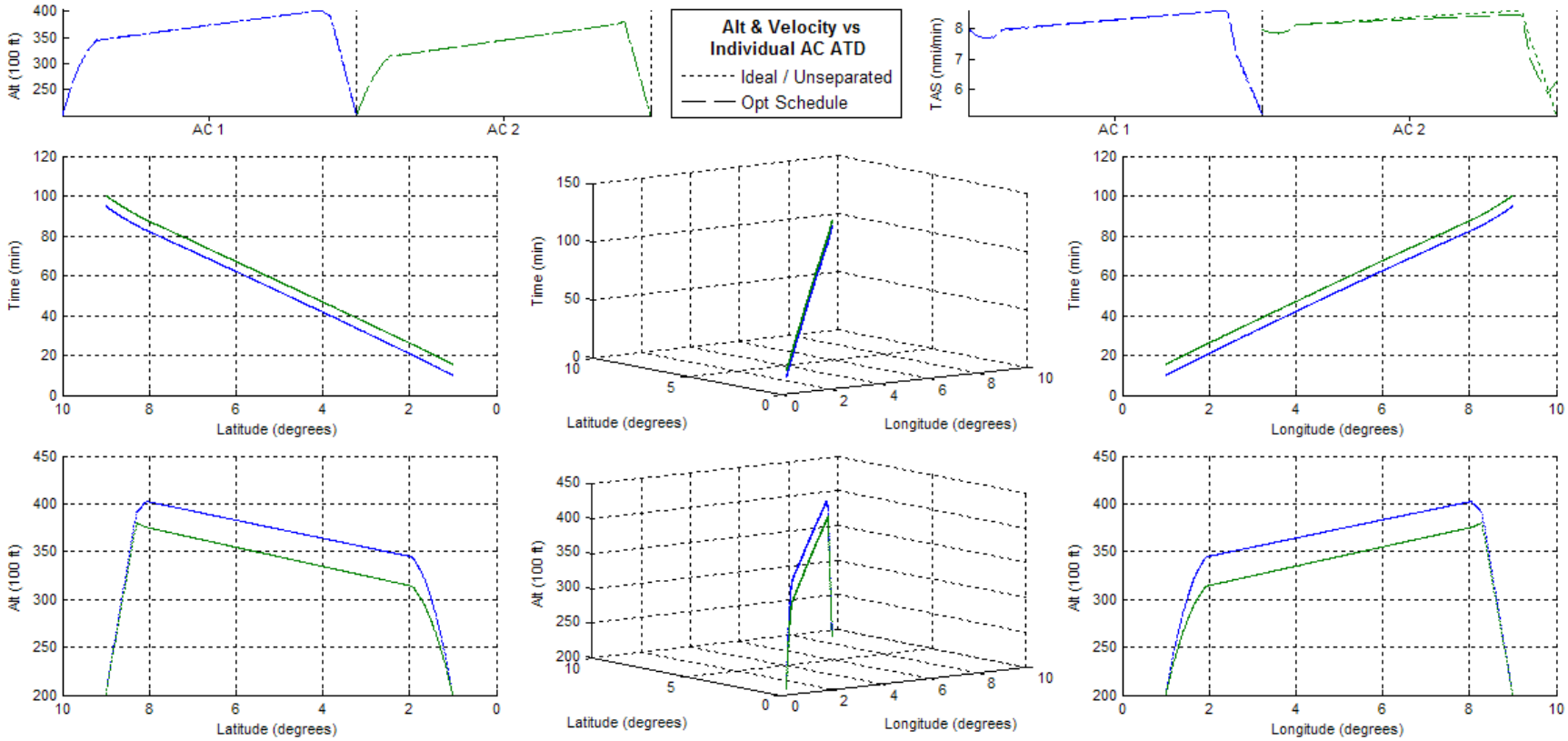

Figure 265 -Schedule Optimized 2acPSd ATD_{R1} Results

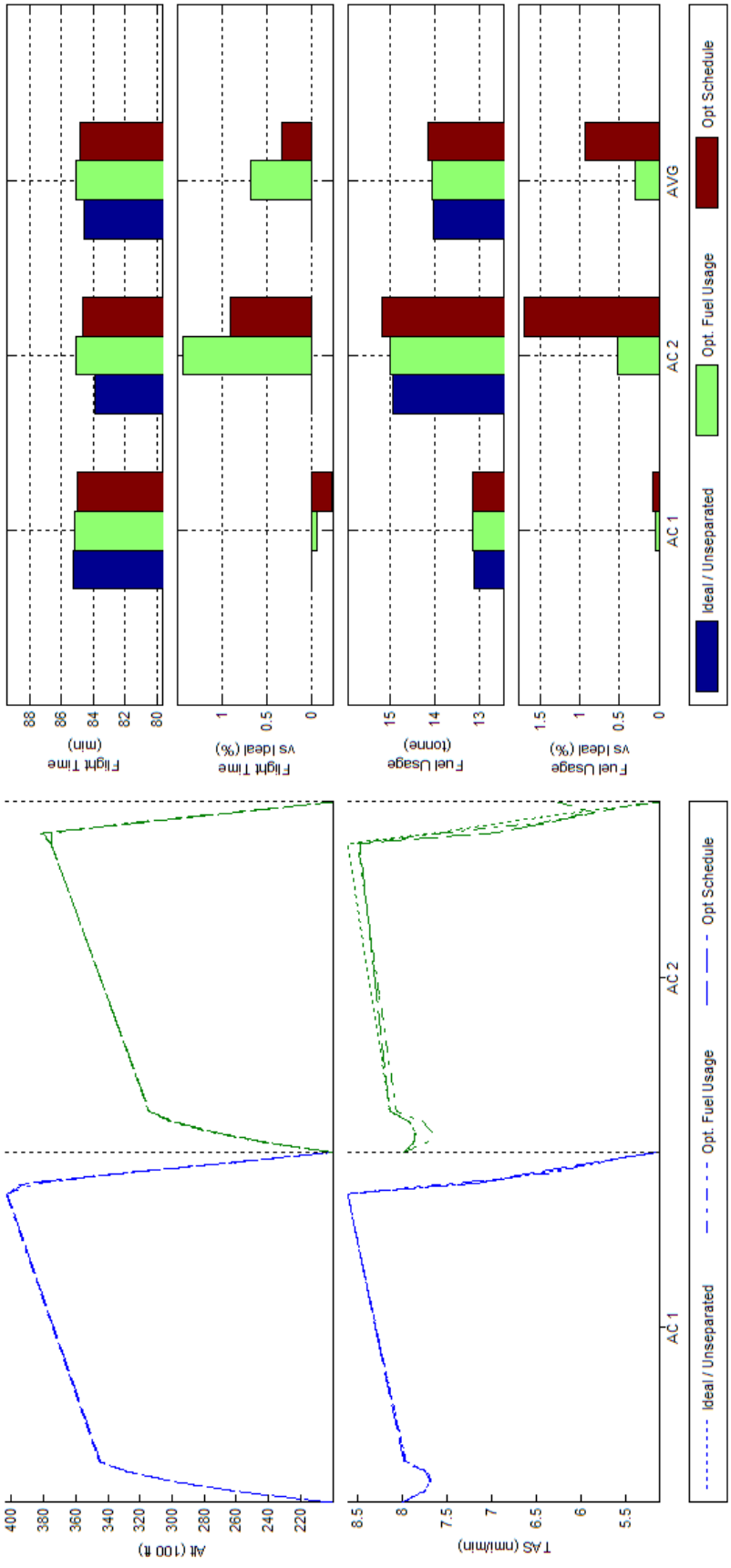

Figure 266 Trajectory Shape, Flight Time, and Fuel Consumption Comparisons of Fuel and Schedule Optimized 2acPSd ATD_{R1} Results

L.2 BADA Boeing 747-300 - Scenario 2acPSd - ATD_{R2}

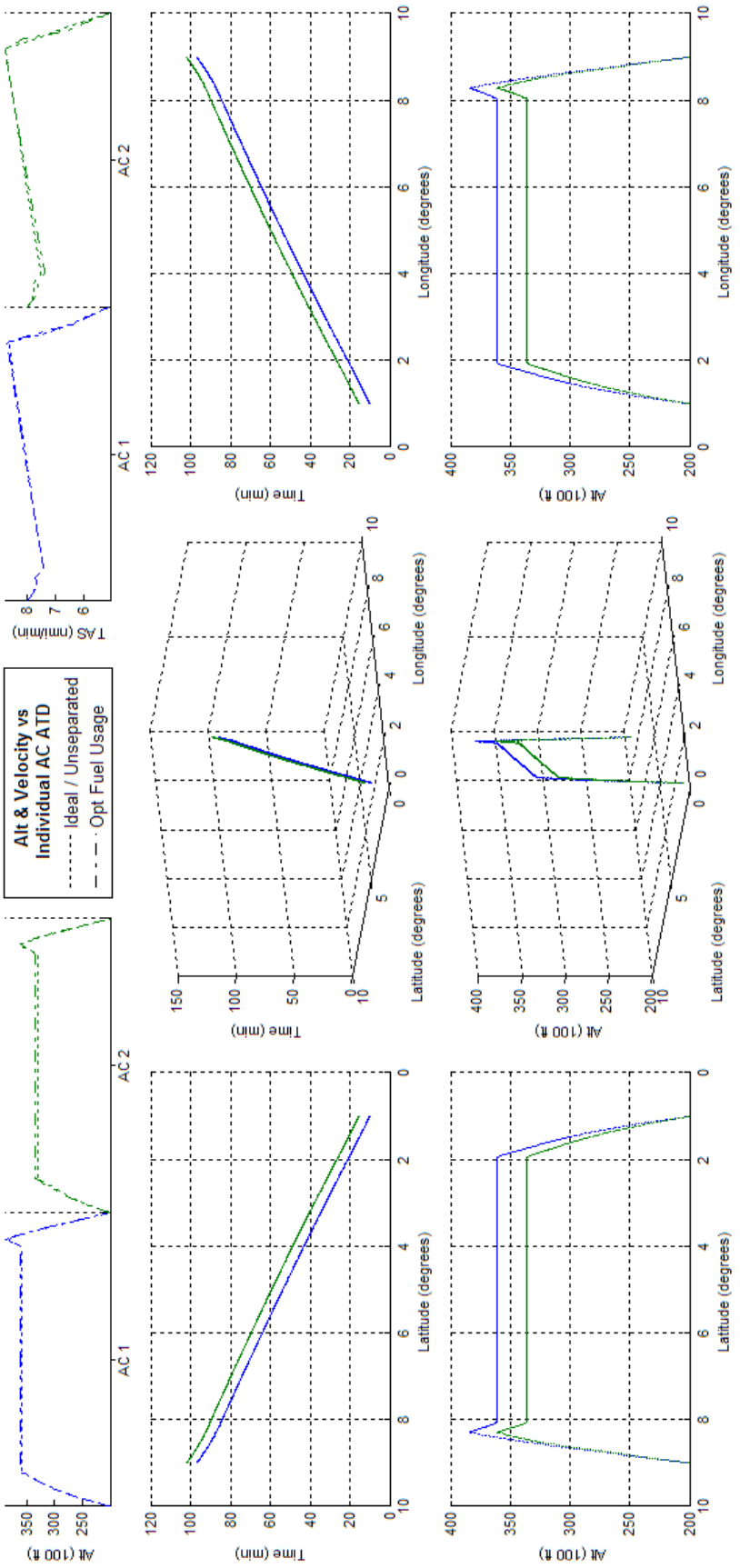

Figure 267 - Fuel Optimized 2acPSd ATD_{R2} Results

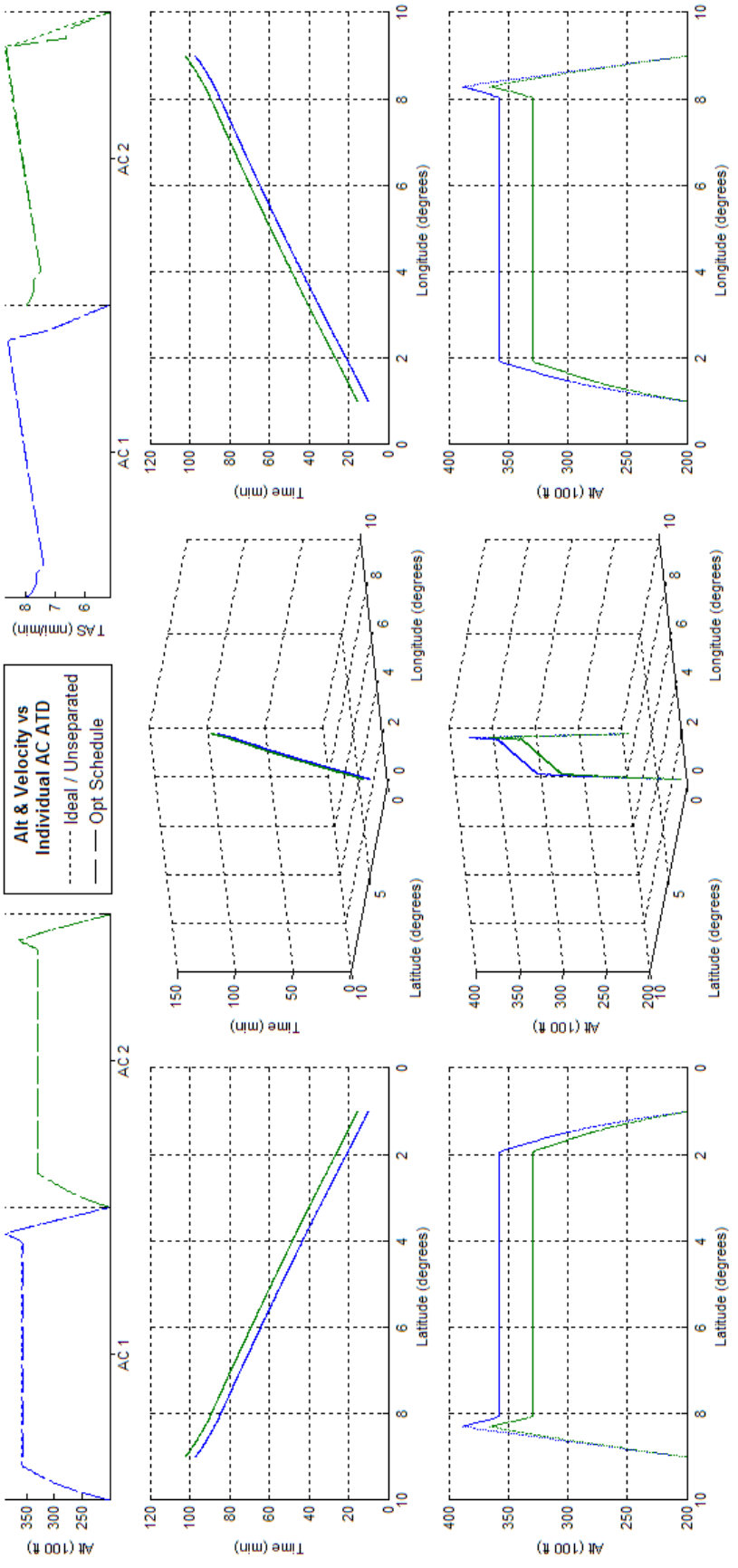

Figure 268 -Schedule Optimized 2acPSd ATD_{R2} Results

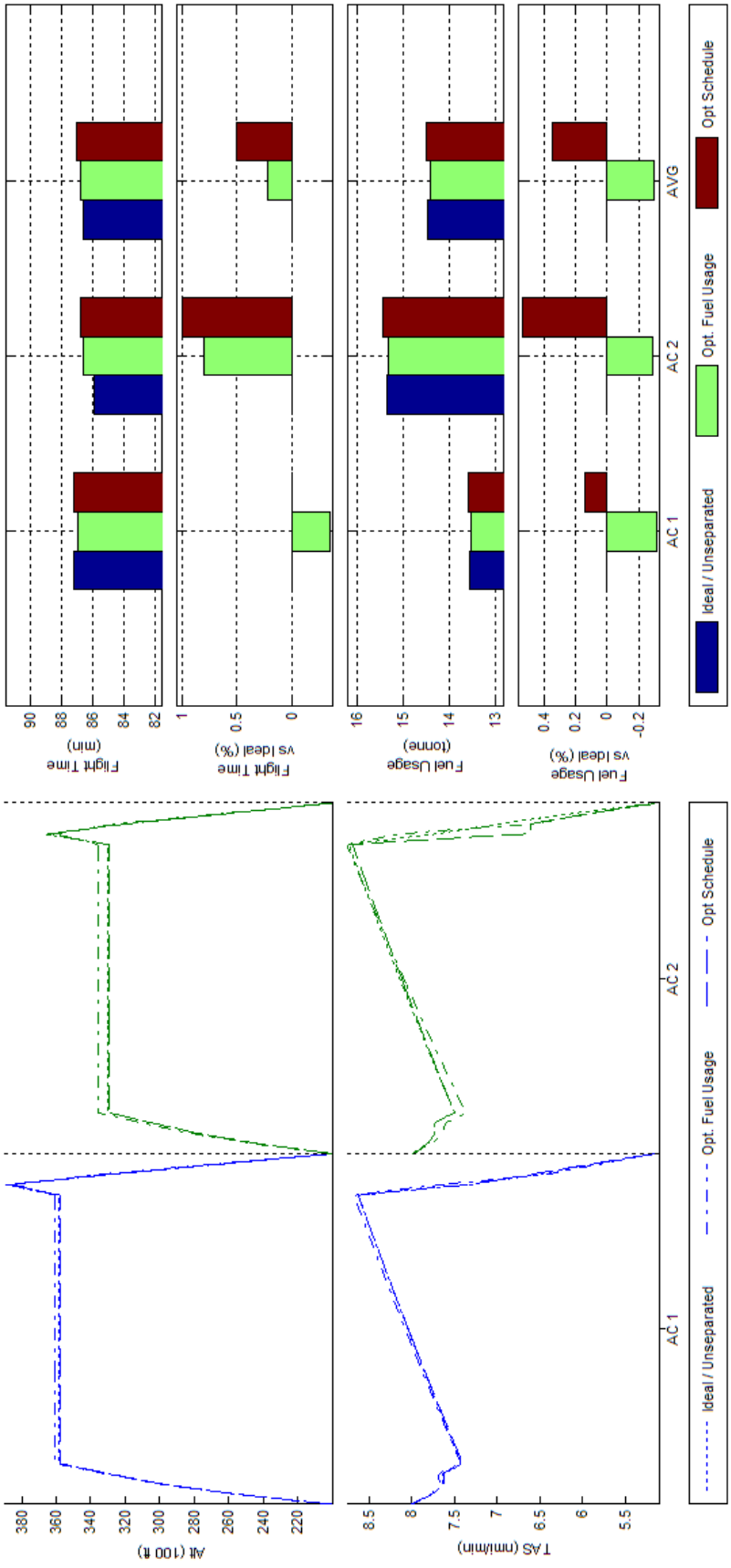

Figure 269 Trajectory Shape, Flight Time, and Fuel Consumption Comparisons of Fuel and Schedule Optimized 2acPSd ATD_{R2} Results

L.3 BADA Boeing 747-300 - Scenario 2acPSd - ATD_{R3}

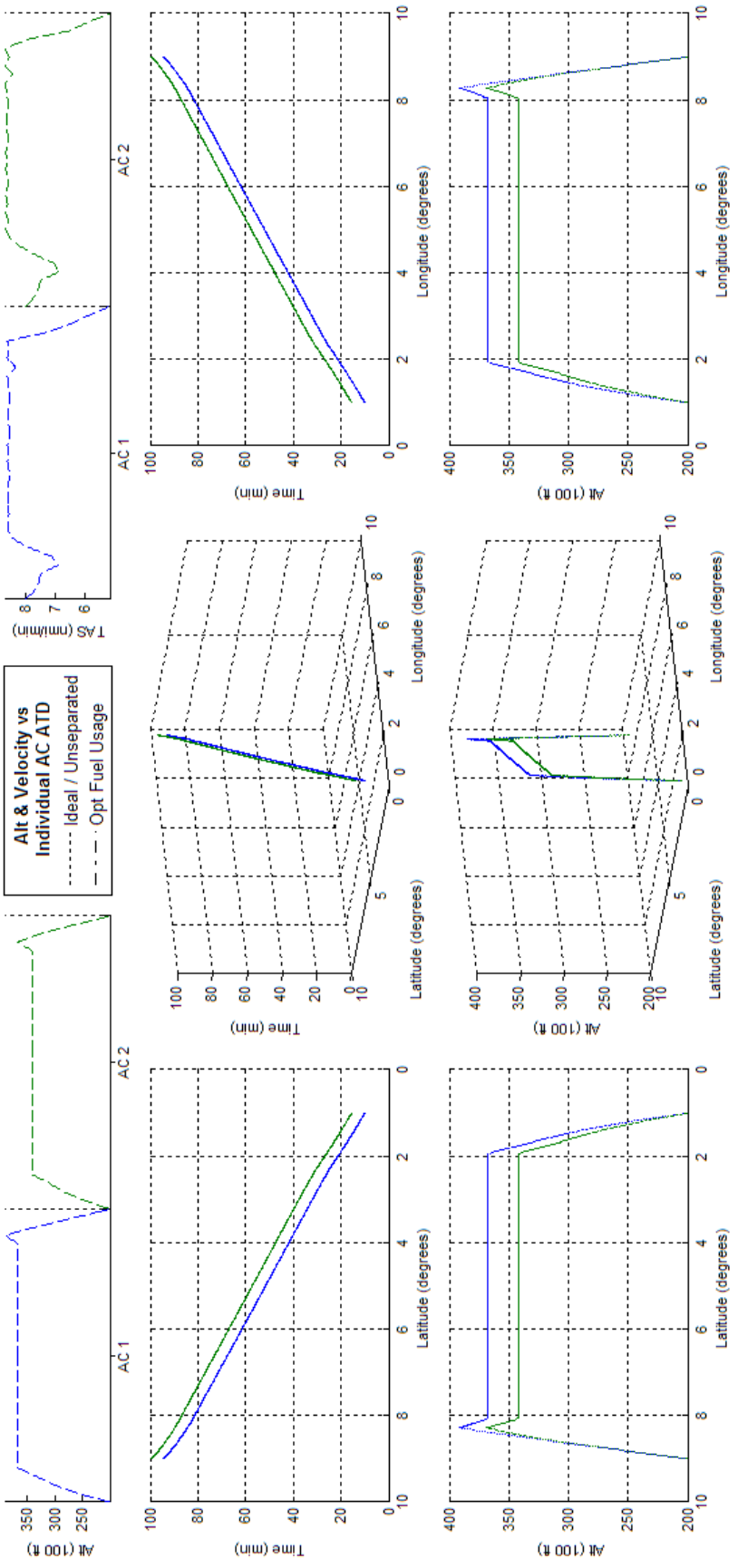

Figure 270 - Fuel Optimized 2acPSd ATD_{R3} Results

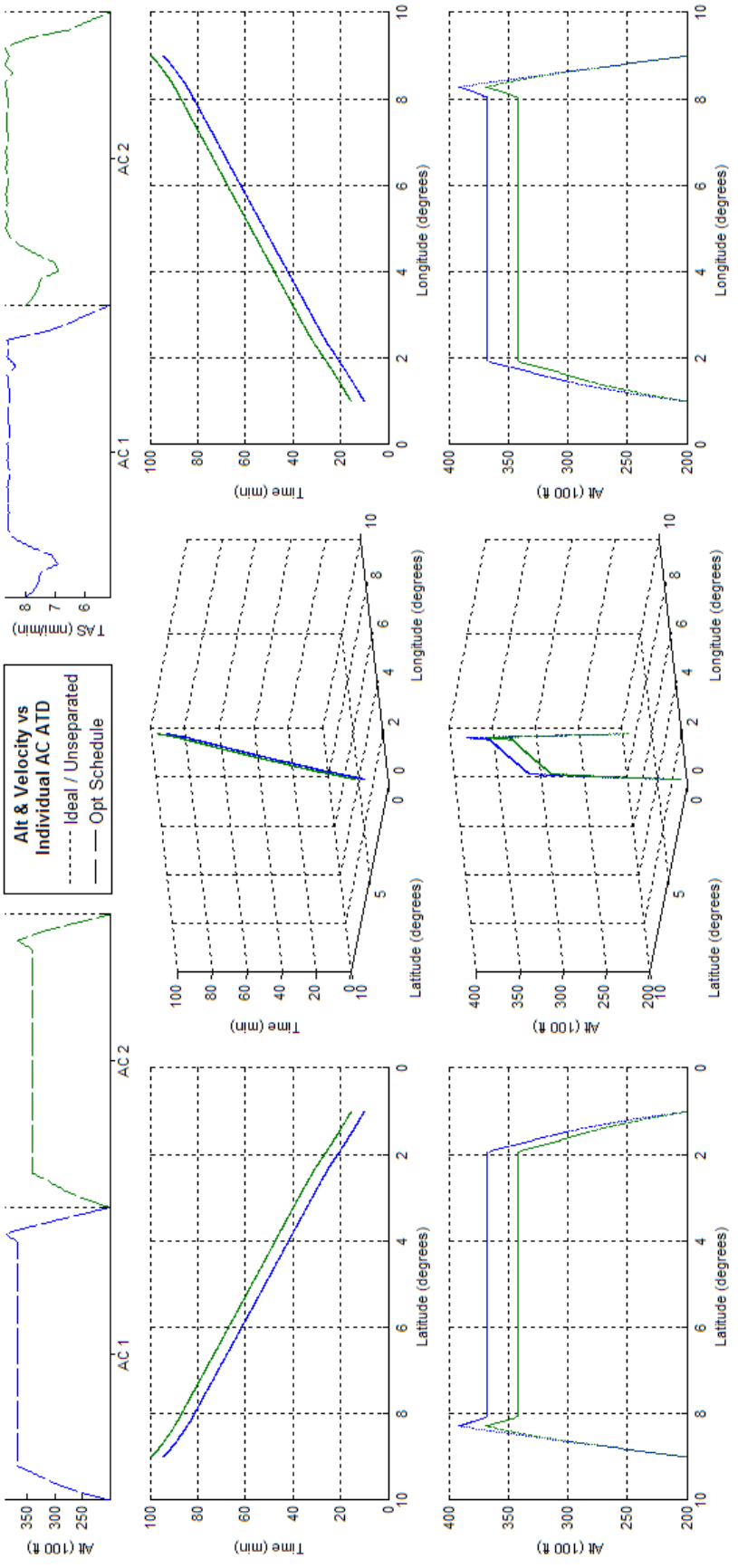

Figure 271 -Schedule Optimized 2acPSd ATD_{R3} Results

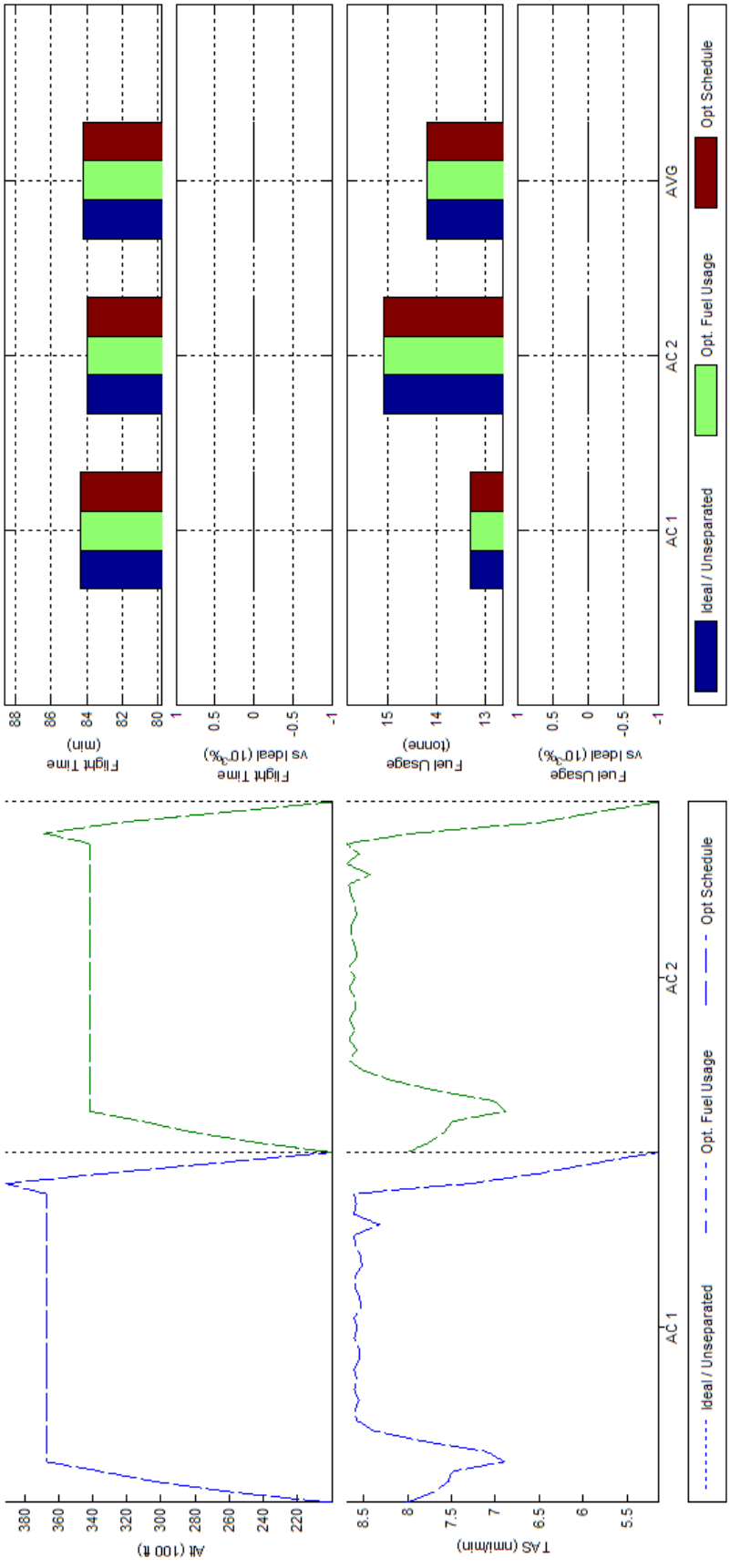

Figure 272 Trajectory Shape, Flight Time, and Fuel Consumption Comparisons of Fuel and Schedule Optimized 2acPSd ATD_{R3} Results

L.4 BADA Boeing 747-300 - Scenario 4acPSd - ATD_{R1}

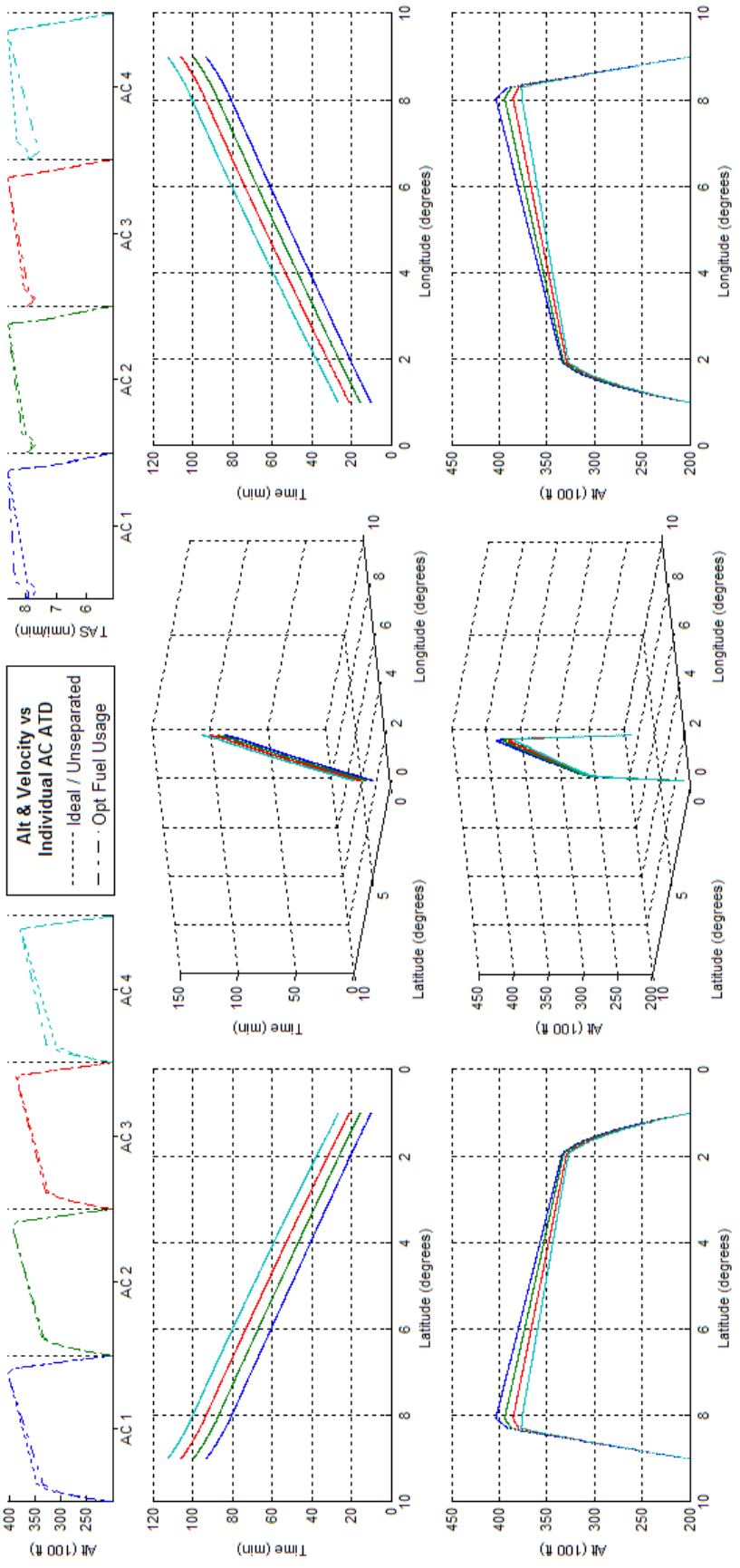

Figure 273 - Fuel Optimized 4acPSd ATD_{R1} Results

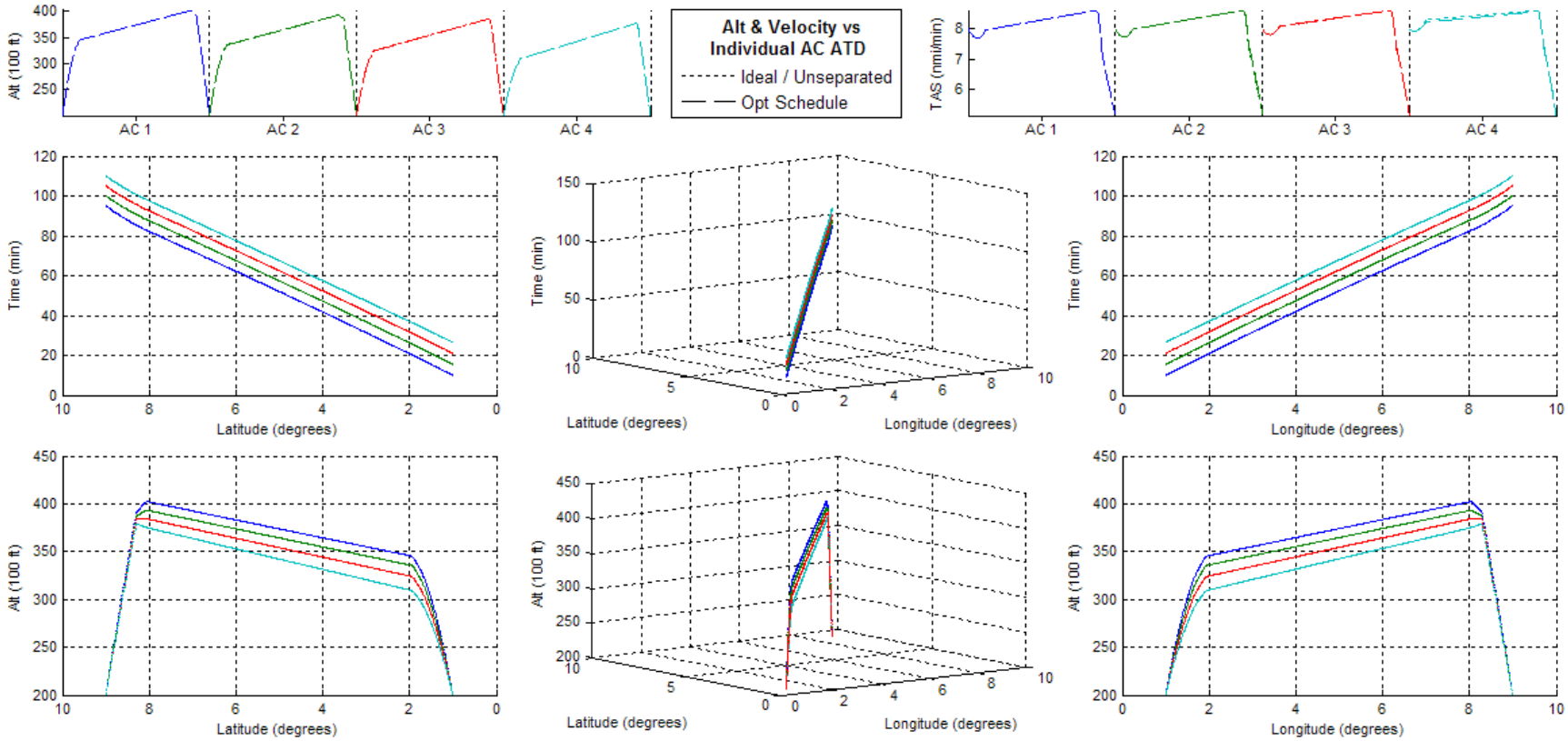

Figure 274 -Schedule Optimized 4acPSd ATD_{R1} Results

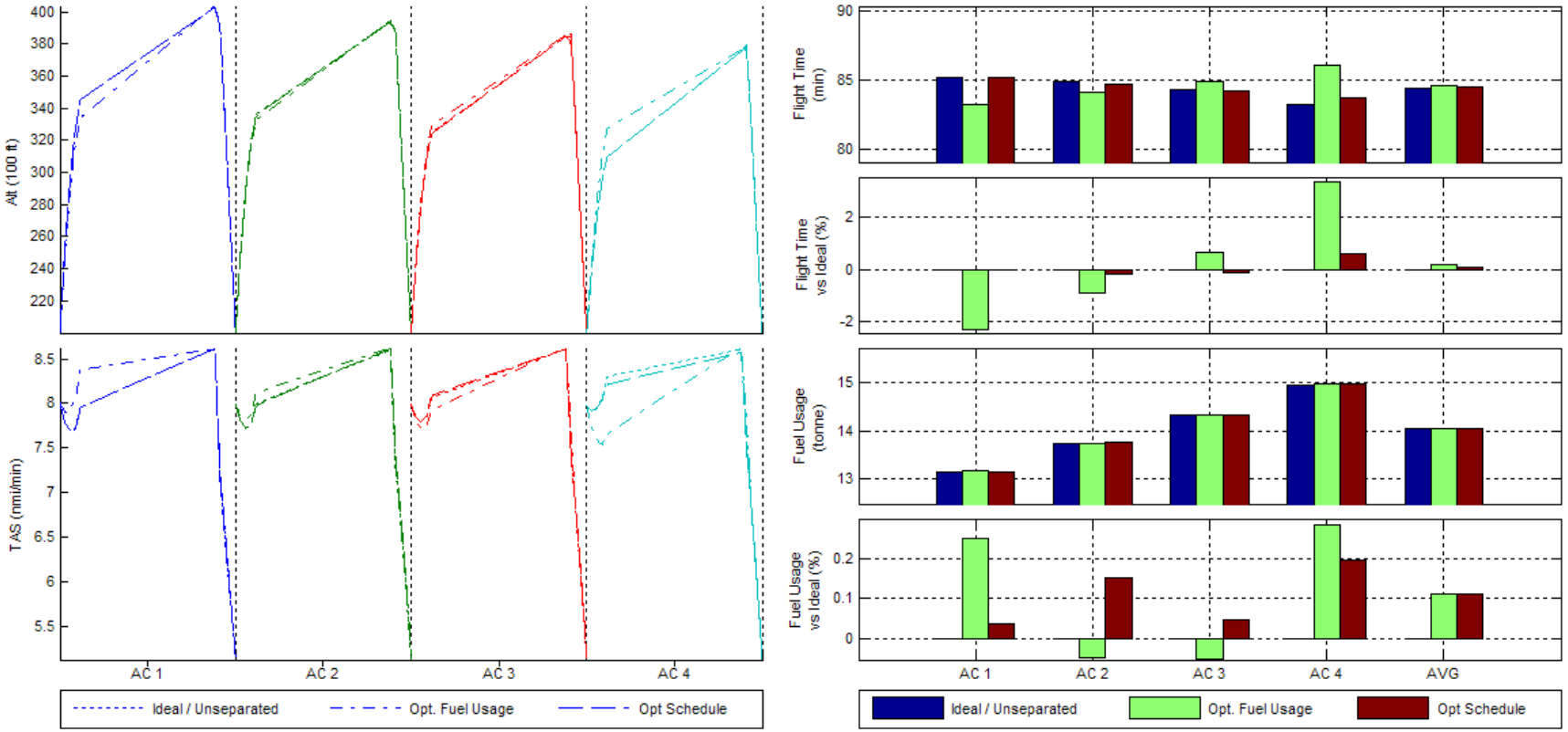

Figure 275 Trajectory Shape, Flight Time, and Fuel Consumption Comparisons of Fuel and Schedule Optimized 4acPSd ATD_{R1} Results

L.5 BADA Boeing 747-300 - Scenario 4acPSd - ATD_{R2}

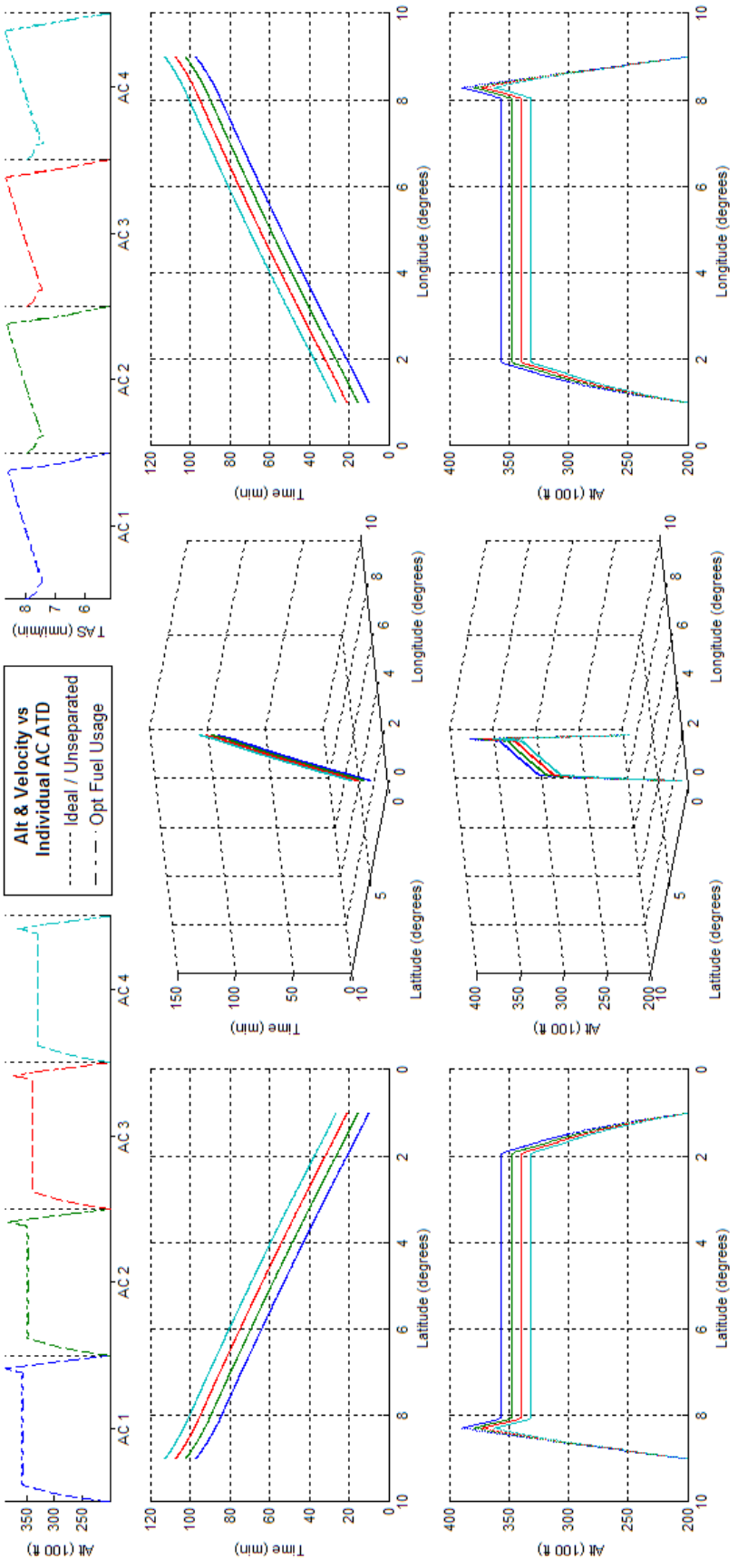

Figure 276 - Fuel Optimized 4acPSd ATD_{R2} Results

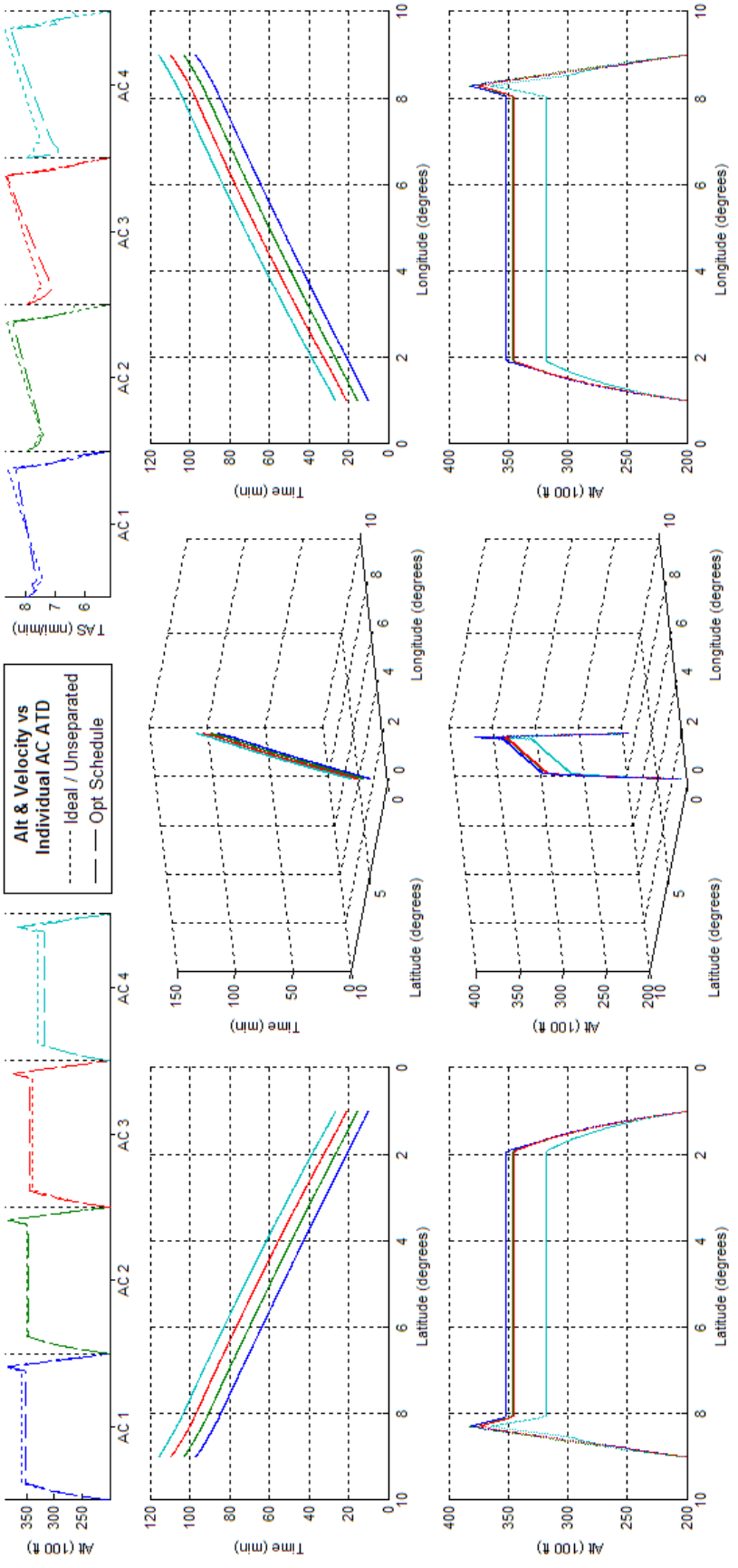

Figure 277 -Schedule Optimized 4acPSd ATD_{R2} Results

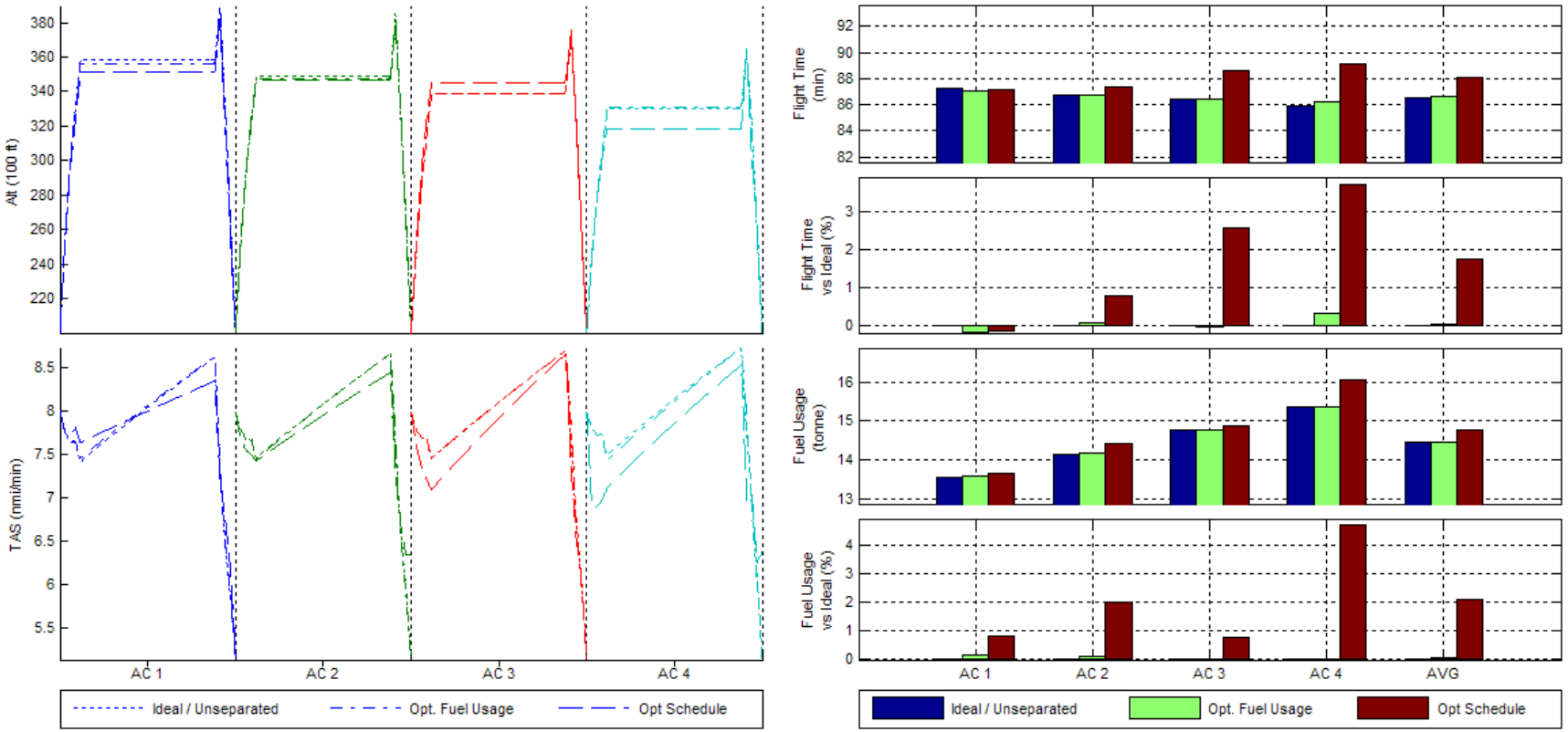

Figure 278 Trajectory Shape, Flight Time, and Fuel Consumption Comparisons of Fuel and Schedule Optimized 4acPSd ATD_{R2} Results

L.6 BADA Boeing 747-300 - Scenario 4acPSd - ATD_{R3}

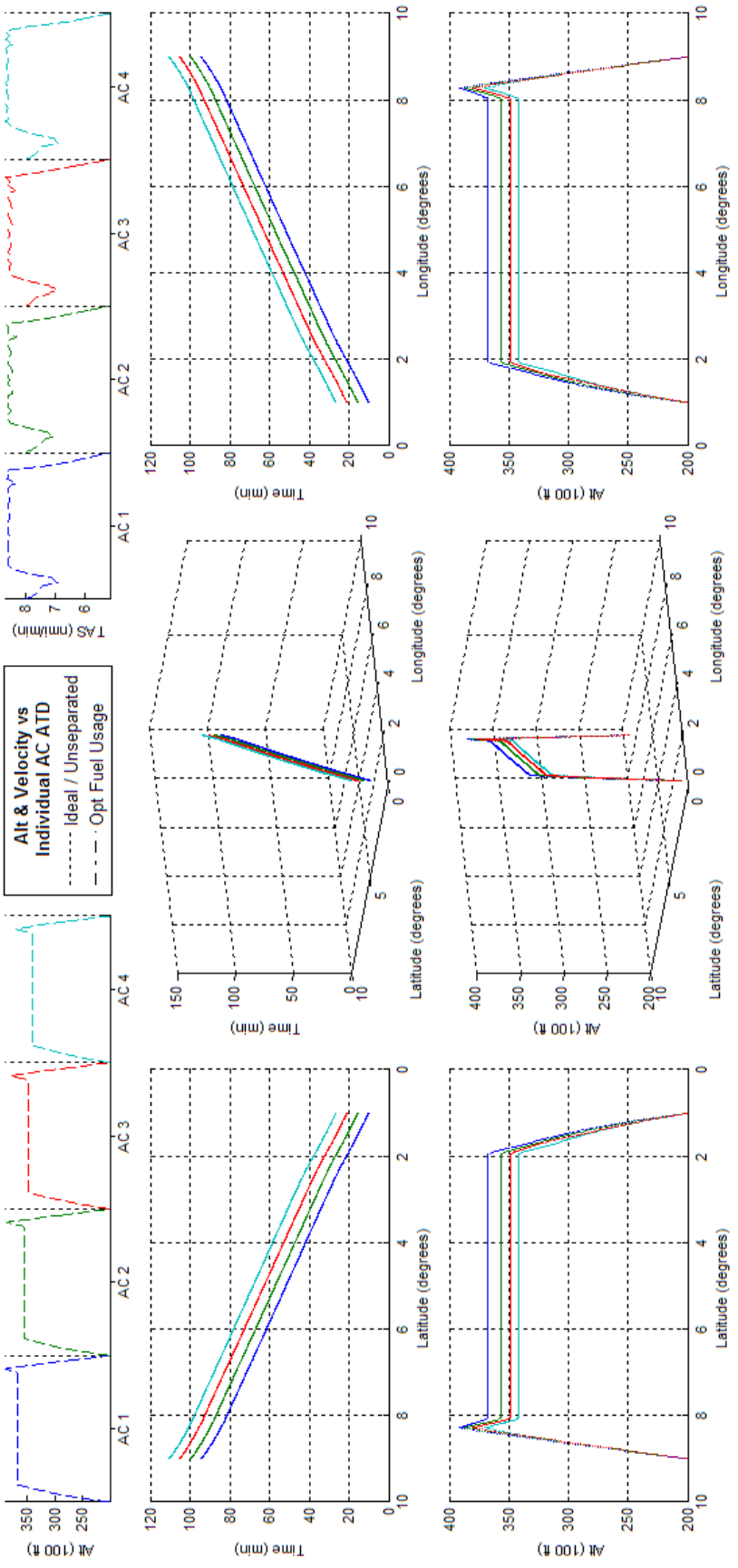

Figure 279 - Fuel Optimized 4acPSd ATD_{R3} Results

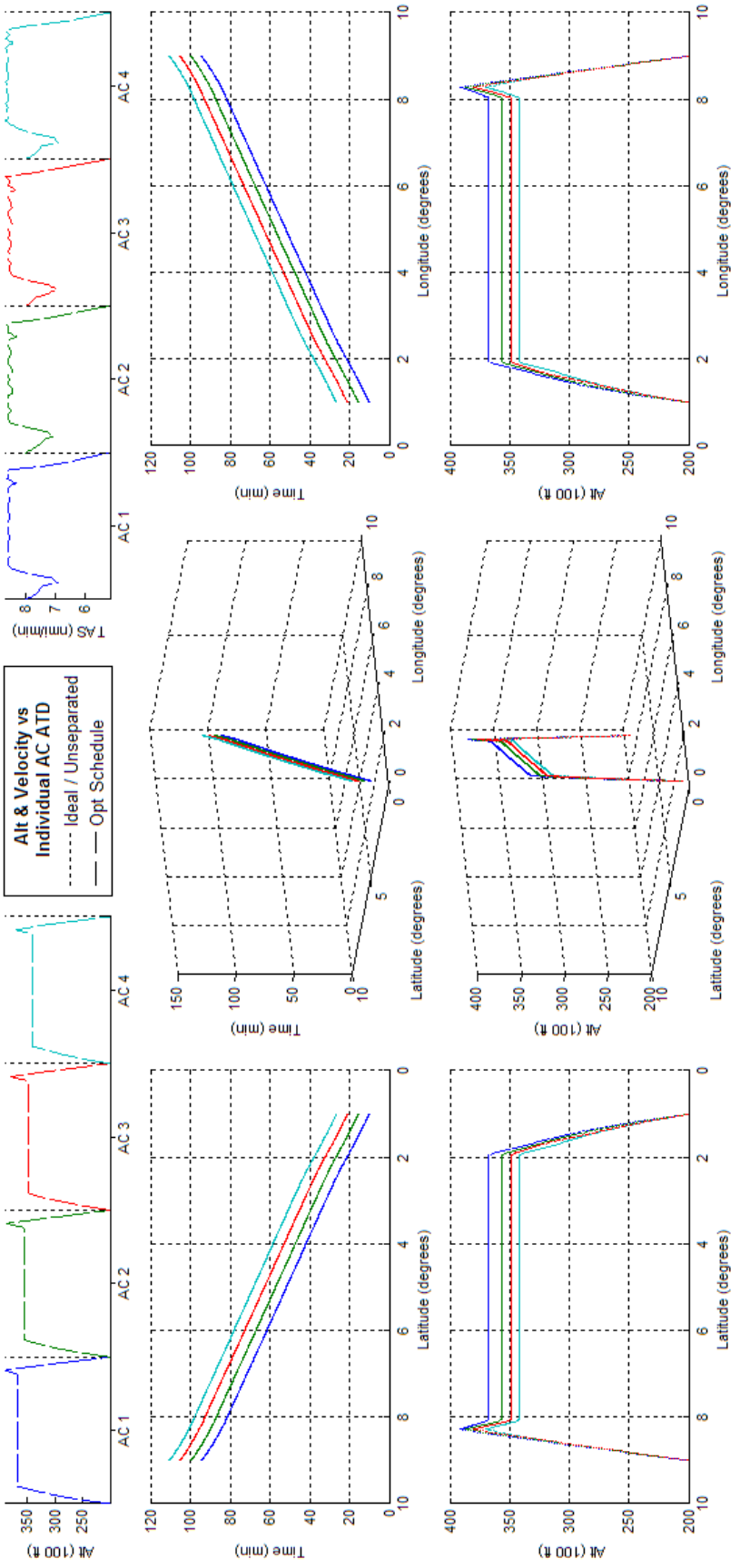

Figure 280 -Schedule Optimized 4acPSd ATD_{R3} Results

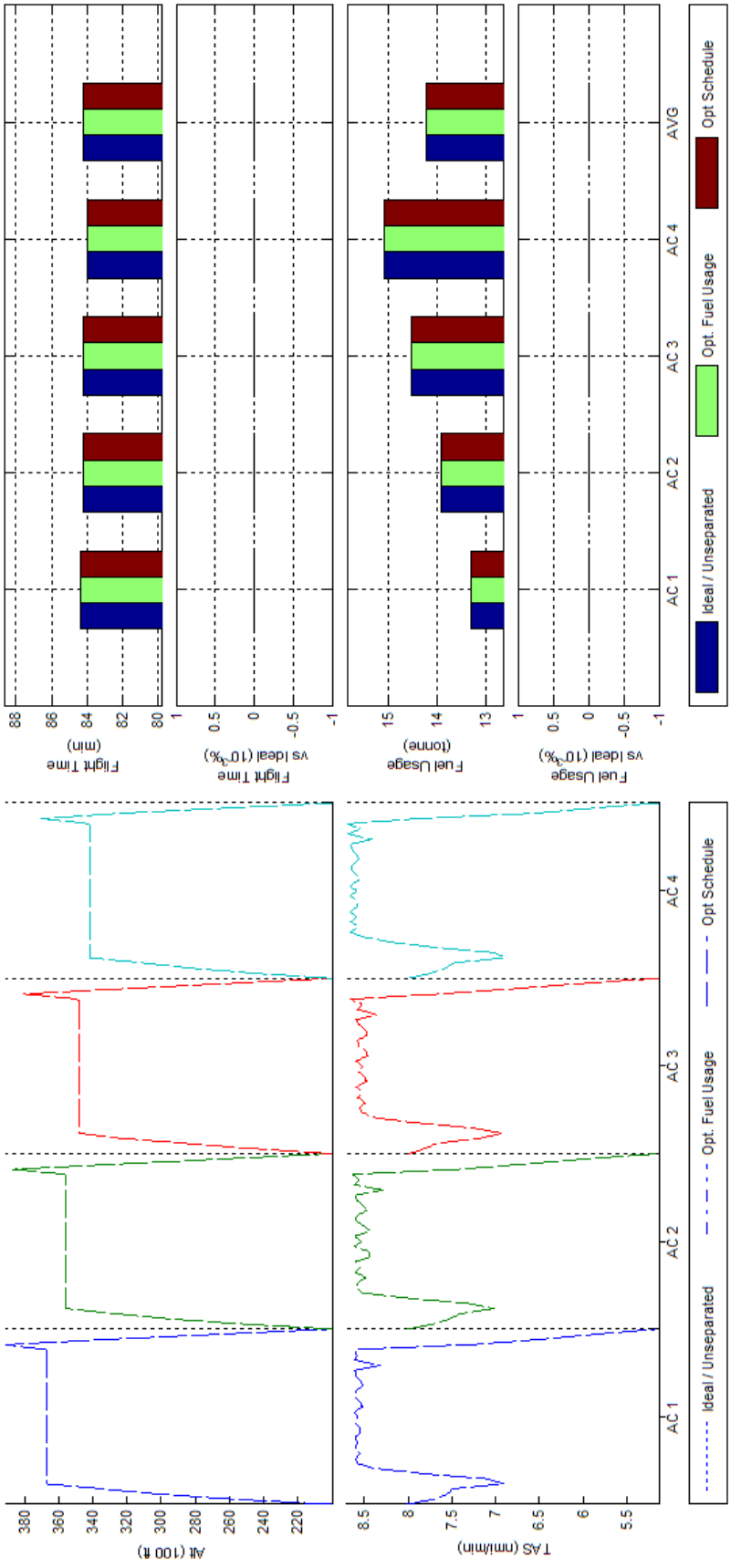

Figure 281 Trajectory Shape, Flight Time, and Fuel Consumption Comparisons of Fuel and Schedule Optimized 4acPSd ATD_{R3} Results

L.7 BADA Boeing 747-300 - Scenario 10acPSd - ATD_{R1}

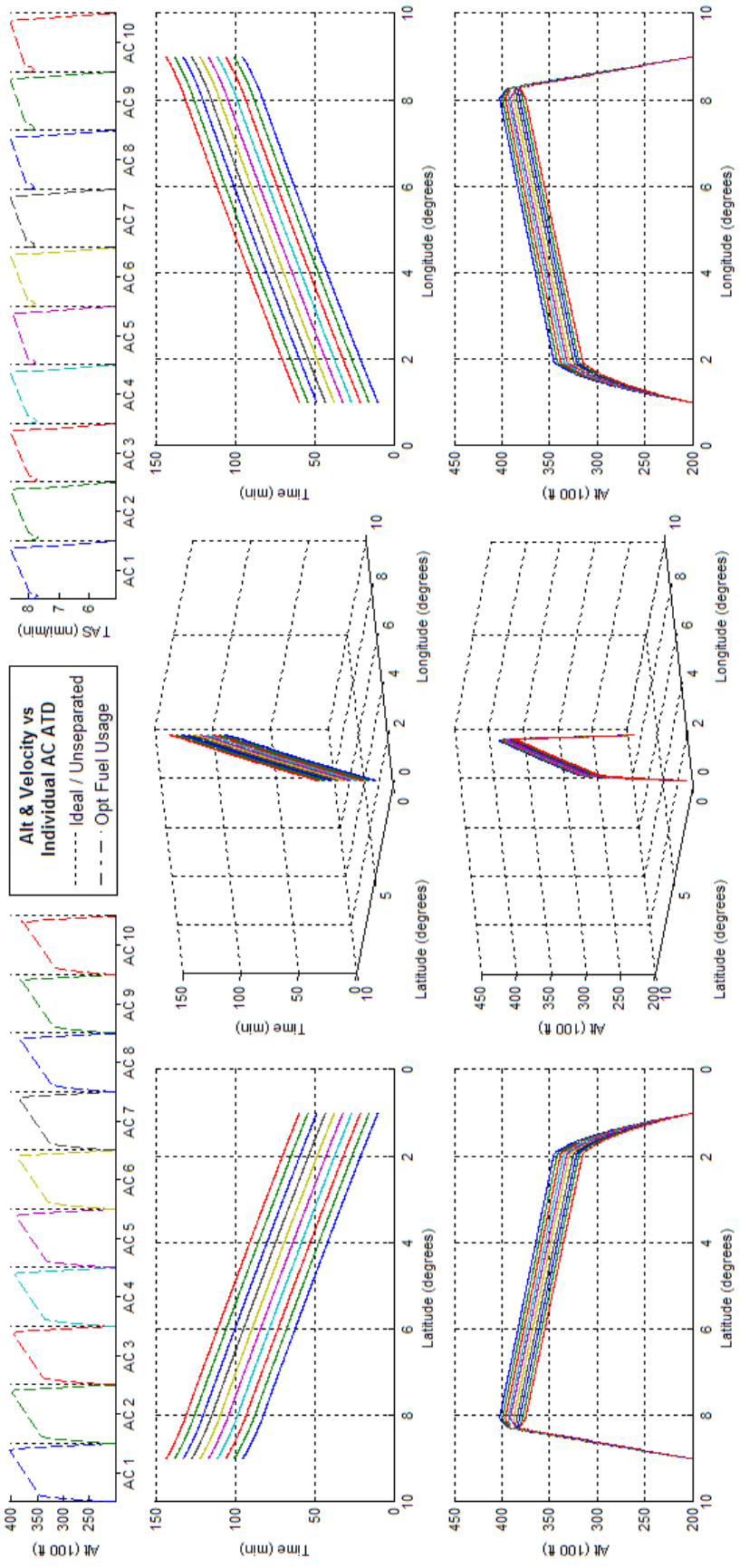

Figure 282 - Fuel Optimized 10acPSd ATD_{R1} Results

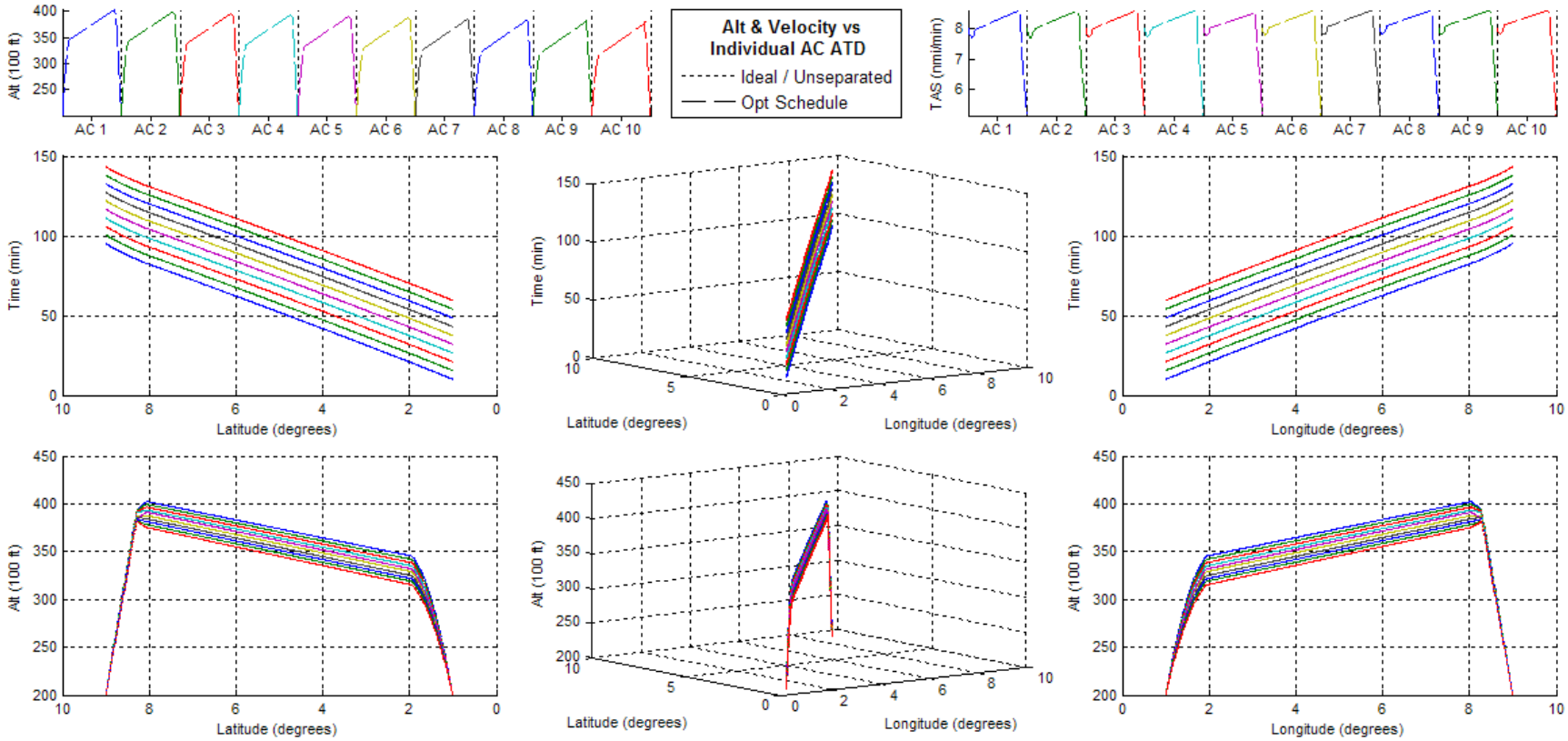

Figure 283 -Schedule Optimized 10acPSd ATD_{R1} Results

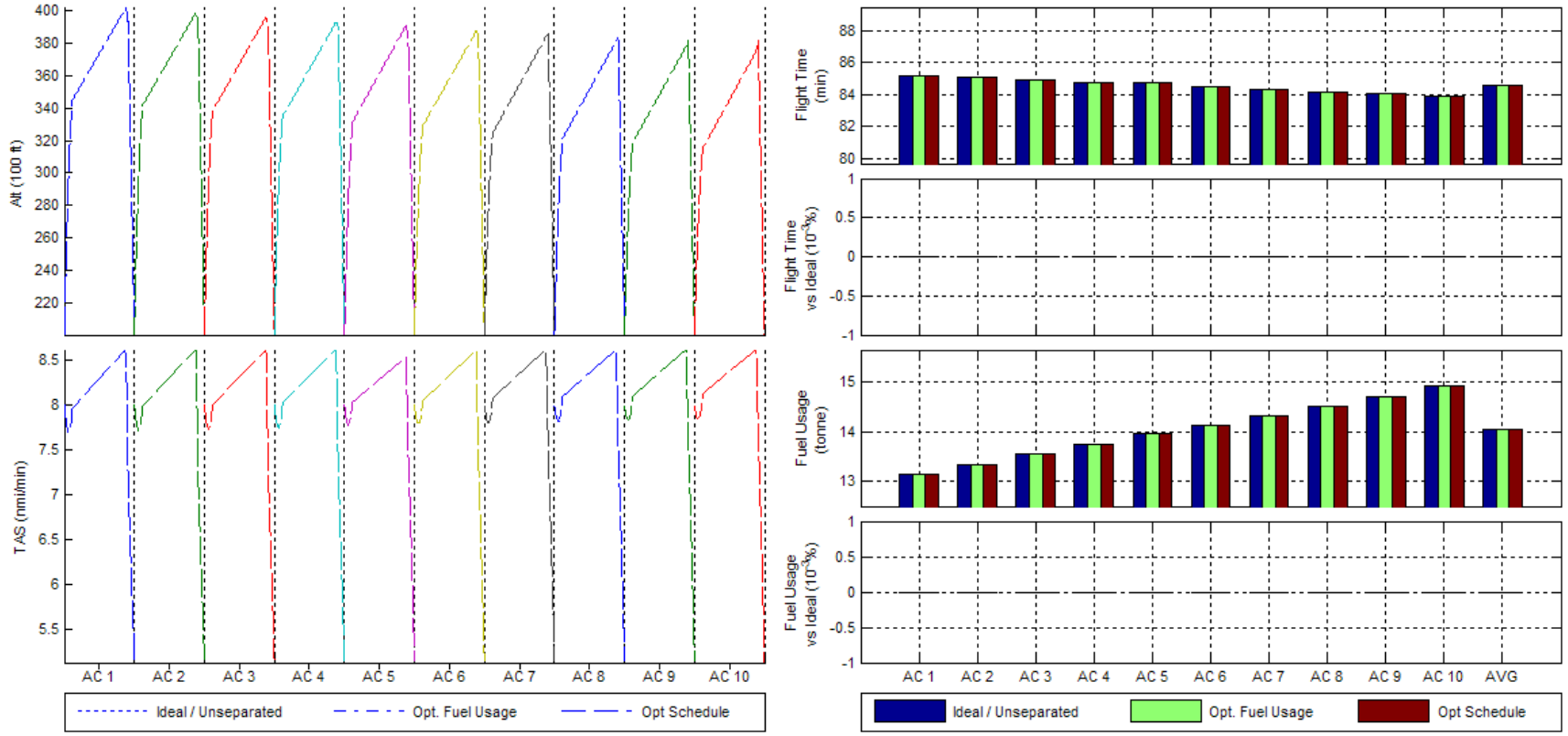

Figure 284 Trajectory Shape, Flight Time, and Fuel Consumption Comparisons of Fuel and Schedule Optimized 10acPSd ATD_{R1} Results

L.8 BADA Boeing 747-300 - Scenario 10acPSd - ATD_{R2}

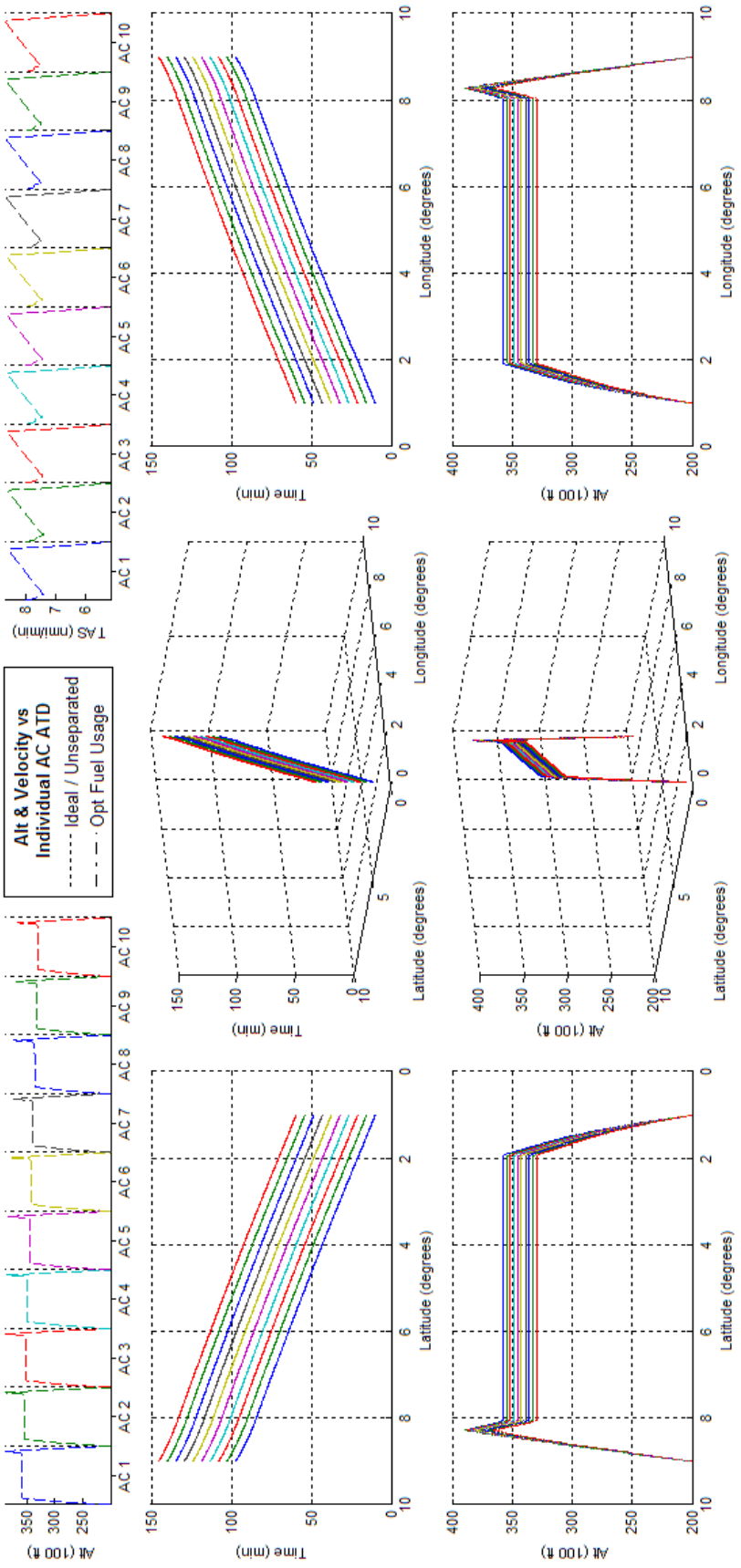

Figure 285 - Fuel Optimized 10acPSd ATD_{R2} Results

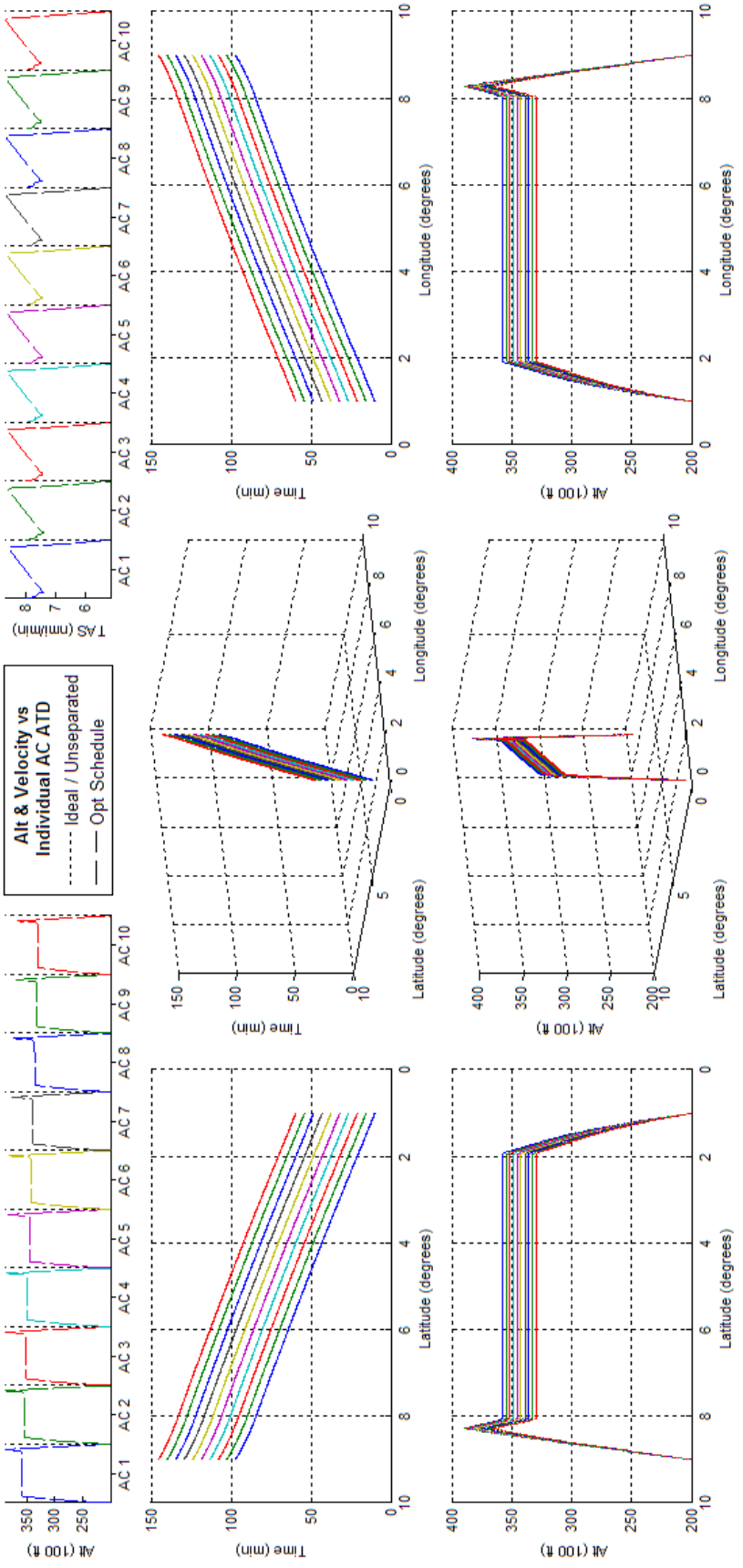

Figure 286 -Schedule Optimized 10acPSd ATD_{R2} Results

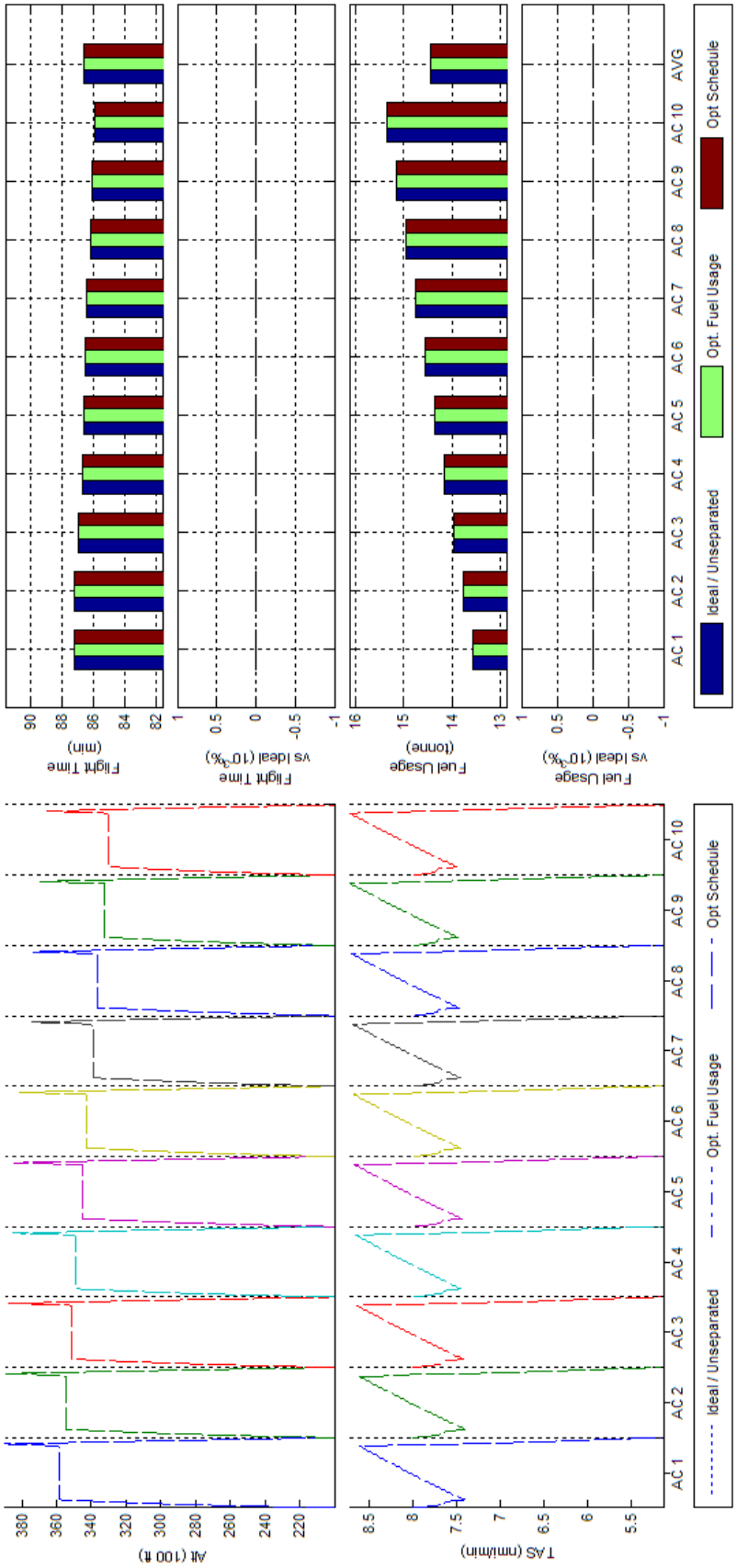

Figure 287 Trajectory Shape, Flight Time, and Fuel Consumption Comparisons of Fuel and Schedule Optimized 10acPSd ATD_{R2} Results

L.9 BADA Boeing 747-300 - Scenario 10acPSd - ATD_{R3}

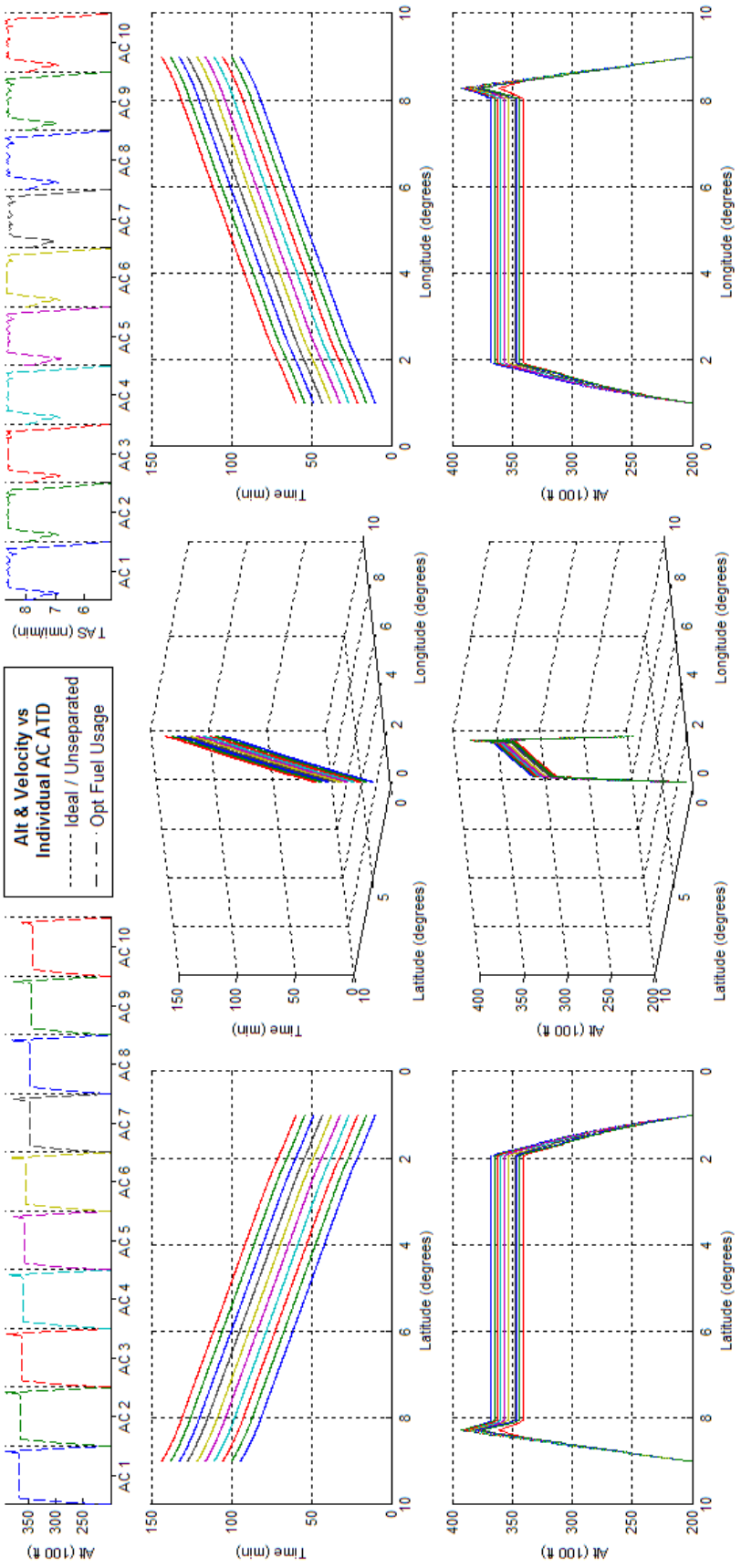

Figure 288 - Fuel Optimized 10acPSd ATD_{R3} Results

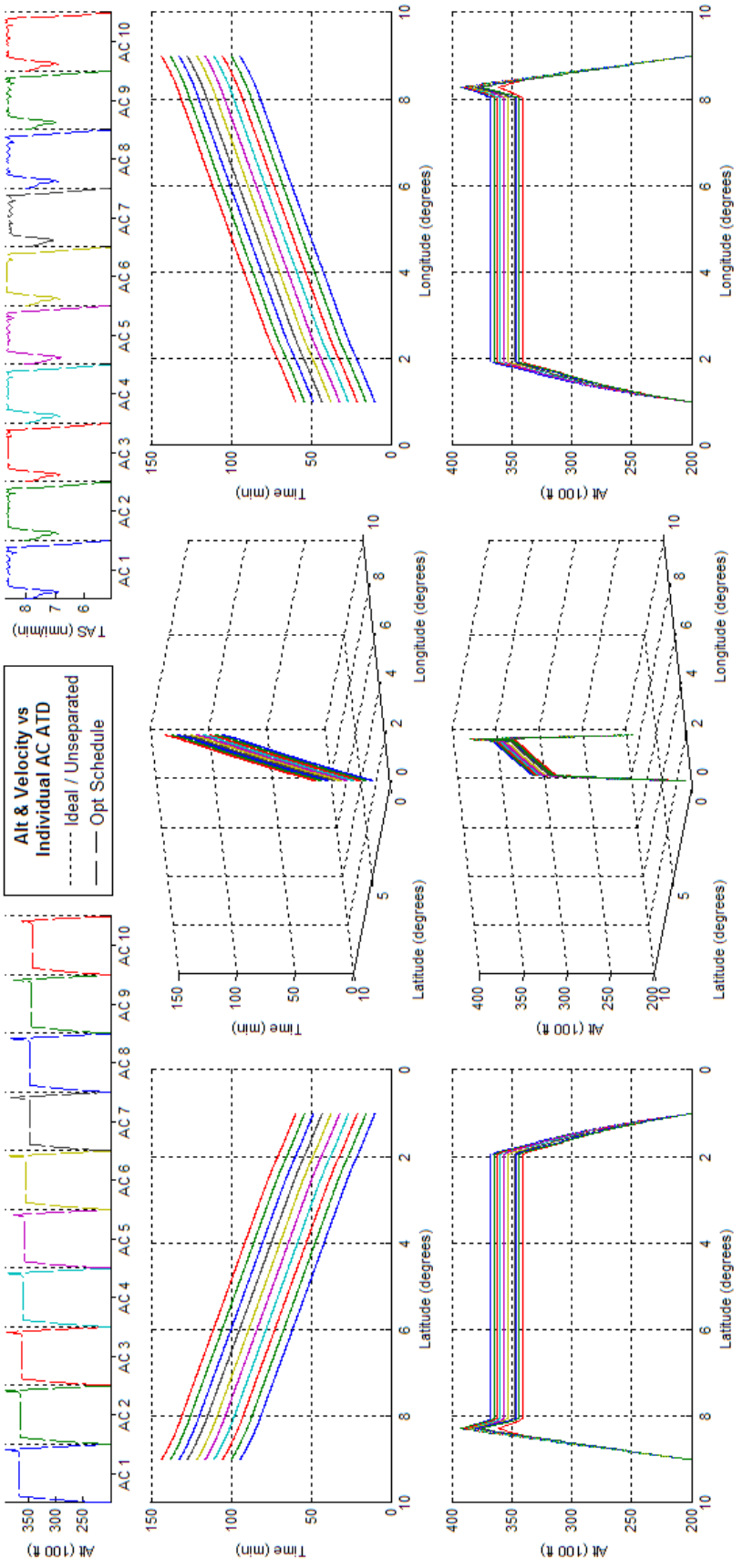

Figure 289 -Schedule Optimized 10acPSd ATD_{R3} Results

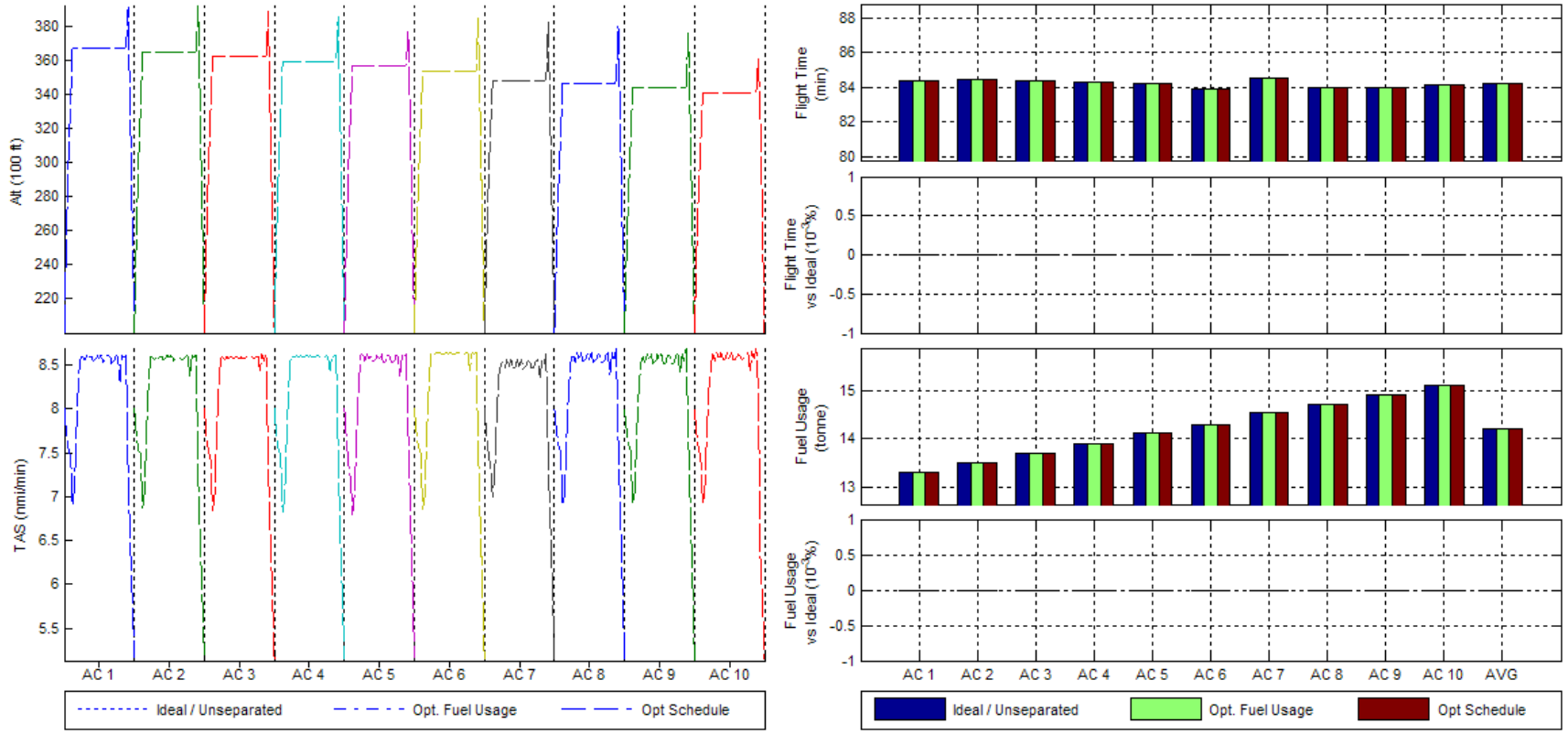

Figure 290 Trajectory Shape, Flight Time, and Fuel Consumption Comparisons of Fuel and Schedule Optimized 10acPSd ATD_{R3} Results

L.10 BADA Boeing 747-300 - Scenario 2acCO - ATD_{R1}

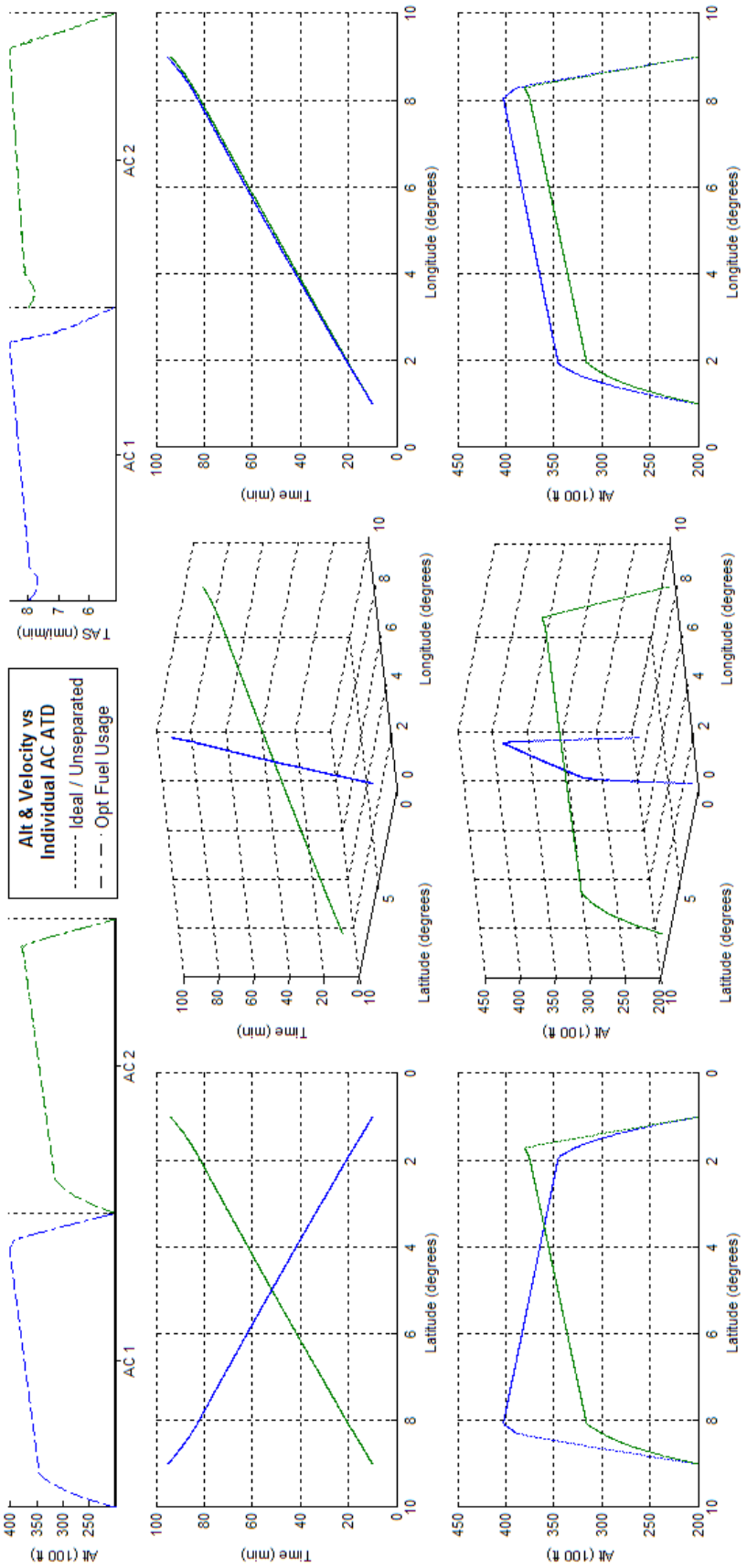

Figure 291 - Fuel Optimized 2acCO ATD_{R1} Results

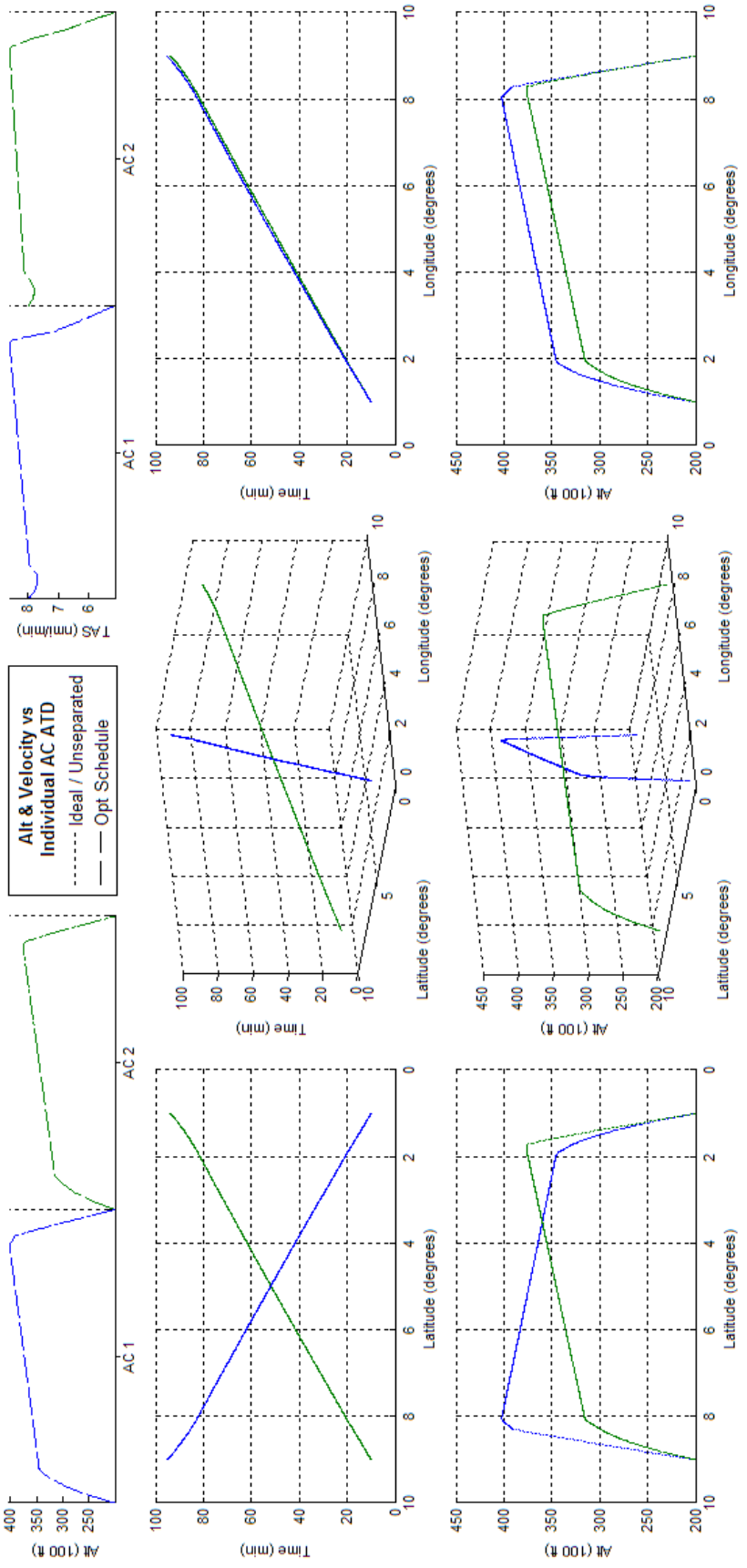

Figure 292 -Schedule Optimized 2acCO ATD_{R1} Results

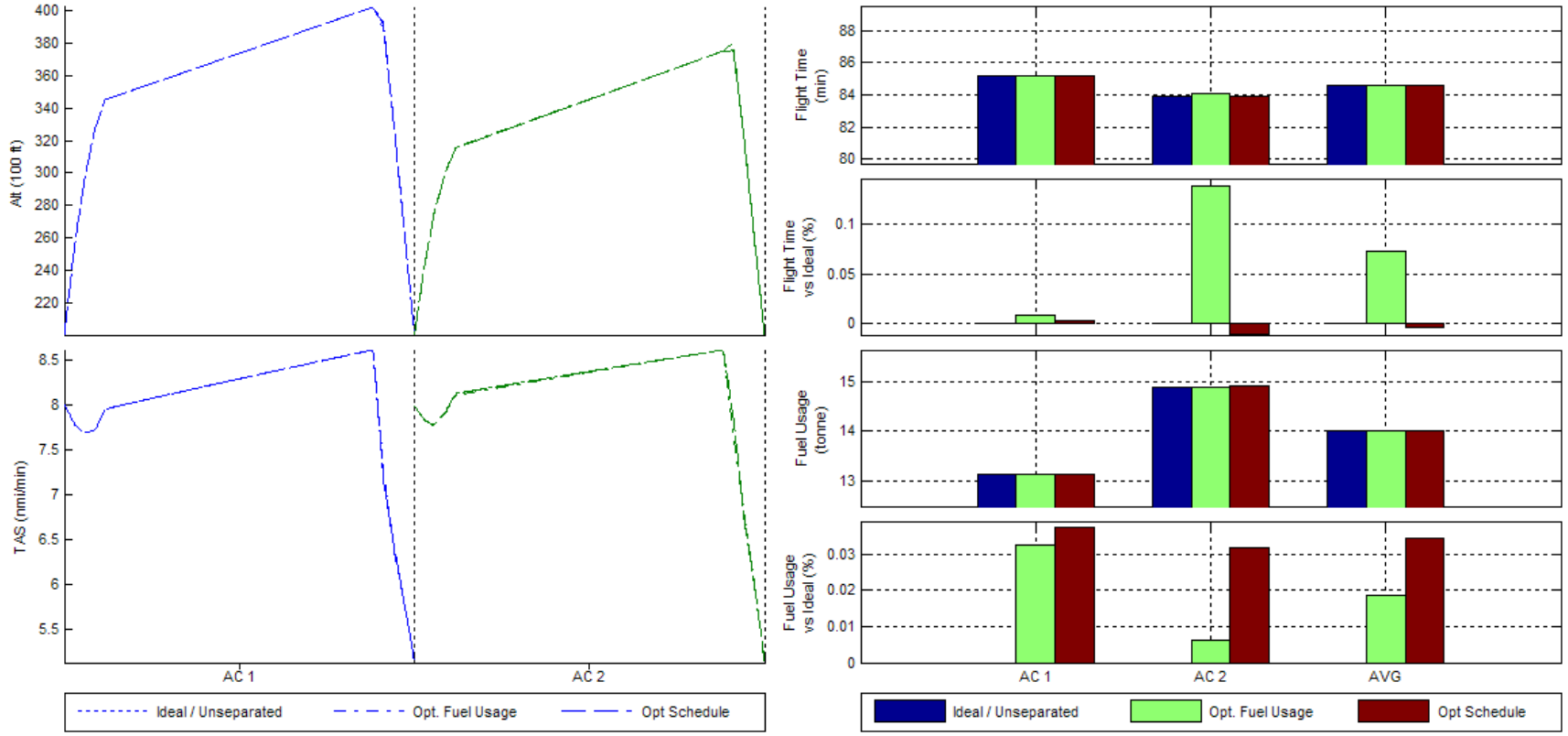

Figure 293 Trajectory Shape, Flight Time, and Fuel Consumption Comparisons of Fuel and Schedule Optimized 2acCO ATD_{R1} Results

L.11 BADA Boeing 747-300 - Scenario 2acCO - ATD_{R2}

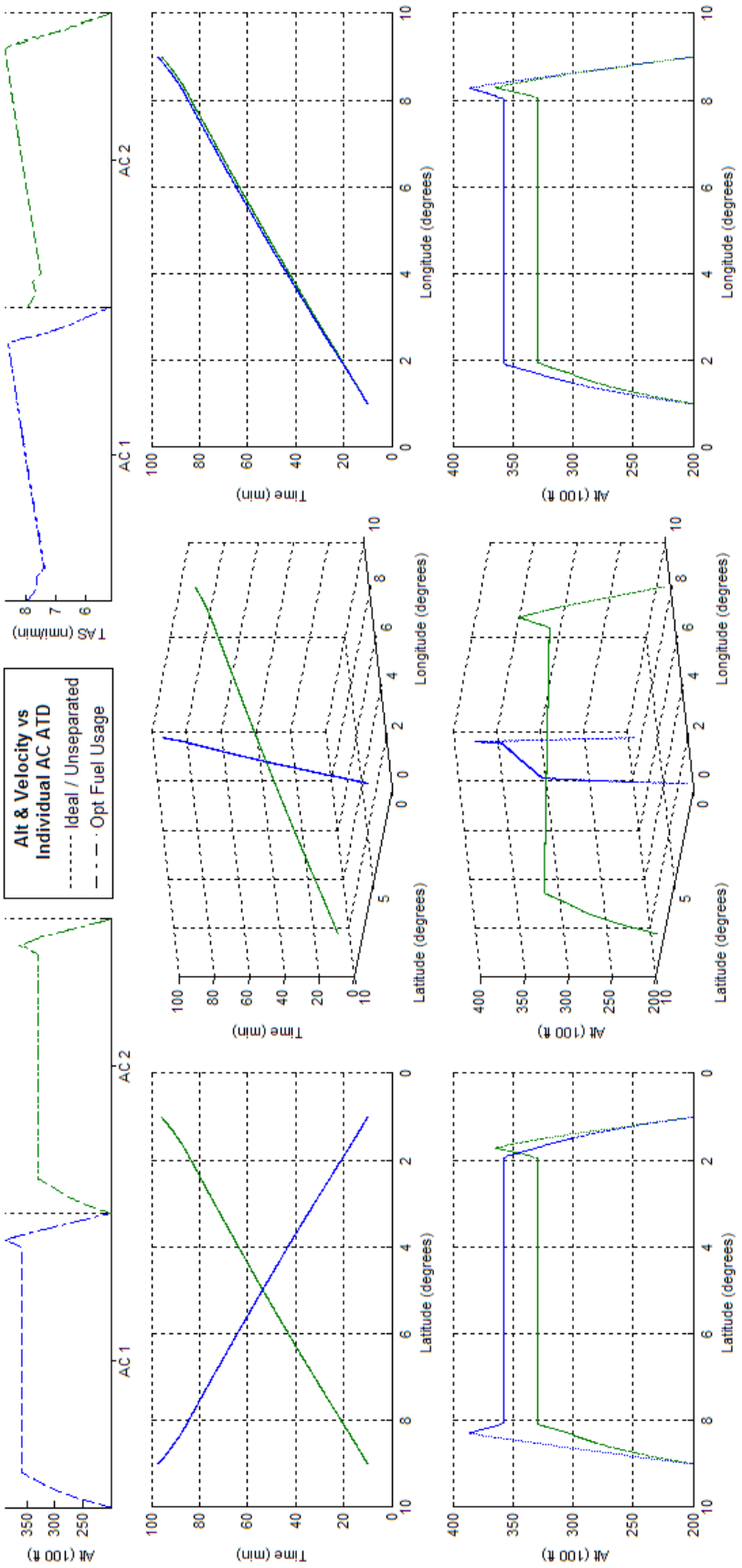

Figure 294 - Fuel Optimized 2acCO ATD_{R2} Results

Figure 295 -Schedule Optimized 2acCO ATD_{R2} Results

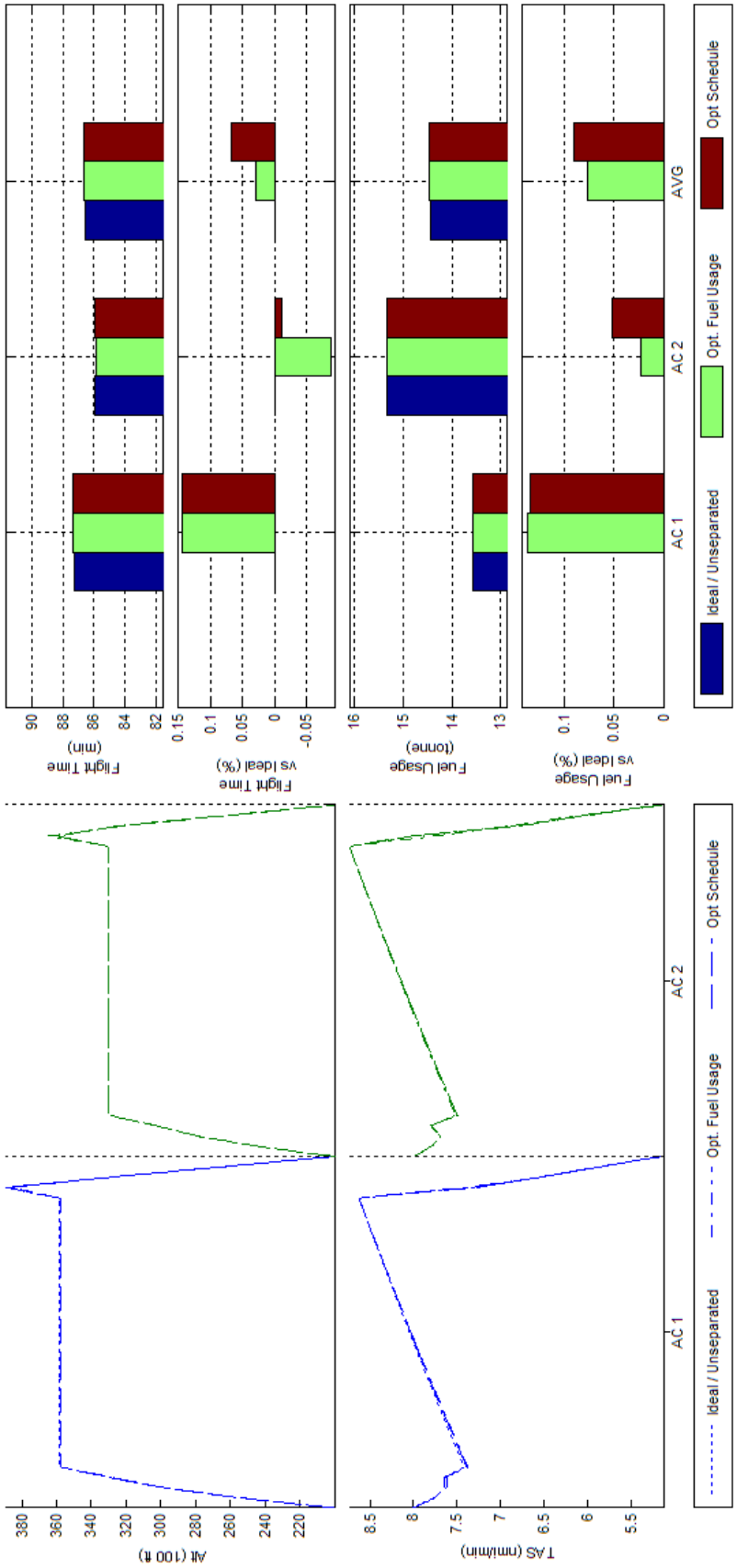

Figure 296 Trajectory Shape, Flight Time, and Fuel Consumption Comparisons of Fuel and Schedule Optimized 2acCO ATD_{R2} Results

L.12 BADA Boeing 747-300 - Scenario 2acCO - ATD_{R3}

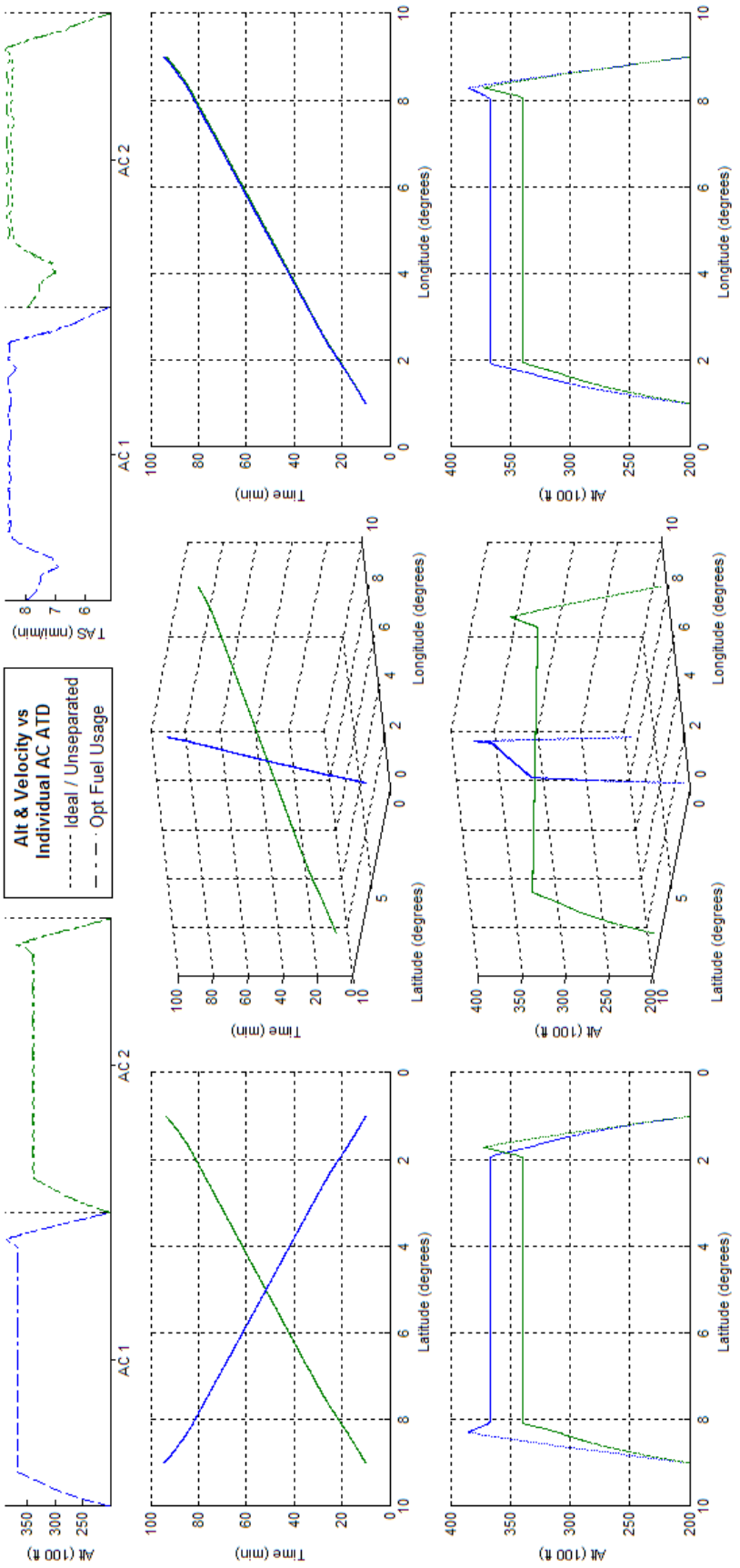

Figure 297 -Schedule Optimized 2acCO ATD_{R3} Results

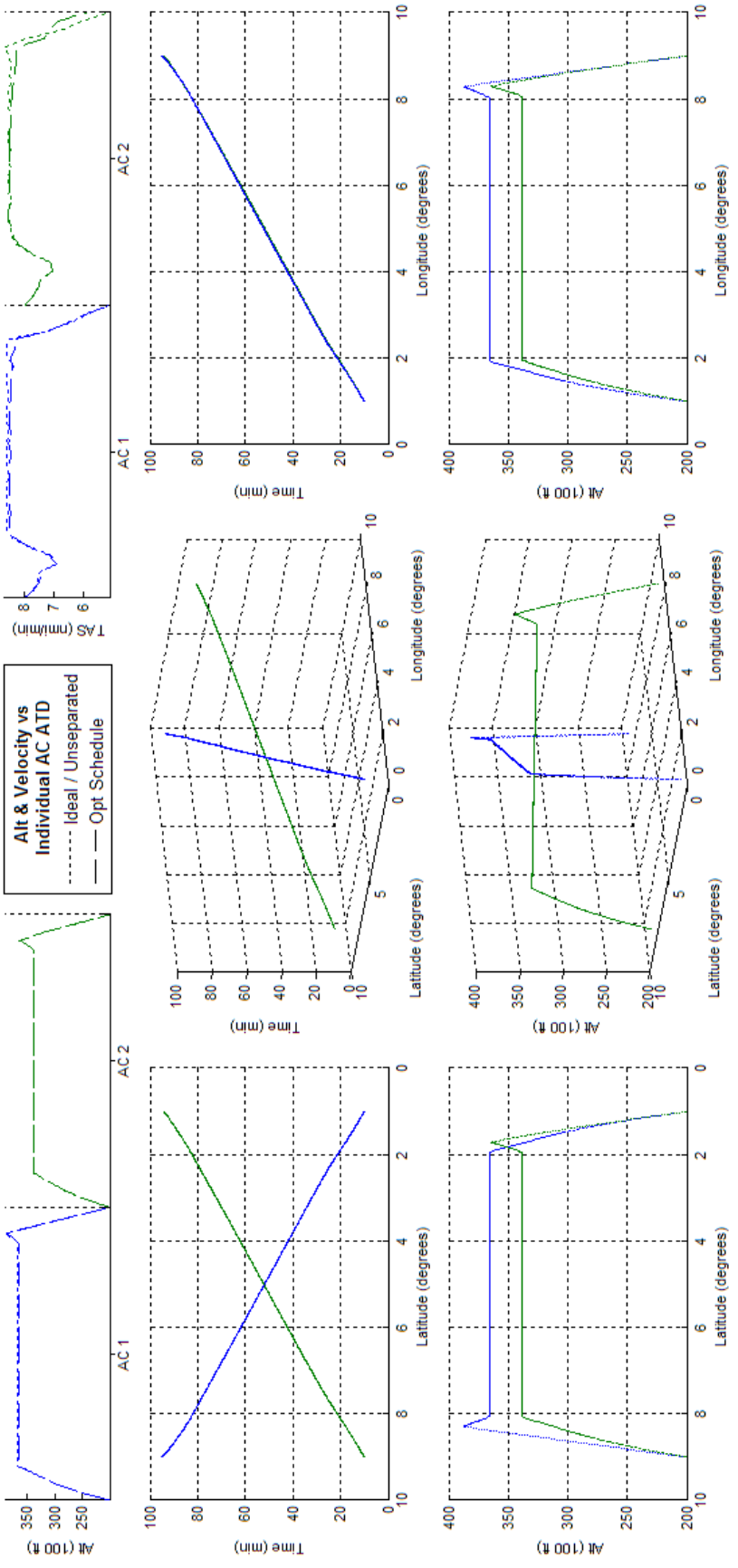

Figure 298 -Schedule Optimized 2acCO ATD_{R3} Results

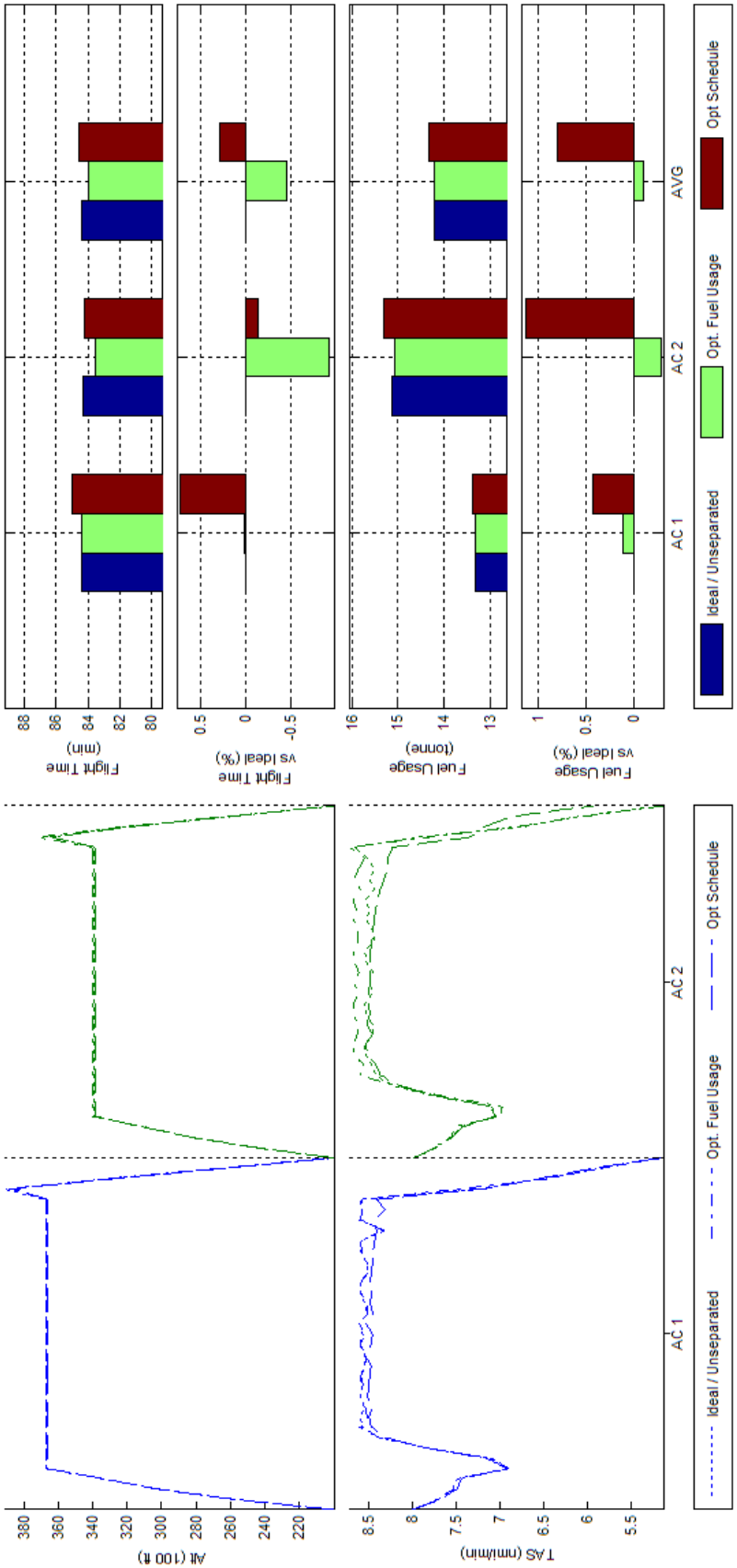

Figure 299 Trajectory Shape, Flight Time, and Fuel Consumption Comparisons of Fuel and Schedule Optimized 2acCO ATD_{R3} Results

L.13 BADA Boeing 747-300 - Scenario 4acCO - ATD_{R1}

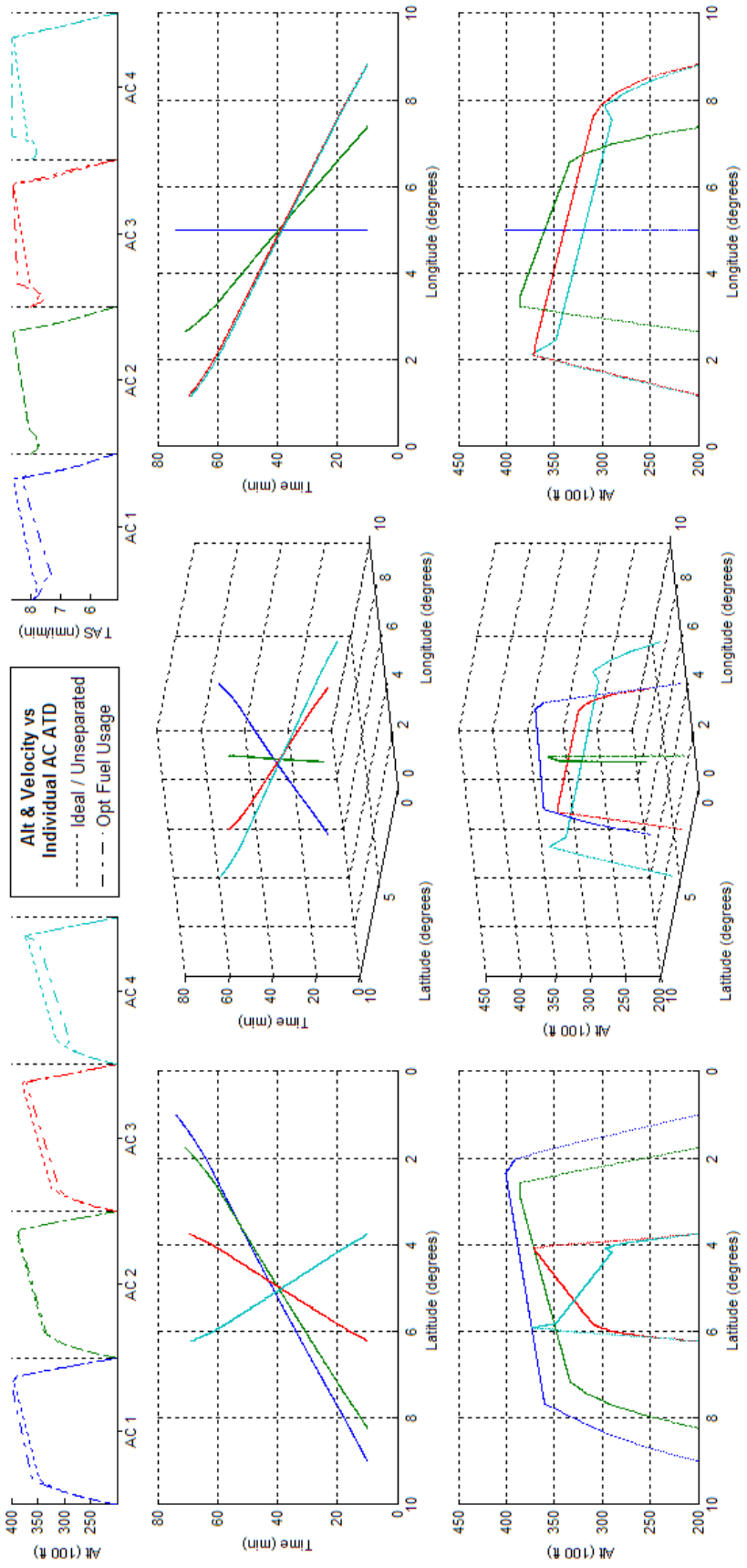

Figure 300 - Fuel Optimized 4acCO ATD_{R1} Results

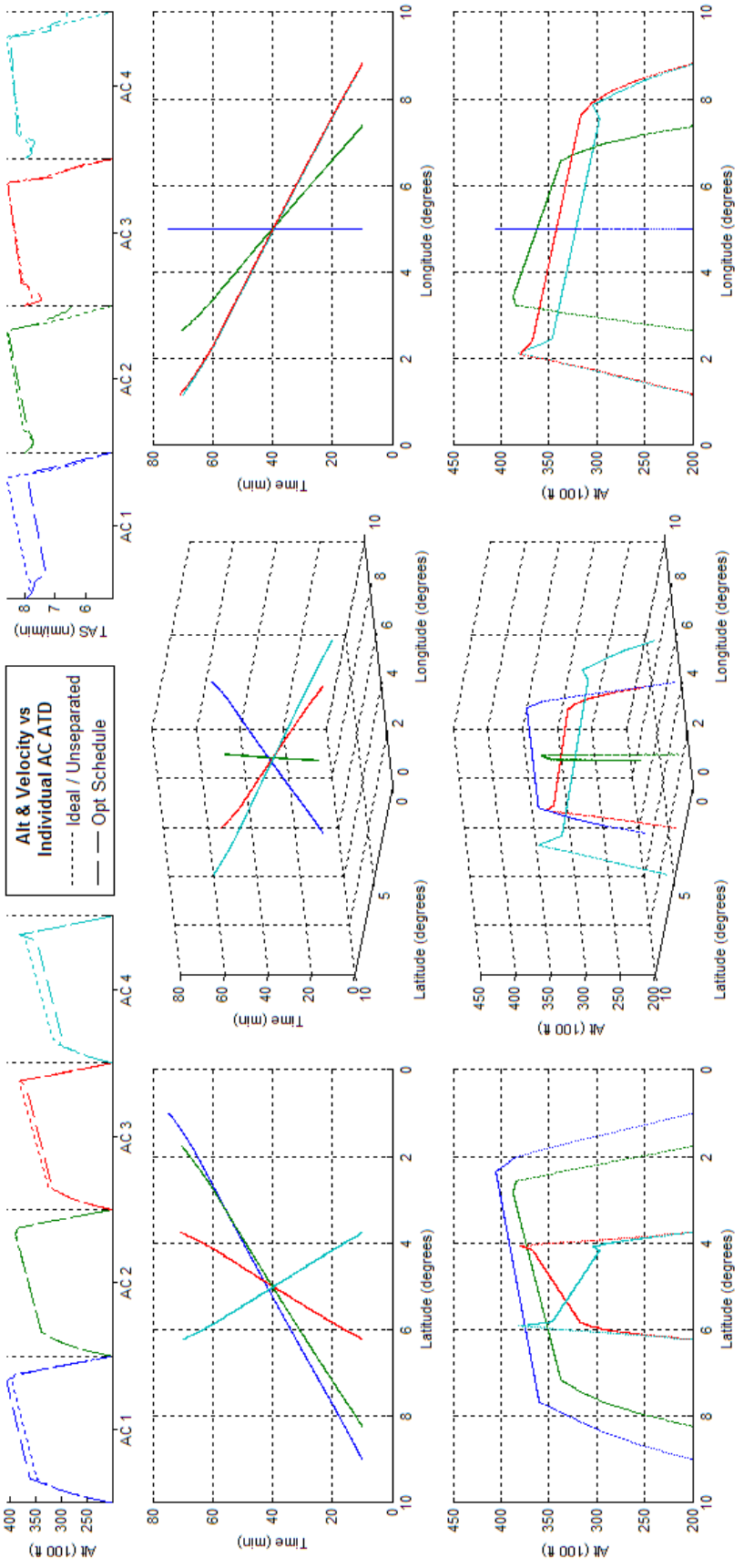

Figure 301 -Schedule Optimized 4acCO ATD_{R1} Results

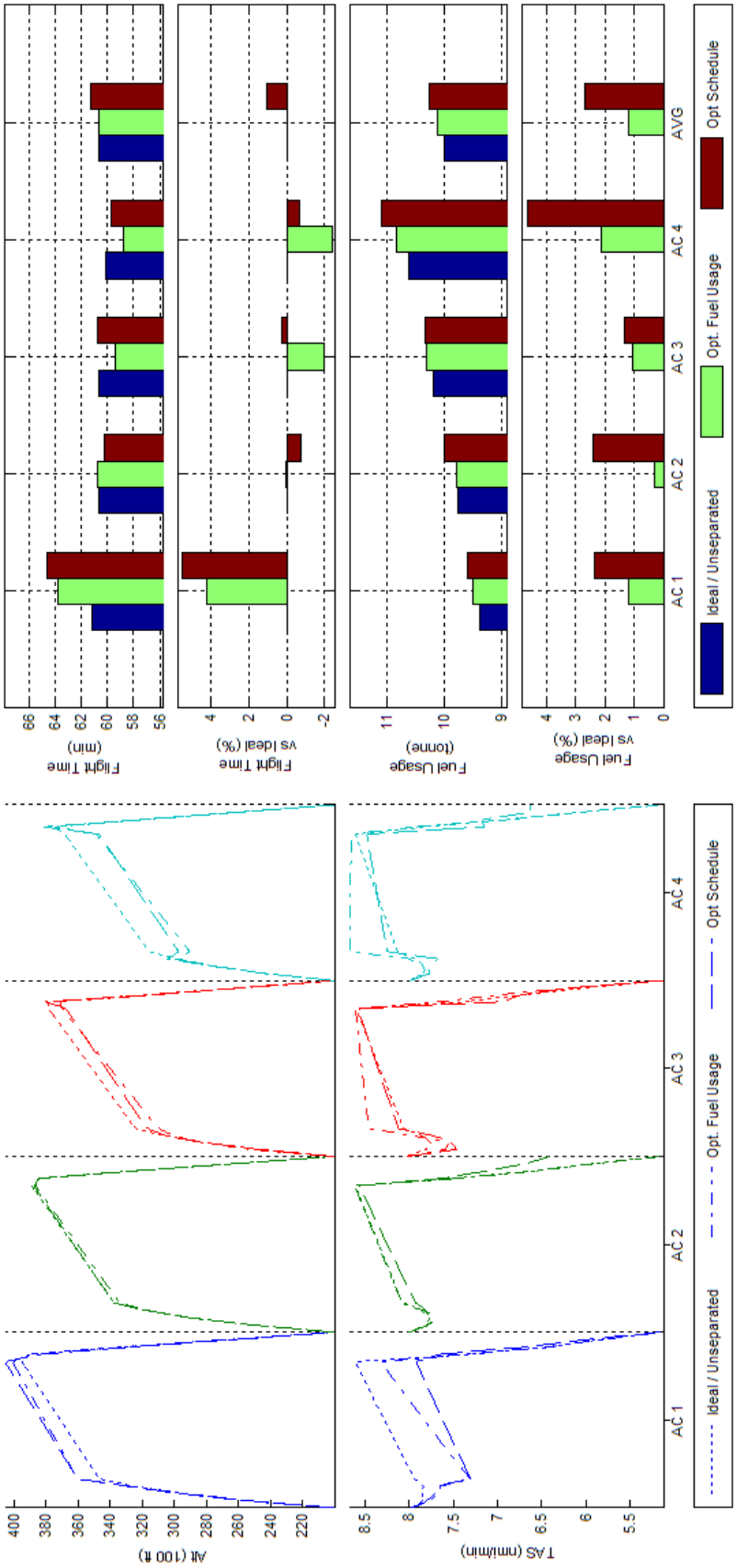

Figure 302 Trajectory Shape, Flight Time, and Fuel Consumption Comparisons of Fuel and Schedule Optimized 4acCO ATD_{R1} Results

L.14 BADA Boeing 747-300 - Scenario 4acCO - ATD_{R2}

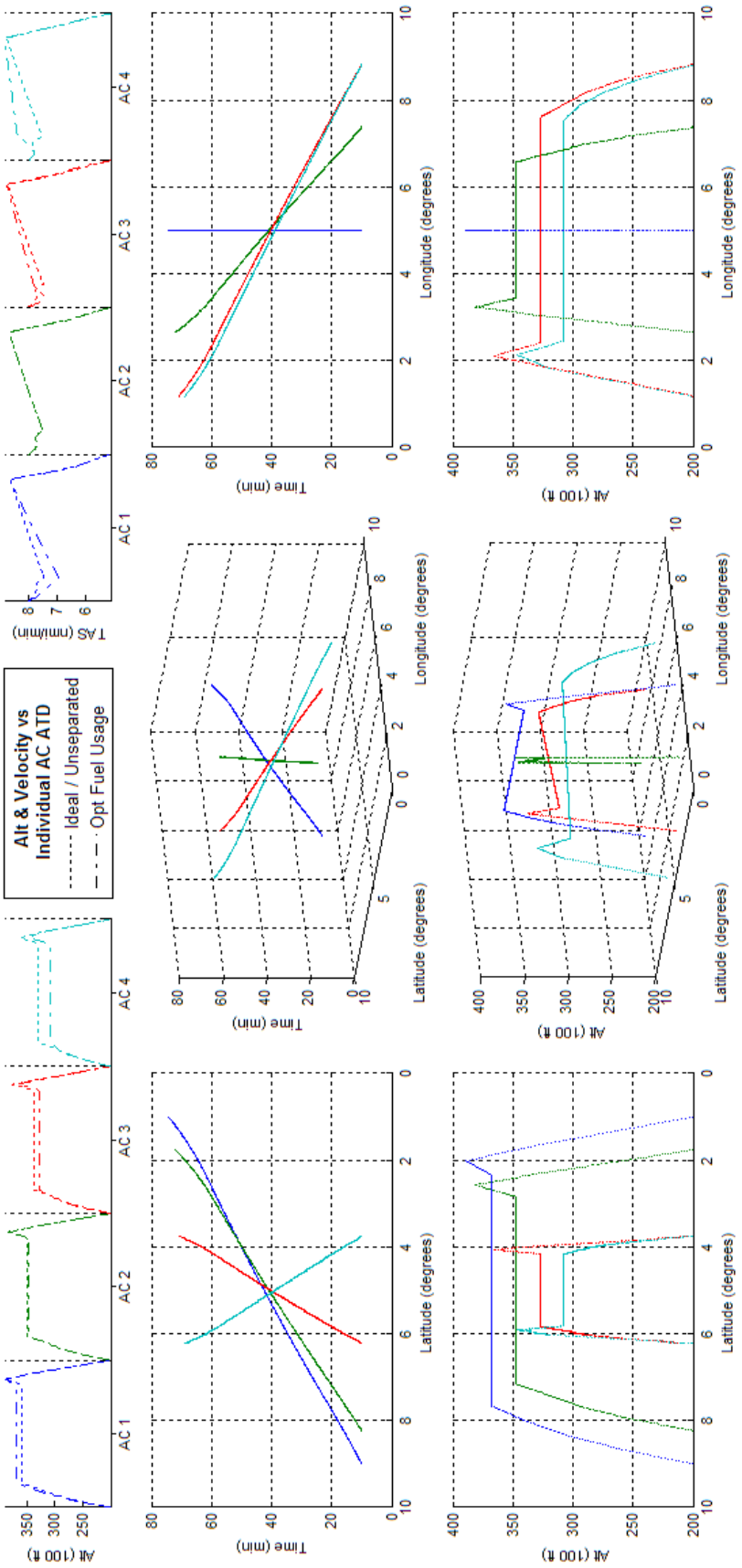

Figure 303 - Fuel Optimized 4acCO ATD_{R2} Results

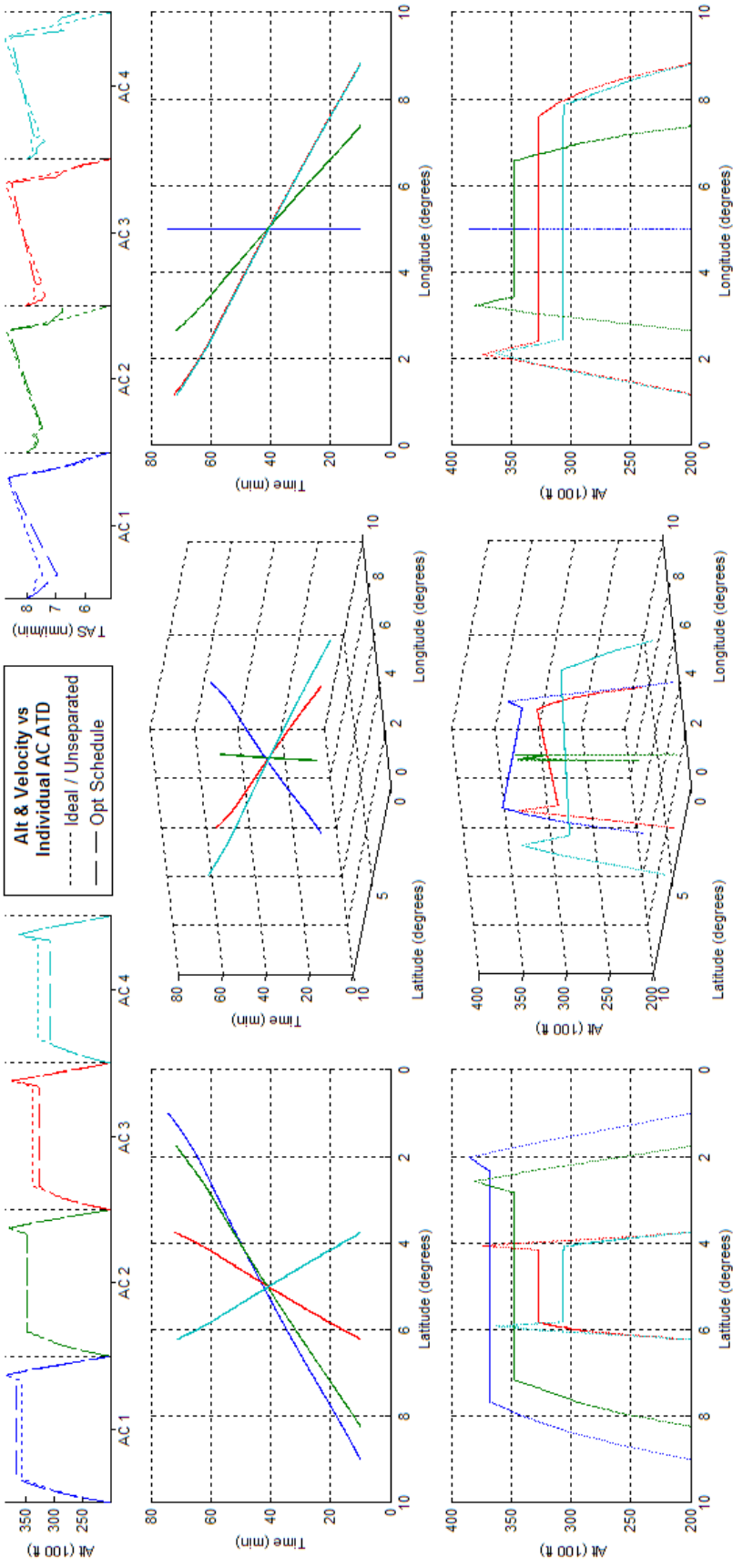

Figure 304 -Schedule Optimized 4acCO ATD_{R2} Results

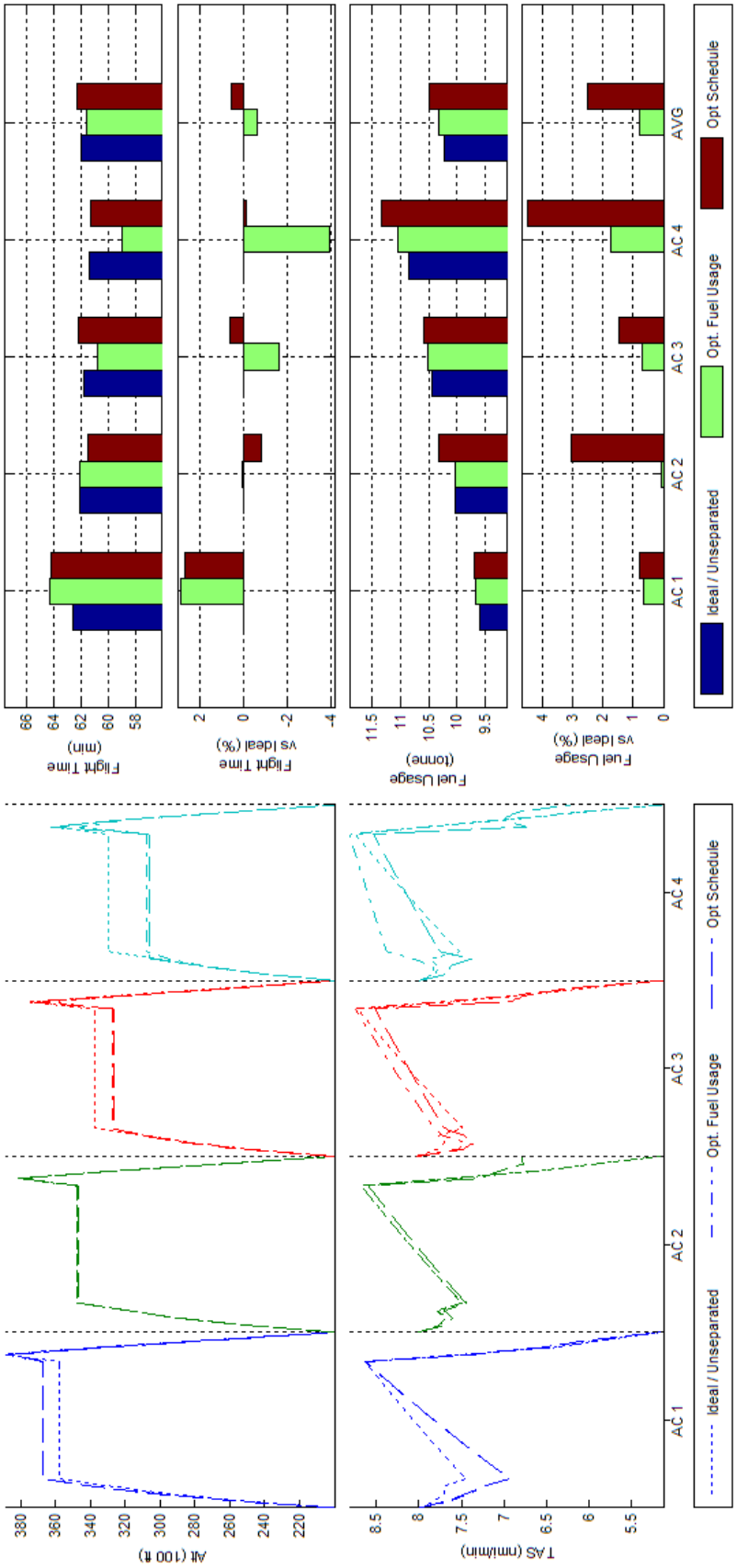

Figure 305 Trajectory Shape, Flight Time, and Fuel Consumption Comparisons of Fuel and Schedule Optimized 4acCO ATD_{R2} Results

L.15 BADA Boeing 747-300 - Scenario 4acCO - ATD_{R3}

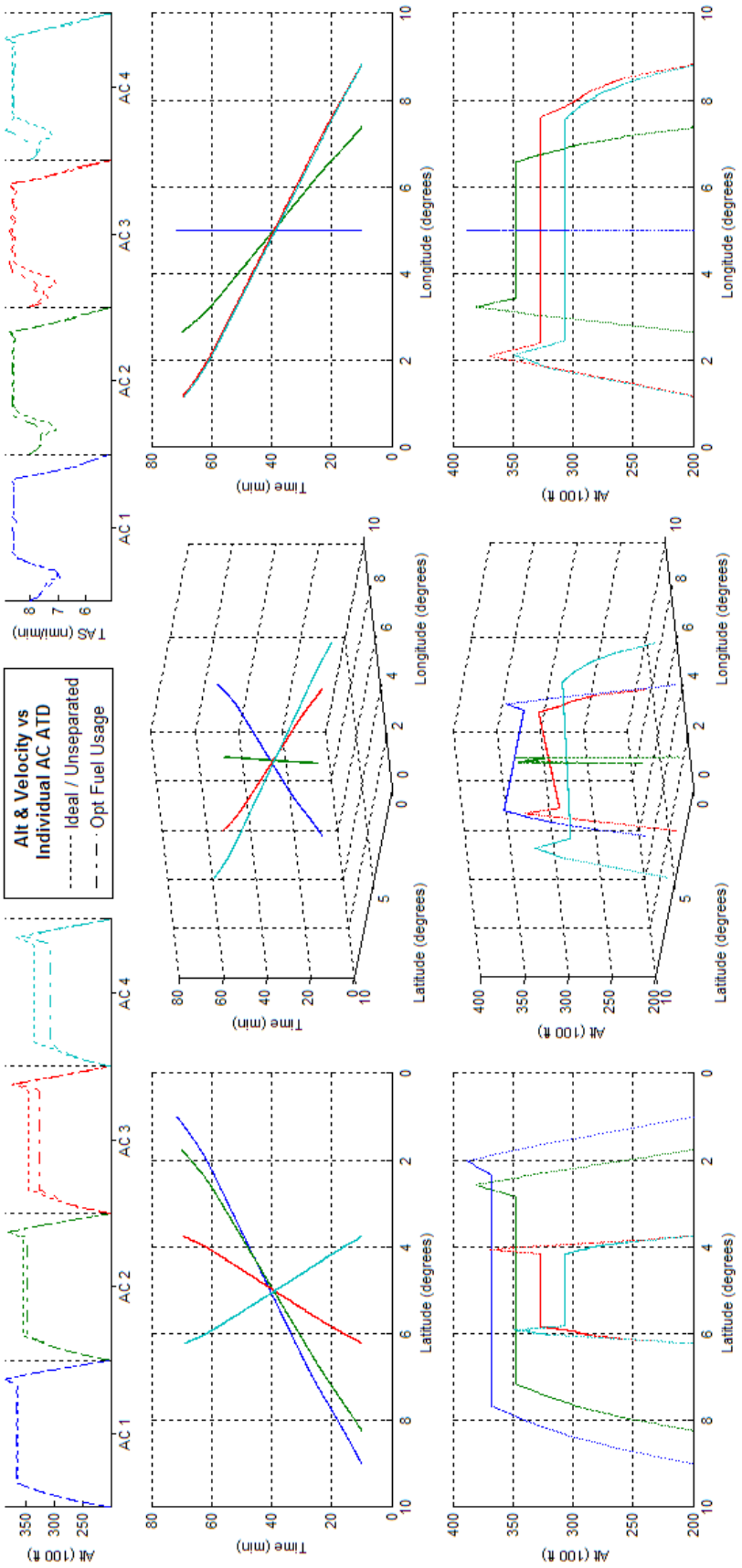

Figure 306 - Fuel Optimized 4acCO ATD_{R3} Results

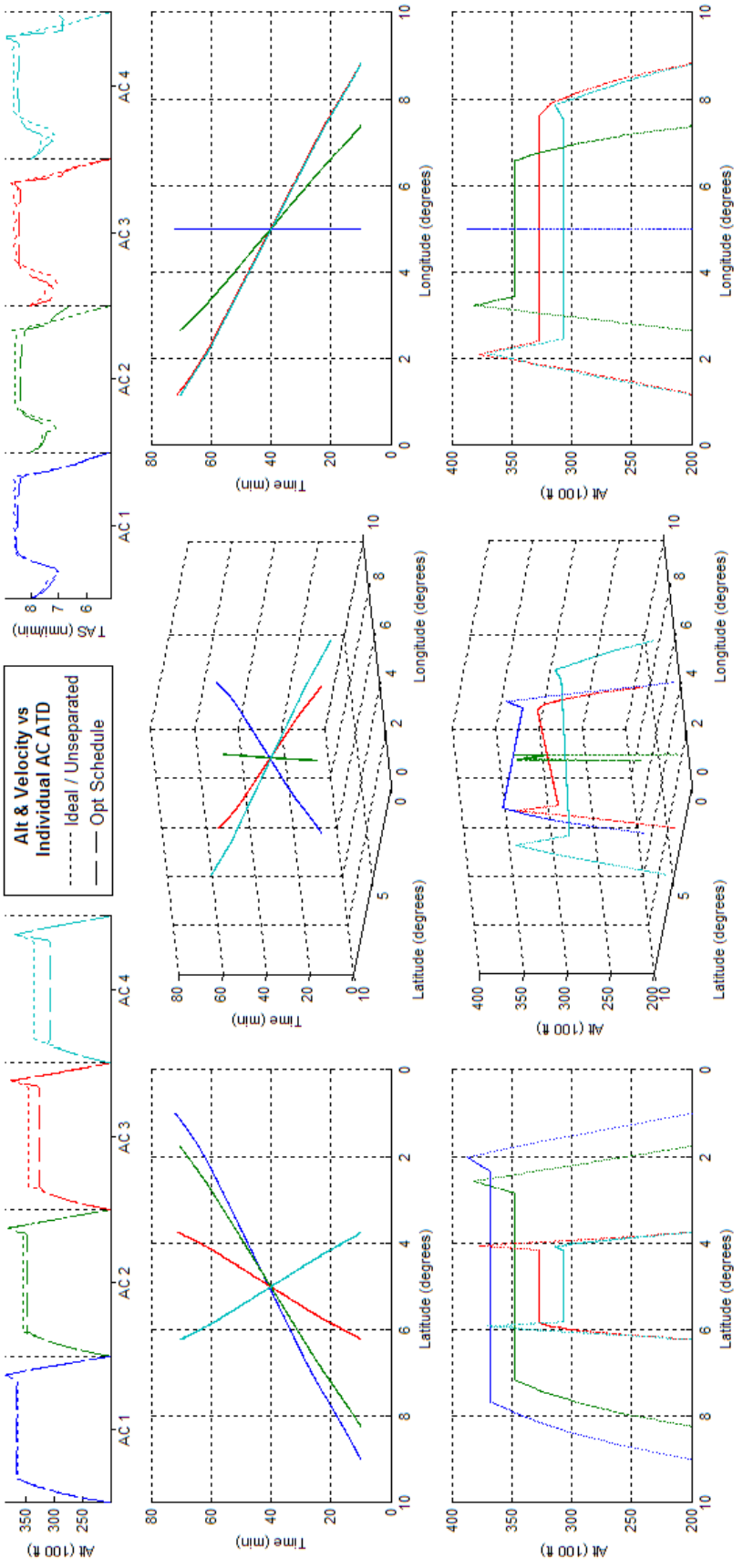

Figure 307 -Schedule Optimized 4acCO ATD_{R3} Results

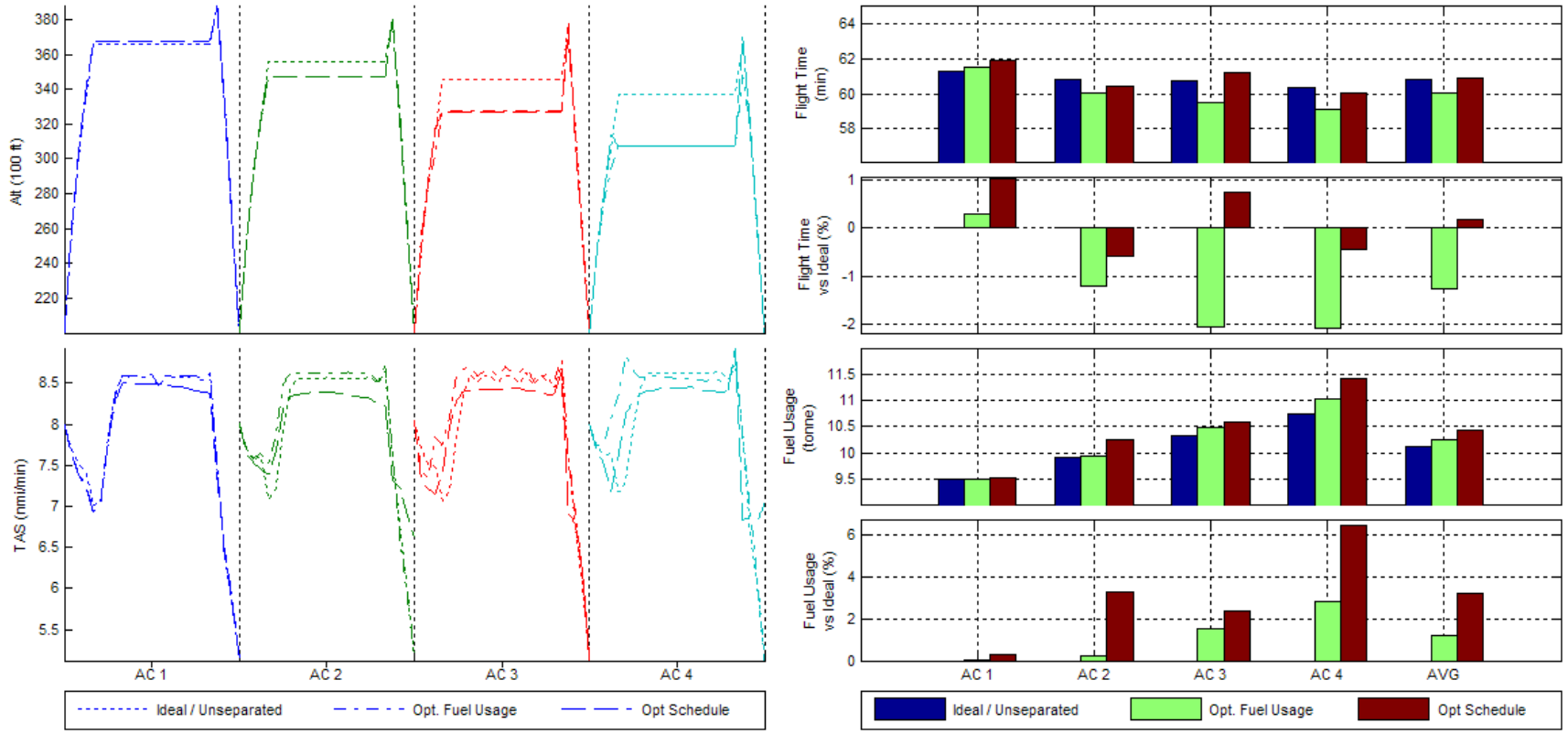

Figure 308 Trajectory Shape, Flight Time, and Fuel Consumption Comparisons of Fuel and Schedule Optimized 4acCO ATD_{R3} Results

L.16 BADA Boeing 747-300 - Scenario 10acCO - ATD_{R1}

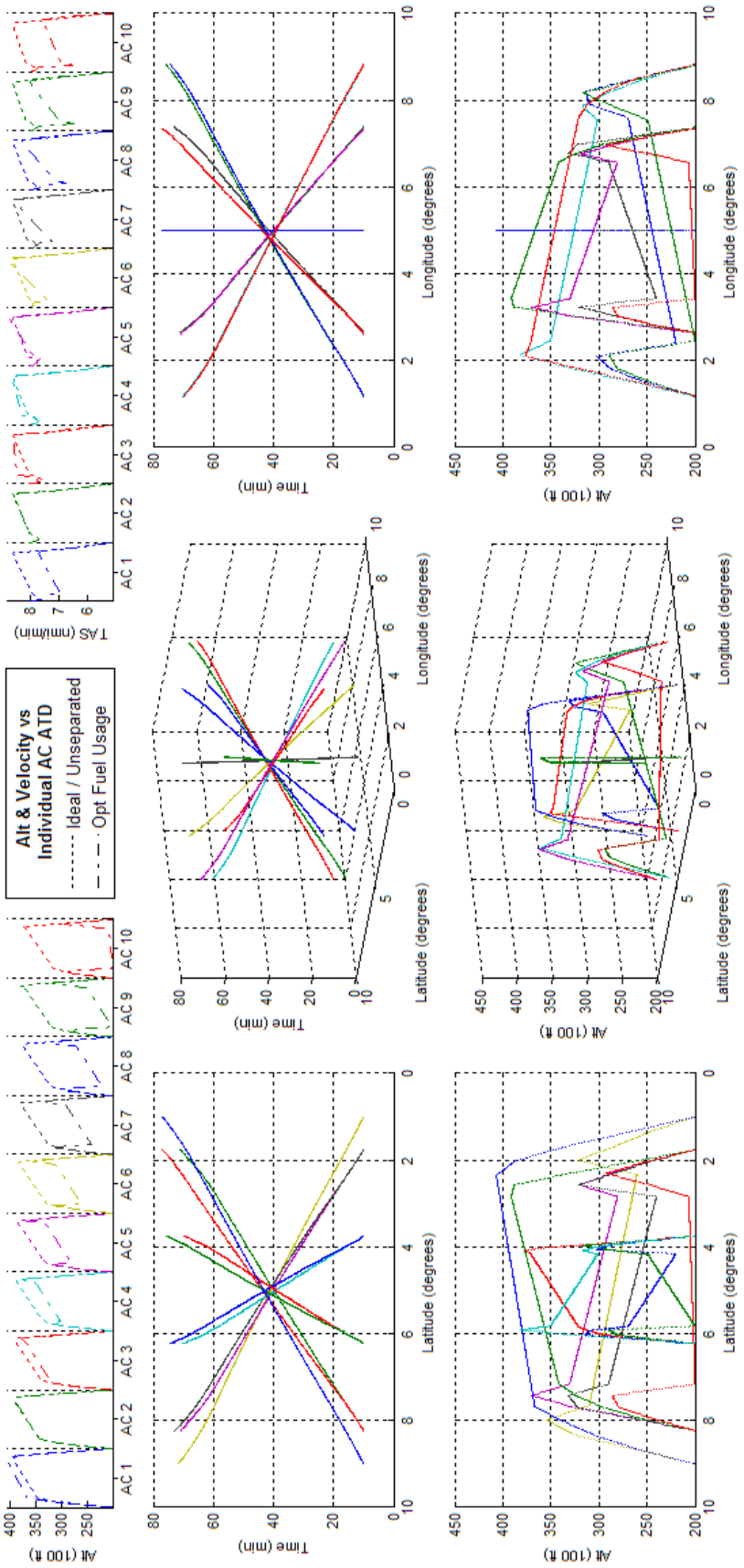

Figure 309 - Fuel Optimized 10acCO ATD_{R1} Results

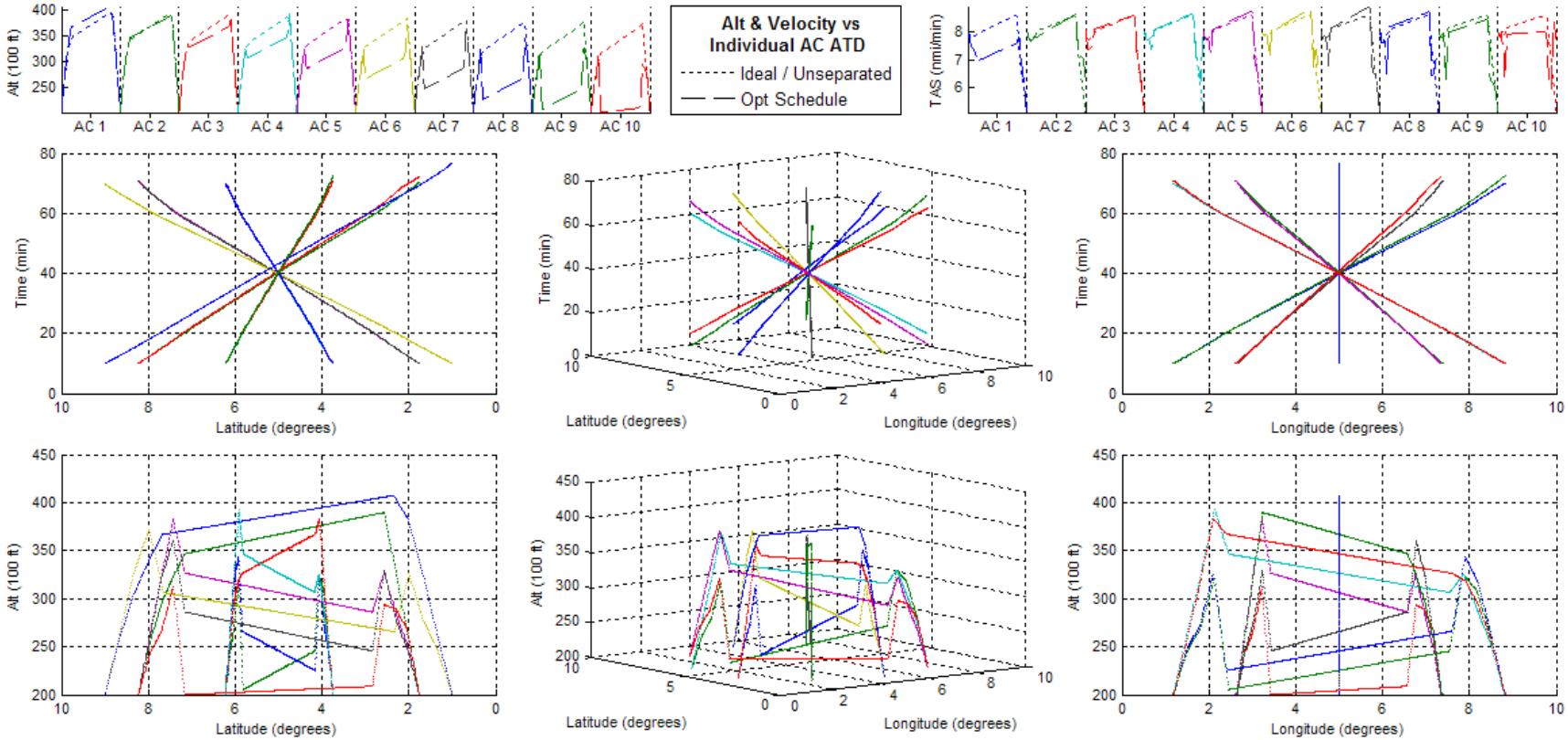

Figure 310 -Schedule Optimized 10acCO ATD_{R1} Results

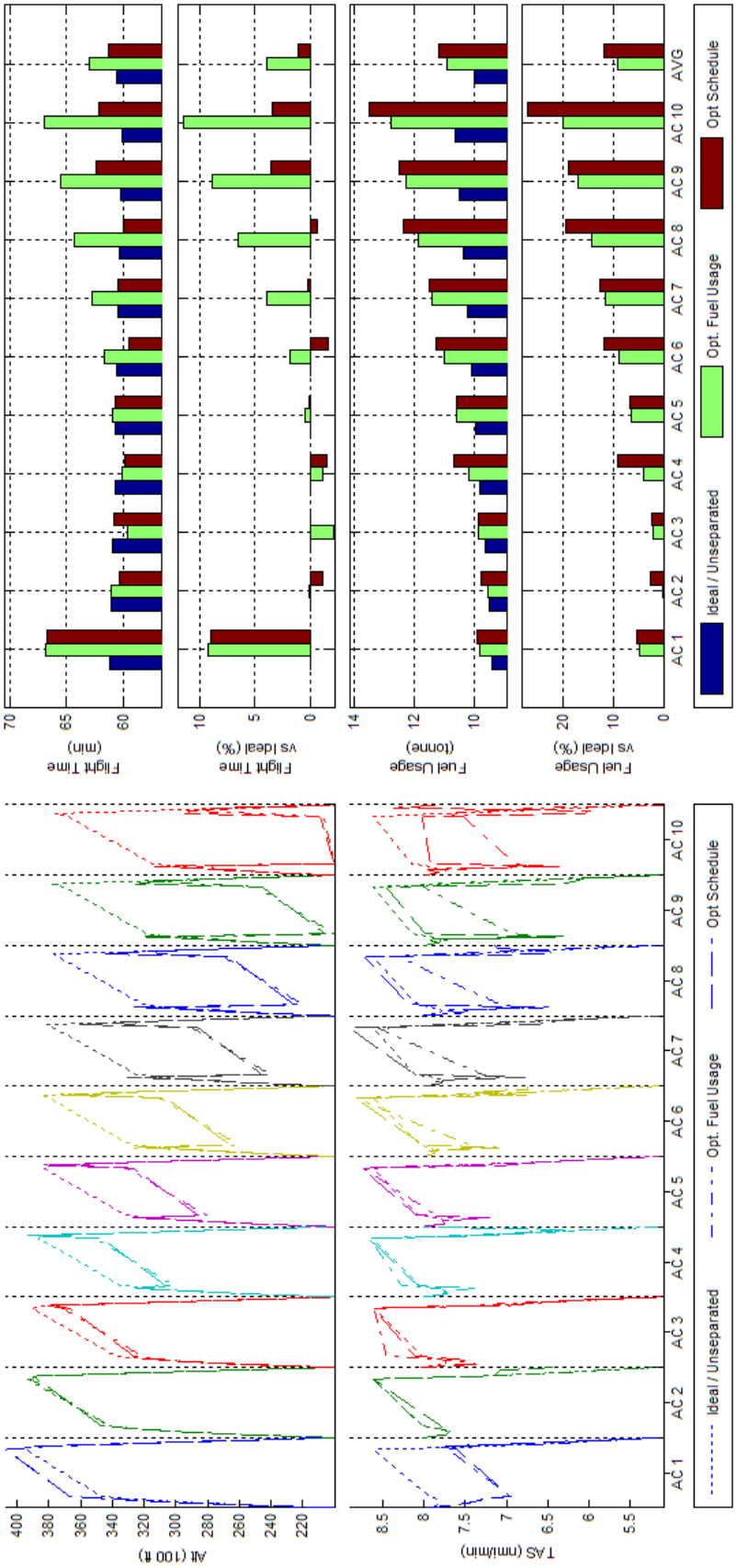

Figure 311 Trajectory Shape, Flight Time, and Fuel Consumption Comparisons of Fuel and Schedule Optimized 10acCO ATD_{RI} Results

L.17 BADA Boeing 747-300 - Scenario 10acCO - ATD_{R2}

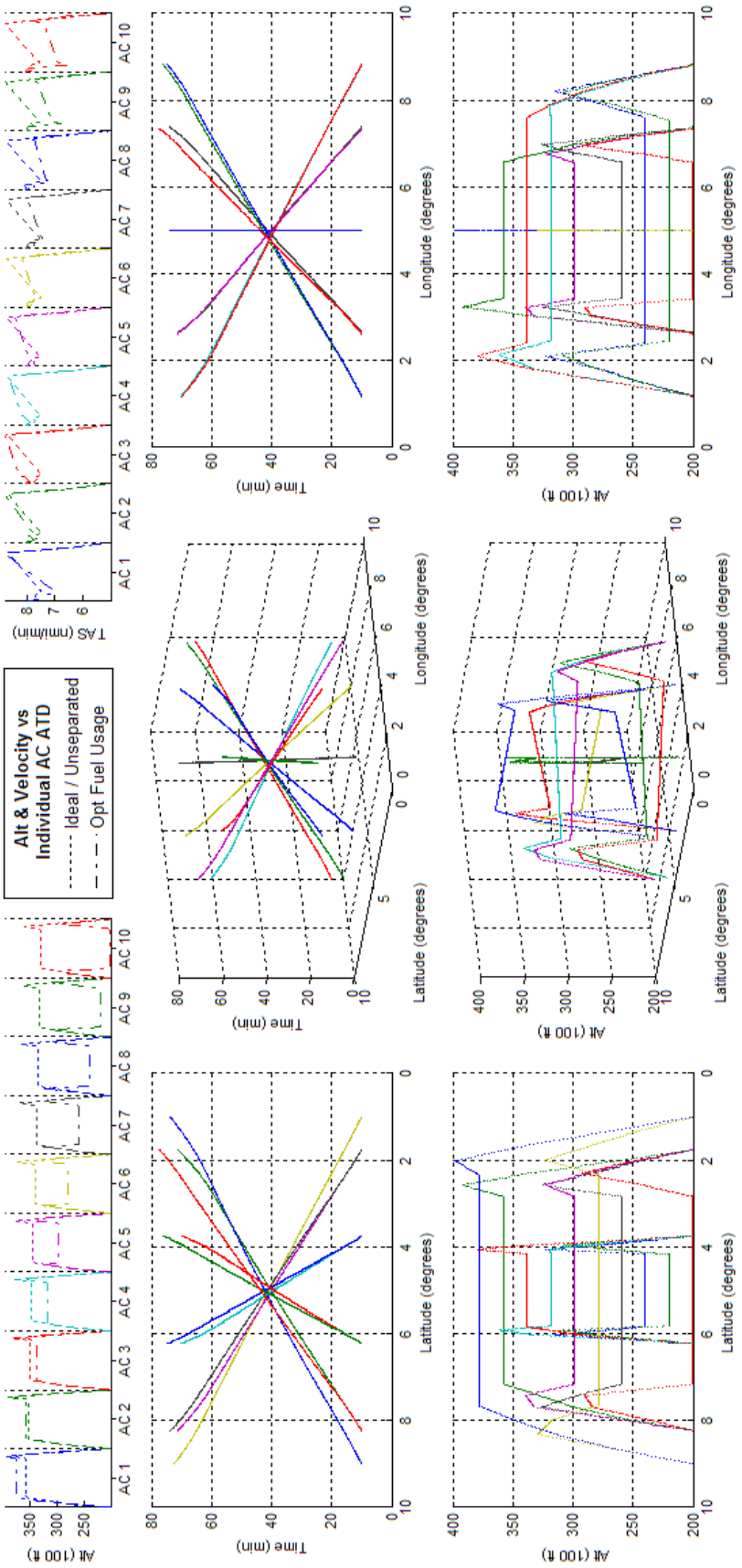

Figure 312 - Fuel Optimized 10acCO ATD_{R2} Results

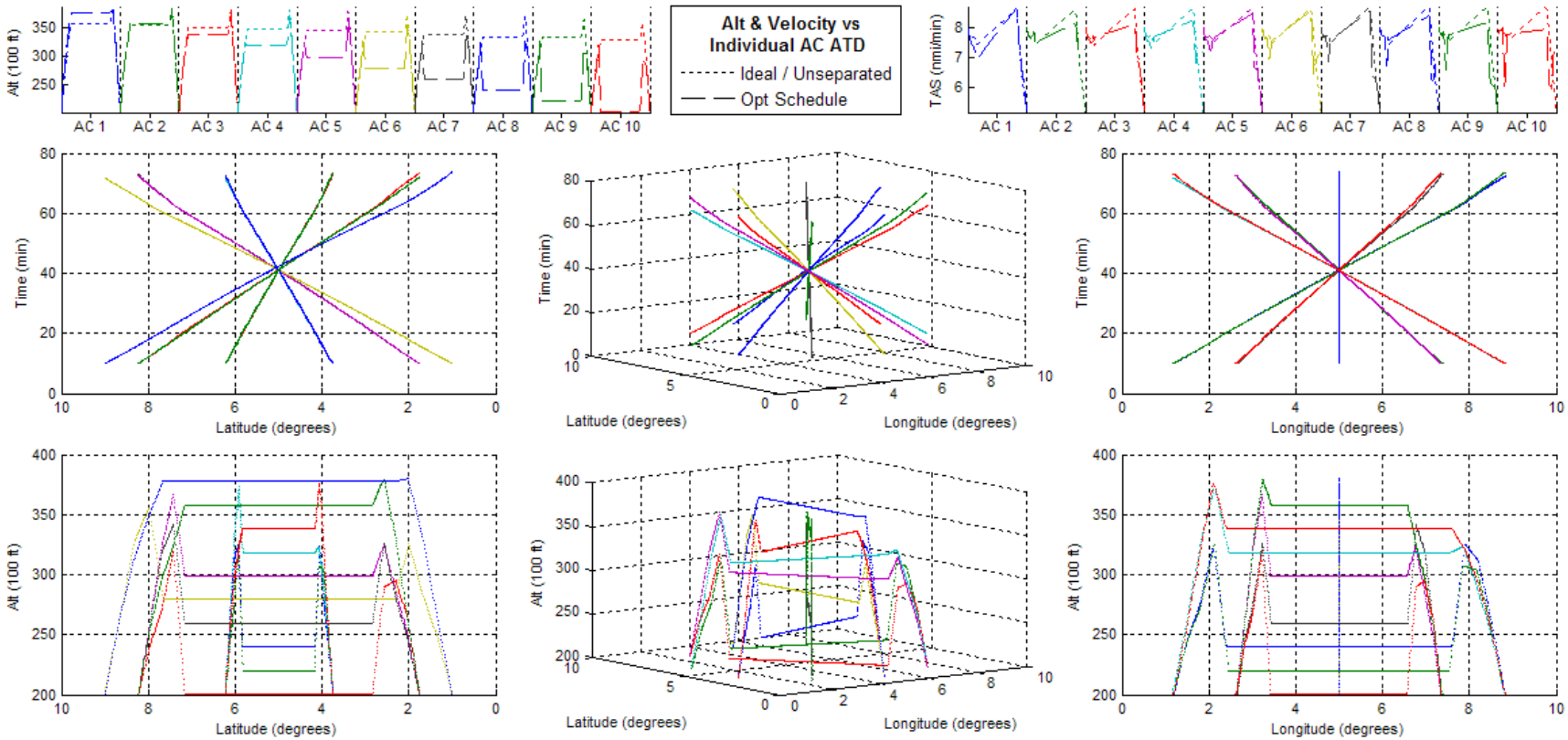

Figure 313 -Schedule Optimized 10acCO ATD_{R2} Results

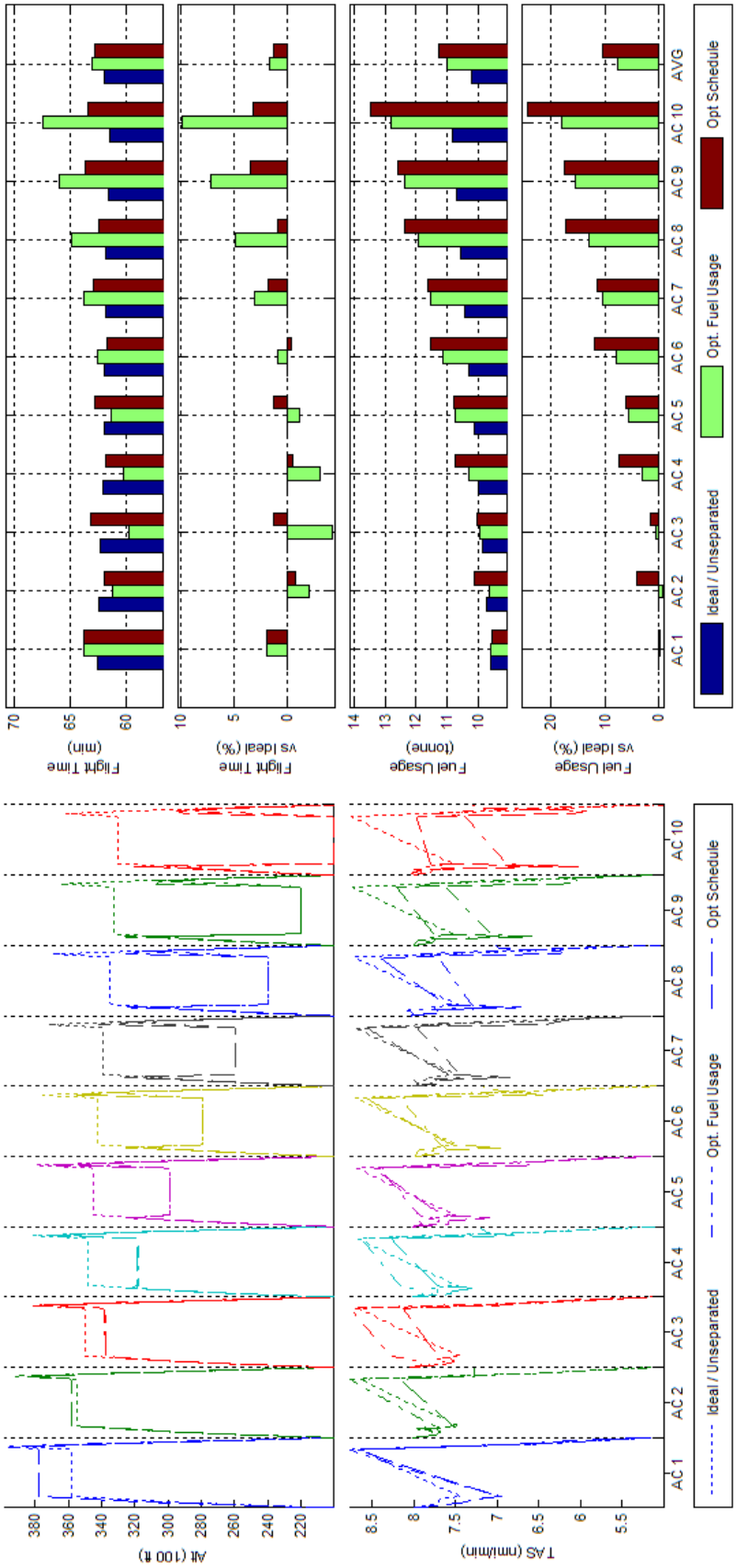

Figure 314 Trajectory Shape, Flight Time, and Fuel Consumption Comparisons of Fuel and Schedule Optimized 10acCO ATD_{R2} Results

L.18 BADA Boeing 747-300 - Scenario 10acCO - ATD_{R3}

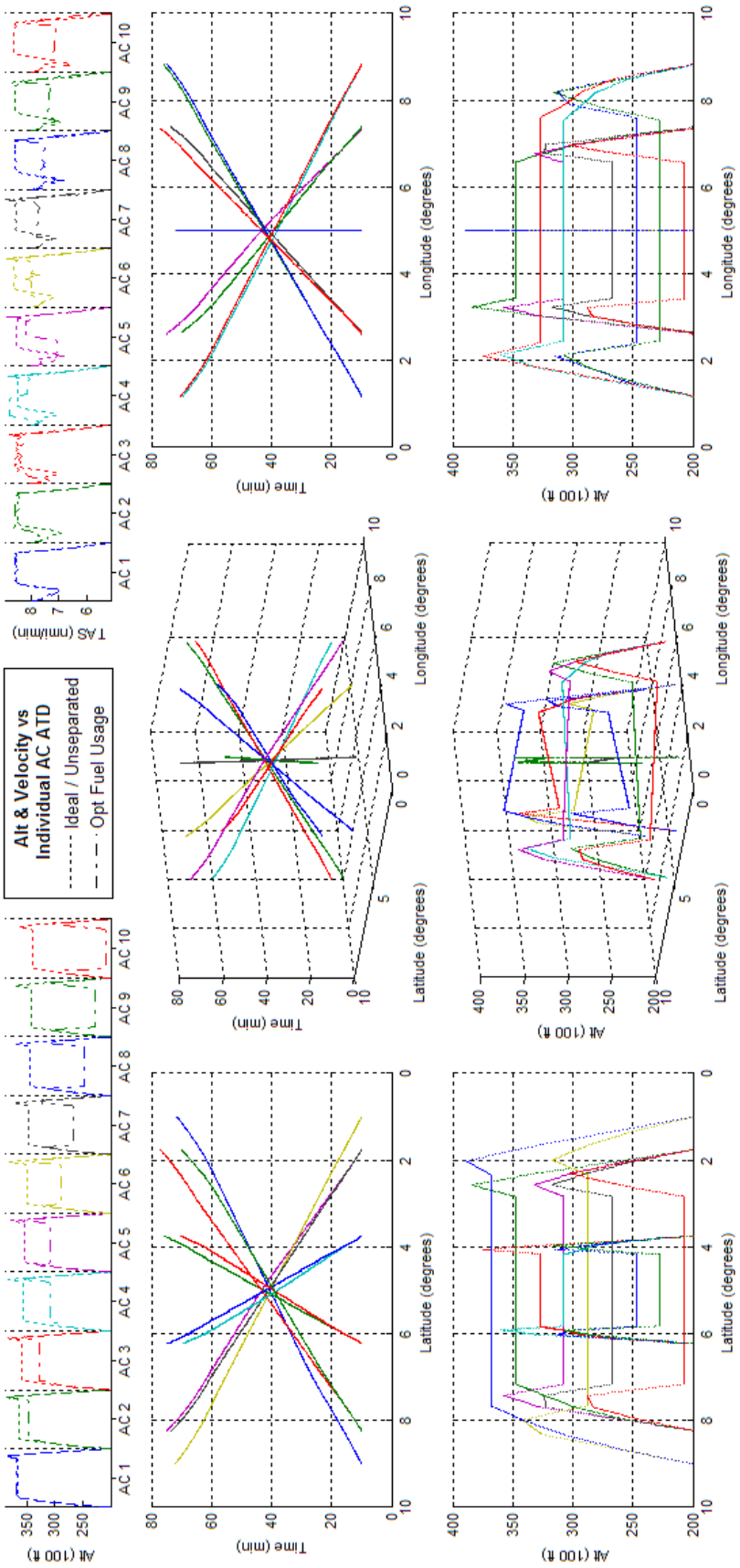

Figure 315 - Fuel Optimized 10acCO ATD_{R3} Results

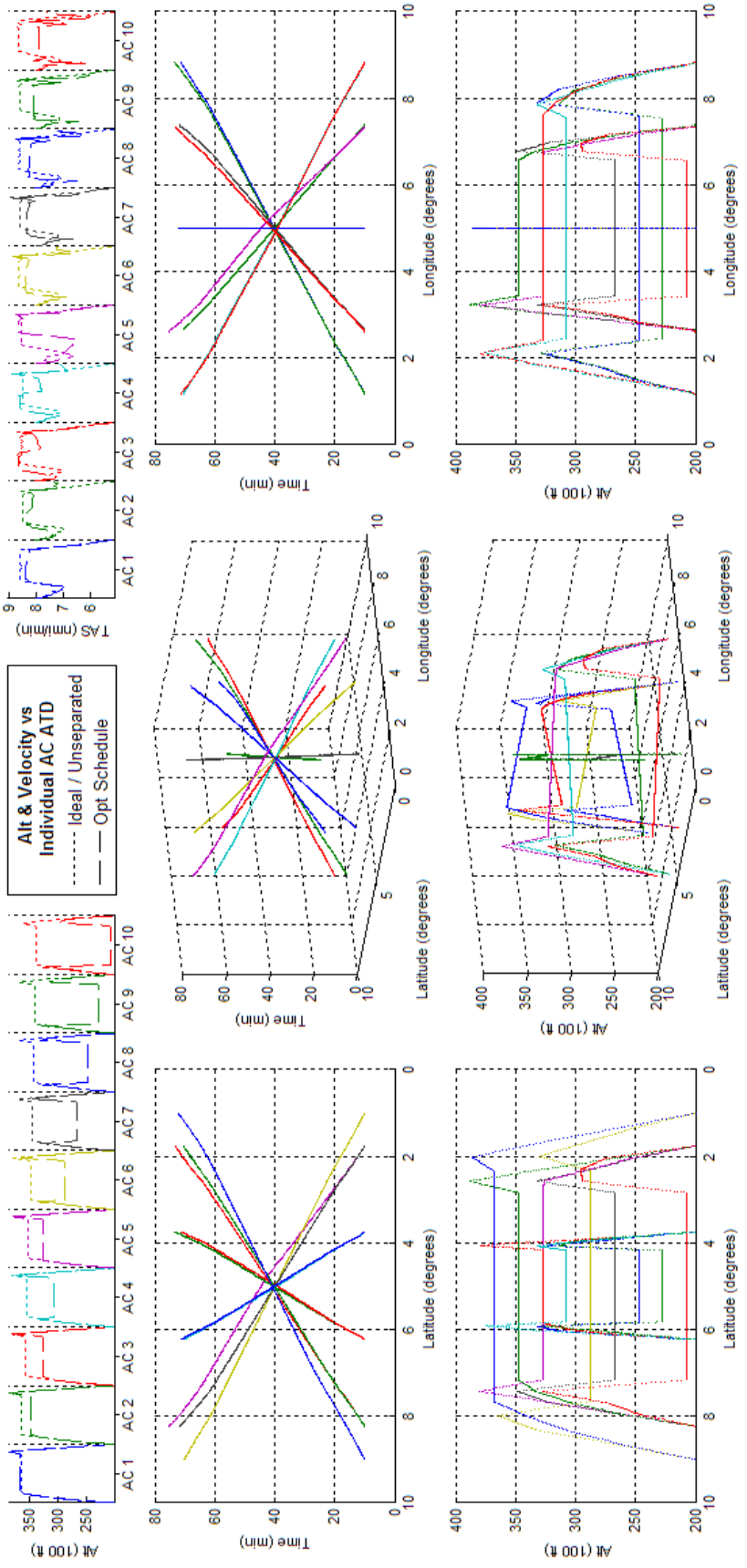

Figure 316 -Schedule Optimized 10acCO ATD_{R3} Results

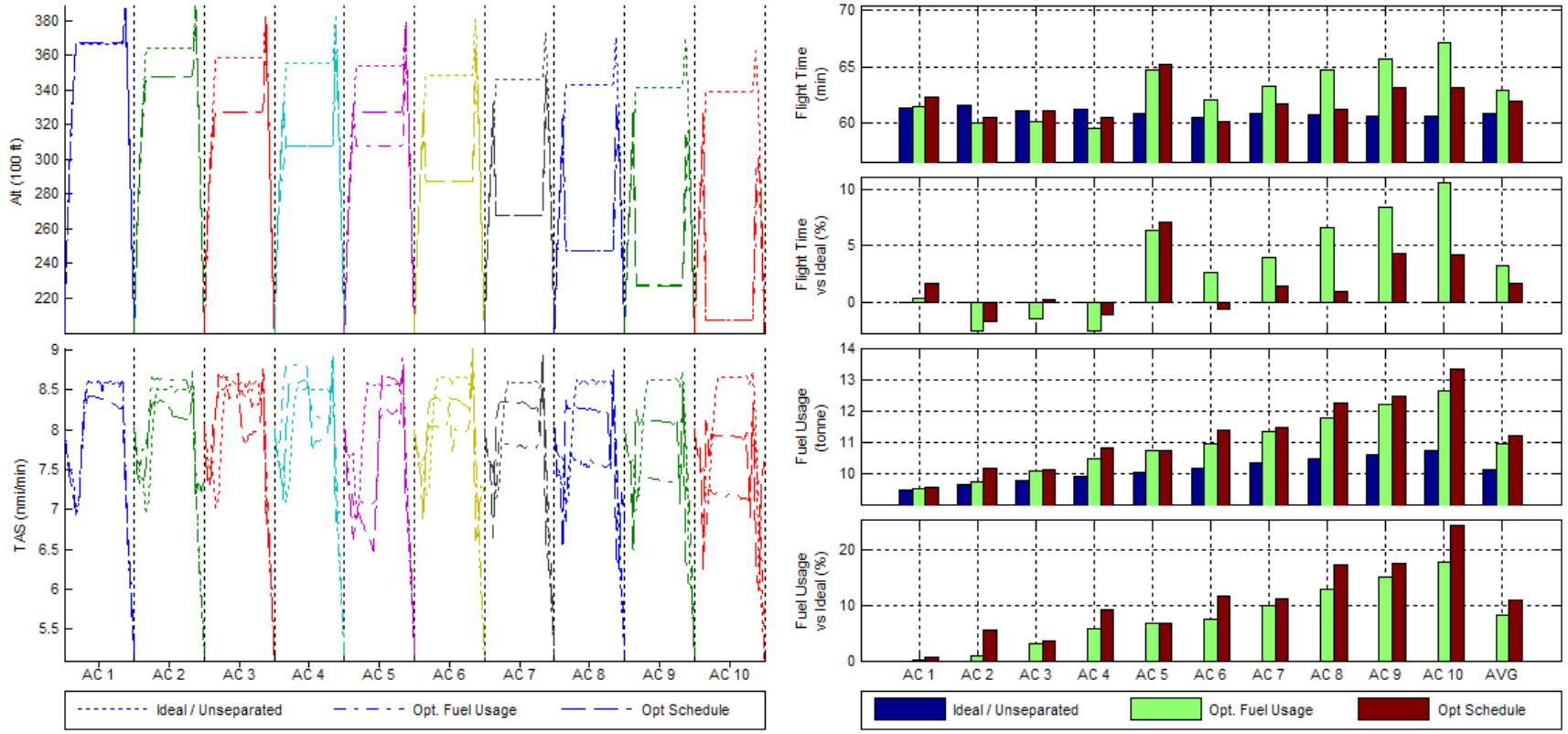

Figure 317 Trajectory Shape, Flight Time, and Fuel Consumption Comparisons of Fuel and Schedule Optimized 10acCO ATD_{R3} Results

L.19 BADA Boeing 747-300 - Scenario 4acCH - ATD_{R1}

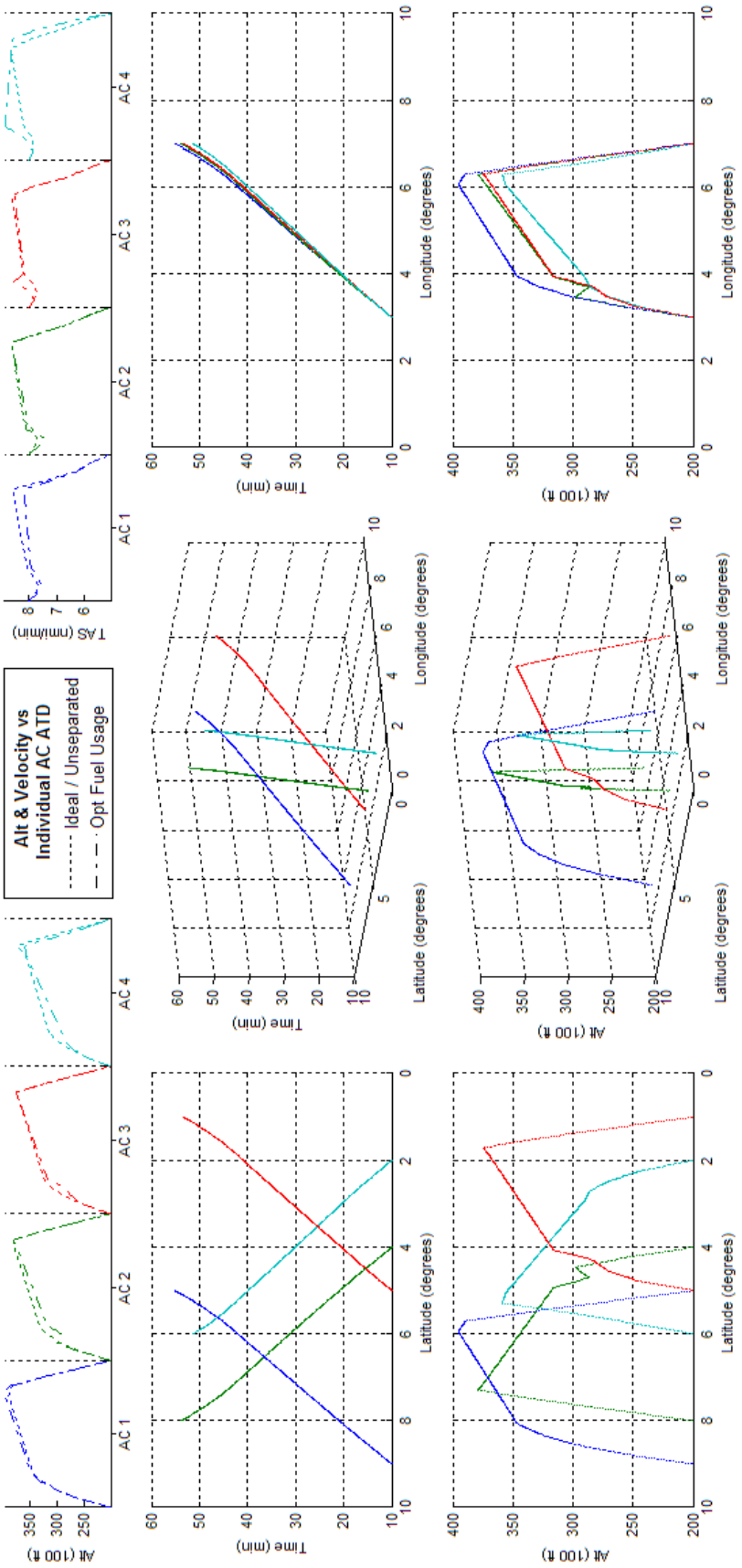

Figure 318 - Fuel Optimized 4acCH ATD_{R1} Results

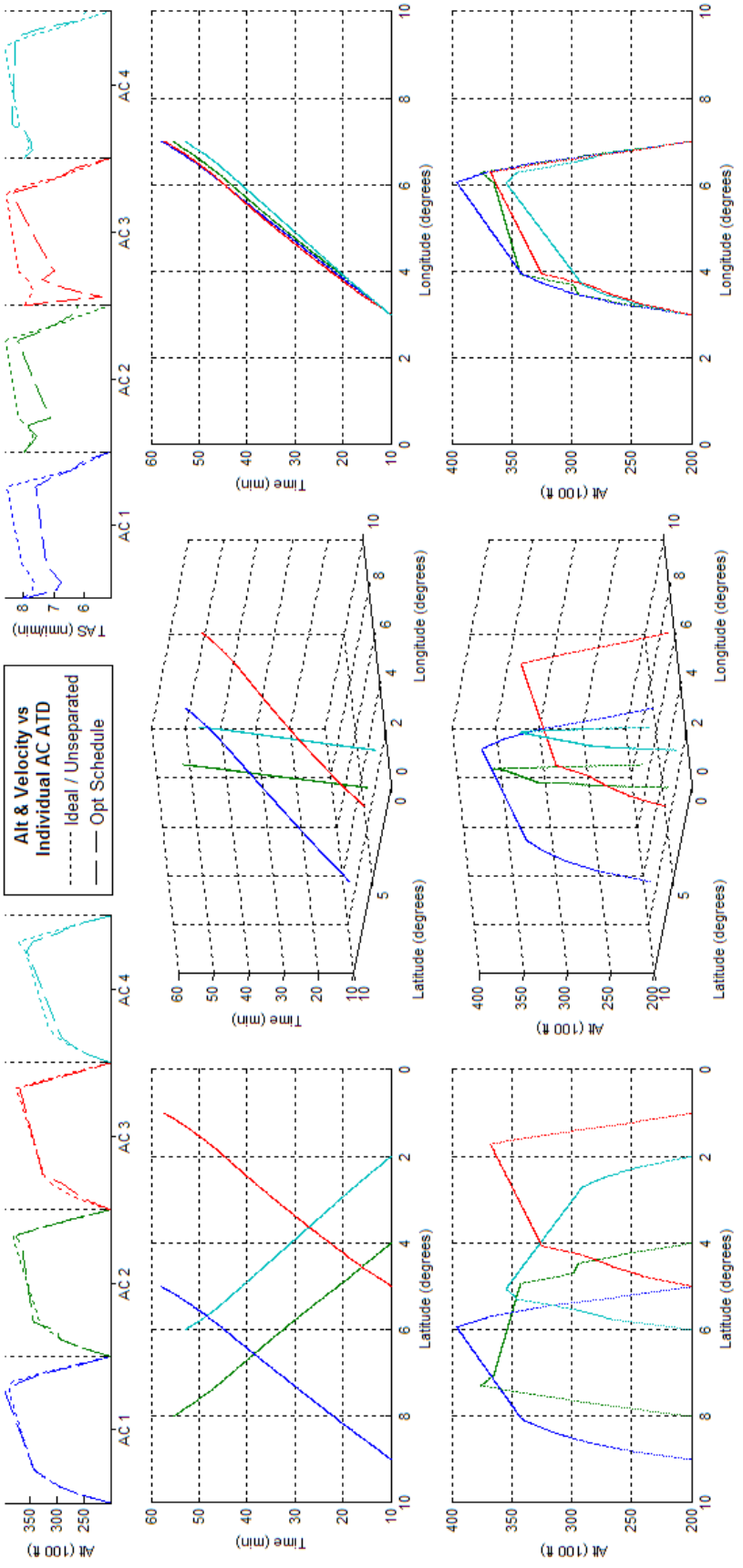

Figure 319 -Schedule Optimized 4acCH ATD_{R1} Results

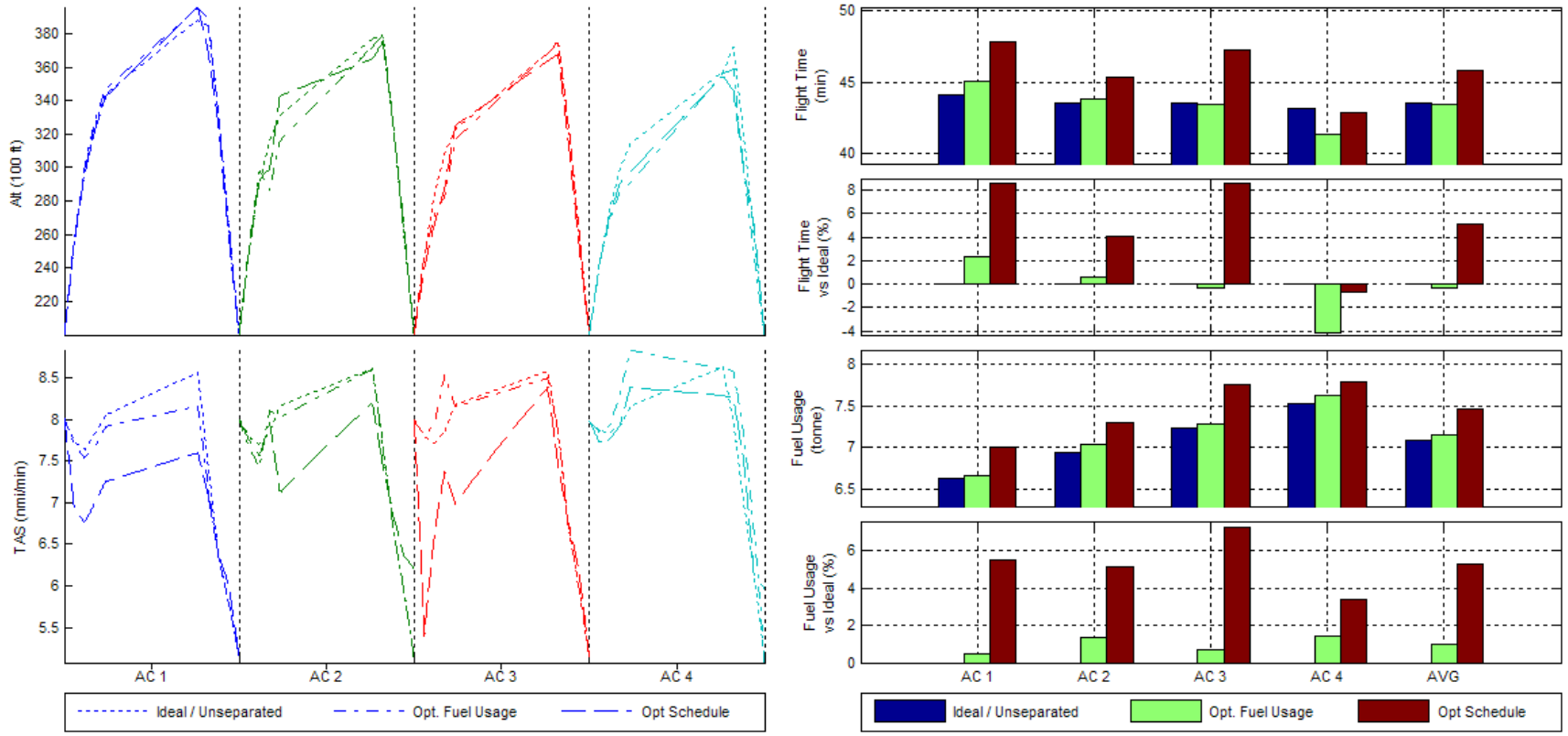

Figure 320 Trajectory Shape, Flight Time, and Fuel Consumption Comparisons of Fuel and Schedule Optimized 4acCH ATD_{R1} Results

L.20 BADA Boeing 747-300 - Scenario 4acCH - ATD_{R2}

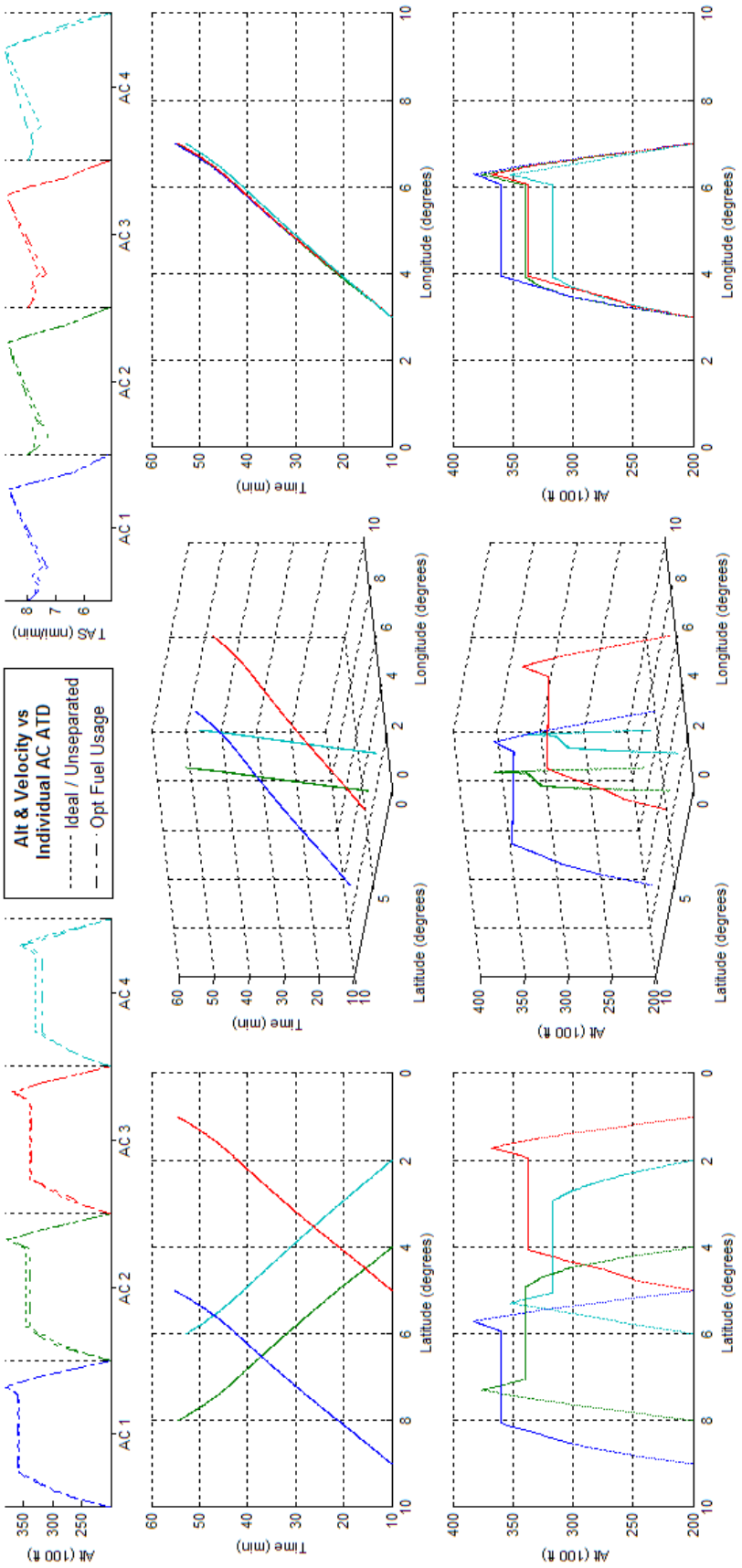

Figure 321 - Fuel Optimized 4acCH ATD_{R2} Results

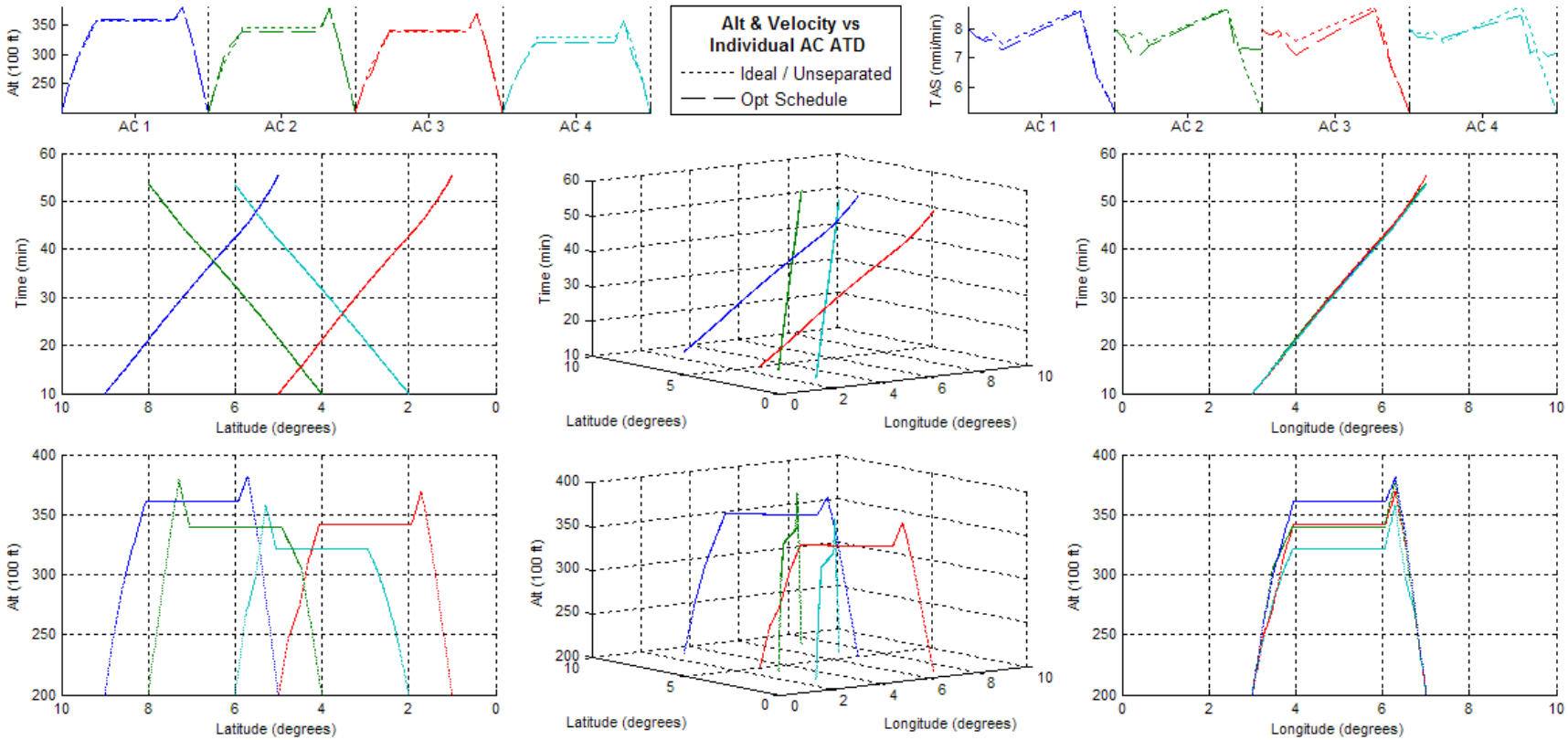

Figure 322 -Schedule Optimized 4acCH ATD_{R2} Results

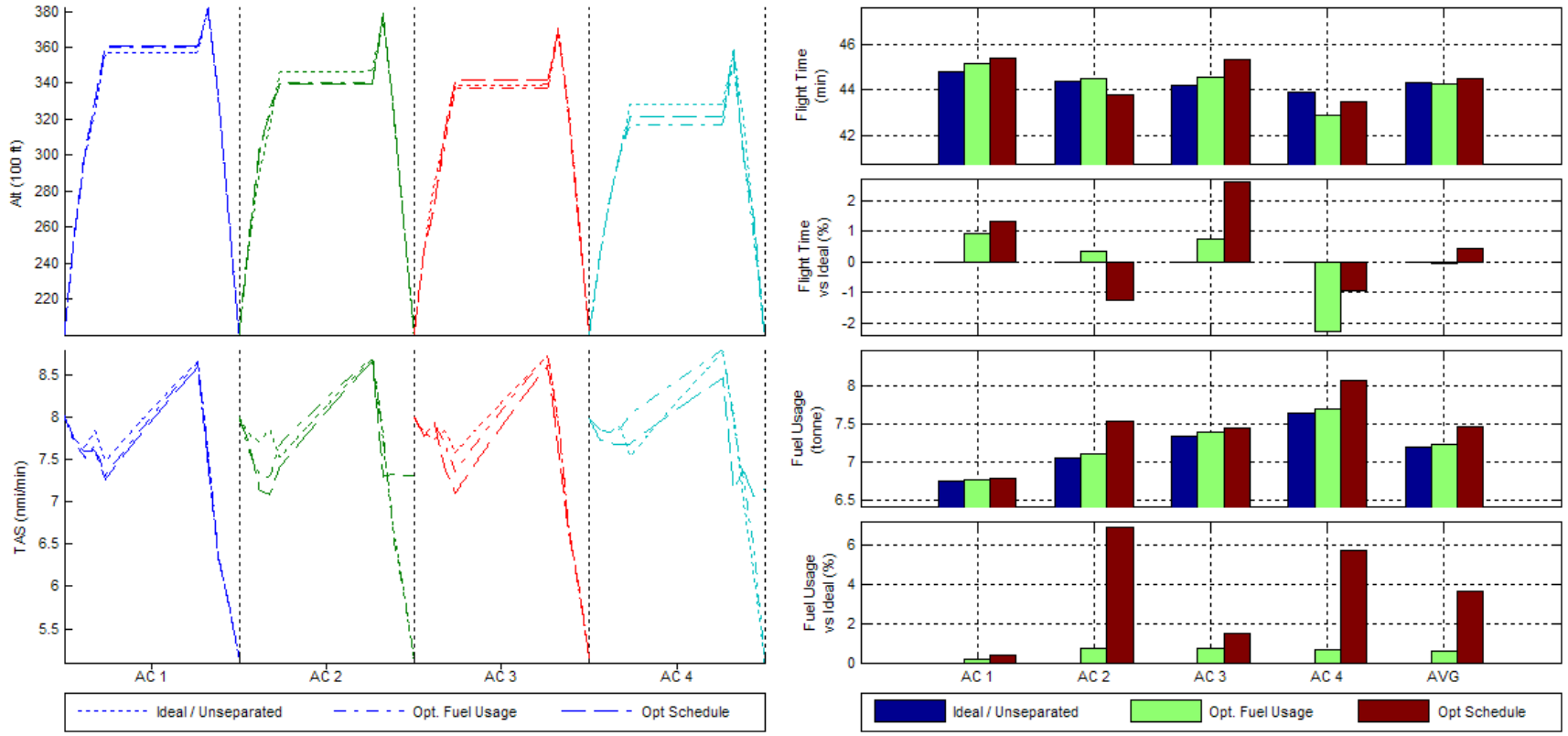

Figure 323 Trajectory Shape, Flight Time, and Fuel Consumption Comparisons of Fuel and Schedule Optimized 4acCH ATD_{R2} Results

L.21 BADA Boeing 747-300 - Scenario 4acCH - ATD_{R3}

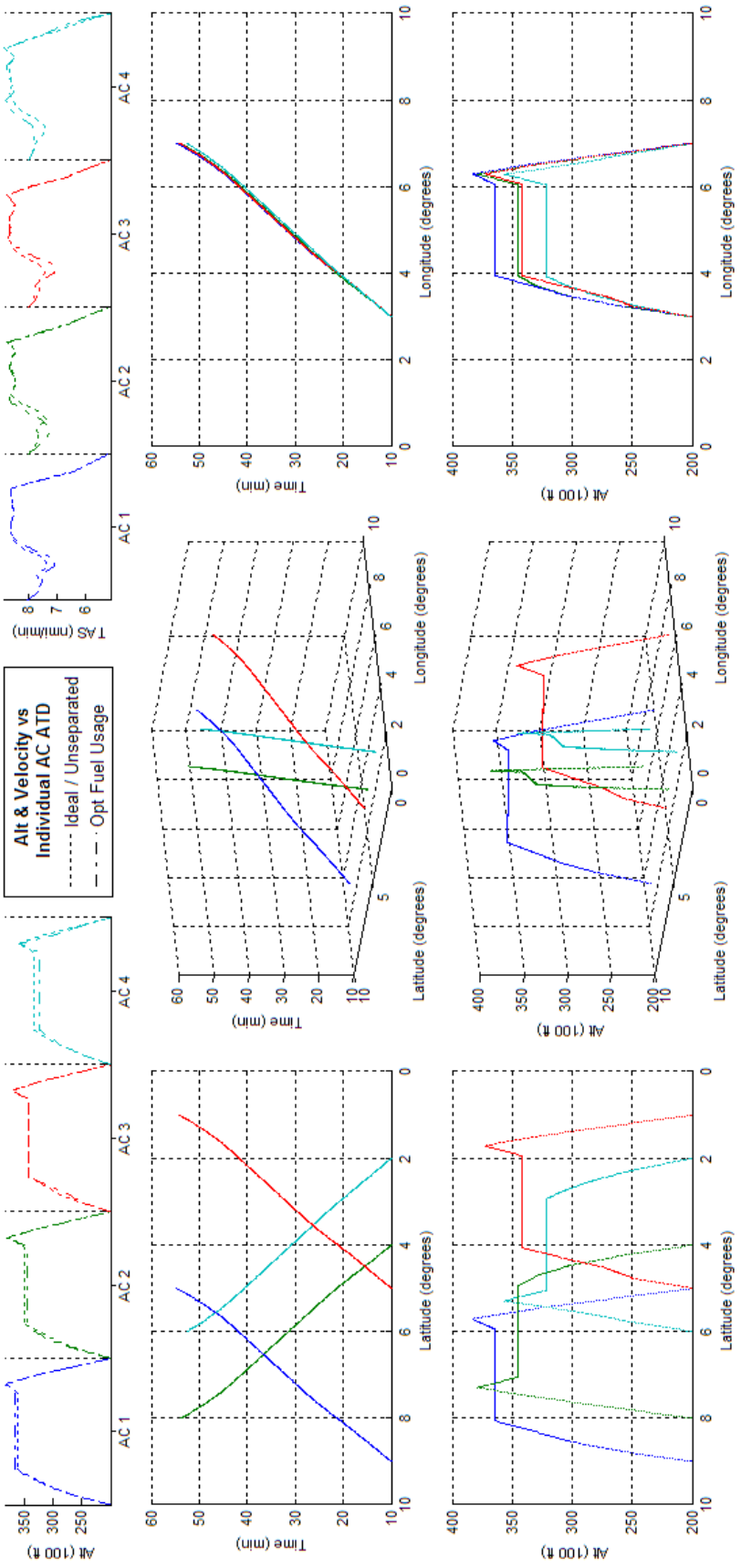

Figure 324 - Fuel Optimized 4acCH ATD_{R3} Results

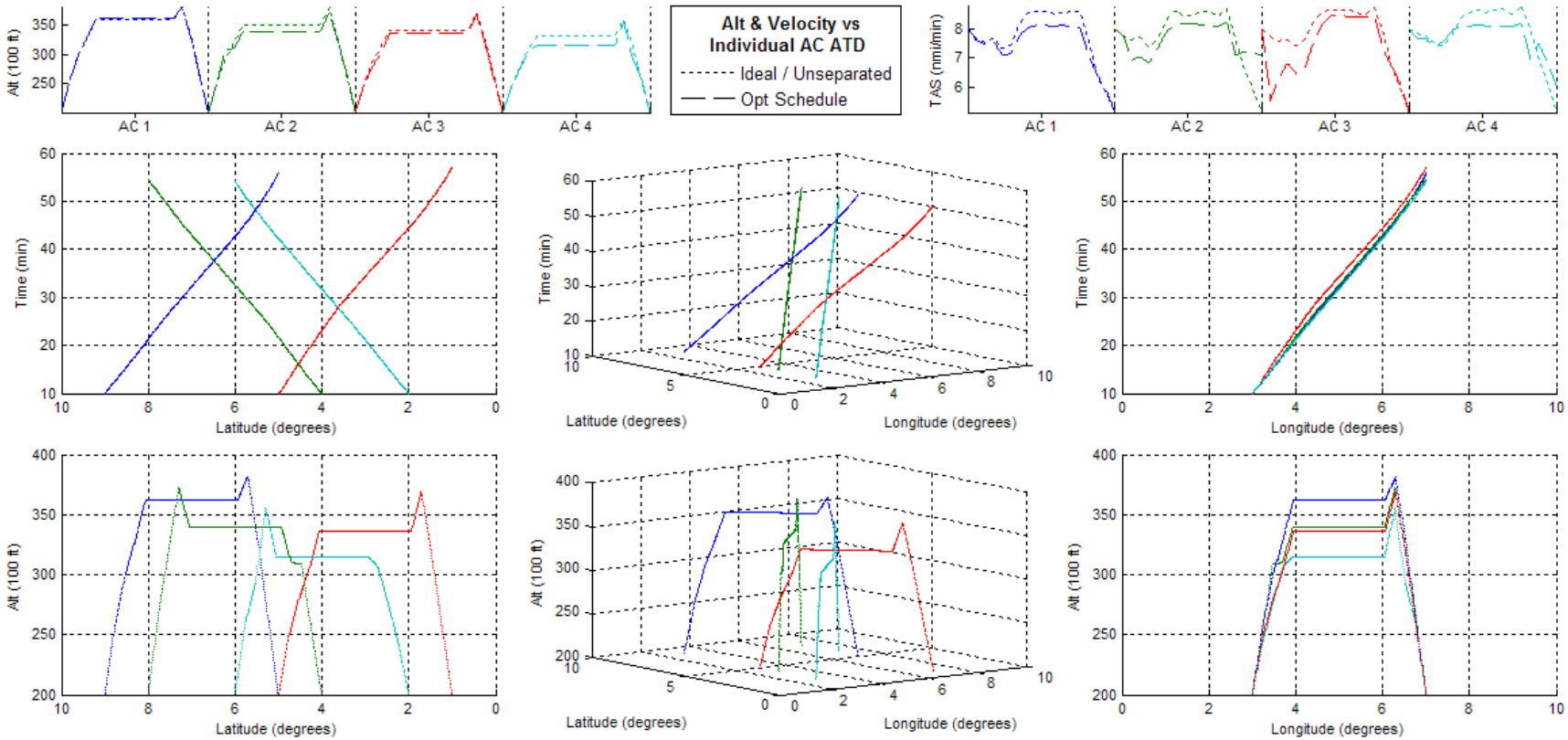

Figure 325 -Schedule Optimized 4acCH ATD_{R3} Results

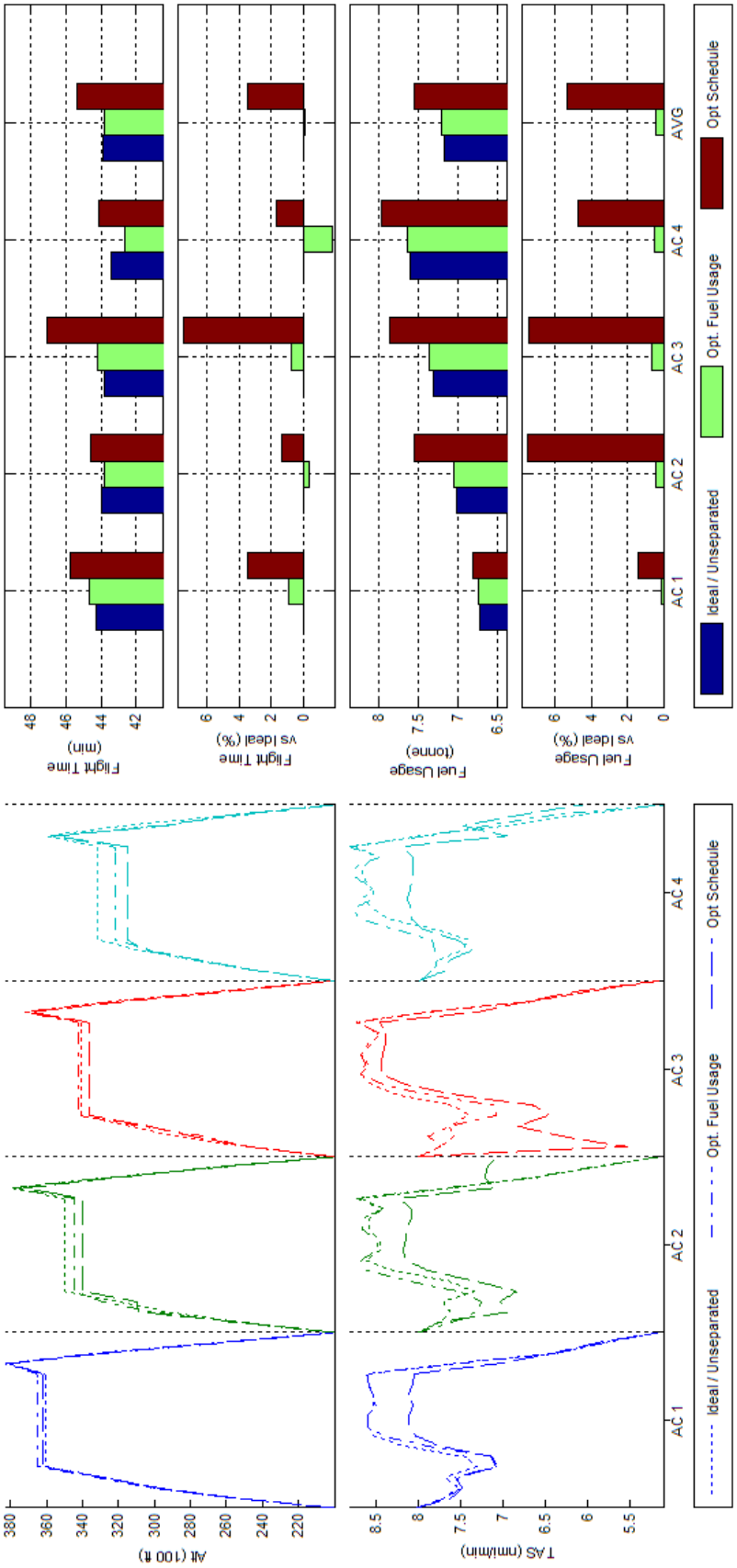

Figure 326 Trajectory Shape, Flight Time, and Fuel Consumption Comparisons of Fuel and Schedule Optimized 4acCH ATD_{R3} Results

L.22 BADA Boeing 747-300 - Scenario 10acCH - ATD_{R1}

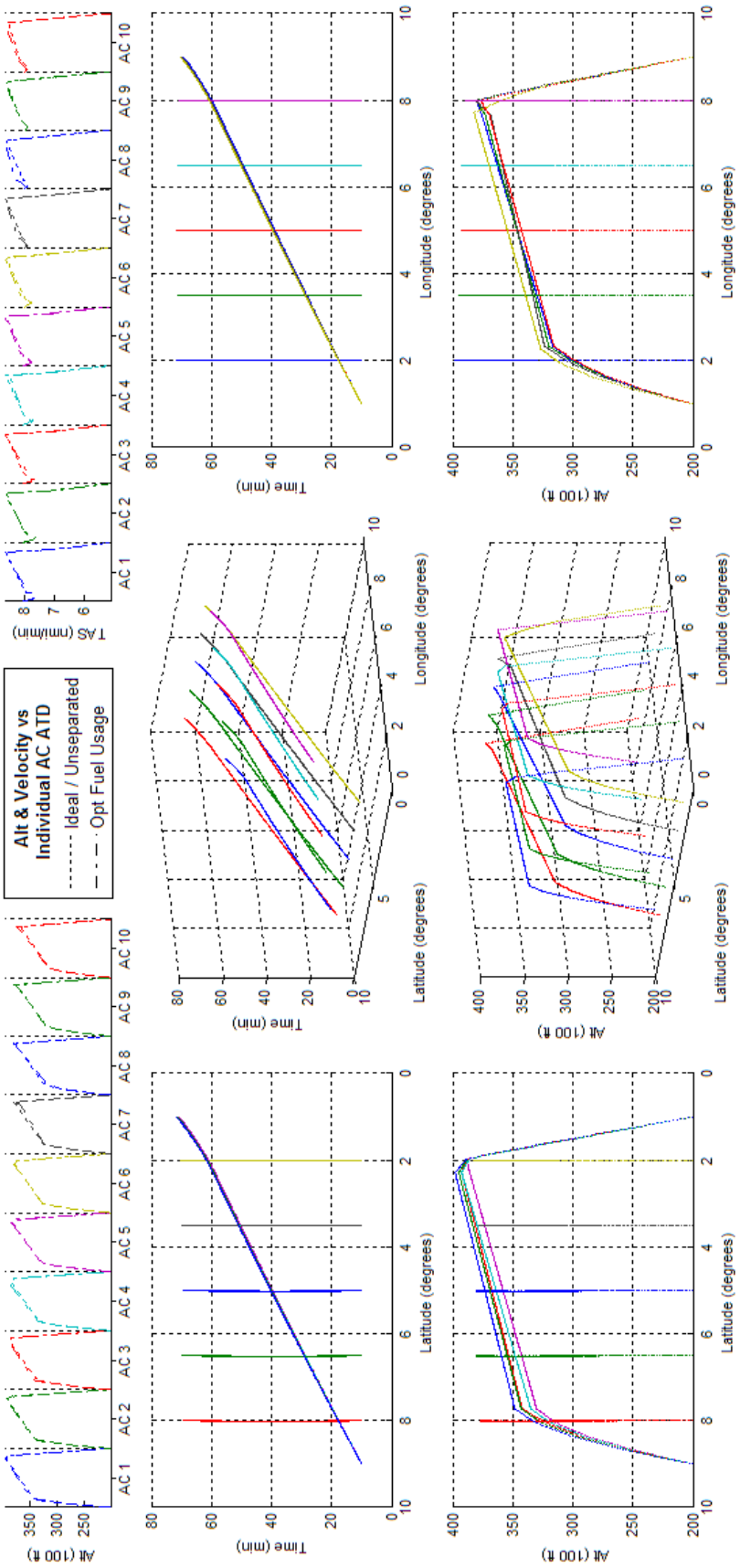

Figure 327 - Fuel Optimized 10acCH ATD_{R1} Results

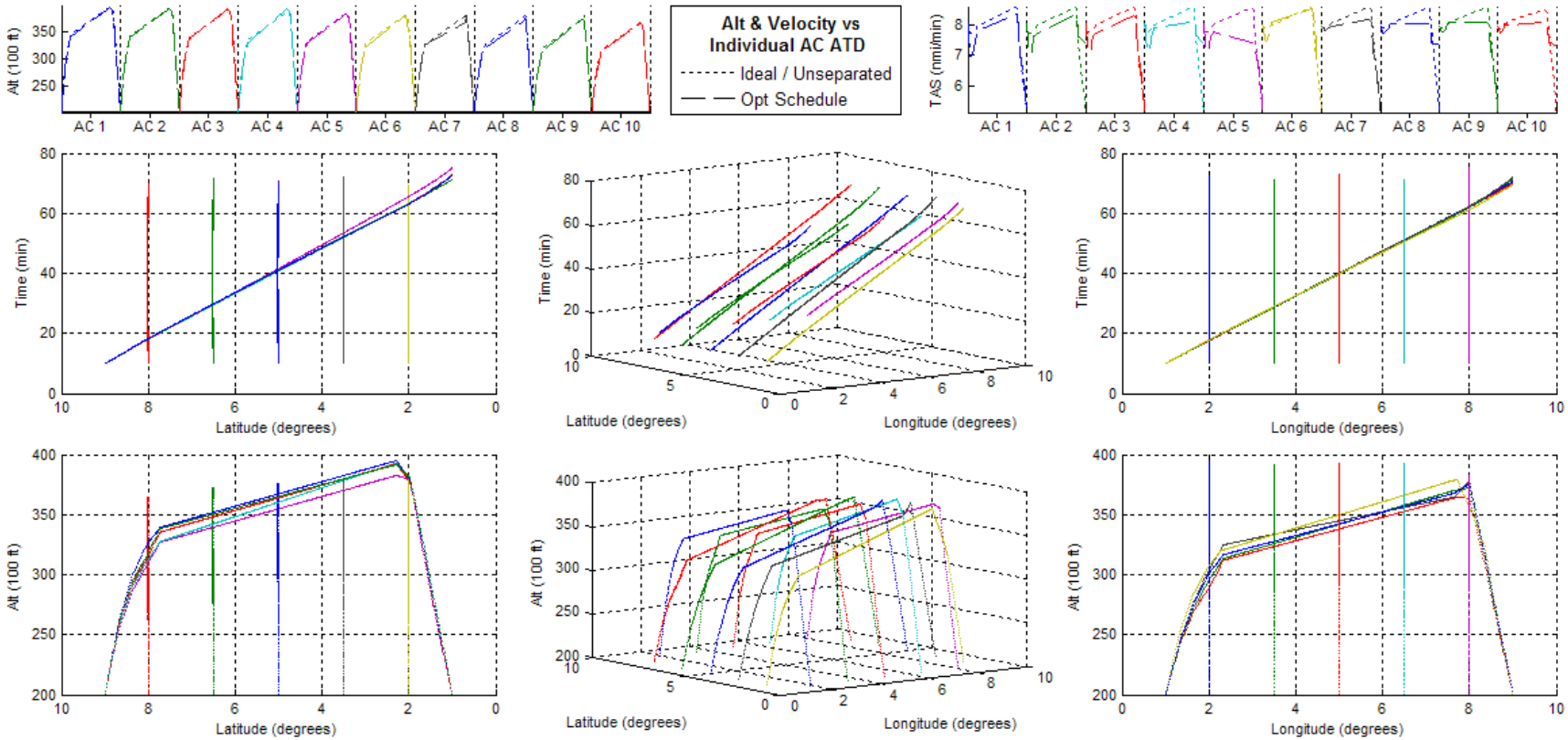

Figure 328 -Schedule Optimized 10acCH ATD_{R1} Results

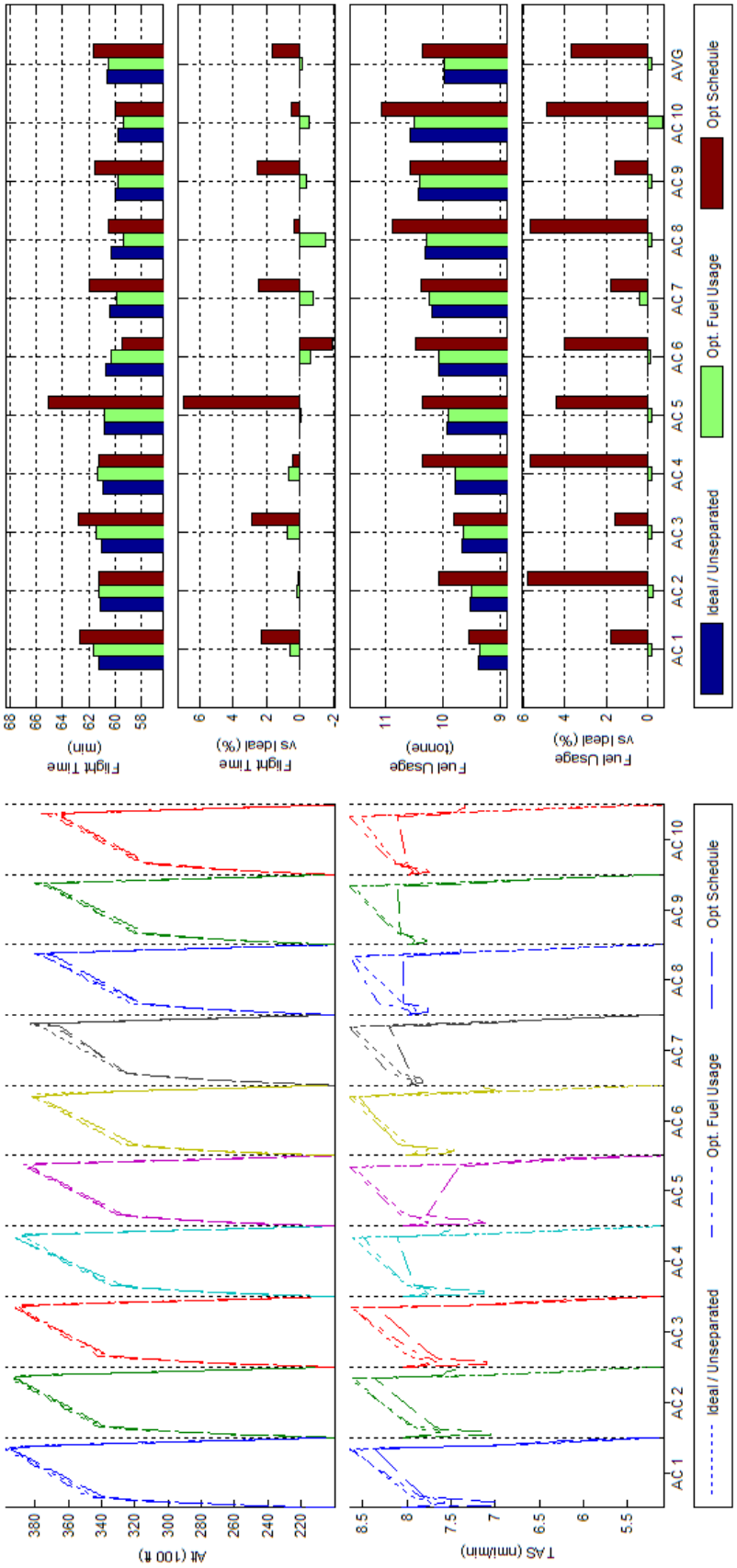

Figure 329 Trajectory Shape, Flight Time, and Fuel Consumption Comparisons of Fuel and Schedule Optimized 10acCH ATD_{RI} Results

L.23 BADA Boeing 747-300 - Scenario 10acCH - ATD_{R2}

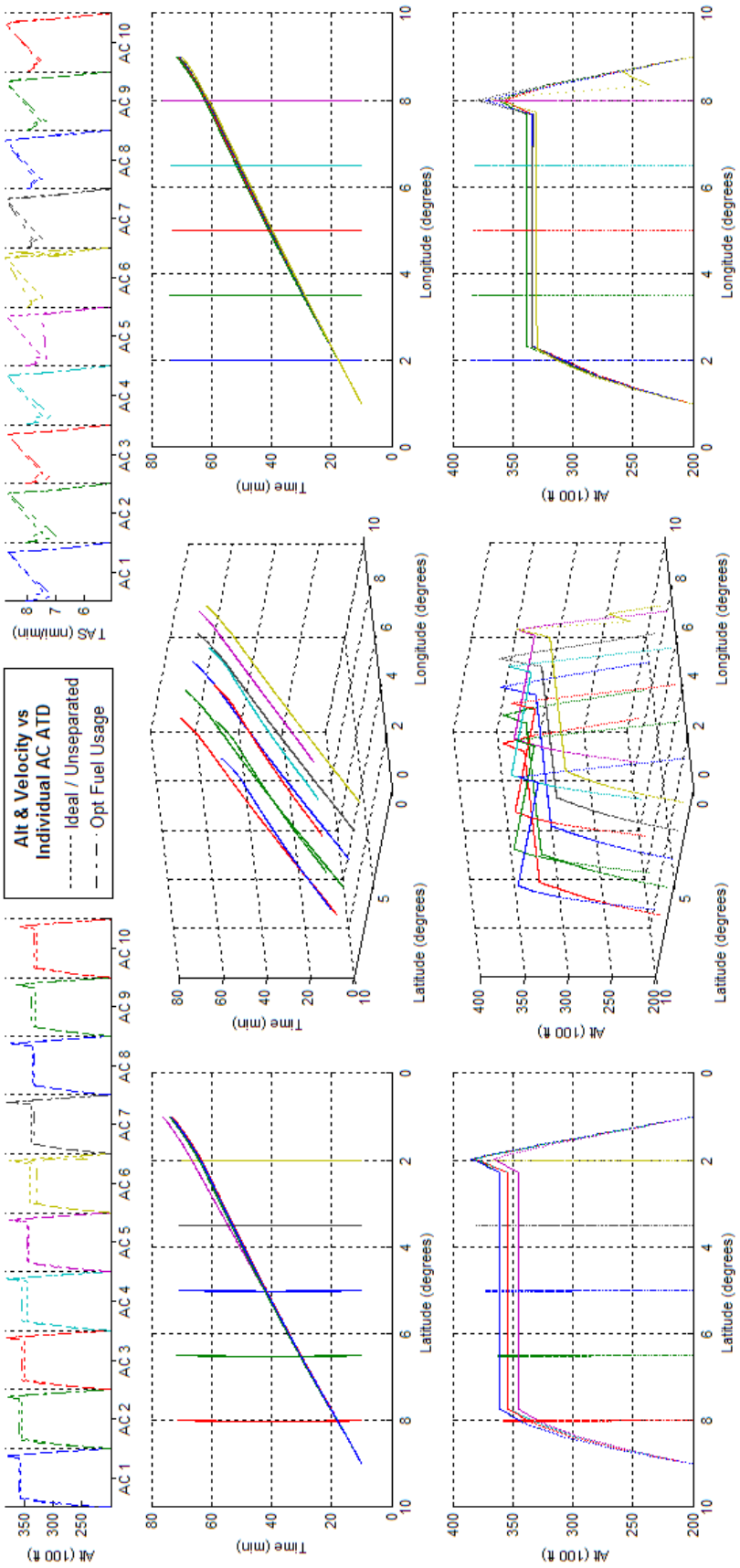

Figure 330 - Fuel Optimized 10acCH ATD_{R2} Results

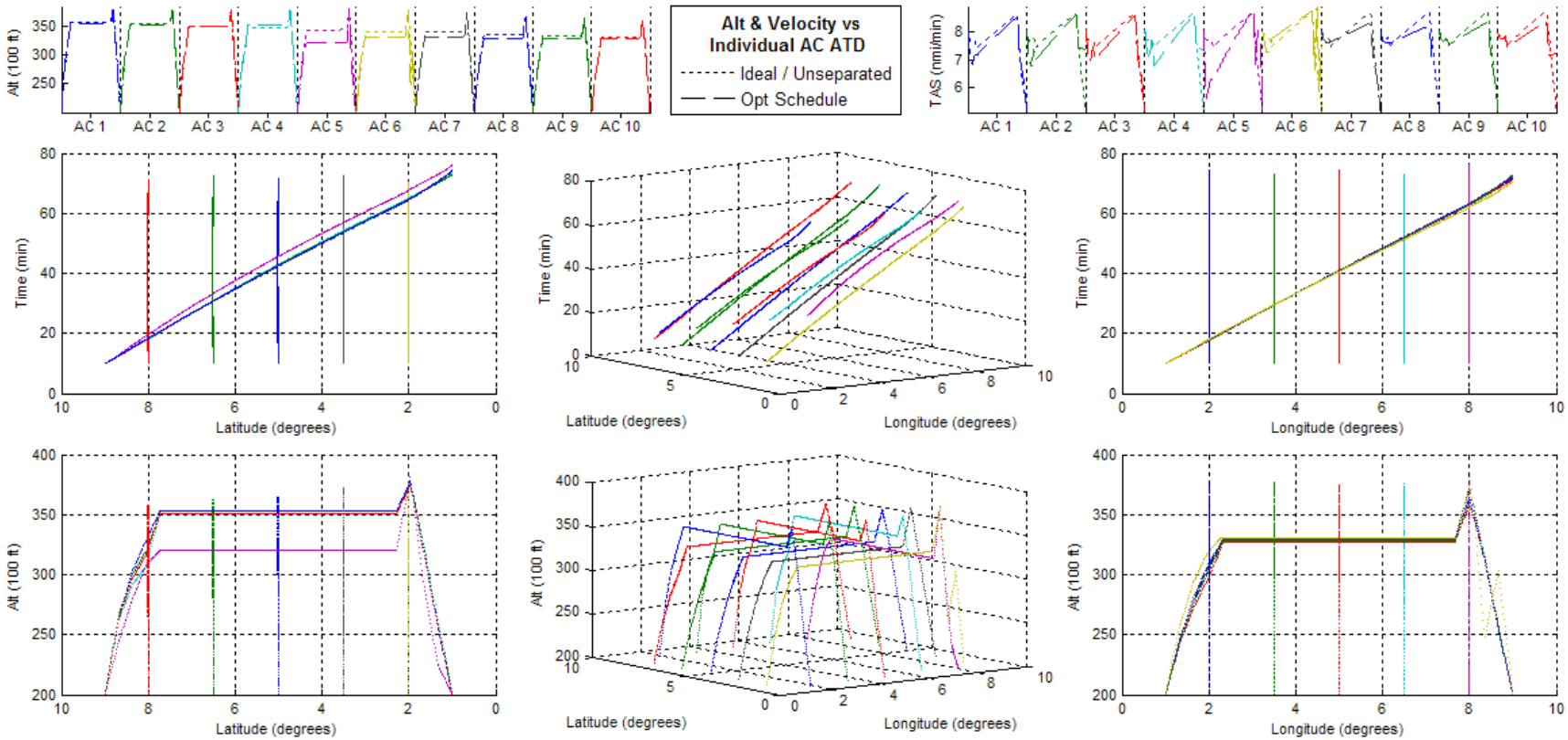

Figure 331 -Schedule Optimized 10acCH ATD_{R2} Results

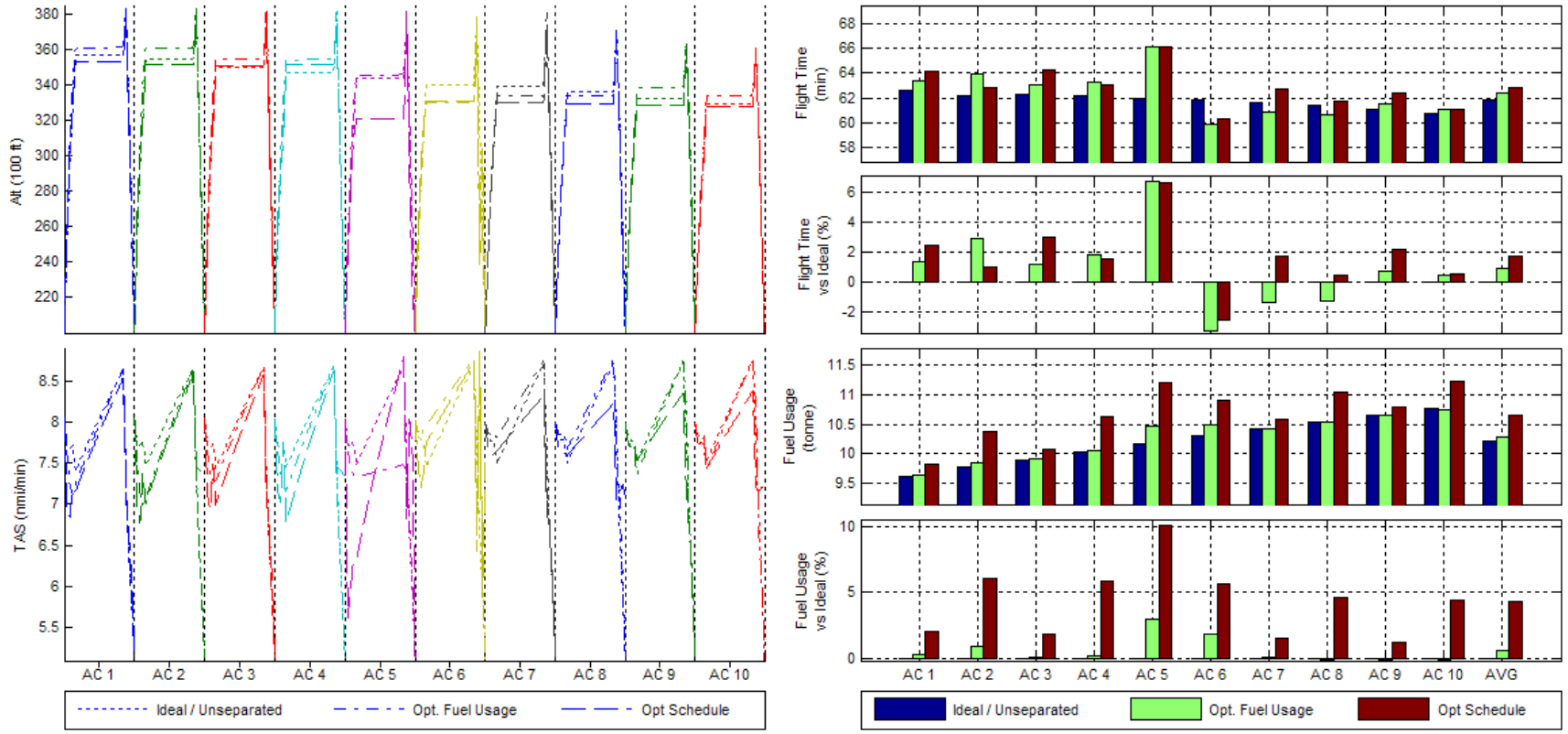

Figure 332 Trajectory Shape, Flight Time, and Fuel Consumption Comparisons of Fuel and Schedule Optimized 10acCH ATD_{R2} Results

L.24 BADA Boeing 747-300 - Scenario 10acCH - ATD_{R3}

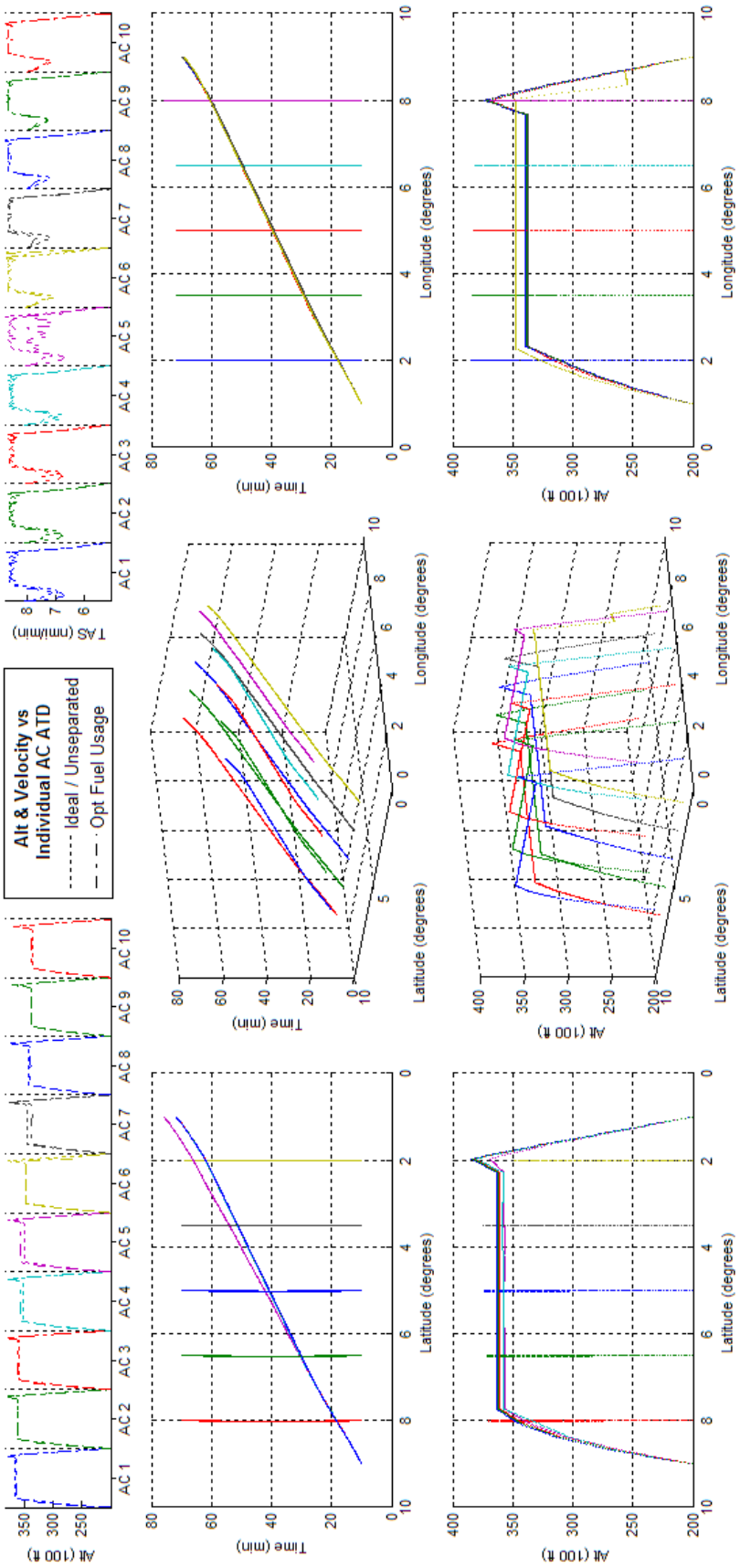

Figure 333 - Fuel Optimized 10acCH ATD_{R3} Results

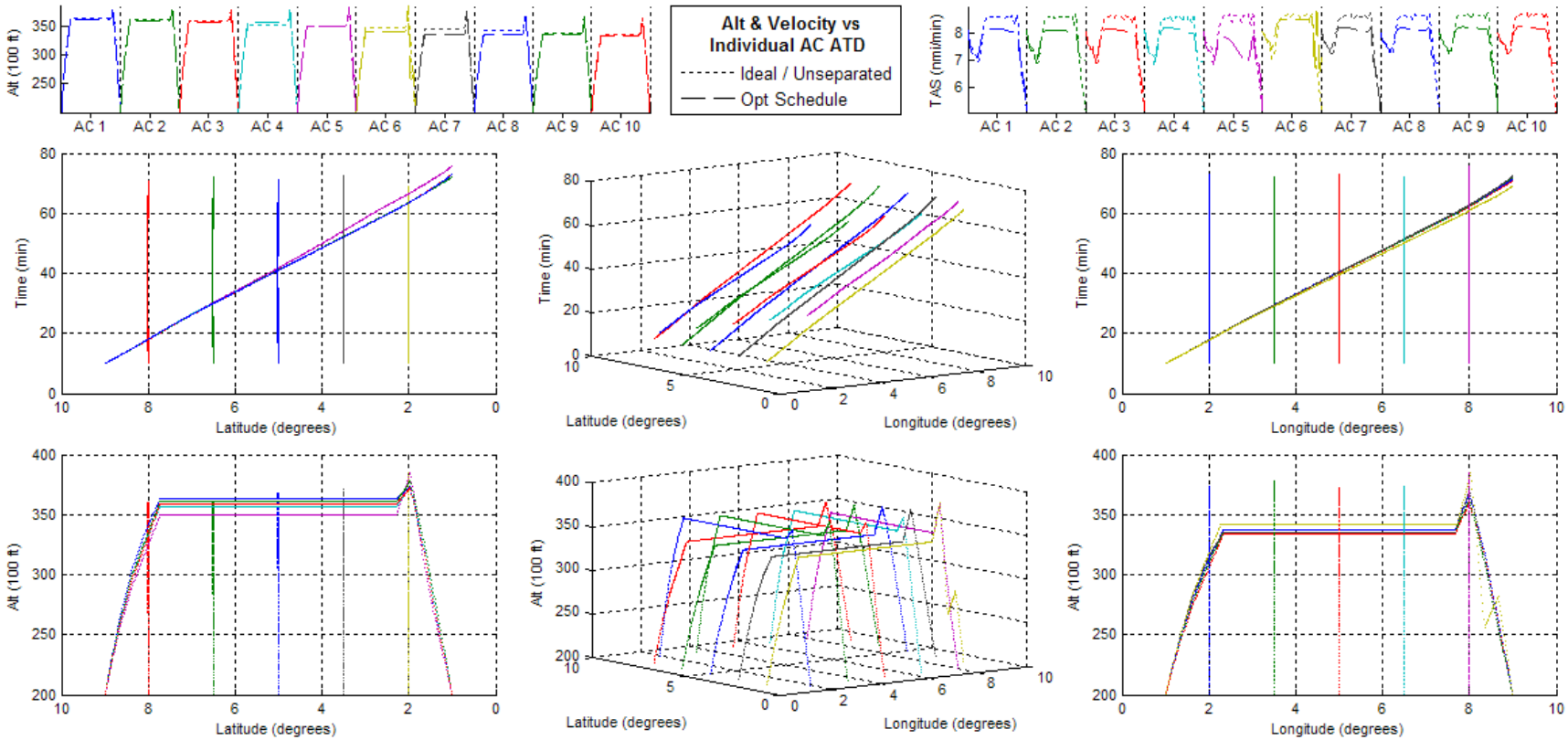

Figure 334 -Schedule Optimized 10acCH ATD_{R3} Results

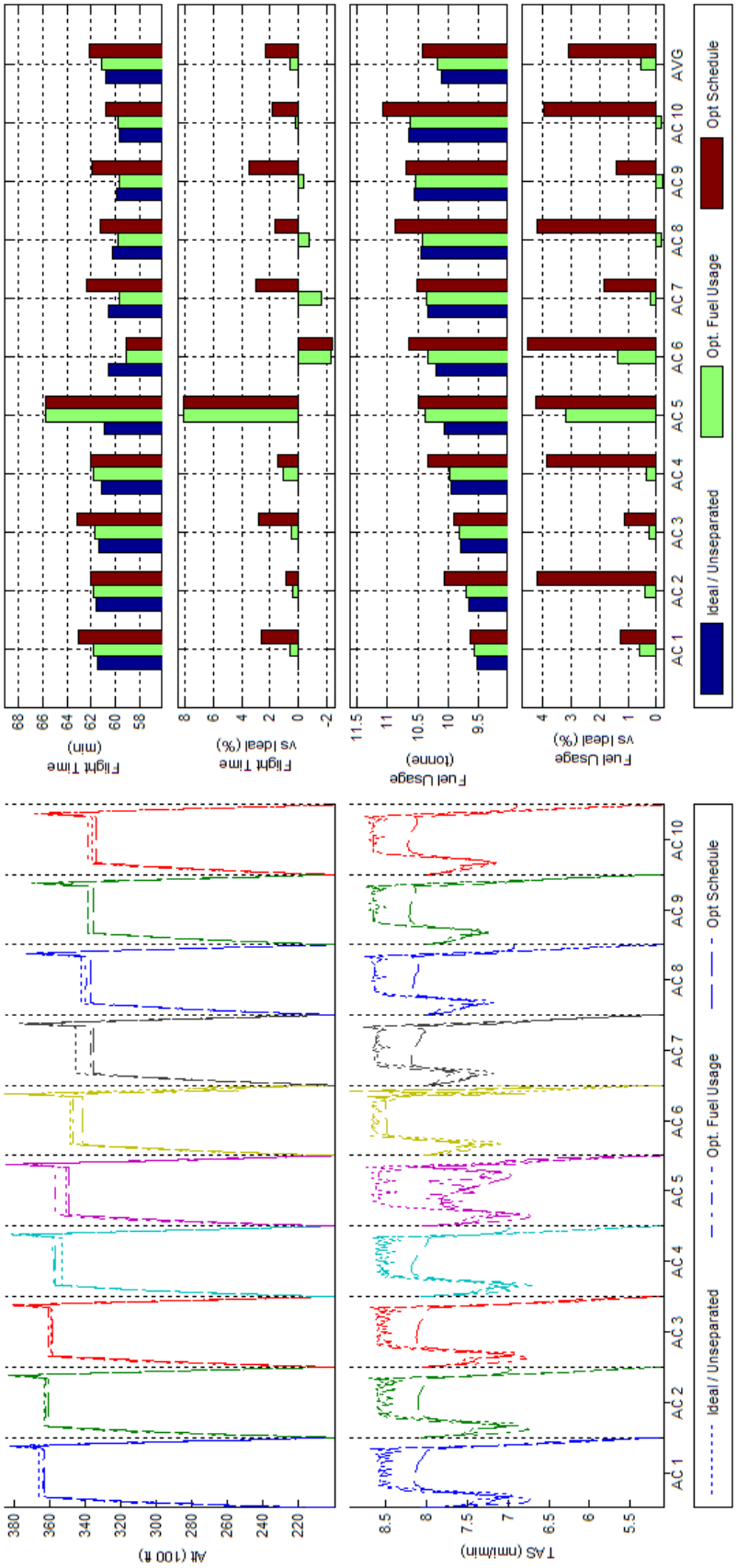

Figure 335 Trajectory Shape, Flight Time, and Fuel Consumption Comparisons of Fuel and Schedule Optimized 10acCH ATD_{R3} Results

L.25 BADA Boeing 747-300 - Scenario 2acPH2H - ATD_{R1}

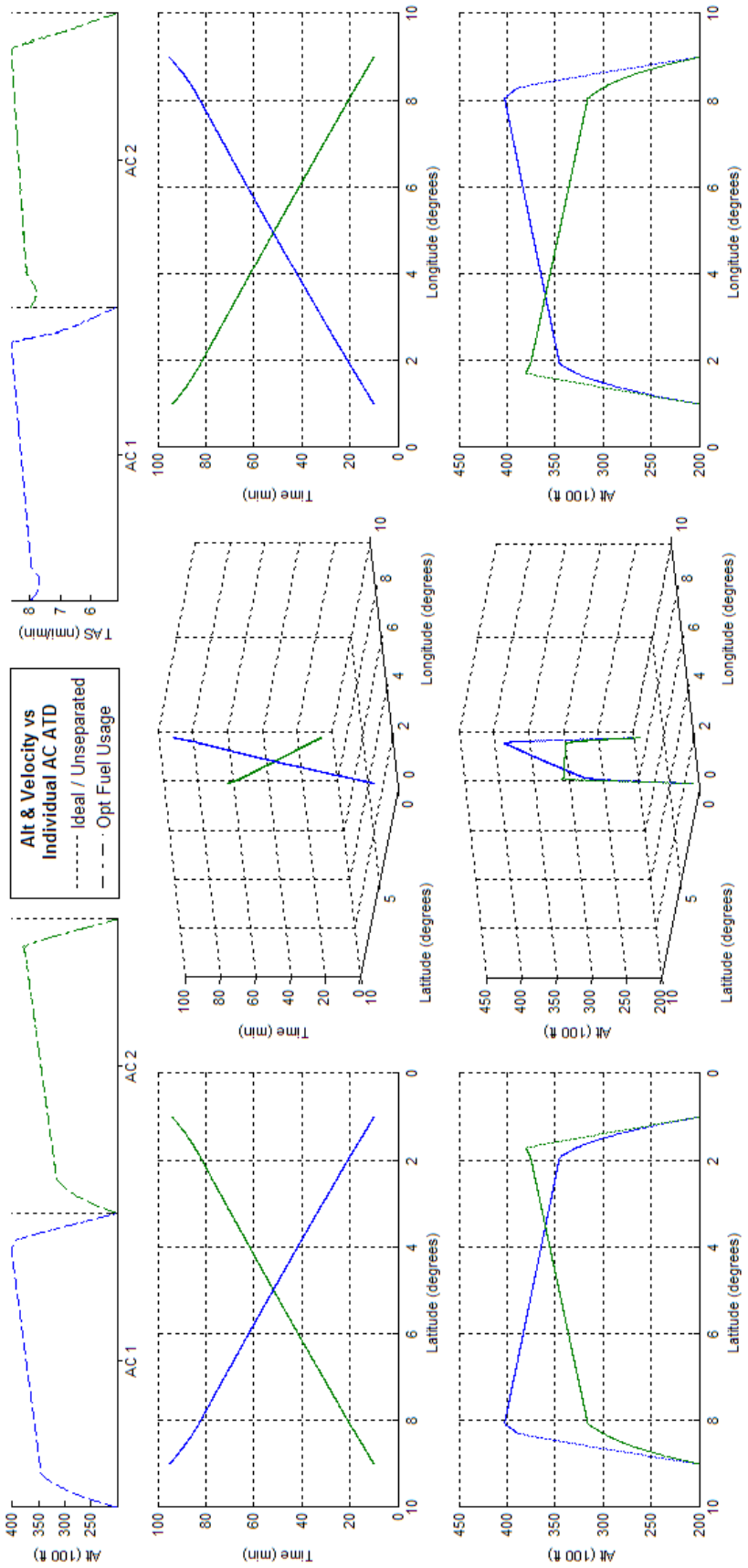

Figure 336 - Fuel Optimized 2acPH2H ATD_{R1} Results

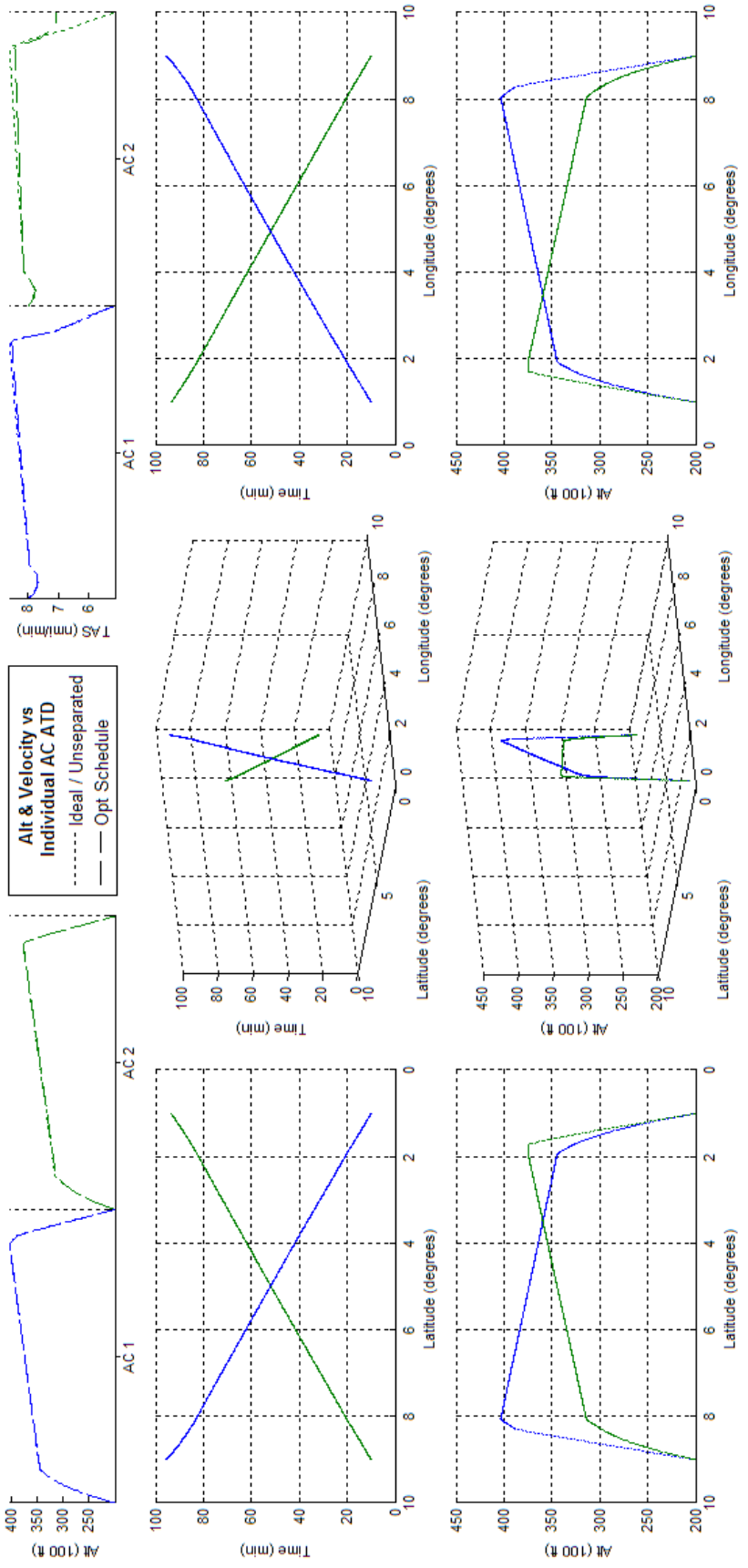

Figure 337 -Schedule Optimized 2acPH2H ATD_{R1} Results

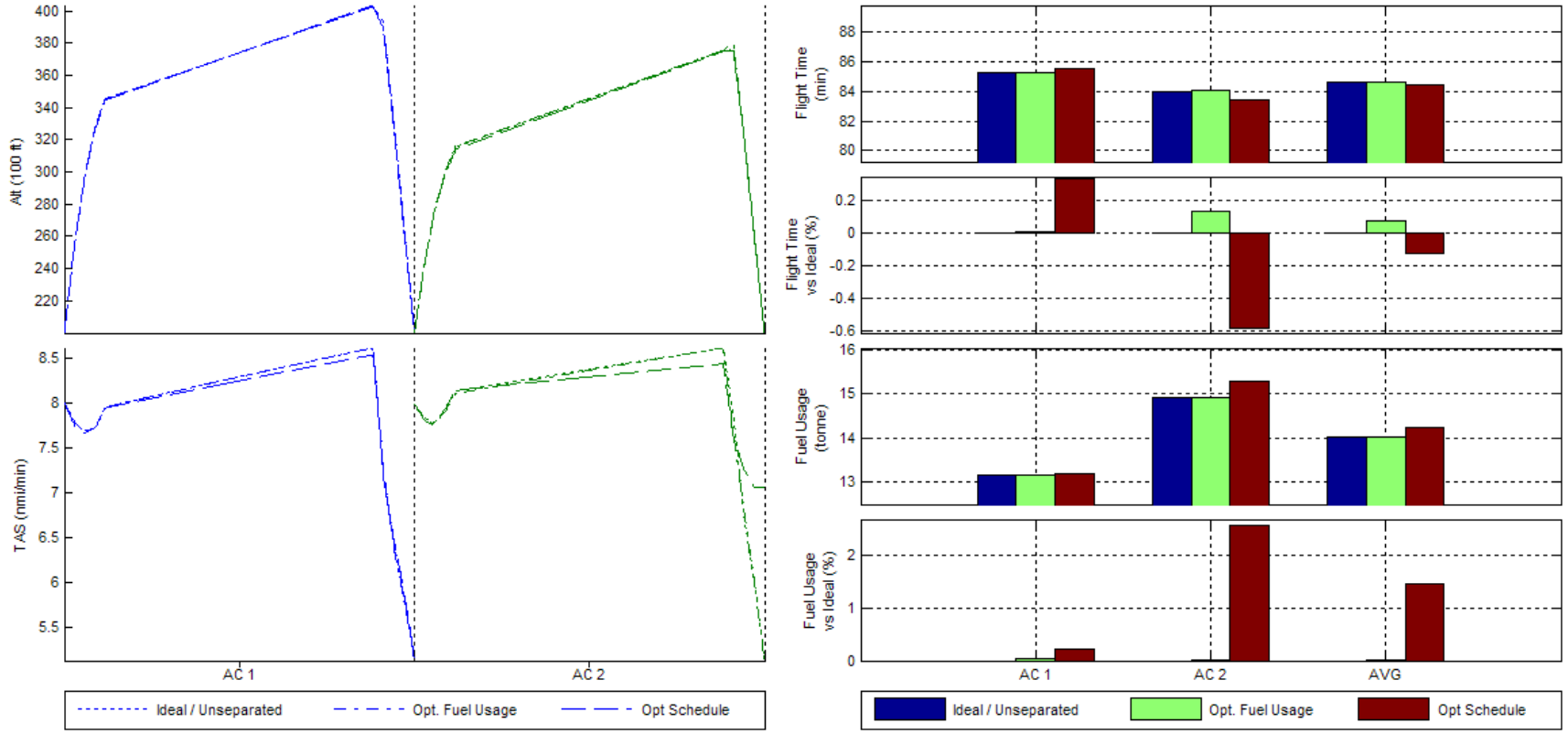

Figure 338 Trajectory Shape, Flight Time, and Fuel Consumption Comparisons of Fuel and Schedule Optimized 2acPH2H ATD_{R1} Results

L.26 BADA Boeing 747-300 - Scenario 2acPH2H - ATD_{R2}

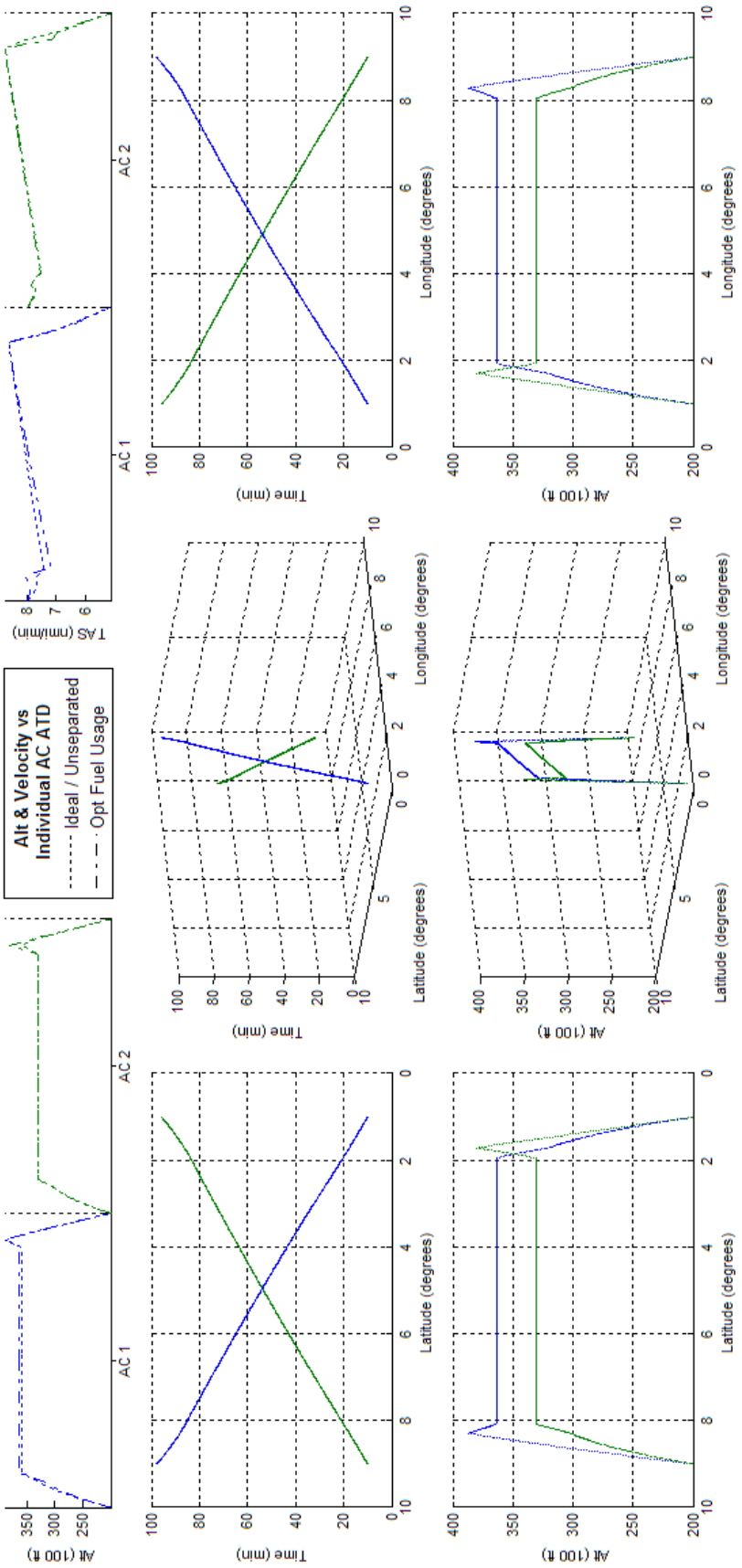

Figure 339 -Fuel Optimized 2acPH2H ATD_{R2} Results

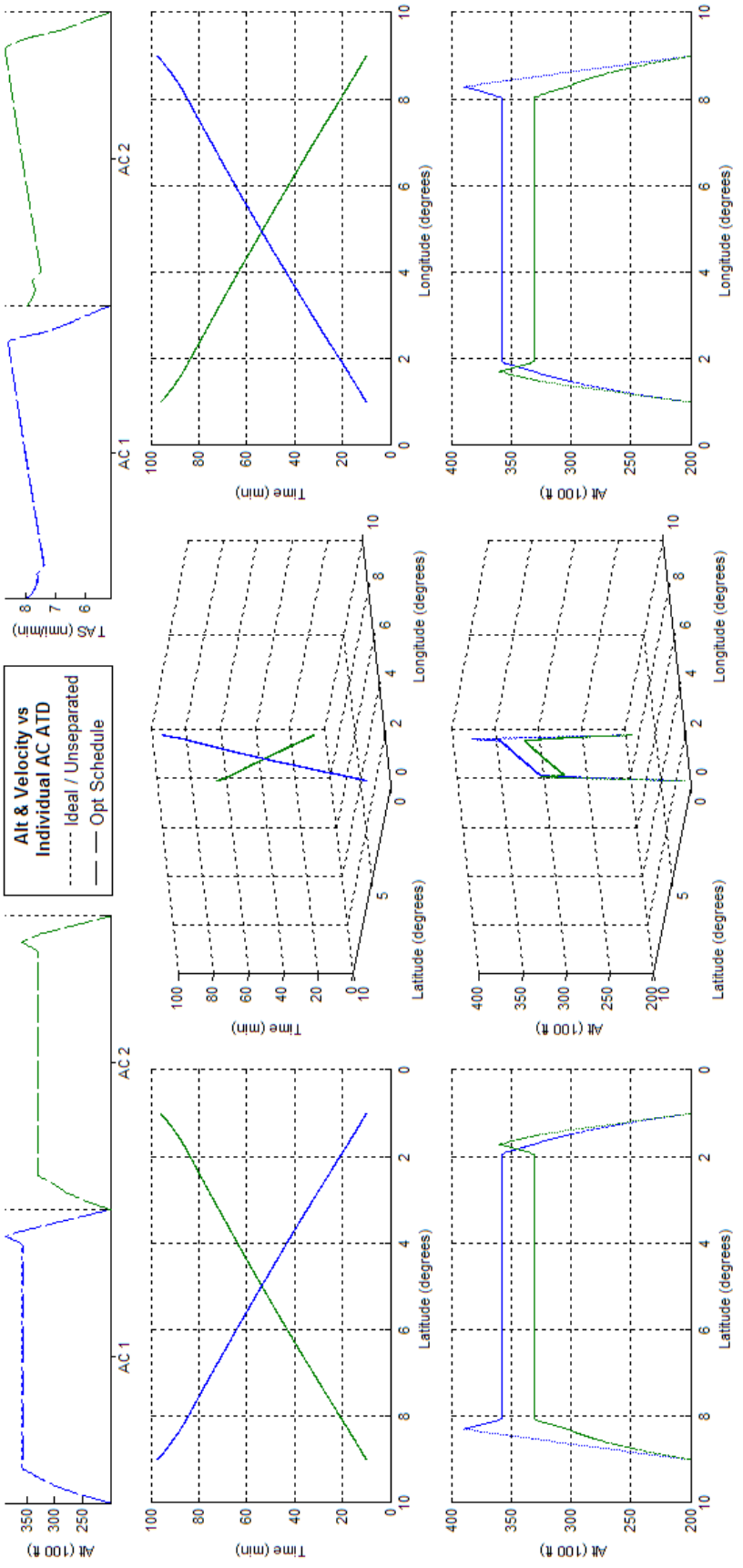

Figure 340 -Schedule Optimized 2acPH2H ATD_{R2} Results

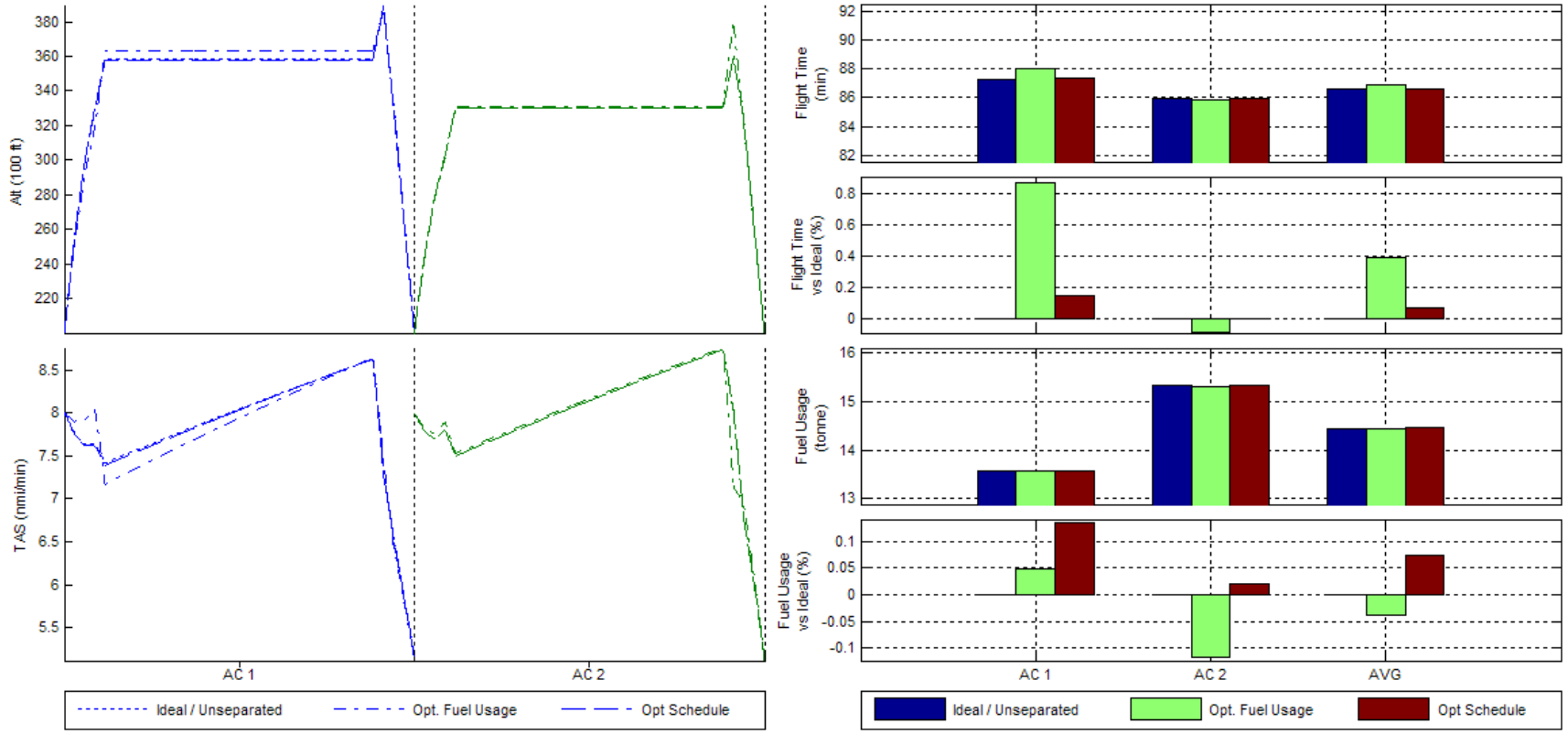

Figure 341 Trajectory Shape, Flight Time, and Fuel Consumption Comparisons of Fuel and Schedule Optimized 2acPH2H ATD_{R2} Results

L.27 BADA Boeing 747-300 - Scenario 2acPH2H - ATD_{R3}

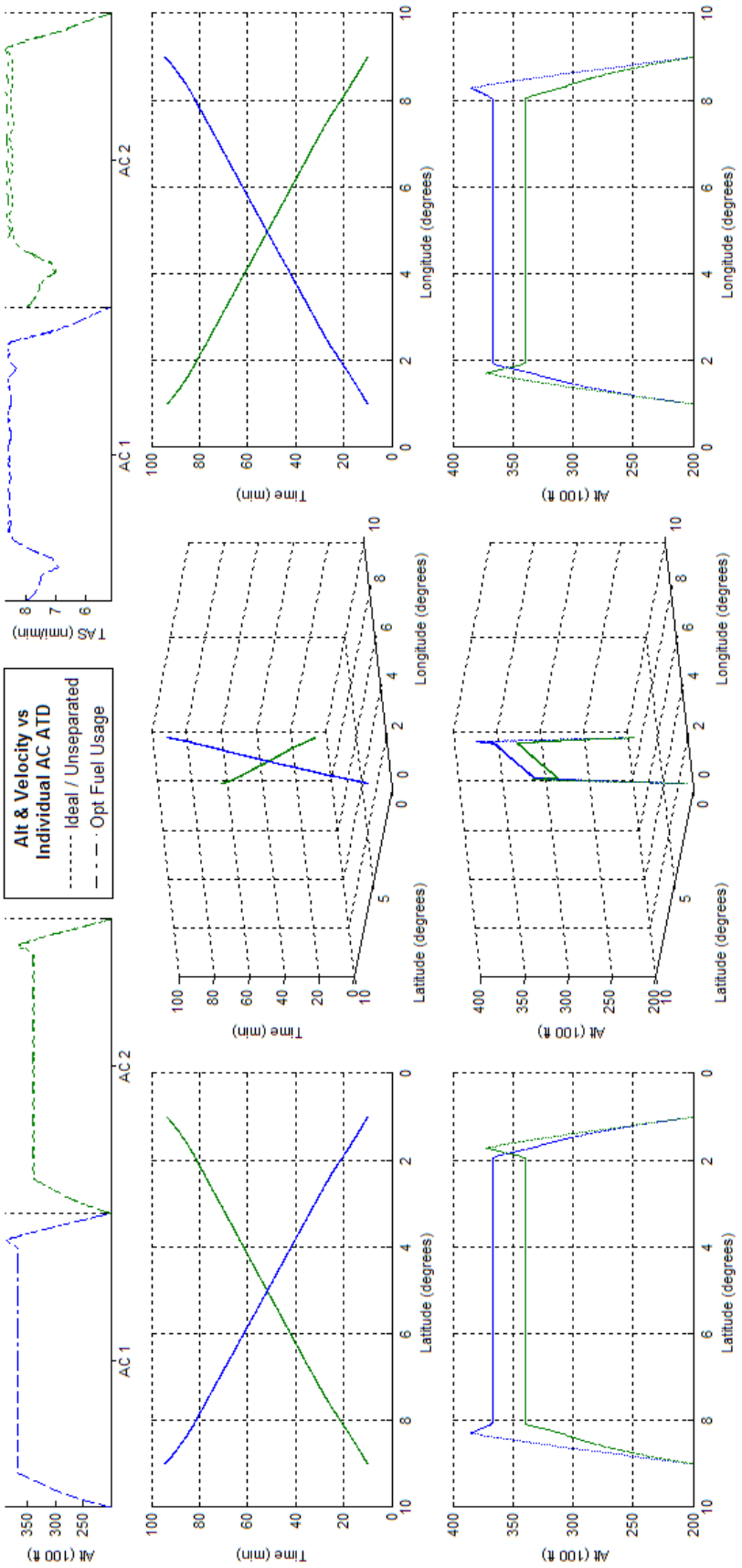

Figure 342 - Fuel Optimized 2acPH2H ATD_{R3} Results

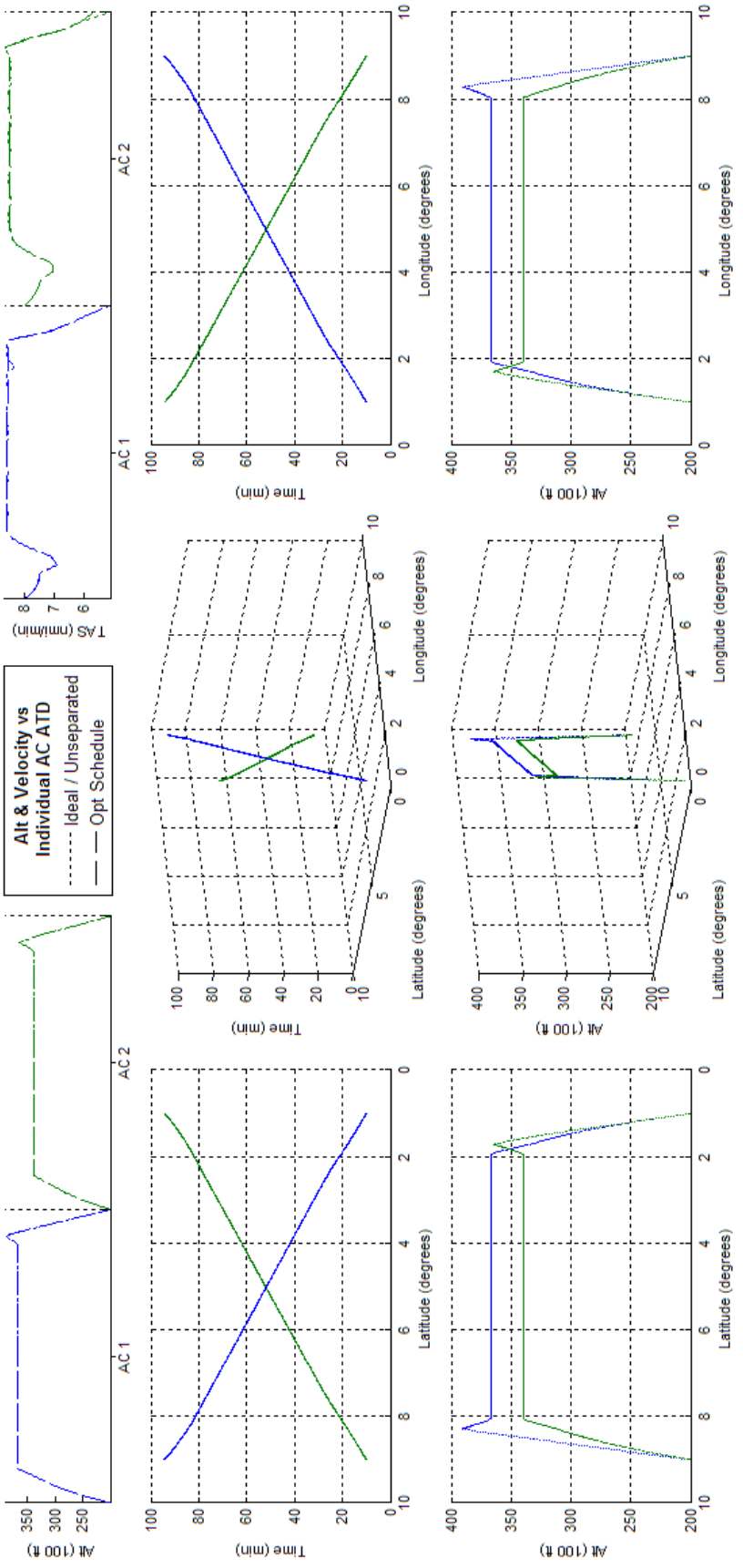

Figure 343 -Schedule Optimized 2acPH2H ATD_{R3} Results

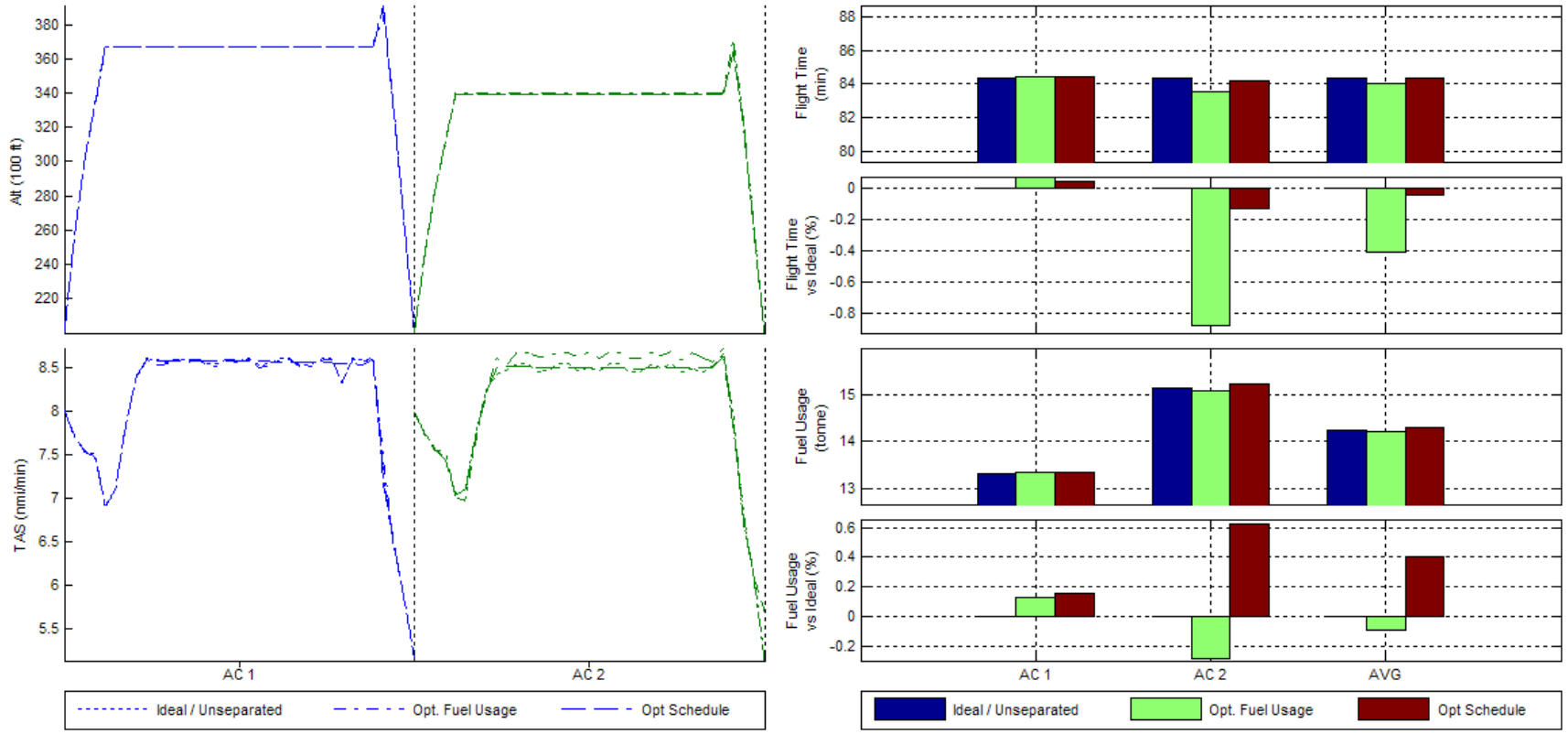

Figure 344 Trajectory Shape, Flight Time, and Fuel Consumption Comparisons of Fuel and Schedule Optimized 2acPH2H ATD_{R3} Results

L.28 BADA Boeing 747-300 - Scenario 4acPH2H - ATD_{R1}

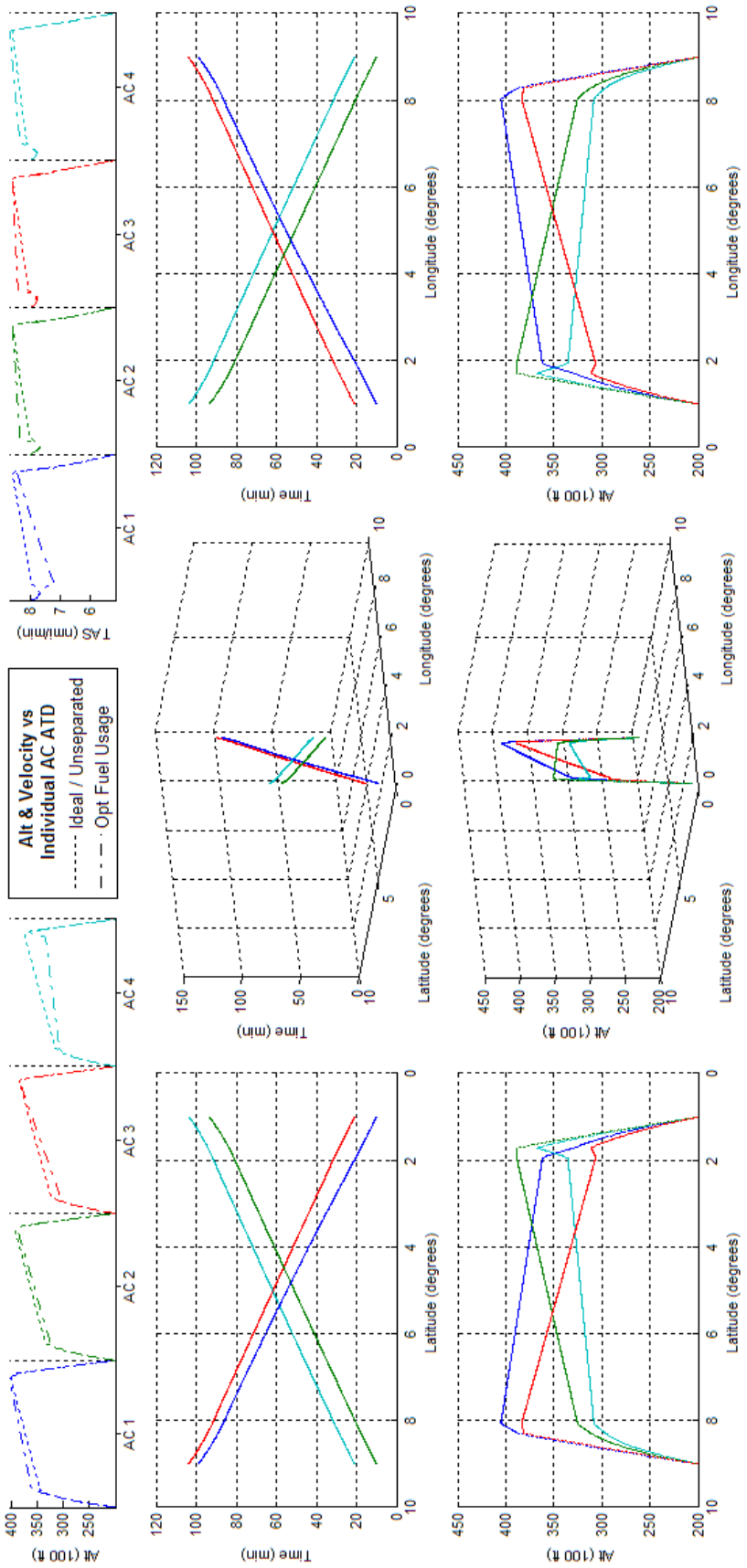

Figure 345 - Fuel Optimized 4acPH2H ATD_{R1} Results

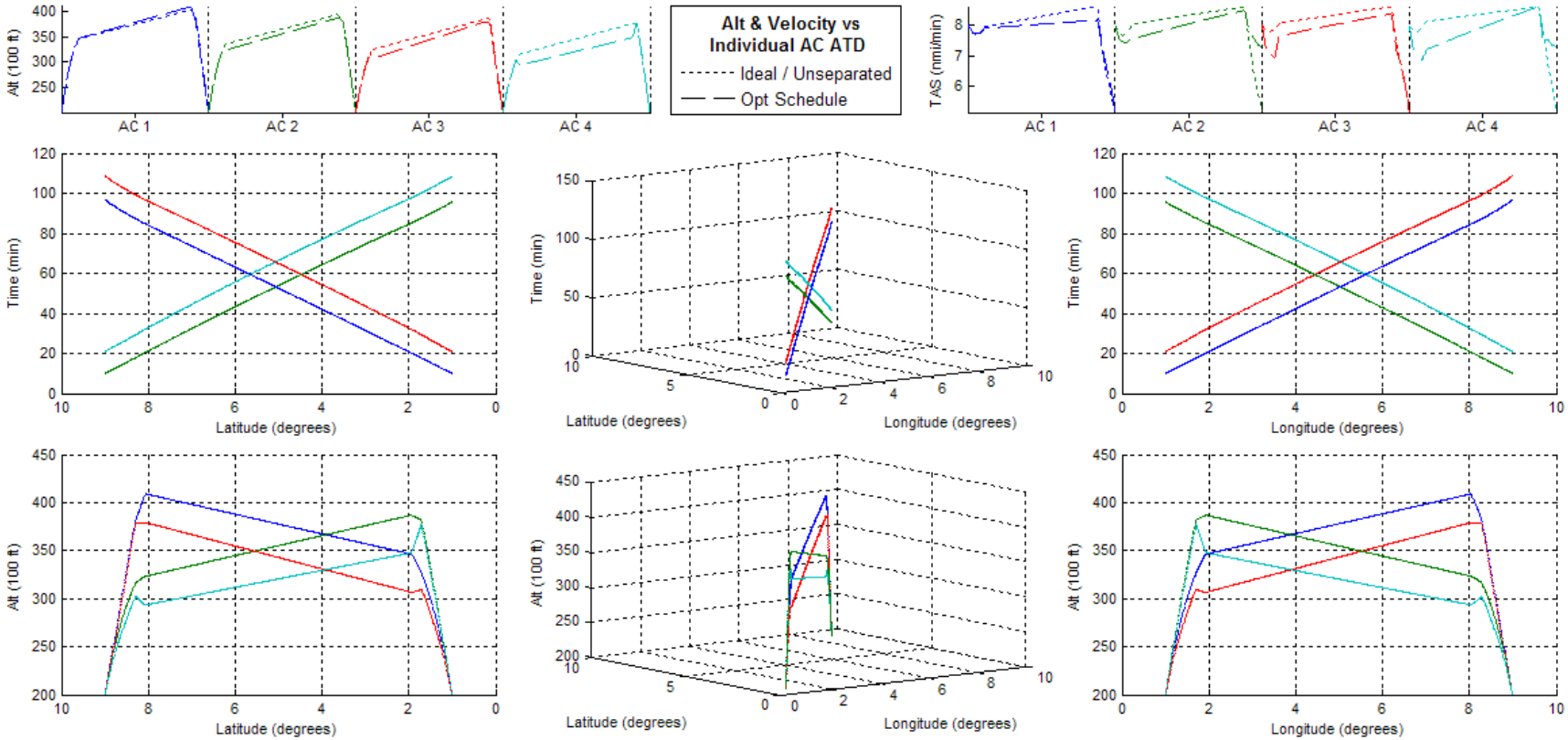

Figure 346 -Schedule Optimized 4acPH2H ATD_{R1} Results

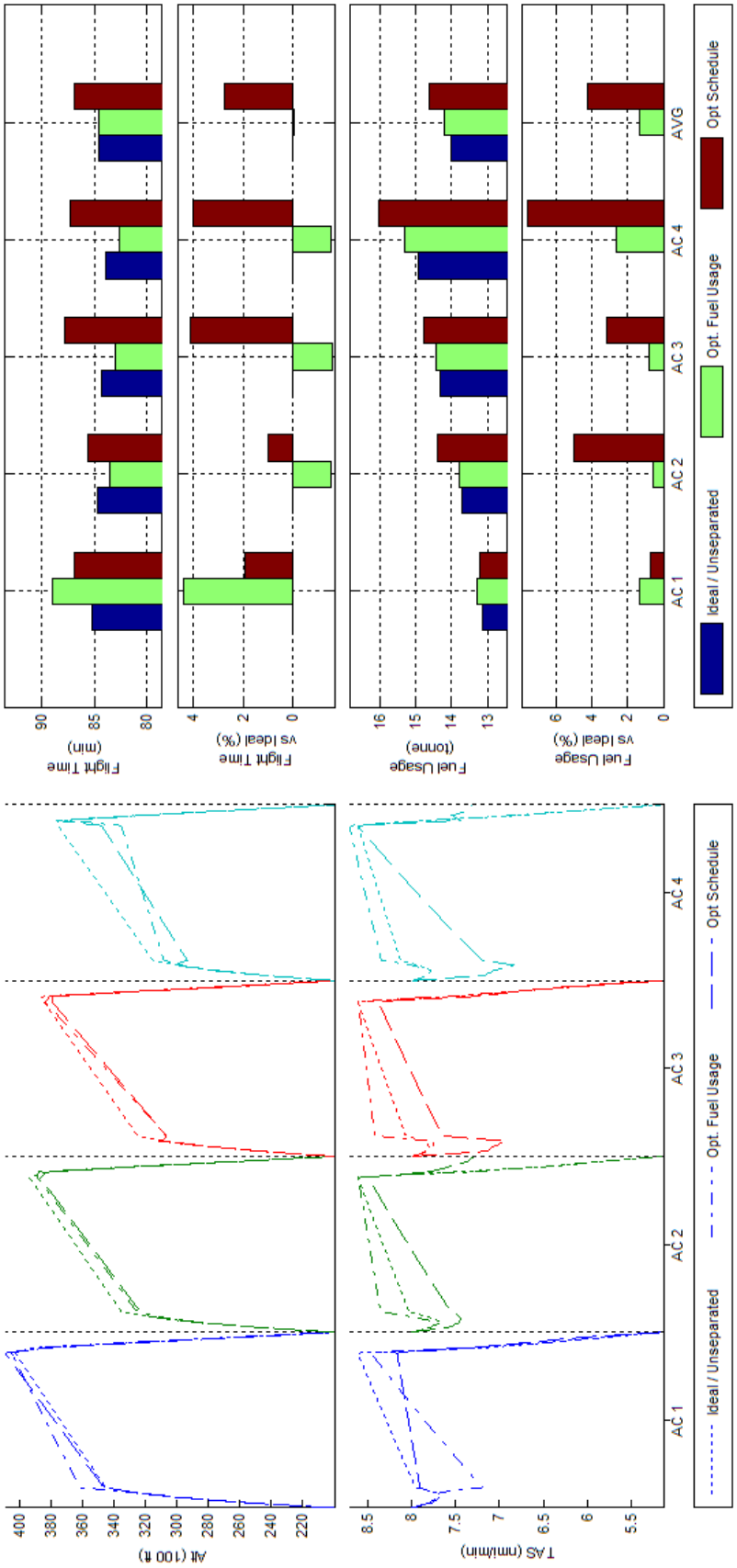

Figure 347 Trajectory Shape, Flight Time, and Fuel Consumption Comparisons of Fuel and Schedule Optimized 4acPH2H ATD_{R1} Results

L.29 BADA Boeing 747-300 - Scenario 4acPH2H - ATD_{R2}

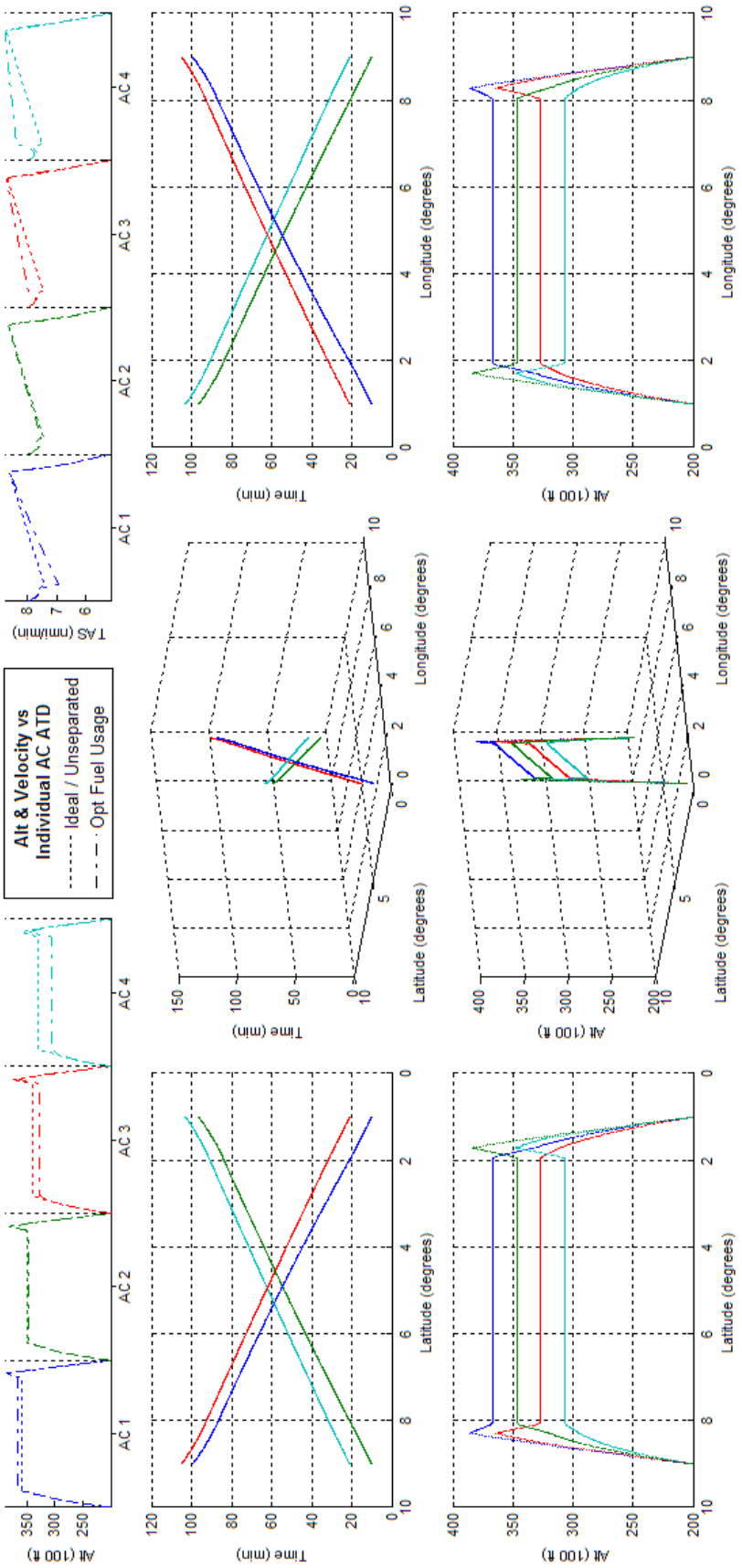

Figure 348 - Fuel Optimized 4acPH2H ATD_{R2} Results

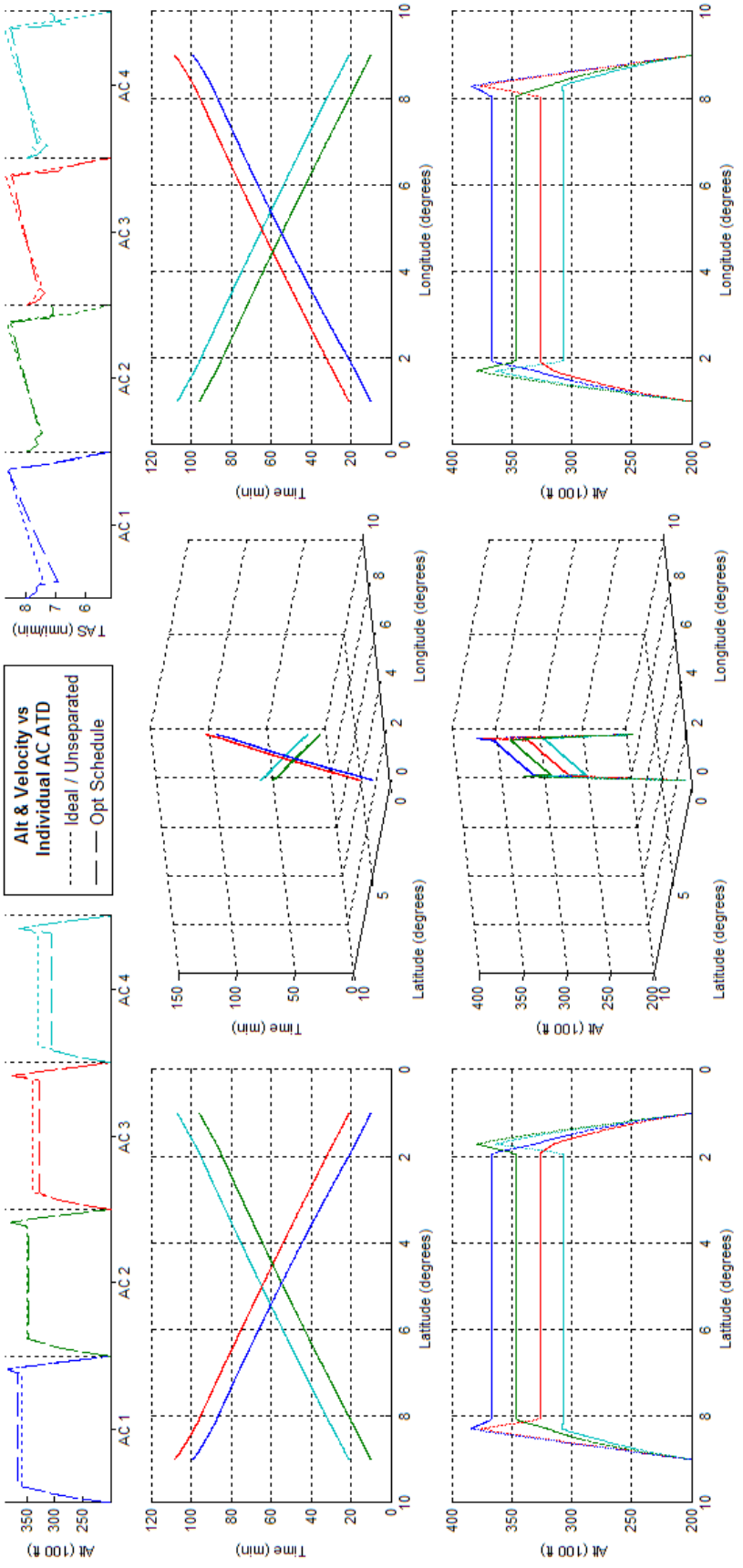

Figure 349 -Schedule Optimized 4acPH2H ATD_{R2} Results

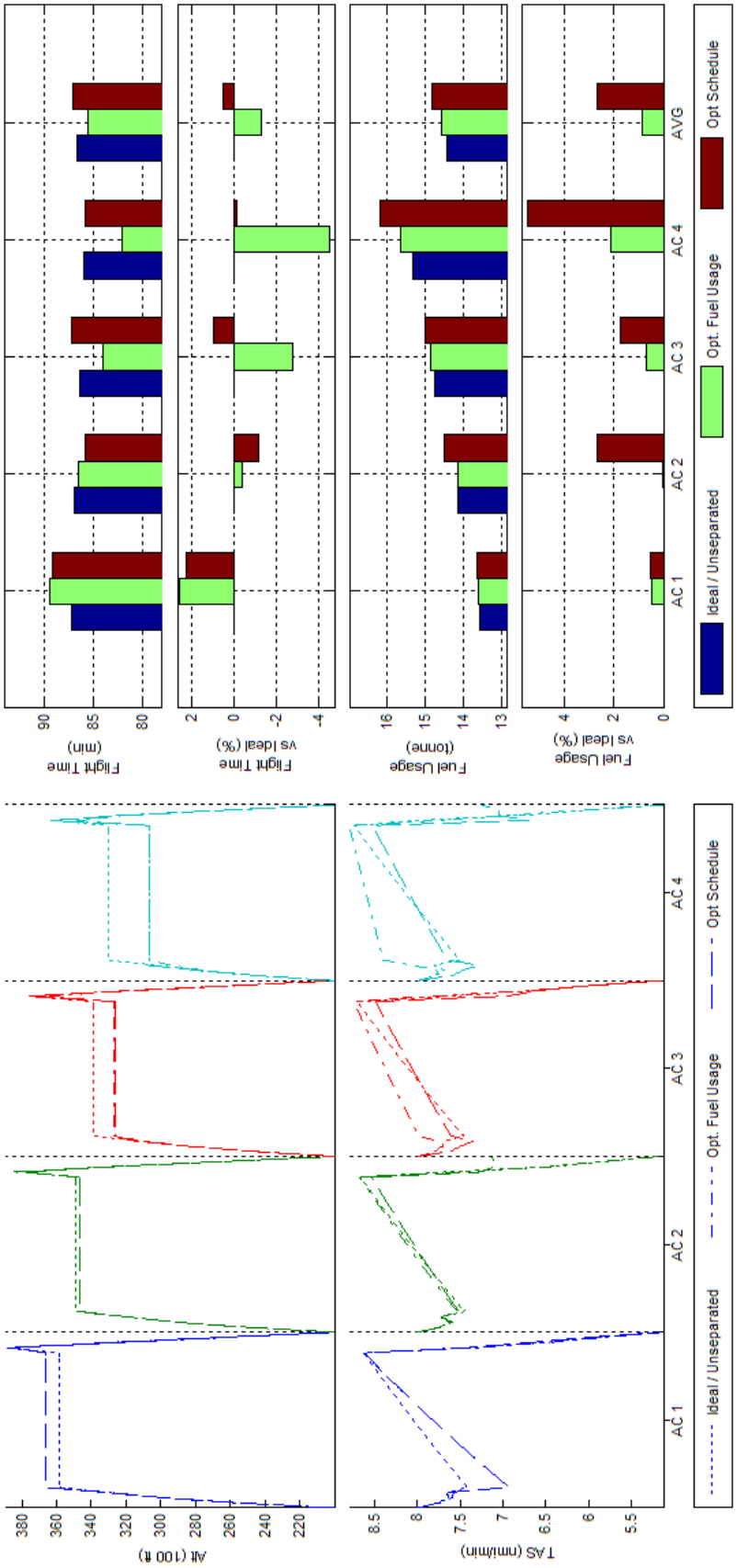

Figure 350 Trajectory Shape, Flight Time, and Fuel Consumption Comparisons of Fuel and Schedule Optimized 4acPH2H ATD_{R2} Results

L.30 BADA Boeing 747-300 - Scenario 4acPH2H - ATD_{R3}

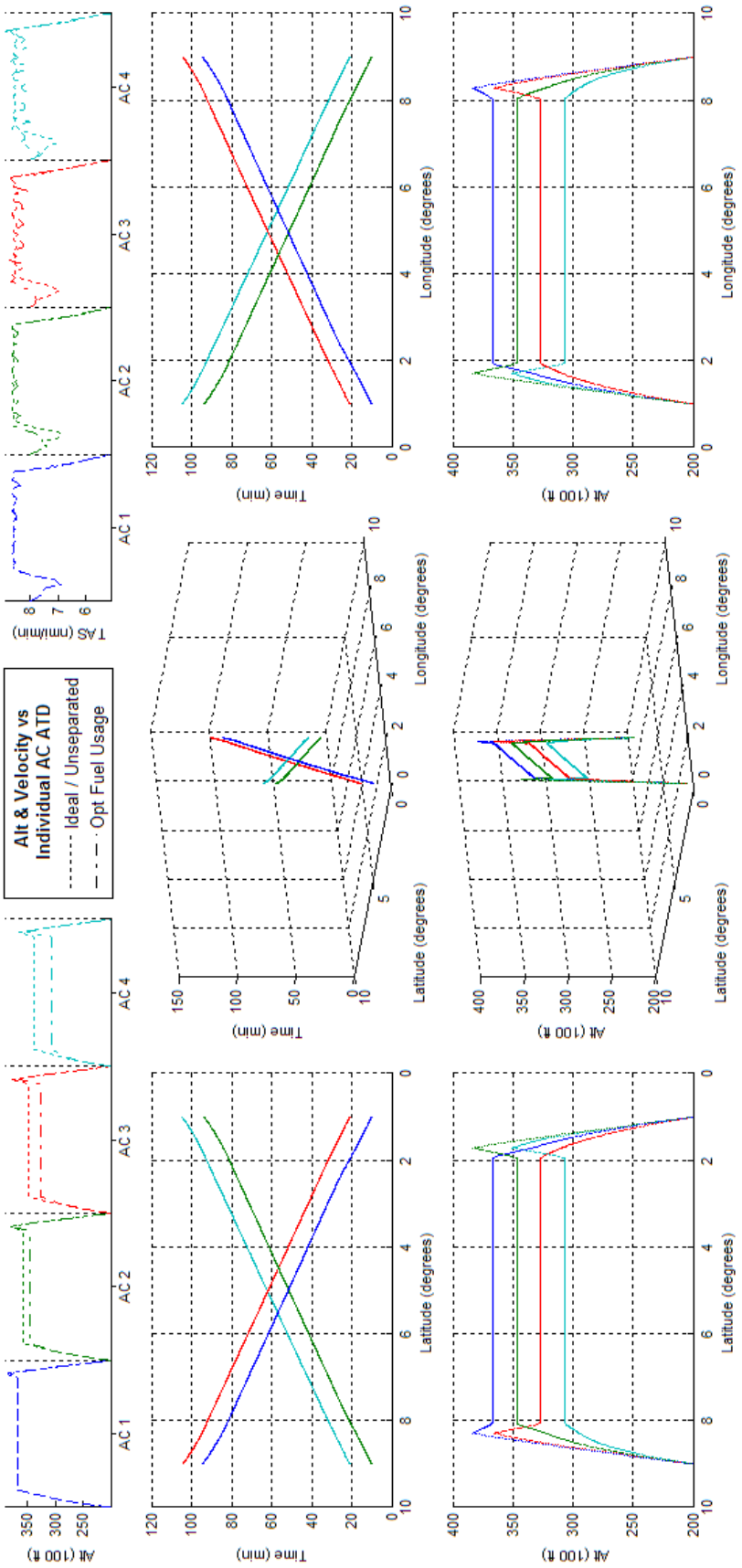

Figure 351 - Fuel Optimized 4acPH2H ATD_{R3} Results

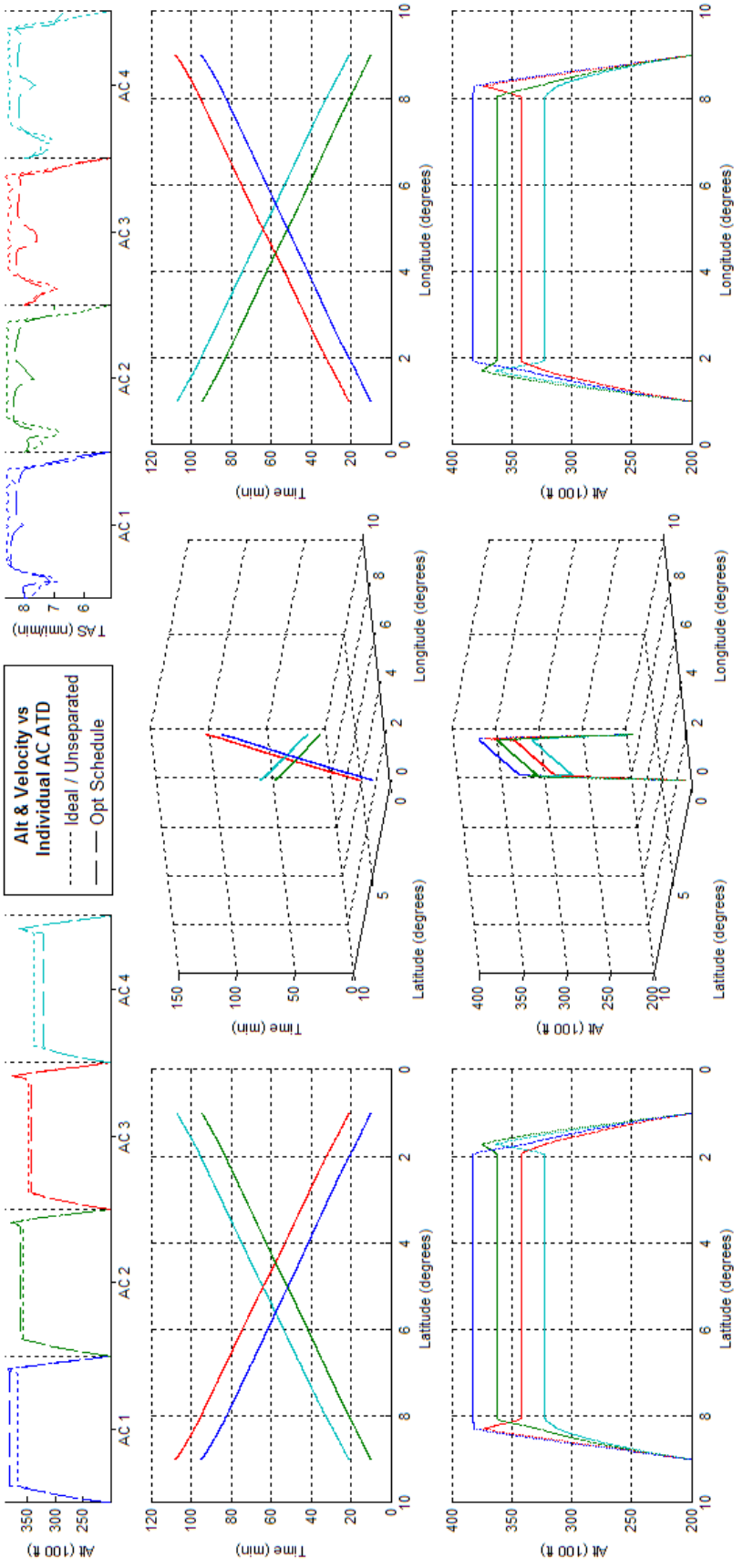

Figure 352 -Schedule Optimized 4acPH2H ATD_{R3} Results

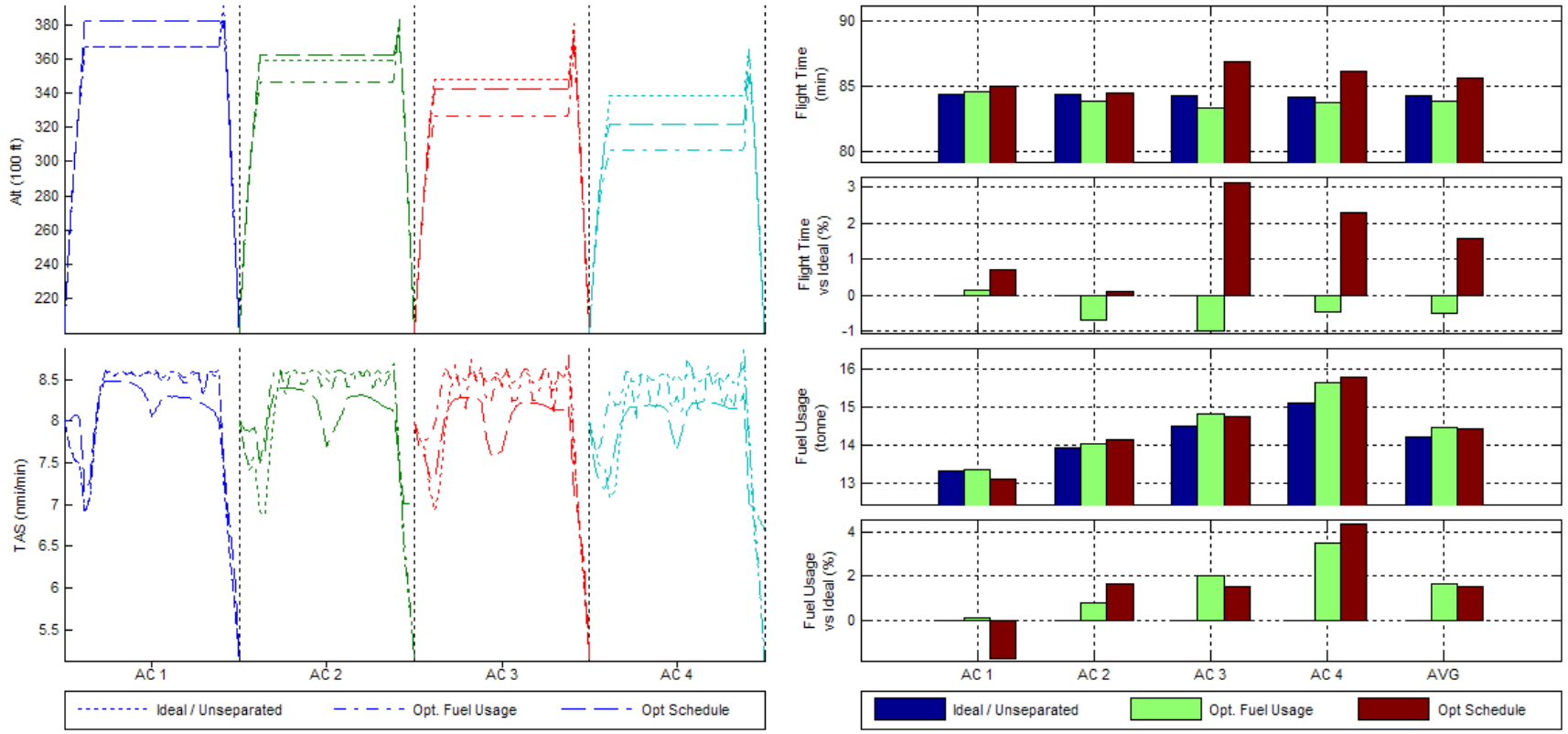

Figure 353 Trajectory Shape, Flight Time, and Fuel Consumption Comparisons of Fuel and Schedule Optimized 4acPH2H ATD_{R3} Results

L.31 BADA Boeing 747-300 - Scenario 10acPH2H - ATD_{R1}

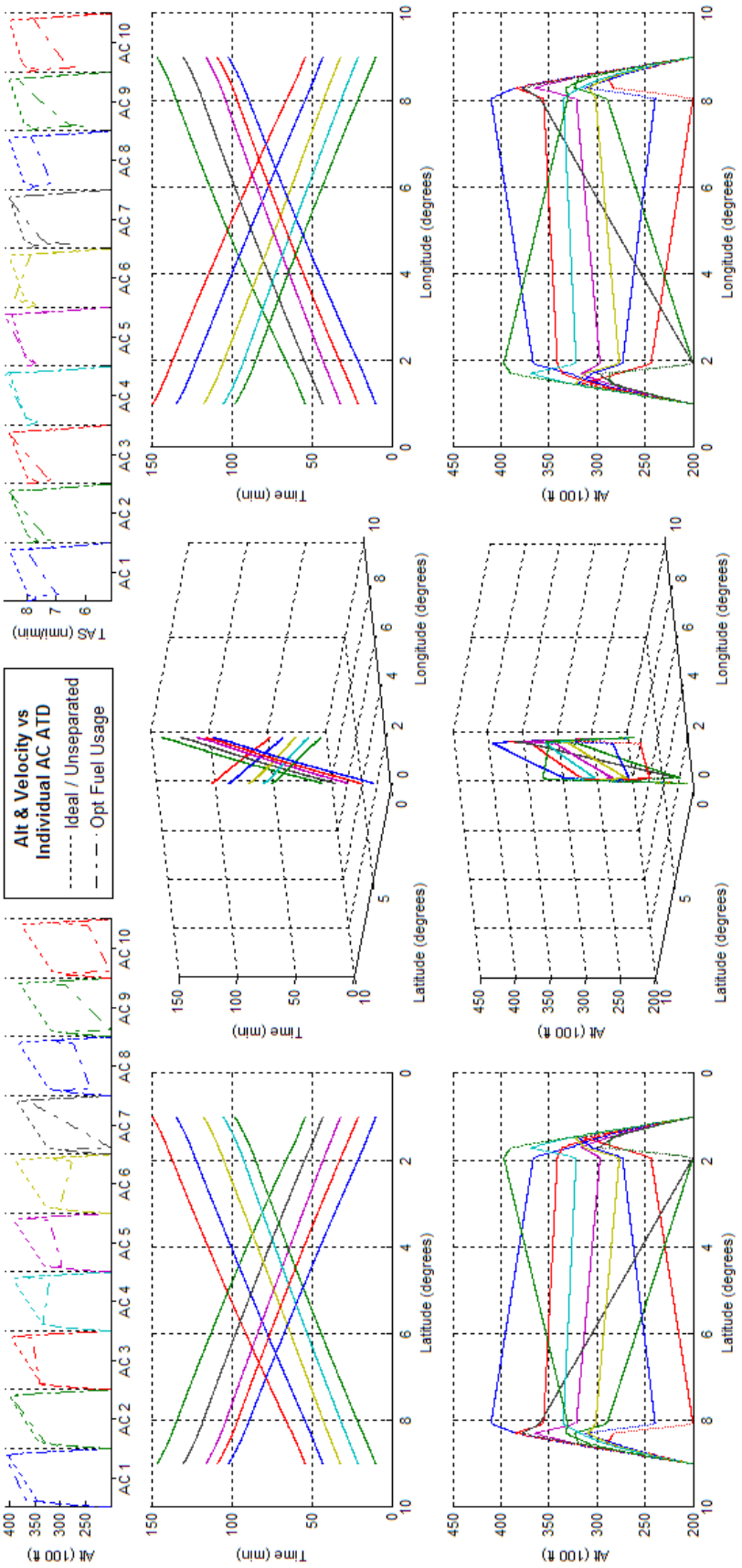

Figure 354 - Fuel Optimized 10acPH2H ATD_{R1} Results

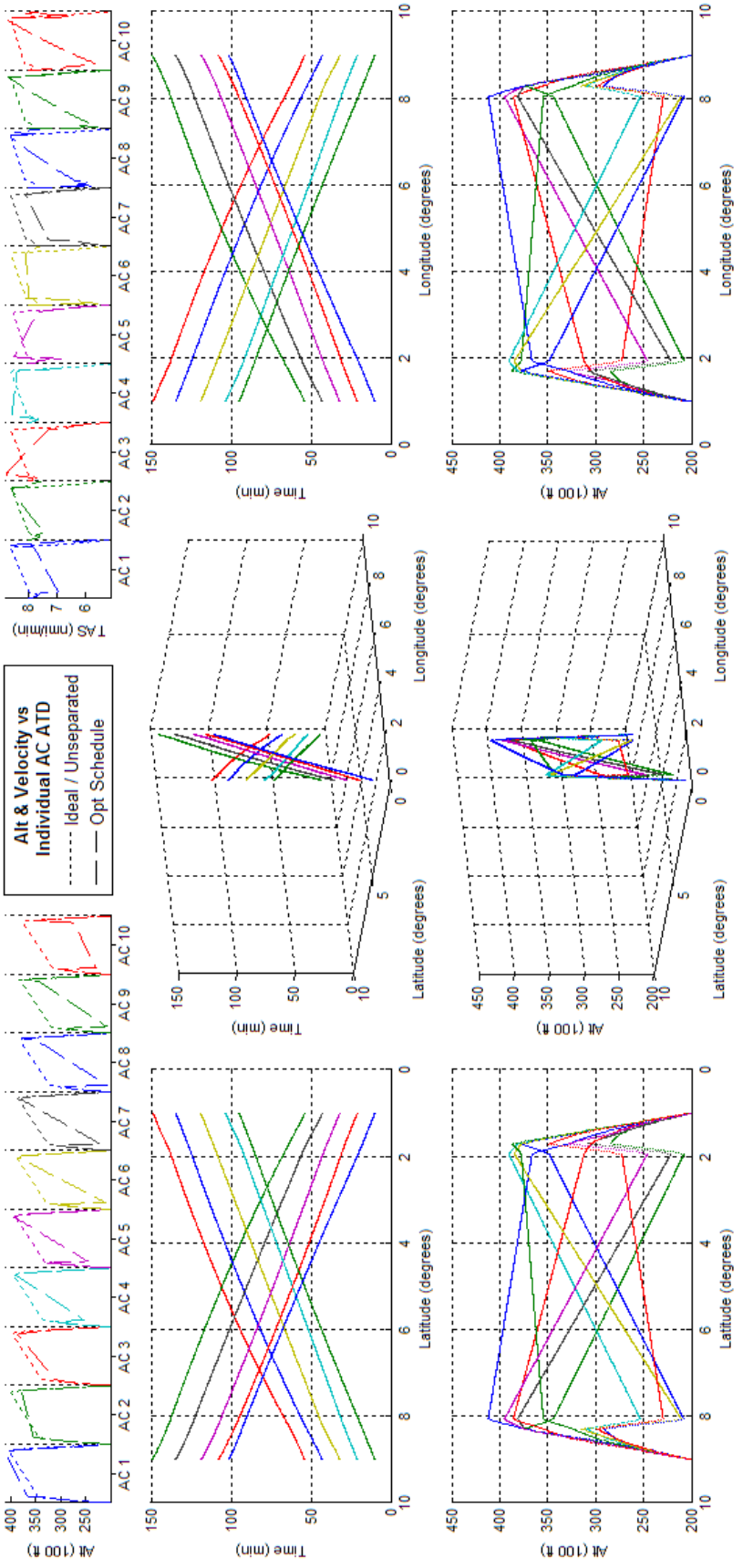

Figure 355 - Fuel Optimized 10acPH2H ATD_{R1} Results

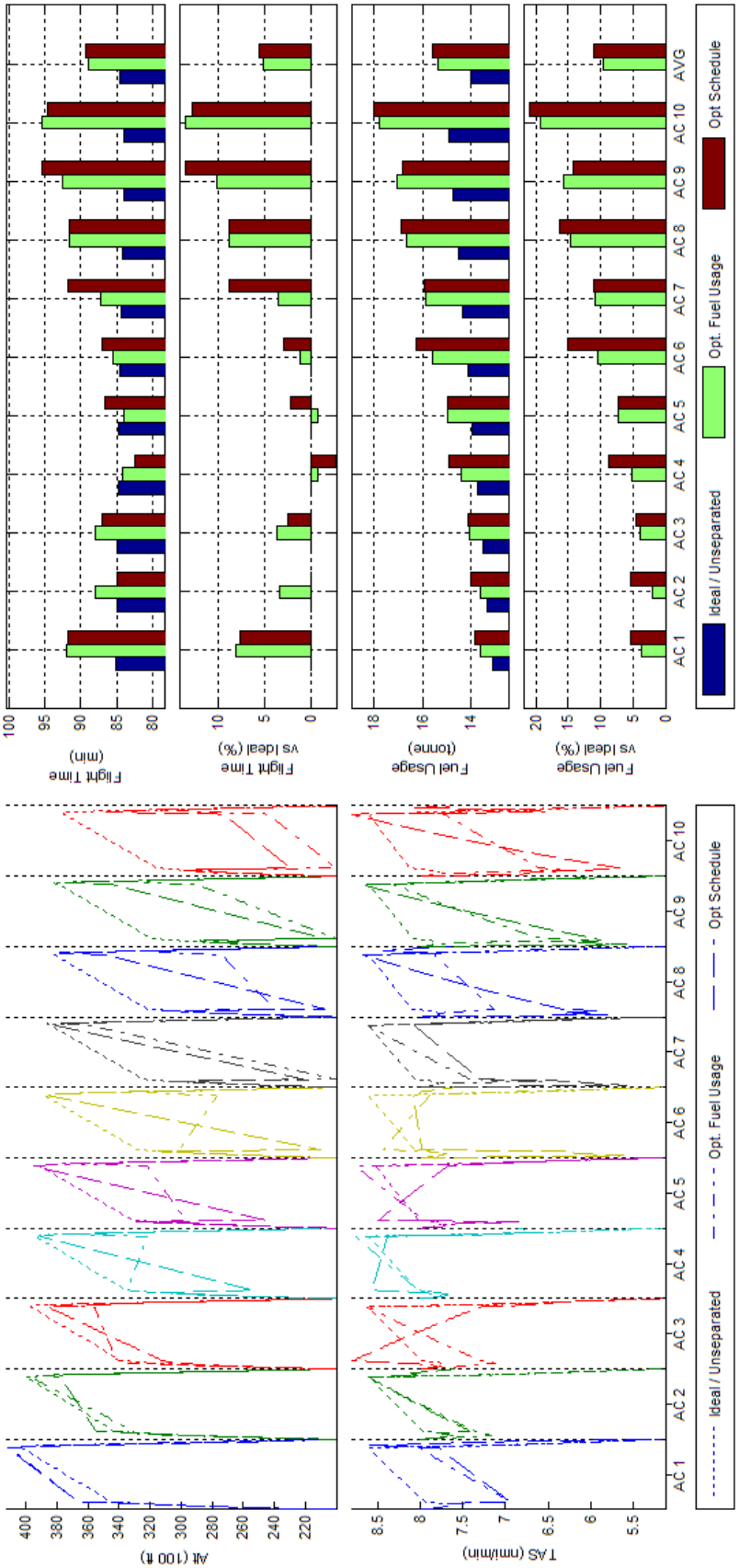

Figure 356 Trajectory Shape, Flight Time, and Fuel Consumption Comparisons of Fuel and Schedule Optimized 10acPH2H ATD_{RI} Results

L.32 BADA Boeing 747-300 - Scenario 10acPH2H - ATD_{R2}

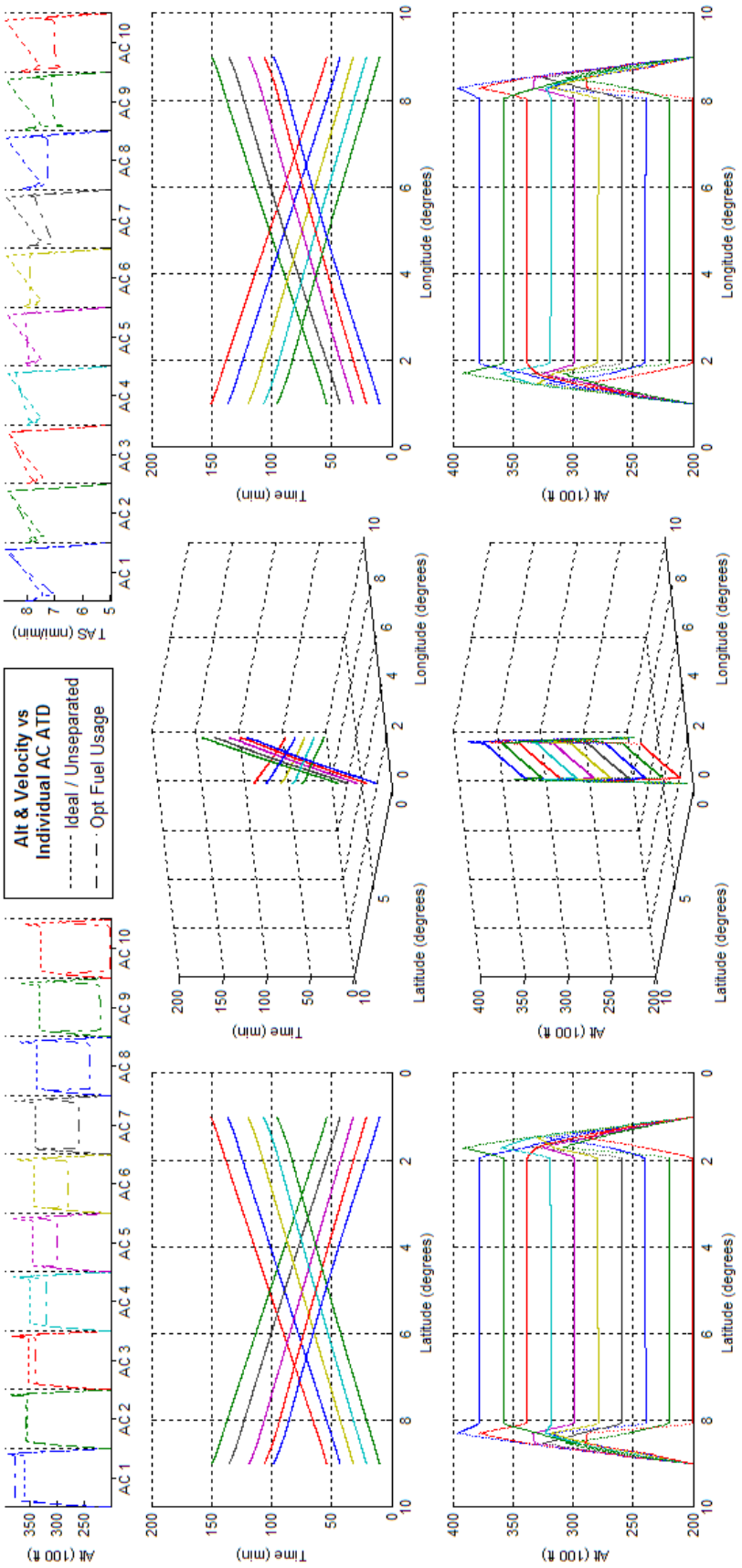

Figure 357 - Fuel Optimized 10acPH2H ATD_{R2} Results

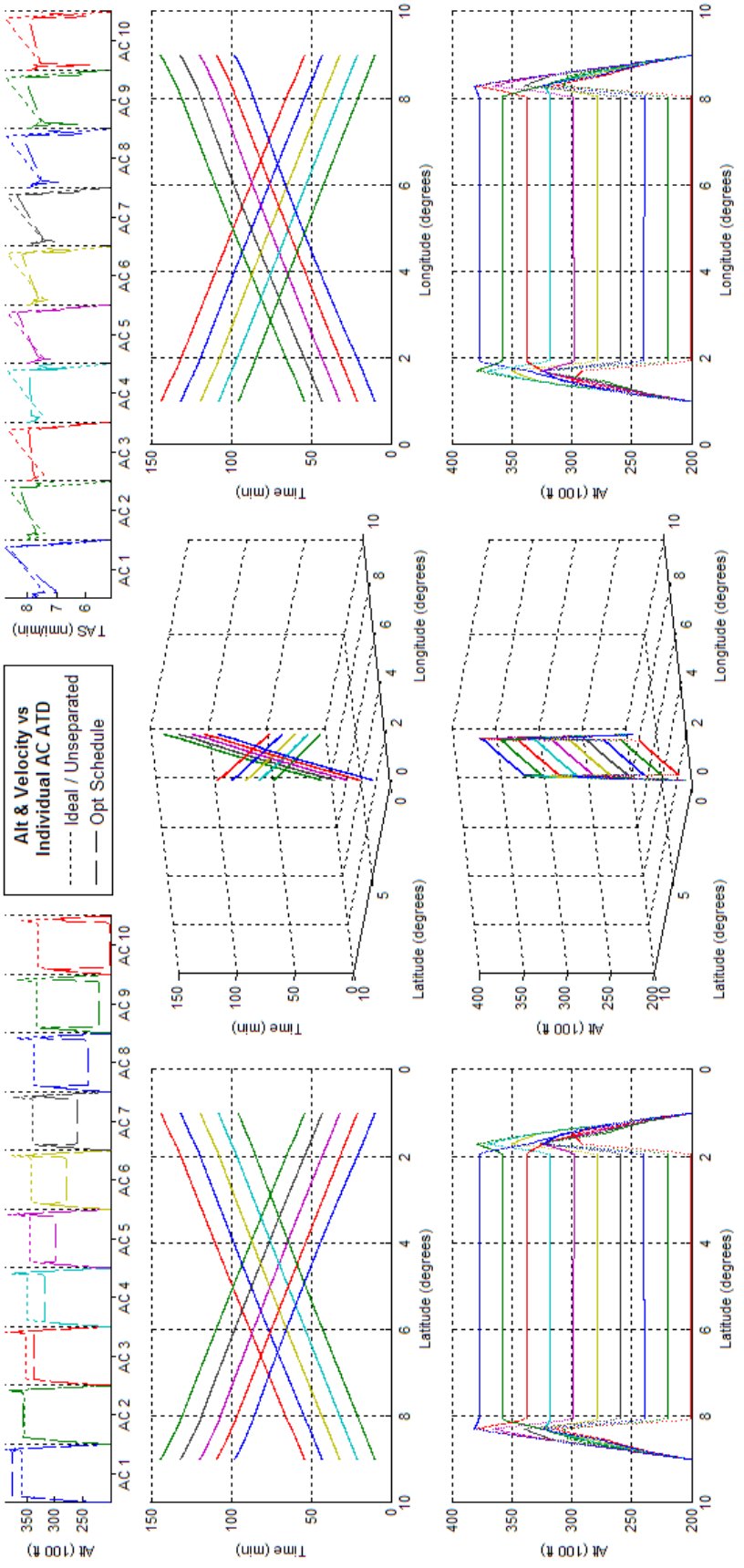

Figure 358 -Schedule Optimized 10acPH2H ATD_{R2} Results

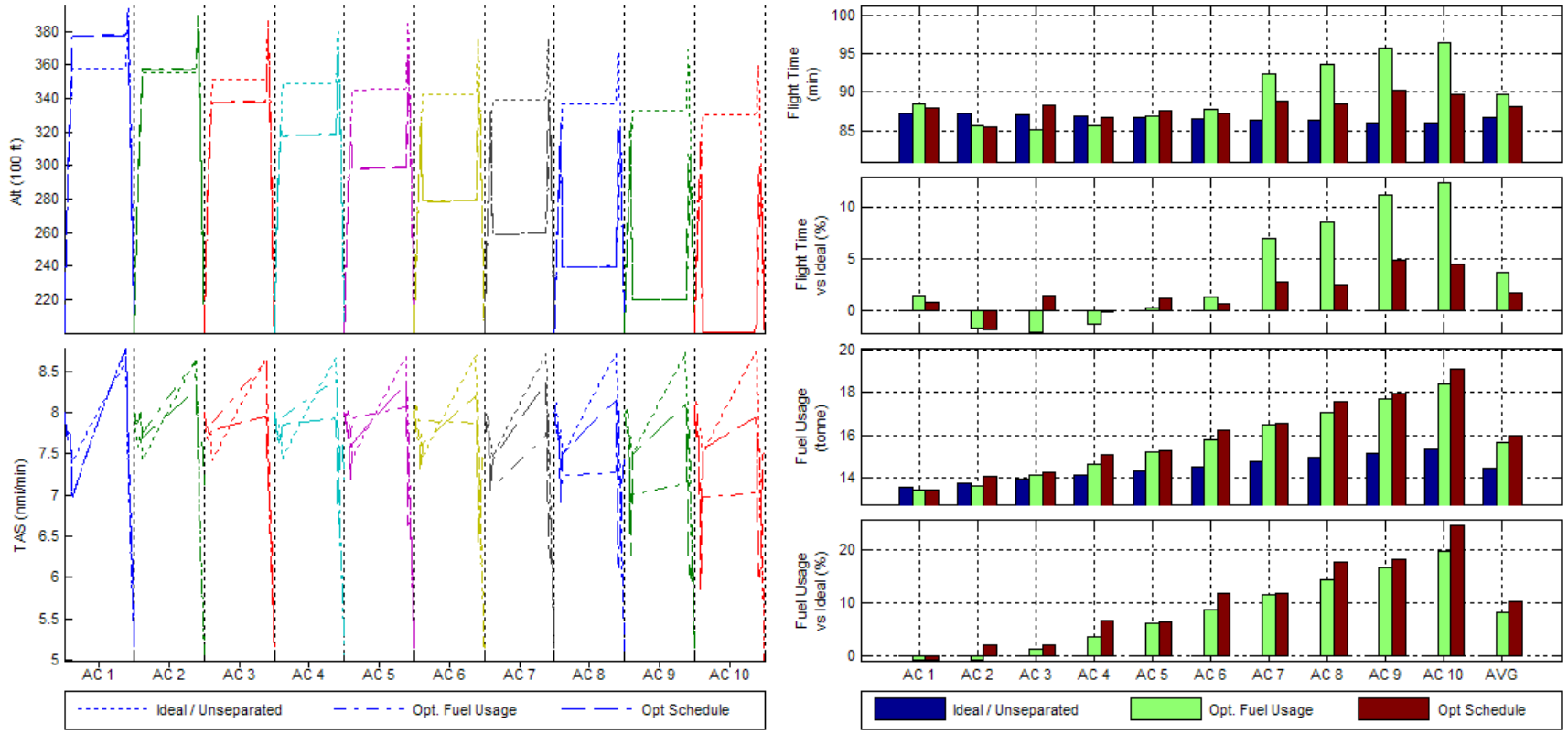

Figure 359 Trajectory Shape, Flight Time, and Fuel Consumption Comparisons of Fuel and Schedule Optimized 10acPH2H ATD_{R2} Results

L.33 BADA Boeing 747-300 - Scenario 10acPH2H - ATD_{R3}

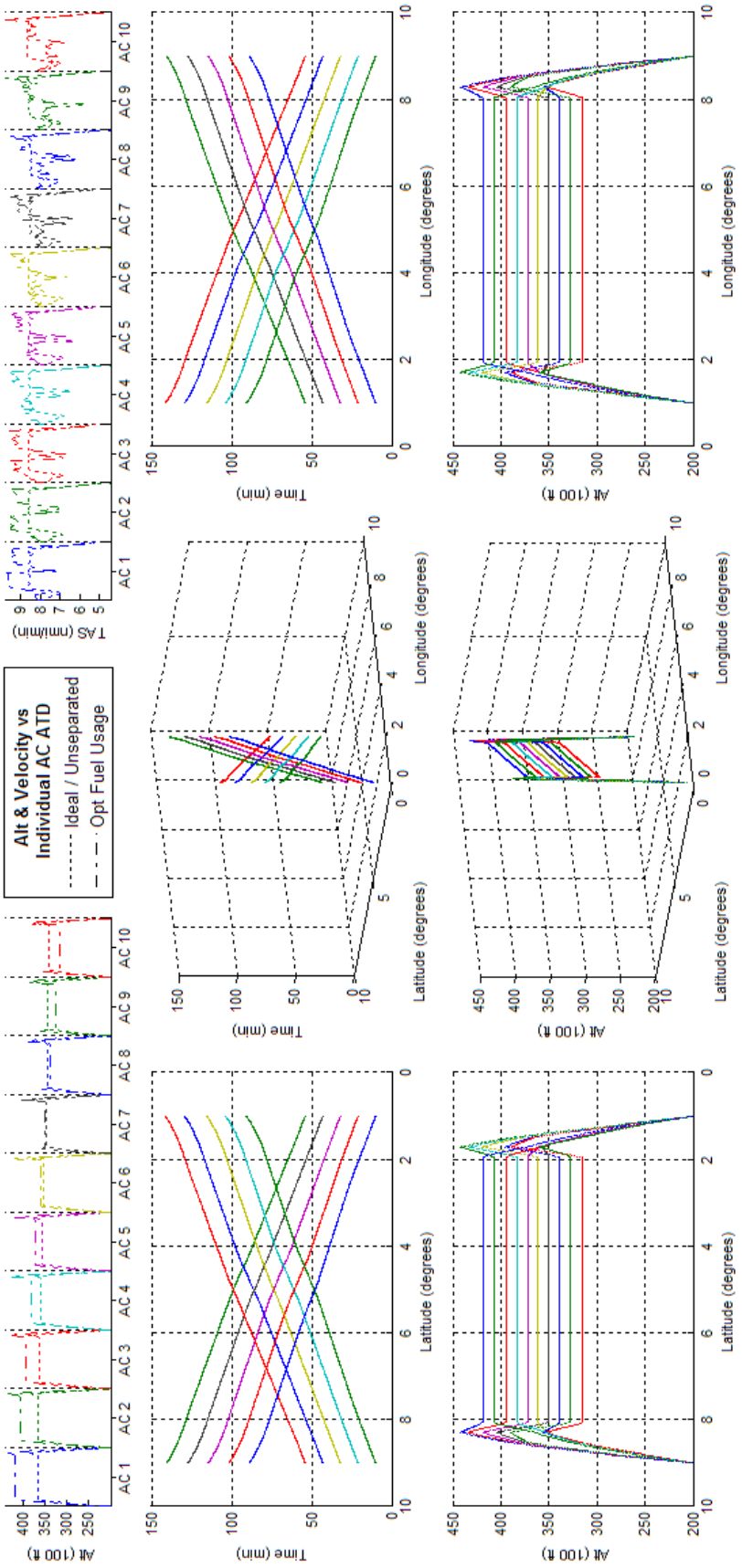

Figure 360 - Fuel Optimized 10acPH2H ATD_{R3} Results

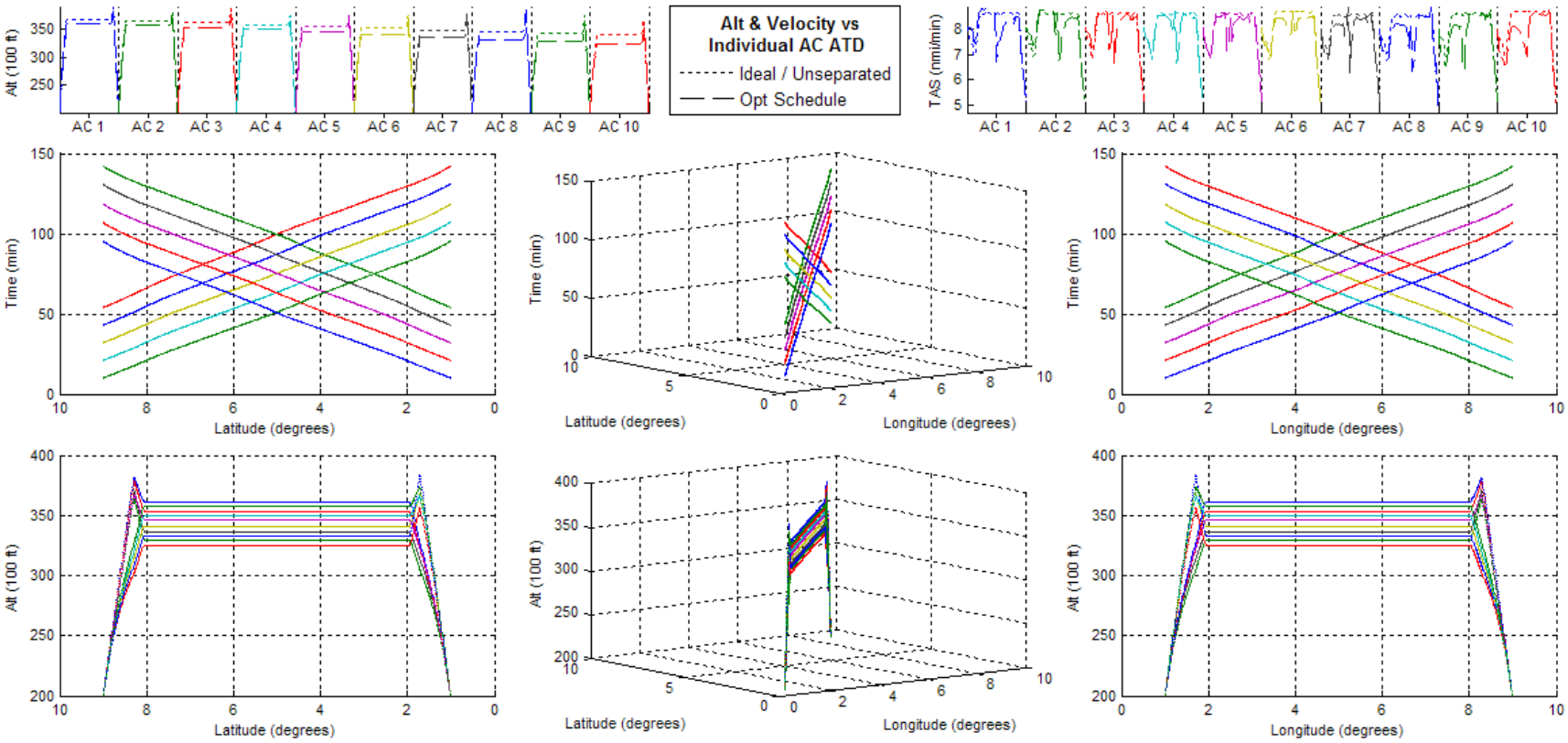

Figure 361 -Schedule Optimized 10acPH2H ATD_{R3} Results

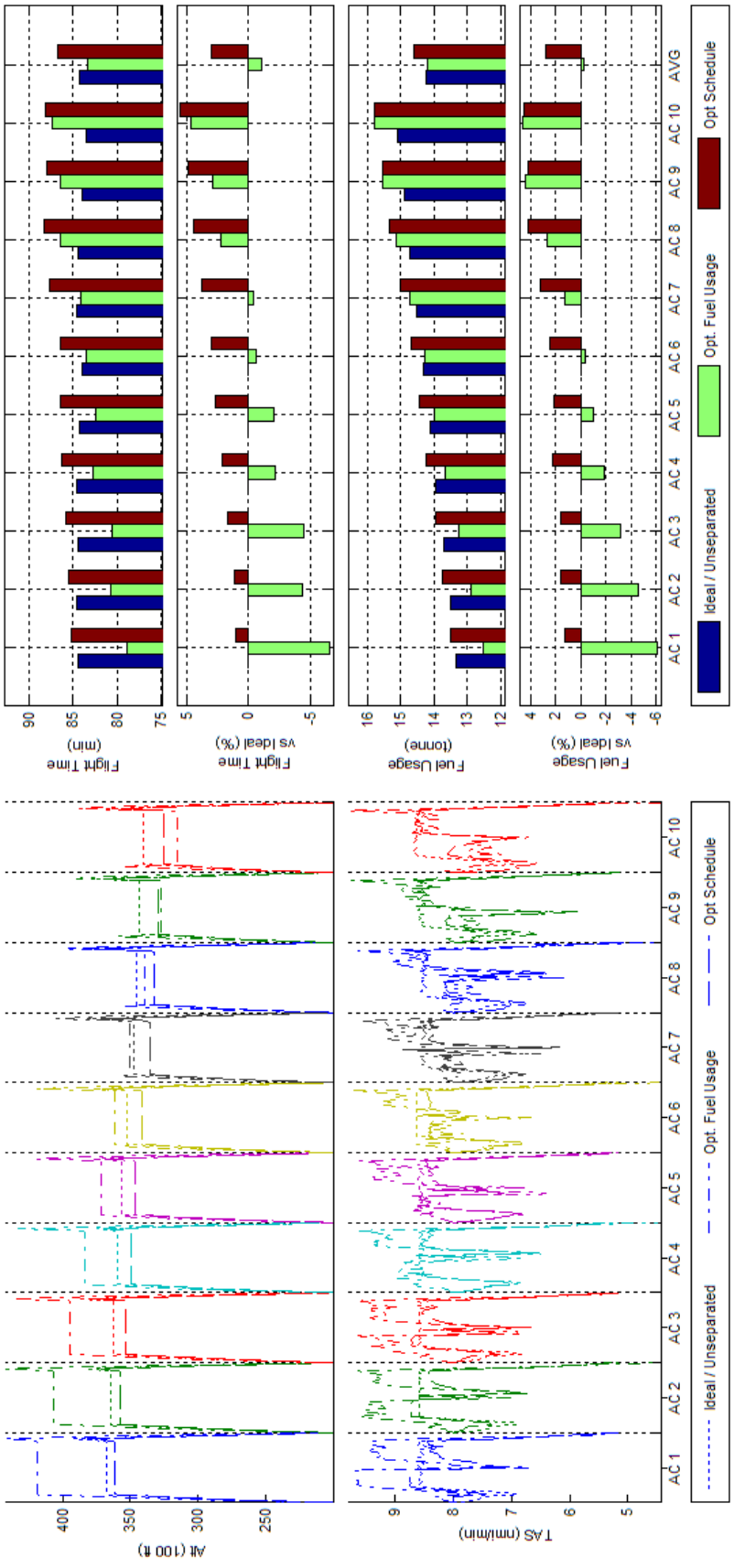

Figure 362 Trajectory Shape, Flight Time, and Fuel Consumption Comparisons of Fuel and Schedule Optimized 10acPH2H ATD_{R3} Results

APPENDIX M Bibliography

The following are documents that have influenced the research shown in this thesis, but for the purposes of clarity have not been directly cited by the work. Consequently, they do not appear in any of the reference lists shown in Chapter 8, Appendix A.6, Appendix B.3, or Appendix C.4.

[M1] Abeloos, A., Mulder, M., van Paassen, R., & Hoffman, E., 2000. "Potential co-operations between the TCAS and the ASAS", *Proceedings of International Conference on Human-Computer Interaction in Aeronautics*, France.

[M2] Bakker, G. J., & Blom, H. A., 1993. "Air traffic collision risk modelling", *Proceedings of the 32nd IEEE Conference on Decision and Control*, pp. 1464-1469, San Antonio, Texas.

[M3] Bayen, A. M., Raffard, R. L., & Tomlin, C. J., 2006. "Adjoint-based control of a new Eulerian network model of air traffic flow", *IEEE Transactions on Control Systems Technology*, Vol. 14(5), pp. 804-818.

[M4] Blin, K., Akian, M., Bonnans, F., Hoffman, E., & Zeghal, K., 2000. "A Stochastic conflict detection method integrating planned heading and velocity changes", *Decision and Control, 2000. Proceedings of the 39th IEEE Conference*, Vol. 5, pp. 4717-4722.

[M5] Blin, K., Akian, M., Bonnans, F., Hoffman, E., Martini, C., & Zeghal, K., 2000. "A stochastic conflict detection model revisited", *AIAA Guidance, Navigation, and Control Conference*, Denver, CO.

[M6] Blin, K., Bonnans, F., Hoffman, E., & Zeghal, K., 2001. "Conflict resolution in presence of uncertainty: A case study of decision making with dynamic programming", *AIAA Guidance, Navigation, and Control Conference and Exhibit*, Montreal, Canada.

[M7] Bonnemaison, B., Casaux, F., & Miquel, T., 1998. "Operational assessment of co-operative ASAS applications", *USA/Europe Air Traffic Management R&D Seminar*.

[M8] Caetano, T., Hoffman, E., & Zeghal, K., 2001. "Model-based evaluation of merging operations in sequence of aircraft", *AIAA Guidance, Navigation, and Control Conference and Exhibit*, Montreal, Canada.

[M9] Casaux, F., & Hasquenoph, B., 1997. "Operational Use of ASAS". *USA/Europe Air Traffic Management R&D Seminar*.

[M10] Cloerec, A., Zeghal, K., & Hoffman, E., 1999. "Traffic complexity analysis to evaluate the potential for limited delegation of separation assurance to the cockpit", *Digital Avionics Systems Conference, 1999. Proceedings. 18th*, Vol. 1, pp. 5-A, IEEE.

[M11] Christien, R., Benkouar, A., Chaboud, T., & Loubieres, P., 2002. "Air traffic complexity indicators & ATC sectors classification", *Proceedings of the 21st Digital Avionics Systems Conference*, Vol. 1, pp. 2D3-1, IEEE.

[M12] Christodoulou, M., & Costoulakis, C., 2004. "Nonlinear mixed integer programming for aircraft collision avoidance in free flight", *Proceedings of the 12th IEEE Mediterranean Electrotechnical Conference*, Vol. 1, pp. 327-330, IEEE.

[M13] Duong, V. N., 1997. "FREER: Free-Route Experimental Encounter Resolution-Initial Results", *10th European Aerospace Conference on Free Flight, Session Systems & Concept*, Amsterdam.

[M14] Duong, V. N., 1997. "FREER - A Solution for European Free Flight Implementation?", *Proceedings of the 1997 Flight International Air Navigation Conference*, Amsterdam.

[M15] Duong, V. N., & Hoffman, E., 1997. "Conflict resolution advisory service in autonomous aircraft operations", *16th Digital Avionics Systems Conference*, Vol. 2, pp. 9-3, IEEE.

[M16] Duong, V. N., Hoffman, E., & Nicolaon, J. P., 1997. "Initial results of investigation into autonomous aircraft concept (freer-1)", *Proceedings of the 1rst USA/Europe Seminar,* Saclay, France.

[M17] Duong, V. N., & Zeghal, K., 1997. "Conflict resolution advisory for autonomous airborne separation in low-density airspace", *Decision and Control, 1997. Proceedings of the 36th IEEE Conference,* Vol. 3, pp. 2429-2434.

[M18] Graham, R., Hoffmann, E., Pusch, C., & Zeghal, K., 2003. "Absolute versus Relative Navigation: Theoretical Considerations from an ATM Perspective", *ATM2003 FAA/Eurocontrol R&D Seminar*, Budapest, Hungary.

[M19] Grimaud, I., Hoffman, E., Pene, N., Rognin, L., & Zeghal, K., 2003. "Towards the use of spacing instruction. Assessing the impact of spacing tolerance on flight crew activity", *Proceedings of AIAA Guidance, Navigation, and Control Conference*, Austin, Texas, USA.

[M20] Grimaud, I., Hoffman, E., Rognin, L., & Zeghal, K., 2003. "Spacing instructions in approach: assessing usability from the air traffic controller perspective", *AIAA Guidance, Navigation, and Control Conference*, Austin, Texas.

[M21] Grimaud, I., Hoffman, E., Rognin, L., & Zeghal, K., 2002. "Limited delegation with arrival streams: more insight on its impact on controller activity", *Conference on Guidance, Navigation and Control,* Monterey, USA.

[M22] Grimaud, I., Hoffman, E., Rognin, L., & Zeghal, K., 2002. "Towards a new task distribution between controller and flight crew to manage aircraft spacing", *IFATCA/The Controller*, Vol. 41, N° 2.

[M23] Grimaud, I., Hoffman, E., Rognin, L., & Zeghal, K., 2001. "Assessing the impact on the flight deck of delegation of separation tasks", *20th Digital Avionics Systems Conference*, Florida, USA.

[M24] Grimaud, I., Hoffman, E., Rognin, L., & Zeghal, K., 2001. "Delegating upstream-Mapping where it happens", *Fourth International Air Traffic Management R&D Seminar*, Santa Fe, USA.

[M25] Grimaud, I., Hoffman, E., Rognin, L., & Zeghal, K., 2001. "Involving pilots and controllers in the

evaluation of the limited delegation concept". *Proceedings of the 11th International Symposium on Aviation Psychology*, Columbus, USA.

[M26] Grimaud, I., Hoffman, E., & Zeghal, K., 2001. "Limited delegation of separation assurance to the flight crew", *Air & Space Europe*, Vol. 3(3), pp. 285-287.

[M27] Grimaud, I., Hoffman, E., & Zeghal, K., 2000. *Evaluation of delegation of sequencing operations to the flight crew from a controller perspective–Preliminary results*. Eurocontrol Experimental Centre, France.

[M28] Hoekstra, J. M., Ruigrok, R. C. J., & Van Gent, R. N. H. W., 2001. "Free flight in a crowded airspace?", *Progress in Astronautics and Aeronautics*, Vol. 193, pp. 533-546.

[M29] Hoekstra, J. M., Ruigrok, R. C. J., van Gent, R. N. H. W., Visser, J., Gijsbers, B., Clari, M. S. V. V., Heesbeen, W. W. M., Hilburn, B. G., & Groeneweg, J., 2000. *Overview of NLR free flight project 1997-1999*, NATIONAAL LUCHT EN RUIMTEVAARTLABORATORIUM-PUBLICATIONS-NLR TP, 227.

[M30] Hoffman, E., Bellman, J., Perret, S. G,, & Zeghal, K., 2000. "Traffic analysis with fast-time simulations to evaluate delegation potentialities of sequencing operations", *Proceedings of the 19th Digital Avionics Systems Conference*, Vol. 2, pp. 5D3-1, IEEE.

[M31] Hoffman, E., Grimaud, I., Rognin, L., & Zeghal, K., 2002. "Impact of delegating spacing tasks on flight crew activities. Preliminary results", *21st Digital Avionics Systems Conference*, Irvine, California.

[M32] Hoffman, E., Grimaud, I., Rognin, L., & Zeghal, K., 2001. "Delegation of Crossing Operations to the Flight Crew: First Quantitative Results", *AIAA Guidance, Navigation, and Control Conference and Exhibit*, Montreal, Canada.

[M33] Hoffman, E., Ivanescu, D., Shaw, C., & Zeghal, K., 2003. "Analysis of constant time delay airborne spacing between aircraft of mixed types in varying wind conditions". *USA/Europe Air Traffic Management R&D Seminar*, Budapest, Hungary.

[M34] Hoffman, E., Ivanescu, D., Shaw, C., & Zeghal, K., 2002. "Analysis of spacing guidance for sequencing aircraft on merging trajectories". *21st Digital Avionics Systems Conference*, California, USA.

[M35] Hoffman, E., Nicolaon, J. P., Pusch, C., & Zeghal, K., 1999. "Limited delegation of separation assurance to aircraft". *Air Traffic Management 1999 Workshop*, Capri, Italy.

[M36] Hoffman, E., Pene, N., Rognin, L., & Zeghal, K., 2003. "Introducing a new spacing instruction: Impact of spacing tolerance on flight crew activity", *Proceedings of the Human Factors and Ergonomics Society Annual Meeting*, Vol. 47, No. 1, pp. 174-178, SAGE Publications.

[M37] Hoffman, E., Perret, S.G., and Zeghal, K., 2000. "Pilot-in-the-Loop Evaluation of Cockpit Assistance for Autonomous Operations", *Proceedings of the 2000 World Aviation Conference*, San Diego, CA.

[M38] Hoffman, E., Zeghal, K., Cloerec, A., Grimaud, I., & Nicolaon, J. P., 1999. "Operational concepts for limited delegation of separation assurance to the cockpit", *Air Traffic Management 1999 Workshop*, Capri, Italy.

[M39] Hoffman, E., Zeghal, K., Cloerec, A., Grimaud, I., & Nicolaon, J., 2000. "Is limited delegation of separation assurance promising?". *Third USA/Europe Air Traffic Management R&D Seminar*, Vol. 10, pp. 2004.

[M40] Hoffman, E., Zeghal, K., & Courtet, G., 1999. "Modeling of the scale of separations in cockpit displays for limited delegation of separation assurance". *1999 World Aviation Conference*, San Francisco, CA.

[M41] Hwang, I., & Seah, C. E., 2008. "Intent-based probabilistic conflict detection for the next generation air transportation system", *Proceedings of the IEEE*, Vol. 96(12), pp. 2040-2059.

[M42] Ivanescu, D., Hoffman, E., & Zeghal, K., 2002. "Impact of ADS-B link characteristics on the performances of in-trail following aircraft", *AIAA Guidance, Navigation and Control Conference*, Monterey, California.

[M43] Ivanescu, D., Shaw, C., Hoffman, E., & Zeghal, K., 2003. "Effect of entry conditions on airborne spacing when sequencing multiple converging aircraft", *AIAA Guidance, Navigation, and Control Conference*, Austin, Texas, USA.

[M44] Ivanescu, D., Shaw, C., Hoffman, E., & Zeghal, K., 2003. "Effect of mixed aircraft types and wind on time based airborne spacing". *AIAA Guidance, Navigation, and Control Conference and Exhibit*, Austin, Texas, USA.

[M45] Kosecka, J., Tomlin, C., Pappas, G., & Sastry, S., 1998. "2½D conflict resolution maneuvers for ATMS", *Proceedings of the 37th IEEE Conference on Decision and Control*, Vol. 3, pp. 2650-2655, Florida, USA.

[M46] Krozel, J., Peters, M., & Bilimoria, K., 2000. "A decentralized control strategy for distributed air/ground traffic separation", *AIAA Guidance, Navigation, and Control Conference and Exhibit*, Denver, CO.

[M47] Loureiro, T., Blin, K., Hoffman, E., & Zeghal, K., 2001. "Development of a tool for comparing conflict detection algorithms for air traffic management", *AIAA Guidance, Navigation, and Control Conference and Exhibit*, Montreal, Canada.

[M48] Loynes, J., Dieudonne, J., Collins, B., Lewis, M., Struth, R., Comitz, P., Holtz, D., & Wilson, I., 2003. "Global communications, navigation, surveillance system (GCNSS) satellite based architecture for air traffic management", *Digital Avionics Systems Conference, 2003. DASC'03*. Vol. 1, pp. 4-A, IEEE.

[M49] Mackintosh, M. A., Dunbar, M., Lozito, S., Cashion, P., McGann, A., Dulchinos, V., Ruigrok, R., Hoekstra, J., & Van Gent, R., 1998. "Self-separation from the air and ground perspective", *2nd USA/Europe Air Traffic Management R&D Seminar*, Orlando, FL.

[M50] Massink, M., & De Francesco, N., 2001. "Modelling free flight with collision avoidance", *Proceedings. Seventh IEEE International Conference on Engineering of Complex Computer Systems*, pp. 270-279, IEEE.

[M51] Paglione, M. M., Oaks, R. D., & Ryan, H. F., 2004. "Methodology for evaluating and regression testing a conflict probe", Proceedings of the 23rd Digital Avionics Systems Conference, Vol. 1, IEEE.

[M52] Pekela, W. D. & Hilburn, B., 1998. "Air traffic controller strategies in resolving free flight traffic conflicts: The effect of enhanced controller displays for situation awareness", *Proceedings of the 1998 World Aviation Conference*, Anaheim, CA.

[M53] Prandini, M., & Hu, J., 2008. "Application of reachability analysis for stochastic hybrid systems to aircraft conflict prediction", Proceedings of the 47th IEEE Conference on Decision and Control, pp. 4036-4041, IEEE.

[M54] Rognin, L., de-Beler, N., Grimaud, I., Hoffmans, E., & Zeghal, K., 2003. "Validating a New Task Distribution between Air Traffic Controllers and Flight Crew", *Proceedings of the Human Factors and Ergonomics Society Annual Meeting*, Vol. 47, No. 1, pp. 86-90, SAGE Publications.

[M55] Rognin, L., Grimaud, I., Hoffman, E., & Zeghal, K., 2002. "Assessing Negative and Positive Dimensions of Safety. A Case Study of a New Air Traffic Controller-Flight crew Task Allocation", *21st European Conference on Human Decision Making and Control*, Glasgow.

[M56] Rognin, L., Grimaud, I., Hoffman, E., & Zeghal, K., 2002. "Impact of delegation of spacing tasks on safety issues. *Proceedings of the 21st Digital Avionics Systems Conference on Air Traffic Management for Commercial and Military Systems*, p. 17.

[M57] Rognin, L., Grimaud, I., Hoffman, E., & Zeghal, K., 2001." Implementing changes in controller-pilot tasks distribution: the introduction of limited delegation of separation assurance", *4th international workshop on Human Error, safety and Systems Development*, Linkoping, Sweden

[M58] Rognin, L., Grimaud, I., Hoffman, E., & Zeghal, K., 2001. "User-centered design of cockpit interfaces involving pilots in sequencing operations", *AIAA Guidance Navigation and Control Conference*, Montreal, Canada.

[M59] Rognin, L., Zeghal, K., Grimaud, I., & Hoffman, E., 2002. "Investigating Delegation of Spacing Tasks from Air Traffic Controllers to Pilots. Impact on Controller Activity", *Proceedings of the Human Factors and Ergonomics Society Annual Meeting*, Vol. 46, No. 1, pp. 71-75, SAGE Publications.

[M60] van Gent, R. N. H. W., Hoekstra, J. M., & Ruigrok, R. C. J., 1997. "Free flight with airborne separation assurance", *Proc. Int. Conf. Human Computer Interaction in Aeronautics*, pp.63 -69 1998, Montreal, Canada.

[M61] Vinken, P., Hoffman, E., & Zeghal, K., 2000. "Influence of speed and altitude profile on the dynamics of in-trail following aircraft", *AIAA Guidance, Navigation and Control Conference*, Denver, CO.

[M62] Wang, C., Ge, J., & Xu, X., 2009. "Analysis of Air Traffic Flow Control through Agent-Based Modeling and Simulation", *Proceedings of the 2009 International Conference on Computer Modeling and Simulation*, pp. 286-290, IEEE Computer Society.

[M63] Warren, A. W., & Ebrahimi, Y. S., 1998. "Vertical path trajectory prediction for next generation ATM", Proceedings of the 17th Digital Avionics Systems Conference, Vol. 2, pp. F11-1, IEEE.

[M64] Work, D. B., & Bayen, A. M., 2008. "Convex formulations of air traffic flow optimization problems", *Proceedings of the IEEE*, Vol. 96(12), pp. 2096-2112.

[M65] Zeitlin, A., & Bonnemaison, B., 2000. "Managing criticality of ASAS applications". *3rd USA/Europe Air Traffic Management R&D Seminar*, Napoli.

[M66] Zeghal, K., Deransy, R., Grimaud, I., Hoffman, E., & Rognin, L., 2001. "Delegation of sequencing operations to the flight crew–First quantitative results", *AIAA Guidance Navigation and Control Conference*, Montreal, Canada.

[M67] Zeghal, K., Grimaud, I., Hoffman, E., Rognin, L., Pellegrin, A., & Rodet, L., 2002. "Delegation of spacing tasks from controllers to flight crew: Impact on controller monitoring tasks", *The 21st Digital Avionics Systems Conference, 2002. Proceedings*, Vol. 1, pp. 2B3-1, IEEE.

[M68] Zeghal, K., & Hoffman, E., 2002. "Delegation of separation assurance to aircraft: towards a framework for analysing the different concepts and underlying principles", *International Council of the Aeronautical Sciences Congress (ICAS)*, Harrogate, UK.

[M69] Zeghal, K., & Hoffman, E., 1999. "Design of cockpit displays for limited delegation of separation assurance", *Digital Avionics Systems Conference, 1999. Proceedings. 18th* , Vol. 1, pp. 4-D. IEEE.

[M70] Zeghal, K., Hoffman, E., Cloerec, A., Grimaud, I., & Nicolaon, J. P., 1999. "Initial evaluation of limited delegation of separation assurance to the cockpit". *SAE Transactions*, Vol. 108(1), pp. 1020-1031.